MERCURY AND ASSOCIATED TRACE ELEMENTS IN THE PRIMARY ENVIRONMENT, KEEL PROSPECT, COUNTY LONGFORD, IRELAND.

A thesis submitted for the degree of Doctor of Philisophy

by

Roger John Watling

Mining Geology Department,
Royal School of Mines,
Imperial College of Science
and Technology, London.

December, 1972.

ERRATA

p. 2		Diagram after Morrissey,C.J., Davis, G.R., and Steed,G.M. 1971.
p. 4	line 21	Friedrich and Hawkes, 1966.,
p. 10		Numbers,corresponding to rock types,are referred to throughout the text.
p. 12		R.T.Z. company diagram.
p. 15	line 17	gouge
p. 66	line 26	horizons
p. 144	line 10	Colorimetric
p. 203	line 11	chalcopyrite and tetrahedrite
p. 211	line 24	Friedrich and Hawkes,1966
p. 237	line 2	which was released in greater amounts the finer the material was crushed.
p. 255	line 7	- 494 um + 210 um fraction 93.3 ppb
	line 18	TOTAL 157 ppb
p. 281	line 12	$2ZnS + 3O_2 = 2ZnO + 2O_2$
p. 285	line 28	Fig. 8.19B.
p. 288	line 1	Fig. 8.19B.
p. 299	line 9	Appendix E gives the results obtained.
p. 340	line 22	Watling,R.J., Davis,G.R., Meyer,W.T., 1972

Analytical precision for all elements analysed by atomic absorption is within $\pm$ 5% relative.

DEDICATED

WITH FONDEST LOVE TO

MY WIFE

HELEN

ABSTRACT

The Keel zinc/cadmium prospect occurs in Lower Carboniferous clastic sediments, on the down-faulted southern flank of a north-east/south-west trending Lower Palaeozoic inlier. The wallrocks of the deposit are predominantly siliceous clastics which are overlain by reef and bioclastic limestones. Mineralization is closely associated with south-easterly dipping normal faults of late Hercynian age with an east-west Caledonian strike, and occurs predominantly in the clastic sequences.

Investigation into the distribution of Cu, Pb, Zn, Ag, Cd and Hg in the prospect area confirmed the absence of any primary dispersion pattern for these elements. The distribution of Ca, Mg, Na and K also gave no indication of even minor wallrock alteration or redistribution of these elements associated with the mineralizing processes.

Chemical analysis of sphalerite, galena and pyrite indicated certain trace element associations. These however were proven to be mainly due to inclusions of chalcopyrite, tetrahedrite and gangue minerals such as quartz and dolomite.

Intensive investigation into the geochemistry and dispersion pattern for mercury in the Keel prospect area ultimately led to the development of an analytical technique whereby identification of mercury compounds in rock material was made possible.

The analysis was carried out by measurement of the atomic absorption of mercury, evolved during controlled heating of samples, in a continuous air flow system. Evolved mercury peaks in natural rock samples were identified at approximately, 170°C, 220°C, 300°C, 520°C, 450°C and 600°C, correlating with artificially prepared standards of

mercurous chloride, mercuric chloride, mercuric sulphide and mercuric oxide respectively. The 450°C and 600°C peaks correspond to mercury released from pyrite and sphalerite lattices respectively. Elemental mercury gave a release peak at 80°C and mercuric sulphate gave a triple release peak at 350°C, 420°C and 510°C; however these two phases did not attain major significance in the Keel area.

Mercuric sulphide was found to be concentrated in the vicinity of base metal sulphides, while mercuric chloride wae the predominant phase in rocks more remote from sulphide ore. These main zones are separated by a mixed zone of mercuric chloride and mercuric sulphide.

Exploration in this area, using rock analysis could thus be aided by identification of the sulphide zone in mercury trace analysis, as the total mercury content does not always appear to be directly releated to the proximity of sulphide ore.

ARRANGEMENT OF TEXT

		PAGE
Abstract		I
Arrangement of text		III
List of figures		VIII
List of tables		XIX
CHAPTER 1	INTRODUCTION	
	1.1 Location of the Keel prospect	1
	1.2 History of the Keel prospect	1
	1.3 Scope of the present study	4
	1.4 Mercury as a geochemical exploration tool	5
	1.5 Acknowledgements	7
CHAPTER 2	GEOLOGY AND MINERALIZATION OF THE KEEL DEPOSIT	
	2.1 Introduction	9
	2.2 Geology of the Longford area	9
	2.3 Structural geology of the Longford area	14
	2.4 Mineralogy and mineralization at Keel	15
	2.5 Ore genesis at Keel	17
CHAPTER 3	PRIMARY DISPERSION OF SELECTED ELEMENTS IN THE KEEL AREA	
	3.1 Introduction	18
	3.2 Initial results and sample preparation	18
	3.3 Primary dispersion of metals in the Keel area	22
	3.3A Calcium, magnesium, sodium & potassium	25
	3.3B Iron and manganese	30
	3.3C Lead and zinc	45
	3.3D Cadmium and copper	66
	3.3E Silver	76
	3.3F Mercury	79

PAGE

CHAPTER 4 PRIMARY DISPERSION STUDIES IN THE UNDERGROUND WORKINGS OF THE KEEL PROSPECT

4.1 Introduction 96

4.2 Interlaboratory comparison of Cu, Pb & Zn analyses 96

4.3 Comparison of polarographic and atomic absorption for lead and cadmium analyses 102

4.3 Comparison of optical spectrograph and atomic absorption for copper , lead , zinc and manganese analyses 107

4.4 Geology and mineralization of the underground workings , Keel mine , County Longford , Ireland . 110

4.5 Primary dispersion in the underground workings , Keel prospect , County Longford , Eire . 118

4.6 Conclusions 134

CHAPTER 5 PRIMARY DISPERSION OF FLUORINE AND CHLORINE IN WALL ROCKS SURROUNDING THE KEEL ZINC-CADMIUM PROSPECT

5.1 Introduction 142

5.2 Cycle of fluorine and chlorine 142

5.3 Method of analysis 144

5.4 Discussion of the method of analysis 146

5.5 Analysis of G.1 & W.1 for chloride 149

5.6 Analysis of rock material from Keel for fluorine and chlorine 150

CHAPTER 6 TRACE ELEMENT DISTRIBUTION IN SPHALERITE GALENA AND PYRITE FROM THE KEEL PROSPECT

6.1 Introduction 155

6.2 Analytical method 155

6.3 Analysis 157

6.4 Mercury in sphalerite, galena and pyrite 164

CHAPTER 6		PAGE
	6.5 Trace elements in sphalerite from Keel	181
	6.6Inter - element relationships in Keel sphalerites	201
	6.7 Trace elements in galena from Keel	203
	6.8 Trace elements in pyrite from Keel	208
	6.9 X - Ray analysis of sphalerite, galena and pyrite	210
	6.10 Summary and conclusions	214
CHAPTER 7	SUMMARY AND CONCLUSIONS	
	7.1 Introduction	217
	7.2 Geology and stratigraphy	217
	7.3 Mineralization	218
	7.4 Ore genesis	218
	7.5 Primary geochemistry	219
	7.6 Trace element distribution in sphalerite galena and pyrite	222
	7.7 Conclusions	223
CHAPTER 8	MERCURY AND MERCURY COMPOUNDS IN THE PRIMARY ENVIRONMENT OF THE KEEL PROSPECT	
	8.1 The geochemistry and abundance of mercury	225
	8.2 Primary dispersion of total mercury at the Keel prospect	226
	8.3 Primary dispersion of mercury compounds at the Keel prospect	231
	8.3a Sample collection and preparation	231
	8.3b Initial analytical results	240
	8.3c Continuous flow, thermal dissociation of mercury compound analysis	246
	8.3d Standardization of equipment	247

CHAPTER 8 PAGE

8.3e One possible reason for the variation in mercury concentration with decreasing particle size in sieved , crushed rock material . 252

8.3f Results 252

8.3g Identification and distribution of mercury compounds in the primary environment at Keel 261

8.3h Mercury in the lattices of sphalerite, galena and pyrite at Keel 278

A) The 600°C - 700°C peak of mercury release 281

B) The 450°C peak of mercury release 288

C) The 520°C peak of mercury release 290

8.4 Summary 290

8.5 Conversion of a Southern Analytical A 3000 atomic absorption spectro - photometer into a continuous mercury and arsenic release monitoring apparatus 291

8.6 Base metal and mercury compound distribution in Keel soils 295

1) Introduction 295

2) Soil geochemistry at Keel 296

3) i) Sampling and sample preparation 296

ii) Sample drying 297

4) Sample analysis 297

5) Results 299

i) Copper 299

ii) Lead 299

iii) Zinc 299

iv) Cadmium 309

v) Iron 309

vi) Manganese 309

CHAPTER 8		PAGE
	8.6 5) vii) Mercury and mercury compounds	309
	a) 270°C peak	318
	b) 430°C peak	319
	c) Results	319
CHAPTER 9	SUMMARY AND CONCLUSIONS	
	9.1 Summary	323
	9.2 Conclusions	324
	9.3 Suggestions for further research	328
	9.4 Suggestions for improvement of mercury thermal dissociation equipment	328
REFERENCES		329 - 341
APPENDICES		i - xxv
A	SAMPLE PREPARATION AND METHOD OF ANALYSIS OF Cu, Pb, Zn, Ag, Fe, Mn, Ca, Mg, Na & K , BY ATOMIC ABSORPTION AND ATOMIC EMISSION	i
B	ANALYTICAL RESULTS FOR INITIAL SAMPLE PREPARATION STUDY	vii
C	POLAROGRAPHIC TECHNIQUE AND PREPARATION OF ATOMIC ABSORPTION STANDARD SOLUTIONS	xvii
D	FLUORINE AND CHLORINE ANALYSIS OF SELECTED DRILL CORE SAMPLES	xx
E	TRACE ELEMENT ANALYSIS OF SOILS IN THE KEEL AREA	xxii

LIST OF FIGURES

FIG. No.	TITLE	PAGE No.
1.1	Map of the known lead-zinc-copper mineralization in Ireland.	2
1.2	Generalised cross section of the Keel prospect.	3
2.1	Stratigraphic succession, Keel.	10
3.1	Keel drillhole location map.	19
3.2	Comparison of the metal concentration of different size fractions of rock material with the true whole rock concentration.	21
3.3	Diagram illustrating lateral metal zoning as indicated by diamond drillhole intersections.	24
3.4	The distribution of Mg/Ca on the 100' level, Keel prospect.	26
3.5	The distribution of Mg/Ca on the 200' level, Keel prospect.	27
3.6	Diagram illustrating the relationship of the magnesium:calcium ratio and the potassium:sodium ratio to mineralization.	28
3.7	The distribution of Mg/Ca on the 500' level, Keel prospect.	29
3.8	The distribution of K/Na on the 100' level, Keel prospect.	31
3.9	A comparison of manganese and iron in rock material from drillcore and underground workings	32
3.10	The distribution of manganese on the 100' level, Keel prospect.	33

FIG.No.	TITLE	PAGE No.
3.11	The distribution of Mn on the 200' level, Keel prospect.	34
3.12	The distribution of Mn on the 300' level, Keel prospect	35
3.13	The distribution of Mn on the 400' level, Keel prospect.	36
3.14	The distribution of Mn on the 500' level, Keel prospect.	37
3.15	The distribution of Fe on the 100' level, Keel prospect.	38
3.16	The distribution of Fe on the 200' level, Keel prospect.	39
3.17	The distribution of Fe on the 300' level, Keel prospect.	40
3.18	The distribution of Fe on the 400' level, Keel prospect.	41
3.19	The distribution of Fe on the 500' level, Keel prospect.	42
3.20	Diagram illustrating the distribution of iron and manganese in the Mixed Beds & Reef Limestone.	44
3.21	Cross section of the Keel prospect showing the association of lead & zinc mineralization with faulting & the association of pyrite bodies with the Reef Limestone.	46
3.22	Relationship between silver content and Zn:Pb ratio in C,D,G,H&K orebodies, Keel prospect.	48
3.23A	Lithological association of lead and zinc mineralization east of the shaft.	49
3.23B	Lithological association of lead and zinc mineralization east of the shaft.	50

FIG.No.	TITLE	PAGE No.
3.24A	Lithological association of lead and zinc mineralization west of the shaft	51
3.24B	Lithological association of lead and zinc mineralization west of the shaft.	52
3.25	Diagram of the thicknesses of beds encountered in selected drillholes east and west of the Keel shaft	53
3.26	The distribution of Zn on the 100' level,Keel prospect.	55
3.27	The distribution of Zn on the 200' level,Keel prospect.	56
3.28	The distribution of Zn on the 300' level,Keel prospect.	57
3.29	The distribution of Zn on the 400' level,Keel prospect.	58
3.30	The distribution of Zn on the 500' level,Keel prospect.	59
3.31	The distribution of Pb on the 100' level,Keel prospect.	60
3.32	The distribution of Pb on the 200' level,Keel prospect.	61
3.33	The distribution of Pb on the 300' level,Keel prospect.	62
3.34	The distribution of Pb on the 400' level,Keel prospect.	63
3.35	The distribution of Pb on the 500' level,Keel prospect.	64
3.36	Cross section of the Keel prospect showing association of lead & zinc mineralization with major faulting.	65
3.37	The distribution of Cd on the 100' level,Keel prospect.	67

FIG.No.	TITLE	PAGE No.
3.38	The distribution of Cd on the 200' level,Keel prospect.	68
3.39	The distribution of Cd on the 300' level,Keel prospect.	69
3.40	The distribution of Cd on the 400' level,Keel prospect,	70
3.41	The distribution of Cd on the 500' level,Keel prospect.	71
3.42	The distribution of Cu on the 200' level,Keel prospect.	72
3.43	The distribution of Cu on the 500' level,Keel prospect.	73
3.44	A comparison of cadmium and zinc in rock material from drillcore and underground workings.	74
3.45	A comparison of cadmium and zinc in rock material from drillcore and underground workings.	75
3.46	Base metal distribution in drillholes,K50 & K61 Keel,Ireland.	77
3.47	A comparison of silver and zinc in rock material from drillcore and underground workings.	78
3.48	Diagram illustrating Sb/Ag relationship in sphalerite and Pb/Ag relationship in drillcore.	80
3.49	Variation in mercury content of drillcore with particle size.	81
3.50	The distribution of Hg on the 100' level,Keel prospect.	84
3.51	The distribution of Hg on the 200' level,Keel prospect.	85
3.52	The distribution of Hg on the 300' level,Keel prospect.	86

FIG.No.	TITLE	PAGE No.
3.53	The distribution of Hg on the 400' level,Keel prospect.	87
3.54	The distribution ofHg on the 500' level,Keel prospect.	88
3.55	Diagram illustrating the relationship between mercury and zinc in material from drillcore and underground workings.	89
3.56	Histogram of the distribution of zinc on five levels of the Keel prospect. (drillcore samples only)	90
3.57	Histogram of the distribution of lead on five levels of the Keel prospect. (drillcore samples only)	91
3.58	Histogram of the distribution of iron on five levels of the Keel prospect. (drillcore samples only)	92
3.59	Histogram of the distribution of manganese on five levels of the Keel prospect. (drillcore samples only)	93
3.60	Histogram of the distribution of cadmium on five levels of the Keel prospect. (drillcore samples only)	94
3.61	Histogram of the distribution of mercury on five levels of the Keel prospect. (drillcore samples only)	95
3.62	Histogram of the combined level distribution of Cd,Pb,Zn,Hg,Fe,Mn, from drillcore samples Keel prospect.	95b
4.1	Sample locations on the 200' level,Keel.	97
4.2	Sample location on the 400' level,Keel.	98
4.3	Sample locations on the 500' level,Keel.	99
4.4	Interlaboratory comparison of copper and lead analyses.	100

FIG.No.	TITLE	PAGE No.
4.5	Diagram of A) interlaboratory comparison of zinc analyses & B) polarograph versus A.A. for lead analyses.	101
4.6	Polarograms of rock material from Keel.	104
4.7	Comparison of polarograph and atomic absorption analyses for cadmium and lead in rock samples from the mine workings.	105
4.8	Comparison of atomic absorption and optical spectrograph analyses for lead and copper in rock samples from the underground workings.	108
4.9	Comparison of atomic absorption and optical spectrograph analyses for zinc and manganese in rock samples from the underground workings.	109
4.10	Relationship of Cu/Pb/Zn/Ag/Hg. on the 200' level,Keel prospect,County Longford,Ireland	111
4.11	Cu distribution on the 200' level,Keel.	113
4.12	Zn distribution on the 200' level,Keel.	114
4.13	Ag distribution on the 200' level,Keel.	115
4.14	Hg distribution on the 200' level,Keel.	116
4.15	Pb distribution on the 200' level,Keel.	117
4.16	Relationship of Cu/Pb/Zn/Ag/Hg. on the 500' level,Keel prospect,County Longford,Ireland.	119
4.17	Zn distribution on the 500' level,Keel.	122
4,18	Hg distribution on the 500' level,Keel.	123
4.19	Cu distribution on the 500' level,Keel.	124
4.20	Ag distribution on the 500' level,Keel.	125
4.21	Pb distribution on the 500' level,Keel.	126

FIG.No.	TITLE	PAGE No.
4.22	Relationship of copper and mercury to zinc on the 500' level,keel prospect.	127
4.23	Diagram illustrating the variation of mercury concentration with particle size on the 200' and 500' levels,Keel.	130
4.24	Relationship of Cu/Pb/Ag/Zn/Hg. on the 400' level Keel prospect, County Longford , Ireland .	135
4.25	Copper distribution on the 400' level,Keel.	136
4.26	Lead distribution on the 400' level,Keel.	137
4.27	Mercury distribution on the 400' level,Keel.	138
4.28	Zinc distribution on the 400' level,Keel.	139
4.29	Silver distribution on the 400' level , Keel.	140
4.30	Histogram plot of the distribution of mercury, zinc,copper,lead & silver on the underground workings , Keel prospect , County Longford.	141
5.1	Diagram of the calibration curves for fluoride and chloride analysis.	145
5.2	Diagram showing the variation with time of optical density of standard colloidal suspensions of silver chloride	147
5.3	Diagram of the relative variation with time of optical density of standard colloidal suspensions of silver chloride.	148
5.4	Diagram illustrating the relationship between zinc sodium , potassium , fluorine & chlorine in D.D.H.1 & D.D.H.14 ,Keel prospect , County Longford , Ireland .	151
5.5	Diagram of relationship of calcium & magnesium to fluorine & chlorine in cold water leaches from Keel drill core .	153

FIG . No.	TITLE	PAGE No.
6.1	Mercury calibration curves for stannous chloride method of mercury analysis .	169
6.2	Diagram illustrating mercury release from a 0.1μg./ml. mercury standard in three different diluting mediums .	171
6.3	Diagram illustrating the effect of Au, Pt & Ag on mercury release from standard solutions	173
6.4	Diagram illustrating the relationship between mercury and iron in sphalerite from the Keel prospect , County Longford .	176
6.5	Effect of water and acidified potassium permanganate solution on the mercury calibration graph .	179
6.6	Diagram illustrating cadmium/iron relations in material from drillcore & underground workings .	185
6.7	Diagram showing trace element distribution in sphalerite , galena & pyrite , Keel prospect .	198
6.8	Diagram illustrating the method of calculating the cell edge of sphalerite and galena crystals .	213
6.9	Diagram illustrating the effect of increasing iron and cadmium concentration on the cell dimensions of sphalerite .	215
8.1	The cycles of mercury	228
8.2	Diagram of apparatus for continuous mercury thermal release analysis	233
8.3	Calibration graph for mercury analysis by the mercury vapour injection method	235

FIG . No .	TITLE	PAGE No.
8.4	Perspex lid design for gas extraction from a sealed grinding mill.	239
8.5	Calibration of mercury analysis apparatus by the mercury pulse method .	242
8.6	Mercury release from crushed rock material under step heating volatilization conditions.	244
8.7	Thermal release curves of mercury vapour from various mercury compounds.	245
8.8	Mercury compound calibration graphs .	250
8.9	Dissociation characteristics of mercuric sulphide .	251
8.10	Diagram illustrating the effect of particle size on mercury thermal dissociation characteristics.	254
8.11	Variation of mercury content with fraction in crushed rock material from chloride - rich and sulphide - rich areas,Keel prospect Ireland .	258
8.12	The variation in mercury thermal release pattern in rock samples from the different mercury compound zones, Keel prospect, County Longford,Ireland.	264
8.13	The distribution of mercury compounds on the 100' level,Keel prospect.	265
8.14	The distribution of mercury compounds on the 200' level,Keel prospect .	266
8.15	The distribution of mercury compounds on the 300' level,Keel prospect.	267
8.16	The distribution of mercury compounds on the 400' level,Keel prospect.	268
8.17	The distribution of mercury compounds on the 500' level,Keel prospect.	269

FIG . No .	TITLE	PAGE No.
8.18	Comparison of total mercury and mercury compound data .	272
8.19	The use of calcium oxide to remove sulphide interference in mercury thermal dissociation analysis .	279
8.20	Diagram of the positions of samples taken for X - Ray analysis of thermal breakdown of rock matrix on heating .	283
8.21	Thermal X - Ray photograph showing dissociation of sphalerite into zinc oxide on heating .	286
8.22	Relationship between zinc and mercury in Keel rock material .	289
8.23	Diagram of apparatus for continuous mercury and arsenic thermal release analysis .	292
8.24	The use of calcium oxide to remove sulphide interference in arsenic thermal dissociation analysis .	294
8.25	Plan of soil sample locations surrounding the Keel shaft .	300
8.26	Sample positions on orientation traverse .	301
8.27	Contour intervals of element concentrations in Keel soil .	302
8.28	Copper distribution in shaft area .	303
8.29	Copper distribution on orientation traverse .	304
8.30	Lead distribution on orientation traverse .	305
8.31	Lead distribution in shaft area .	306
8.32	Zinc distribution on orientation traverse .	307
8.33	Zinc distribution in shaft area .	308

FIG . No .	TITLE	PAGE No,
8.34	Cadmium distribution on orientation traverse.	310
8.35	Cadmium distribution in shaft area .	311
8.36	Iron distribution in shaft area .	312
8.37	Iron distribution on orientation traverse .	313
8.38	Manganese distribution on orientation traverse.	314
8.39	Manganese distribution in shaft area .	315
8.40	Mercury and mercury compound distribution on orientation survey .	316
8.41	Mercury and mercury compound distribution in shaft area .	317
8.42	Mercury thermal release characteristics of clay minerals and iron oxides .	320

LIST OF TABLES

TABLE No.	TITLE	PAGE No.
3.1	Mercury content in different size fractions of rock samples : A) from underground workings B) from drillcore.	23
3.2	Comparison of duplicate mercury analyses.	83
4.1	Zn/Pb , Zn/Cd & Zn/Ag ratios in the F,E,D & C faults , Keel prospect, County Longford ,Eire.	120
4.2	Variation of mercury content with fraction size of rock from the underground workings.	128
4.3	Zn/Pb , Zn/Cd & Zn/Ag ratios in the F,E,D & C faults Keel prospect,County Longford,Eire.	132
6.1	Semiquantitative spectrographic analysis of selected sphalerites from Keel prospect, County Longford,Ireland.	159
6.2	Semiquantitative spectrographic analysis of selected sphalerites from Keel prospect, County Longford , Ireland.	160
6.3	Semiquantitative spectrographic analysis of selected sphalerites from Keel prospect, County Longford,Ireland.	161
6.4	Semiquantitative spectrographic analysis of selected sphalerites , galenas & pyrites from Keel prospect , County Longford,Ireland.	162
6.5	Comparison of spectrographic and atomic absorption analysis for selected elements in sphalerites from Keel prospect,County Longford,Ireland.	163
6.6	Wavelengths of the spectral lines used in the determination of minor element concentrations in sphalerite from Keel.	182

TABLE No.	TITLE	PAGE No.
6.7	Gallium , germanium , cadmium & iron concentrations of two selected series of Keel sphalerite.	187
6.8	Antimony , silver & copper concentrations in two selected series of Keel sphalerites.	189
6.9	Mean and standard deviation values for trace element concentrations in Keel sphalerites.	190
6.10	Diagram of the relative abundances of trace elements in sphalerite , galena & pyrite, Keel prospect,County Longford,Ireland.	199
6.11	Variation in trace element assemblage in sphalerite with depth.	201
6.12	Table illustrating the correlation coefficients of trace elements in sphalerite from the Keel prospect,County Longford,Ireland.	202
6.13	Wavelengths of the spectral lines used in the determination of minor elements in pyrite and galena samples from Keel Ireland.	205
6.14	Unit cell characteristics of selected minerals from Keel and the literature.	214
8.1	Average content of mercury in sedimentary and igneous rocks.	227
8.2	Mercury content in different size fractions of rock samples.	236
8.3	Comparison of the mercury content of ground and unground -1550 μ + 494 μ material from Keel.	238

TABLE No.	TITLE	PAGE No.
8.4	Calibration of mercury meter by the mercury pulse method using various chart recorder/ voltmeter settings to obtain maximum sensitivity.	243
8.5	Composition of rock standard bases used in mercury compound analysis.	248
8.6	Temperatures of mercury release peaks.	248
8.7	The effect of heat on the reactions: $Hg^{2+} + S^{2-} = HgS$ & $Hg^{2+} + 2Cl^{-} = HgCl_2$ and on anion activities.	277
8.8	The effect of heat on mercury loss in sample drying.	298
8.9	Analysis of mercury and mercury compounds in Keel soils.	321

CHAPTER 1

INTRODUCTION

1.1. LOCATION OF THE KEEL PROSPECT.

The Keel zinc-cadmium prospect is located, Fig. 1.1., towards the north of the Central Irish Plain at longitude 7° 44' W. latitude 53° 39' N., some 70 miles west of Dublin and 7 miles south of Longford town. The surrounding countryside of Keel is low lying agricultural and grazing land, with generally high water table. The Keel prospect, however, is sited on the southern flank of an elevated quartzitic and conglomeratic inlier with folded and faulted lower Palaeozoic rocks at its core and consequently the water-table here is much lower. This allows migration of water through the fractured siliceous wallrocks of the deposit.

1.2. HISTORY OF THE KEEL PROSPECT.

In 1962 reconnaissance parties of Rio Tinto Finance and Exploration Ltd. detected high values of lead and zinc in soils and stream sediments in the Longford area. Geophysical and geological work followed, leading to a diamond drilling programme which outlined a zinc/cadmium deposit. In the light of information obtained from the first twenty-eight drillholes, the control of mineralization at Keel was considered stratigraphic with an unknown amount of lateral metal migration into the fault zones. In 1965 an exploration shaft was sunk to expose the mineralization. Some 4,500 ft. of underground workings were excavated. As a result of this, a definite structural control of mineralization was established, Fig. 1.2. The Keel prospect was put on a care and maintenance basis in 1968.

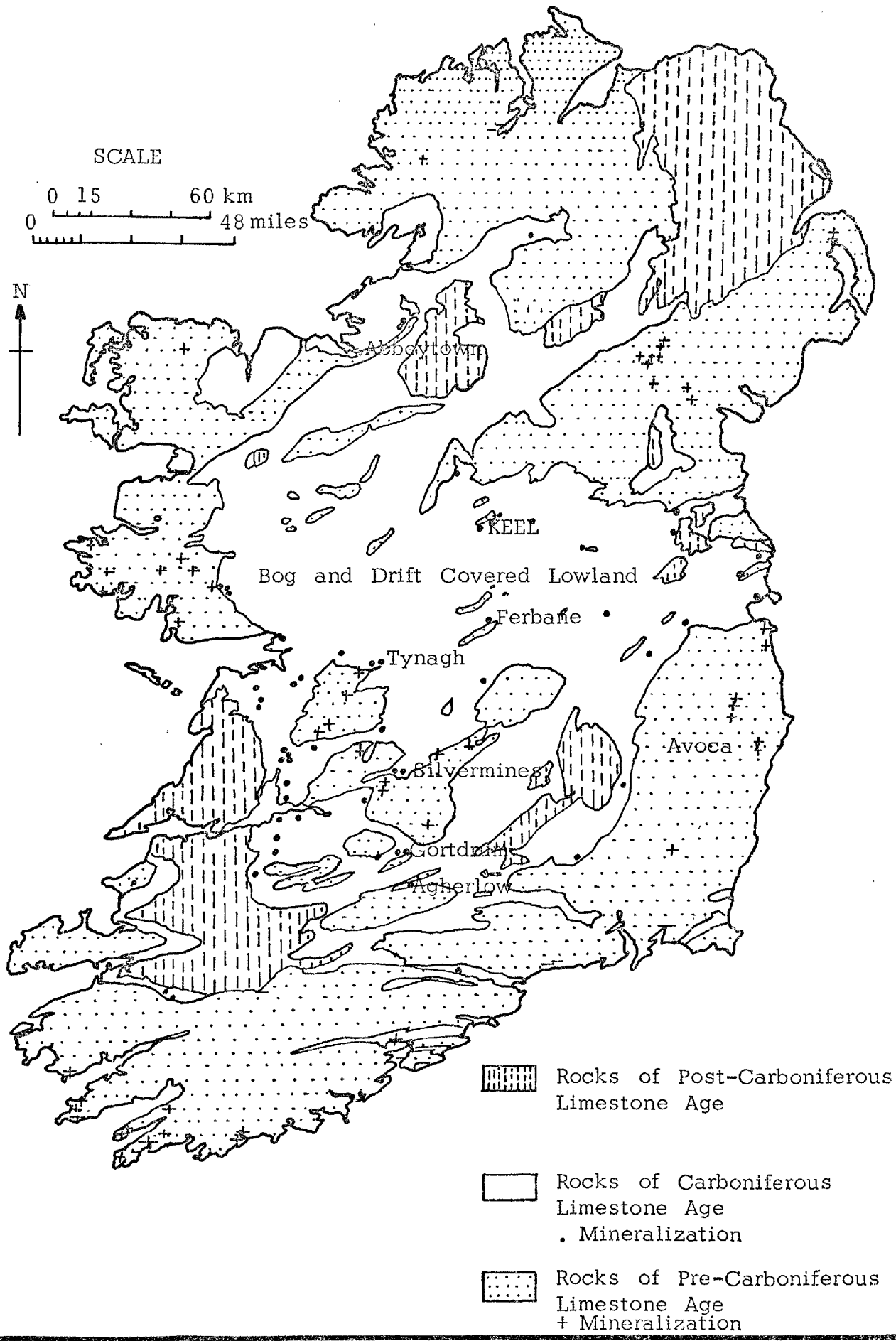
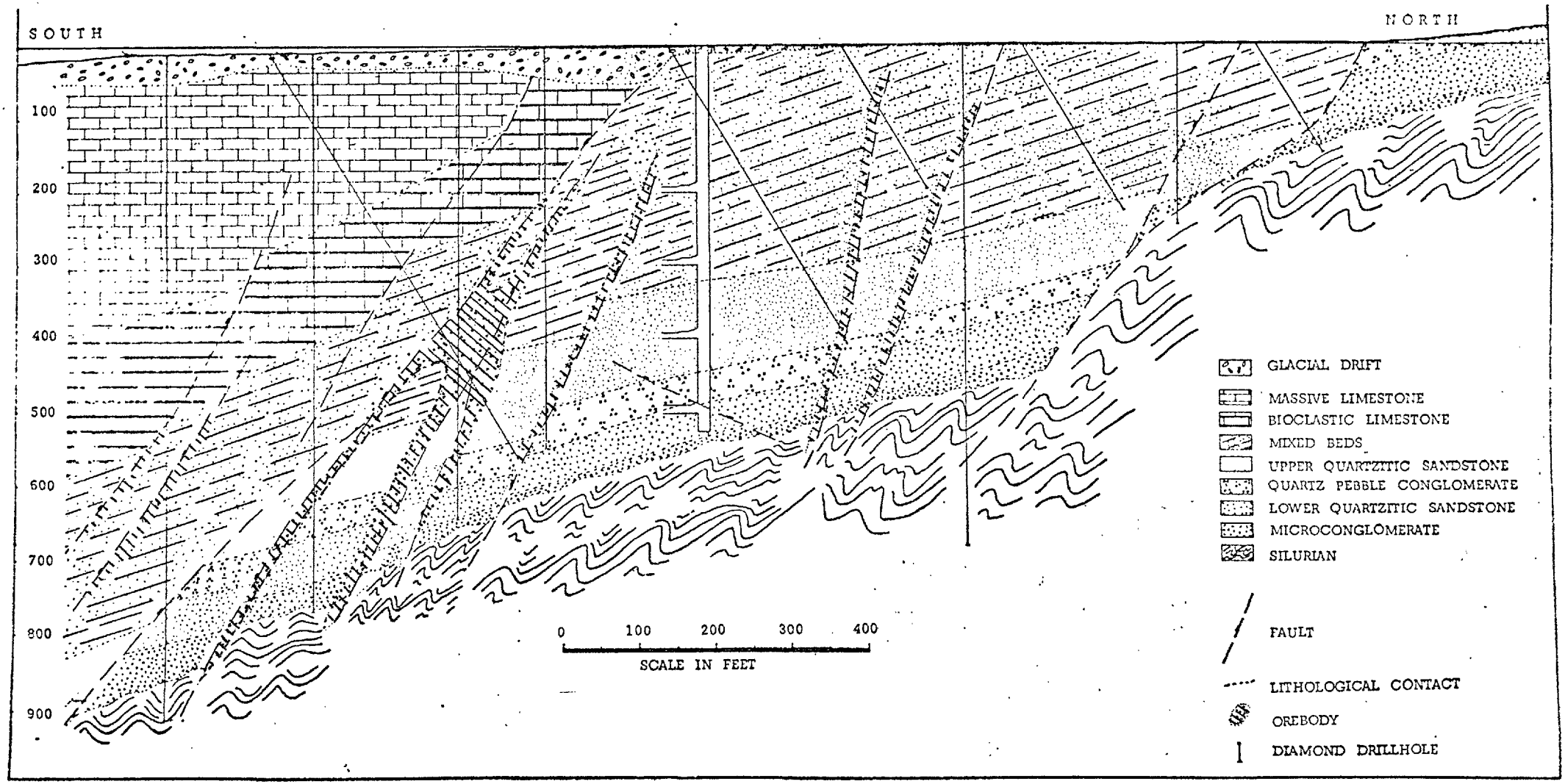


FIG ...1.1

MAP OF THE KNOWN LEAD-ZINC-COPPER MINERALIZATION IN IRELAND

FIG ... 1.2 GENERALISED CROSS SECTION OF THE KEEL PROSPECT



In late 1970 American Smelting and Refining Company (A.S.A.R.C.O.) agreed with Rio Tinto Zinc (R.T.Z.) to carry out further drilling in the area in order to investigate the possible lateral extensions of the known mineralization. In August 1971, after leaving submersible pumps underground, pumping stopped and the water-table was left to find its own level. In December 1971 A.S.A.R.C.O. ceased drilling activities in the Keel area and no exploration activity has occurred subsequently.

1.3. SCOPE OF THE PRESENT STUDY.

This study forms part of an interdisciplinary research programme on the Keel zinc/cadmium deposit by the Royal School of Mines. The particular aspect of the research programme covered by this study is the investigation of the trace element geochemistry of the primary environment surrounding the Keel prospect. It was also hoped, by analysing selected trace elements and minerals, to discover something about the mechanism of ore emplacement and the effects of mineralization on the surrounding rocks. As the importance of mercury as a geochemical pathfinder element for potential areas of base metal mineralization has increased enormously in recent years, (Fursov, 1958., Ozerova, 1959., Hawkes and Williston, 1962., Frederick and Hawkes, 1961., James, 1964., and Barringer, 1965), due to new analytical techniques and a better understanding of its geochemistry, this element has tended to assume predominance in this study.

In the latter part of the research, a technique which enabled trace amounts of various mercury compounds to be identified and

measured in rock material was developed, and using this technique, the distribution of mercury compounds around the Keel deposit was worked out. An explanation of the genesis of the deposit on the basis of the mercury compounds distribution has been put forward.

Other elements investigated during the course of this study were as follows:-

In whole rock material: Cu, Pb, Zn, Cd, Fe, Mn, Na, K, Ca, Mg.

In the ore minerals, sphalerite, pyrite and galena: (Zn), (Fe), (Pb), Cu, Cd, Mn, Na, K, Ca, Mg, As, Sb, Bi, Ba, Co, Ni, Cr, Sn, Mo, Si, V, Ga, Ge, In, Ti.

1.4. MERCURY AS A GEOCHEMICAL EXPLORATION TOOL.

Many authors have discussed the use of the mercury halo method of geochemical exploration for base metal deposits. James (1962) states "Broad patterns of primary dispersion are frequently formed by mercury around both mercury and polymetallic deposits. These halos are believed to reflect predominantly gaseous dispersion and may be expected to be most marked where the rocks are most porous or where fracturing has occurred prior to, or simultaneous with mineralization".

Although the writer is not in complete agreement with this view, with respect to the Keel deposit, the above statement admirably summarizes the reasons for using mercury as a geochemical prospecting guide.

Techniques for mercury analysis have now vastly increased in sophistication and many of the initial problems of interferences from sulphur and organic material have been overcome. Consequently the use of mercury as a geochemical pathfinder technique has become far more dependable.

Airborne detection of mercury gas is at present being carried out by Barringer Research Ltd. using a helicopter mounted mercury spectrometer. This technique enables vast areas of sometimes comparatively inaccessible terrain to be covered quickly, accurately and cheaply, and the mineralization potential to be assessed before the expence of a ground survey. The results of the research described in this thesis provide a possible follow-up technique to investigate target areas identified by such reconnaissance surveys.

1.5. ACKNOWLEDGEMENTS.

The author wishes to express his gratitude to Dr. A.R. Barringer, Visiting Professor of Economic Geology at Imperial College, for both initiating and financing the entire project. To Professor G.R. Davis, Professor of Mining Geology, Imperial College, as senior supervisor throughout the entire project, for his continued help, support and advice and for reading the manuscript. To Mr. W.T. Meyer, Applied Geochemistry Research Group, Imperial College, for supervising a major part of the analytical programme and for his advice and support throughout the programme and for reading the manuscript. To Dr. C. J. Morrissey for supervising the initial period of the research and for his continued support and interest. To Mr. A. J. Thompson of the departmental Geochemistry Laboratory for his invaluable help, advice and interest throughout the analytical programme, and to many other colleagues in both Mining Geology and Applied Geochemistry Departments at the Royal School of Mines for helpful discussion and assistance.

The author also wishes to express his gratitude to Mr.J. Sample and Mr. D. Toft of A.S.A.R.C.O. for their assistance during the field sample collection programme and to R.T.Z. for allowing unlimited access to their information concerning the Keel prospect.

Polished sections were excellently prepared by Mrs. K. Irving and Mr. B. Foster in the Mining Geology laboratories, and advice on X-Ray technique was given by Mr. R. Curtis and Mrs. S. Bird of the Departmental X-Ray laboratory. Mr. R. Berlin provided technical advice on optical spectrograph technique and Mr. K. Lam Shang Leen on atomic absorption technique. The assistance of these people is acknowledged with great pleasure.

The photographic department, under Mr. J. Gee advised on illustrations and Miss Helen O'Brien skilfully reduced many of the trace element distribution maps. Their generous help is also gratefully acknowledged.

CHAPTER 2.

GEOLOGY AND MINERALIZATION OF THE KEEL DEPOSIT.

2.1. INTRODUCTION

This chapter is based primarily on a recent Ph.D. thesis (1971) in Mining Geology at the Royal School of Mines by J.M. Patterson entitled, "Geology and Mineralization of the Keel Area, Co. Longford, Republic of Ireland".

2.2. GEOLOGY OF THE LONGFORD AREA.

Longford is a shelf area situated between the Lower Palaeozoic Longford Down Massif to the north and a deep water facies to the south. Consequently it is in the zone of maximum sedimentary variation.

The stratigraphy of the area was surveyed in great detail by Patterson (1971) and is here only briefly reviewed. Fig. 2.1. shows a simplified stratigraphic section at Keel. The Silurian at the base is in excess of 250' thick and overlying this with strong unconformity is the microconglomerate, which varies in thickness from 0-50'. The Lower Quartz Sandstone overlies this and is regarded as being of Lower Carboniferous age by Patterson; the microconglomerate is consequently the only possible Devonian in the area. The Quartz Pebble Conglomerate, a very distinctive lithological unit with rounded pebbles of quartzite in a siliceous matrix, occurs next in the stratigraphic sequence and is exposed in both the Keel and Longford inliers. In the underground workings of the prospect, it is well represented on both the 400' and 500' levels.

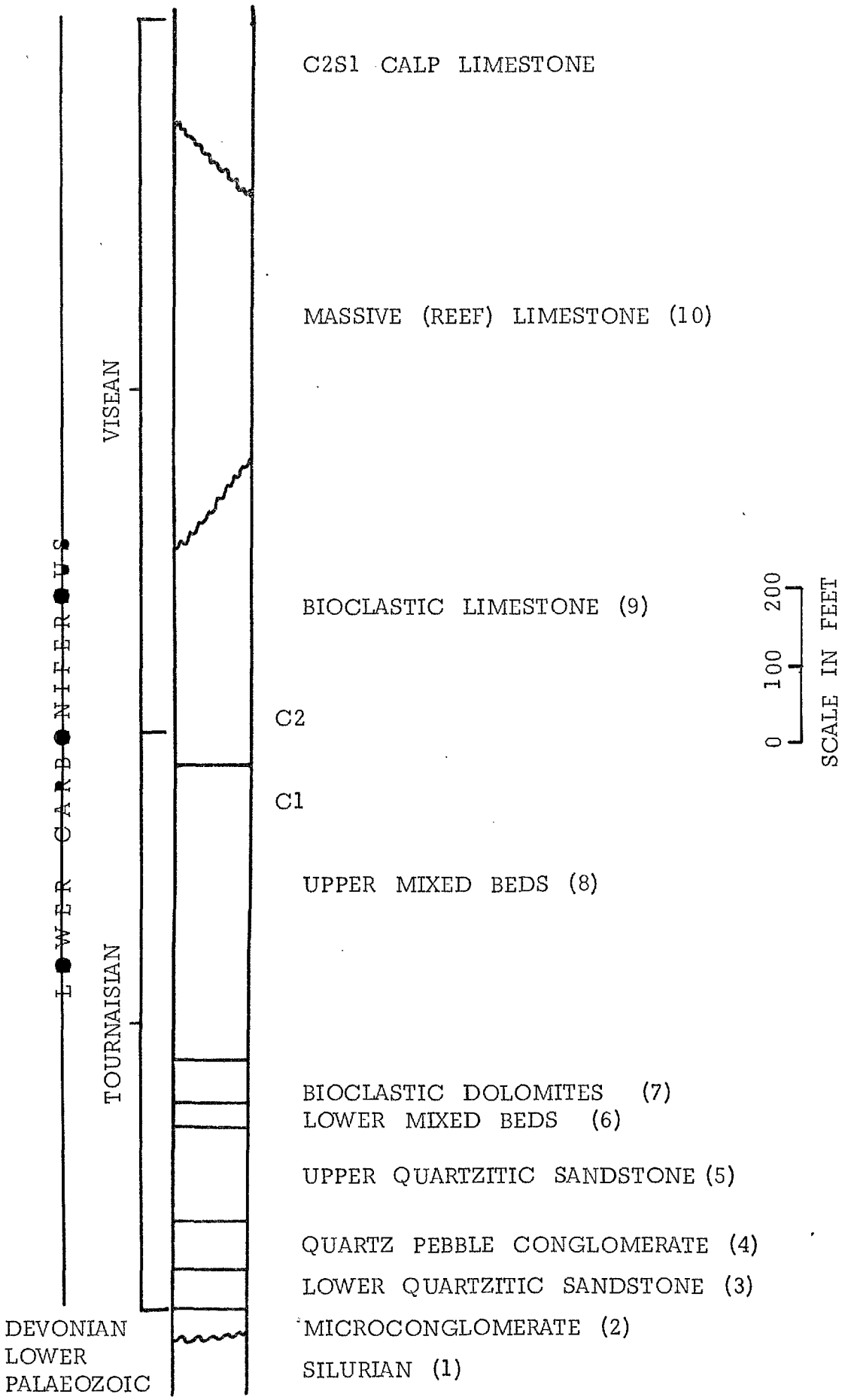


FIG ... 2.1 STRATIGRAPHIC SUCCESSION, KEEL

A transitional conglomeratic sandstone passes up into the overlying Upper Quartz Sandstone which in turn passes transitionally up into the Mixed Beds.

This last unit consists of some 400 feet of interbedded and intercalated muddy sandstones, sandy mudstones, mudstones, sandstones, shales and limestones, commonly dolomitic and bioclastic. Overlying the Mixed Beds is a Bioclastic Limestone unit with a maximum thickness of some 350 feet. This unit is a fossiliferous muddy limestone exhibiting many sedimentary features including slumping and brecciation. A definite relationship exists between this fossiliferous limestone and the overlying reef limestone, a dense, fine grained, highly organic limestone with chert nodules and calcite or dolomite vugs. Further physical characteristics of the sedimentary rock units are summarised below.

(a) Silurian

The Silurian crops out in the core of the Keel inlier and is represented by a sequence of dark grey, green and red shaley mudstones and interbedded coarser grits. Numerous tight folds are common and incipient shaley cleavage is present. The rock is fissile and breaks up easily into small fragments and it is cut by later quartz filled fractures which,in some instances,have a carbonate core. Metamorphic grade is low, as evidenced by the sericitization of the mica and the presence of small quantities of chlorite which appear to have grown in place.

(b) Microconglomerate

This distinctive rock type is seen by Patterson as a basal Carboniferous conglomerate on both sides of the Keel Inlier. Its rapid variation in thickness indicates that it was initially a transgressive infilling in an uneven Silurian sea floor. One interesting characteristic is that it contains reworked fragments of Silurian grits which in some cases contain galena.

(c) Lower Quartz Sandstone

The basal contact with the microconglomerate is usually of transitional nature with thin stringers of microconglomerate and green shale. The sandstone is well bedded and of medium grain-size and although cross-bedding is present it is far from common.

(d) Quartz Pebble Conglomerate

The resistant nature of this rock is the main reason for the Keel inlier forming a topographic high. The base is well defined and shows both faulted and sedimentary contact with the underlying Lower Quartz Sandstone. Pebble size varies from 8" x 6" to 1" x 1" with smaller and more angular pebbles in the matrix. The unit is well jointed with sphalerite along joint planes and its extremely hard nature allows many fractures to develop.

(e) Upper Quartz Sandstone

The top member of the Basal Clastic Group comprises an interbedded series of clean quartzitic, feldspathic, white and grey sandstones and green and black shales. The sandstone is a well jointed competent rock.

(f) Mixed Beds

These beds are interpreted as representing a transition between the clean higher energy clastics below and the overlying muddy lower energy chemical sediments. The Mixed Beds are represented by an interbedded series of sandstones, mudstones and limestones with both dolomitic and siliceous cement. The Upper and Lower Mixed Beds are split by a Bioclastic Dolomite sequence, the rocks of which exhibit a distinctive vuggy appearance and are characteristically very porous. The unit is well bedded with abundant fossils, vugs and fractures and small solution and tensional breccias filled with secondary dolomite. Weathering is very much in evidence along east-west and north-south joints with complete decomposition of the beds when intense weathering is encountered.

(g) Bioclastic Limestone

These beds mark the Tournaisian/Visean boundary and consist of a series of black fine-grained mudstones and dark grey, medium to course-grained limestones. Slump features are common and fossils abound.

(h) Reef Limestone

This is a pale grey fine-grained calc-mudstone with abundant fractures ,joints and bryozoan debris. It passes transitionally into the Bioclastic Limestone.

(i) Calp Limestone

The Calp Limestone shows abundant slumping and folding which may reflect Nassauian earth movements. There is however, no indication of Calp Limestone sub-outcrop in the Keel area although excellent exposures are found at Ardagh village to the east and near Kenagh to the west.

2.3. STRUCTURAL GEOLOGY OF THE LONGFORD AREA.

2.3a. FOLDING.

(i) Caledonian Orogeny

The Caledonian orogeny, with its predominantly northeast-southwest trend, initiated the inliers of the Central Irish Plain. In the Longford area, the anticlinal crests which had been left as positive features after the orogeny, were quickly covered by a transgressive Lower Carboniferous sea. At Keel, the occurrence of a microconglomerate on both sides of the inlier is evidence, according to Patterson, that this was a very low topographic feature.

(ii) Nassauian Earth Movements

The Hercynian orogeny is heralded in Mid-Dinantian times by minor earth movements. In the Longford area the effects of these movements are minor and consist of only slumping and wedging of beds of Calp Limestone age.

(iii) Hercynian (Variscan) Orogeny

The main effects of this orogeny in the Longford area were to rejuvenate the old Caledonian folds and raise them once more to predominance.

2.3b. FAULTING.

Patterson has been able to recognise three major fault systems in the Keel area, which he subdivides as:-

(i) Low angle, very tight, normal faults dipping at $25\text{-}30^{\circ}$ to the north, striking more or less east-west.

(ii) High angle east-west normal faults dipping south-east, with the associated conjugate joint system dipping north with minor throws.

(iii) North-south faults and associated joint systems throwing both east and west. These are post-ore faults.

2.4. MINERALOGY AND MINERALIZATION AT KEEL.

2.4a. CONTROLS OF MINERALIZATION.

A close structural correlation between faults of class (ii) of Patterson and mineralization exists at Keel. Some lithological control is also apparent in that the ore is predominantly confined to the clastic sediments. The faults, along which the ore solutions were introduced, are post-depositional in age and the contact between the Mixed Beds and Bioclastic Limestone is also faulted. At the base of the Bioclastic Limestone, a fault gouge, up to three feet thick, has provided an impermeable barrier to any mineralizing solutions and consequently very minor dispersion of zinc and lead occurs across this barrier. This clay gauge is well developed on the 200' level of the prospect where high grade mineralization is completely truncated by the fault. The main ore control at Keel is consequently structural, the ore being introduced and emplaced along faults, Fig. 1.2. Although disseminated mineralization does occur, this can also be shown to be controlled by structure. Thus the concept of remobilization of originally sedimentary sulphides is an unacceptable hypothesis for ore genesis at Keel.

2.4b. MINERALOGY.

Sphalerite is the predominant ore mineral in the Keel deposit although galena and pyrite do attain local significance. The sphalerite varies in colour from true honey-coloured "honeyblende" to black, and in texture from fine, disseminated intergranular intergrowths to coarse, well terminated crystals in vugs. Colour variation can be attributed in part to variation in iron content from 0.7% Fe in the light sphalerites to 3.0% Fe in the dark sphalerites. This information is based on atomic absorption and optical spectrograph analysis of 113 sphalerite crystals, Chapter 6.

Galena, as already stated, attains local significance in the deposit occurring as disseminated intergrowths, vein deposits or well formed crystals in vugs associated with sphalerite. The trace element assemblage of galena is discussed in Chapter 6.

Tetrahedrite is widely distributed throughout the deposit as inclusions in both galena and sphalerite. Patterson concludes on the basis of electron-probe microanalysis that the tetrahedrite contains Cu, Fe, Zn, Ag, Sb and S. Chalcopyrite occurs as inclusions in the sphalerite but nowhere reaches economic importance and, as with tetrahedrite, chalcopyrite was not present in large enough quantities to be separated for chemical analysis. Jalpaite, ($Cu_{0.45}$ $Ag_{1.55}$ S) and Bournonite (Pb. Cu Sb_2 S_3) are also reported to occur at Keel by Patterson but again, no large enough quantities could be found for analysis in this study.

Pyrite, as already stated, attains local significance and its trace element assemblage is also discussed in Chapter 6.

Calcite, dolomite, baryte and quartz are the predominant gangue minerals occurring as fracture and breccia fillings, joint coatings and terminated crystals in vugs.

2.5. ORE GENESIS AT KEEL.

After the Hercynian orogeny, ore solutions invaded the east-west trending faults and deposited base metal sulphides, apparently with marked rapidity, as the total available space for mineralization was not used.

On the 500' level the hanging wall of the orebody passes out from a high grade breccia, by gradual stages, into unmineralized ground. Evidence suggests that the ore solutions were originally hypersaline brines (Patterson, 1971) carrying metals in the form of complex ions and chlorides.

Patterson concludes that the source of the ore solutions at Keel is conjectural. However, on the basis of information obtained during the course of this study, it is considered that the metals were gathered by scavenging brine solutions from the surrounding rocks and deposited in an area of high sulphur activity in the fault zones. These brines probably originated in the Silurian (Chapter 8) and migrated into and along the fault zones, depositing base metals as they went. This would give rise to a structurally controlled orebody, together with areas of disseminated mineralization spread over great distances but nonetheless associated with the minor fractures and fissures in the rocks, a set of parameters which are found in the Keel prospect area.

CHAPTER 3

PRIMARY DISPERSION OF SELECTED ELEMENTS IN THE KEEL AREA.

(An interpretation of drill core information)

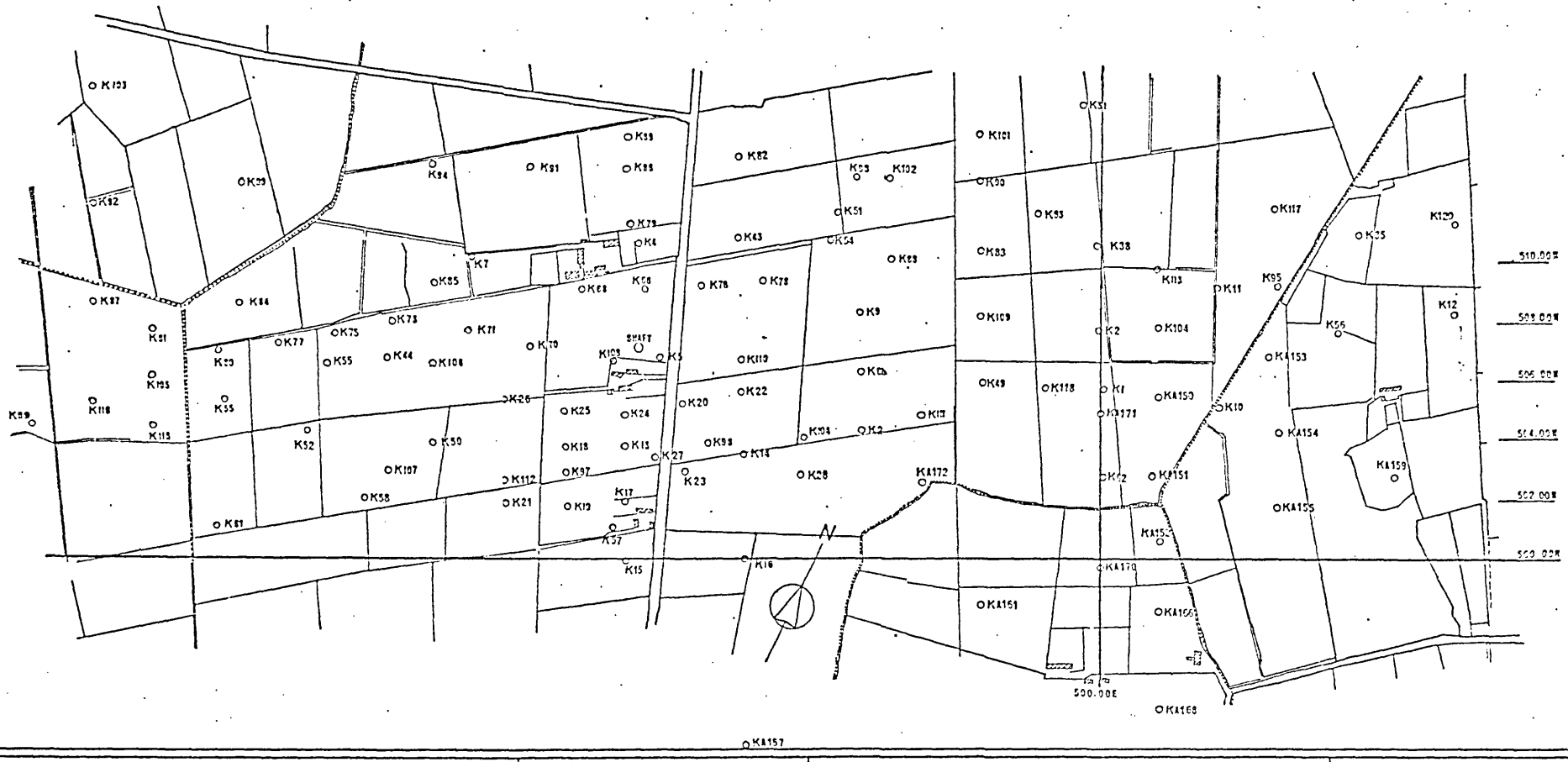
3.1. INTRODUCTION

This chapter deals with the information gained from the analysis of eight hundred samples of drill core material for Cu, Pb, Zn, Ag, Cd, Hg, Fe, Mn, Na, K, Ca and Mg, by the atomic absorption techniques described in Appendix A. Additional information was gained from the analysis of one hundred and fifty samples of drillcore by optical spectrograph for Pb, Sn, Ga, V, Mo, Cu, Zn, Ti, Ag, Ni, Co, Mn, Cr and Ba. It was hoped that this analytical programme would yield information about the primary dispersion of these elements in the rocks in the vicinity of the Keel prospect. The distribution of drill holes sampled is shown in Fig. 3.1.

The approach to the problem of investigating primary dispersion in the Keel area was twofold. Stage one was the collection of samples from positions where the drill core itself intersected the elevations of the 100ft., 200ft., 300ft., 400ft., and 500ft. levels of the prospect. Stage two was to collect samples at close intervals from selected drill cores in order to investigate changes in trace element content over much smaller distances. Thus a large and small scale picture of the primary dispersion in this area could be built up.

3.2. INITIAL RESULTS AND SAMPLE PREPARATION

All analytical work was carried out at the Royal School of Mines and initially consisted of evaluation of sample preparation methods. This work was carried out on two kilogramme samples of rock material which were



KEEL DRILLHOLE LOCATION MAP

O K 99 RTZ DRILLHOLE
O KA 170 ASARCO DRILLHOLE

SCALE :- 1:6000
SCALE IN FEET

FIG...3.1

reduced to - 1550 μm in a manganese-steel jaw-crusher. The samples were then homogenised and split into two equal halves. One half was then reduced to - 53.5 μm in a Tema grinding mill and reserved for analysis; this is known throughout the text as the "true"total sample. The remaining half was then sieved into three size fractions, - 210 μm., - 494 μm. + 210 μm. and - 1550 μm. + 494 μm. These three size fractions and the pulverised half were then analysed separately for Cu, Pb, Zn, Ag, Cd, Hg, Fe, Mn, K, Na, Ca and Mg as described in Appendix A. The results obtained are summarized in Appendix B. A graphical interpretation of some of these results is shown in Fig. 3.2.

From this information it can be seen that Na, K, Ca and Mg show only very minor variations in concentration between different size fractions. Copper shows a slight increase in concentration with decreasing size fraction, the - 1550 μm. + 494 μm. fraction being lower than the "true" whole rock value indicating a possible depletion in copper from this fraction. Iron shows a similar trend and here again the - 1550 μm. + 494 μm fraction has lower iron values than the "true" total. The manganese results show a different series of curves, Fig. 3.2E.; both the - 494 μm. + 210 μm. and - 1550 μm. + 494 μm. fractions exhibit lower manganese values than the "true" total, while the - 210 μm. fraction switches from having a concentration greater than the "true" total to values lower than it at approximately 0.55% Mn.

Zinc and lead show considerable increases in concentration with decreasing size fraction, although here too the - 1550 μm. + 494 μm. fraction appears to show values lower than those obtained from the pulverised half. This increase in zinc and lead content with decreasing particle size is probably due to the fact that in the Keel

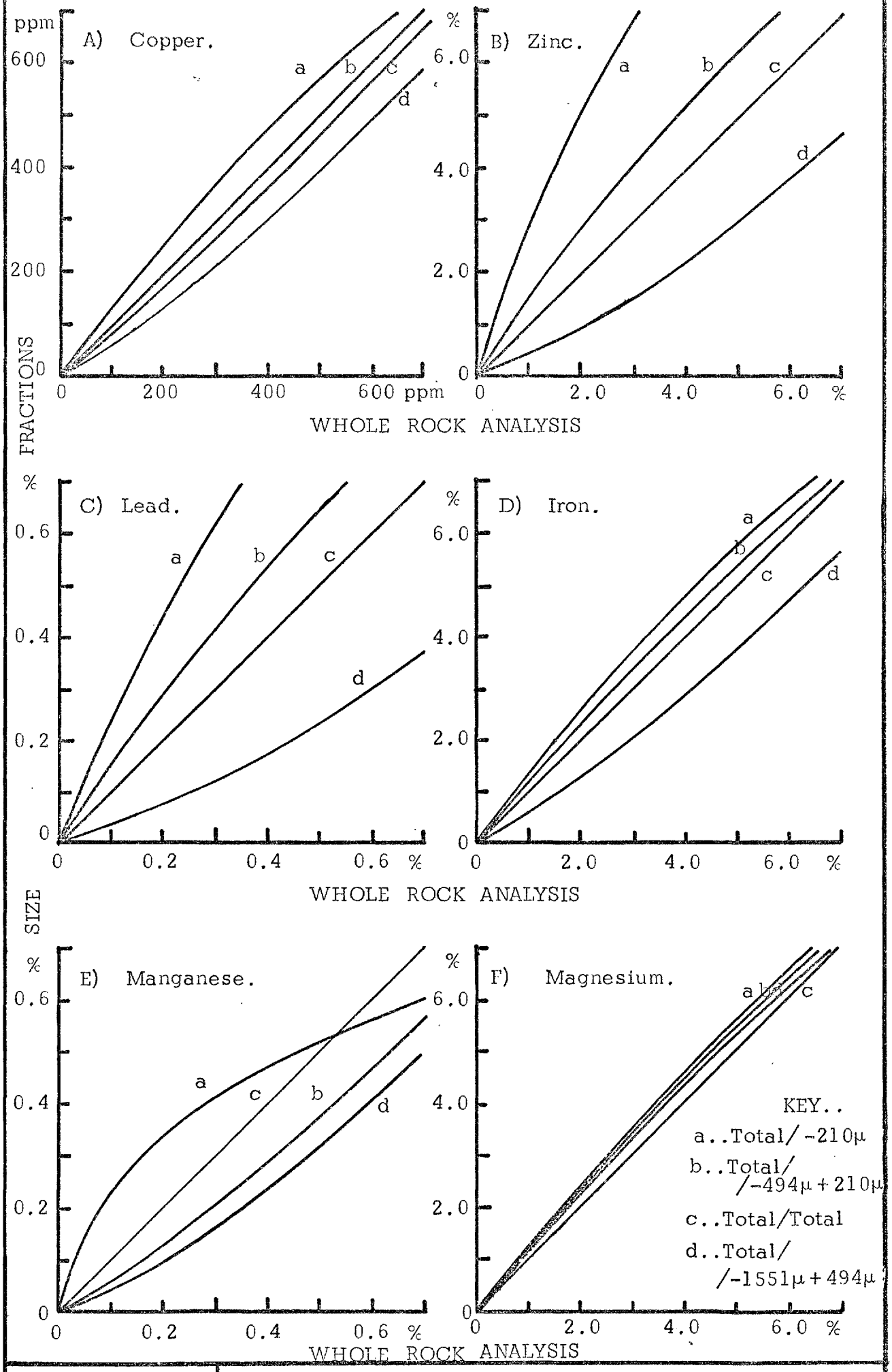


FIG... 3.2

Comparison of the metal concentration of different size fractions of rock material with the true whole rock concentration

area, both sphalerite and galena are friable minerals and consequently will easily concentrate, on crushing, in the finer fractions. As copper is concentrated in the sphalerite as chalcopyrite inclusions, it also follows this trend.

This increase in the zinc and lead content of the finer fractions of the sieved, crushed rock material poses two problems. The first is that unrepresentative results will be obtained by analysis of these fractions. The second is that mercury, being concentrated primarily in the lattices of the sulphide minerals, can also be expected to increase in concentration with decreasing particle size. Table 3.1A. for crushed material from the underground workings of the mine shows the relationship quite clearly; however Table 3.1B and Fig. 3.49 indicate that the opposite relationship is true for material from drill cores. The complexities suggested by these figures are fully dealt with in Chapter 8, but do not form part of this present study.

Resulting upon this initial survey of sample preparation techniques, it was decided that an homogenised, ground - 53.5 µm. size fraction would be used for general trace analysis.

From the results shown in Tables 3.1A and 3.1B. it was decided to use the - 494 µm. + 210 µm. fraction for mercury analysis. This fraction also shows the smallest enrichment factor of the other metals and therefore inter-element/mercury correlations will still be valid, although different sample preparation techniques were used for both.

3.3. PRIMARY DISPERSION OF METALS IN THE KEEL AREA

Previous work by Patterson (1970) in conjunction with Rio Tinto Finance and Exploration Company indicated a marked degree of lateral metal zonation for the Keel prospect, Fig. 3.3. This picture,

TABLE ... 3.1

MERCURY CONTENT IN DIFFERENT SIZE FRACTIONS OF ROCK SAMPLES

A) FROM UNDERGROUND WORKINGS

SAMPLE	- 210 μ	- 494 μ + 210 μ	- 1550 μ + 494 μ
K 1	665	152	90
K 2	2575	280	174
K 3	2420	144	84
K 4	300	140	106
K 5	525	206	16
K 6	240	170	130
K 7	2855	1180	720
K 8	1330	160	80
K 9	705	184	116
K 10	2460	390	49
K 11	1075	216	139

B) FROM DRILLCORE

K 12	998	1560	1020
K 13	28	48	28
K 14	22	32	36
K 15	35	96	14
K 16	166	210	110
K 17	70	85	50
K 18	14	42	15
K 19	103	310	80
K 20	60	130	52
K 21	219	560	27
K 22	169	700	150
K 23	318	496	130
K 24	44	210	27
K 25	49	326	20
K 26	160	172	110
K 27	1675	2593	1020
K 28	66	74	30
K 29	44	236	25
K 30	33	57	14
K 31	141	280	100

RESULTS EXPRESSED AS p p b

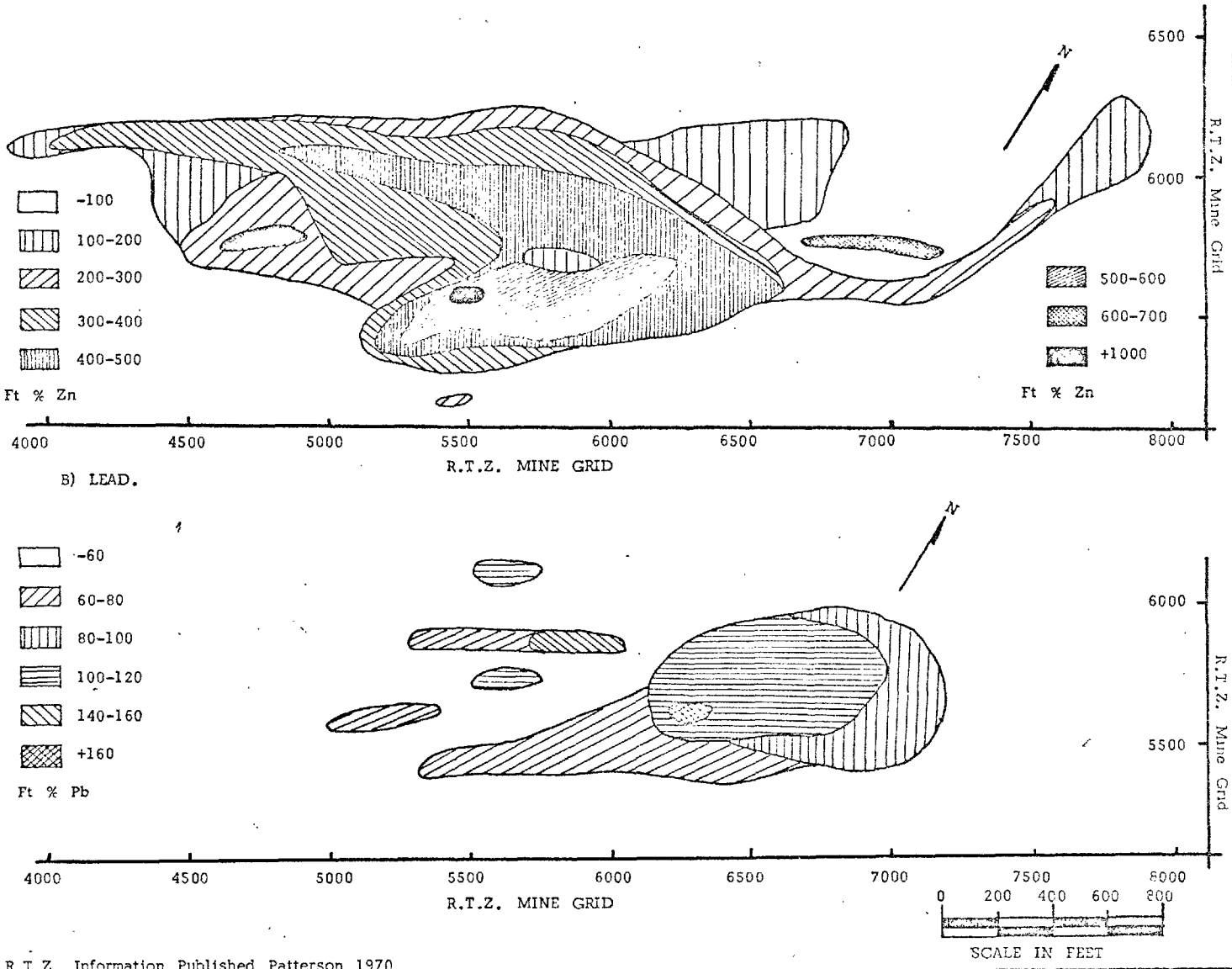


FIG ...3.3 DIAGRAM ILLUSTRATING LATERAL METAL ZONING AS INDICATED BY DIAMOND DRILLHOLE INTERSECTIONS

as will be indicated throughout this chapter, is oversimplified and suggests a primary dispersion pattern for lead and zinc at least of reasonable simplicity. When looked at in detail however, broad dispersion of base metals in the Keel area is not apparent. Such dispersion as there is, is closely associated with faulting, and lateral migration of cations into wallrocks, during, or subsequent to mineralization at Keel, did not take place to any marked degree.

3.3A. CALCIUM, MAGNESIUM, SODIUM AND POTASSIUM

Rock types in the Keel area consist of carbonate and clastic sediments, with mineralization occurring predominantly in the latter. An investigation into the wallrocks was carried out to discover if dolomitization was in any way associated with mineralization.

The Reef and Bioclastic Limestones show little evidence, chemically, of dolomitization, although dolomite is present in both thin and polished sections of these units; usually the Mg/Ca ratio is $< 0.1 : 1$. The clastic sediments, in which mineralization occurs, have much higher Mg/Ca ratios although, in these lithologies, both magnesium and calcium are generally present in quantities $< 1{,}000$ p p m. The fact that in some cases high Mg/Ca ratios occur in association with base metal build-up is, in the author's opinion, purely fortuitous. Figs. 3.4, 3.5 and 3.7, show the relationship of the Mg/Ca ratio to the extent of known mineralization in the Keel area and from this it can be seen that the highest Mg/Ca ratios correspond to the Upper Mixed Beds and Bioclastic Dolomite. When looked at in detail, Fig. 3.6, it can be seen that this initial association of high Mg/Ca ratio with rock type does not always hold true and low values do occur in the Upper Mixed Beds, even in direct association with 5,000 p p m zinc. The correlation of high

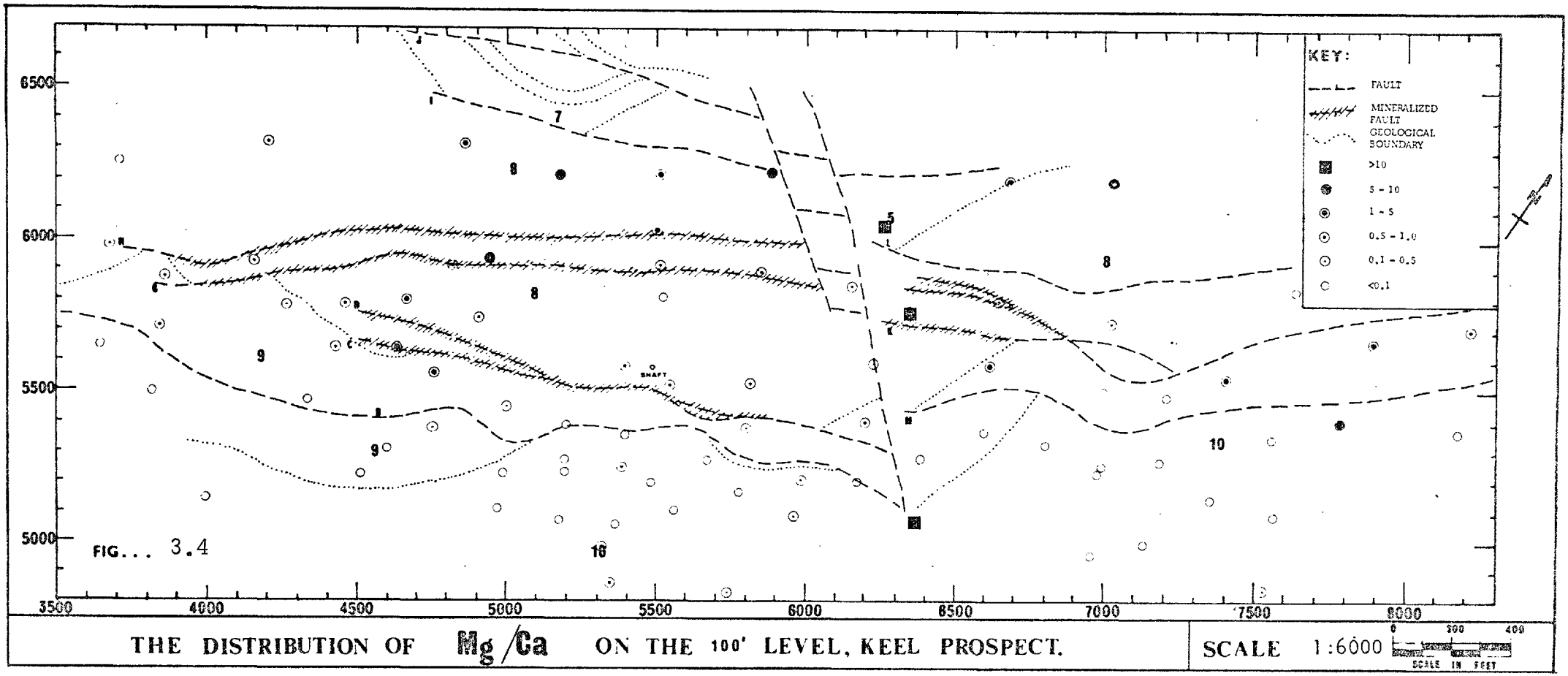
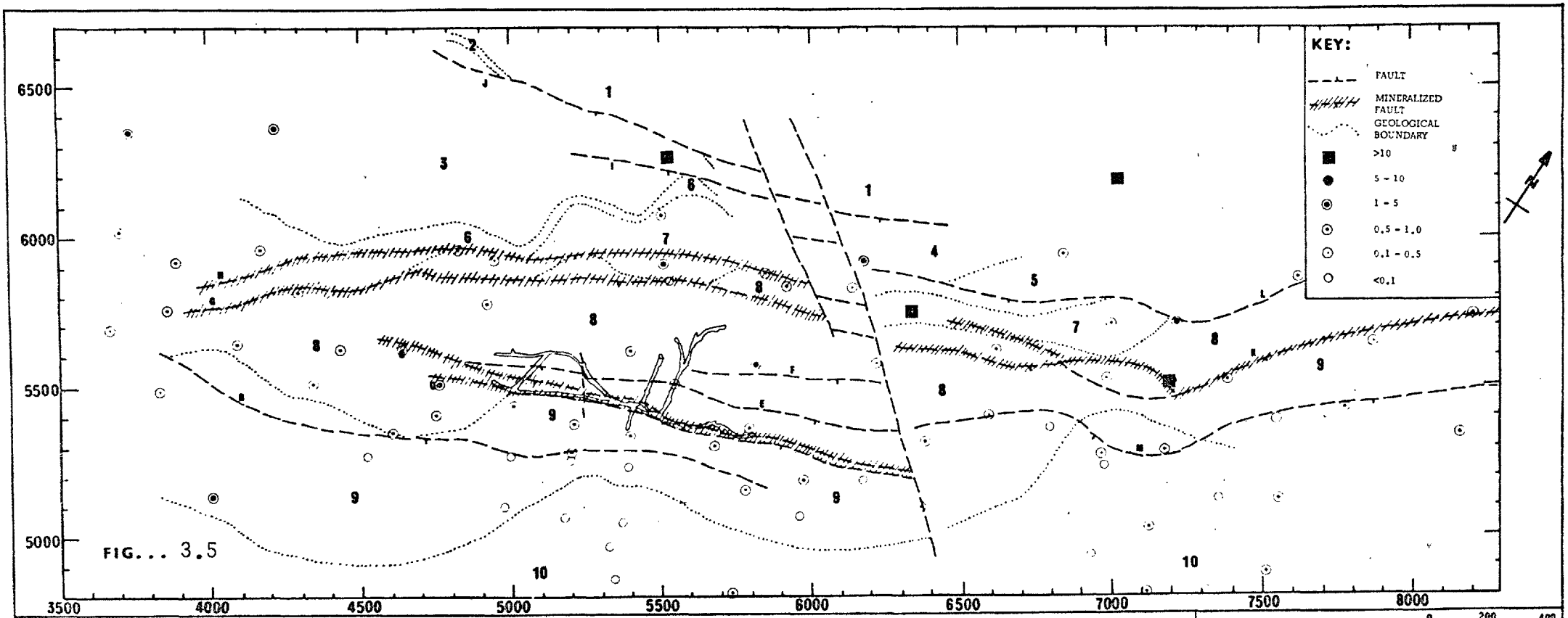


FIG... 3.4

THE DISTRIBUTION OF **Mg/Ca** ON THE 100' LEVEL, KEEL PROSPECT.

SCALE 1:6000


KEY:
FAULT
MINERALIZED FAULT
GEOLOGICAL BOUNDARY
>10
5 - 10
1 - 5
0.5 - 1.0
0.1 - 0.5
<0.1
6500
6000
5500
5000
3500
4000
4500
5000
5500
6000
6500
7000
7500
8000
FIG... 3.5
THE DISTRIBUTION OF Mg/Ca ON THE 200' LEVEL, KEEL PROSPECT.
SCALE :- 1:6000
0
200
400
FEET

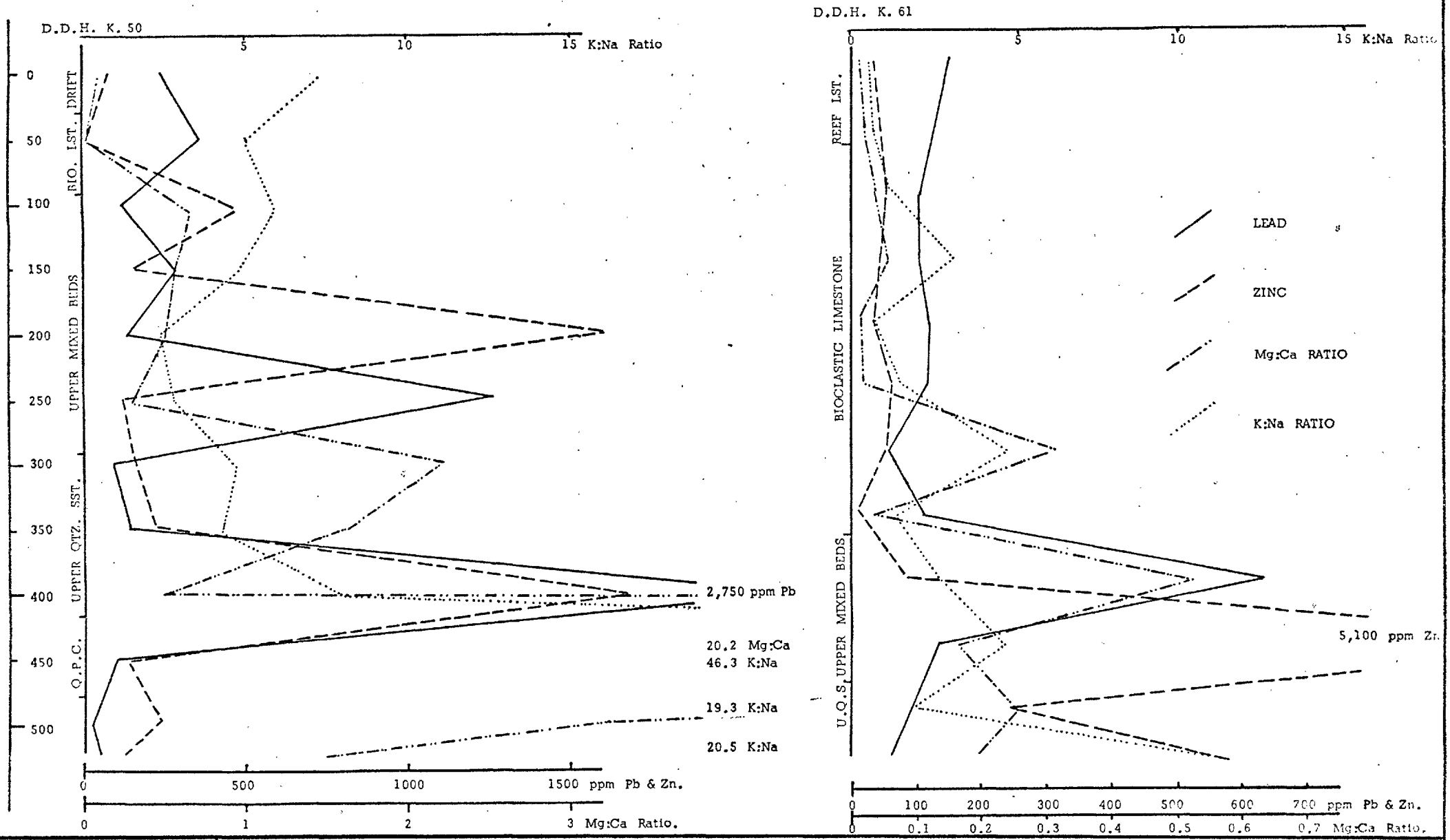
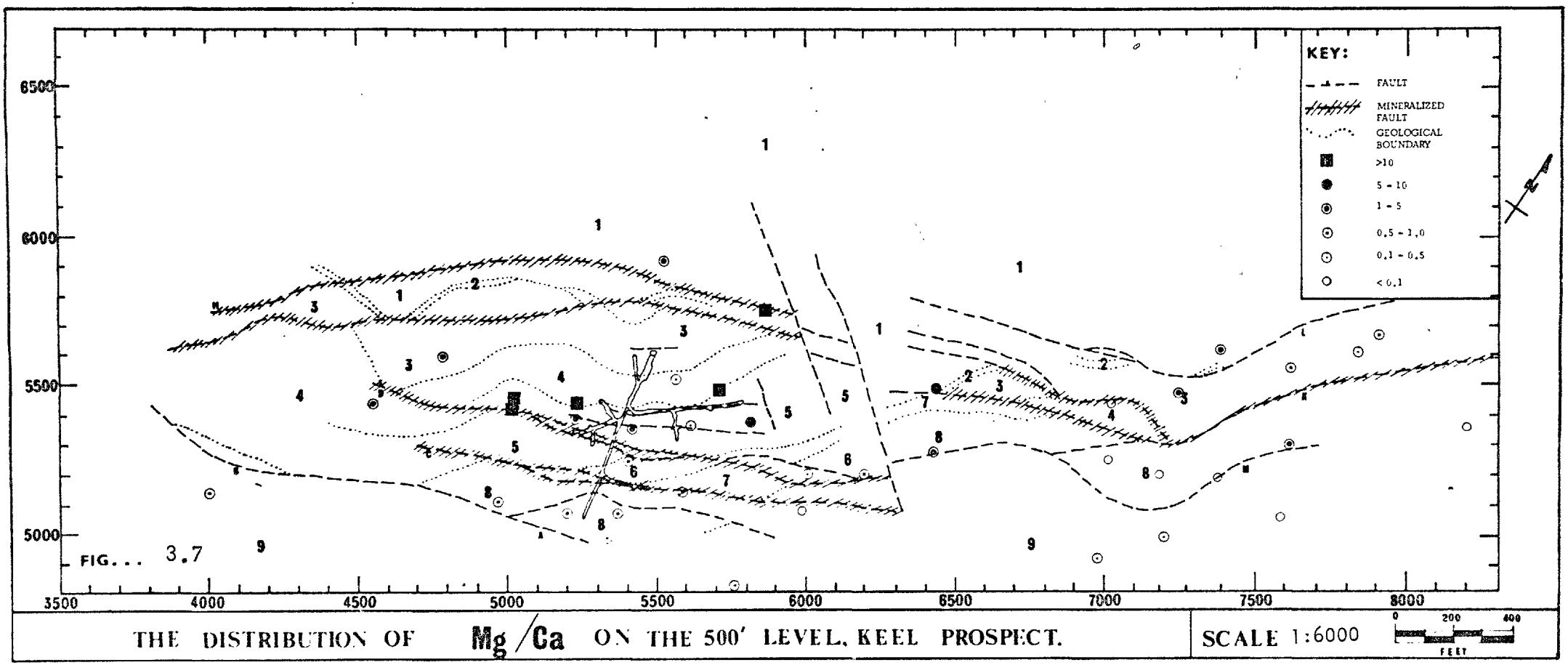


FIG ... 3.6

DIAGRAM ILLUSTRATING THE RELATIONSHIP OF THE MAGNESIUM:CALCIUM RATIO AND THE POTASSIUM:SODIUM RATIO TO MINERALIZATION IN BOREHOLES K.50 & K.61 KEEL PROSPECT, IRELAND


KEY:
FAULT
MINERALIZED FAULT
GEOLOGICAL BOUNDARY
>10
5 - 10
1 - 5
0.5 - 1.0
0.1 - 0.5
< 0.1
6500
6000
5500
5000
3500
4000
4500
5000
5500
6000
6500
7000
7500
8000
FIG... 3.7
THE DISTRIBUTION OF Mg/Ca ON THE 500' LEVEL, KEEL PROSPECT.
SCALE 1:6000
0
200
400
FEET

Mg/Ca ratio with build up of base metal sulphides that is indicated in Figs. 3.4. and 3.5, represents only a very broad association with rock type and cannot be said to be directly associated with mineralization.

The K/Na ratio in Keel rocks is, in many cases, > 10:1, values of 2% K being common in both carbonate and clastic sequences. However, only a haphazard distribution of high K/Na values becomes apparent when these ratios are plotted graphically. Fig. 3.8. displays this lack of relationship between high K/Na ratio and mineralization. When looked at in greater detail, Fig. 3.6, it can be seen that, even when exact figures are used, there is still no relationship between the K/Na ratio and build up of base metal sulphides.

3.3B. IRON AND MANGANESE

Rankama and Sahama, (1950) suggest that the average concentration of iron and manganese in sediments is as follows:-

	Mn	Fe
Sandstone	Trace	1.41%
Limestone	1.86%	0.54%
Shale	0.85%	6.73%

The relation of iron to manganese at Keel is shown in Fig. 3.9, and varies between 10:1 and 500:1, Fe:Mn. For manganese values below 1,000 p.p m., a completely random relationship between Mn and Fe exists and it is not until manganese values of above 5,000 p p m. that any definite relationship can be seen. These values suggest that there has possibly been a remobilization and enrichment of manganese and to some extent a remobilization of iron with precipitation from a manganese enriched solution in association with constant iron values. As can be seen from Figs. 3.10 to 3.19, high iron and manganese values

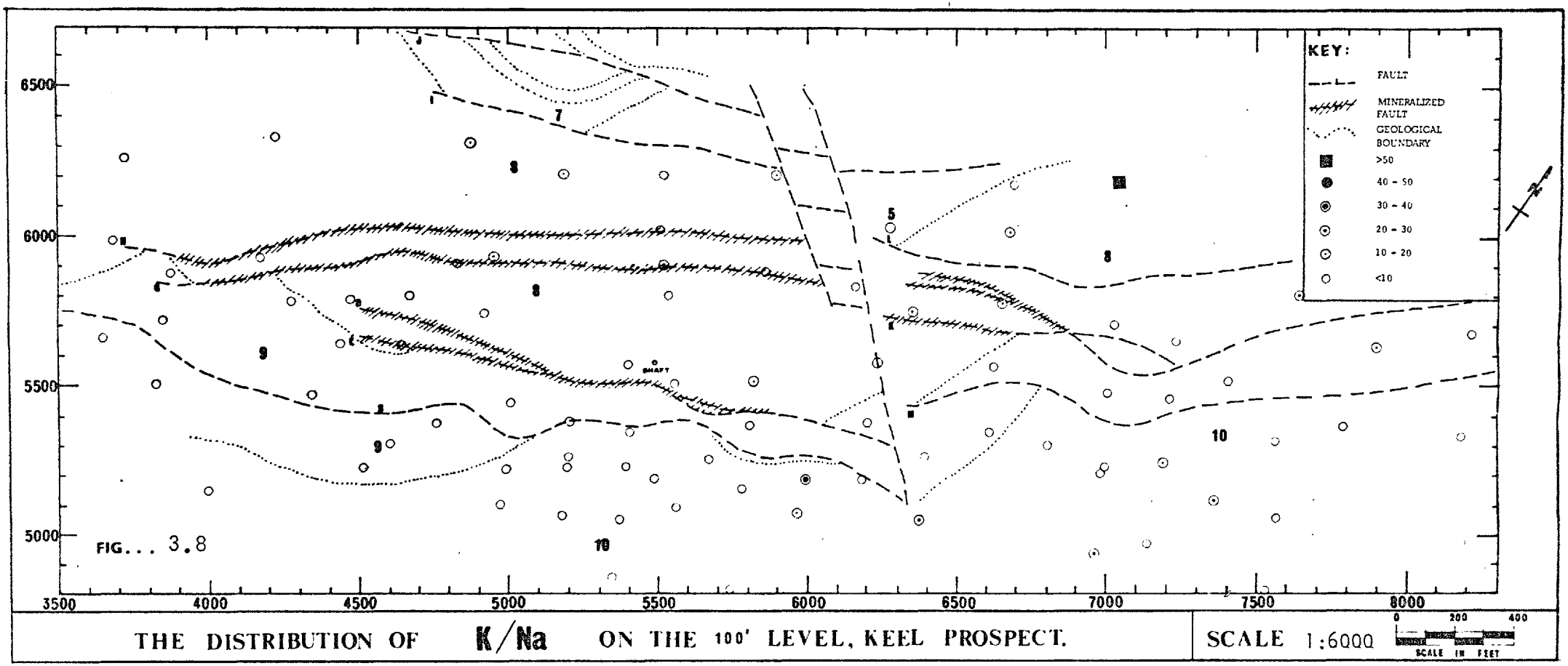
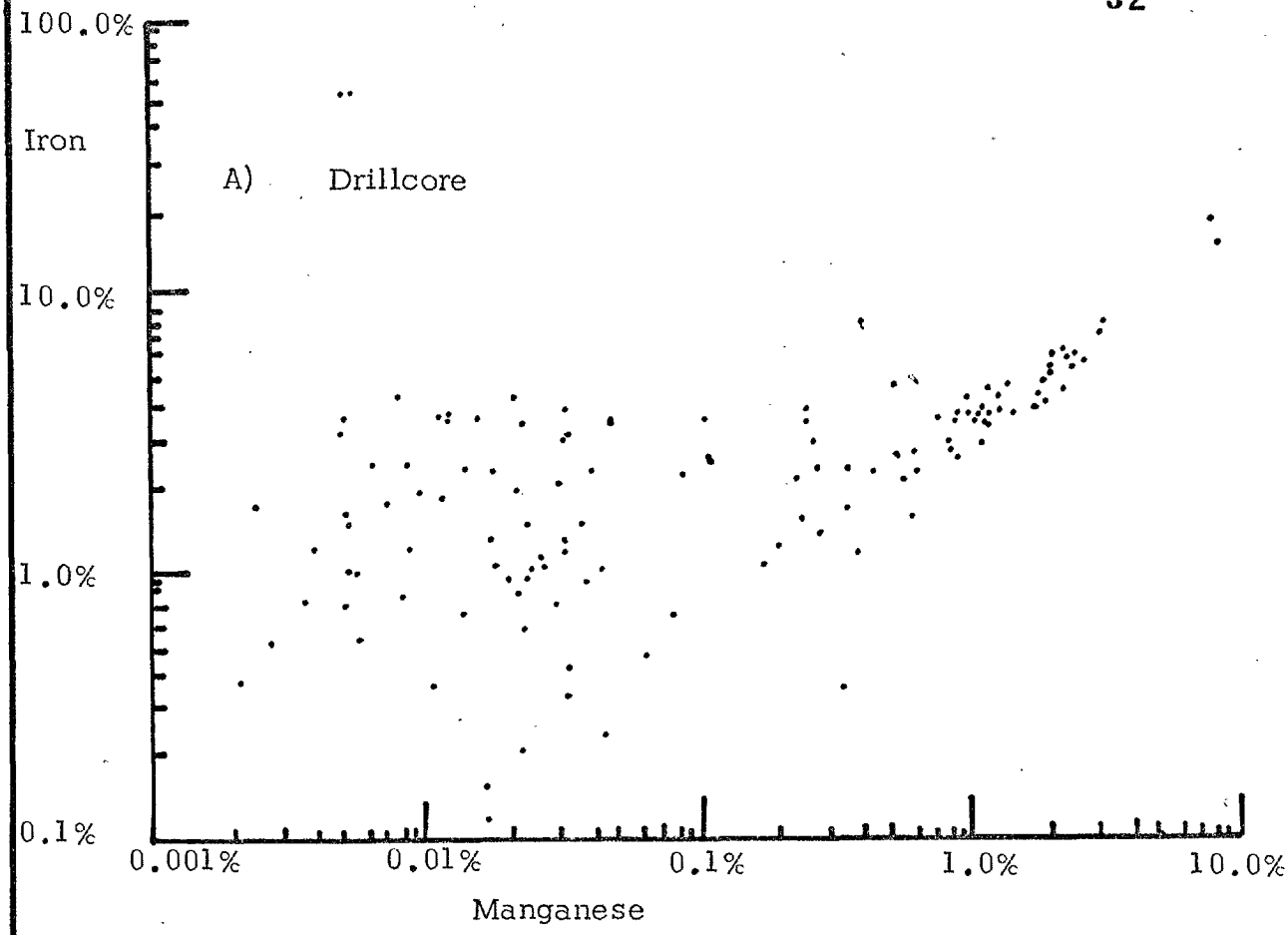


FIG... 3.8

THE DISTRIBUTION OF **K/Na** ON THE 100' LEVEL, KEEL PROSPECT.

SCALE 1:6000



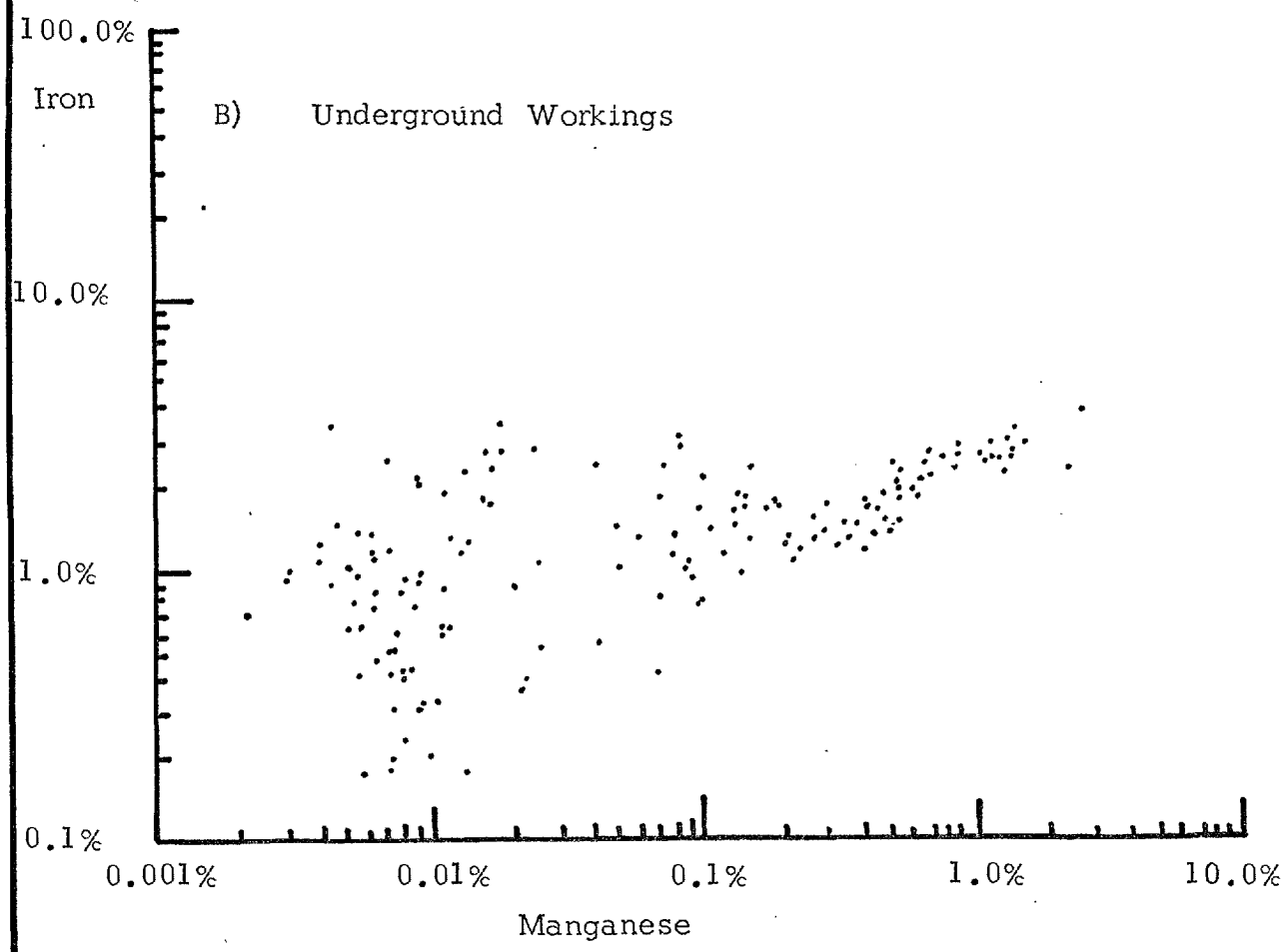


FIG... 3.9

A Comparison of Manganese and Iron in Rock Material from Drillcore and underground Workings

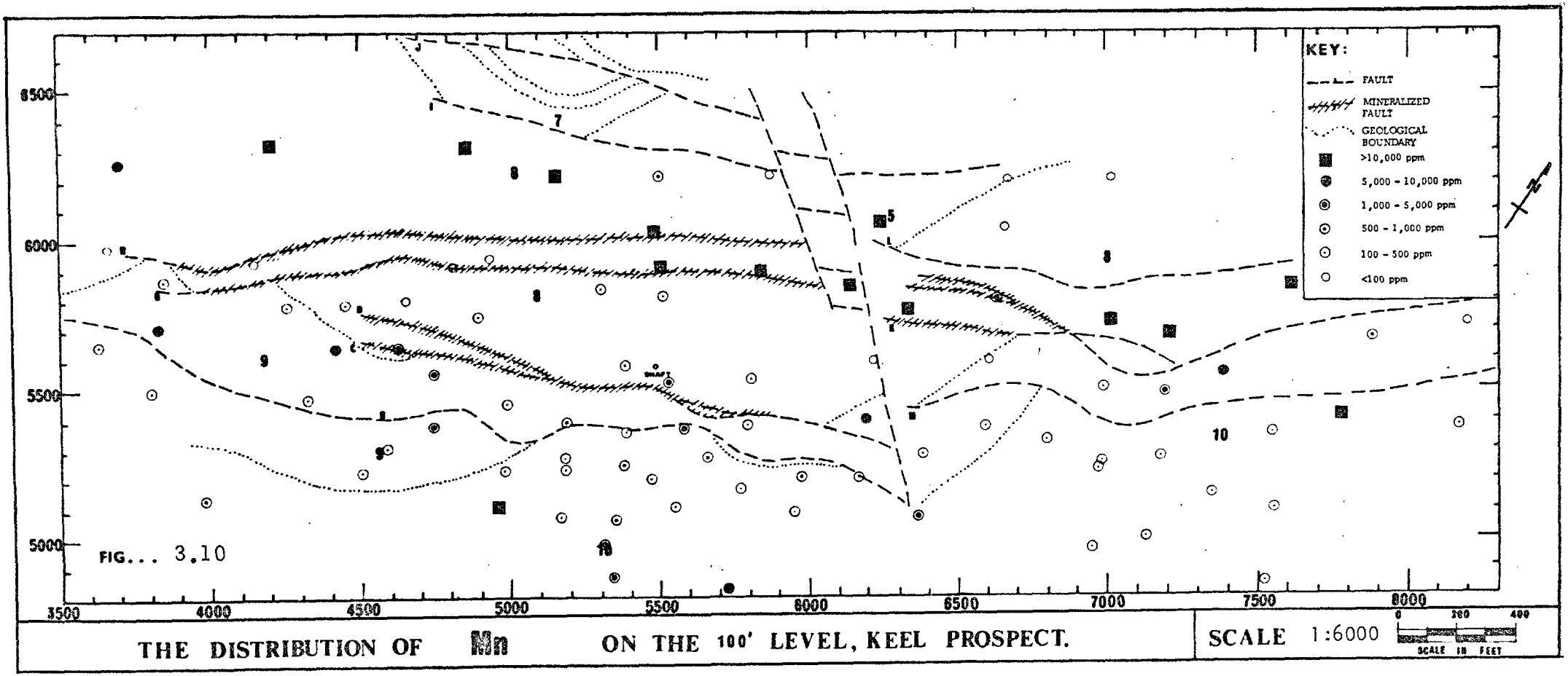


FIG... 3.10

THE DISTRIBUTION OF Mn ON THE 100' LEVEL, KEEL PROSPECT.

SCALE 1:6000

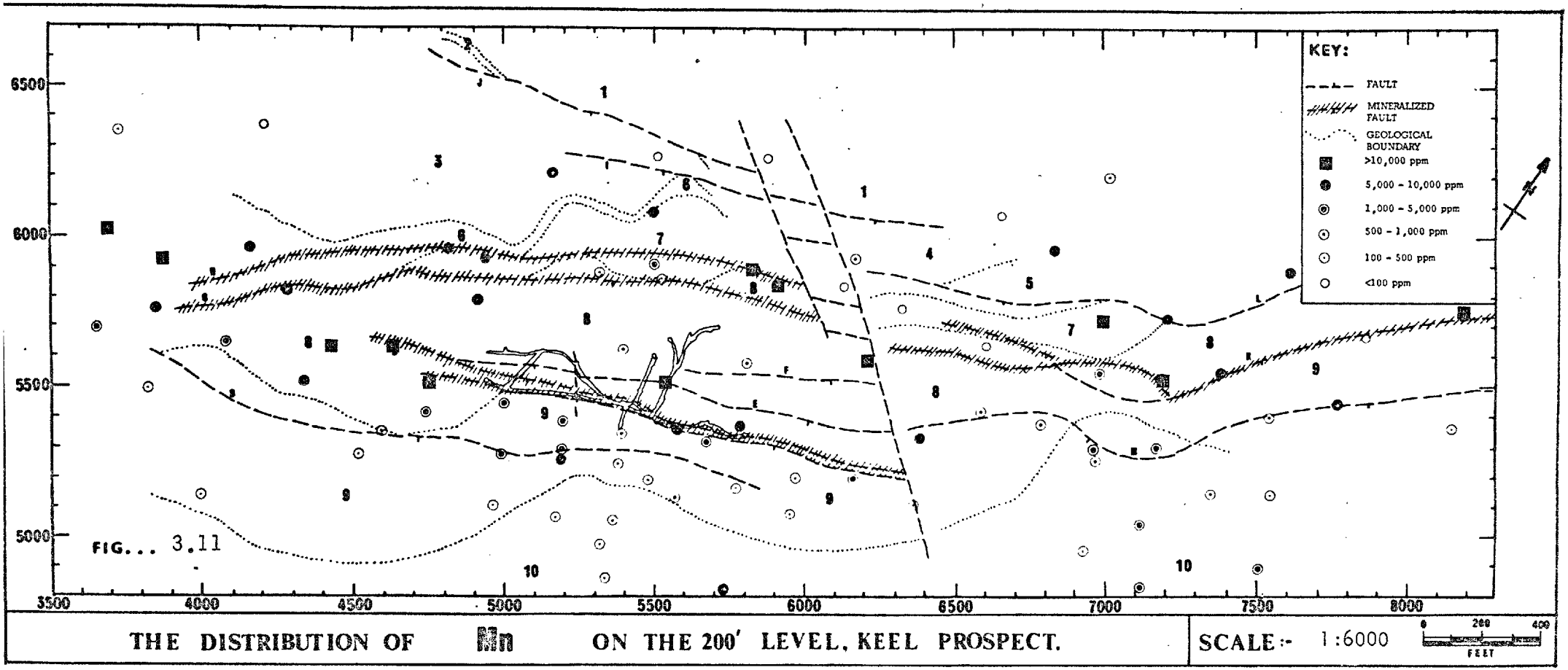
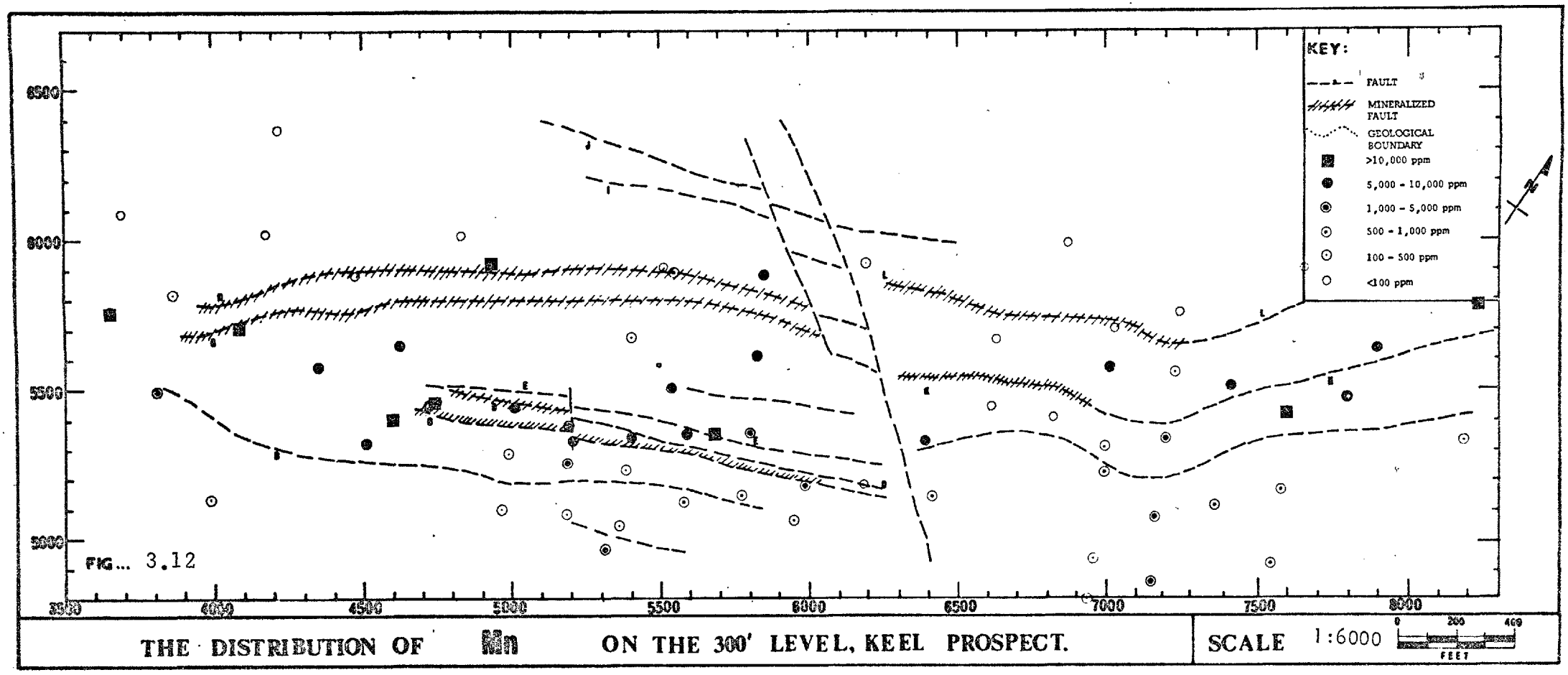


FIG... 3.11

THE DISTRIBUTION OF Mn ON THE 200' LEVEL, KEEL PROSPECT.

SCALE :- 1:6000


KEY:
FAULT
MINERALIZED FAULT
GEOLOGICAL BOUNDARY
>10,000 ppm
5,000 - 10,000 ppm
1,000 - 5,000 ppm
500 - 1,000 ppm
100 - 500 ppm
<100 ppm
8500
8000
5500
5000
4000
4500
5000
5500
6000
6500
7000
7500
8000
FIG... 3.12
THE DISTRIBUTION OF Mn ON THE 300' LEVEL, KEEL PROSPECT.
SCALE 1:6000
0 200 400
FEET

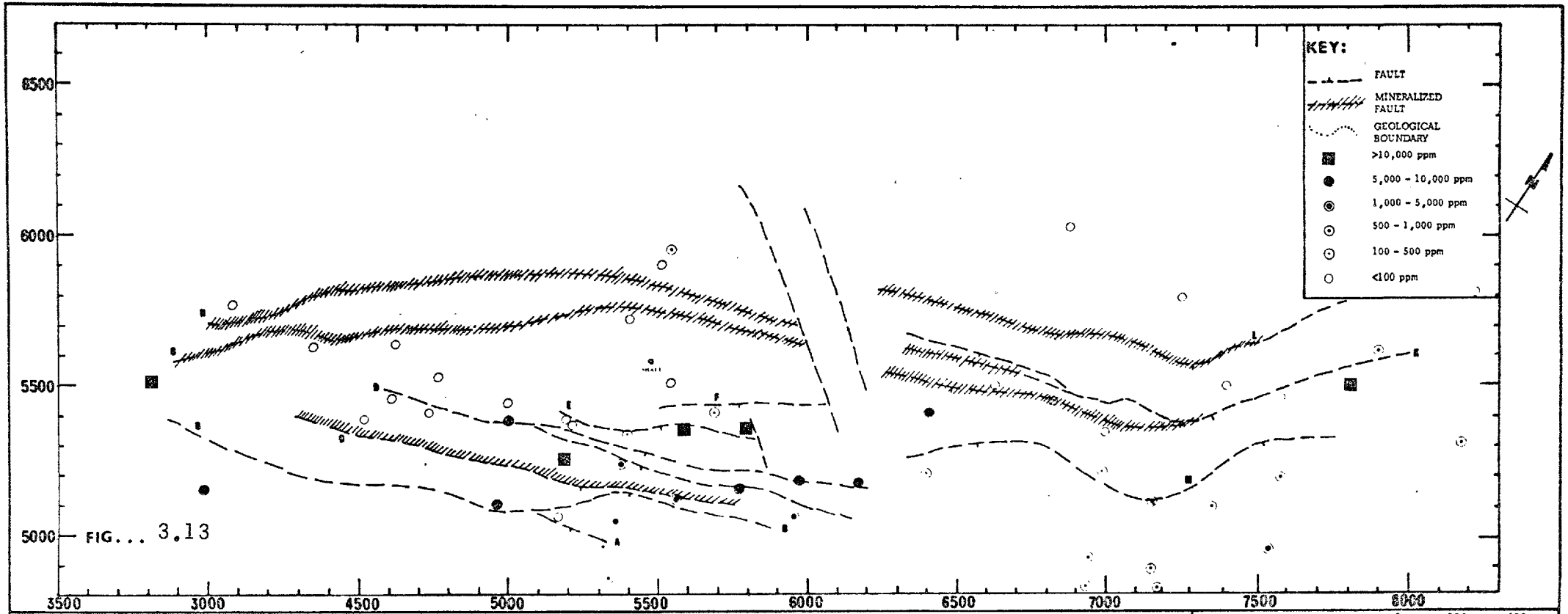
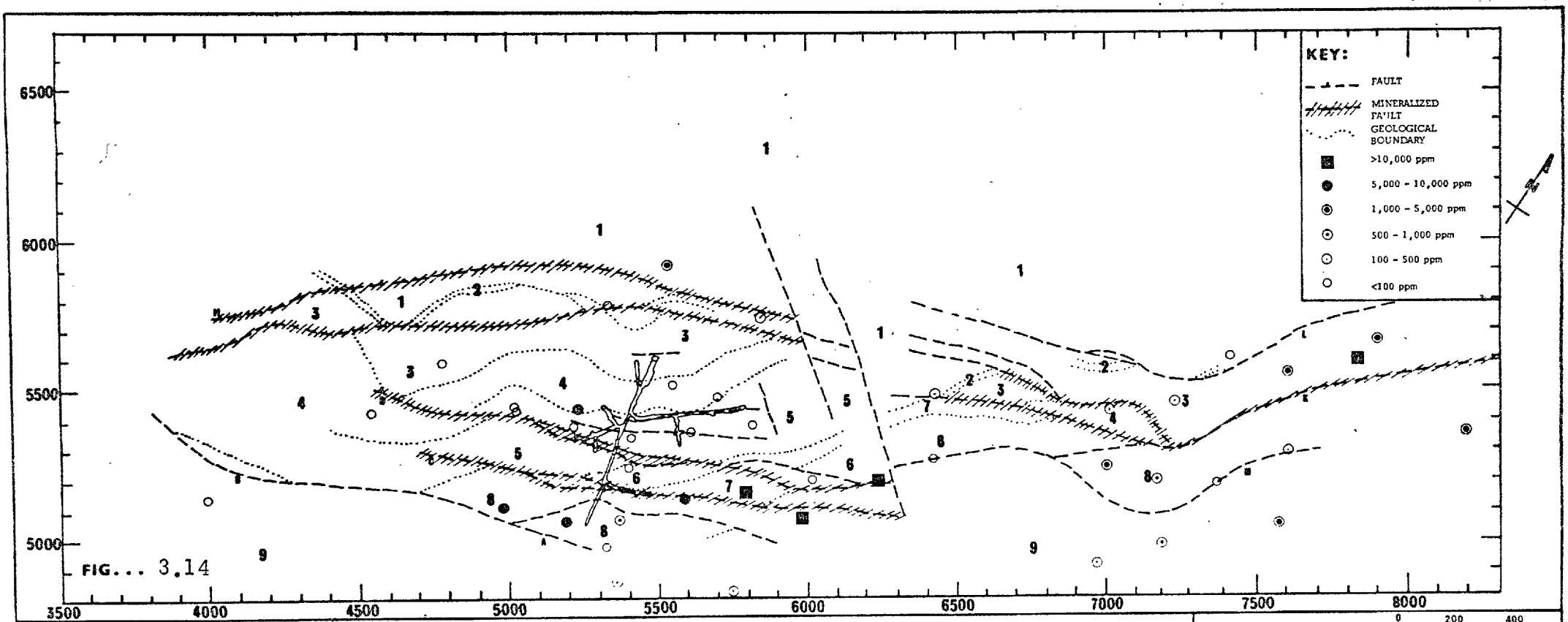


FIG... 3.13

THE DISTRIBUTION OF Mn ON THE 400' LEVEL, KEEL PROSPECT.

SCALE: 1:6000



THE DISTRIBUTION OF Mn ON THE 500' LEVEL, KEEL PROSPECT.

SCALE: 1:6000 0 200 400 FEET

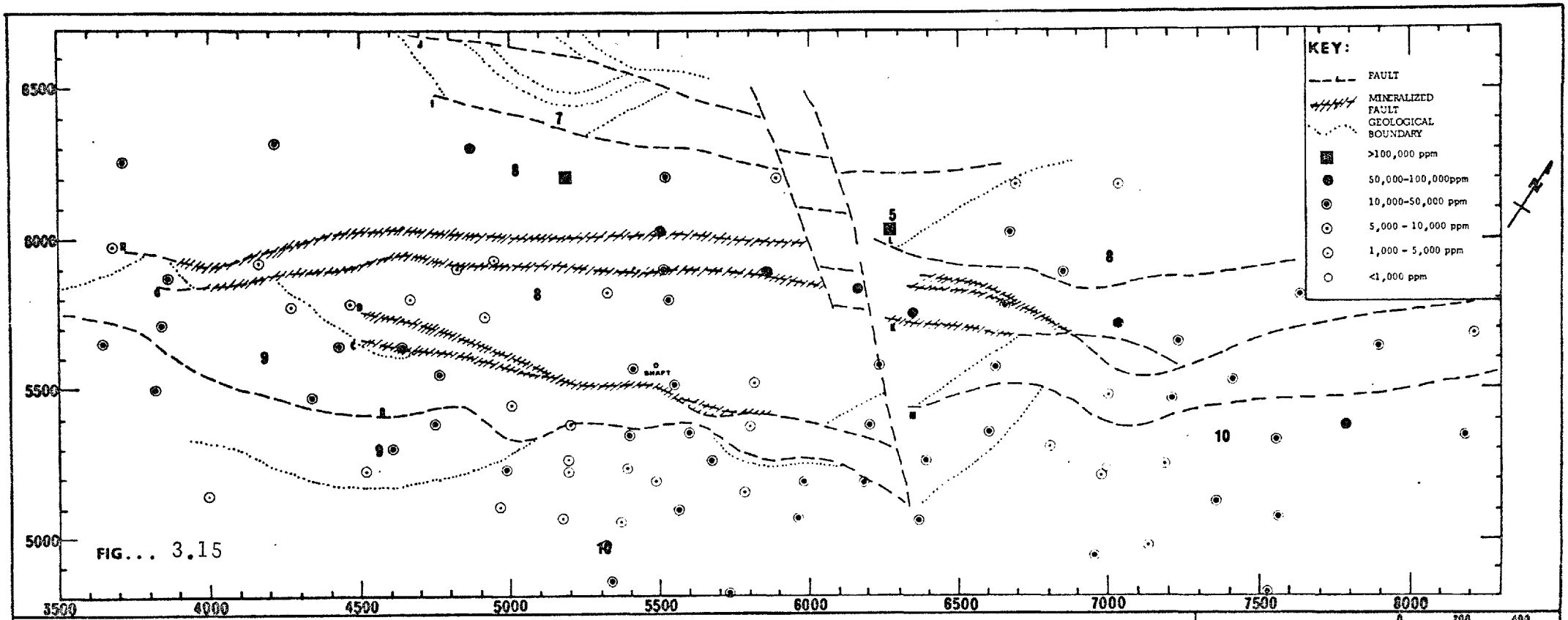
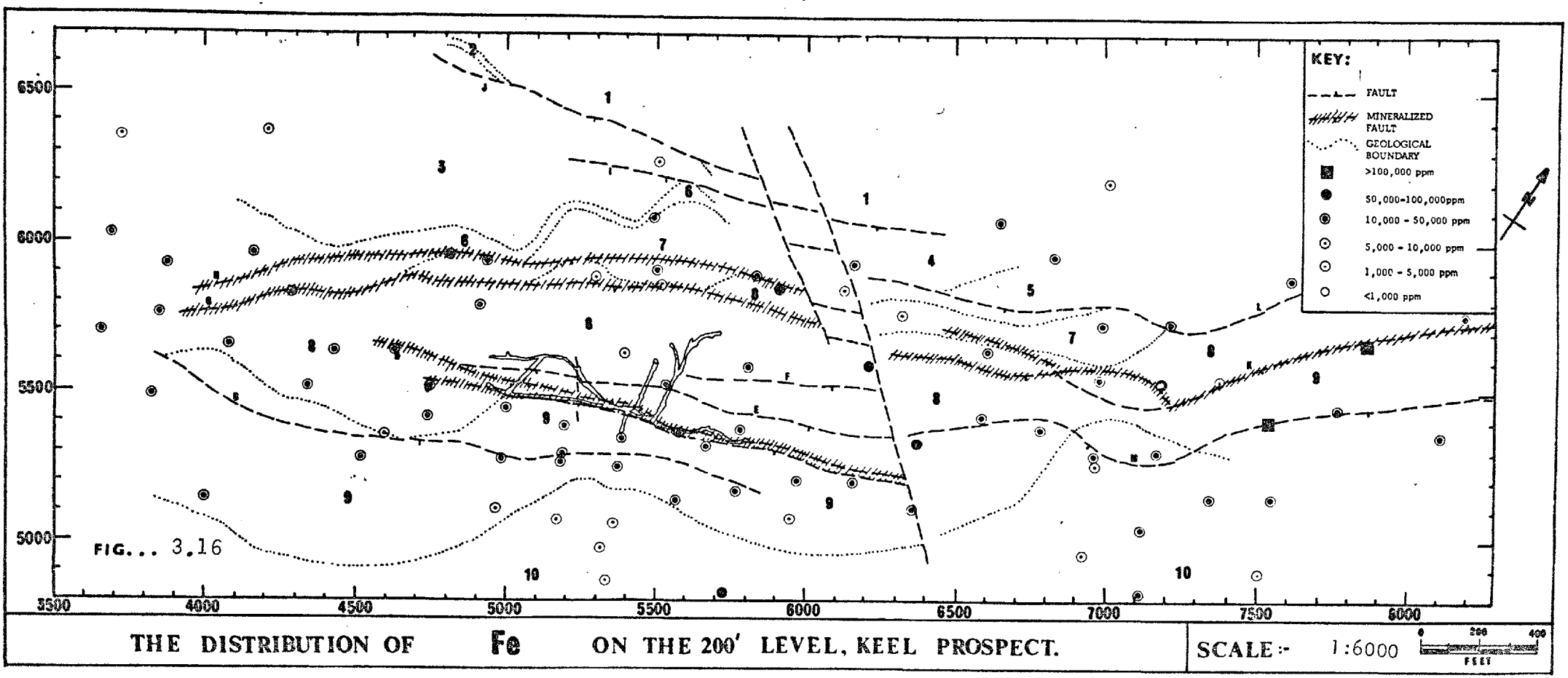


FIG... 3.15

THE DISTRIBUTION OF Fe ON THE 100' LEVEL, KEEL PROSPECT.

SCALE 1:6000


KEY:
FAULT
MINERALIZED FAULT
GEOLOGICAL BOUNDARY
>100,000 ppm
50,000-100,000ppm
10,000 - 50,000 ppm
5,000 - 10,000 ppm
1,000 - 5,000 ppm
<1,000 ppm
6500
6000
5500
5000
3500
4000
4500
5000
5500
6000
6500
7000
7500
8000
FIG... 3.16
THE DISTRIBUTION OF Fe ON THE 200' LEVEL, KEEL PROSPECT.
SCALE:- 1:6000
FEET

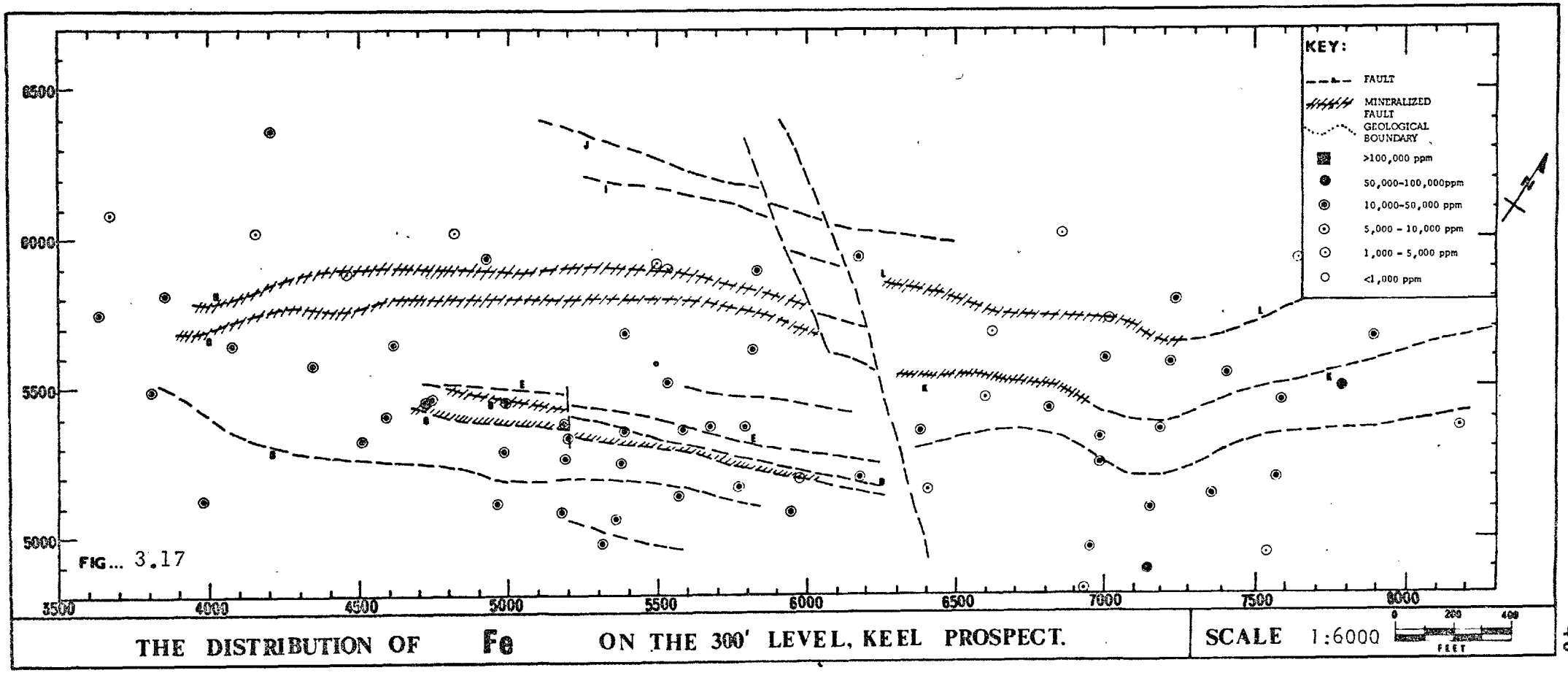


FIG... 3.17

THE DISTRIBUTION OF Fe ON THE 300' LEVEL, KEEL PROSPECT.

SCALE 1:6000

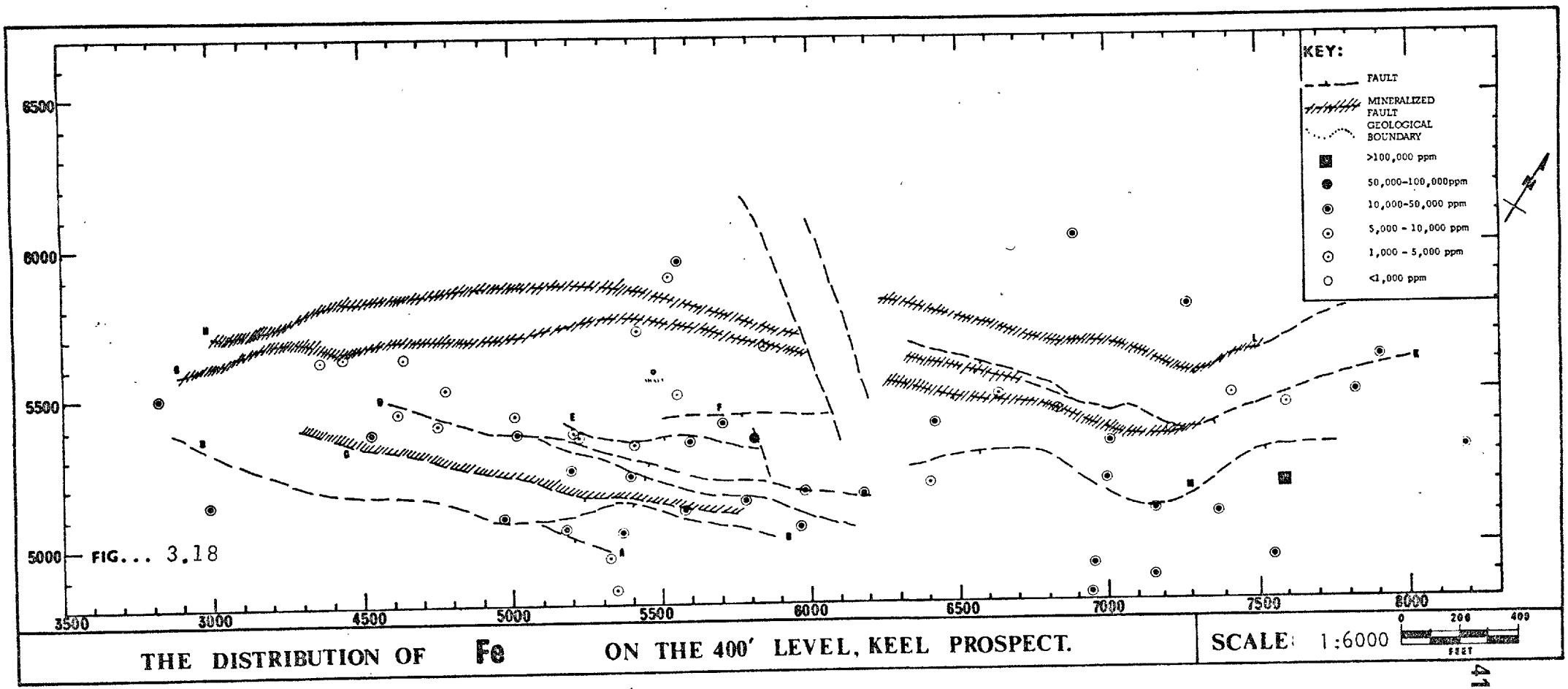


FIG... 3.18

THE DISTRIBUTION OF Fe ON THE 400' LEVEL, KEEL PROSPECT.

SCALE: 1:6000

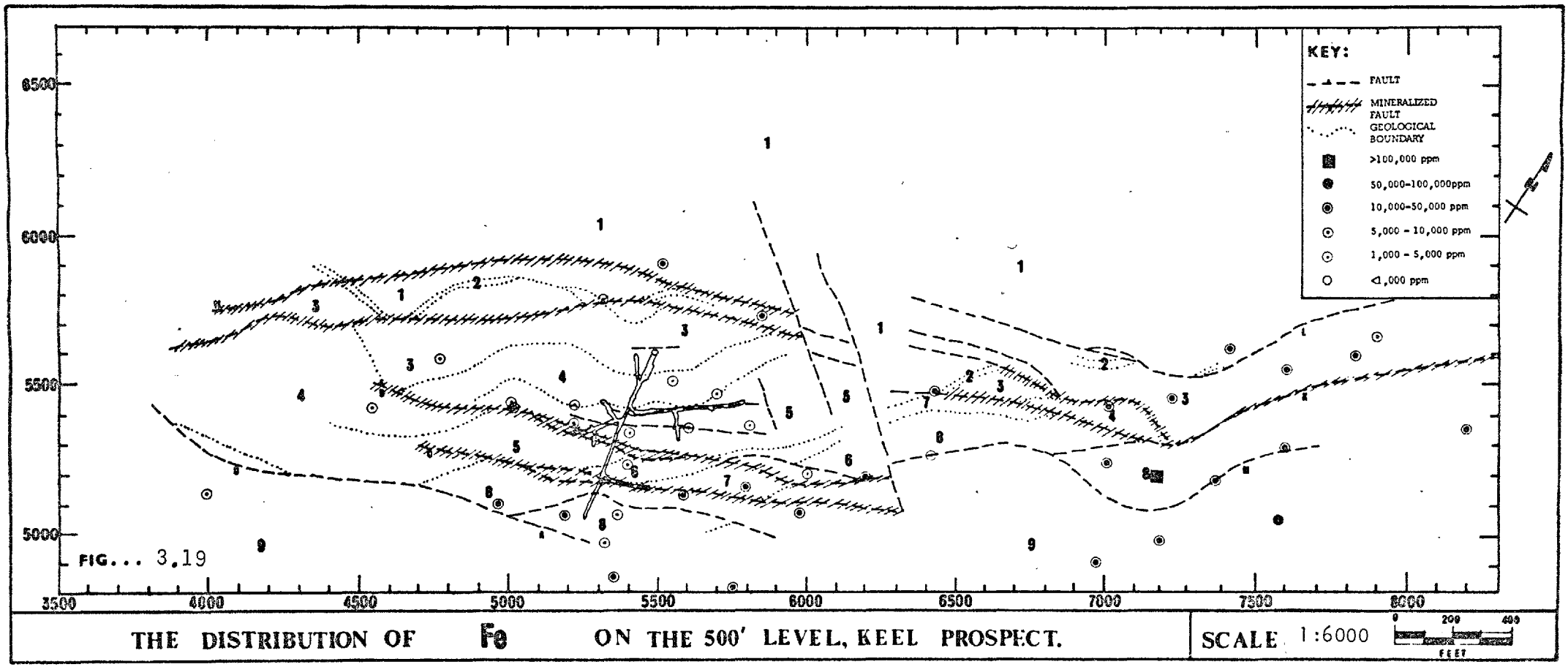


FIG... 3.19

THE DISTRIBUTION OF Fe ON THE 500' LEVEL, KEEL PROSPECT.

SCALE 1:6000

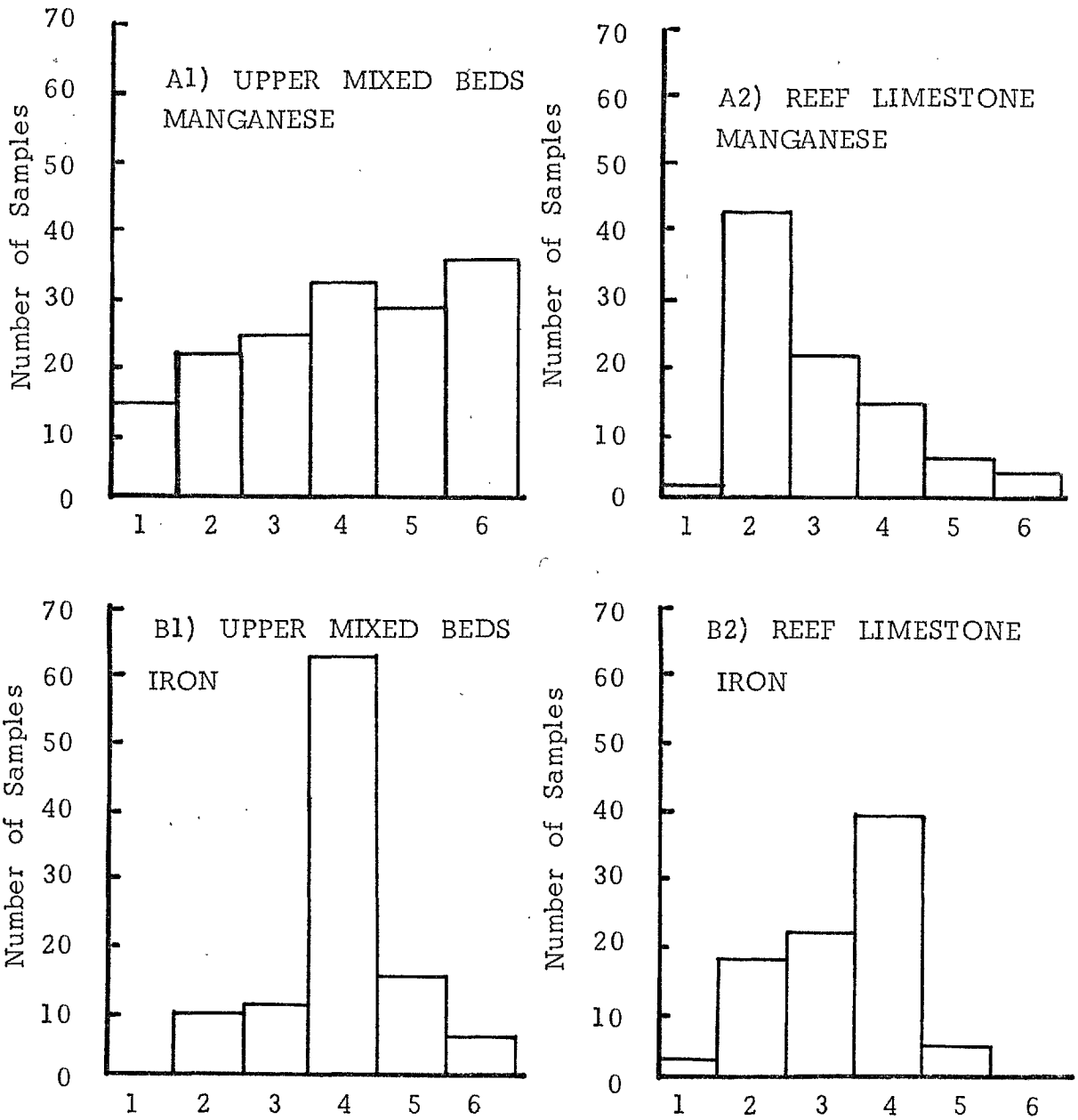
occur in the Upper Mixed Beds somewhat in association with mineralization and faulting and low values occur in the limestones where no mineralization is usually found.

Fig. 3.20 shows a histogram plot of the manganese and iron concentrations in the Mixed Beds and Reef Limestone. Figures correspond to the concentration ranges on Figs. 3.10 - 3.19. The highest concentrations of iron occur in the Mixed Beds, the predominant concentration interval being from 1% - 5%. In the Upper Mixed Beds some 7% of the samples have iron concentrations $>10\%$ while no values greater than this occur in the limestones.

Manganese shows a far more striking concentration in the Mixed Beds with 60% of the samples having manganese concentrations $>1{,}000$ p p m, whereas only 30% of the samples show this range in the Reef Limestone.

Rankama and Sahama suggest that in carbonate sediments manganese may become enriched with respect to iron. At Keel, the reverse is true, Fig. 3.20; here manganese enrichment is in the clastic sediments. This could be due to the fact that under the influence of migrating ground waters, which in the Keel area would be rich in dissolved CO_2 and organic acids, manganese could be taken into solution as the bicarbonate, while pyrite and iron oxides could not be attacked in this way. Another process which may lead to the solution and mobilization of manganese takes place by the action of solutions containing ferrous and ferric sulphate derived from the weathering of iron sulphides. The process may be represented by the following equation.

$$6FeSO_4 + 3MnO_2 + 6H_2O = Fe_2(SO_4)_3 + 4Fe(OH)_2 + 3MnSO_4$$



KEY :

		IRON	MANGANESE
(6)	■	> 100,000 ppm	> 10,000 ppm
(5)	◉	50,000 - 99,999 ppm	5,000 - 9,999 ppm
(4)	◉	10,000 - 49,999 ppm	1,000 - 4,999 ppm
(3)	⊙	5,000 - 9,999 ppm	500 - 999 ppm
(2)	⊙	1,000 - 4,999 ppm	100 - 499 ppm
(1)	○	< 1,000 ppm	< 100 ppm

FIG ... 3.20 DIAGRAM ILLUSTRATING THE DISTRIBUTION OF IRON & MANGANESE IN THE MIXED BEDS & REEF LST.

If the manganese content of sphalerite is examined it is usually below 100 p p m and thus direct co-precipitation of manganese and zinc from ore solutions does not appear to have taken place. Manganese values greater than 1% occur primarily in the Mixed Beds and Decomposed Zone. This latter has been extensively dealt with by Evans, (1971).

Sporadic bodies of pyrite occur throughout the Reef Limestone, Fig. 3.21, and these can contain up to 5% zinc and 0.7% lead. These bodies are responsible for the high Mn and Fe values in the Reef Limestone. Trace element analysis of this pyrite has been carried out and the results are discussed in Chapter 6.

3.3C. LEAD AND ZINC

The Keel prospect is regarded as primarily a zinc-cadmium deposit, with lead of overall minor importance. The conclusions reached in this section are based on analyses of one thousand samples for lead and zinc and the interpretation takes into account both lithological and structural controls. Analytical information obtained by Rio Tinto Zinc Corporation and American Smelting and Refining Company was made available to the author and, where relevant, this is included in the chapter.

Fig. 3.3. shows Patterson's interpretation of lateral metal zoning as indicated by diamond drillhole intersections. Patterson states that in the central part of the area mineralization extends over a greater vertical extent with good grade intersections down into the Silurian. The K orebody extends to the east and is seen to be higher in lead than the other orebodies with a Zn:Pb ratio of 3:1. (Patterson 1971).

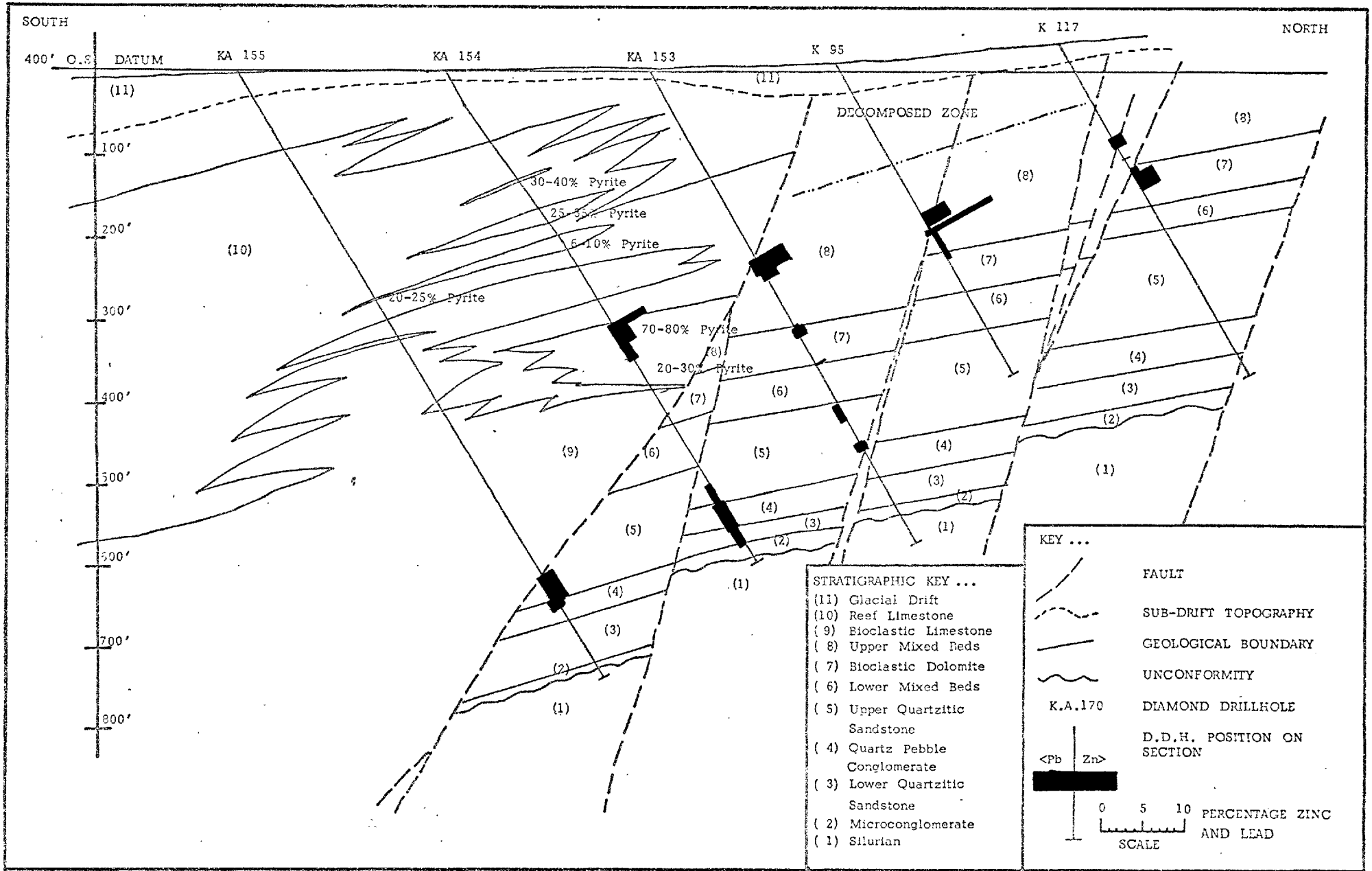


FIG ... 3.21

CROSS SECTION OF THE KEEL PROSPECT SHOWING THE ASSOCIATION OF LEAD AND ZINC MINERALIZATION WITH FAULTING AND THE ASSOCIATION OF PYRITE BODIES WITH THE REEF LIMESTONE.

SCALE ...

To further investigate Patterson's statement, mineralized drill core samples from the C, D, G, H and K faults were taken and analysed for zinc, lead and silver; the results are expressed graphically in Fig. 3.22. The Zn:Pb ratio for each orebody is expressed below:

Orebody	Number of Values	Mean $^{Zn}/_{Pb}$	Standard Deviation
C	84	39.95	52.54
D	44	34.50	49.35
G	52	32.81	36.95
H	44	31.77	44.24
K	62	33.87	29.23

From these results it can be seen that the variation of the Zn:Pb ratio between orebodies is negligible, the only significant difference being a smaller standard deviation for the K orebody, implying that the ratio of 33.87:1 for Zn:Pb is more consistent than for other orebodies. The figure of 3:1 for Zn:Pb obtained by Patterson for the K orebody is not corroborated. Nonetheless a significant increase in lead values east of the shaft was detected and is represented in Figs. 3.23 and 3.24.

Frequency diagrams for lead and zinc concentrations east and west of the shaft were constructed on the basis of drill core analyses carried out by R.T.Z. and A.S.A.R.C.O. and the author to illustrate the variation of metal concentration, Figs. 3.23A and 3.23B, and 3.24A and 3.24B. As some 43% of total drilling was in the Mixed Bed lithology, selected drill holes only were taken so as not to bias results, Fig. 3.25 shows the footage and lithology of beds intersected and used in this study.

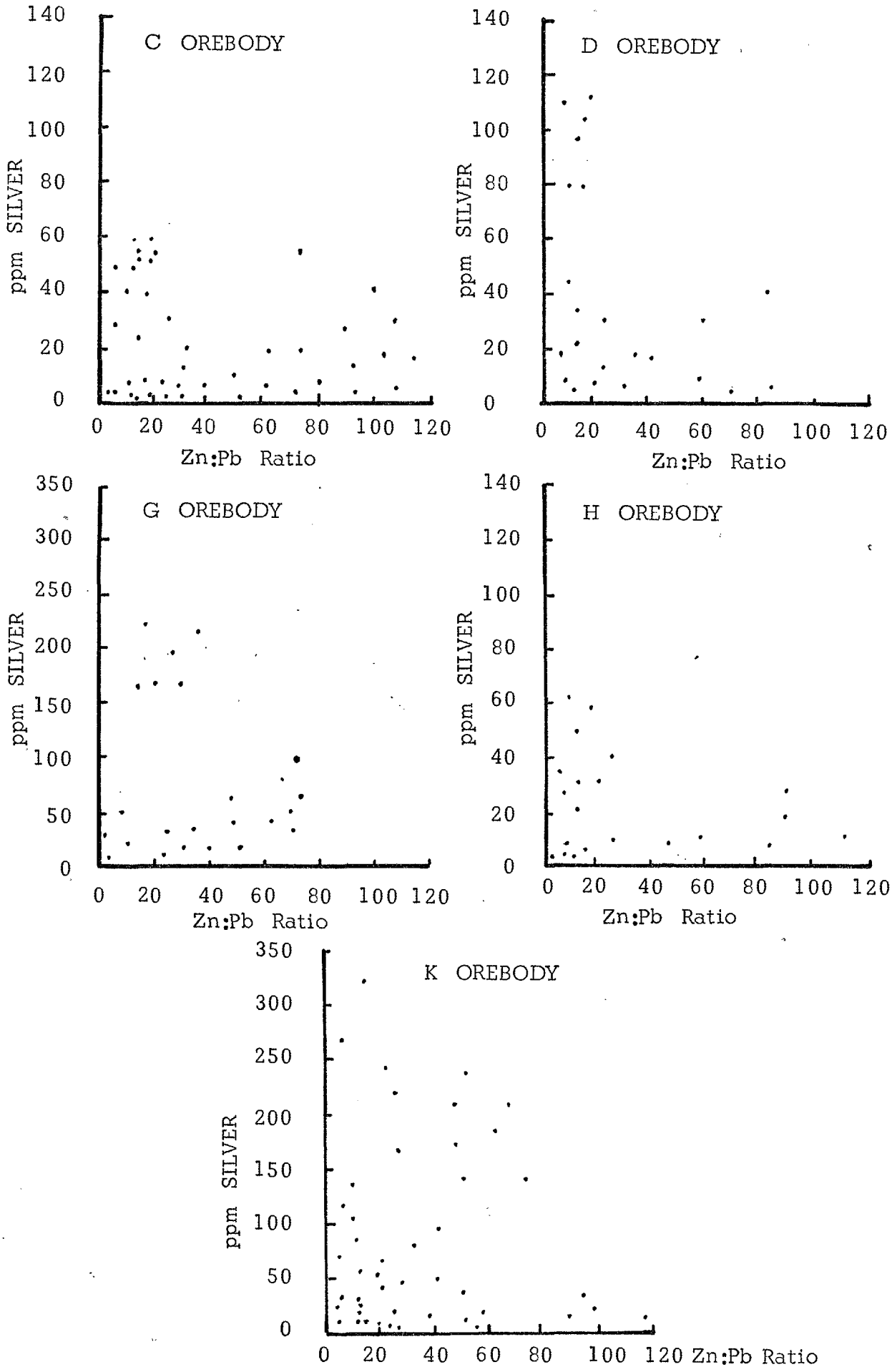


FIG ... 3.22 RELATIONSHIP BETWEEN SILVER CONTENT & Zn:Pb RATIO IN C,D,G,H,K. OREBODIES KEEL PROSPECT

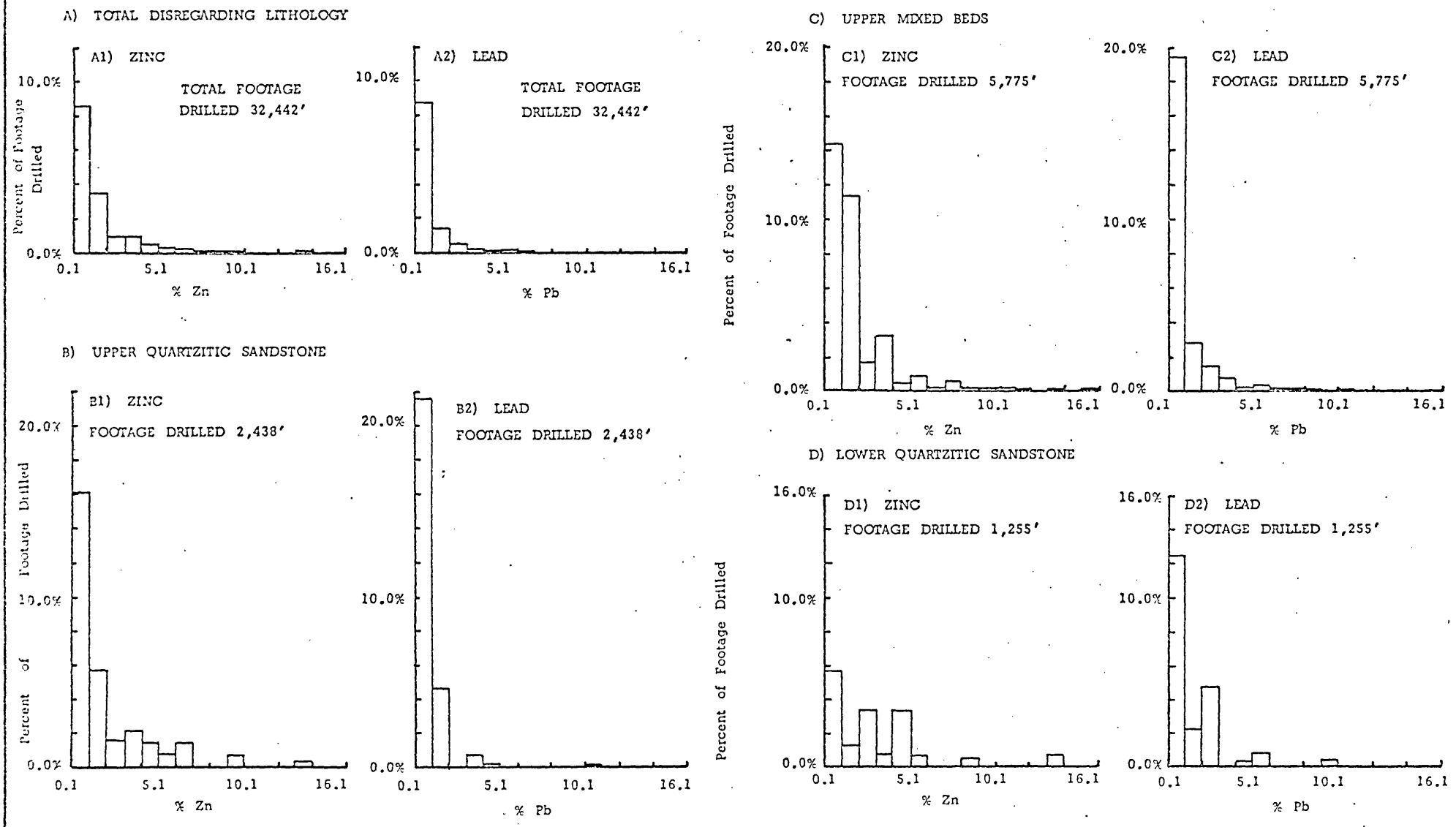


FIG. . . 3.23A

LITHOLOGICAL ASSOCIATION OF LEAD & ZINC MINERALIZATION EAST OF SHAFT

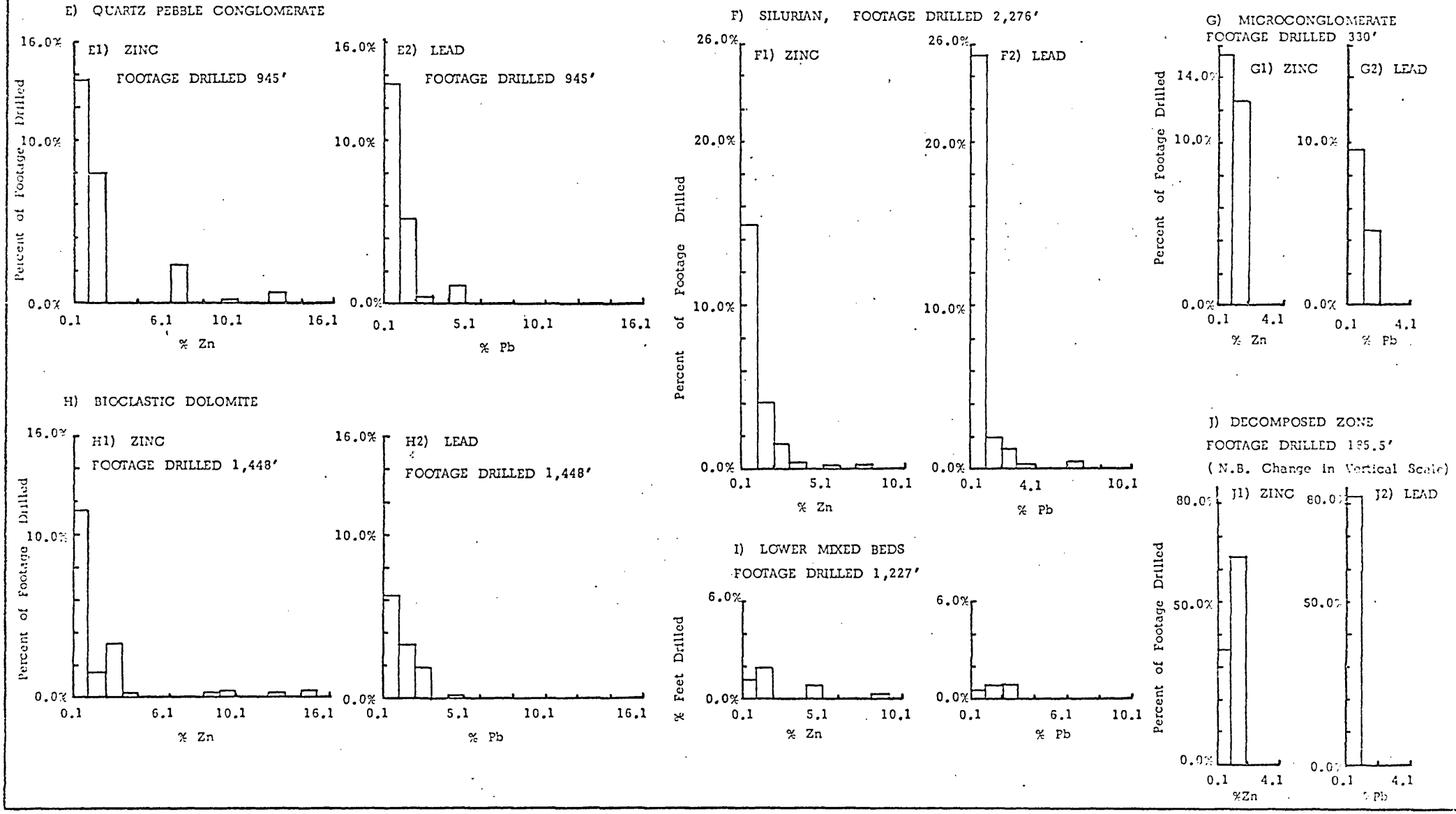


FIG...3.23B

LITHOLOGICAL ASSOCIATION OF LEAD & ZINC MINERALIZATION EAST OF SHAFT

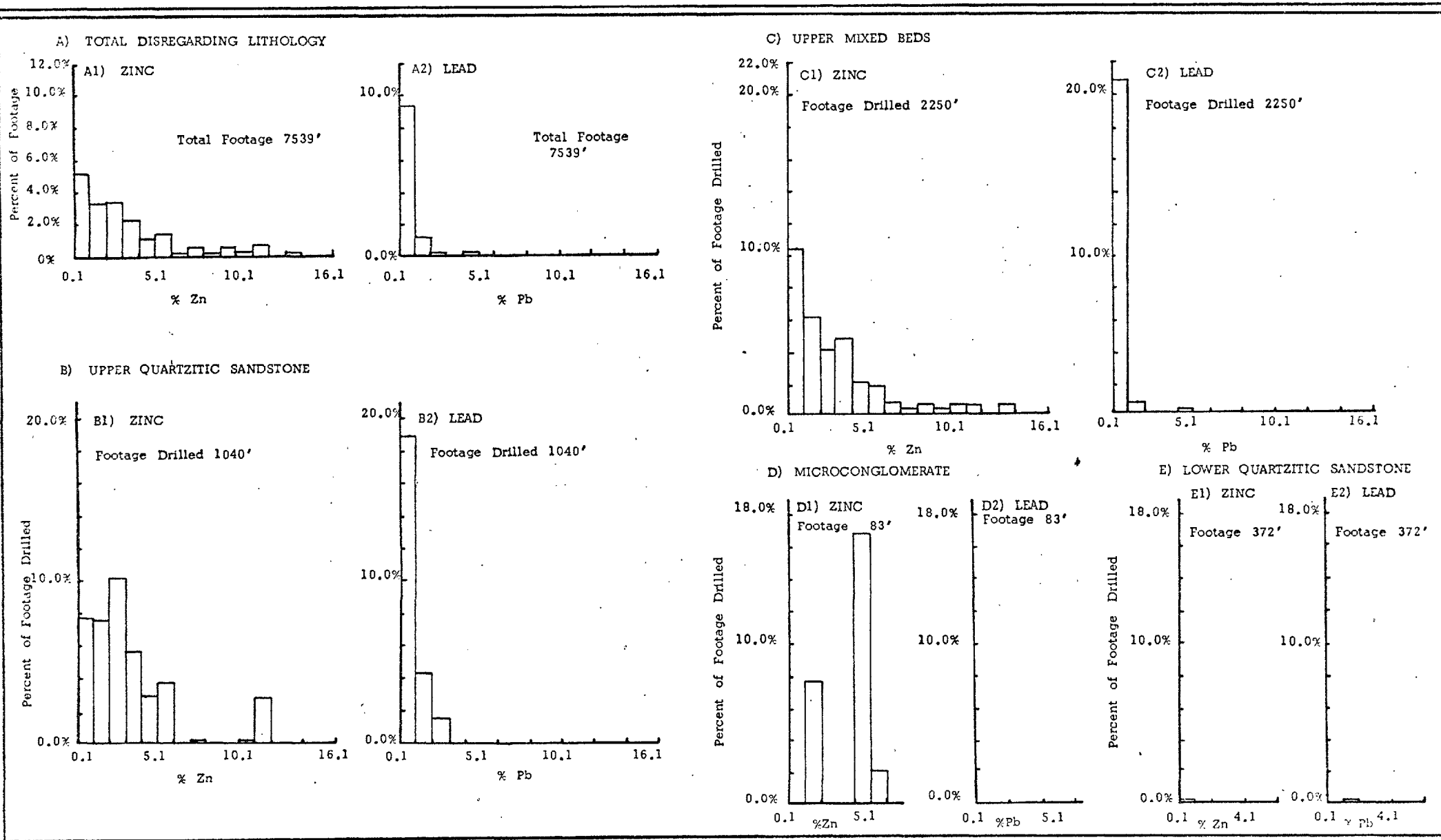
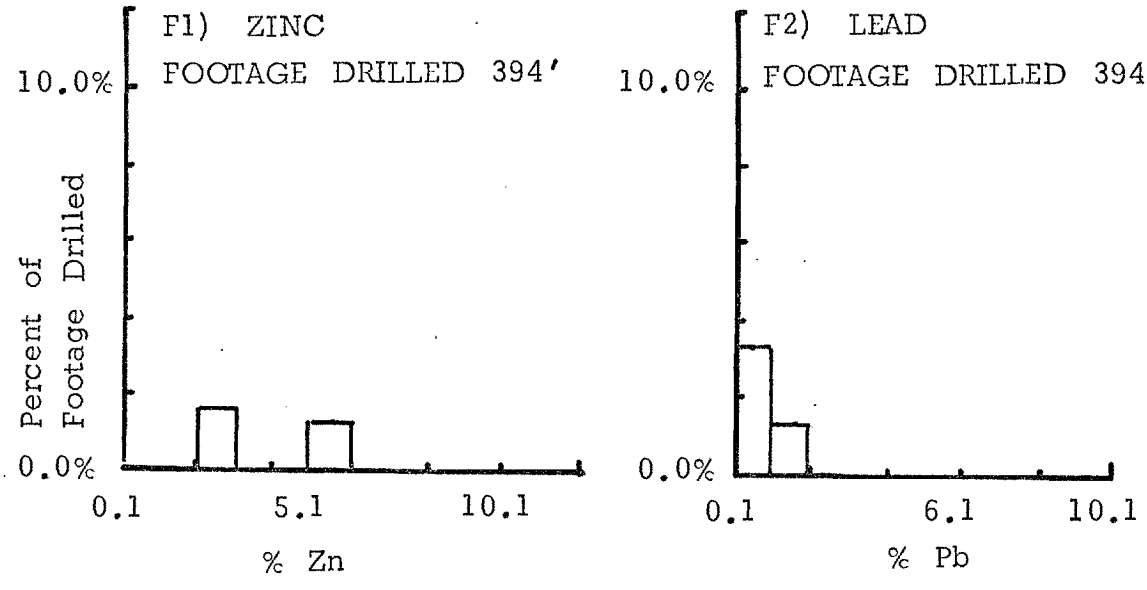


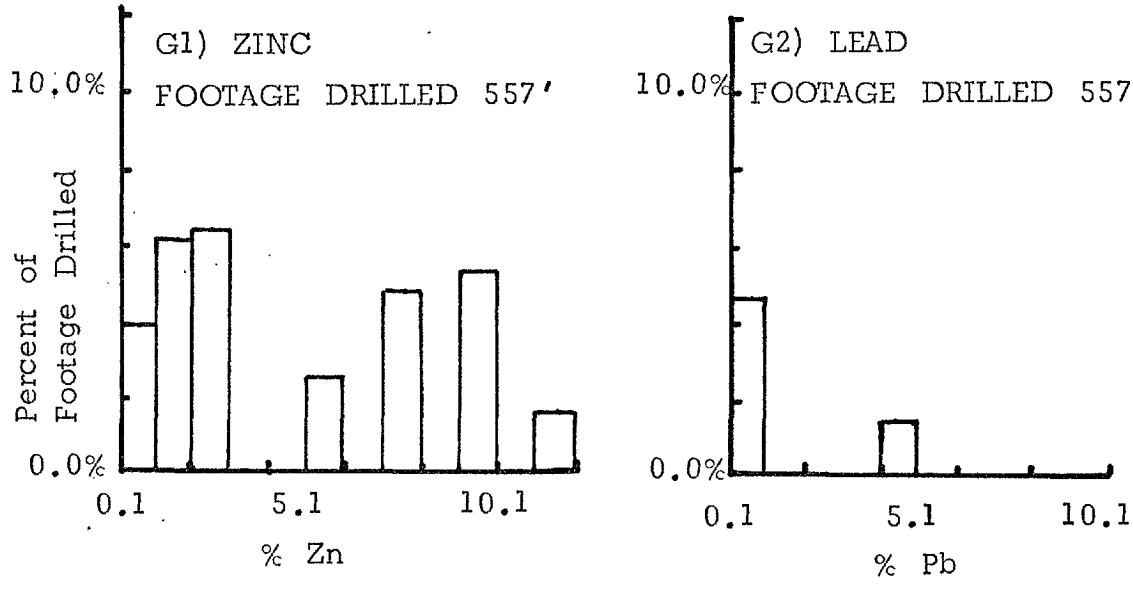
FIG. . . 3.24A

LITHOLOGICAL ASSOCIATION OF LEAD & ZINC MINERALIZATION WEST OF SHAFT

F) QUARTZ PEBBLE CONGLOMERATE



G) BIOCLASTIC DOLOMITE



H) GLACIAL DRIFT

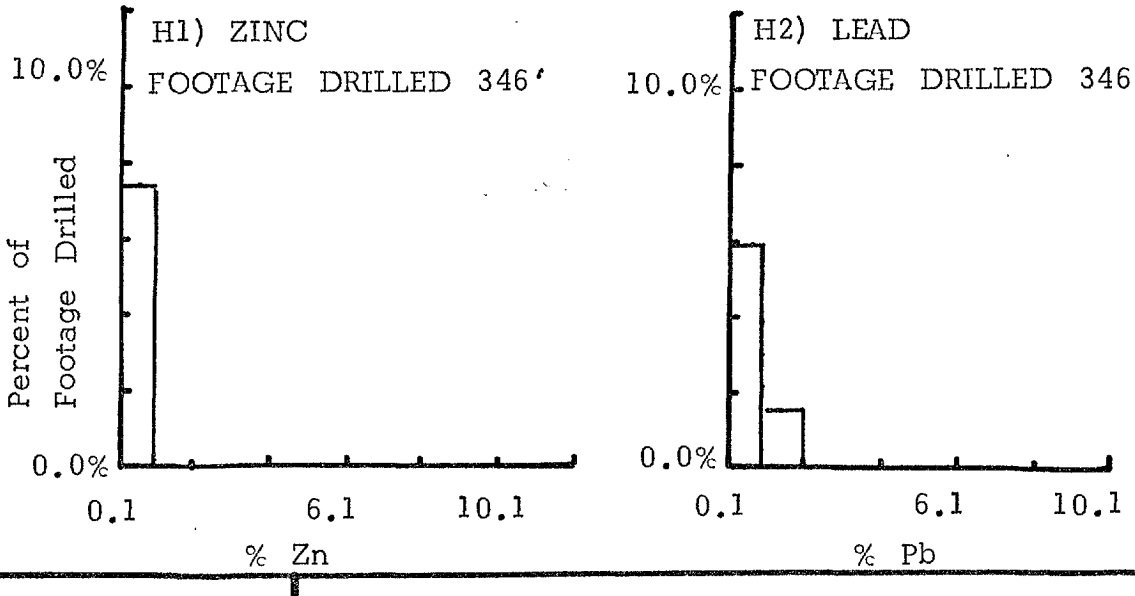
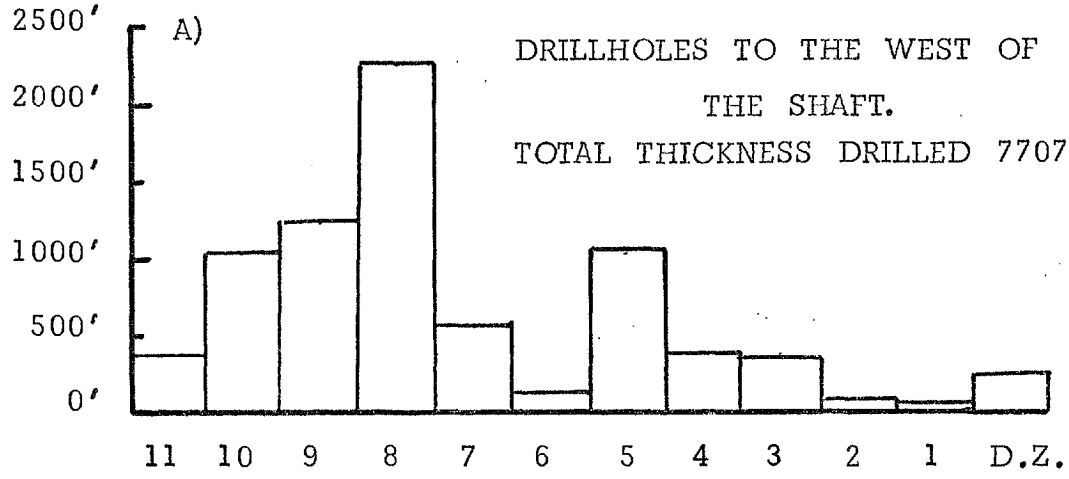


FIG ... 3.24b

LITHOLOGICAL ASSOCIATION OF LEAD & ZINC MINERALIZATION WEST OF SHAFT



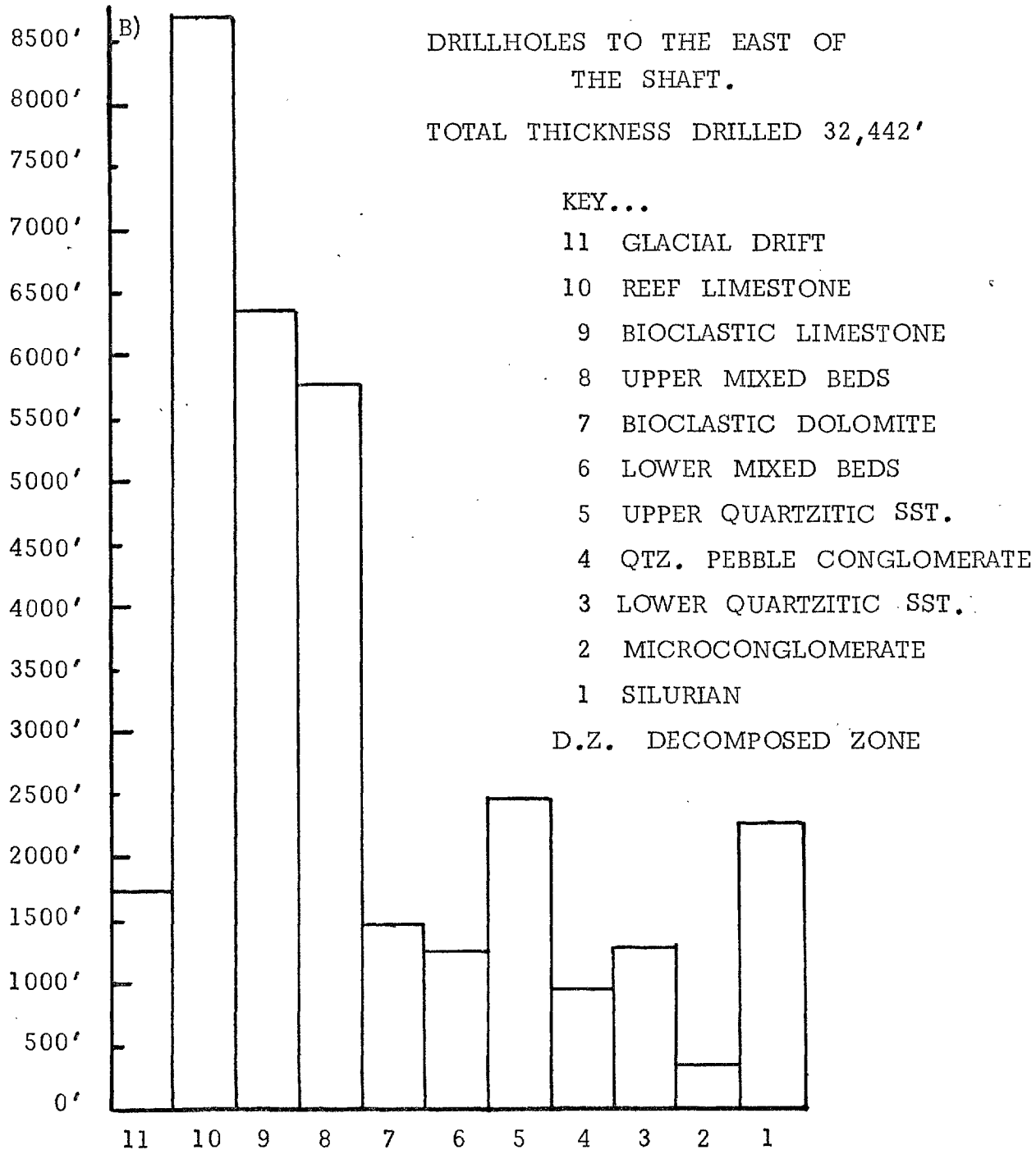


FIG... 3.25

DIAGRAM OF THE THICKNESSES OF THE BEDS ENCOUNTERED IN SELECTED DRILLHOLES TO THE EAST & WEST OF THE KEEL SHAFT.

From Figs. 3.23 and 3.24 it can be seen that there is a definite enrichment of lead to the east of the shaft. The lower quartz sandstone shows an extreme difference from west to east, with a Zn:Pb ratio in the east in many cases < 1:1. The microconglomerate also increases in lead eastwards, so too does the Silurian, being mineralized in some cases to depths of 200 feet.

Mineralization in the limestones is confined to isolated pyrite bodies with associated galena and sphalerite, Fig. 3.36 and to occasional ZnS grains. Sporadic high grade mineralization occurs throughout the bioclastic dolomite to the west of the shaft; to the east, grade is lower, but intersections far more frequent. 185.5' of decomposed zone to the east of the shaft was examined and found to assay 83% of its length between 0.1% and 1.0% Pb and 35% of its length between 0.1% and 1.0% Zn and 62% between 1.1% and 2.1% Zn.

Figs. 3.26 - 3.35 show the horizontal distribution of zinc and lead on the 100', 200', 300', 400' and 500' levels of Keel and from these a close association of metal distribution and faulting is very apparent. Figs. 3.36 and 3.21 also show this fault association to an even greater extent; the occurrence of pyritic bodies throughout the limestone is also shown in Fig. 3.21.

Broad primary dispersion patterns of lead and zinc in this despoit are really non-existant; mineralization is confined to faults and faulted zones. Fragments of barren wallrock surrounded by high grade mineralization contain < 25 p p m Zn and < 10 p p m Pb. It is true that Zn:Pb ratio decreases with depth, but this is due to an increase in lead with depth rather than a corresponding decrease in zinc. In the author's opinion the Keel deposit does not represent a situation where migration of ore fluids led to a precipitation of

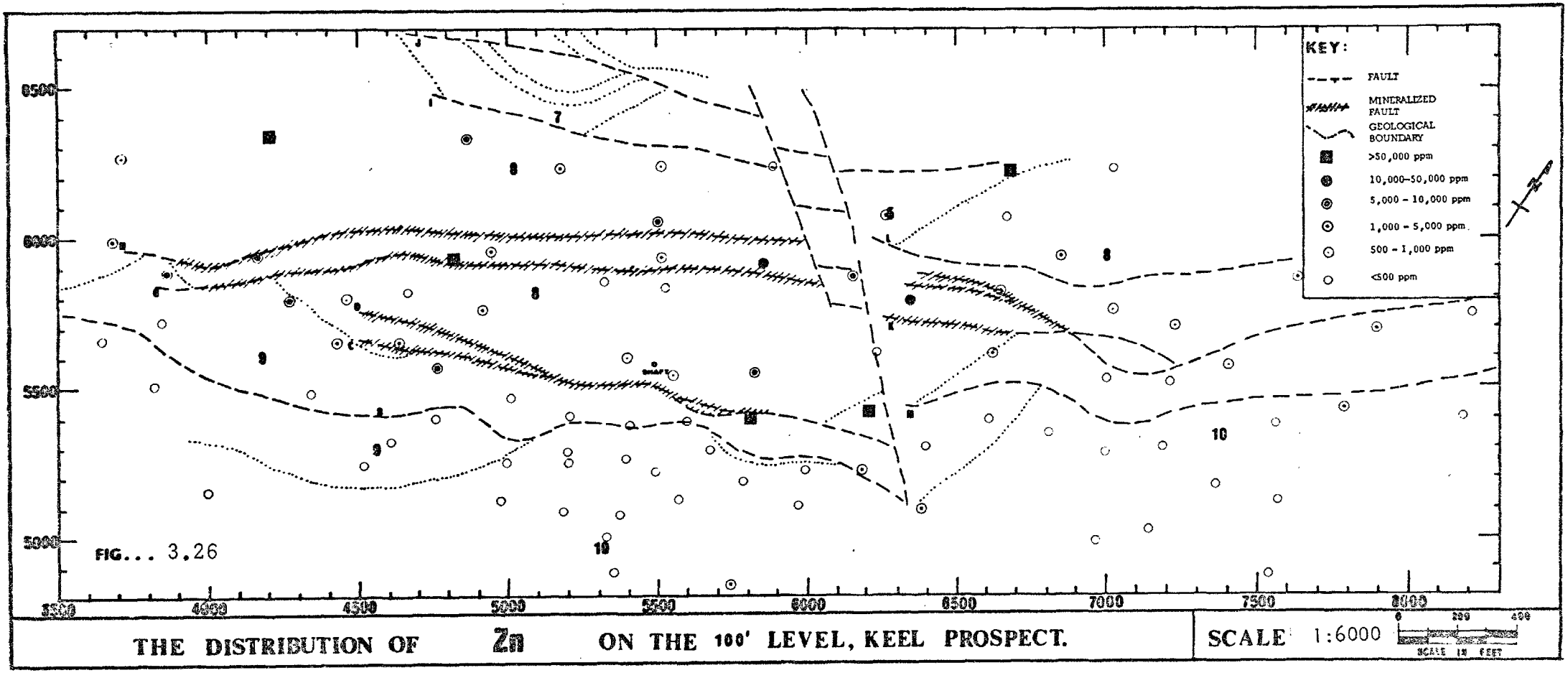
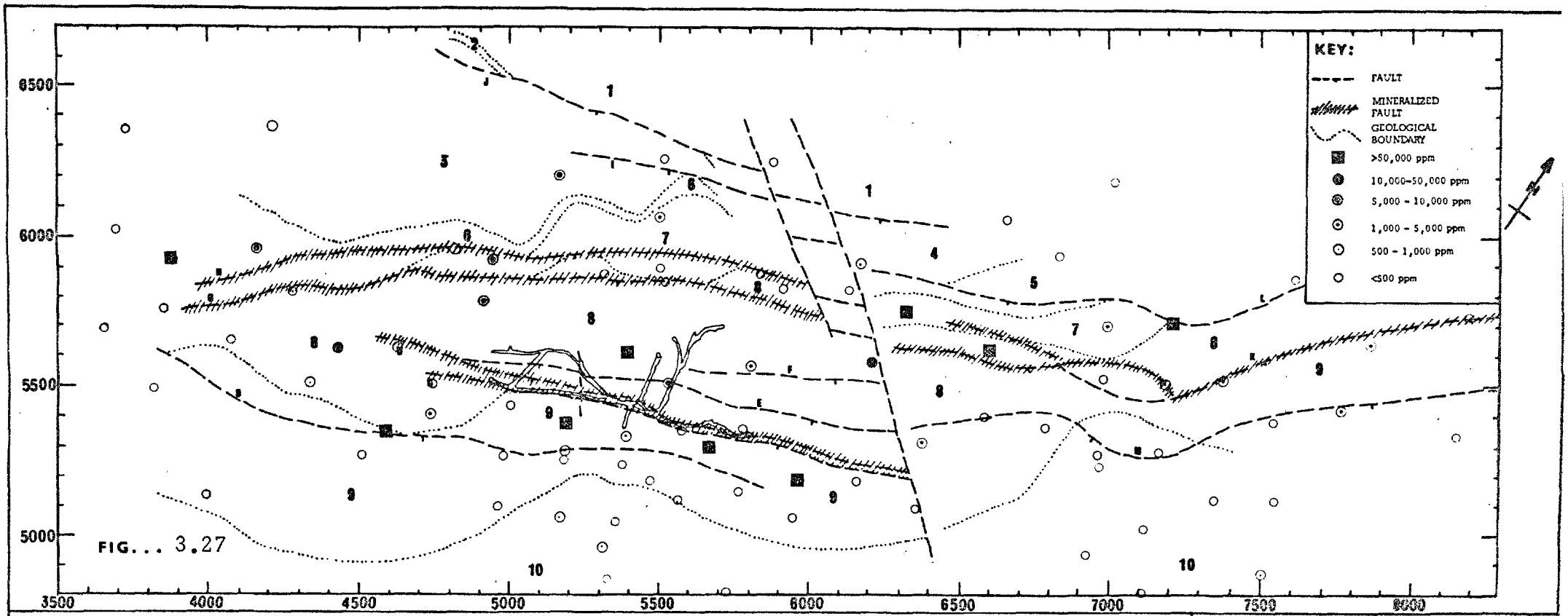


FIG... 3.26

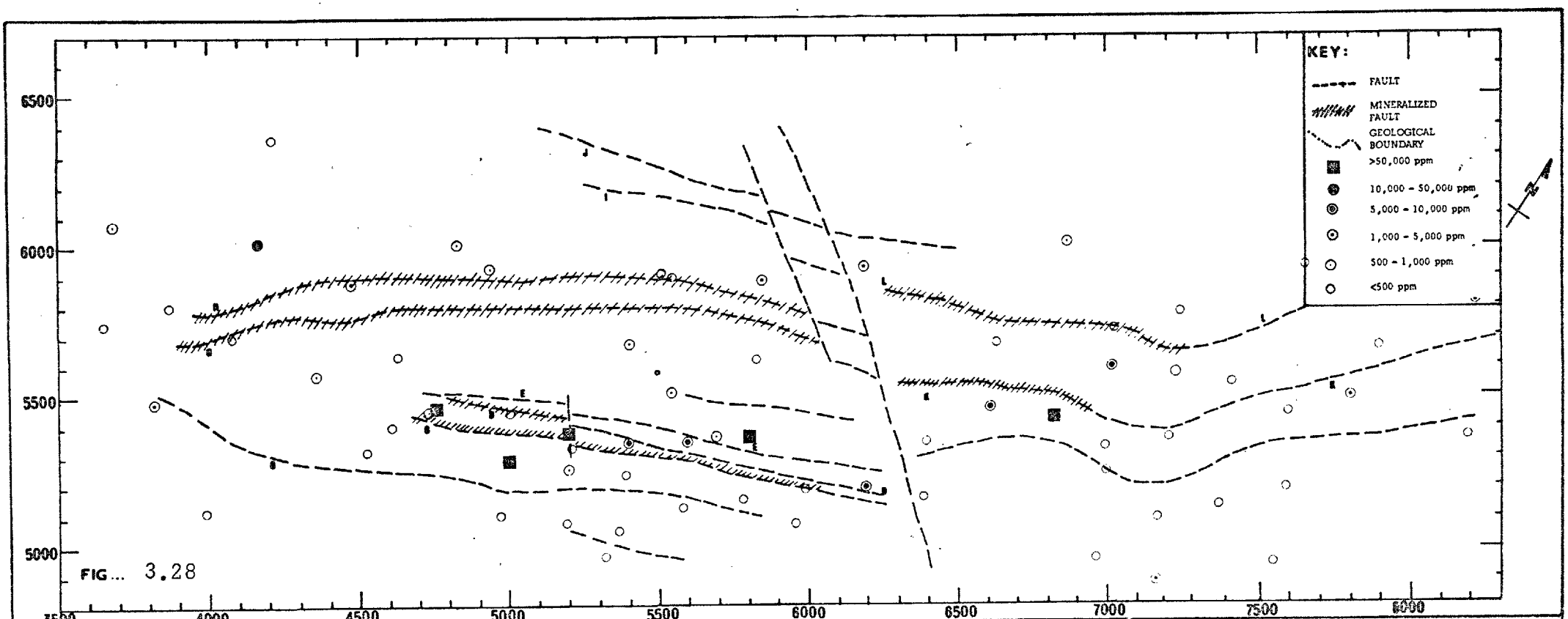
THE DISTRIBUTION OF Zn ON THE 100' LEVEL, KEEL PROSPECT.

SCALE 1:6000



THE DISTRIBUTION OF Zn ON THE 200' LEVEL, KEEL PROSPECT.

SCALE :- 1:6000


KEY:
FAULT
MINERALIZED FAULT
GEOLOGICAL BOUNDARY
>50,000 ppm
10,000 - 50,000 ppm
5,000 - 10,000 ppm
1,000 - 5,000 ppm
500 - 1,000 ppm
<500 ppm
6500
6000
5500
5000
3500
4000
4500
5000
5500
6000
6500
7000
7500
8000
FIG... 3.28
THE DISTRIBUTION OF Zn ON THE 300' LEVEL, KEEL PROSPECT.
SCALE 1:6000
0
200
400
FEET

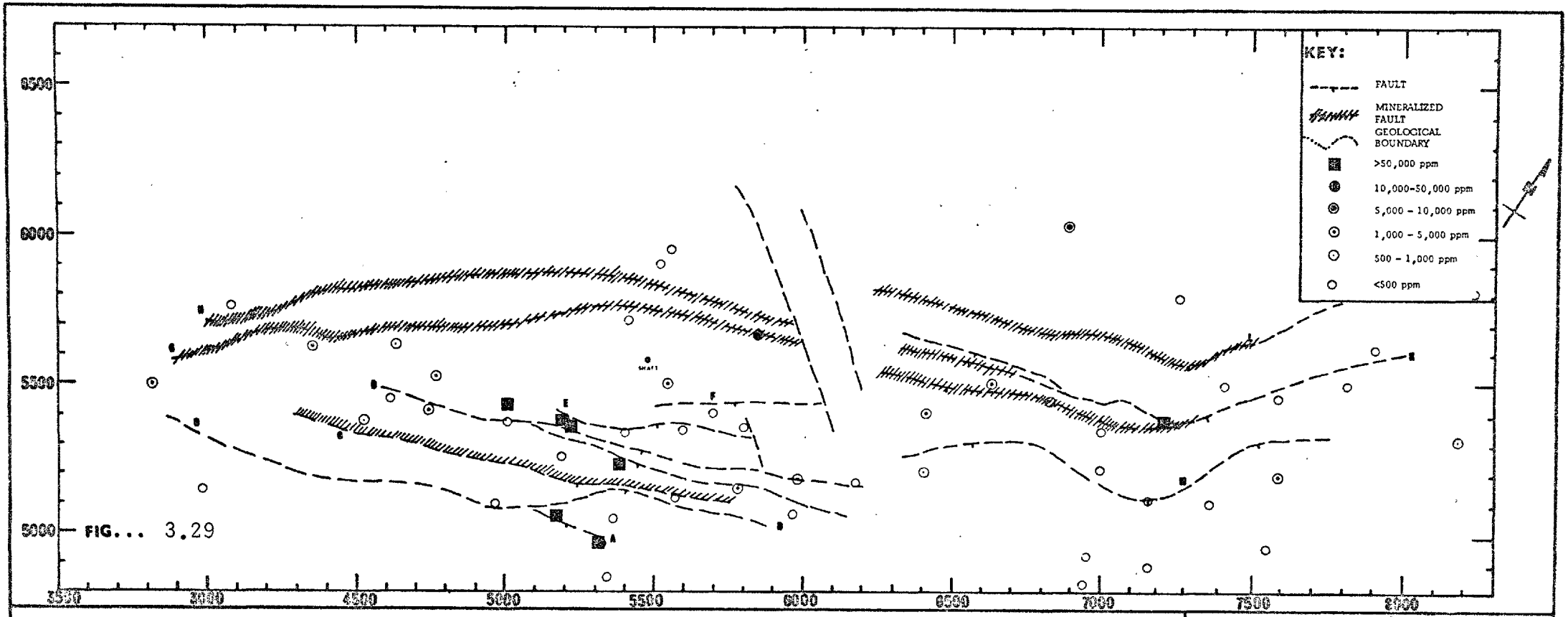


FIG... 3.29

THE DISTRIBUTION OF Zn ON THE 400' LEVEL, KEEL PROSPECT.

SCALE 1:6000

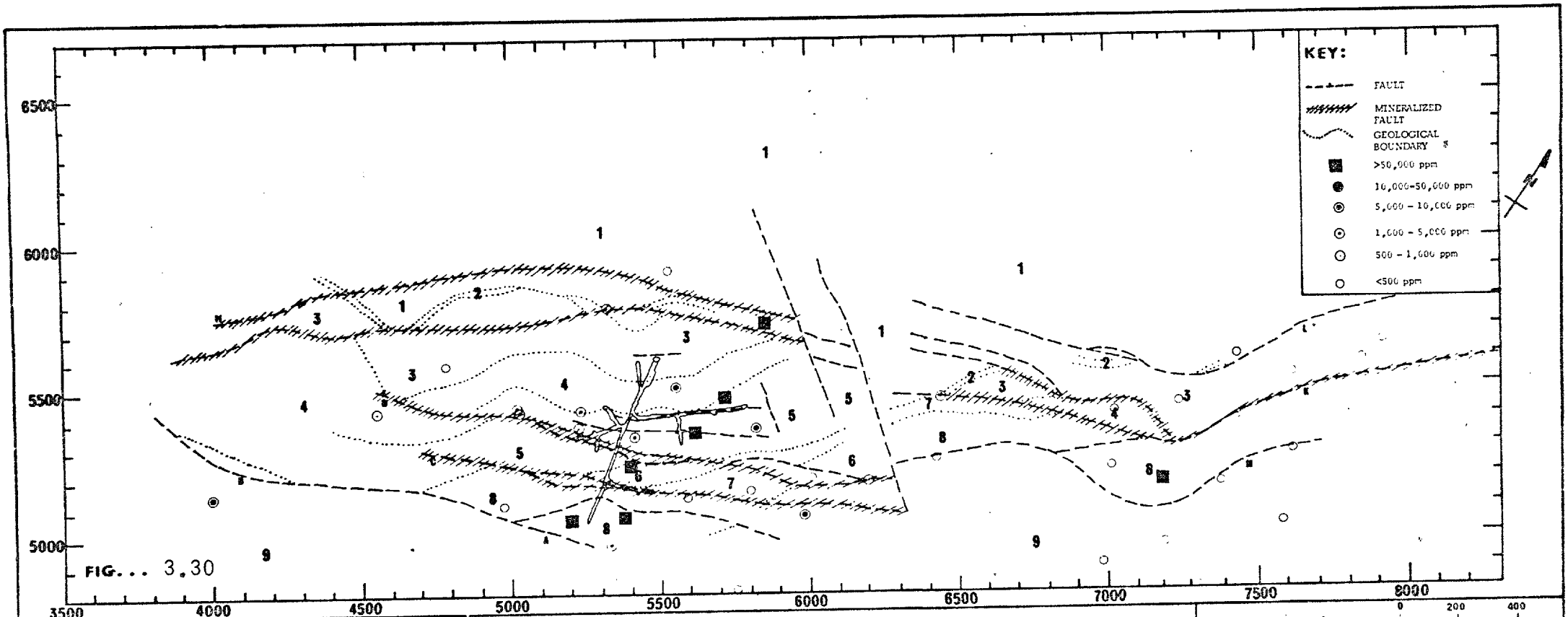


FIG... 3.30

THE DISTRIBUTION OF **Zn** ON THE 500' LEVEL, KEEL PROSPECT.

SCALE 1:6000

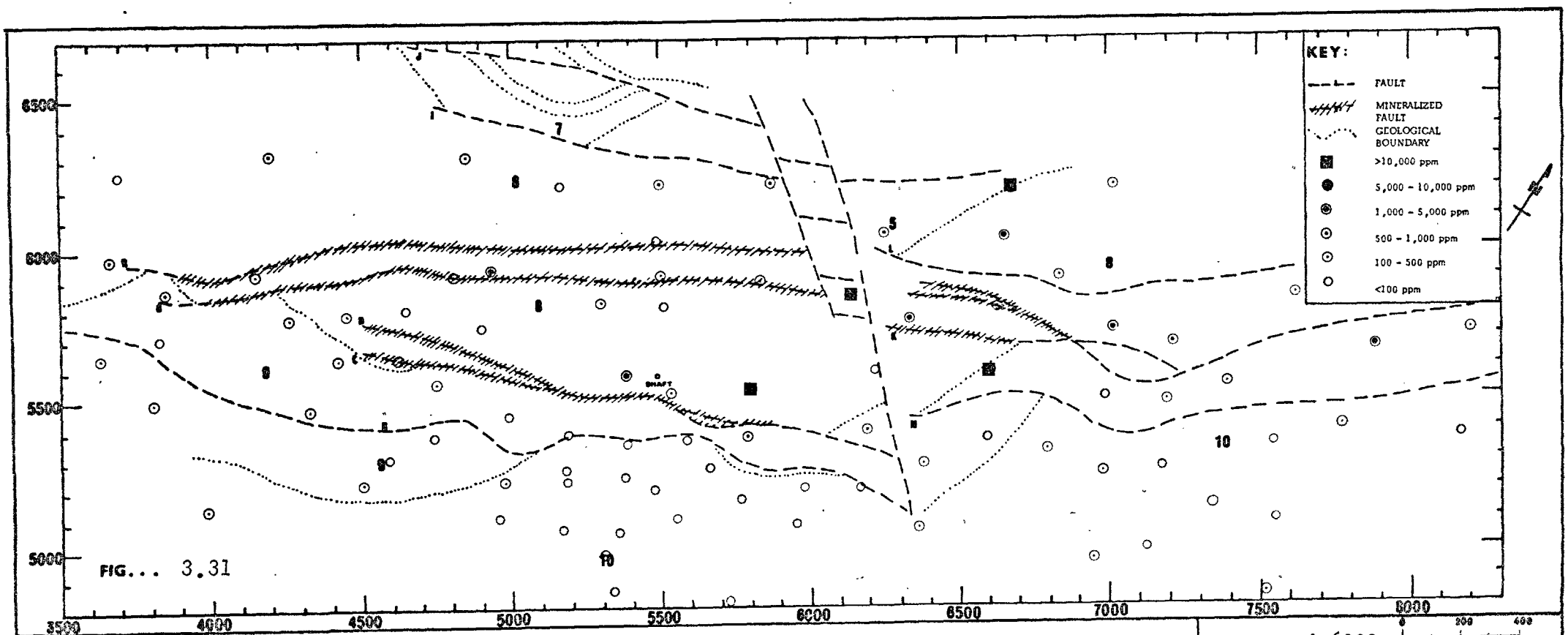
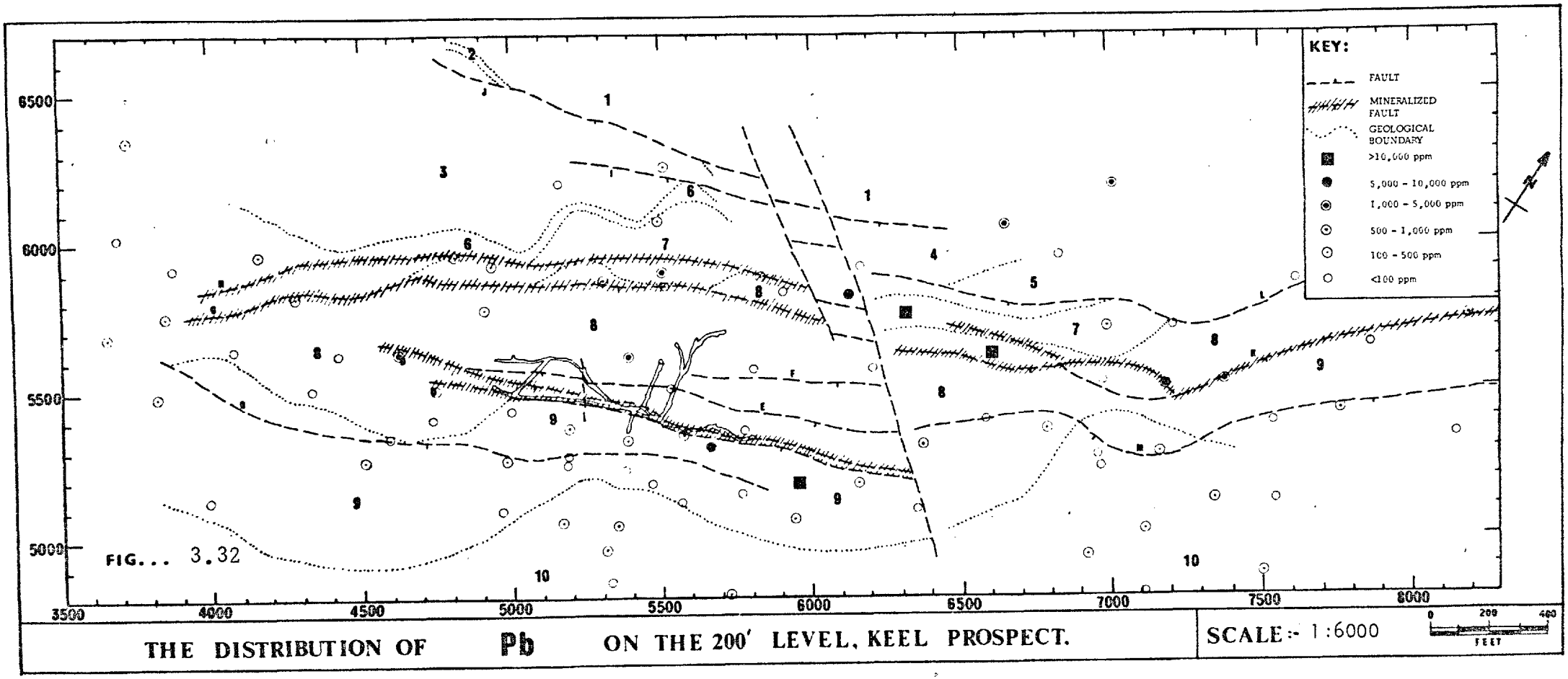
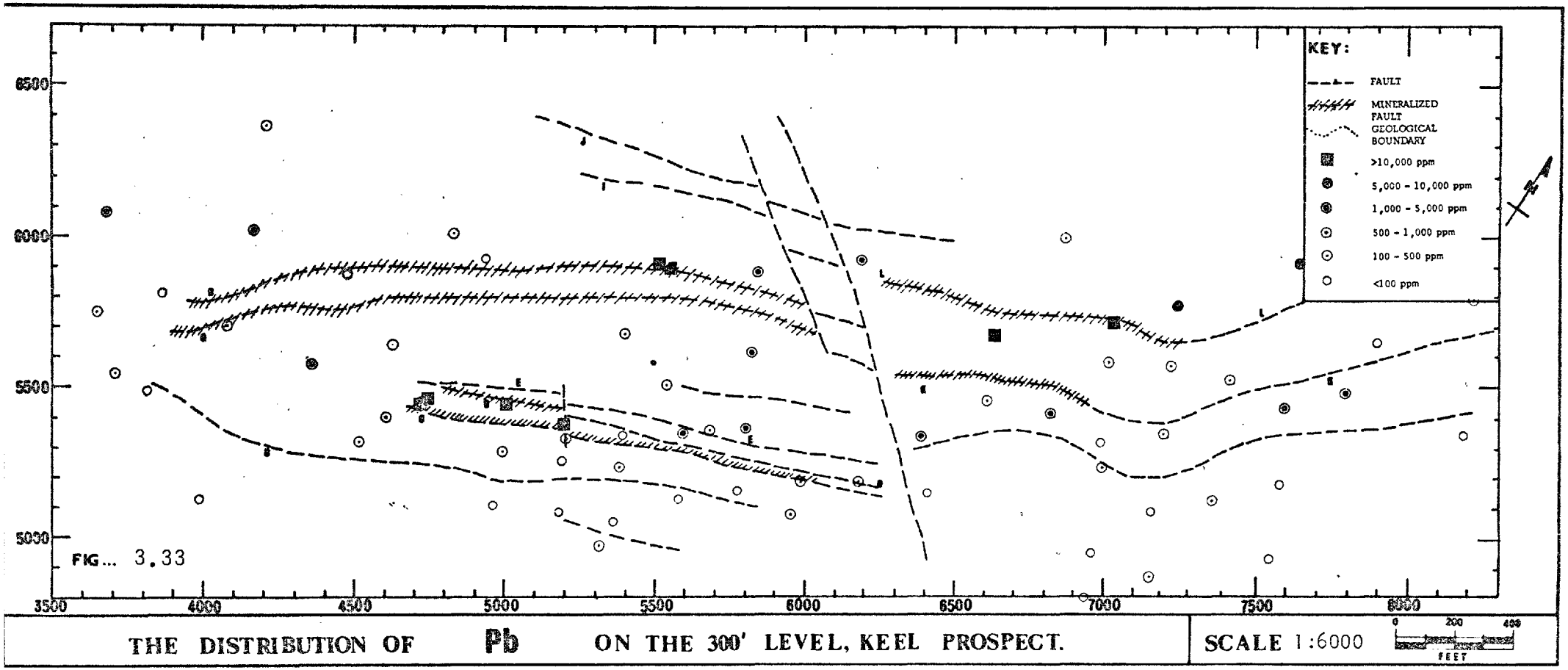


FIG... 3.31

THE DISTRIBUTION OF Pb ON THE 100' LEVEL, KEEL PROSPECT.


KEY:
FAULT
MINERALIZED FAULT
GEOLOGICAL BOUNDARY
>10,000 ppm
5,000 - 10,000 ppm
1,000 - 5,000 ppm
500 - 1,000 ppm
100 - 500 ppm
<100 ppm
N
6500
6000
5500
5000
3500
4000
4500
5000
5500
6000
6500
7000
7500
8000
FIG... 3.32
THE DISTRIBUTION OF Pb ON THE 200' LEVEL, KEEL PROSPECT.
SCALE :- 1:6000
0
200
400
FEET


KEY:
FAULT
MINERALIZED FAULT
GEOLOGICAL BOUNDARY
>10,000 ppm
5,000 - 10,000 ppm
1,000 - 5,000 ppm
500 - 1,000 ppm
100 - 500 ppm
<100 ppm
6500
6000
5500
5000
3500
4000
4500
5000
5500
6000
6500
7000
7500
8000
FIG... 3.33
THE DISTRIBUTION OF Pb ON THE 300' LEVEL, KEEL PROSPECT.
SCALE 1:6000
0
200
400
FEET

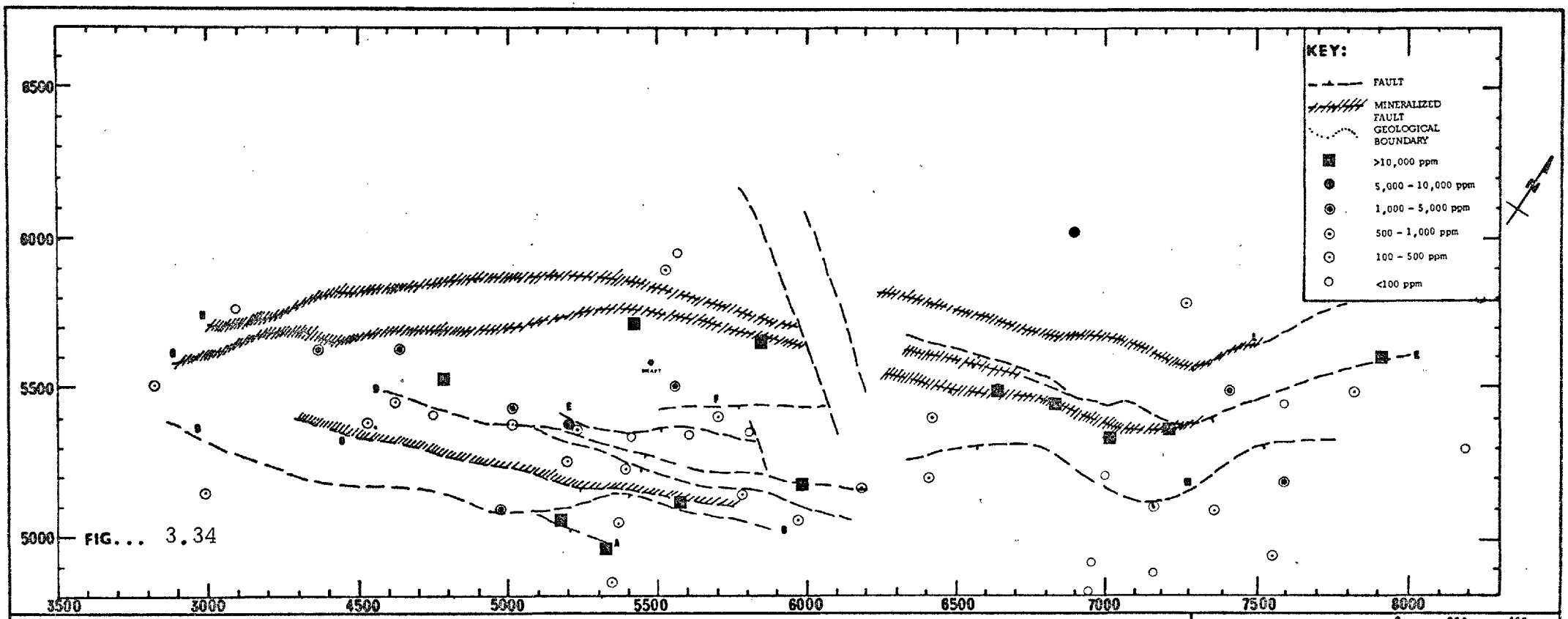


FIG... 3.34

THE DISTRIBUTION OF Pb ON THE 400' LEVEL, KEEL PROSPECT.

SCALE 1:6000

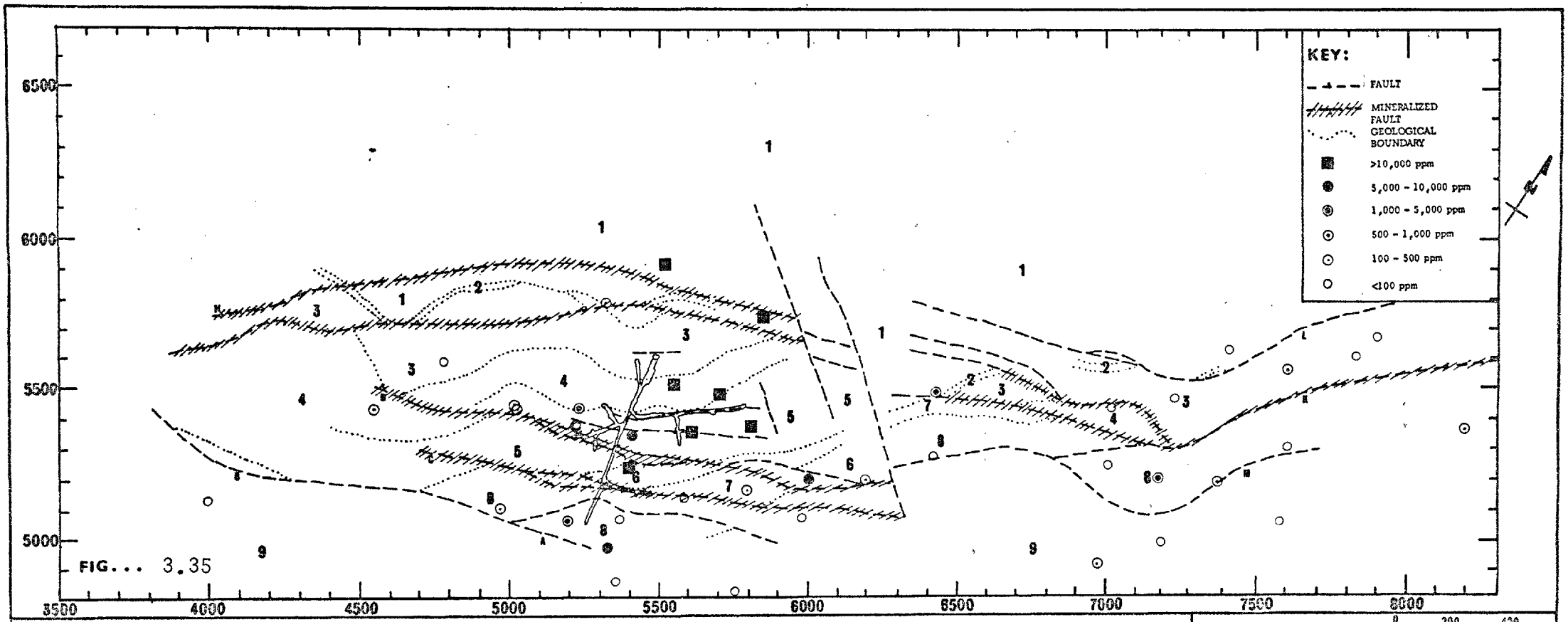


FIG... 3.35

THE DISTRIBUTION OF Pb ON THE 500' LEVEL, KEEL PROSPECT.

SCALE: 1:6000

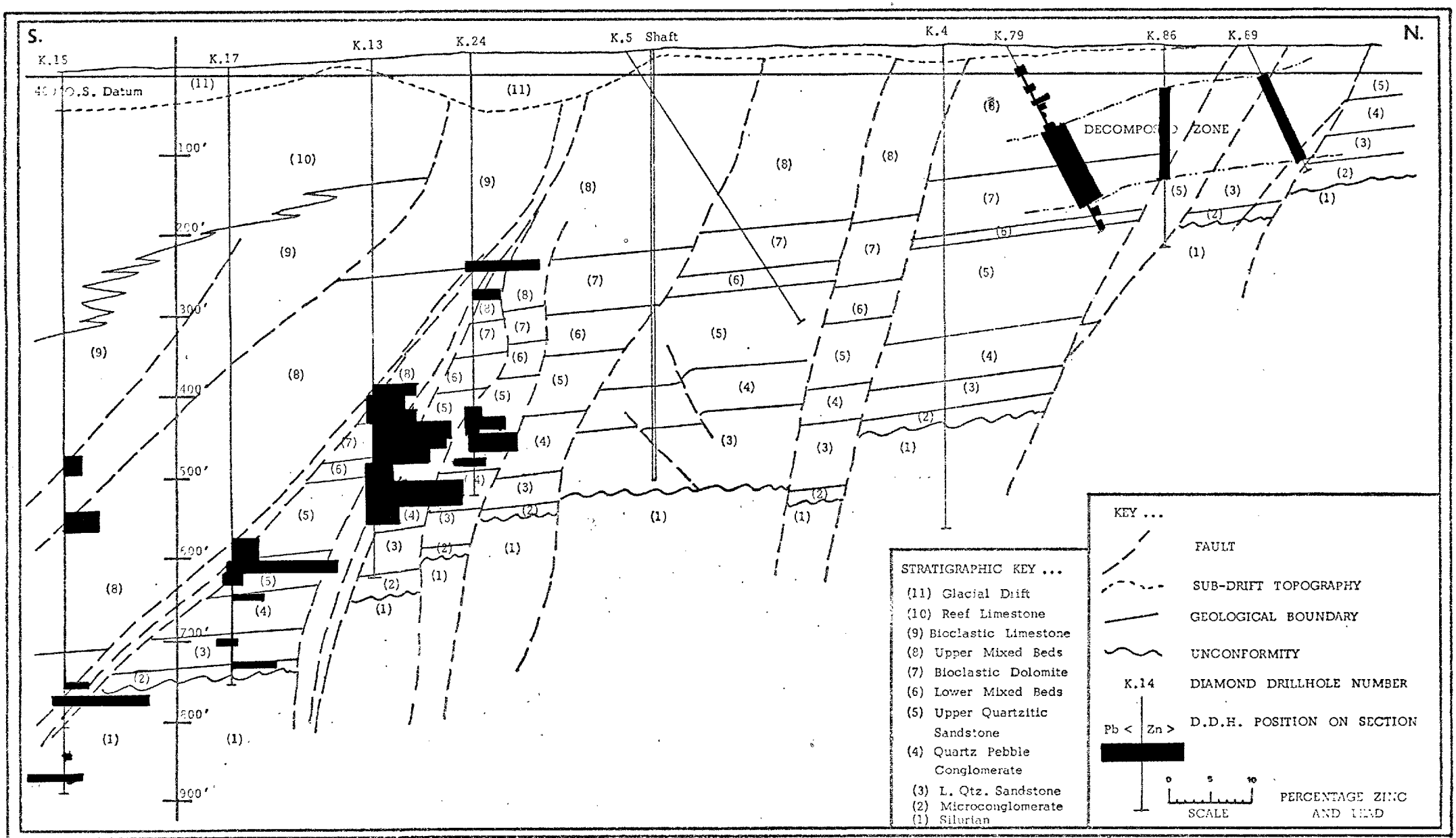


FIG ... 3.36

CROSS SECTION OF THE KEEL PROSPECT SHOWING ASSOCIATION OF LEAD & ZINC MINERALIZATION WITH MAJOR FAULTING

SCALE ... 0 100 200
SCALE IN FEET

lead near the source and a more distant migration and precipitation of zinc. The fluctuations in metal ratio are purely due to local increases and decrease in lead concentration. Thus mineralization in the Keel area is confined to faults and fracture and chemical dispersion of zinc and lead throughout the Keel wallrocks is negligible.

3.3D. CADMIUM AND COPPER

The content of cadmium in the Keel sphalerite varies between 0.5% and 2.1% and as such, is extremely high for the Irish Deposits. Trace element content of the sphalerite is discussed in chapter. 6. Both cadmium and copper follow the zinc pattern as they are predominantly associated with sphalerite Figs. 3.37 - 3.41, illustrate the horizontal distribution of cadmium on the 100', 200', 300', 400' and 500' levels and Figs. 3.42 and 3.43 illustrate the horizontal distribution of copper on the 200' and 500' levels. Their association with the C, D, G, H and K orebodies can be clearly seen.

Figs. 3.44 and 3.45 show zinc cadmium relationships for the C and F orebodies, for material from drillcore and from the underground workings of the prospect. The straight line represents an association of cadmium and zinc in which 1% cadmium is contained in the sphalerite lattice and the sphalerite has 62% zinc, this figure is an average from fifty sphalerite samples analysed for a variety of trace elements. A distinct association of cadmium and zinc can be seen, but a variation between orebodies is not apparent. One very important fact does emerge however, and is illustrated in both the C and F orebodies in the underground workings. Very high values of cadmium to zinc occur, as much as 10:1 for Zn:Cd, when sphalerites from these ore horizones are

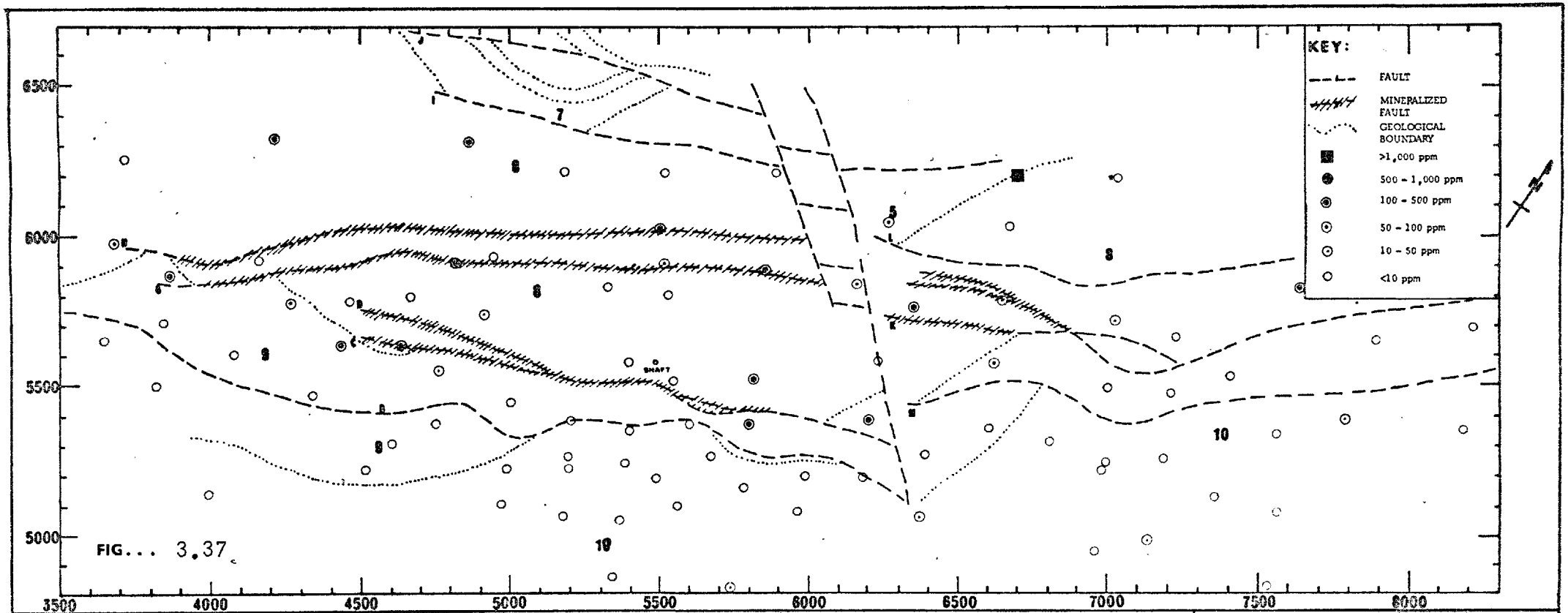
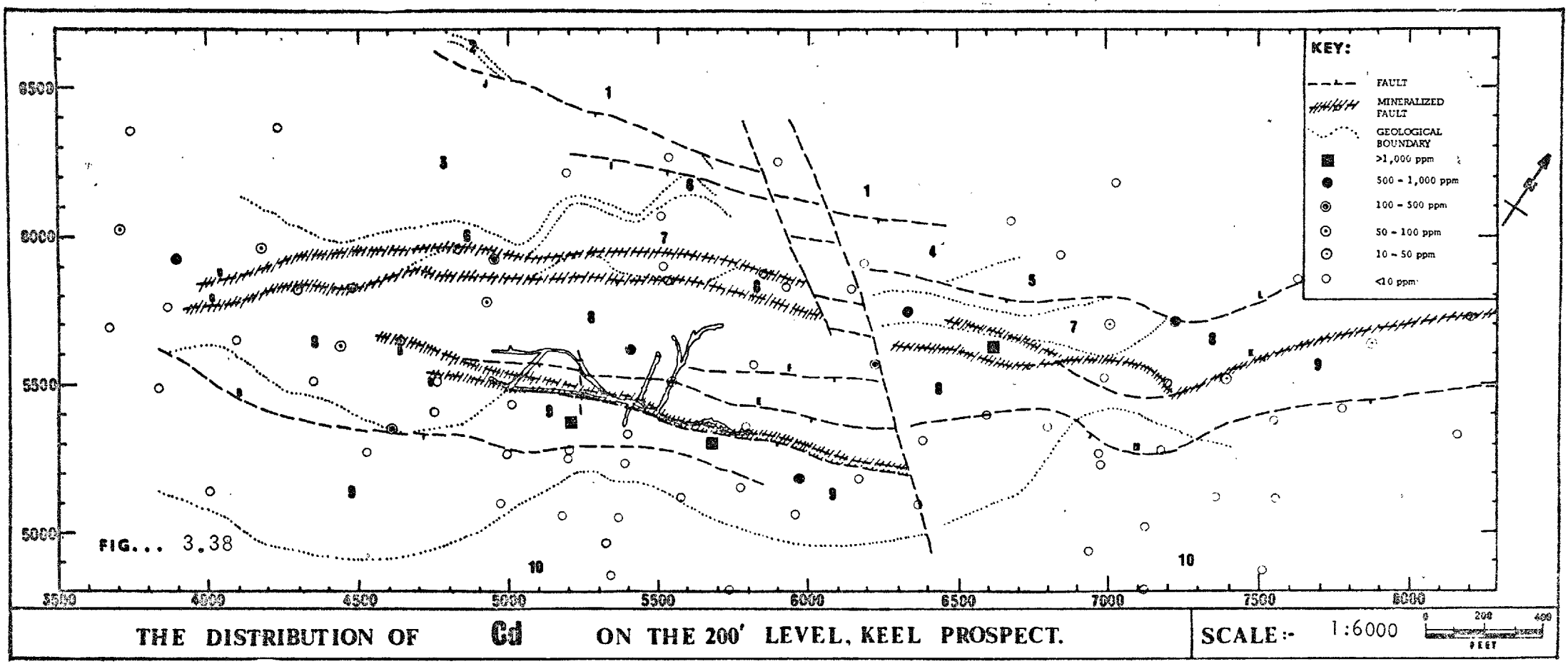


FIG... 3.37

THE DISTRIBUTION OF **Cd** ON THE 100' LEVEL, KEEL PROSPECT.

SCALE 1:6000


KEY:
FAULT
MINERALIZED FAULT
GEOLOGICAL BOUNDARY
>1,000 ppm
500 - 1,000 ppm
100 - 500 ppm
50 - 100 ppm
10 - 50 ppm
<10 ppm
8500
8000
5500
5000
4000
4500
5000
5500
6000
6500
7000
7500
8000
FIG... 3.38
THE DISTRIBUTION OF Cd ON THE 200' LEVEL, KEEL PROSPECT.
SCALE:- 1:6000
FEET

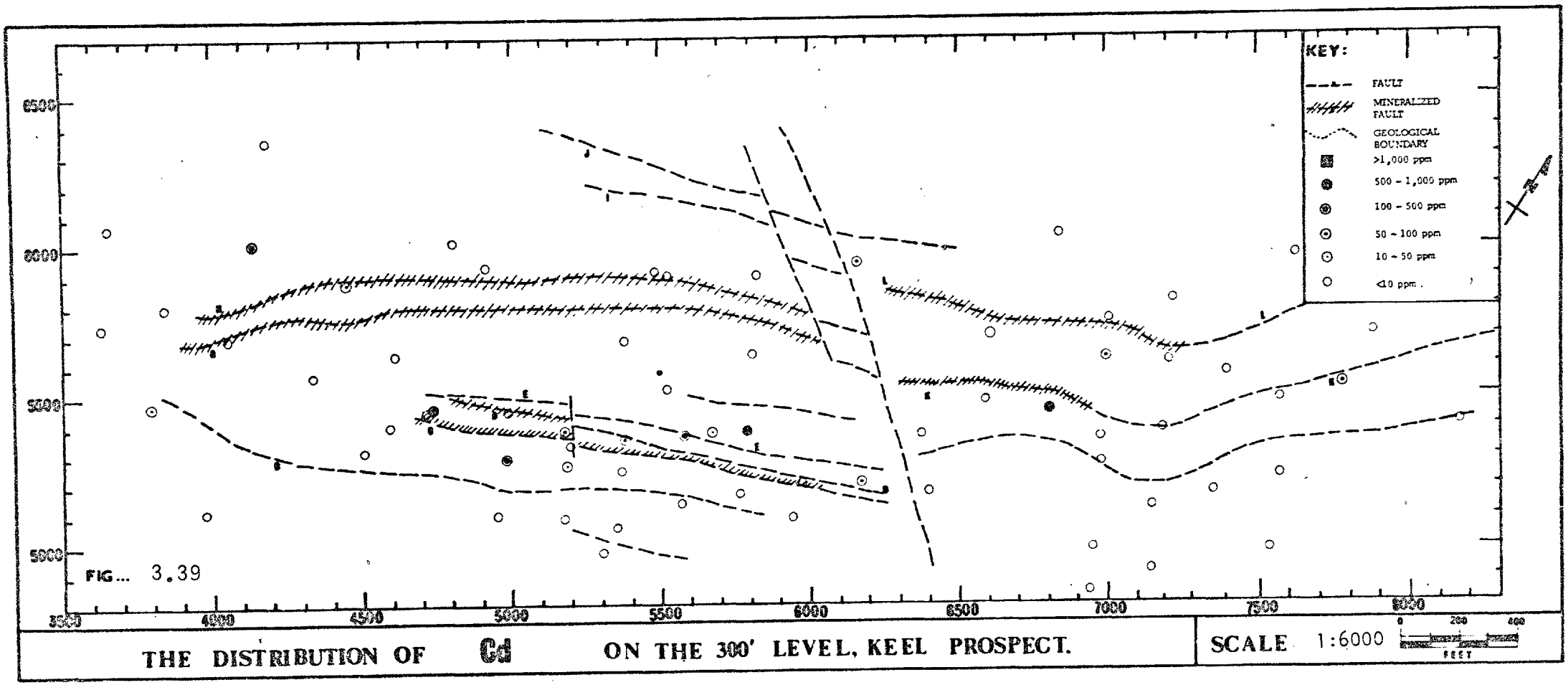


FIG... 3.39

THE DISTRIBUTION OF Cd ON THE 300' LEVEL, KEEL PROSPECT.

SCALE 1:6000

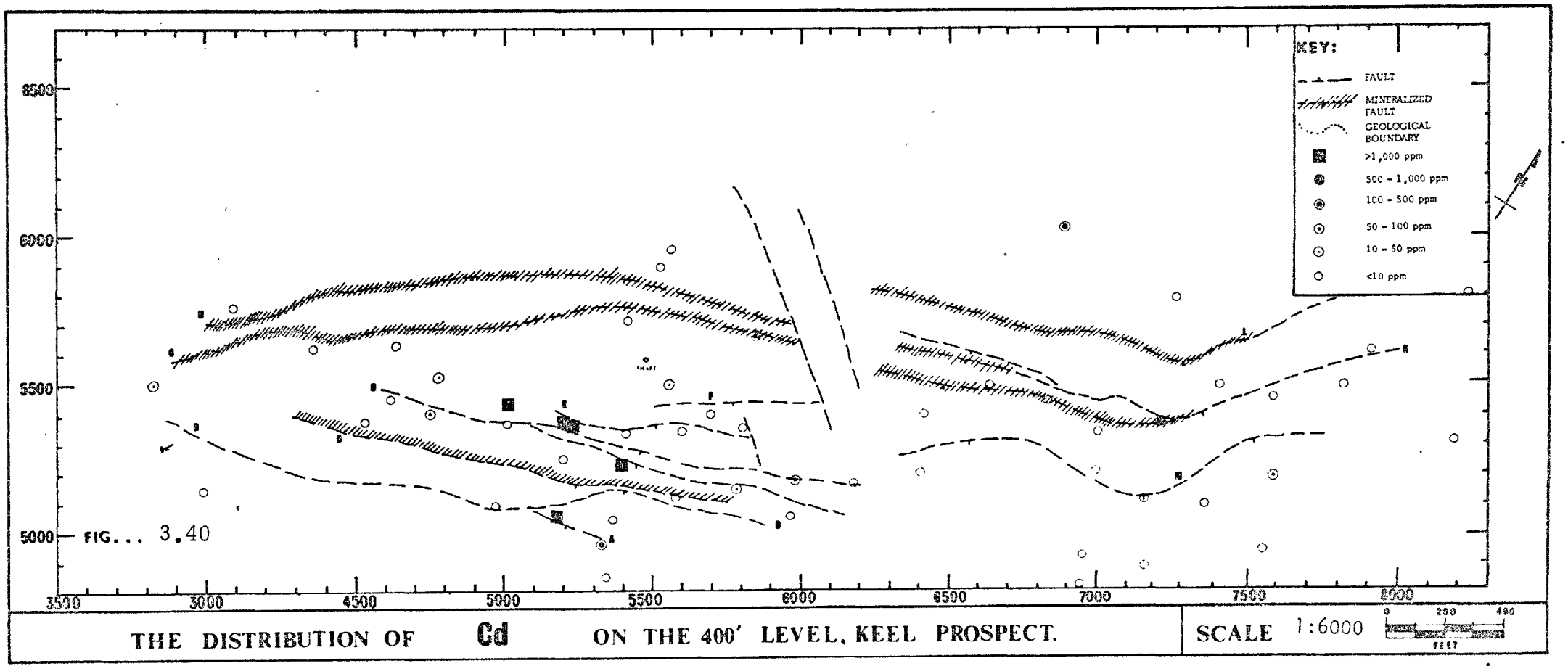


FIG... 3.40

THE DISTRIBUTION OF Cd ON THE 400' LEVEL, KEEL PROSPECT.

SCALE 1:6000

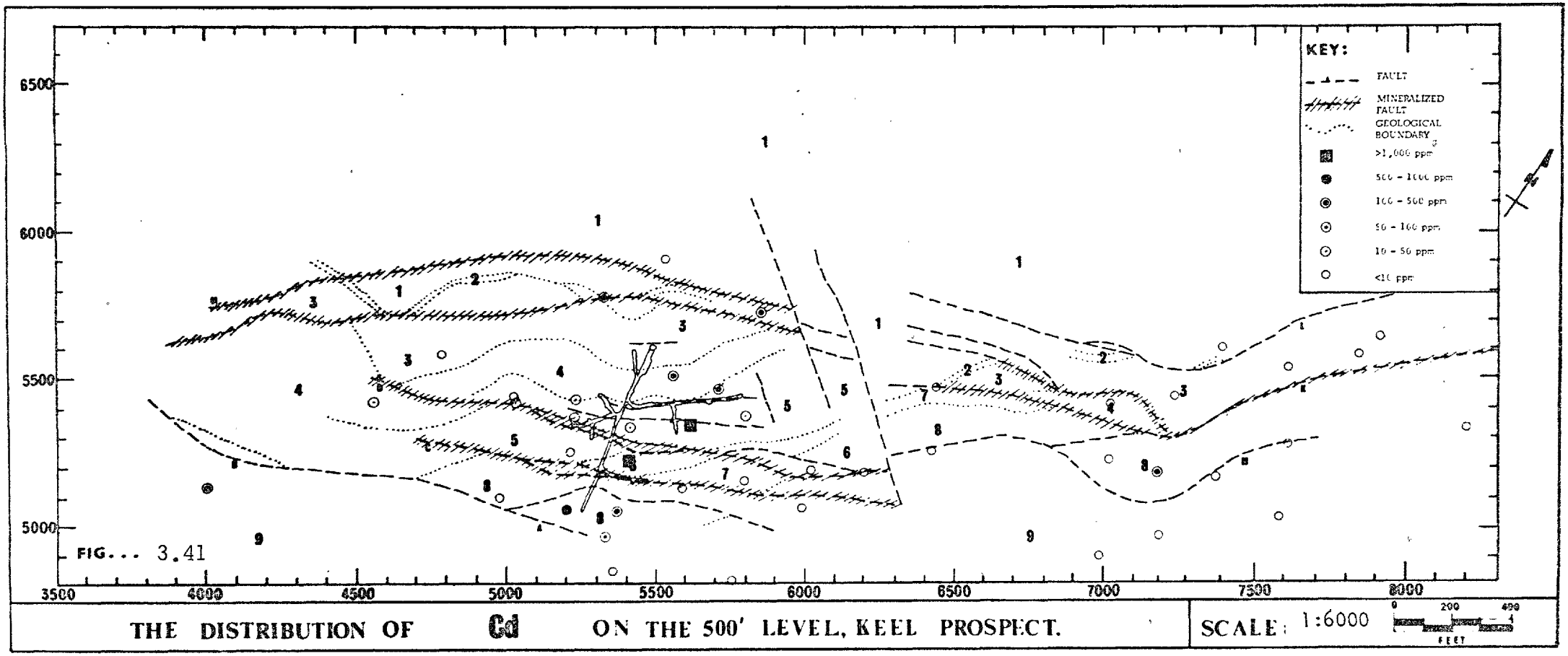
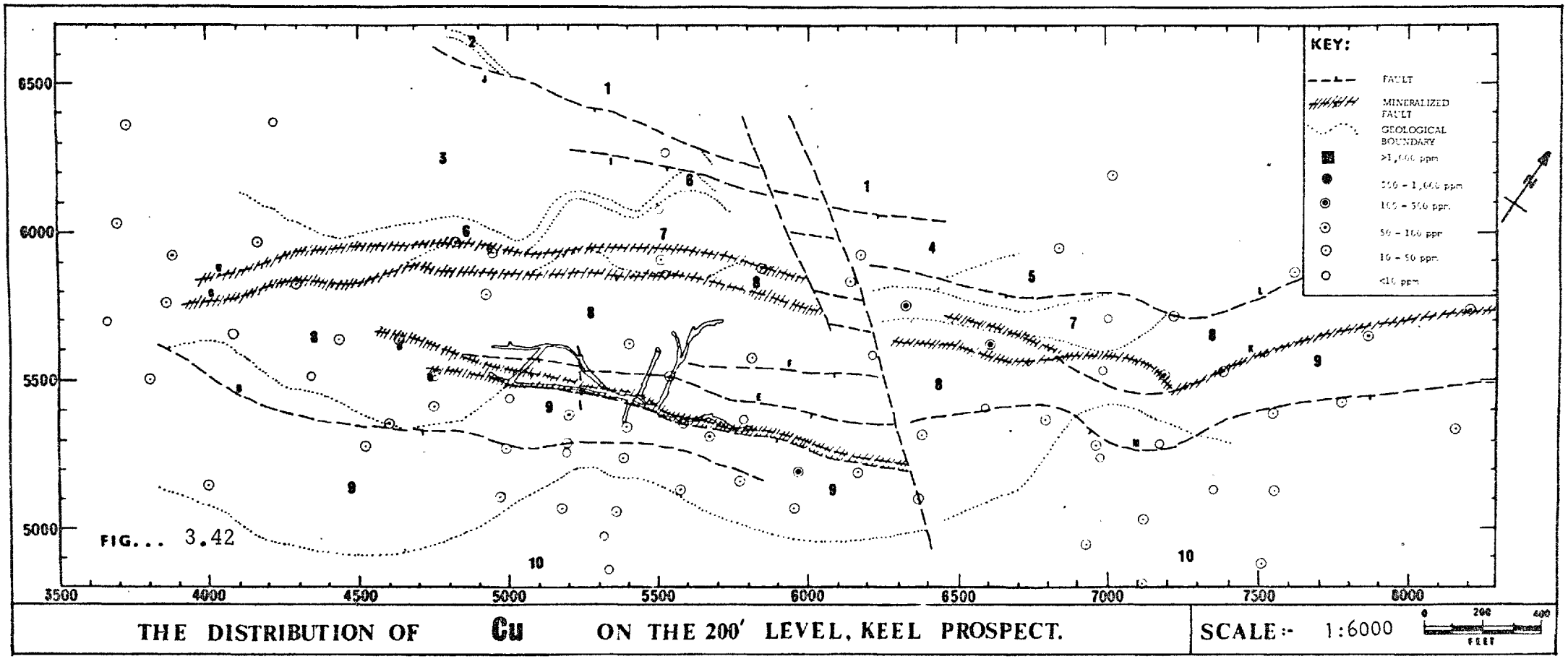


FIG... 3.41

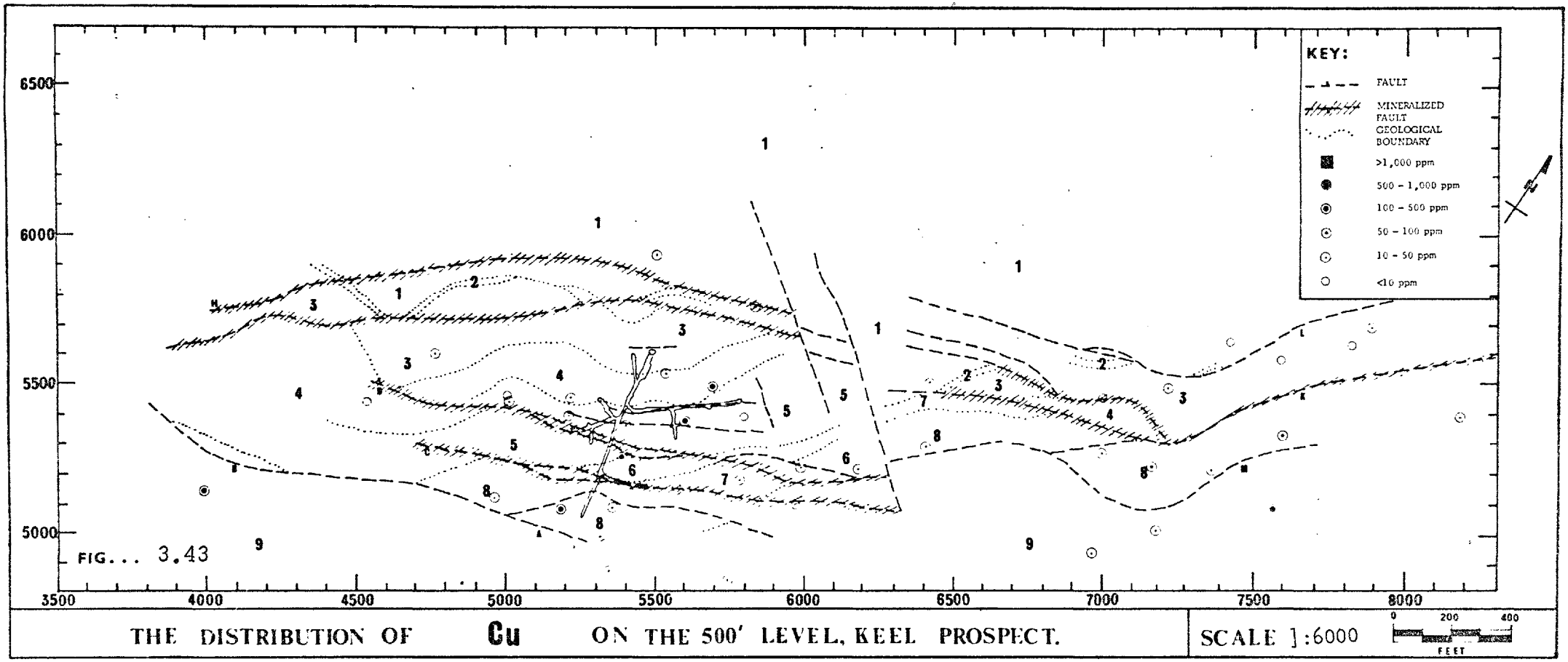
THE DISTRIBUTION OF Cd ON THE 500' LEVEL, KEEL PROSPECT.

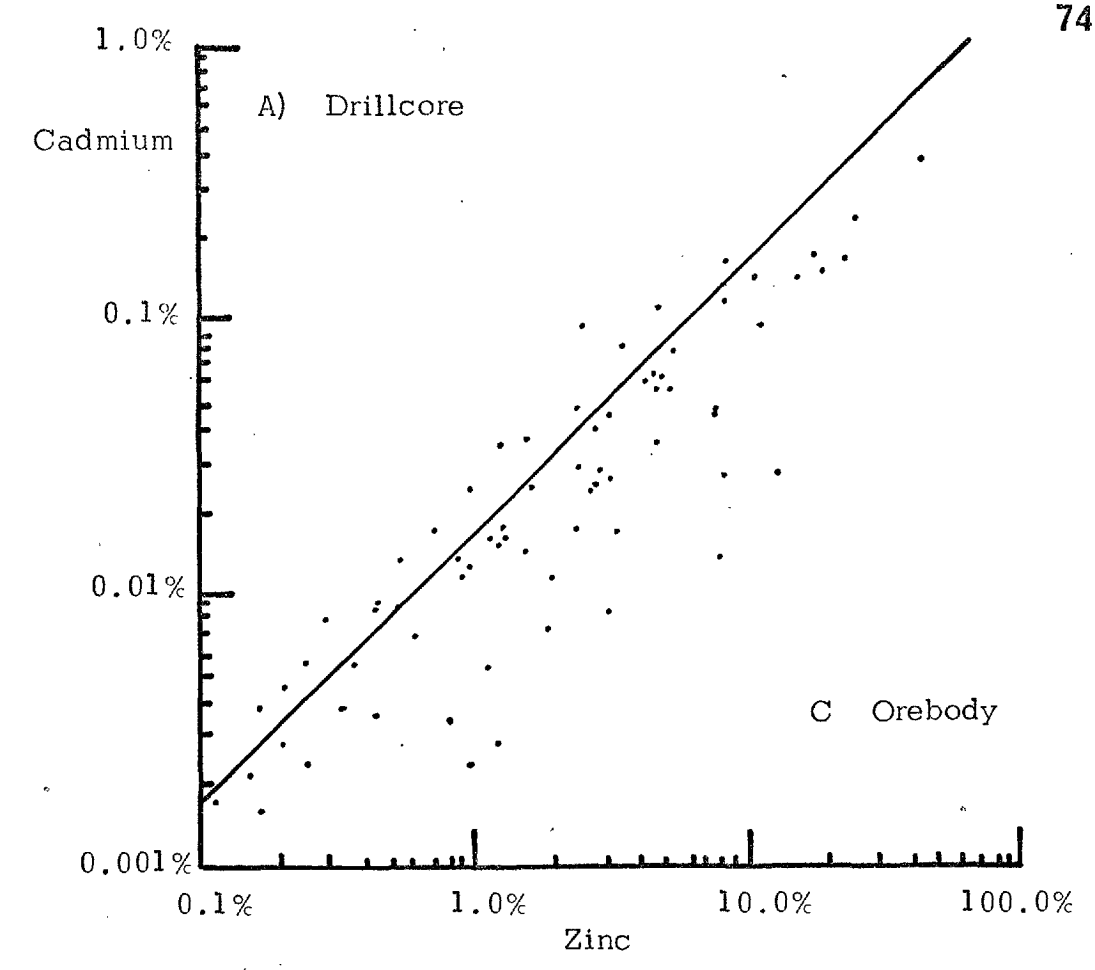
SCALE: 1:6000



THE DISTRIBUTION OF **Cu** ON THE 200' LEVEL, KEEL PROSPECT.

SCALE:- 1:6000


KEY:
FAULT
MINERALIZED FAULT
GEOLOGICAL BOUNDARY
>1,000 ppm
500 - 1,000 ppm
100 - 500 ppm
50 - 100 ppm
10 - 50 ppm
<10 ppm
6500
6000
5500
5000
3500
4000
4500
5000
5500
6000
6500
7000
7500
8000
FIG... 3.43
THE DISTRIBUTION OF Cu ON THE 500' LEVEL, KEEL PROSPECT.
SCALE 1:6000
0
200
400
FEET



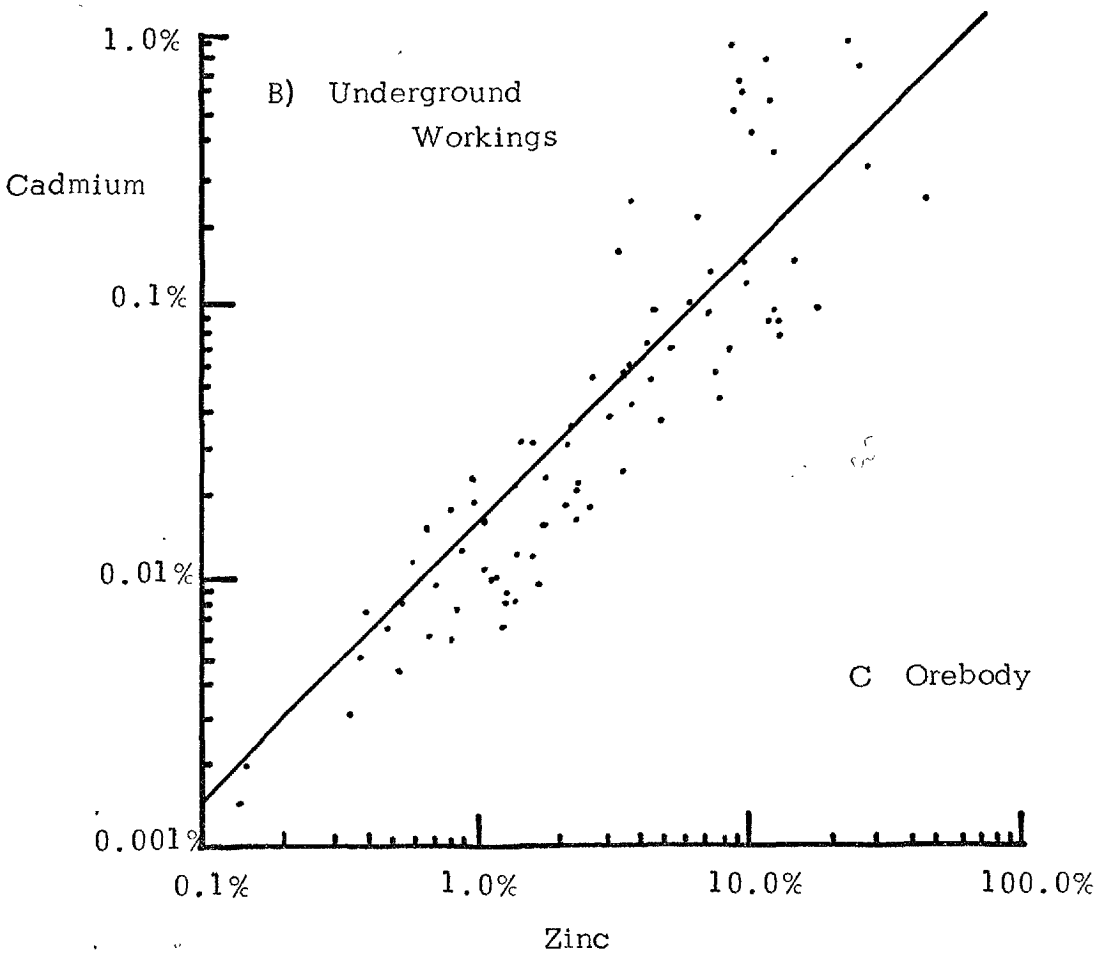
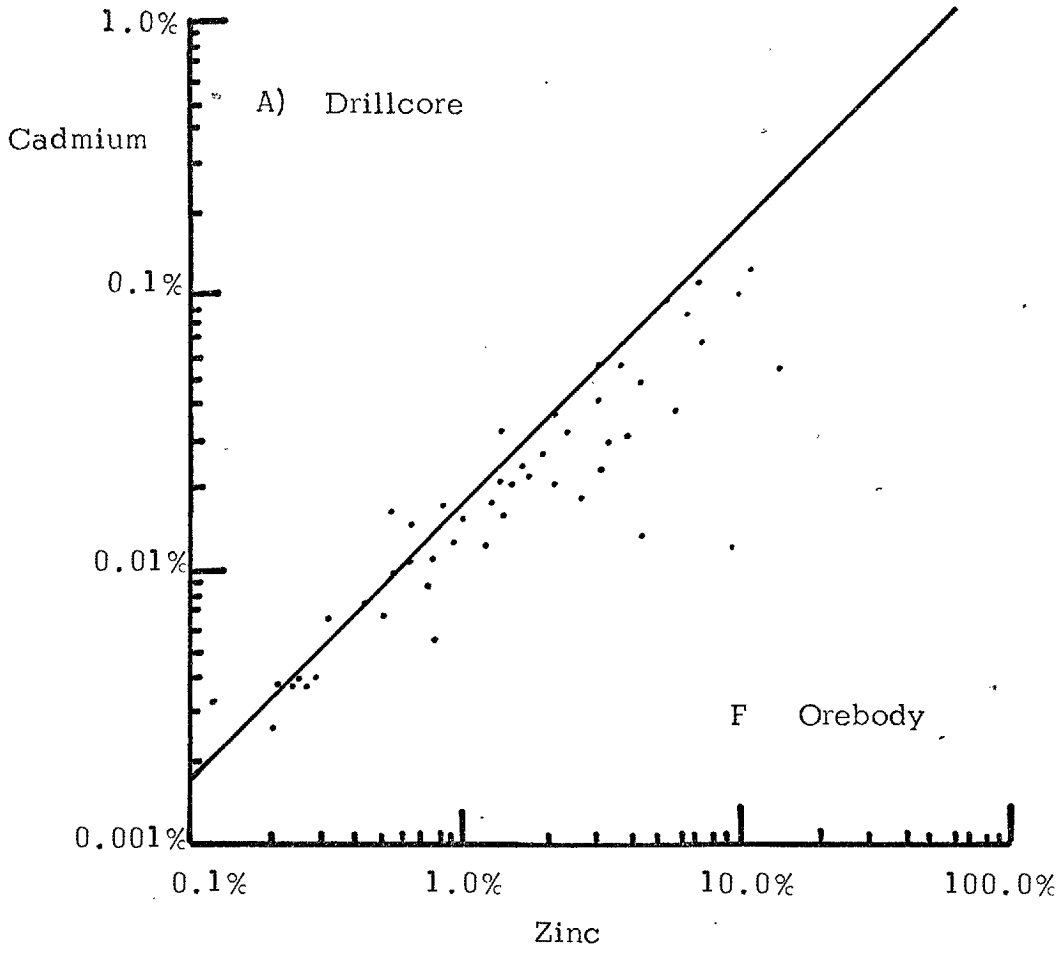


FIG... 3.44 A Comparison of Cadmium and Zinc in Rock Material from Drillcore and Underground



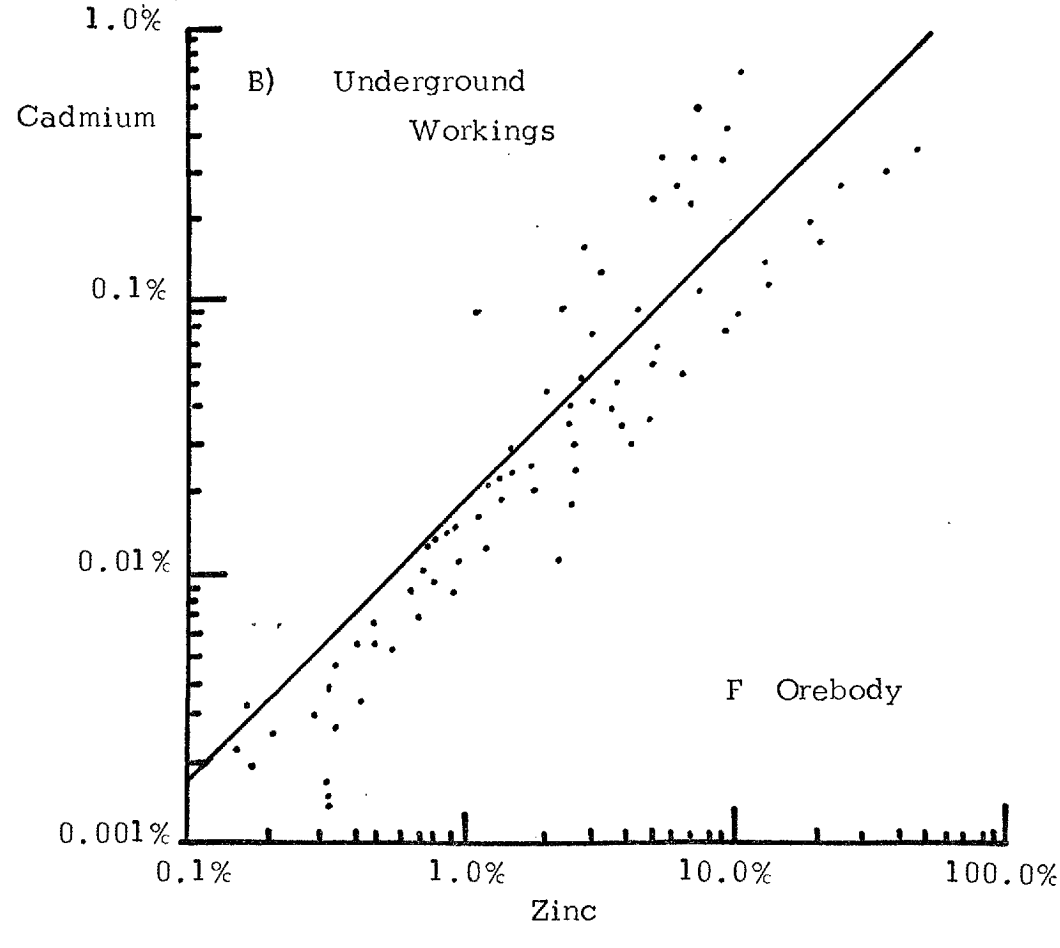


FIG... 3.45

A Comparison of Cadmium and Zinc in Rock Material from Drillcore and Underground Workings

separated and analysed they contain a maximum of 2% cadmium for 62% zinc and an average of approximately 1% cadmium. This indicated the presence of a cadmium phase in the wallrocks immediately surrounding mineralization and the possible existence of greenockite in the underground workings. A cadmium bloom on the C fault plane on the 200' level adds further weight to this conclusion.

Fig. 3.46. shows the vertical distribution of Cu, Pb, Zn and Mg down drillholes. K50 and K61. The high values of Zn and Pb are completely associated with the clastic lithologies. This being especially apparent in drillhole K61. and mercury too shows high values in the clastic sediments although in K50 very high concentrations of mercury occur at the base of the bioclastic dolomite with only minor lead and zinc concentrations. Copper attains only minor importance. The relationship between zinc and lead is seen in these diagrams to be both sympathetic and antipathetic. This point is an example of the complex trace element associations that exist throughout this prospect area.

3.3E. SILVER

The association of zinc and silver is apparent in Fig. 3.47b, however, in Fig. 3.47a when the same diagram is drawn using drillcore material the relationship breaks down. The far superior correlation of zinc with silver in samples from the underground workings is discussed in detail in Chapter 4.

Patterson states that the majority of the silver in the Keel sphalerite is held in solid solution inside minute inclusions of tetrahedrite. The theoretical formula of tetrahedrite is $R_{3-4}Sb_{1-1.5}S_4$ where R is (Cu, Ag, Fe, Zn). To test the possibility that the silver is contained predominantly in the

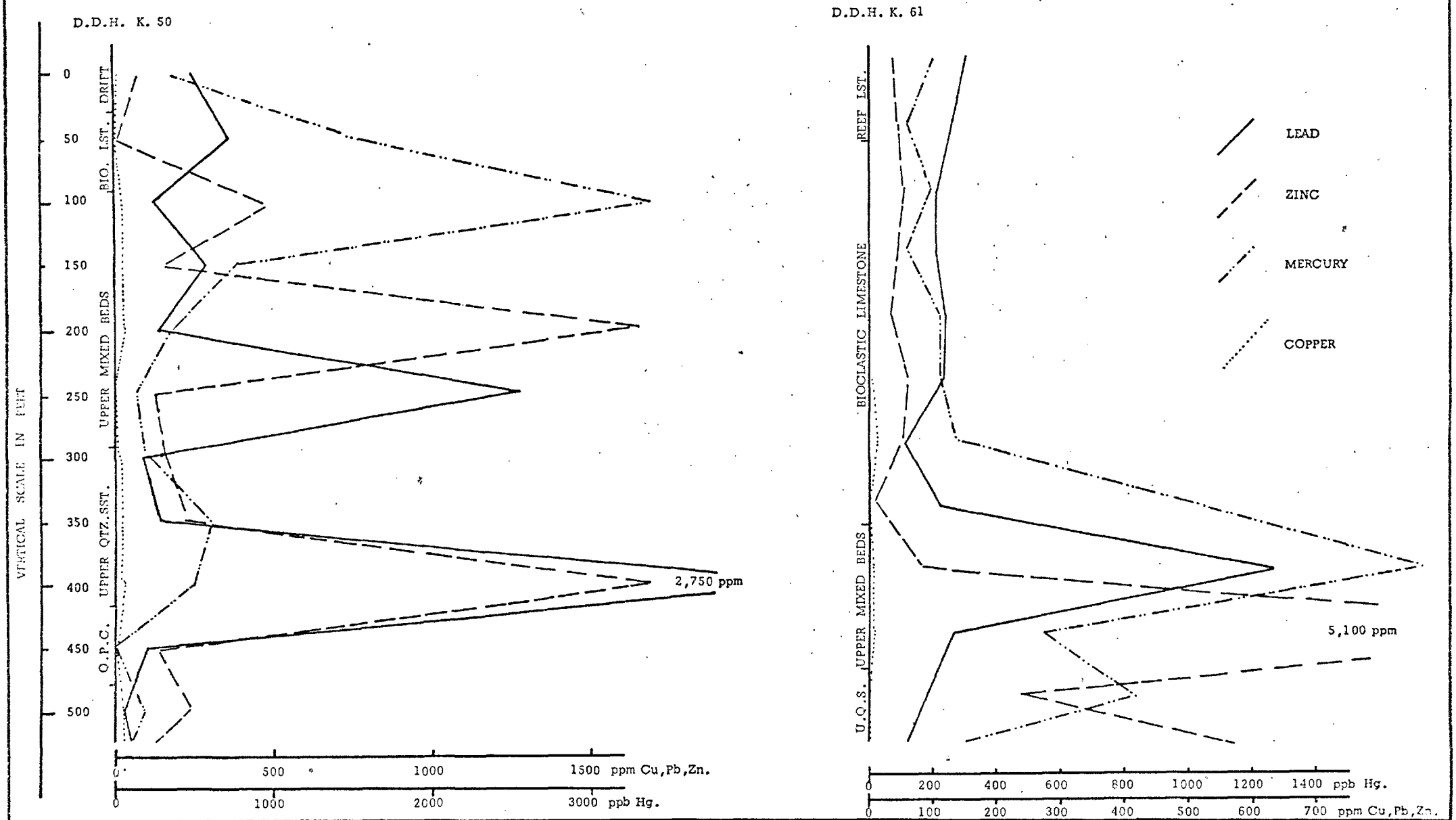
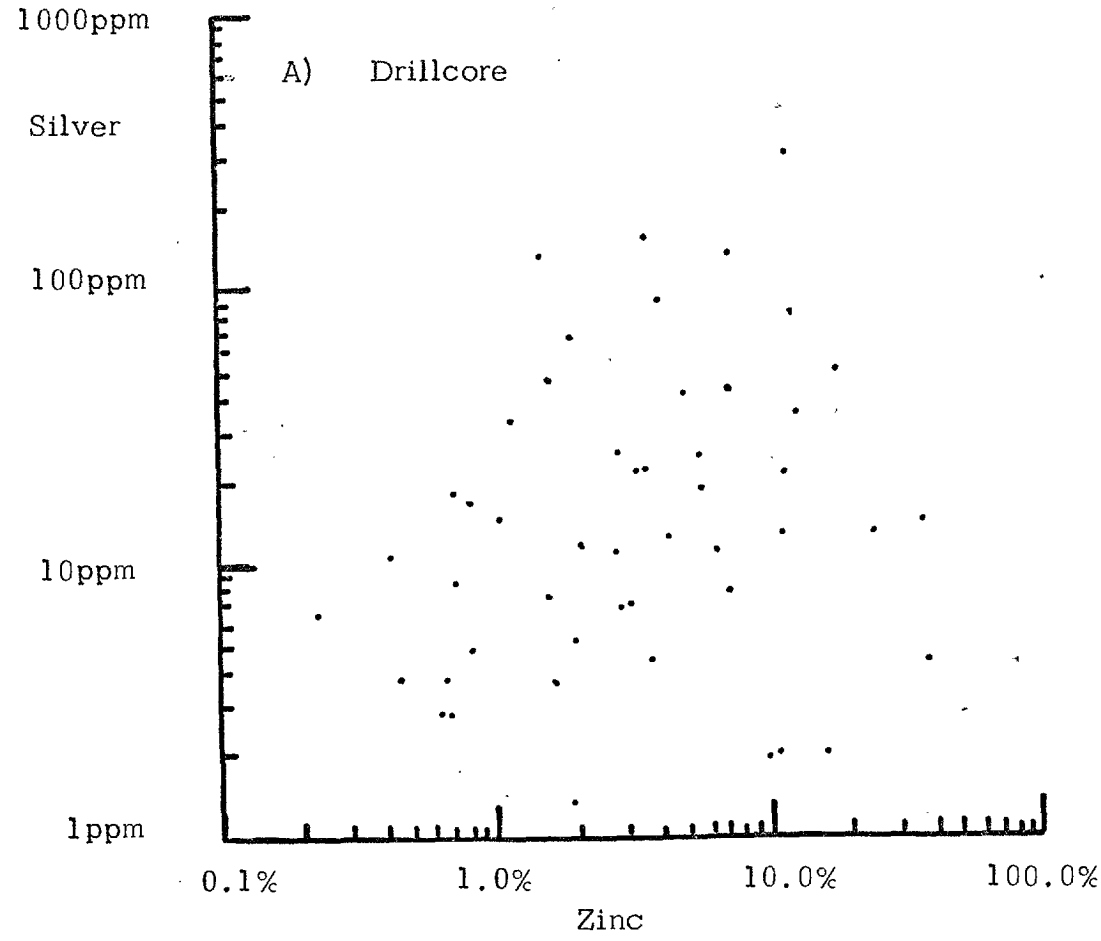


FIG . . . 3.46 BASE METAL DISTRIBUTION IN DRILLHOLES K50 & K61 KEEL IRELAND



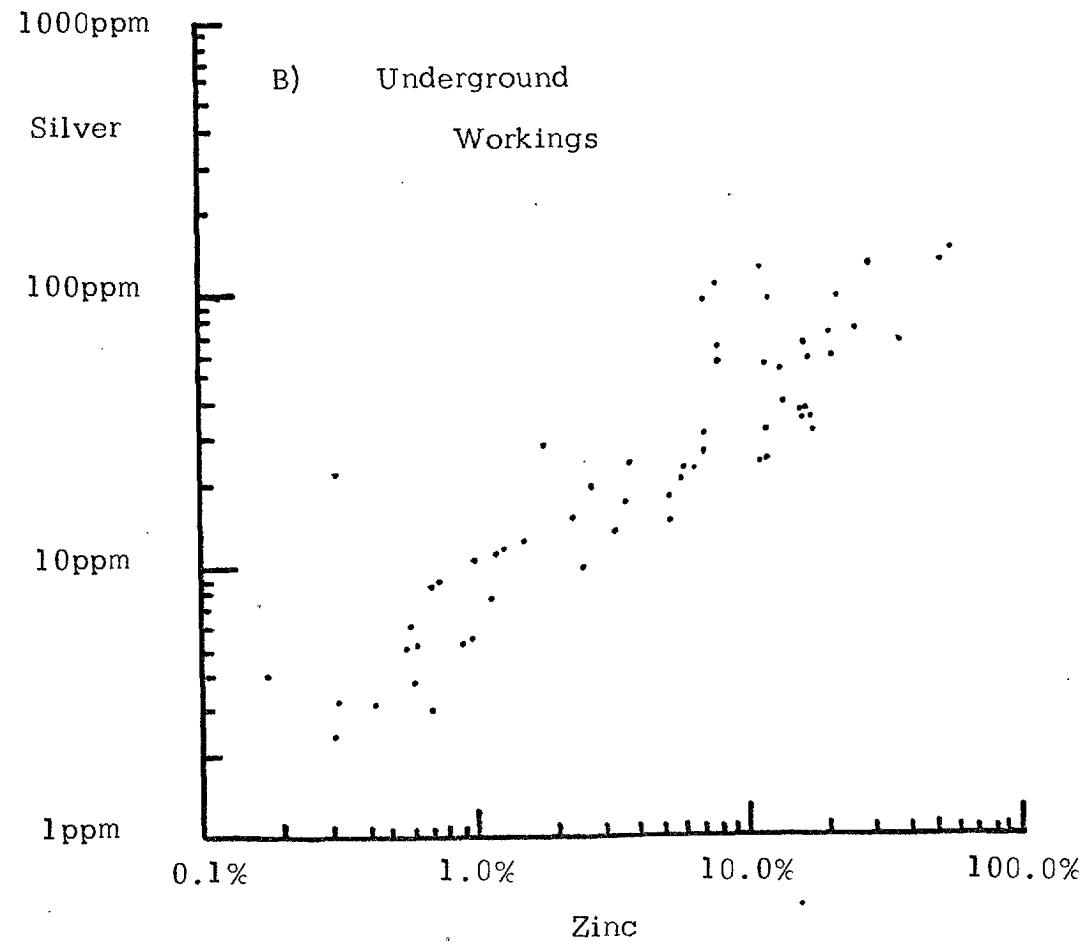


FIG... 3.47

A Comparison of Silver and Zinc in Rock Material from Drillcore and Underground Workings

tetrahedrite, antimony/silver relationships for 57 sphalerites were plotted, Fig. 3.48a. This figure to some extent confirms Patterson's opinion.

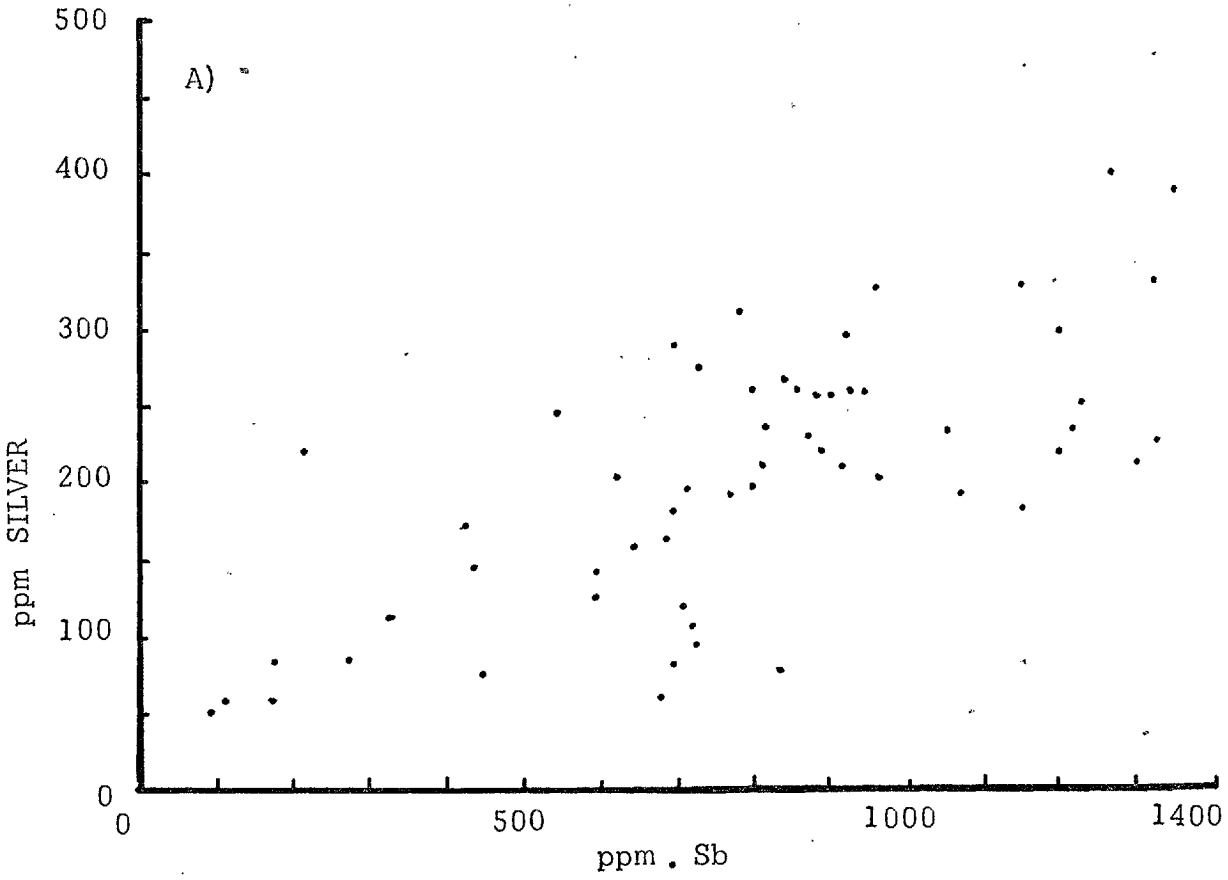
It is concluded that in the case of silver, it is known from mineral studies on selected samples, that the concentration in sphalerite is usually < 100 p p m and in the case of galena > 1000 p p m As no increase in correlation between zinc and silver in the drillcore material was found by plotting the $^{Pb}/_{Ag}$: Zn ratio, there must, as for mercury in Chapter 8, exist the possibility of compounds or complexes outside the area of high base metal build up, which have been removed and redeposited to give rise to the picture indicated in Fig. 3.47a.

The lead:silver relationship is shown in Fig. 3.48B and from this no readily discernible association is present.

3.3F. MERCURY

The distribution of mercury in the primary environment has been discussed at length in the literature. It has been suggested that in permeable rocks such as sandstone and limestone or dolomite, mercury can move rather great distances from its source as a vapour or soluble mercuric chloride (Hawkes and Webb, 1962). It would therefore be reasonable to expect a broad halo of dispersed mercury in wallrocks of lead and zinc ores in these environments. On the basis of this hypothesis it could be assumed that the shape of the resulting mercury anomaly will depend upon such physical characteristics of the rocks as fracturing, faulting and permeability.

Initial studies on the analysis of mercury in the Keel rocks have been described at the beginning of this chapter. Fig. 3.49 shows vertical sections down drillholes K50 and K61 and the effect of fraction size on mercury content. This should be compared with Fig. 4.23 for the



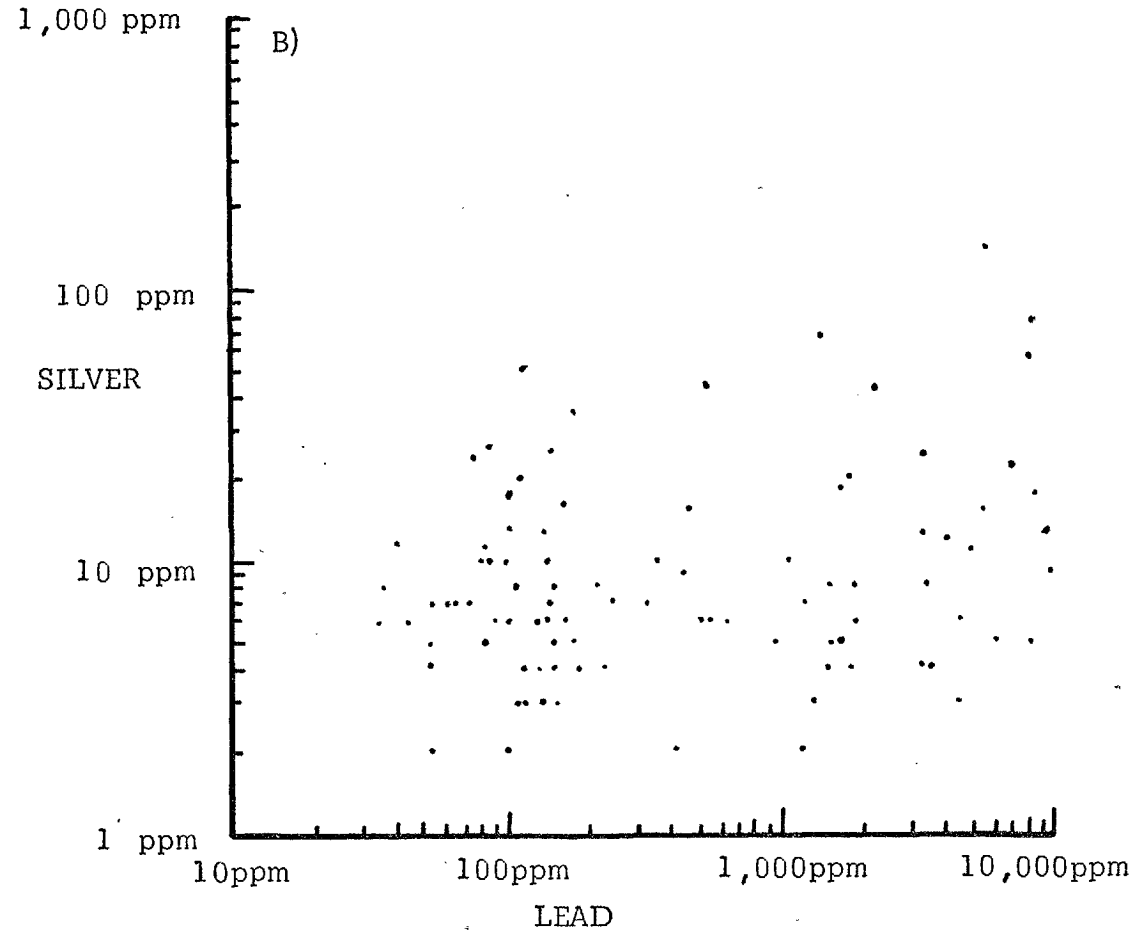


FIG ... 3.48

DIAGRAM ILLUSTRATING Sb/Ag RELATIONSHIP IN SPHALERITE & Pb/Ag RELATIONSHIP IN DRILLCORE

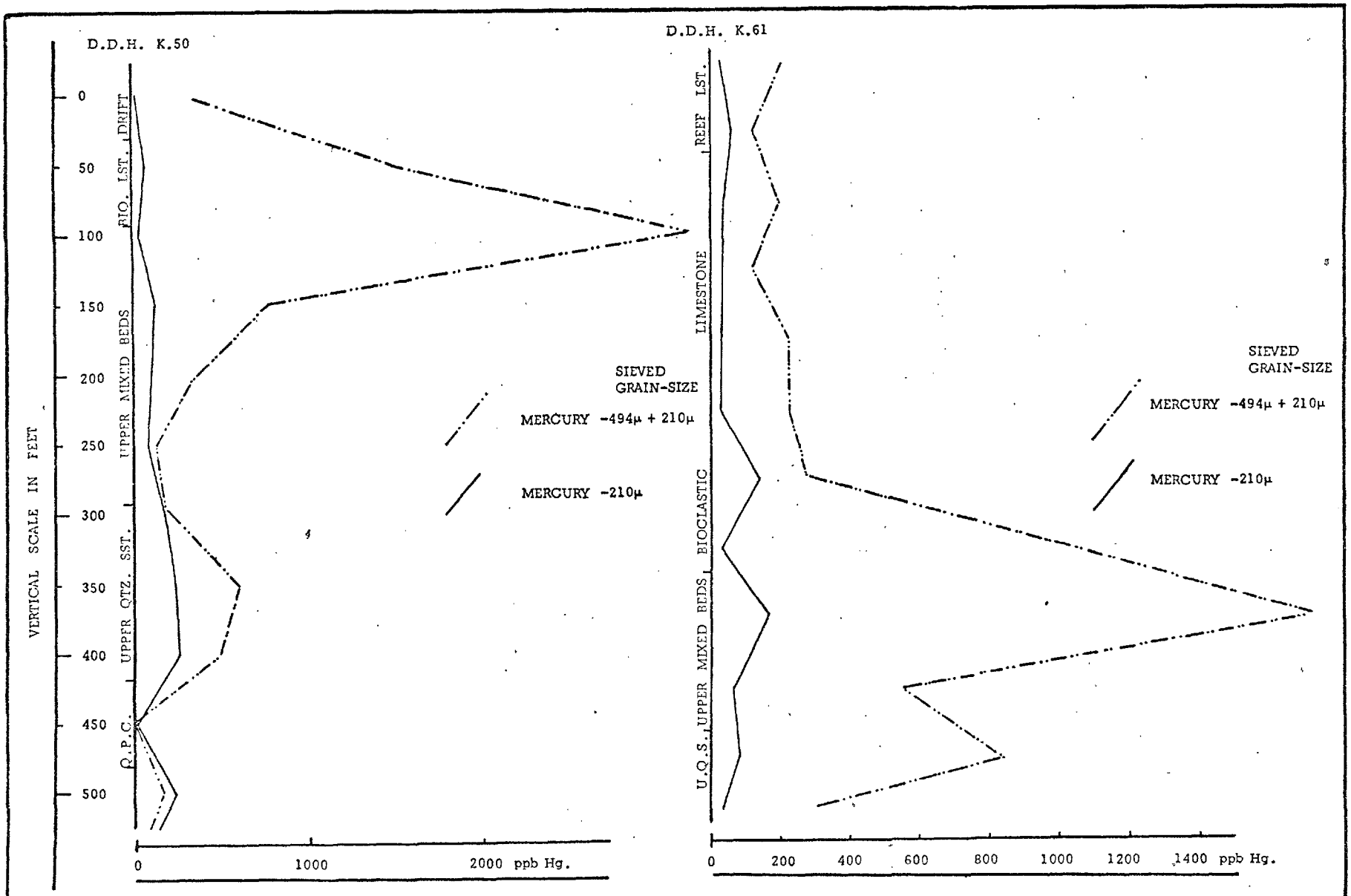


FIG... 3.49 VARIATION IN MERCURY CONTENT OF DRILLCORE WITH PARTICLE SIZE

corresponding effect of fraction size on rocks from the underground workings of the prospect. The initial investigation has led to the use of the - 494 μ + 210 μ fraction in mercury analysis.

The initial mercury analyses were carried out by Barringer Research Ltd. in Toronto. Duplicate analyses gave the following information on the precision of the method. Table 3.2.

From these results it must be concluded that no importance can be placed on the accuracy of the analyses or on any inter-element relationships.

Total mercury analyses have been used to compile Figs. 3.50 - 3.54. Here there can be seen to be only a vague relationship of mercury and the proximity of ore. Fig. 3.55 shows Zn:Hg in drill core and underground workings and Fig. 3.46., the relationship of total mercury to base metal mineralization down drill holes K.50 and K.61 and here again there is absolutely no specific relationship of mercury to lead and zinc, both sympathetic and antipathetic associations being shown.

Figs. 3.56 - 3.62 give combined histogram interpretations of Mn, Zn, Cd, Fe, Pb and Hg on each of the five level elevations at Keel. From these there can be seen to be no marked zonation in metal distribution either, although they do help to clarify the element relationships discussed in the text.

It is impossible to say at Keel that there is any wide primary dispersion associated with the base metal build up of the area; nor is there any broad primary dispersion halo of total mercury around the deposit. The investigation has led to the conclusion that dispersion patterns of any major significance do not exist.

TABLE ... 3.2

COMPARISON OF DUPLICATE MERCURY ANALYSES .

SAMPLENUMBER	FIRST RESULT	SECOND RESULT	% DIFFERENCE
CK 1	945	200	- 80
CK 2	665	1300	+ 97
CK 3	6550	2405	- 63
CK 4	6400	3325	- 48
CK 5	665	1605	+ 141
CK 6	485	360	- 26
CK 7	4850	2208	- 54
CK 8	5000	2880	- 42
CK 9	4550	2585	- 43
CK 10	6550	9725	+ 48
CK 11	6000	5625	- 6
CK 12	190	220	+ 16
CK 13	320	432	+ 35
CK 14	450	240	- 47
CK 15	235	1345	+ 472
CK 16	1576	2695	+ 71
CK 17	6025	11525	+ 91
CK 18	300	395	+ 32
CK 19	6150	750	- 88

Results expressed in parts per billion .

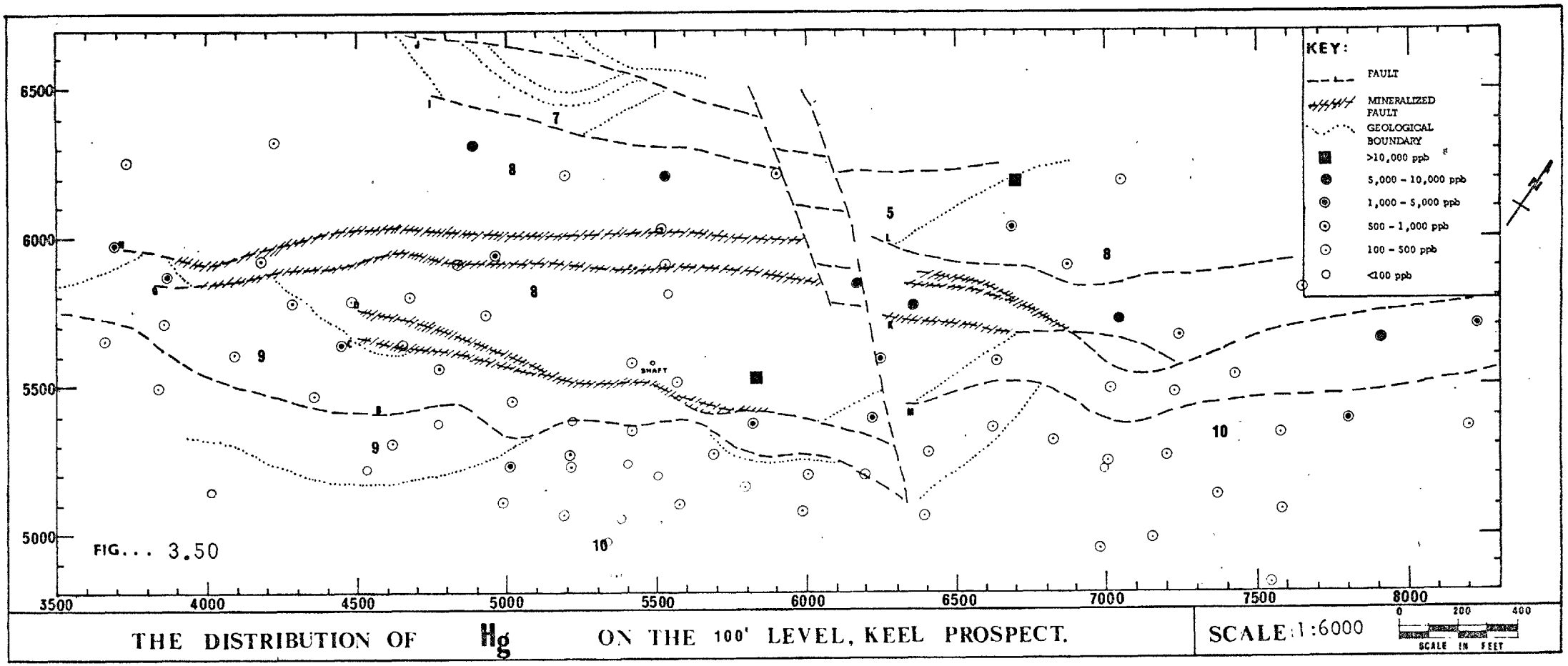
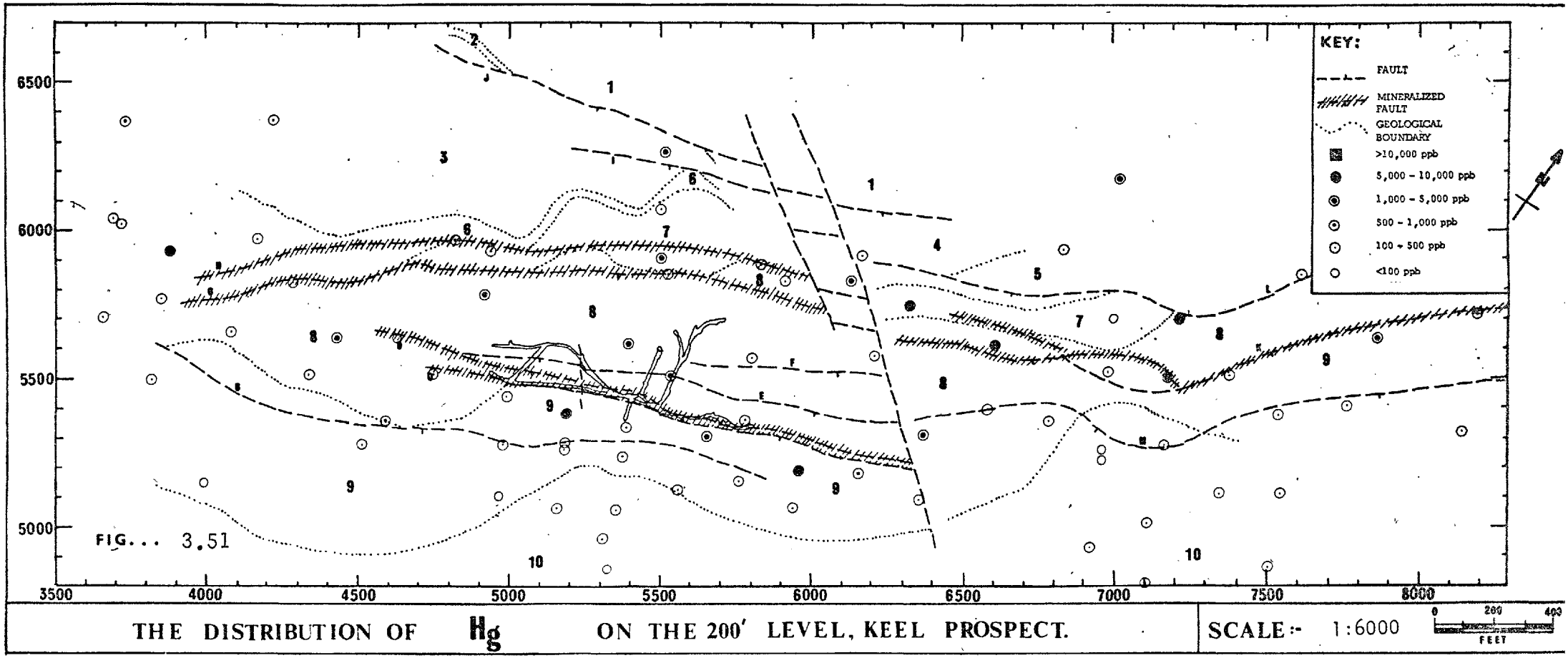
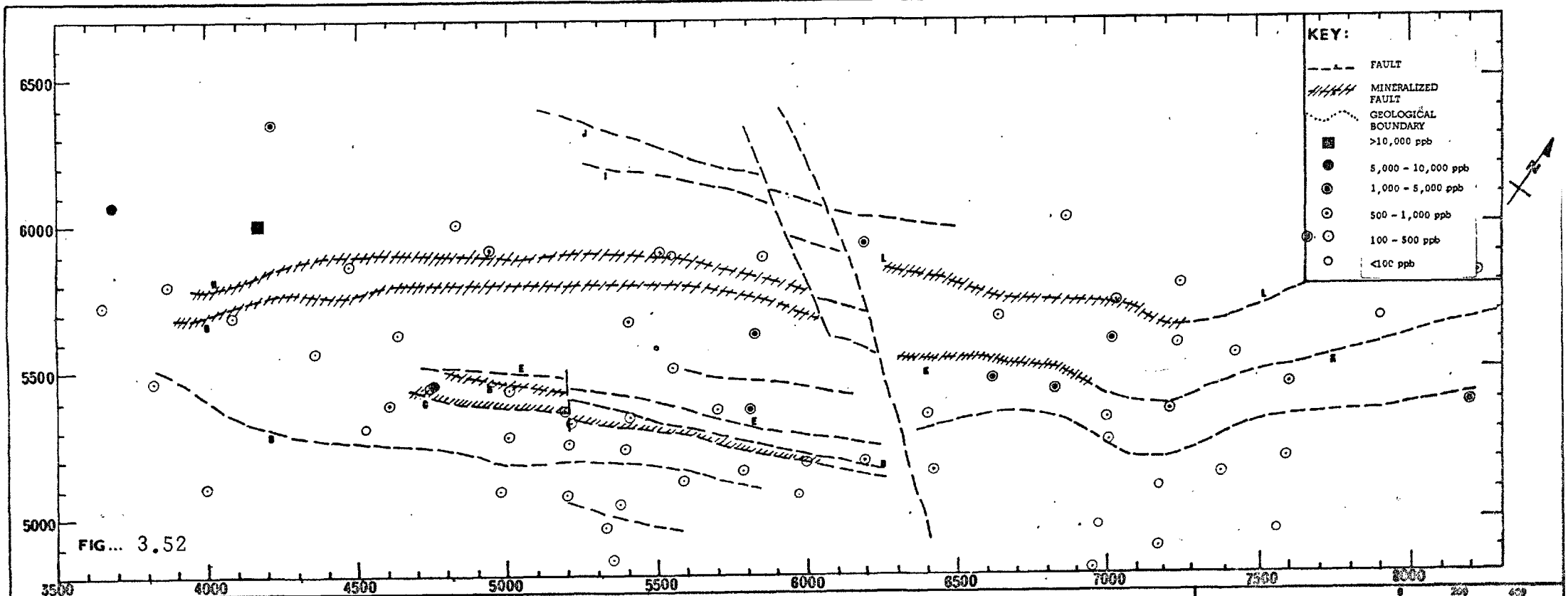


FIG... 3.50

THE DISTRIBUTION OF Hg ON THE 100' LEVEL, KEEL PROSPECT.

SCALE 1:6000


KEY:
FAULT
MINERALIZED FAULT
GEOLOGICAL BOUNDARY
>10,000 ppb
5,000 - 10,000 ppb
1,000 - 5,000 ppb
500 - 1,000 ppb
100 - 500 ppb
<100 ppb
6500
6000
5500
5000
3500
4000
4500
5000
5500
6000
6500
7000
7500
8000
FIG... 3.51
THE DISTRIBUTION OF Hg ON THE 200' LEVEL, KEEL PROSPECT.
SCALE:- 1:6000
0
200
400
FEET


KEY:
FAULT
MINERALIZED FAULT
GEOLOGICAL BOUNDARY
>10,000 ppb
5,000 - 10,000 ppb
1,000 - 5,000 ppb
500 - 1,000 ppb
100 - 500 ppb
<100 ppb
6500
6000
5500
5000
3500
4000
4500
5000
5500
6000
6500
7000
7500
8000
FIG... 3.52
THE DISTRIBUTION OF Hg ON THE 300' LEVEL, KEEL PROSPECT.
SCALE 1:6000
FEET

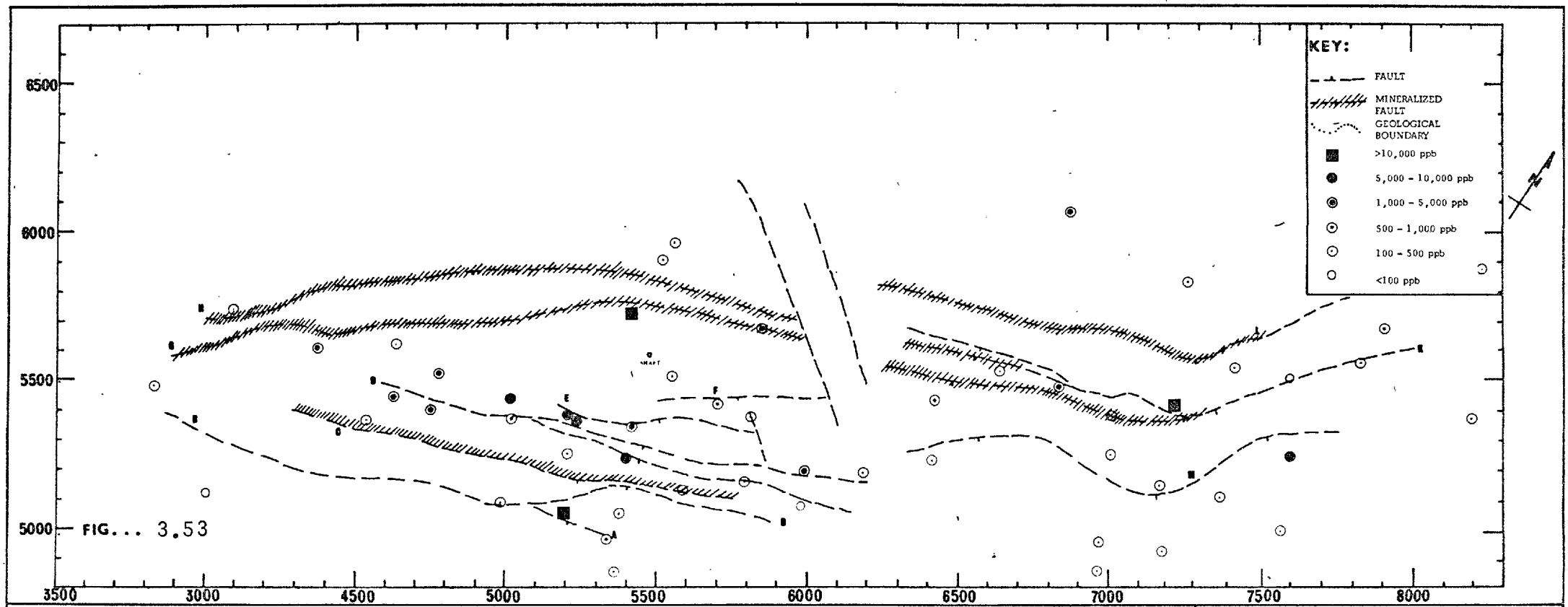


FIG... 3.53

THE DISTRIBUTION OF Hg ON THE 400' LEVEL, KEEL PROSPECT.

SCALE 1:6000

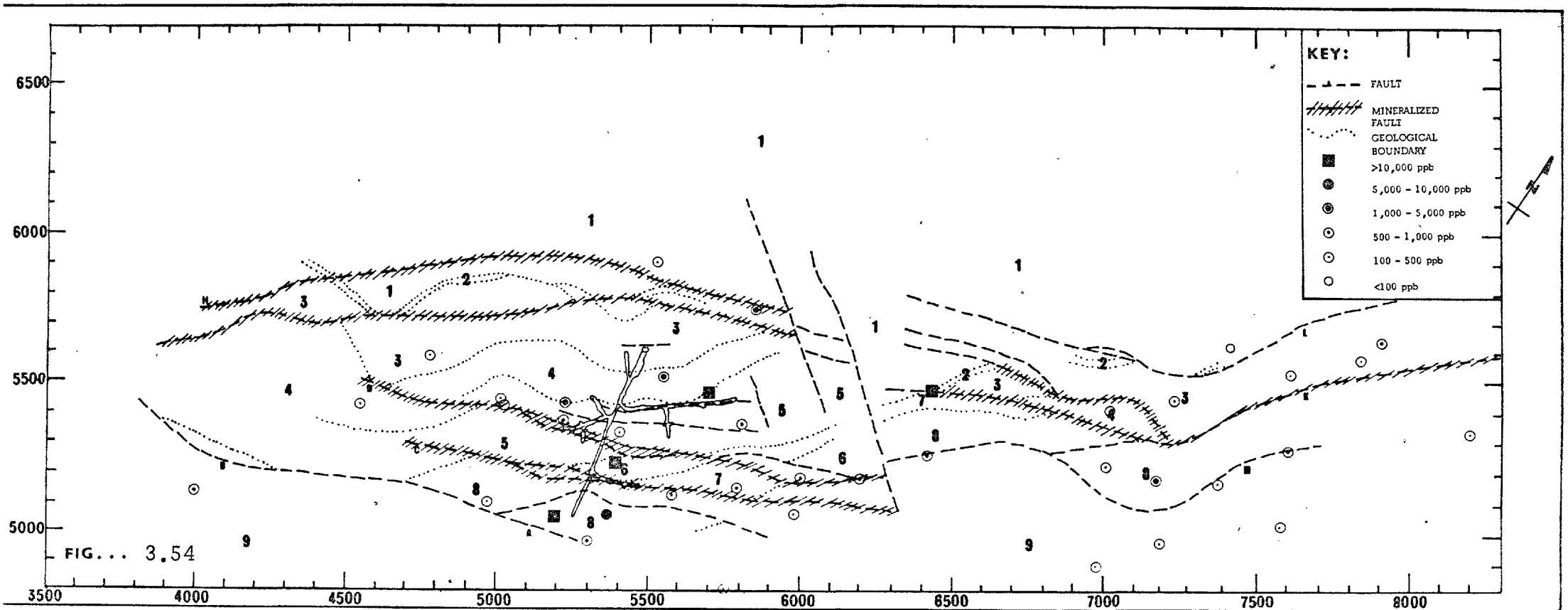
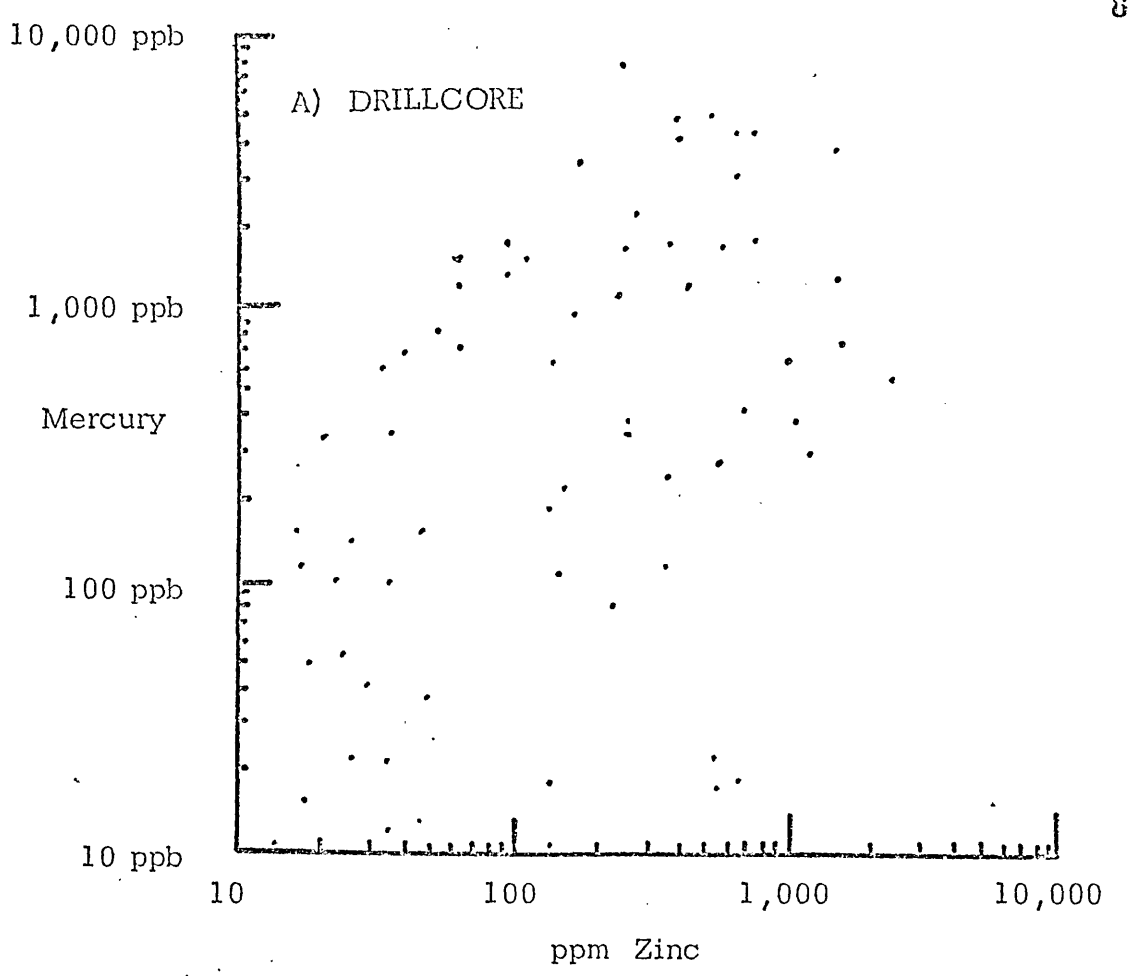


FIG... 3.54

THE DISTRIBUTION OF Hg ON THE 500' LEVEL, KEEL PROSPECT.

SCALE 1:6000 0 200 400 FEET



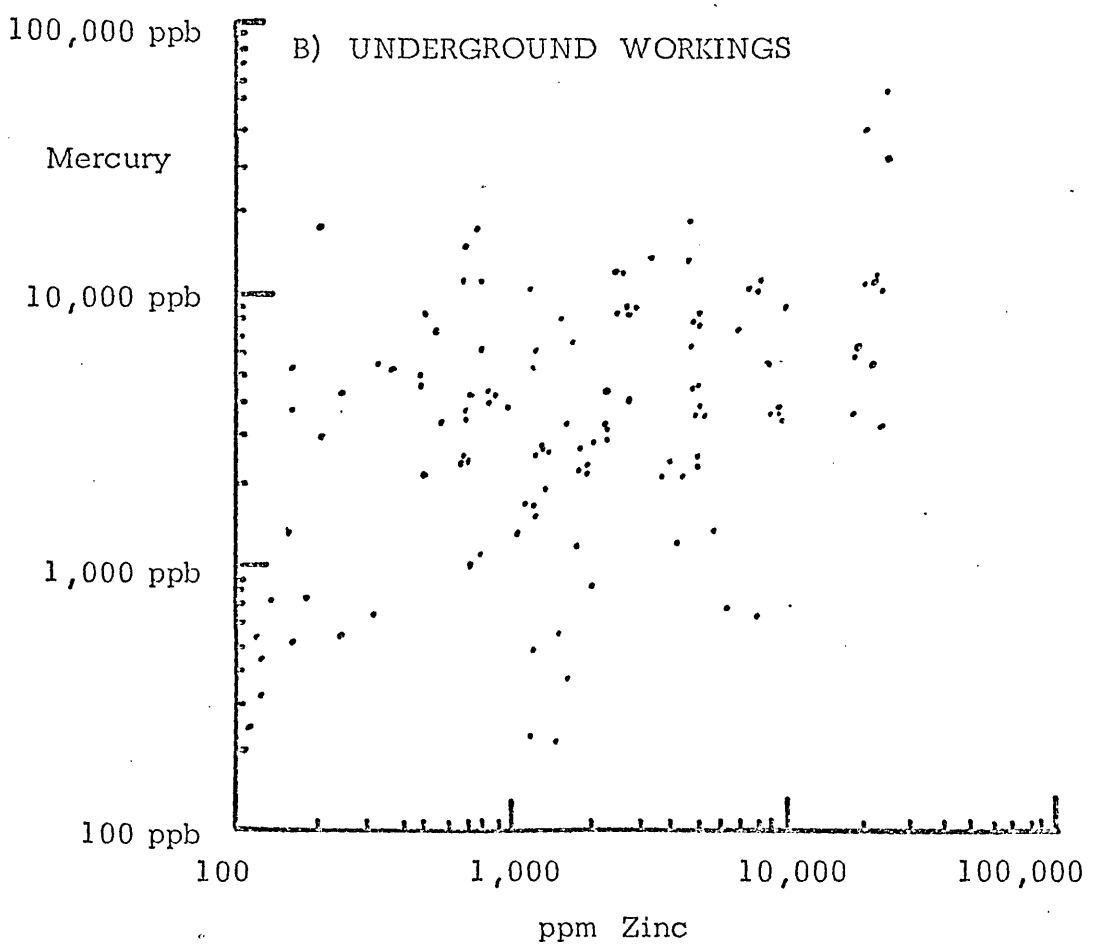


FIG ... 3.55 DIAGRAM ILLUSTRATING THE RELATIONSHIP BETWEEN MERCURY & ZINC IN MATERIAL FROM DRILLCORE & UNDERGROUND WORKINGS

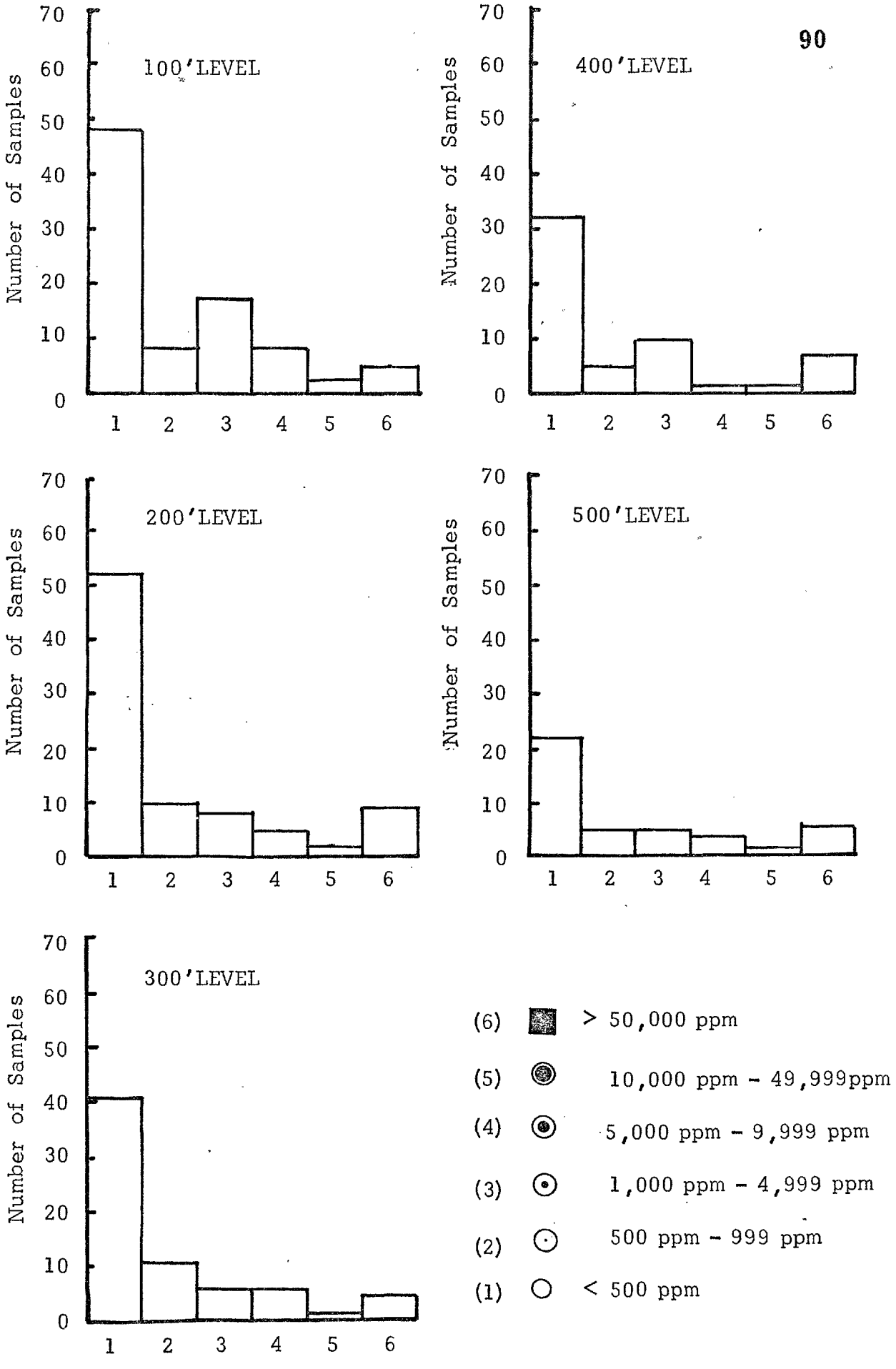


FIG ... 3.56 HISTOGRAM OF THE DISTRIBUTION OF ZINC ON FIVE LEVELS OF THE KEEL PROSPECT: (DRILLCORE SAMPLES ONLY)

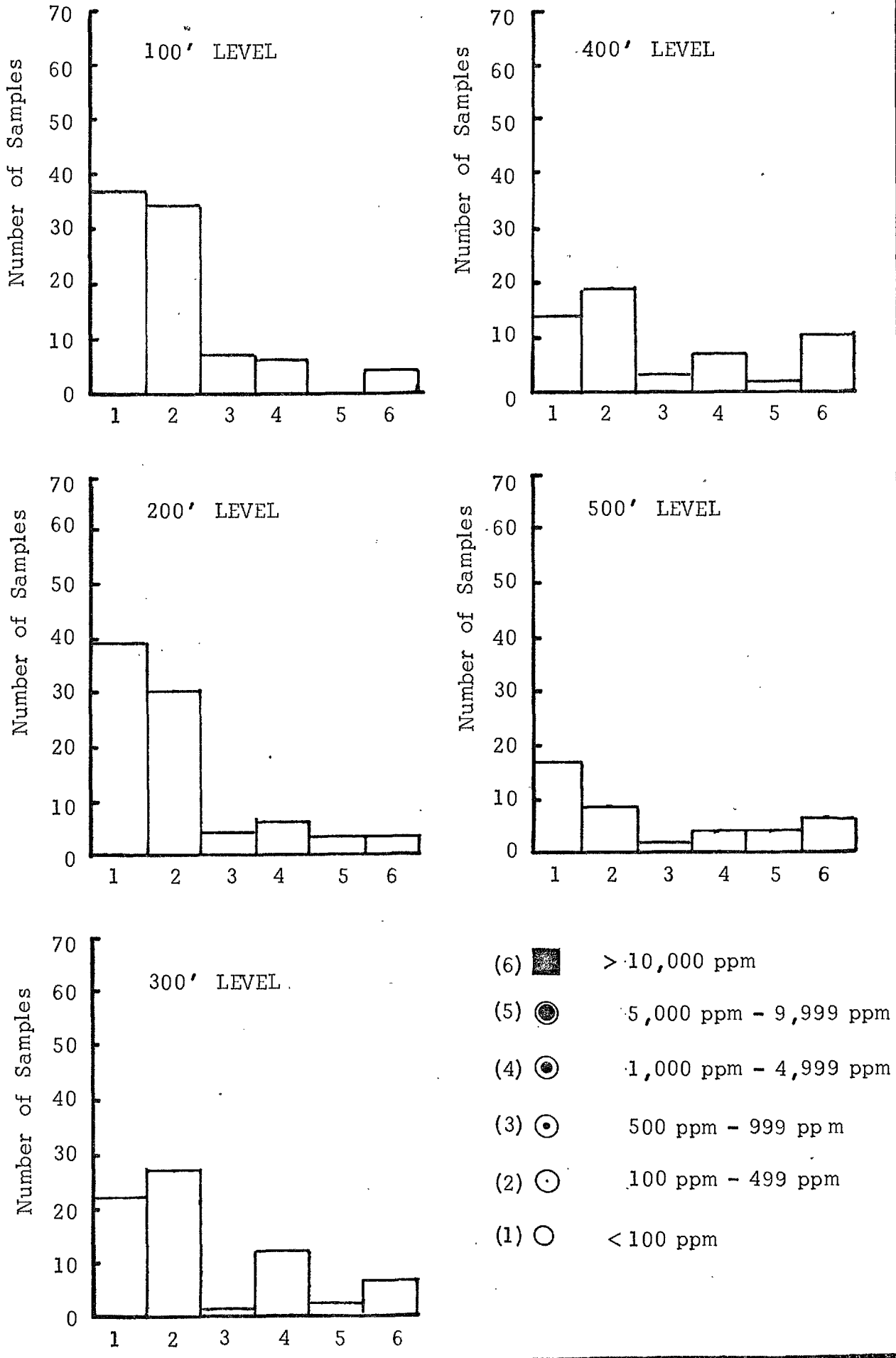


FIG ... 3.57

HISTOGRAM OF THE DISTRIBUTION OF LEAD ON FIVE LEVELS OF THE KEEL PROSPECT: (DRILLCORE SAMPLES ONLY)

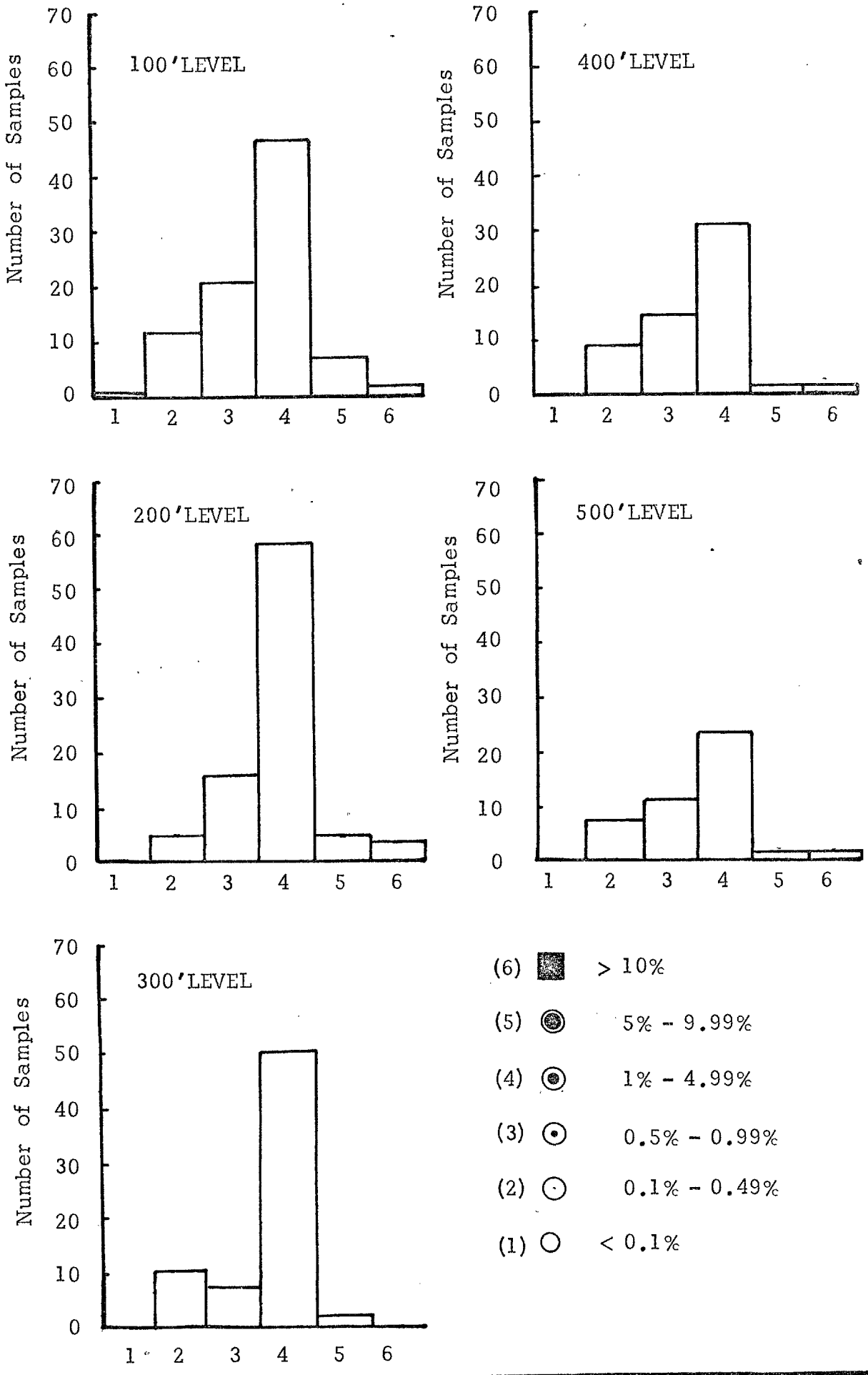


FIG ... 3.58

HISTOGRAM OF THE DISTRIBUTION OF IRON ON FIVE LEVELS OF THE KEEL PROSPECT: (DRILLCORE SAMPLES ONLY)

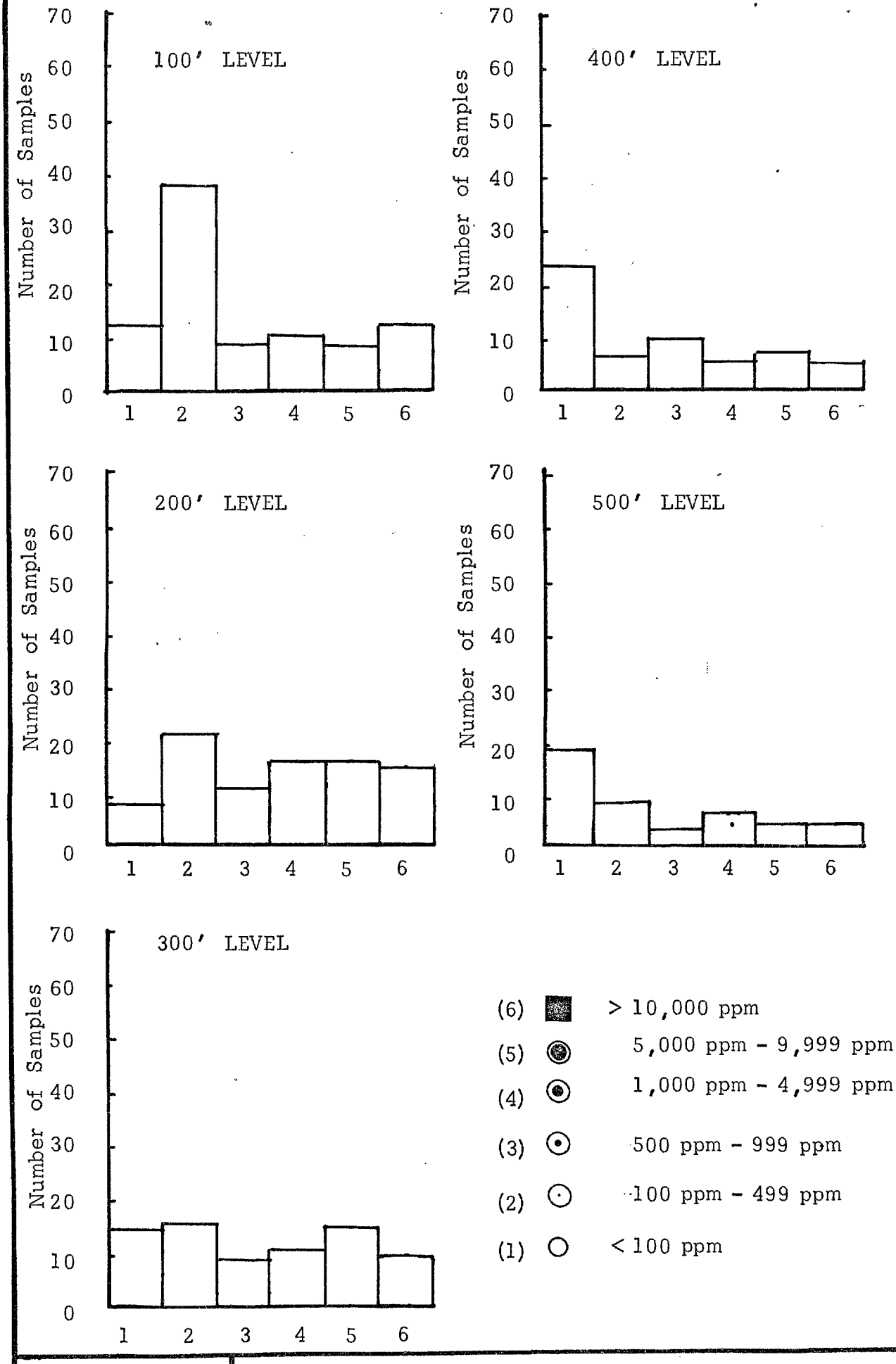


FIG ... 3.59

HISTOGRAM OF THE DISTRIBUTION OF MANGANESE ON FIVE LEVELS OF THE KEEL PROSPECT: (DRILLCORE SAMPLES ONLY)

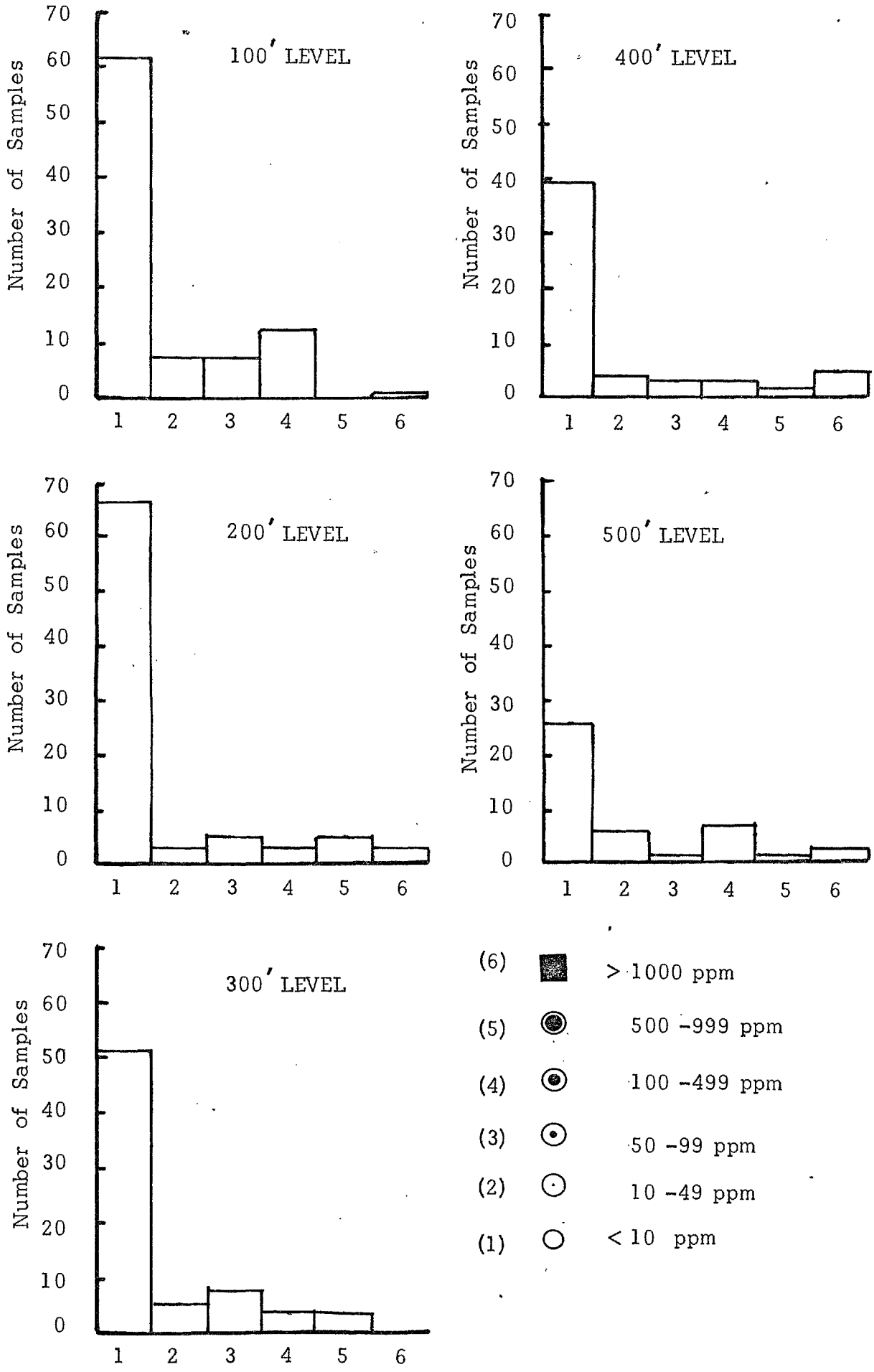


FIG ... 3.60

HISTOGRAM OF THE DISTRIBUTION OF CADMIUM ON FIVE LEVELS OF THE KEEL PROSPECT: (DRILLCORE SAMPLES ONLY)

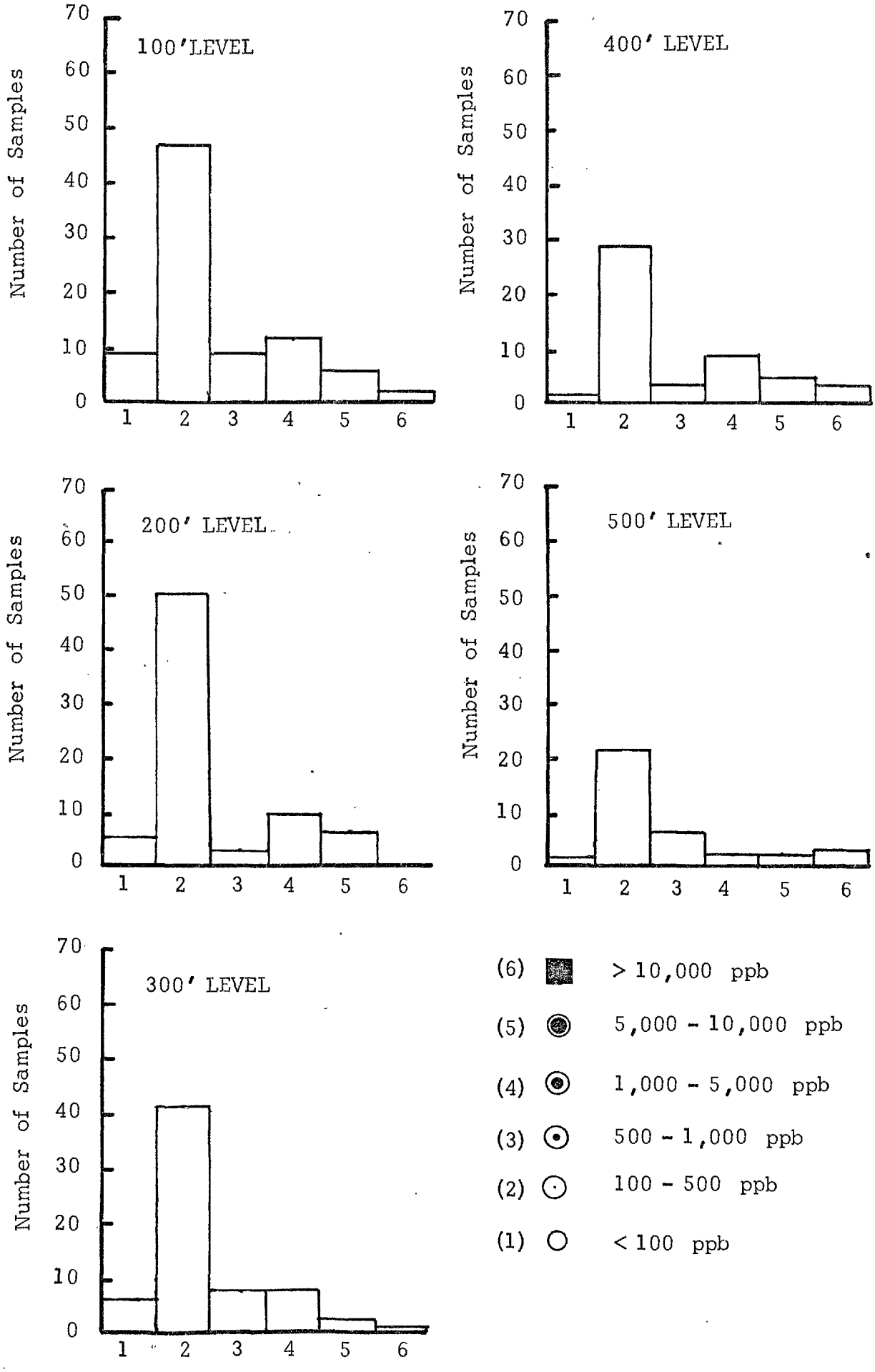


FIG ... 3.61 HISTOGRAM OF THE DISTRIBUTION OF MERCURY ON FIVE LEVELS OF THE KEEL PROSPECT (DRILLCORE SAMPLES ONLY)

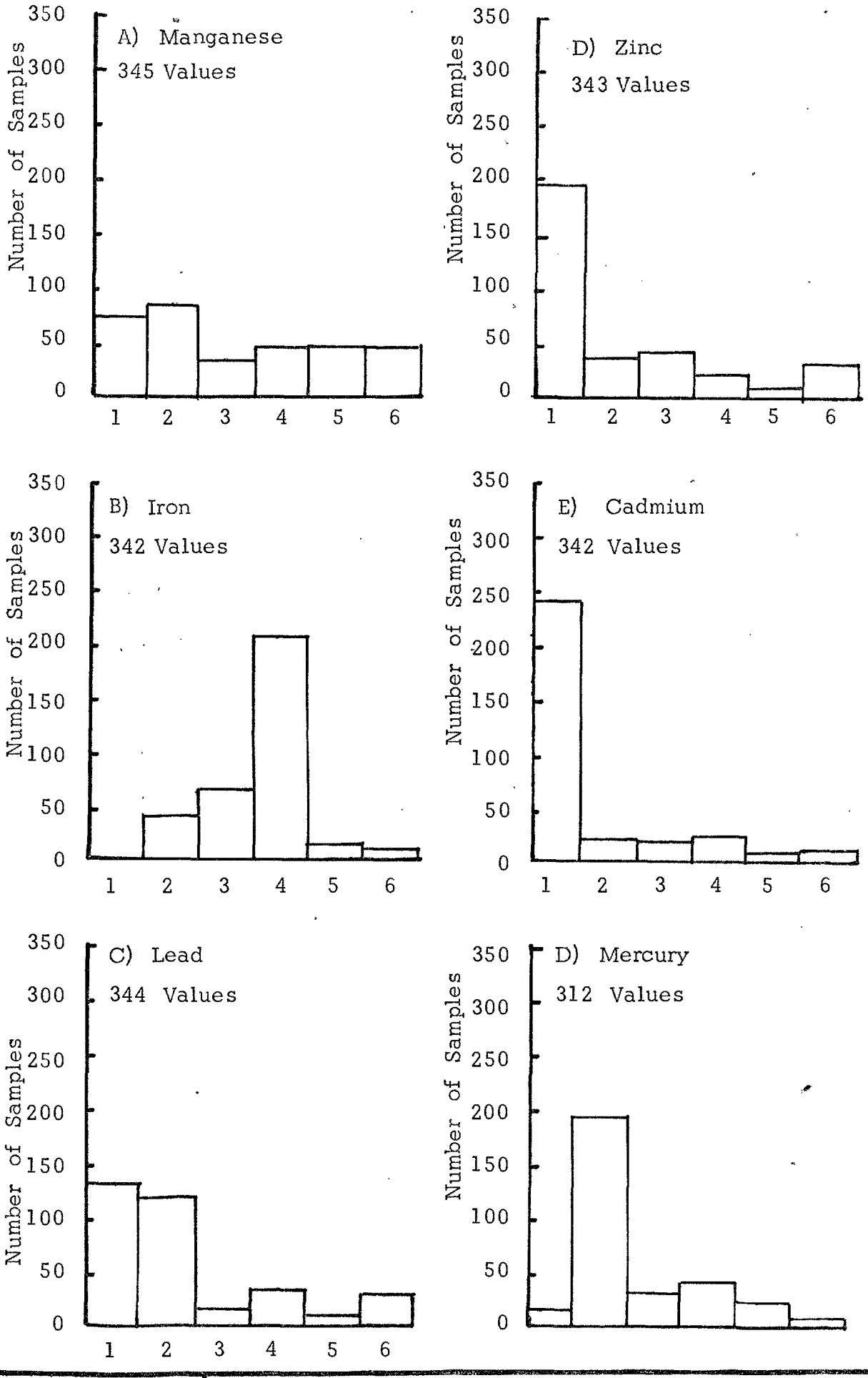


FIG ... 3.62

HISTOGRAM OF THE COMBINED LEVEL DISTRIBUTION OF Cd, Pb, Zn, Hg, Fe, Mn. FROM DRILLCORE SAMPLES KEEL PROSPECT

CHAPTER 4

PRIMARY DISPERSION STUDIES IN THE UNDERGROUND WORKINGS OF THE KEEL PROSPECT

4.1. INTRODUCTION

Three hundred and five rock samples, each weighing in excess of one kilogramme, were collected from the underground workings of the Keel prospect. The sample distribution was as follows:- 101 samples from the 500' level, 142 samples from the 200' level and 62 samples from the 400' level. Figs. 4.1 - 4.3 show the position of these samples on the plans of the underground workings. The samples were stored separately in sealed polythene bags and an effort was made to keep obviously mineralized and unmineralized samples apart, in order to avoid inter-contamination.

Each sample was analysed for Cu, Pb, Zn, Cd, Hg, Ag, Fe, Mn, Ca, Mg, Na and K, using atomic absorption techniques. Initial work consisted of an interlaboratory study on 37 samples for Cu, Pb, and Zn, and comparative studies of optical spectograph and polarograph with atomic absorption were also carried out.

4.2. INTERLABORATORY COMPARISON OF Cu, Pb, and Zn ANALYSES

Thirty seven samples of ground, $-53.5\mu m$ rock material were sent to Loughrea, County Galway, Ireland, for analysis of Cu, Pb and Zn. Half of each ground sample was retained and analysed in the Royal School of Mines laboratories by the procedure outlined in Appendix A. The results are summarized in Figs. 4.4a, 4.4b and Fig. 4.5a. Samples were carefully chosen so as to be relatively low in base metals, thus negating the need for laboratory dilution and hence overcoming a major source of imprecision.

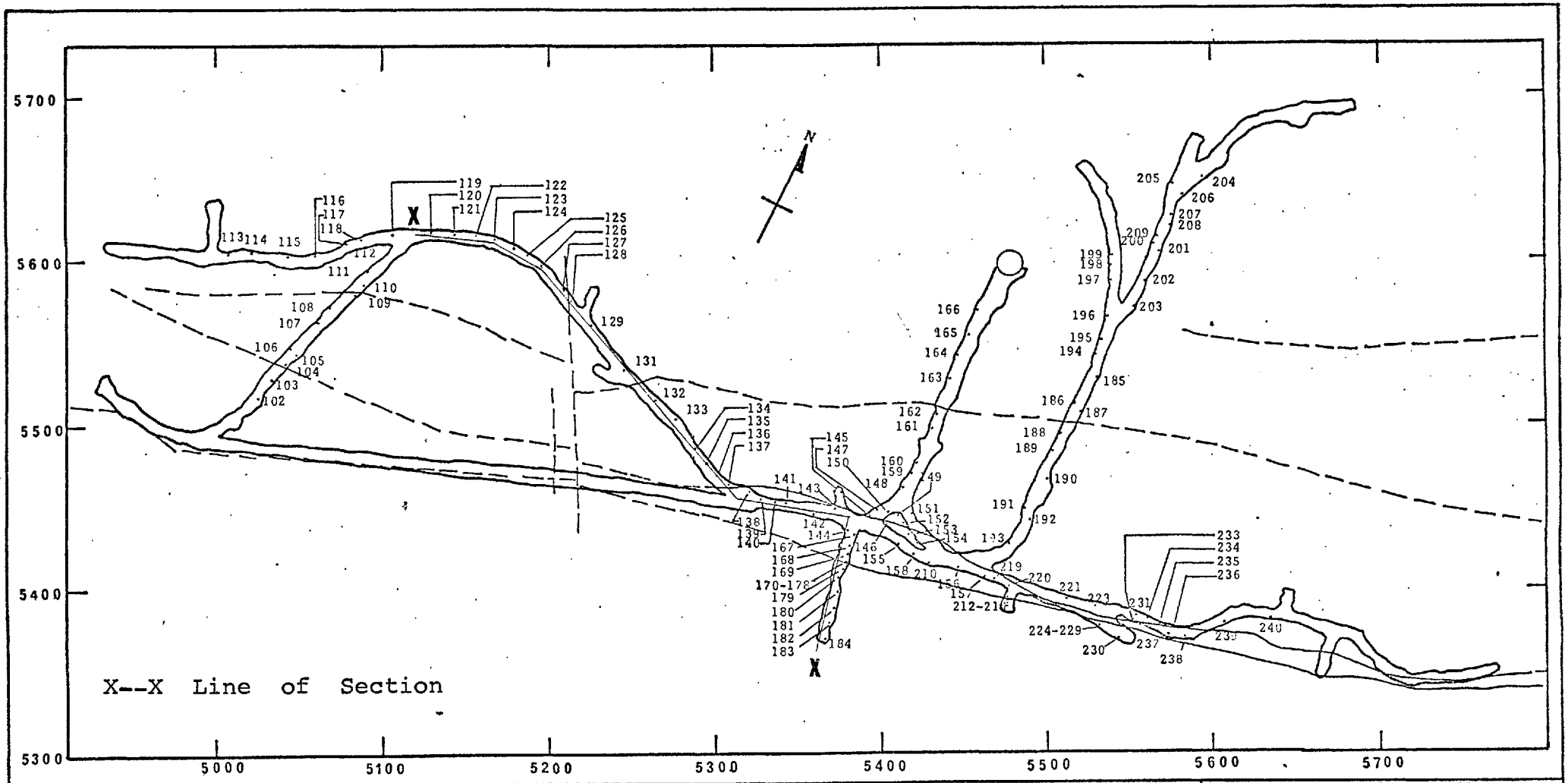


FIG ... 4.1 SAMPLE LOCATIONS ON THE 200' LEVEL, KEEL SCALE :- 0 50 100 FEET

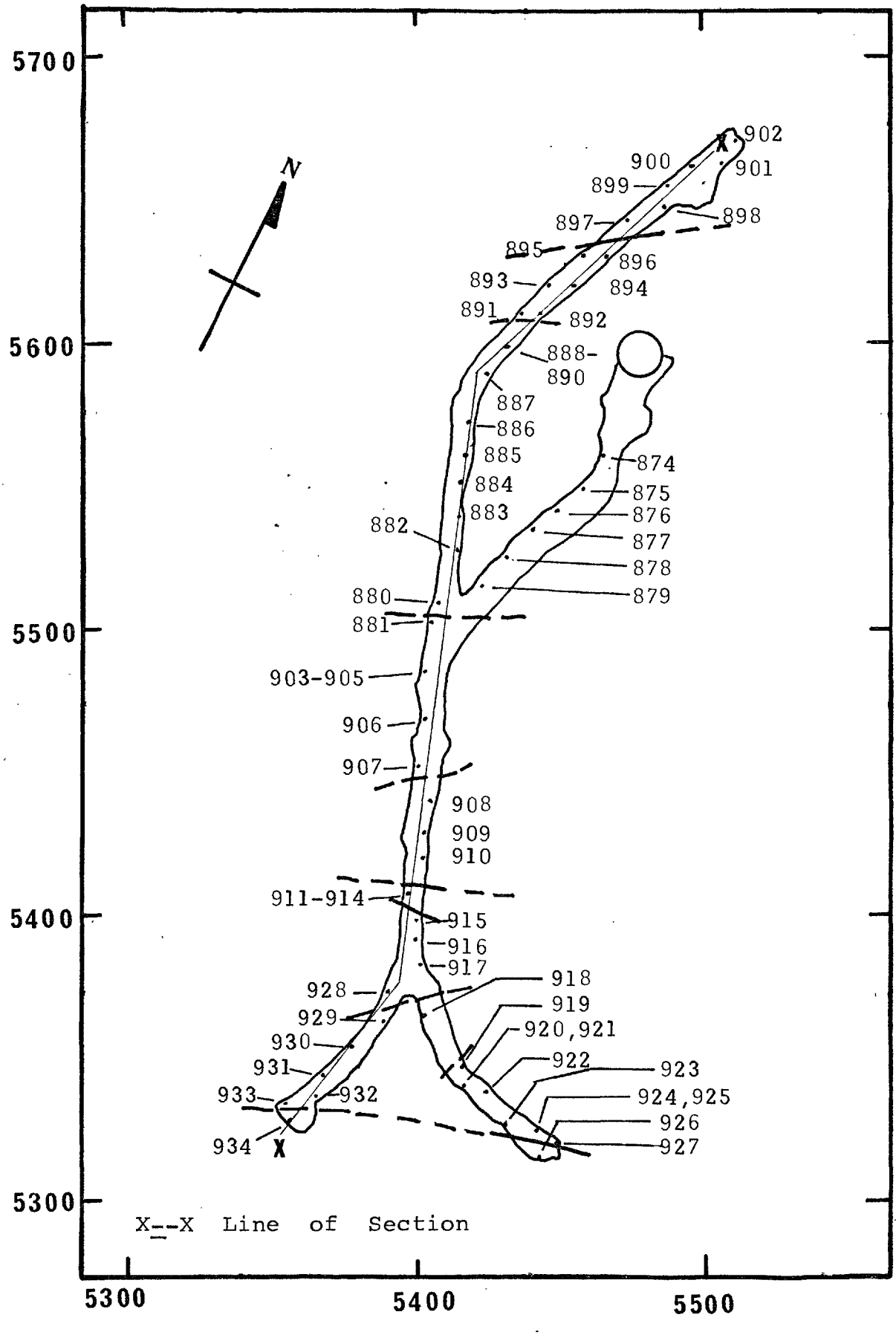


FIG... 4.2	SAMPLE LOCATIONS ON THE 400 LEVEL, KEEL.	0 50 100 SCALE IN FEET

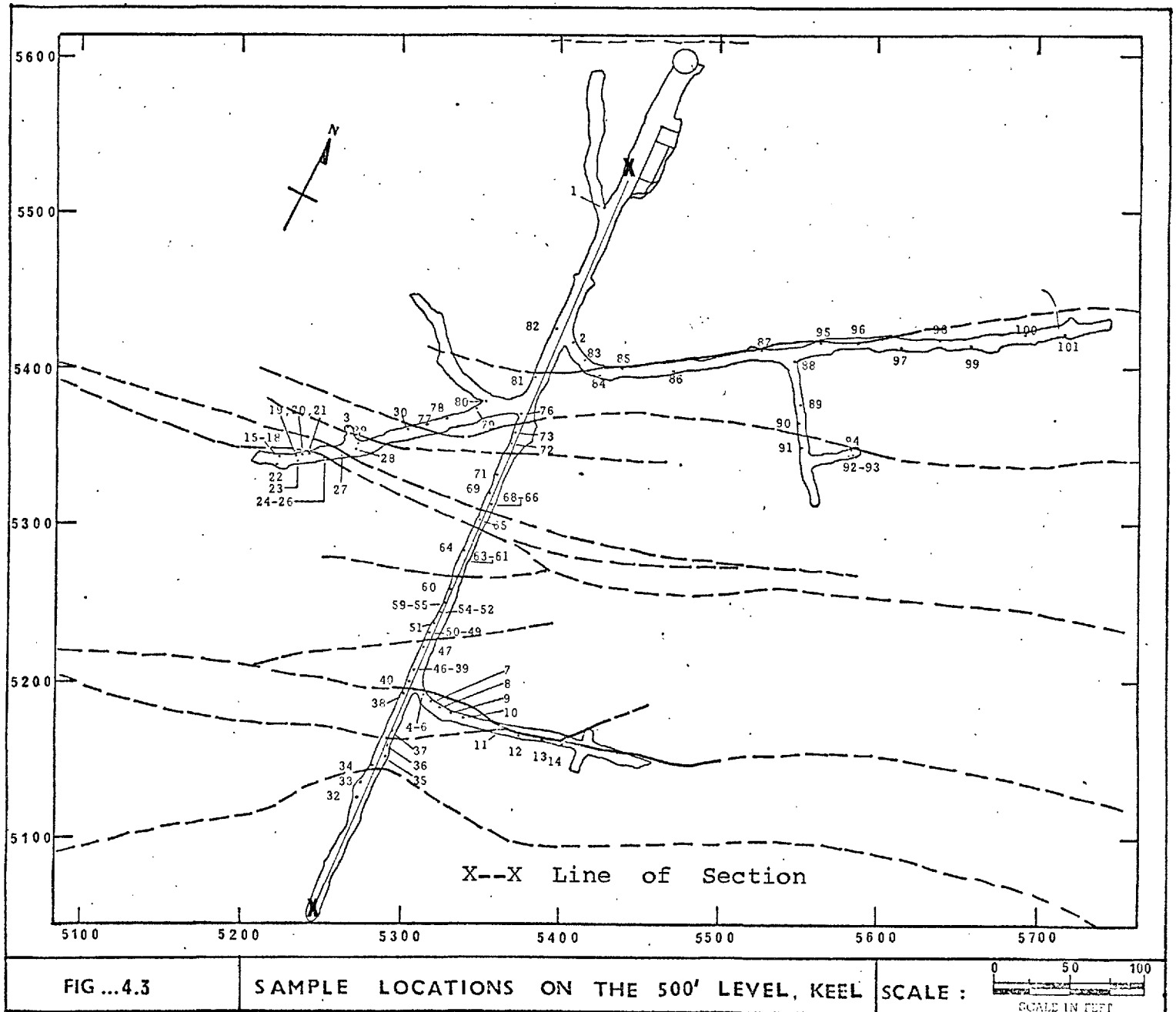
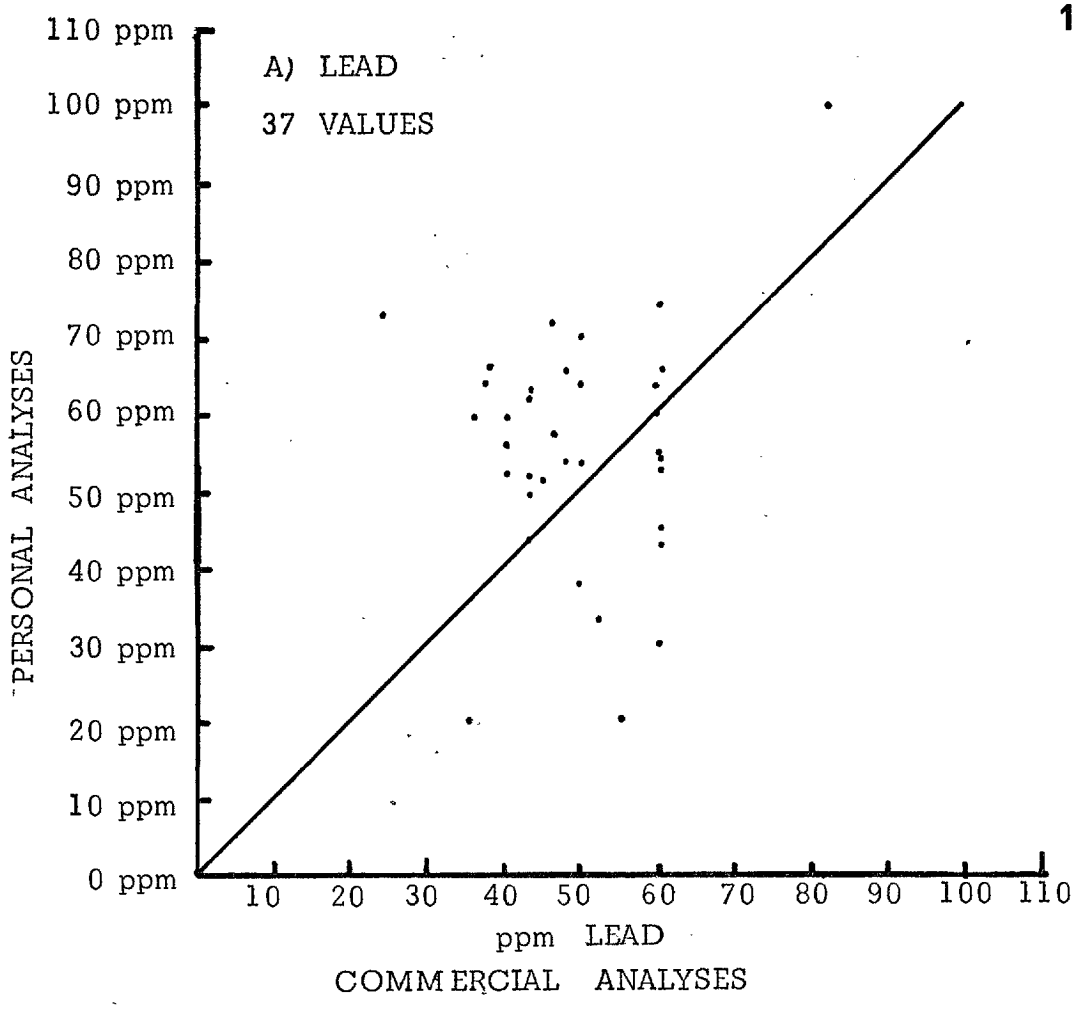


FIG ...4.3 | SAMPLE LOCATIONS ON THE 500' LEVEL, KEEL | SCALE :



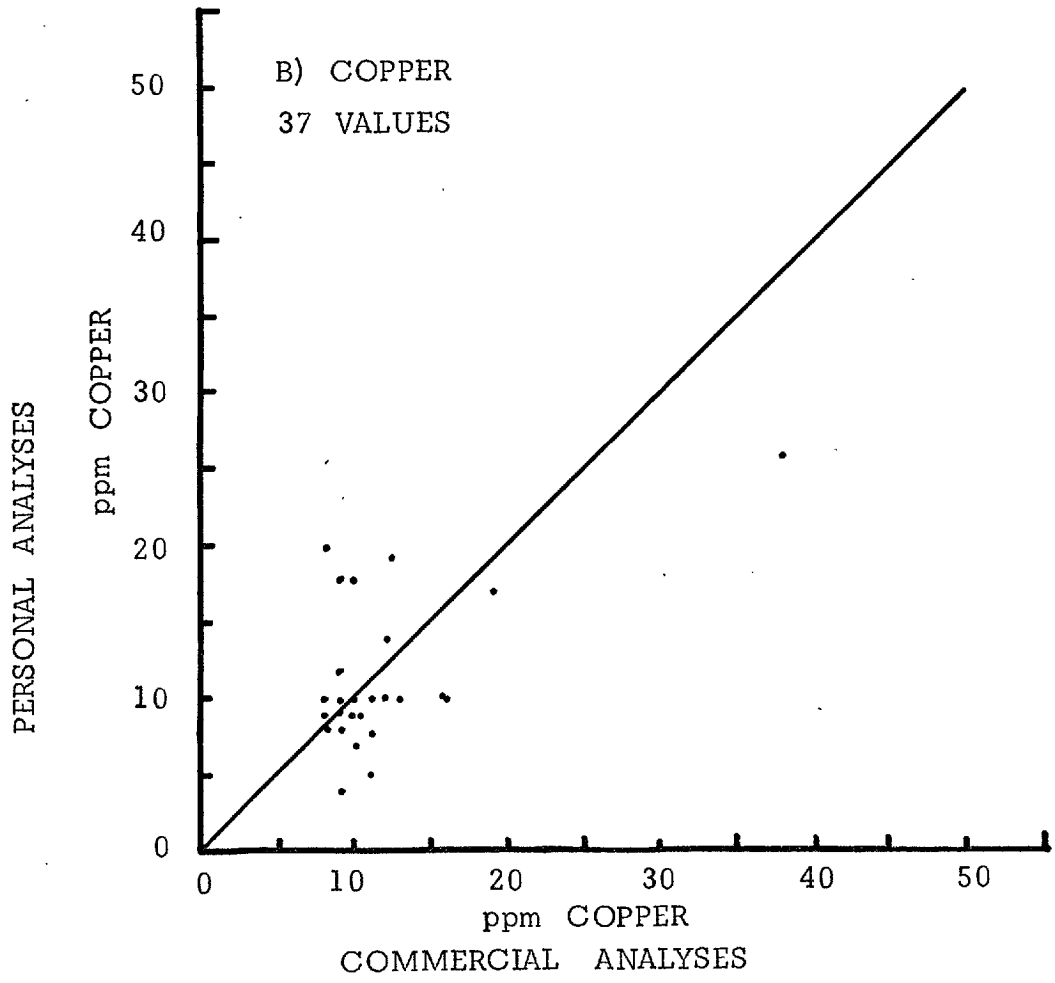
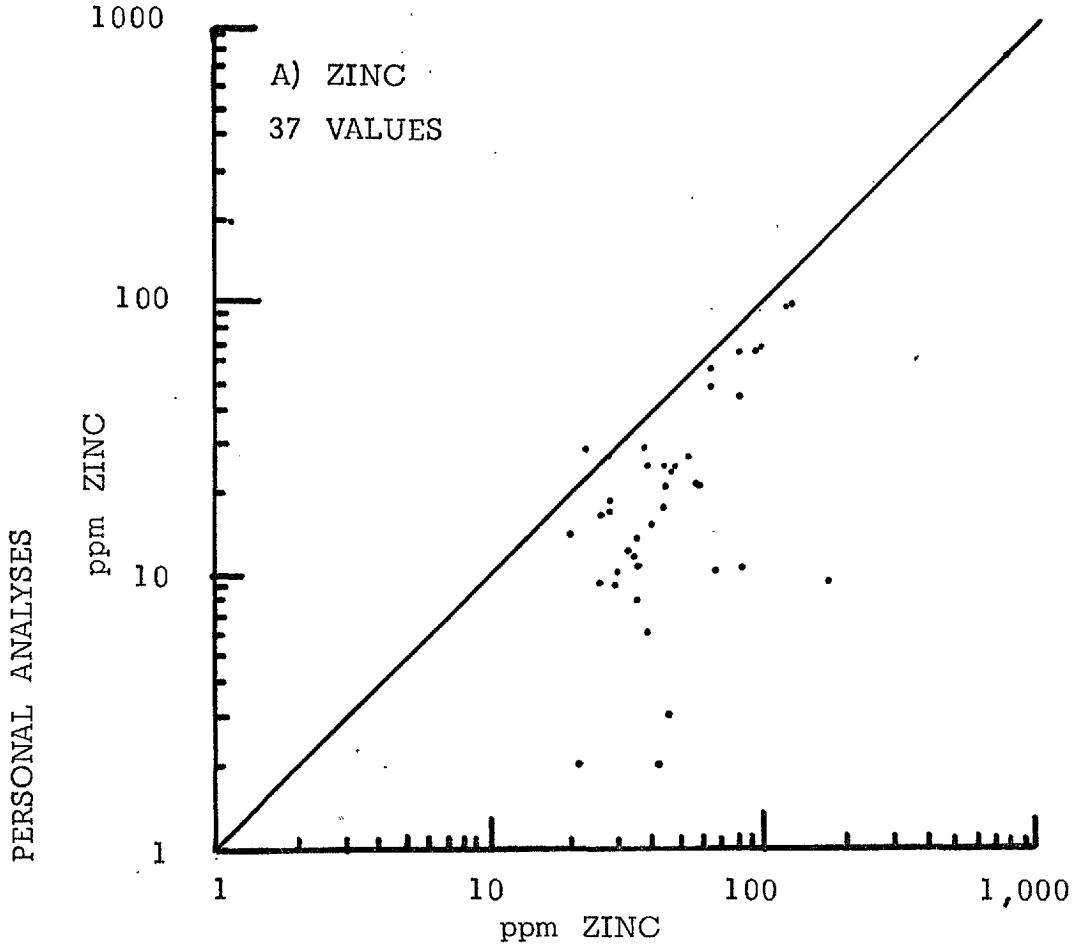


FIG ... 4.4

INTERLABORATORY COMPARISON OF COPPER & LEAD ANALYSES



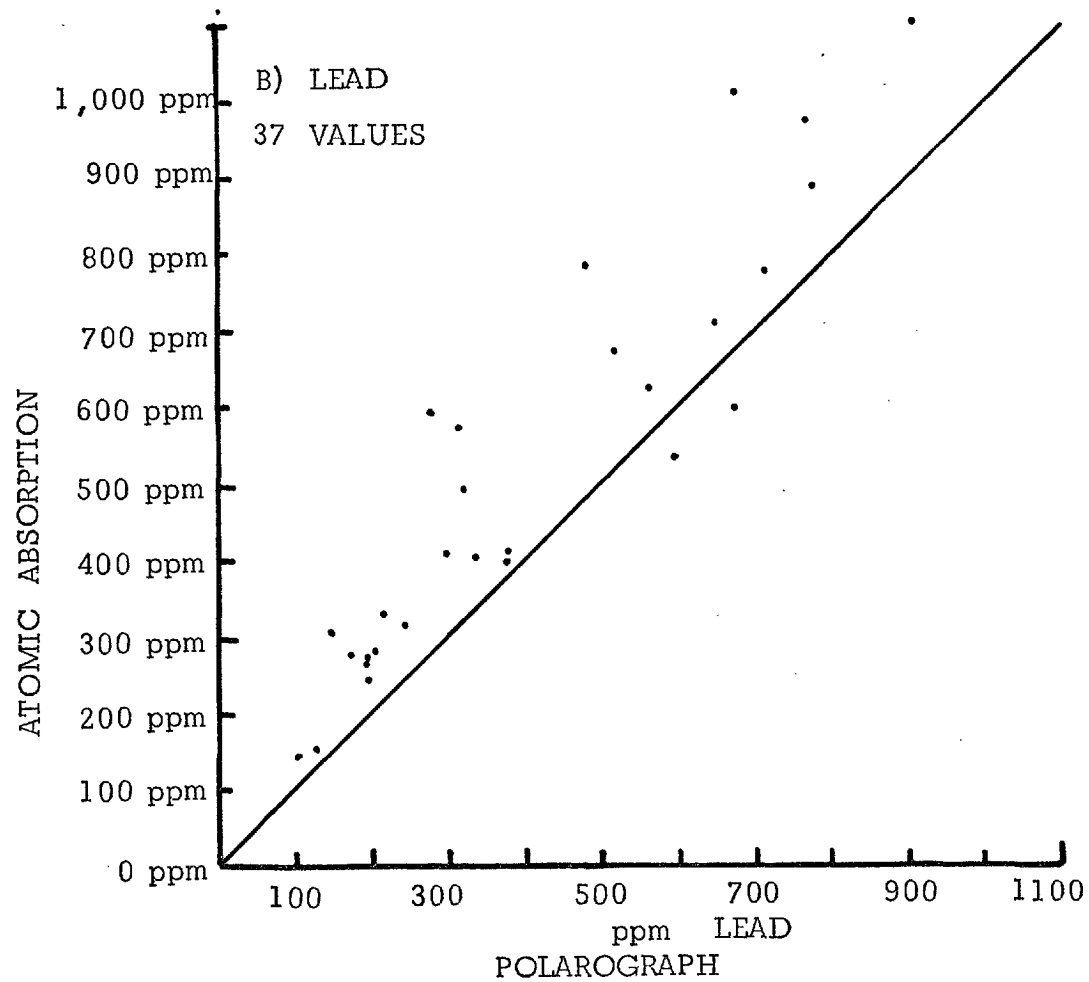


FIG ... 4.5

DIAGRAM OF
A..INTERLABORATORY COMPARISON OF ZINC ANALYSES
B..POLAROGRAPH VERSUS A.A. FOR LEAD ANALYSES

As can be seen from the lead values in Fig. 4.4a, there appears to be no correlation whatsoever between results. The commercial analysee appear to be low with respect to those carried out at R.S.M., the diagonal 45^{o} line representing an ideal 1:1 ratio of results in all casee. Copper appears to be evenly distributed either side of this line, although correlation is also poor. Zinc, however, appears to be almost uniformly high with respect to the equivalent analyses carried out at R.S.M., in some cases fifteen times higher. This is an extremely bad correlation and does not reflect any inhomogeneity of sample, but rather inaccuracies in analytical technique at one of the laboratories. It must be noted here that the author has taken into account interferences such as Ca, Mg, Na and K, and also viscosity effects. This was accomplished by analysing the Ca, Mg, Na and K content of the rocks and using Cu, Pb and Zn standards made up in equivalent concentrations to obtain calibration curves specific for each rock type. A commercial laboratory would not take these precautions.

To further check the accuracy of the analytical technique it was decided to run two other series of comparative tests.

4.3. COMPARISON OF POLAROGRAPH AND ATOMIC ABSORPTION FOR LEAD AND CADMIUM ANALYSIS

One hundred samples of mine rock were ground to - 53.5 μm and taken into solution after a complete acid digestion (Appendix A). The residue was then taken up in IM HCl and then split into two halves. One half was analysed by polarography, and the other half by atomic absorption spectrophotometry.

For the polarographic analyses a Cambridge Polarograph was used, and was fitted with a univector accessory unit. This enables a pure A.C. voltage to be superimposed on the standard D.C. voltage applied to the dropping mercury system, thus producing polarograms of much greater sensitivity, which are simpler to resolve. (Fig. 4.6.).

For polarographic analyses a very small quantity of solution was required which, since it is practically unaffected, could be used for repeated tests. The method used was that largely developed by Heyrovsky and his co-workers, (Heyrovsky, 1935) and is described in Appendix C.

Comparative analytical results obtained by atomic absorption and polarograph are shown in Figs. 4.7 and 4.5b. It can be seen from these figures that there is a very good correlation between these results. However the results obtained by atomic absorption are usually higher than from the polarograph. If the best line through these points is drawn it would be very nearly parallel to the 45^{o} line already drawn. This indicates that there is a more logical explanation than just interference or viscosity increasing readings on atomic absorption. A normal/normal plot of results, Fig. 4.5b, shows more clearly that there appears to be a greater relative increase in atomic absorption over polarograph results with increasing concentration. This suggests that the discrepancy may be due simply to a standard error in dilution of the atomic absorption samples. The polarographic samples were not diluted, but the readout signal reduced by variable resistors with a tolerance of $\pm$ 2%, and hence the reduction in amplitude of the readout signal is very accurate.

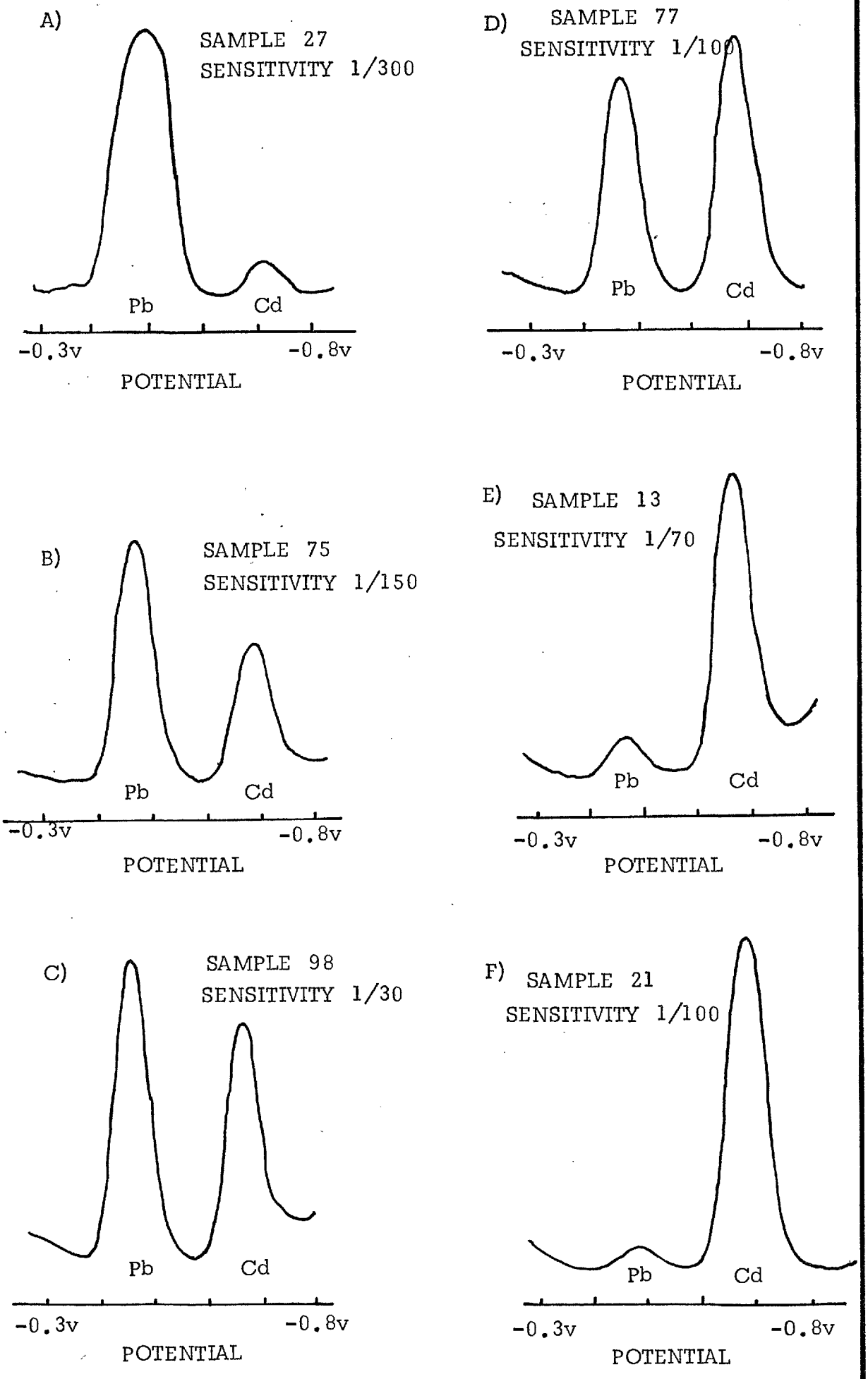
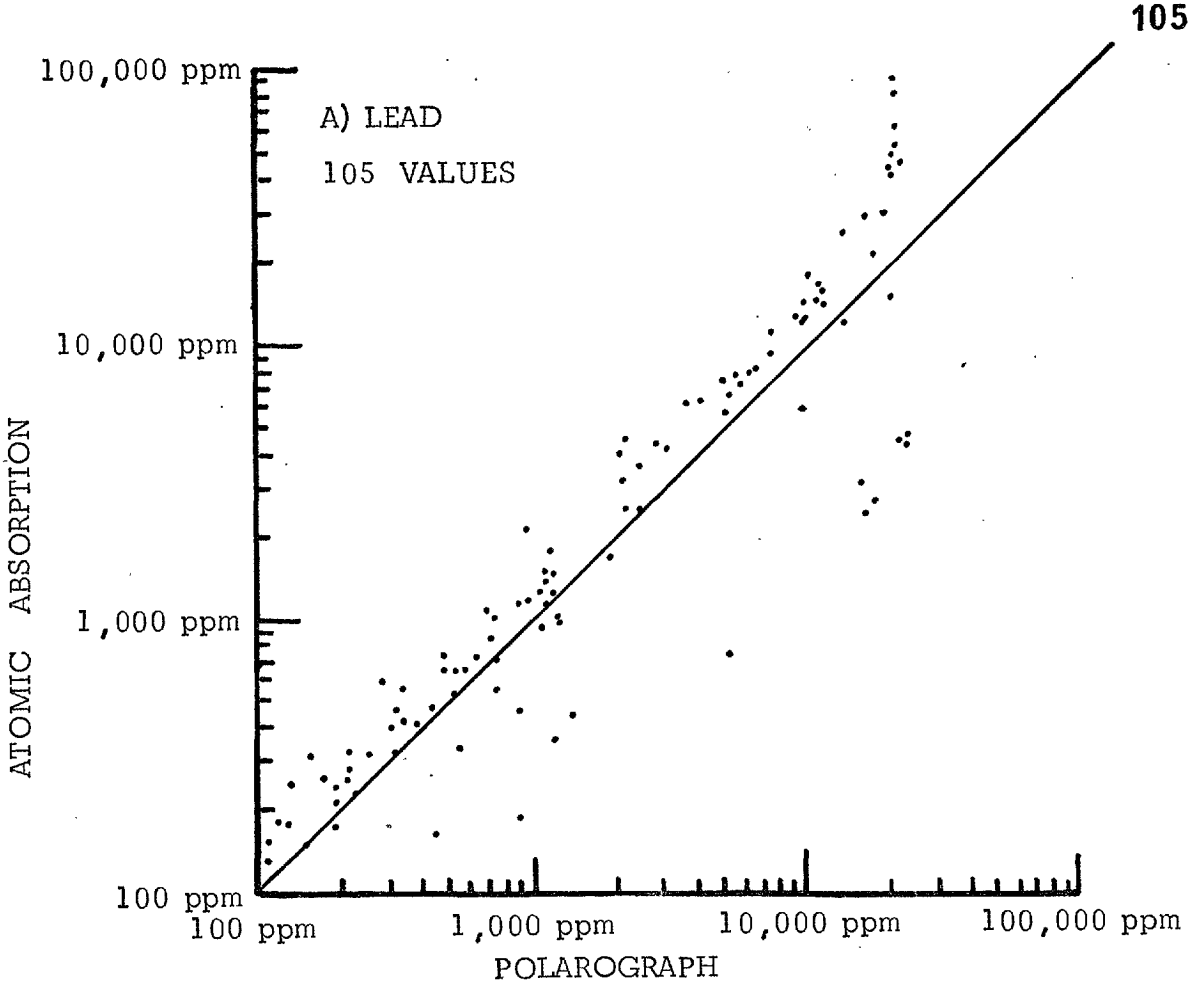


FIG ... 4.6 POLAROGRAMS OF ROCK MATERIAL FROM KEEL.



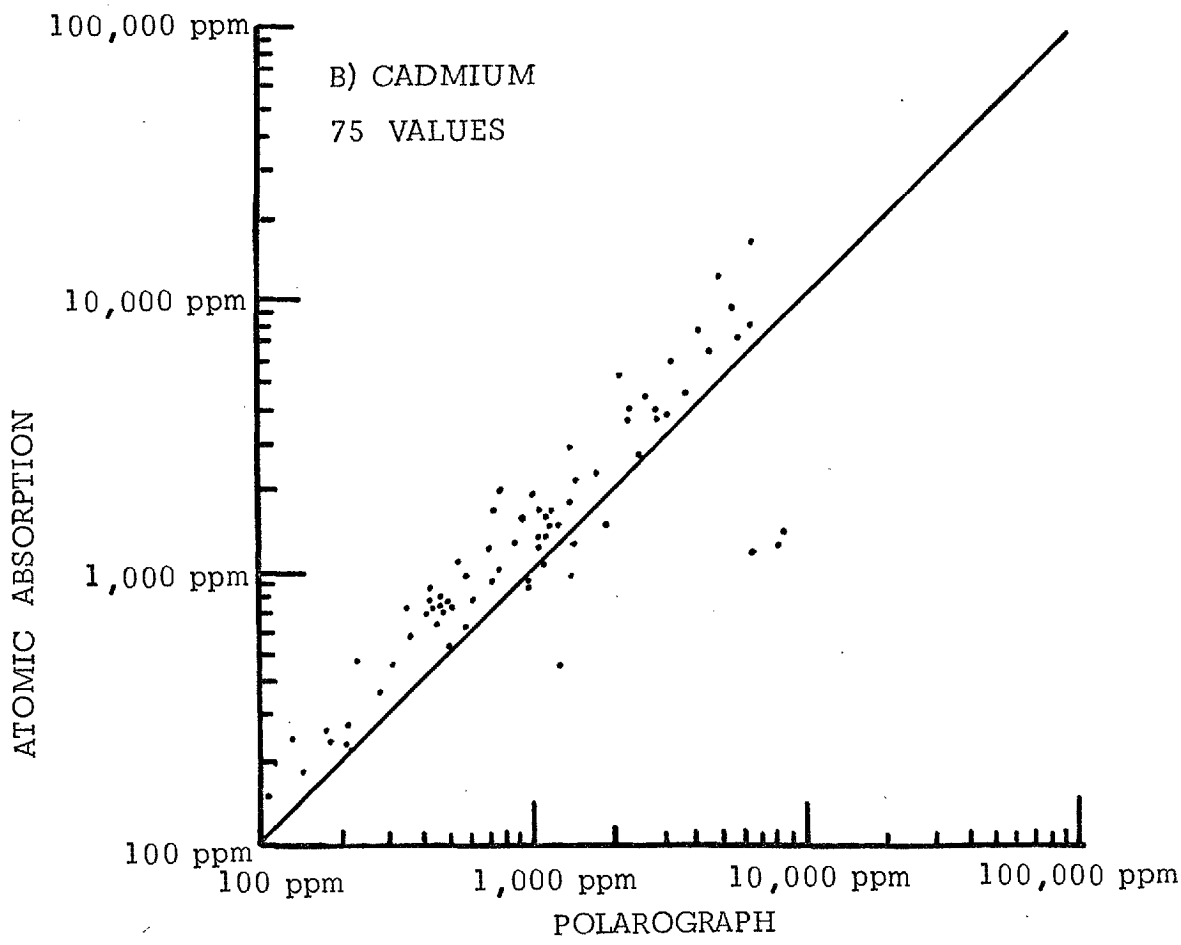


FIG ... 4.7

COMPARISON OF POLAROGRAPH & ATOMIC ABSORPTION ANALYSES FOR CADMIUM & LEAD IN ROCK SAMPLES FROM THE MINE WORKINGS

An extremely interesting point is apparent on the lead graph, Fig. 4.7a. At lead values over 10,000 ppm in the sample, i.e., 100ppm in solution, (dilution factor in solution is 1:100) the tie up between the two methods is extremely poor; at 200 µg/ml, the correlation breaks down completely. Here it must be stressed that the solutions are made up in 1N HCl and the solubility of $PbCl_2$ in IN HCl becomes highly suspect after 100 µg/ml (J. Angus, pers. comm.) with chloride complexes, complex ions and suspensions of the salt. If solutions of $PbCl_2$ with lead potentially in excess of 100 µg/ml were sprayed into an atomic absorption flame, the flame temperature would be sufficient to break down any colloid or suspension present and allow this to be read as ionic lead. However polarographic techniques are non destructive and only the lead in true solution would be read. Thus it appears that the limiting solubility of $PbCl_2$ in IN HCl is approximately 200 µg per ml. One conclusion from this is that solutions of lead in the form of chloride, with concentrations greater than 100 µg/ml, should not be analysed or diluted and subsequently analysed for fear of incorrect results.

Cadmium suffers from none of these effects and the correspondence of the two techniques for cadmium analysis is very good. Cadmium, however, appears higher on atomic absorption than polarograph and the same explanation for this discrepancy as for the lead results is envisaged.

4.3. COMPARISON OF OPTICAL SPECTROGRAPH AND ATOMIC ABSORPTION FOR COPPER, LEAD, ZINC AND MANGANESE ANALYSIS

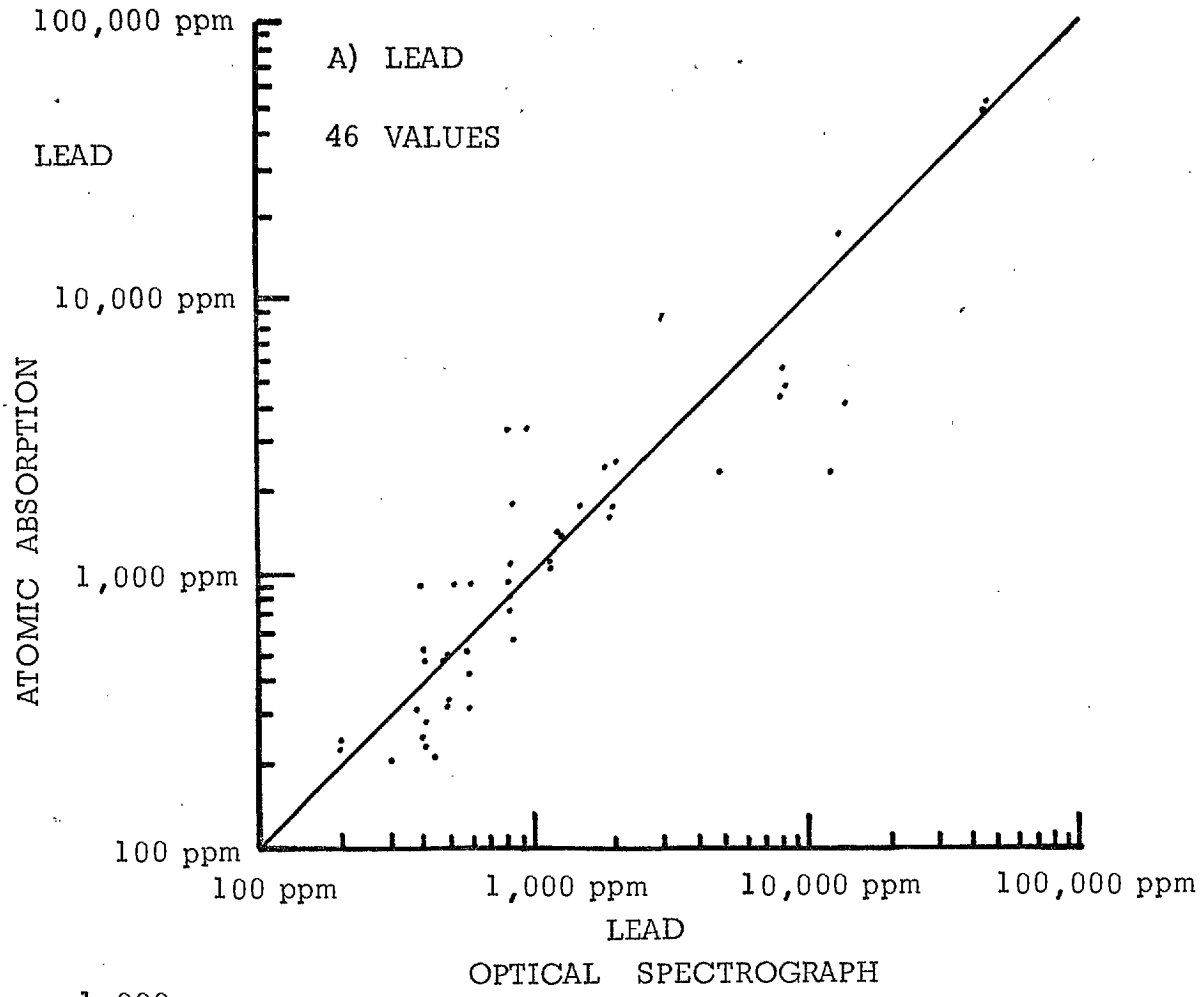
A Hilger large quartz spectrograph E.742, was used to determine Cu, Pb, Zn and Mn in 150 samples of mine rock. The method of analysis is briefly described as follows: 100 milligrammes of the finely ground sample was added to an equal weight of high purity carbon in a plastic vial and shaken with two small plastic balls for 1 min.30 secs. This mixture was then pressed into a carbon electrode and burnt to completion at a current of 9 amp. Spectra were recorded on Kodak N40 plates and a seven step sector was used.

Working curves were constructed by burning standards of mixes of specpure elemental oxides and specpure silica. The precision of the method was calculated as within $\pm$ 15% relative.

The results, shown in Figs. 4.8 and 4.9, indicate manganese to have good correlation between methods. Zinc, lead and copper, although showing a general relationship, have no close correspondence between methods. This lack of correlation could be due to incompatibility of matrices between standards, which are predominantly oxides, and samples, in which the copper, lead and zinc are predominantly in the form of sulphides.

These comparative studies indicate two things:

(1) The analyses obtained by atomic absorption in the Royal School of Mines laboratories can be expected to be of reasonable accuracy. Therefore conclusions drawn from them can be made with reasonable confidence.



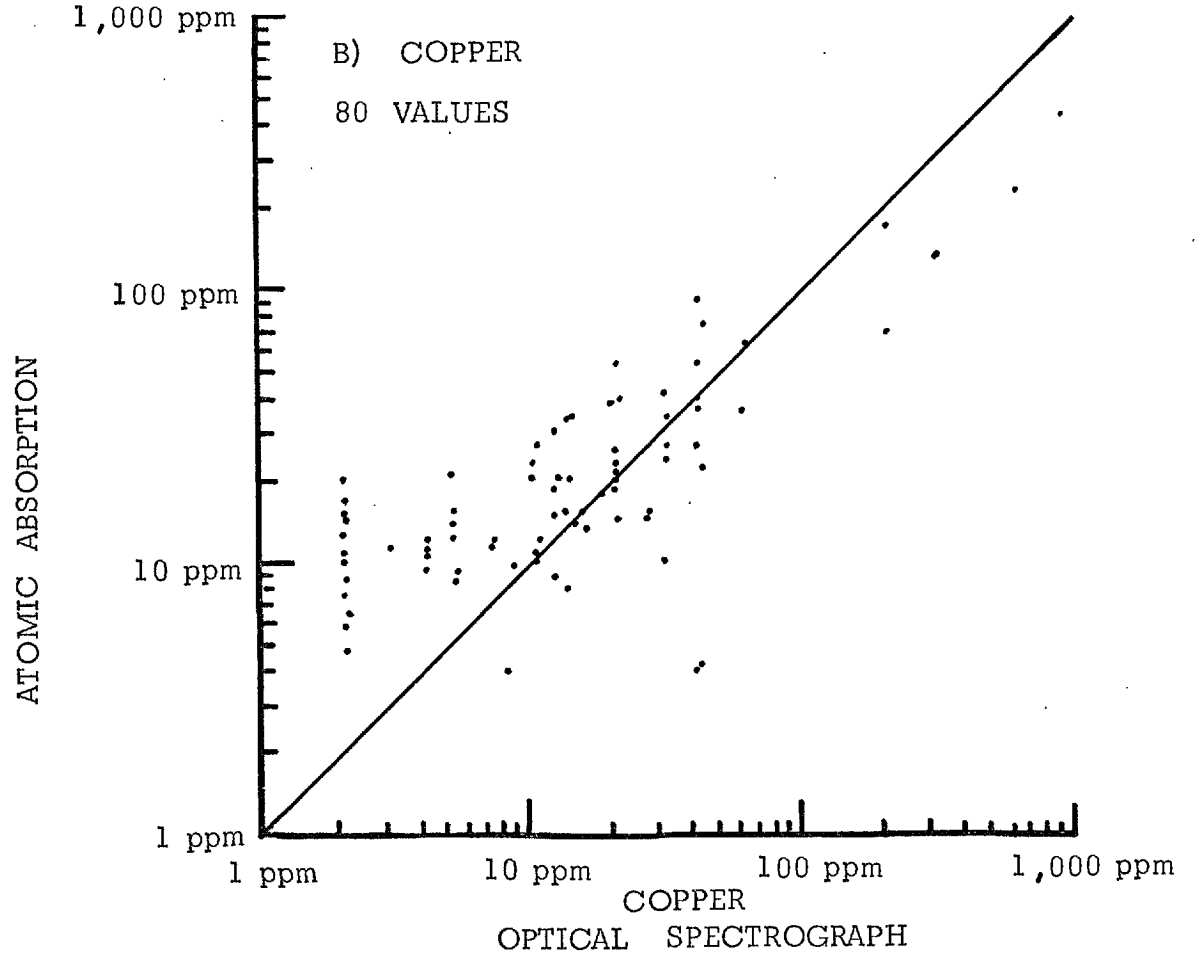
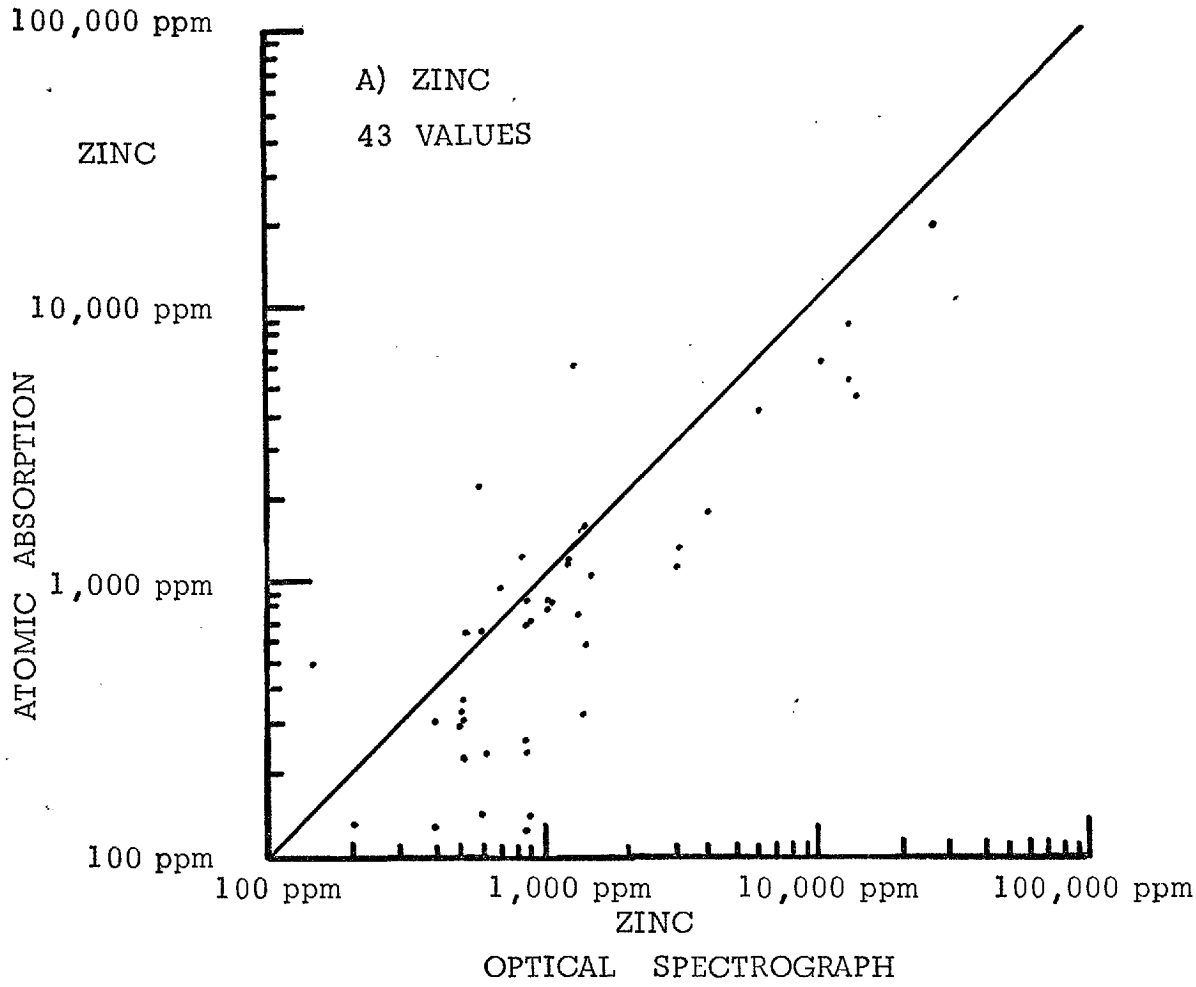


FIG ... 4.8 COMPARISON OF ATOMIC ABSORPTION & OPTICAL SPECTROGRAPH ANALYSES FOR LEAD & COPPER IN ROCK SAMPLES FROM THE UNDERGROUND WORKINGS



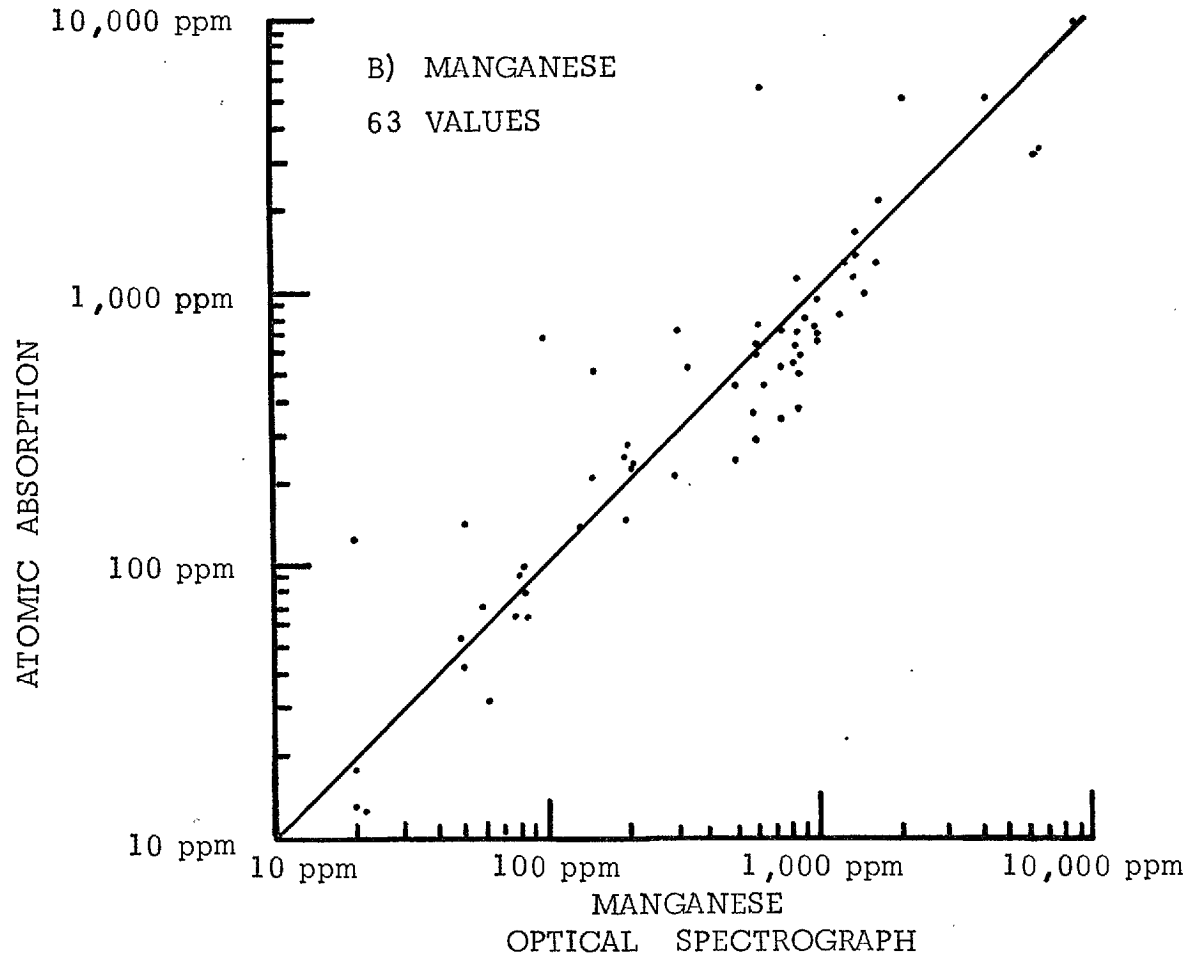


FIG ... 4.9

COMPARISON OF ATOMIC ABSORPTION & OPTICAL SPECTROGRAPH ANALYSES FOR ZINC & MANGANESE IN ROCK SAMPLES FROM THE UNDERGROUND WORKINGS

(2) The standards for optical spectrograph, although predominantly oxides, can be used in the quantitative determination of trace elements in Keel rocks. These standards cannot be used in determination of the trace element content of high grade ore due to incompatibility of matrices.

4.4. GEOLOGY AND MINERALIZATION OF THE UNDERGROUND WORKINGS KEEL MINE, COUNTY LONGFORD, EIRE.

In 1965 a decision was taken to sink a 16' diameter, concrete lined shaft at Keel to evaluate the controls of mineralization within the deposit. The shaft was sunk to 535' and a total of 4500 feet of exploratory tunnelling carried out predominantly on the 200' and 500' levels with only minor work on the 400' level.

The 200' level at Keel is predominantly cut in two rock units, the Upper Mixed Beds and the Bioclastic Limestone. Mineralization on this level is solely confined to the Upper Mixed Beds. Main ore zones occur in breccias along the southerly dipping normal faults, trending east north east to west south west. The contact between the Upper Mixed Beds and the Bioclastic Limestone is faulted and at the base of the Bioclastic Limestone is a fault gouge, up to two feet thick, which according to Patterson, provided an impermeable barrier to any ore solutions. Primary dispersion of lead, zinc, silver, copper and mercury across this fault is negligible, as is convincingly exhibited in Fig. 4.10.

Stratigraphic control exists to some extent, in that mineralized fractures in sandstone die out almost entirely on penetrating a shaley

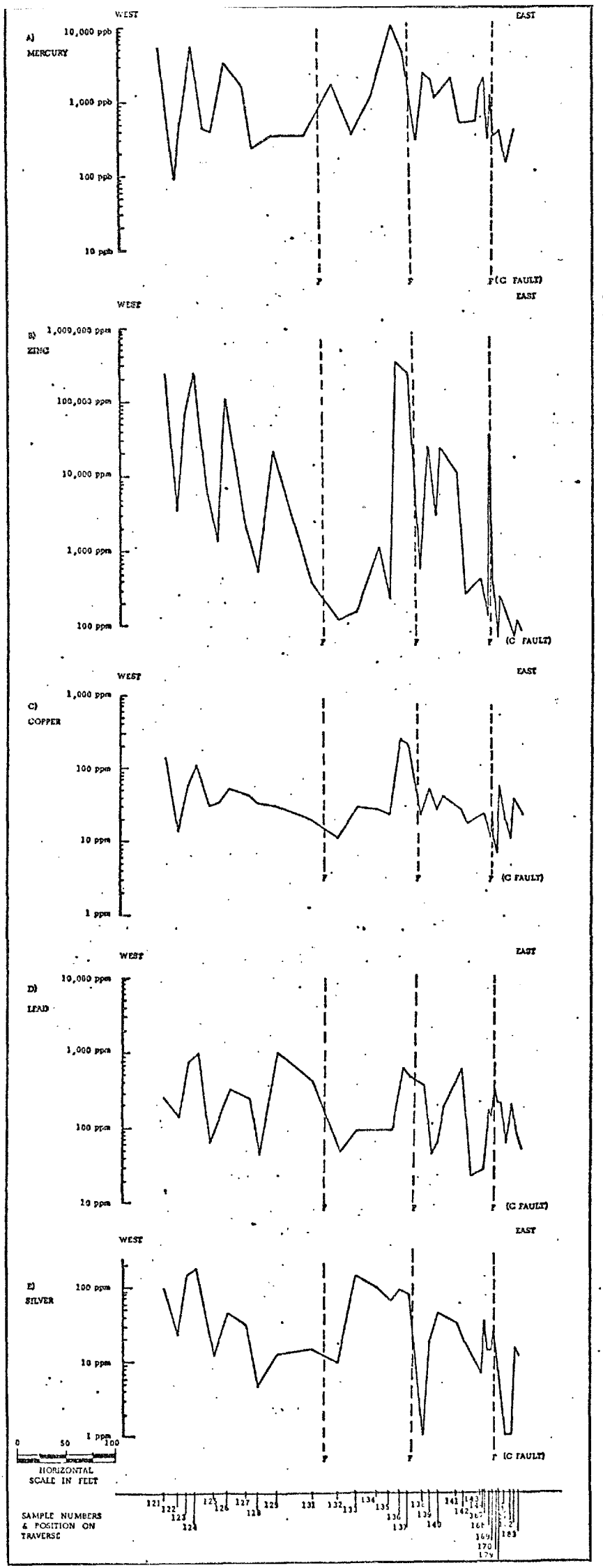


FIG ... 4.10

RELATIONSHIP OF Cu/Pb/Zn/Ag/Hg. ON THE 200' LEVEL KEEL PROSPECT, COUNTY LONGFORD, IRELAND.

horizon. From the primary dispersion maps in this chapter, it is possible to see the structural control of the deposit, the ore obviously having been emplaced along fault planes. Figs. 4.11 - 4.15 show the distribution of Cu, Pb, Zn, Ag and Hg on the 200' level.

The C orebody is excellently exposed on both the 200' and 500' levels. On the 500' level the foot wall of this orebody is fault-controlled. The reverse situation is seen on the 200' level, where the hanging wall is fault-controlled with high grade breccia ore dammed up against bamen bioclastic limestone. The C and D orebodies come very close together on the 200' level, both orebodies pinching and swelling along strike.

The 500' level is more complex with Upper Mixed Beds, Bioclastic Dolomite, Upper Quartz Sandstone, Quartz Pebble Conglomerate and Lower Quartz Sandstone being represented . Mineralization occurs in all units although evidence of mineralization in the Lower Quartz Sandstone could not be found, owing to lack of exposure.

In Chapter 3 it has been seen that primary dispersion is not very much in evidence in the Keel area; maps of the primary dispersion of selected elements on various levels have done little to clarify the overall picture. In Chapter 4 the primary dispersion of copper, lead, zinc, silver and mercury on the 500', 400' and 200' levels will be discussed.

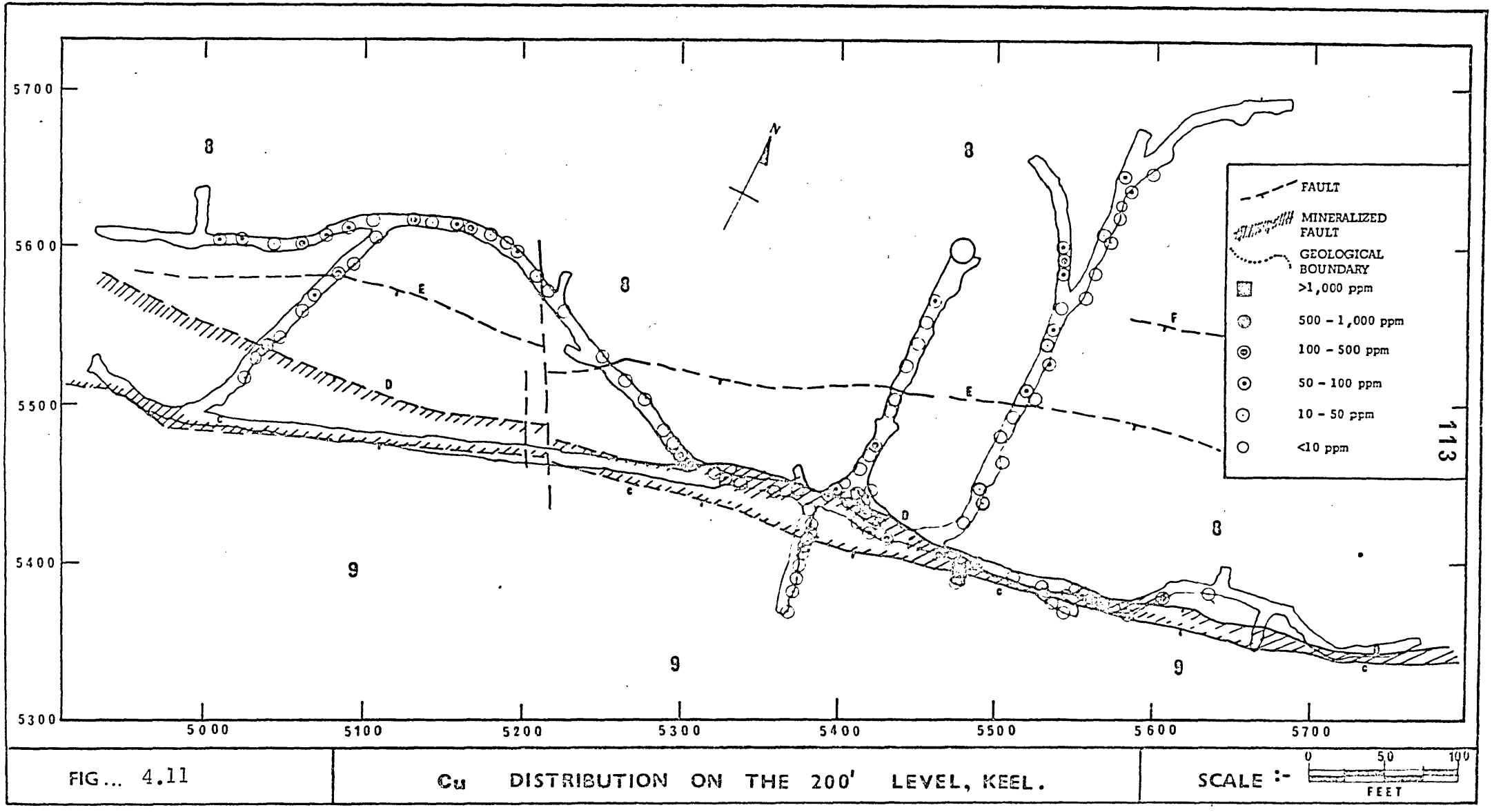


FIG... 4.11

Cu DISTRIBUTION ON THE 200' LEVEL, KEEL.

SCALE :-

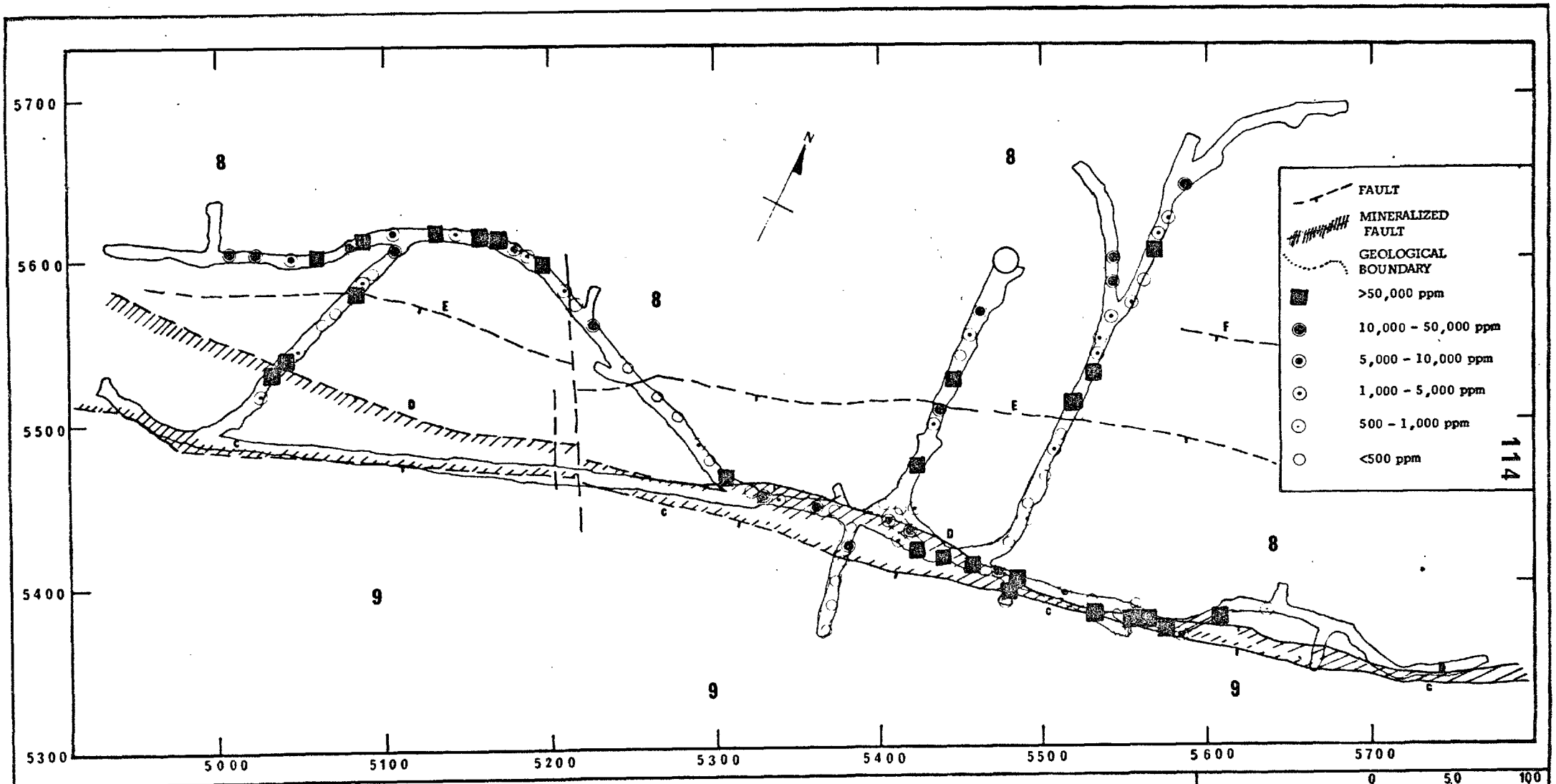


FIG ... 4.12 | Zn DISTRIBUTION ON THE 200' LEVEL, KEEL. | SCALE :-

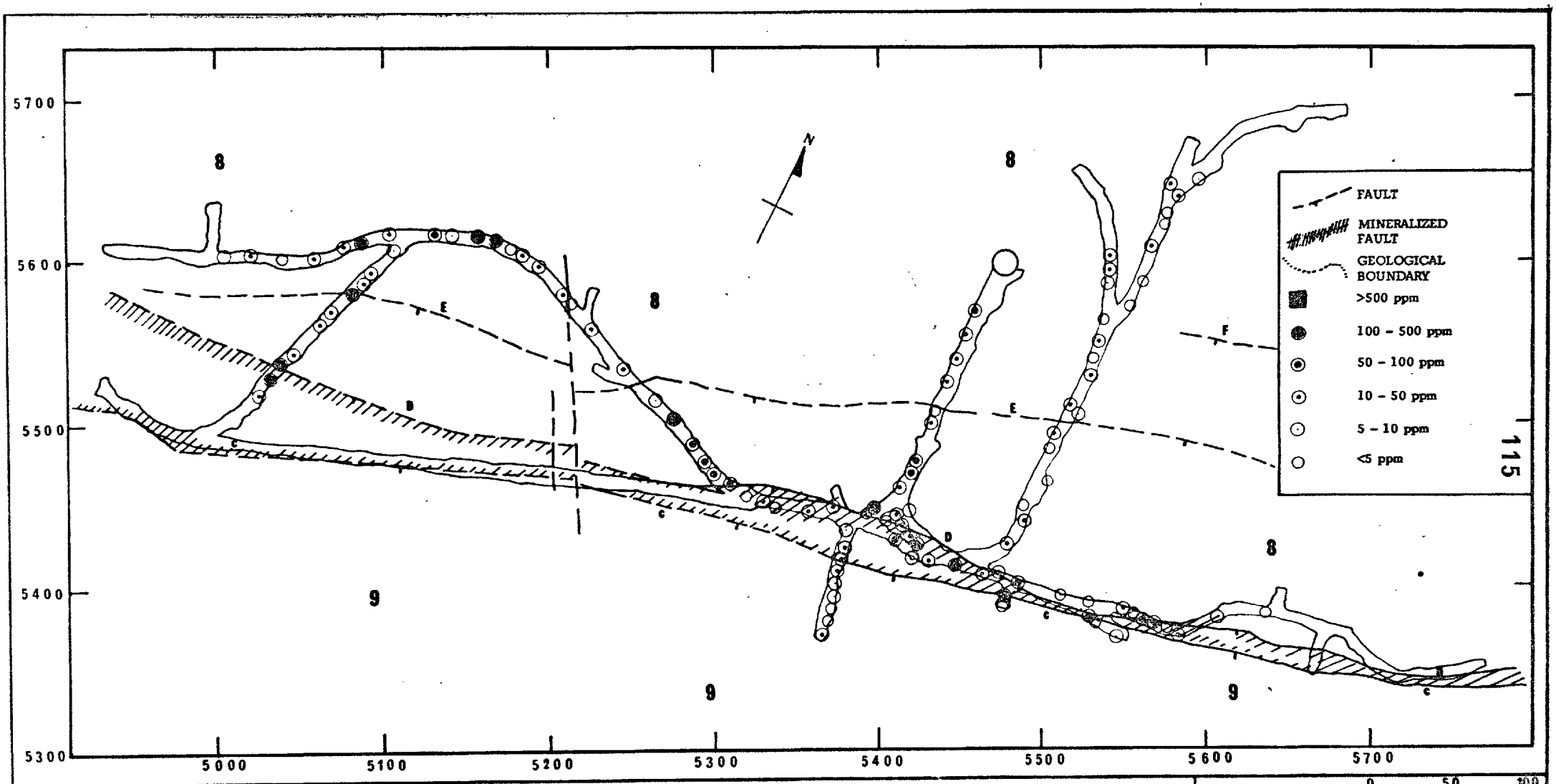


FIG... 4.13

Ag DISTRIBUTION ON THE 200' LEVEL, KEEL.

SCALE :- 0 50 100 FEET

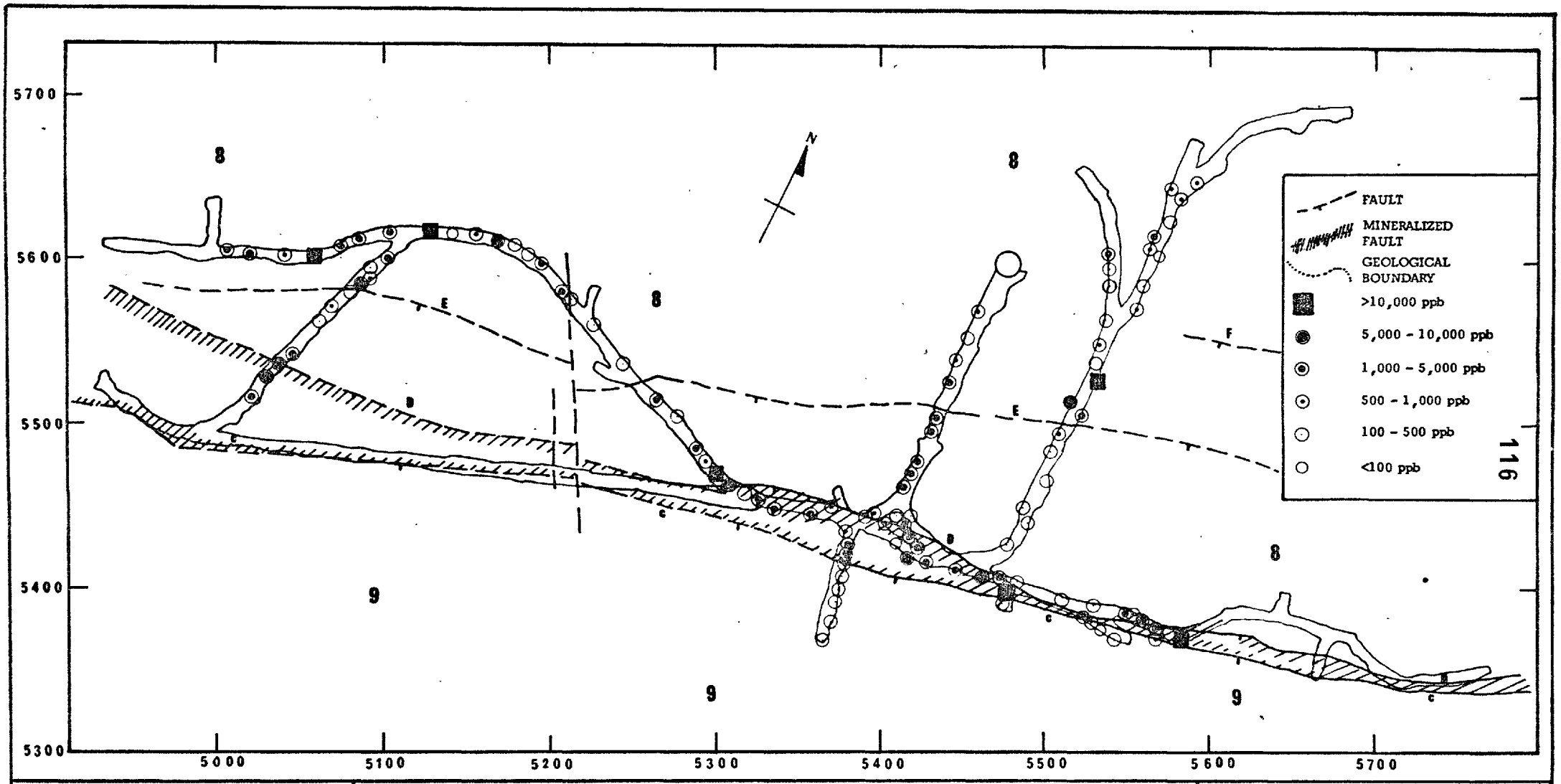


FIG... 4.14

Hg DISTRIBUTION ON THE 200' LEVEL, KEEL.

SCALE :-

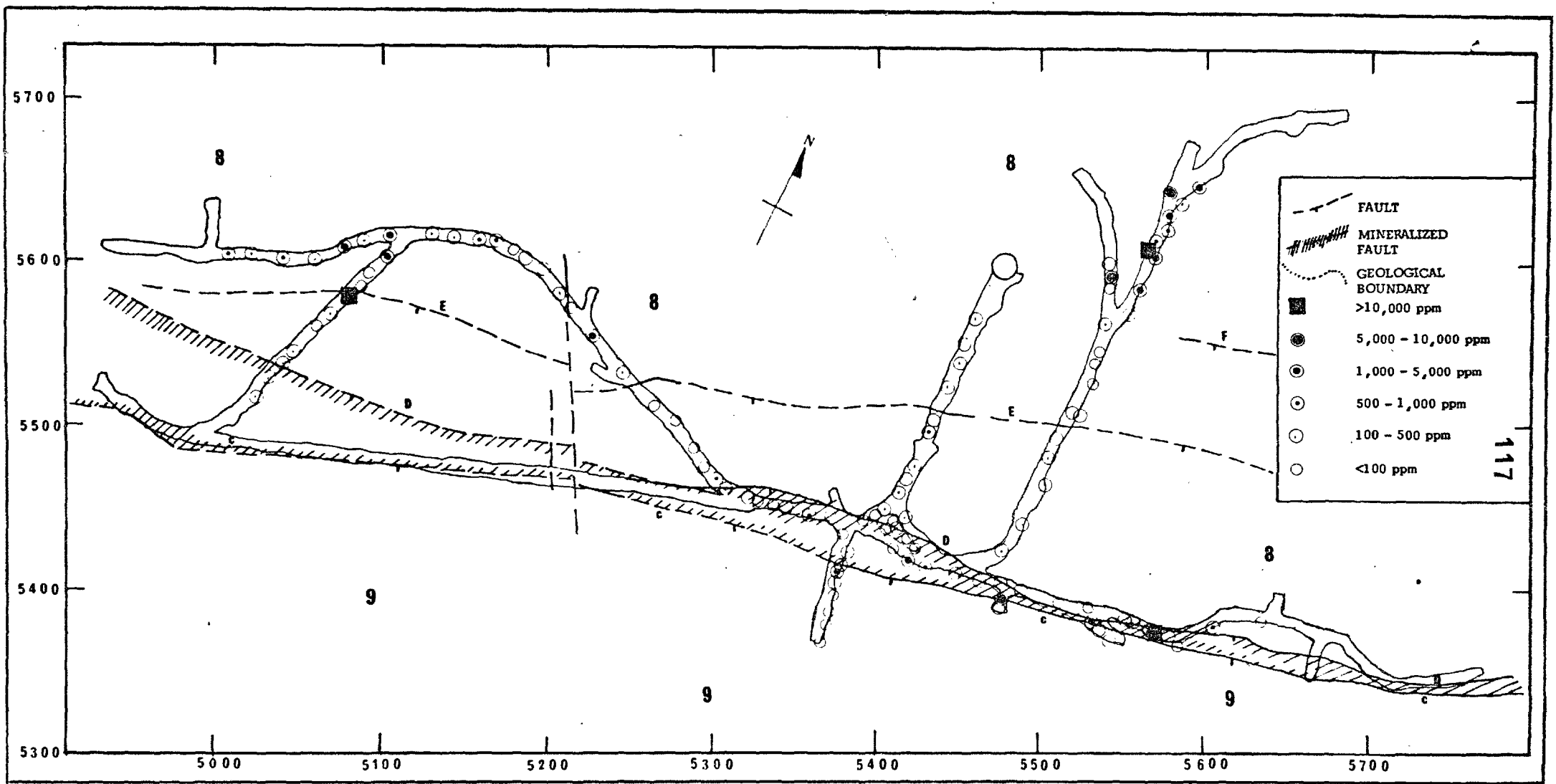


FIG... 4.15 | Pb DISTRIBUTION ON THE 200' LEVEL, KEEL. | SCALE :- 0 50 100 FEET

4.5. PRIMARY DISPERSION IN THE UNDERGROUND WORKINGS

KEEL PROSPECT, COUNTY LONGFORD, EIRE.

The 500' level is the deepest level of the Keel Prospect. Primary dispersion studies are complicated on this, as in all other levels, by the abundance of different lithologies, and thus a simple pattern is extremely difficult to interpret. Fig. 4.16. represents the distribution of Hg, Zn, Cu, Pb and Ag along a traverse from south to north on the main cross cut, south of the 500' level. The position of the traverse is marked on Fig. 4.3.

A broad sympathetic relationship between all the base metals is indicated in Figs. 4.17 - 4.21 and when plotted graphically this relationship is confirmed in Fig. 4.16. Zinc values vary from a few hundred p p m to 50% over very small distances and mercury values from 400 p p b (4×10^{-7} g./g.) to 20 p p m Primary dispersion, however, appears to be very limited and ore-grade mineralization drops to background in distances less than one inch. Mercury also appears to have had little mobility and values of 50 p p b occur in fragments of wallrock, completely surrounded by massive sphalerite with a mercury content of 100 p p m Isolated crystals of galena are not much in evidence on the 500' level and silver is seen to follow zinc to an appreciable extent, Fig. 3.47B.

A marked variation in Zn/Pb, Zn/Cd and Zn/Ag in Table 4.1.

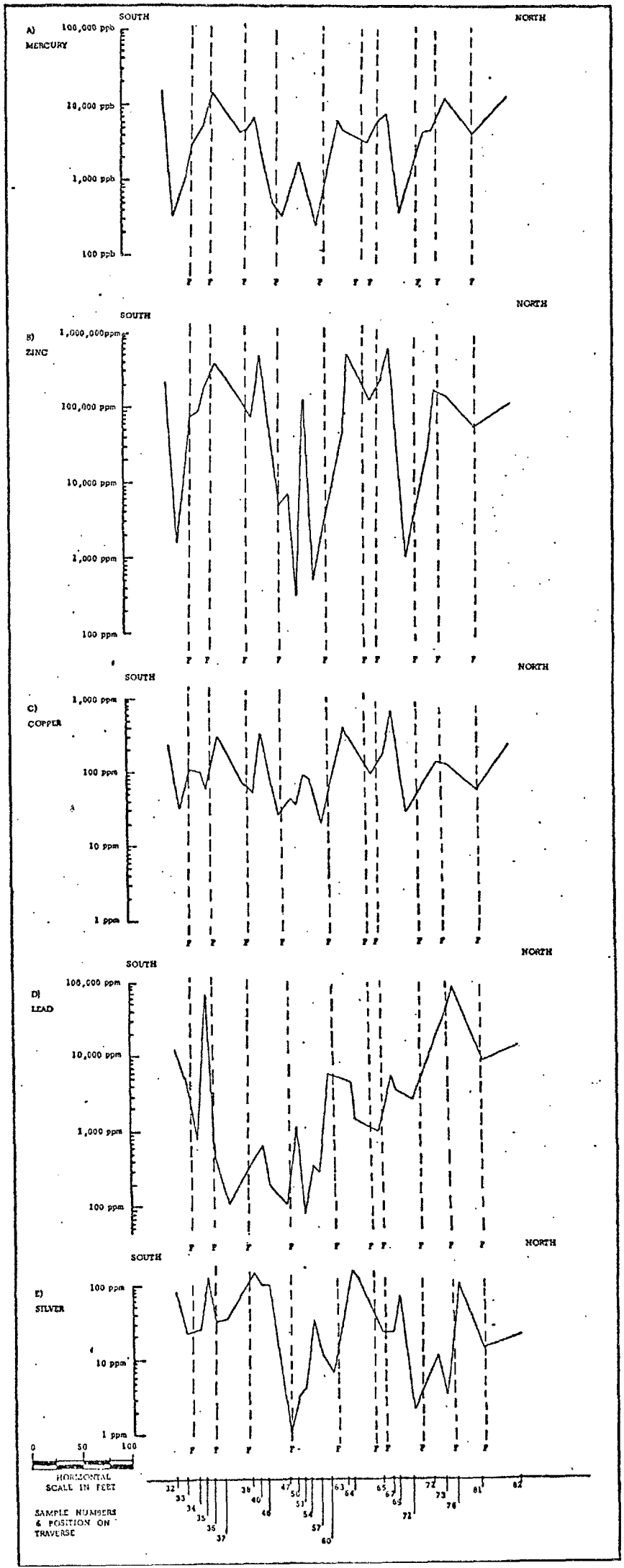


FIG ... 4.16

RELATIONSHIP OF Cu/Pb/Zn/Ag/Hg. ON THE 500' LEVEL KEEL PROSPECT, COUNTY LONGFORD, IRELAND.

TABLE 4.1. Zn/Pb, Zn/Cd and Zn/Ag Ratios in the F, E, D and C Faults, Keel Prospect, County Longford, Eire.

Fault	Zn/Pb		Zn/Cd		Zn/Ag		Number of Samples
	Mean	Standard Deviation	Mean	Standard Deviation	Mean	Standard Deviation	
F	10.92	13.98	95.0	71.18	4003	2527	15
E	19.91	20.33	25.48	3.27	4745	3624	12
D	418.6	125.3	57.07	67.33	3277	2854	16
C	221.2	265.8	94.63	60.81	3223	2600	12

From this it can be seen that the Zn/Pb ratio decreases northwards towards the Silurian inlier and that the Zn/Cd ratio for the E and D faults is much lower than the 62.0 indicated from the optical spectrograph analysis of sphalerite in Chapter 6. This suggests the presence of greenockite as a distinct mineral phase in the rocks of the 500 ft. level. When analyses of bulk samples from the F and C orebodies were taken and plotted graphically, their cadmium values show the same relationship as the F and C orebodies in Figs. 3.44 and 3.45.

When the distribution of Hg, Zn, Cu, Pb and Ag are plotted on plans of the 500' level, a distinct relationship to the extent of faulting can be seen, Figs. 4.17 - 4.21. Zinc mineralization is predominantly associated with the F, E, D and C faults, Fig. 4.17; so too is lead, although it increases in concentration dramatically in the E and F faults, Fig. 4.21. Mercury, Fig. 4.18, shows a sympathetic relationship to zinc and lead, although, unless mineralization is actually present in the sample analysed, mercury levels are very low, suggesting only minor lateral migration of this element.

Silver distribution on the 500' level, Fig. 4.20, appears to be somewhat the reverse of lead, the $^{Zn}/_{Ag}$ ratio decreasing southwards. Copper distribution is also fault associated, Fig. 4.19 although its specific relationship to zinc concentration is extremely tenuous, Fig. 4.22b. The mainly clastic sediments of the 500' level do not really appear to have any marked effect on the distribution of ore.

Experiments were carrried out on each level of the prospect, using rock samples which had been crushed and sieved into three mesh

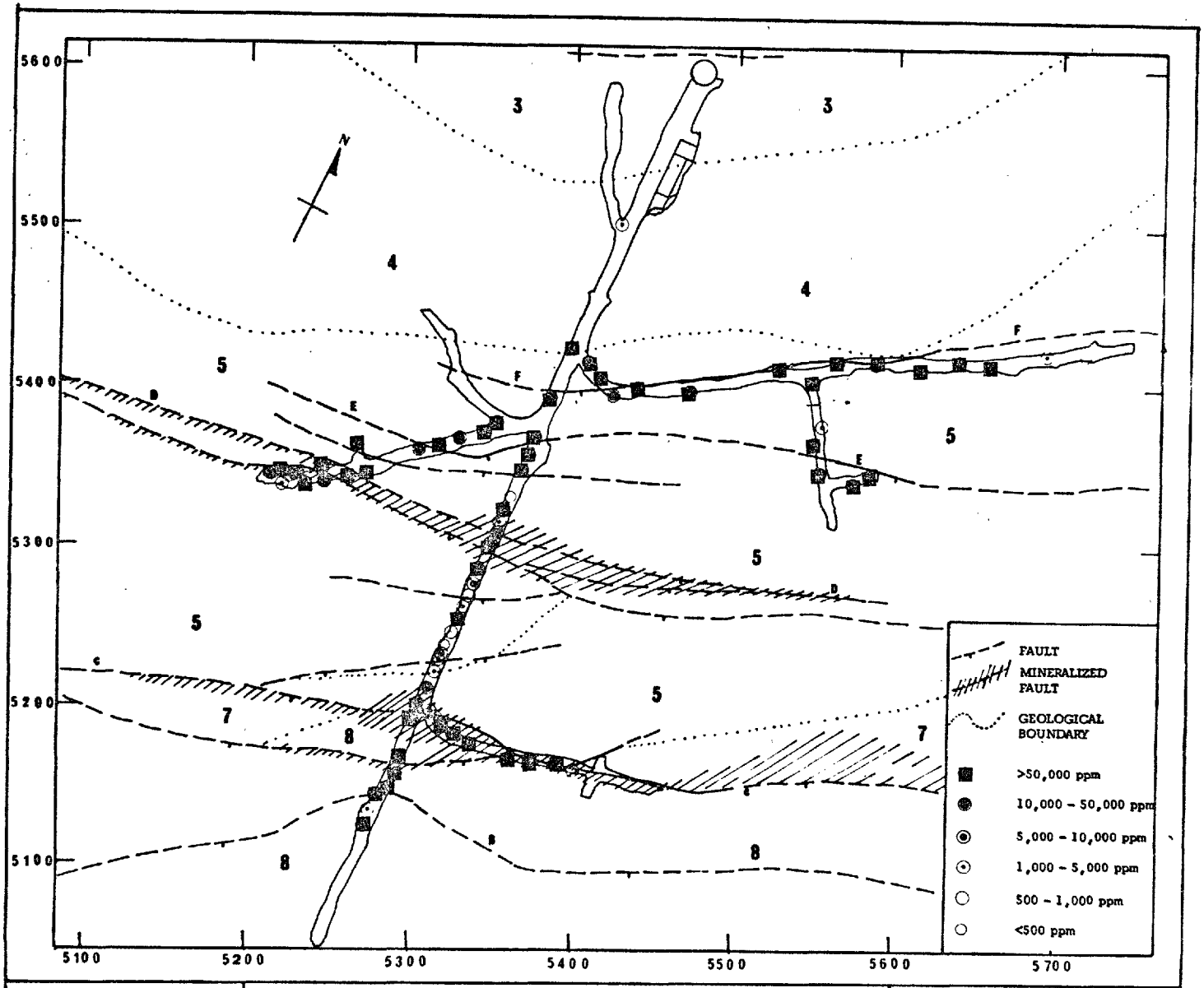


FIG ... 4.17 Zn DISTRIBUTION ON THE 500' LEVEL, KEEL. SCALE : 0 50 100 FEET

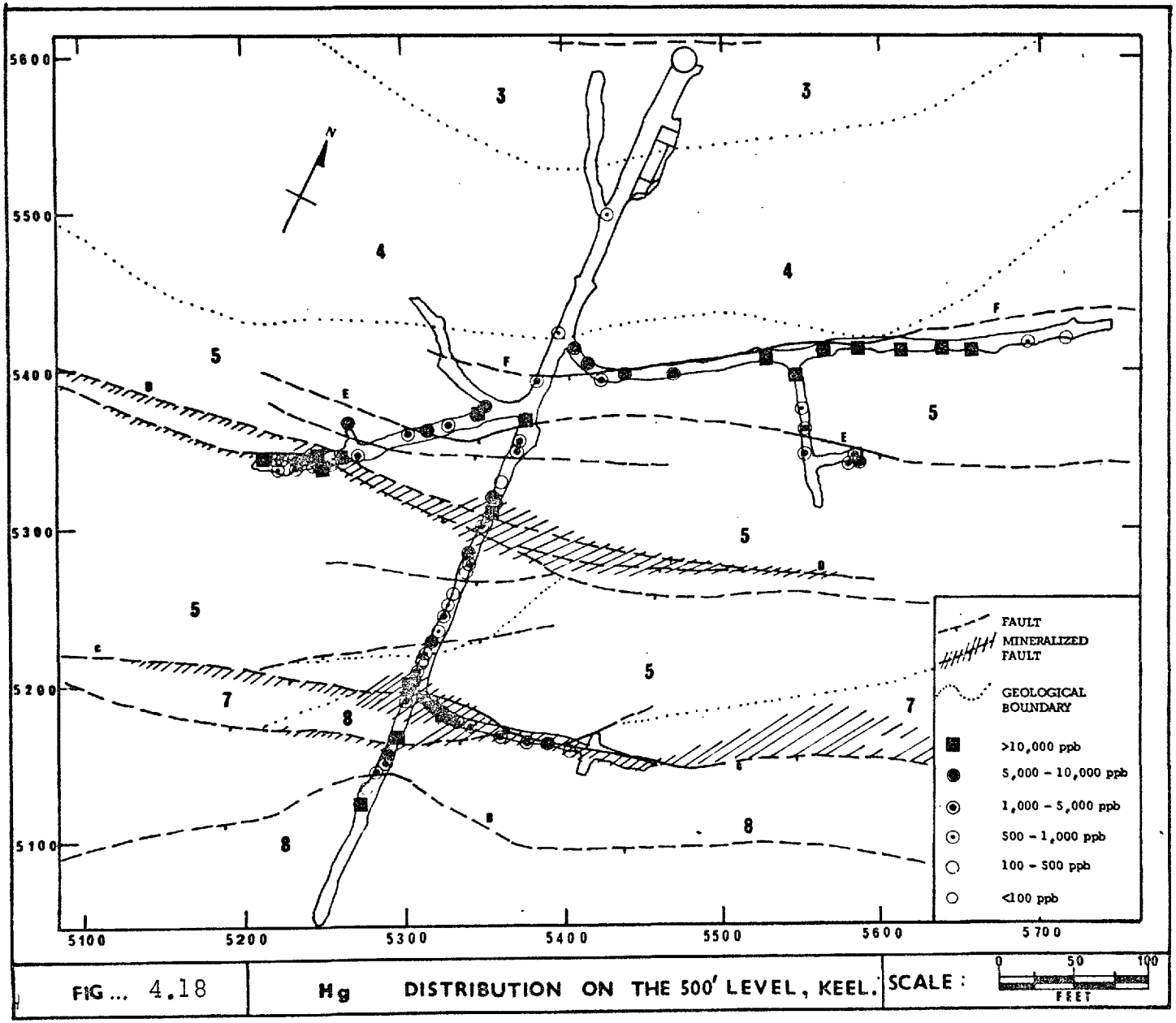


FIG... 4.18 Hg DISTRIBUTION ON THE 500' LEVEL, KEEL. SCALE :

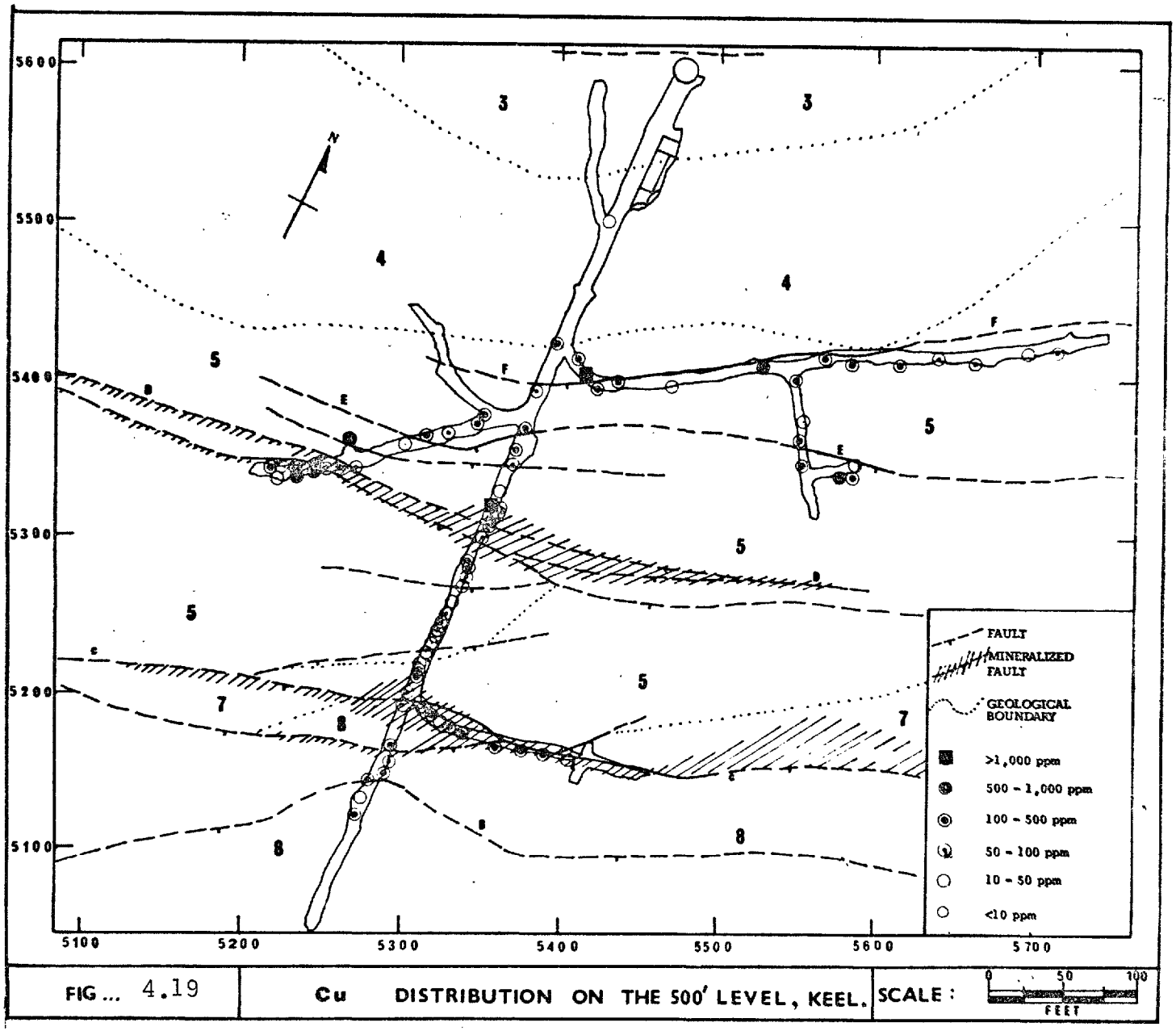


FIG... 4.19 Cu DISTRIBUTION ON THE 500' LEVEL, KEEL. SCALE :

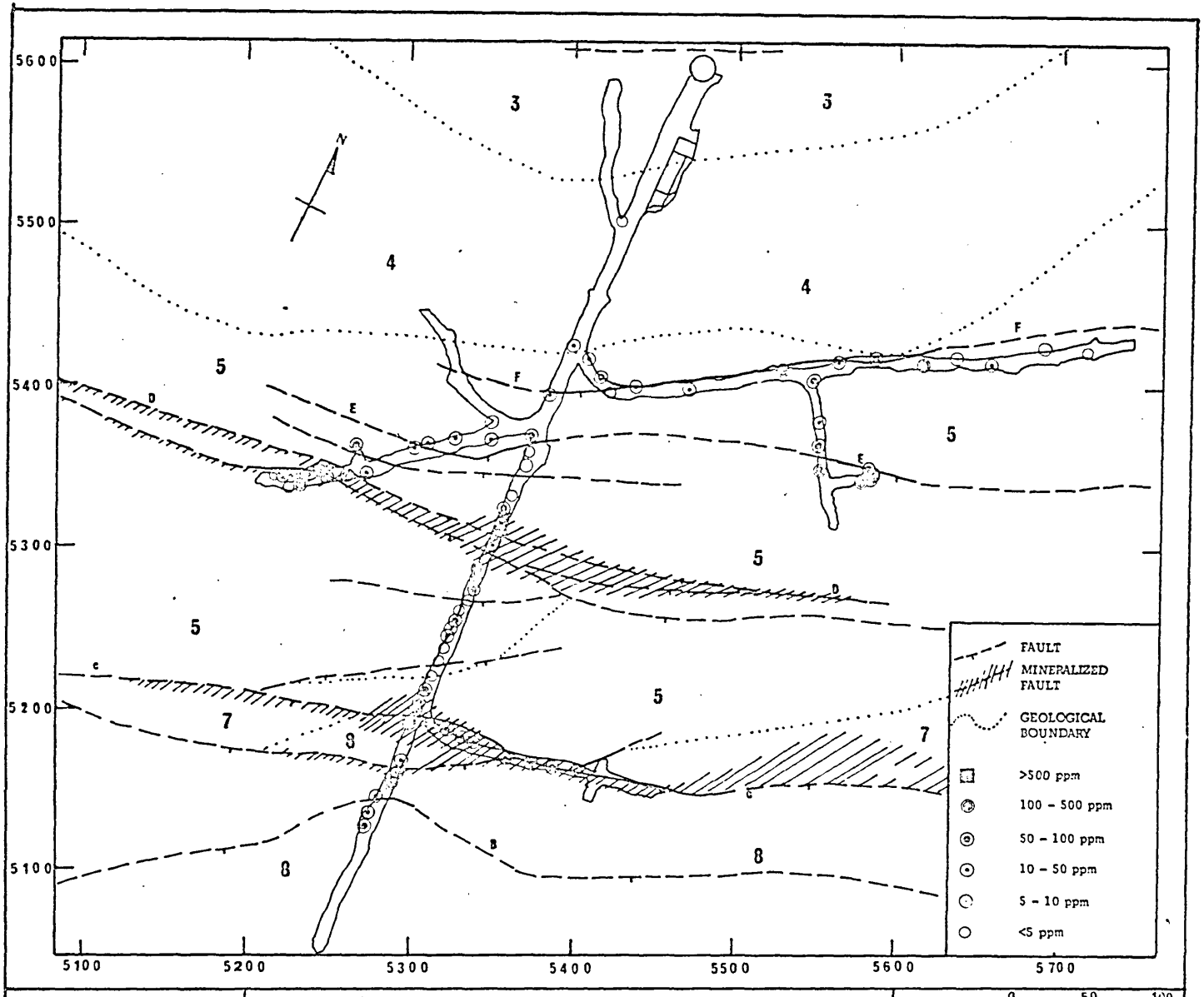


FIG... 4.20 | Ag DISTRIBUTION ON THE 500' LEVEL, KEEL. | SCALE :

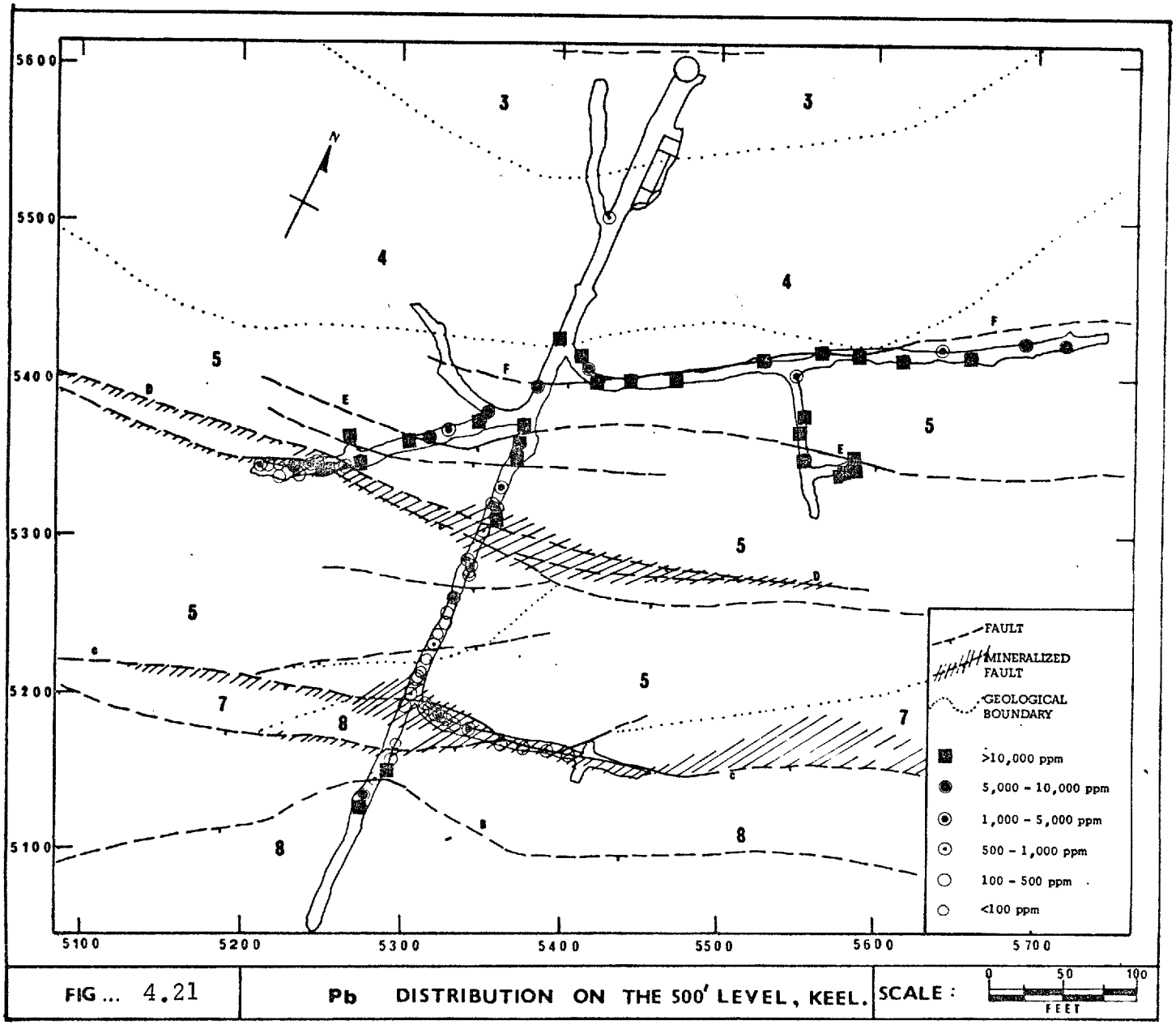
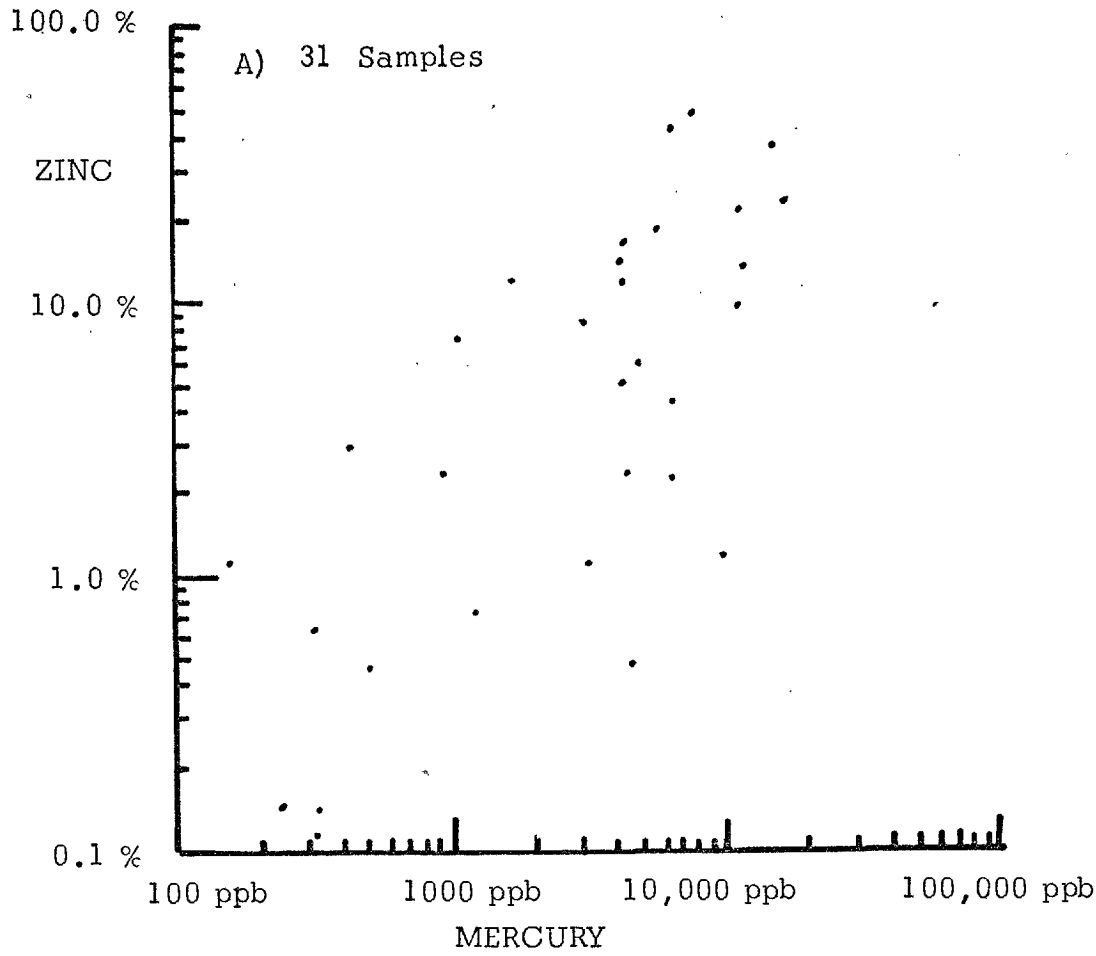


FIG ... 4.21 | Pb DISTRIBUTION ON THE 500' LEVEL, KEEL. | SCALE :



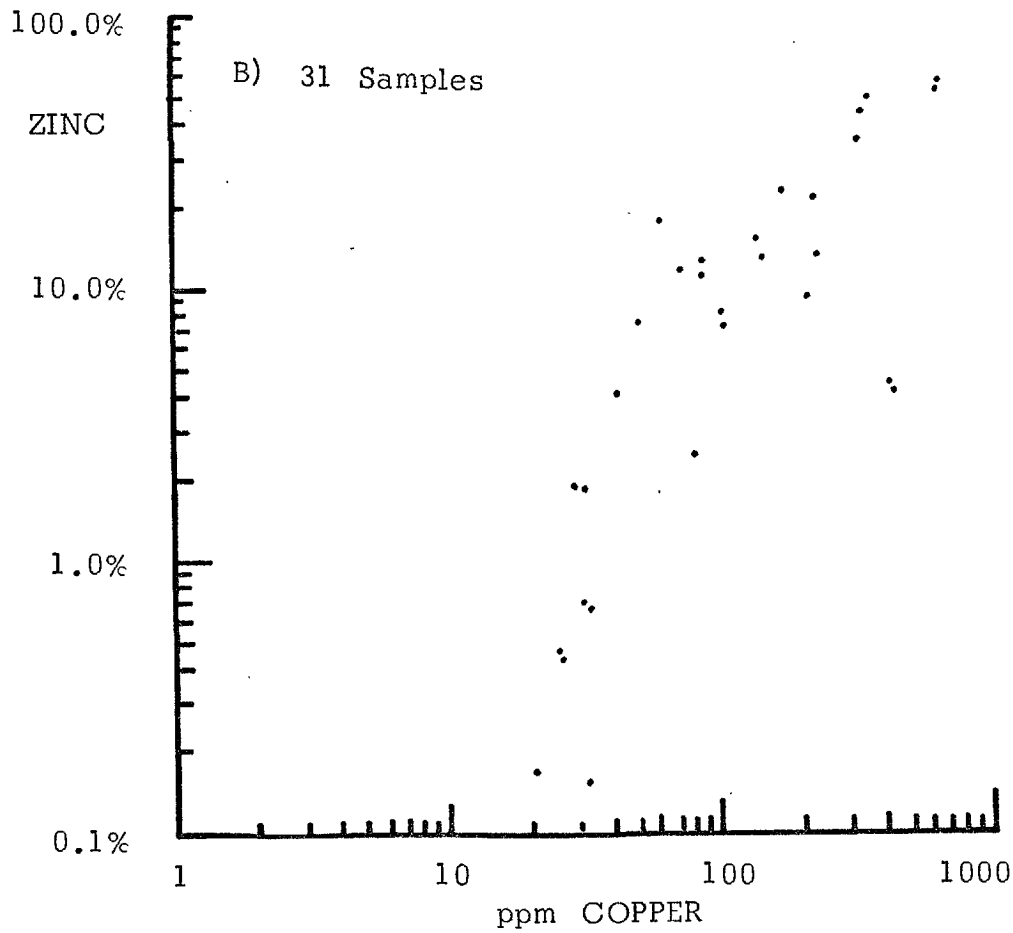


FIG ... 4.22

RELATIONSHIP OF COPPER & MERCURY TO ZINC ON THE 500' LEVEL, KEEL PROSPECT

sizes to ascertain the effect of fraction size on the distribution of trace elements in the rock. The three mesh sizes used were as follows: - 210 µm, - 494 µm + 210 µm and - 1550 µm + 494 µm. A ground, - 53.5 µm sample of the same rock was analysed as a standard against which each mesh size was compared. The results of this survey have been discussed in Chapter 3.

Mercury however, displayed differences between the results obtained respectively from drill core and underground samples. The results are tabulated in Table 4.2.

TABLE 4.2. Variation of mercury content with fraction size of rock from the underground workings, Keel prospect.

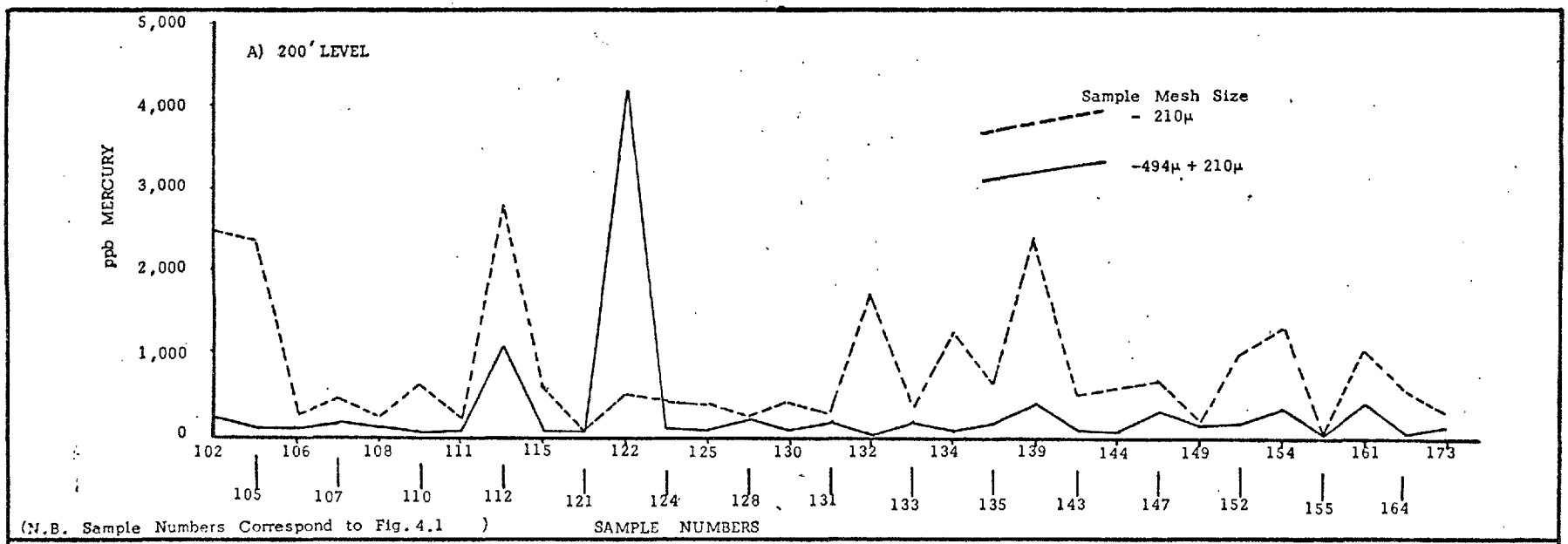
Sample	- 210 µm	- 494 + 210 µm	-1550 + 494 µm
DK1	665	152	90
DK2	2575	280	174
DK3	2420	144	84
DK4	300	140	106
DK5	525	206	16
DK6	240	170	130
DK7	2855	1180	720
DK8	1330	160	80
DK9	705	184	116
DK10	2460	390	49
DK11	1075	216	139

Results expressed as p p b

From these results it can be seen that, unlike the drillcore material, there is a definite increase in mercury content with decreasing fraction size. This observation was attributed to the increase in zinc and lead with decreasing fraction size. When a series of samples from the 500' level were analysed in this way, the picture illustrated in Fig. 4.23 emerged. Sample numbers correspond to samples on Fig. 4.3, the horizontal scale being entirely arbitrary. Here it can be seen that generally the - 210μm mesh size has higher mercury values than the - 494 μm+ 210μm, however occasionally very high values for the - 494μm + 210μm mesh size swamp lower values for the equivalent - 210μm mesh. It was concluded that the main cause of this discrepancy was because mercury must be held in a different way in these samples than in the others from the underground workings. These samples were thought to contain a predominance of pore and fracture held mercury gas which was released on crushing. The validity of this conclusion is discussed in Chapter 8.

If the 200' level is now considered, the main feature on this level is the C fault at the southern end of the main cross-cut south. This is a normal fault down thrown to the south bringing Bioclastic limestone against the Upper Mixed Beds and separating the two by a thick fault gouge. Patterson (1970) suggests that mineralization was dammed up against this fault, a conclusion corroborated by the distribution of zinc on the traverse, Fig. 4.10b.

A traverse, Fig. 4.10, was taken from west to east along the underground workings on the 200' level and the distribution of Hg, Zn, Cu, Pb and Ag along it plotted. Again there appears to be a reasonable sympathetic relationship between all base metals although when plotted graphically no close correlation is obtained. Zinc shows



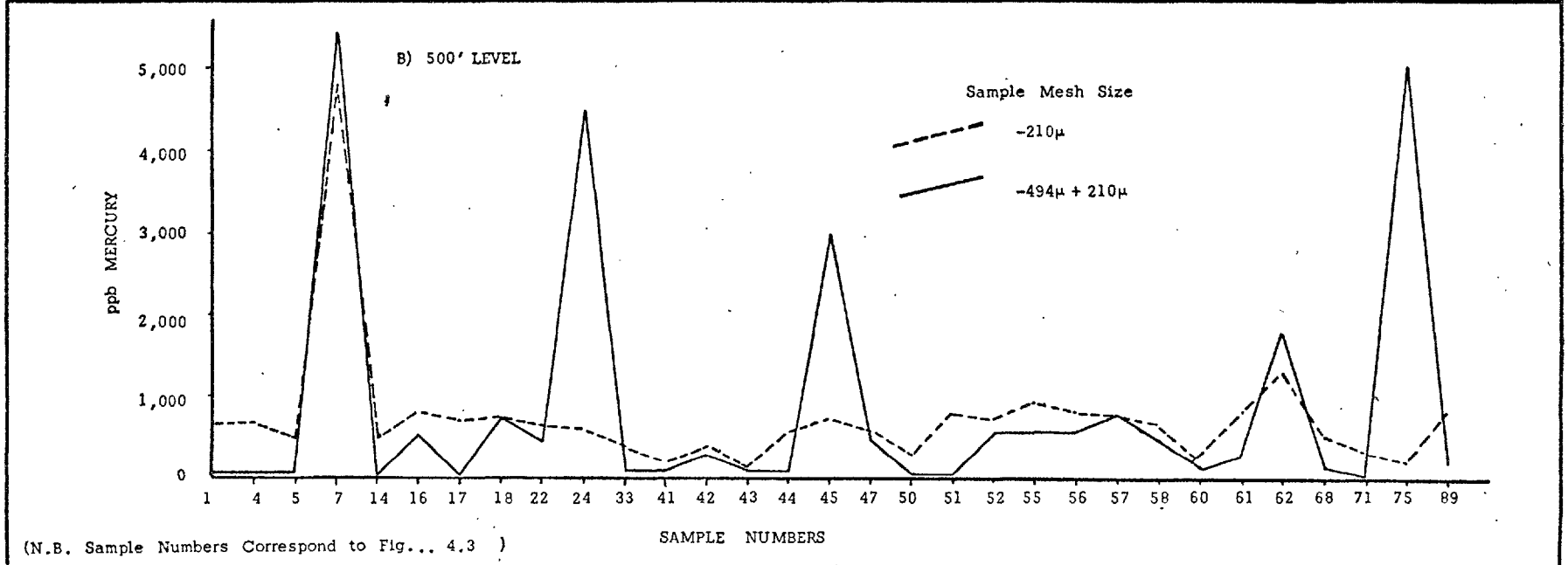


FIG ... 4.23	DIAGRAM ILLUSTRATING THE VARIATION OF MERCURY CONCENTRATION WITH GRAINSIZE ON THE 200' & 500' LEVELS, KEEL.

major fluctuations in concentration and abundant evidence of a build-up towards the C fault is present, together with a sharp fall off of concentration in the Bioclastic Limestone, Fig. 4.10b. Lead, too, exhibits these changes, but to a lesser degree, Fig. 4.10d. Copper, while diminishing in concentration in the fault gouge, reaches average values again some 20' into the Bioclastic Limestone, Fig. 4.10c. Silver and mercury can also be seen to follow the copper trend, Figs. 4.10b and 4.10a respectively.

When maps of the distribution of Cu, Pb, Zn, Hg and Ag on the underground workings of the 200' level are plotted, a similar picture emerges, Figs. 4.11 - 4.15. Zinc is predominantly associated with the F, E, D and C faults and the $^{Zn}/_{Pb}$, $^{Zn}/_{Cd}$ and $^{Zn}/_{Ag}$ relationships of these faults are shown in Table 4.3 for the 200' level.

TABLE 4.3. Zn/Pb, Zn/Cd and Zn/Ag Ratios in the F, E, D and C Faults, Keel Prospect, County Longford, Eire.

Fault	Zn/Pb		Zn/Cd		Zn/Ag		Number of Samples
	Mean	Standard Deviation	Mean	Standard Deviation	Mean	Standard Deviation	
F	51.83	71.94	162.8	122.9	573.0	906.5	11
E	59.54	86.10	185.3	141.1	573.0	1021.7	13
D	784.4	981.5	447.0	1136.0	4597.0	8776.0	9
C	53.56	73.84	186.3	60.58	2861.0	1945.0	16

The $^{Zn}/_{Pb}$ ratio nowhere attains the low values of the F and E faults on the 500' level and generally, there appears to be far more lead on the 500' level than the 200' level. Cadmium also appears to be more abundant on the 500' level than the 200' level although cadmium bloom is seen on the fault plane of the C and D faults on the 200' level. This bloom is probably not due, on the 200' level, to solution of greenockite from the wallrocks, but to solution of cadmium from the sphalerite by the abundant circulating groundwater down the C and D faults. The $^{Zn}/_{Ag}$ ratio of the 200' level appears to be lower for the F and E faults by nearly an order of magnitude over anything on the 500' level, suggesting that either silver-rich sphalerite is more abundant in this region or that a separate silver phase exists in the wallrocks.

The plans of the trace element distribution on the 200' level indicate that lead is far less abundant here than the 500' level. Mercury too appears to be in lower concentration on the 200' level, Fig. 4.14, although the sphalerite contains approximately the same amount of mercury in its lattice (Chapter 6).

Comparisons of mercury content of various fractions were also carried out on this level and the results are shown in Fig. 4.23a. Here there is illustrated a far more uniform result, the finer mesh size almost invariably containing more mercury. This suggests that, if pore and fracture held mercury is the reason for periodic increases in mercury content with increasing particle size, then there is less pore and fracture held mercury on the 200' level than on the 500' level. The validity of this statement is discussed in Chapter 8.

The underground workings on the 400' level have by far the smallest extent. They are mainly cut in Upper Quartz Sandstone and

mineralization is abundant with high grade lead mineralization to the north of the shaft. Lead appears to be more abundant on the 400' and 500' levels than on the 200' level and this further suggests a greater relative concentration of lead to zinc with depth. Fig. 4.24 shows the distribution of Hg, Zn, Cu, Pb and Ag on a traverse along the 400' level from south to north. Here again a good sympathetic relationship between base metals is seen, although an area of very high lead values and very low silver values just west of the shaft presents an anomaly to this pattern. However, zinc values are low here and as the silver-zinc relationship is relatively good,then this low silver could be a function of low zinc.

Figs. 4.25 - 4.29, show the distribution of Hg, Zn, Cu, Pb and Ag on the 400' level. Relationships are the same as with the 500' and 200' levels; mercury shows closer association with zinc than lead and so does silver. Copper is fairly uniform although it too shows closer association with zinc than lead. Fig. 4.30 shows a histogram plot of the distribution of Cu, Pb, Zn, Ag and Hg on the 200', 400' and 500' levels and it too indicates an increasing abundance of base metals with depth.

4.6. CONCLUSION

In conclusion it can be said that little clear cut primary dispersion is in evidence on the underground workings of the Keel prospect, and really only very broad, general trends can be inferred from a study of the geochemistry of the primary environment of this deposit.

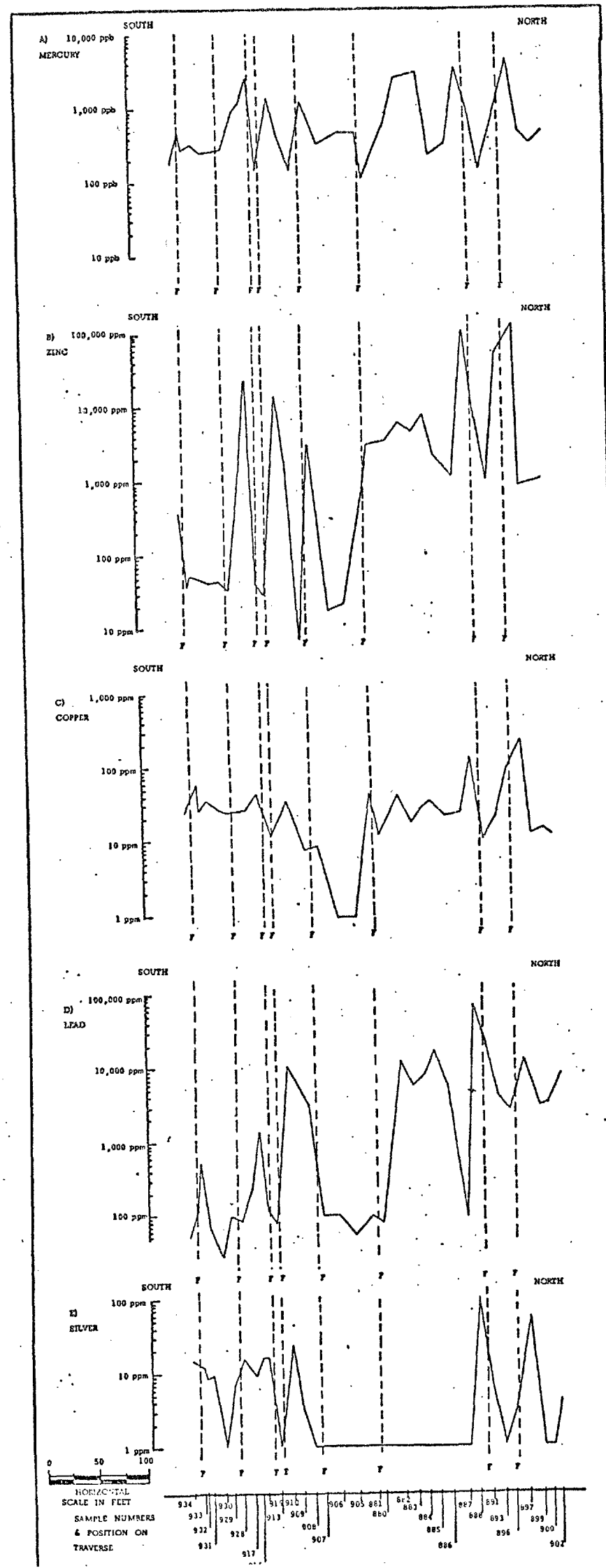


FIG ... 4.24

RELATIONSHIP OF Cu/Pb/Ag/Zn/Hg. ON THE 400' LEVEL KEEL PROSPECT, COUNTY LONGFORD, IRELAND.

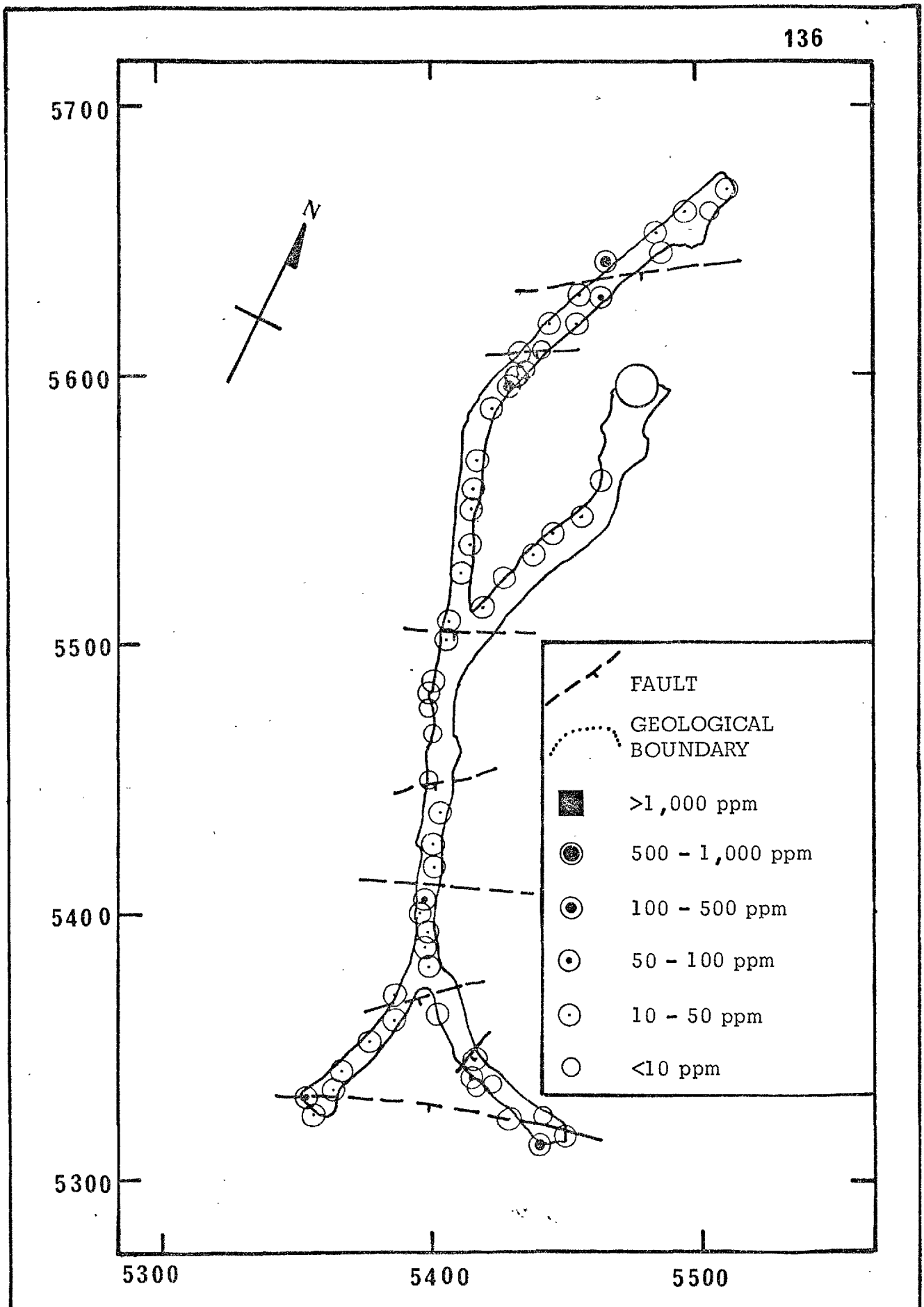


FIG ... 4.25

COPPER DISTRIBUTION ON THE 400' LEVEL, KEEL.

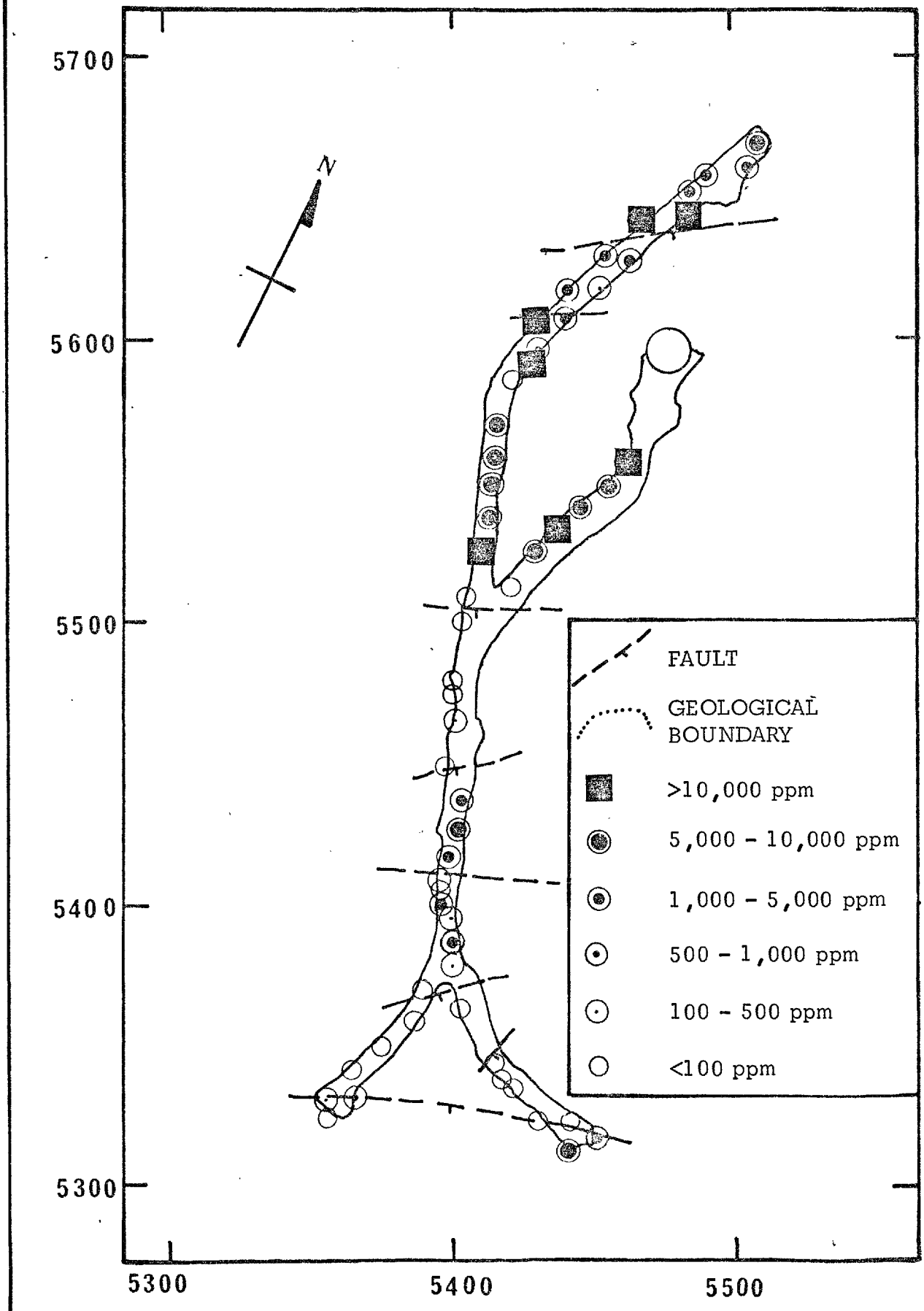


FIG ... 4.26

LEAD DISTRIBUTION ON THE 400' LEVEL, KEEL.

0 50 100

SCALE IN FEET

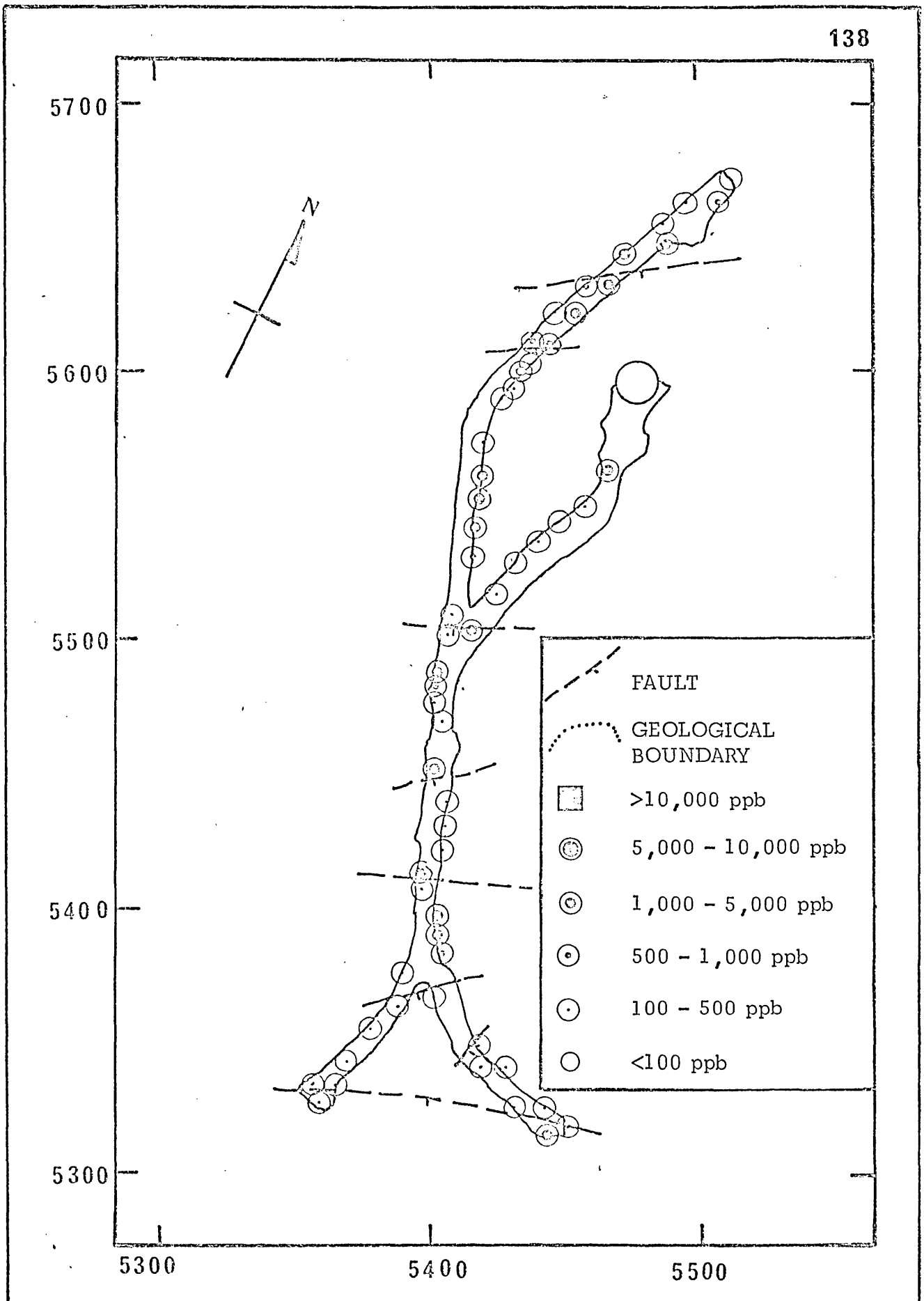


FIG ... 4.27

MERCURY DISTRIBUTION ON THE 400' LEVEL, KEEL.

0 50 100

SCALE IN FEET

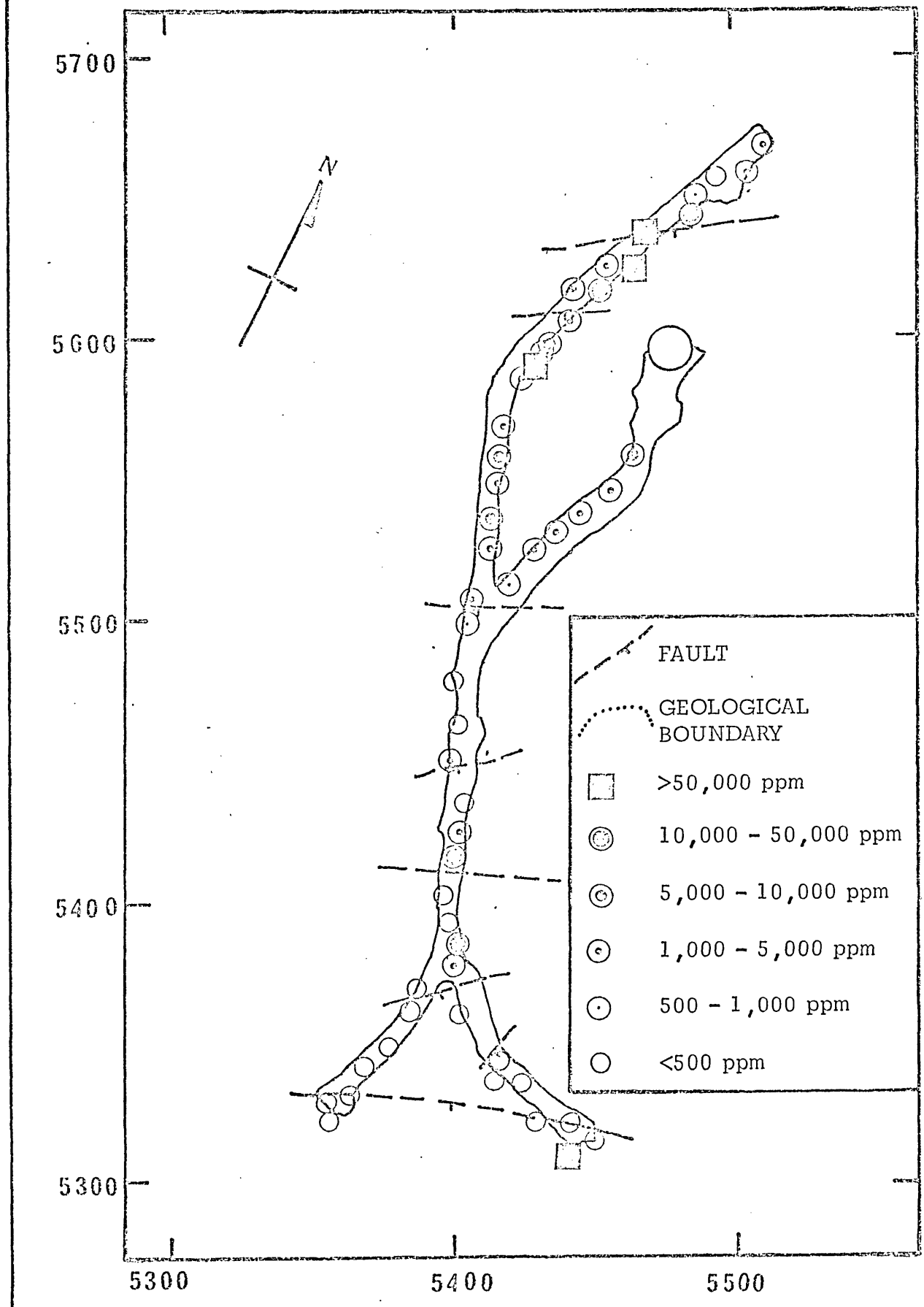


FIG ... 4.28

ZINC DISTRIBUTION ON THE 400' LEVEL, KEEL.

0 50 100
SCALE IN FEET

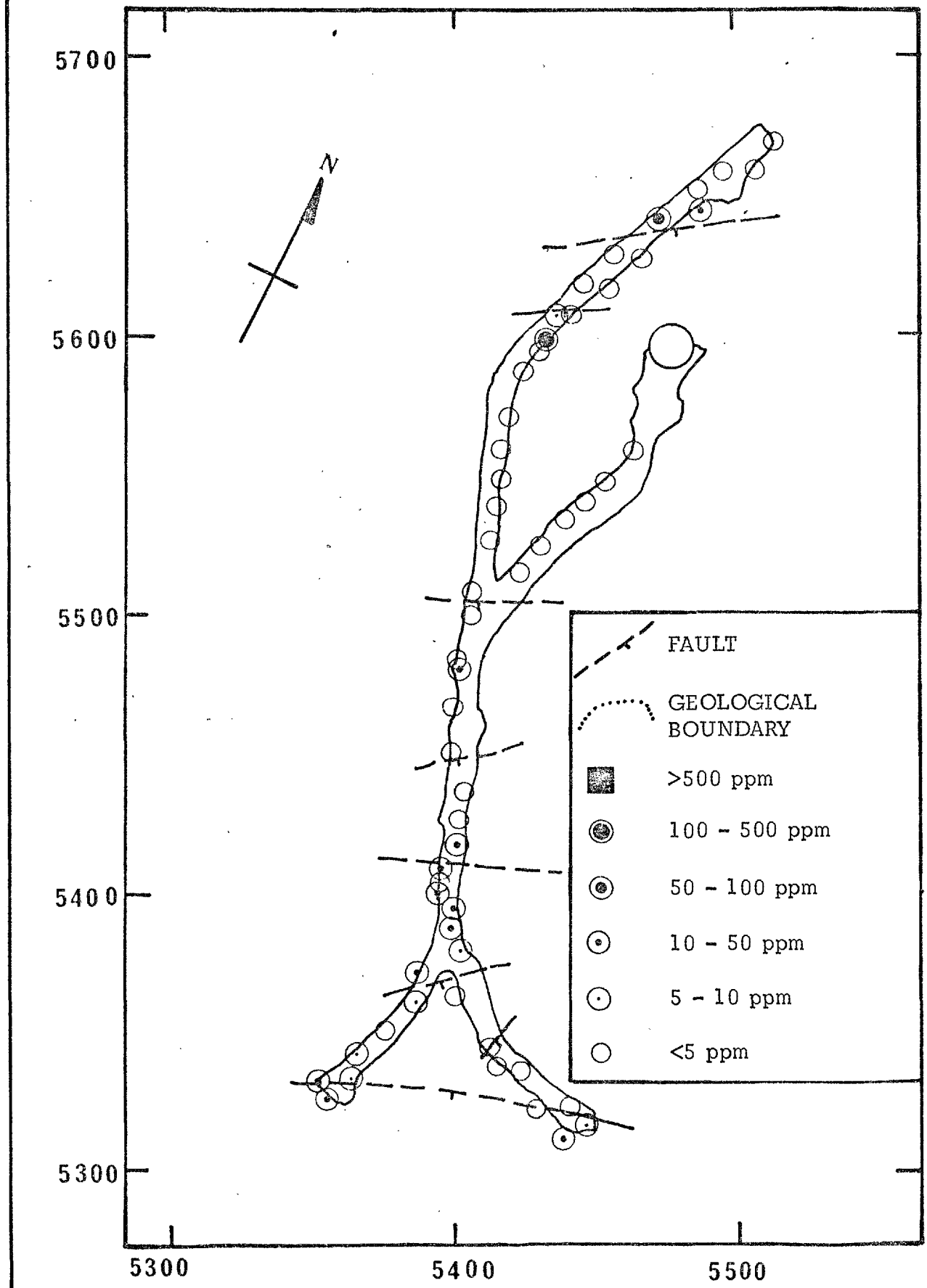


FIG ... 4.29

SILVER DISTRIBUTION ON THE 400' LEVEL, KEEL.

0 50 100

SCALE IN FEET

Numbers Indicating Class Distribution of the Various Elements Correspond to Concentration Levels on Fig...4.11 - Fig...4.15

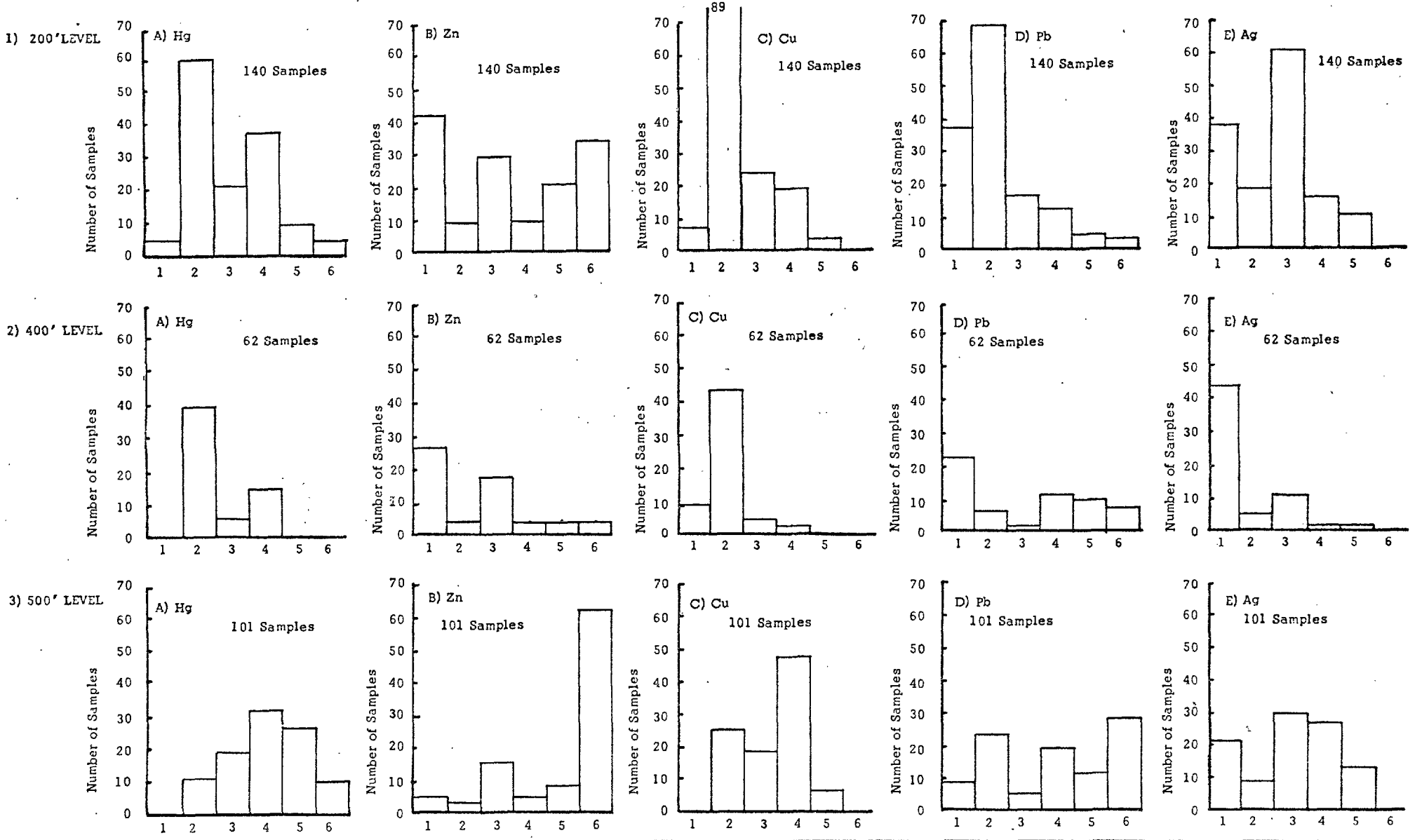


FIG ... 4.30

HISTOGRAM PLOT OF THE DISTRIBUTION OF MERCURY, ZINC, COPPER, LEAD, SILVER ON THE UNDERGROUND WORKINGS, KEEL PROSPECT, COUNTY LONGFORD.

CHAPTER 5

PRIMARY DISPERSION OF FLUORINE AND CHLORINE IN WALL ROCKS SURROUNDING THE KEEL ZINC-CADMIUM PROSPECT.

5.1. INTRODUCTION

Mineralization at Keel, as already stated, is epigenetic and hydrothermally introduced along southerly dipping east-west fault planes. The primary dispersion halo of copper, lead, zinc, silver, mercury and other selected trace elements has already been shown in Chapters 3 and 4 to be almost negligible. Because of this lack of primary dispersion it was decided to investigate the primary dispersion of fluorine and chlorine. These elements were chosen for investigation because of their possible importance as constituents of the hydrothermal solutions carrying the base metals in the Keel area.

A considerable amount of research has been carried out on hydrothermal solutions and brines and their relationship to base metal sulphide mineralization, Barnes and Czamanske (1967), Dunham (1966), Follingshee (1967) etc. Here therefore, it is necessary to first consider the cycle of fluorine and chlorine before commenting on the distribution of these elements in the Keel area.

5.2. CYCLE OF FLUORINE AND CHLORINE.

An interesting feature of the halogens is that they form few insoluble salts, therefore they are not easily precipitated and consequently have great mobility.

Fluorite is the most common fluorine mineral and is very resistant to weathering processes. However the fluorite which does

dissolve, can be transported as alkali fluorides into both seas and rivers, where it can be deposited as calcium fluoride or in evaporate sediments. Calcium fluoride may be removed by co-precipitation with barium sulphate, calcium carbonate and calcium phosphate and consequently may be present in many marine sediments. Fluoride can be strongly adsorbed onto clay minerals and up to 8,000 p p m fluorine in bentonite has been reported (Robinson and Edgington, 1946). Shepherd (1935) found 1,200 p p m fluorine in a bottom mud from the Pacific Ocean, while Barth and Brunn (1945) reported 280 p p m fluorine in Ordovician limestones and 540 p p m fluorine in Ordovician and Cambrian shales.

Chlorine is associated with volcanic activity and hydrogen chloride is a common constituent of volcanic gases.

Chlorine goes readily into solution on weathering as alkali and alkaline earth chlorides. Rankama and Sahama suggest that when chloride solutions are brought into contact with heavy metals, particularly mercury, silver, copper and lead in the surficial parts of orebodies, insoluble, or sparingly soluble chlorides of these metals will be precipitated, e.g., chlorargyrite, Ag Cl; cotunnite, $PbCl_2$; nantokite, CuCl; calomel, Hg_2Cl_2.

On weathering, however, the majority of chloride is carried into the sea and only a minute fraction of that found in the oceans will ever crystallize as halite, NaCl.

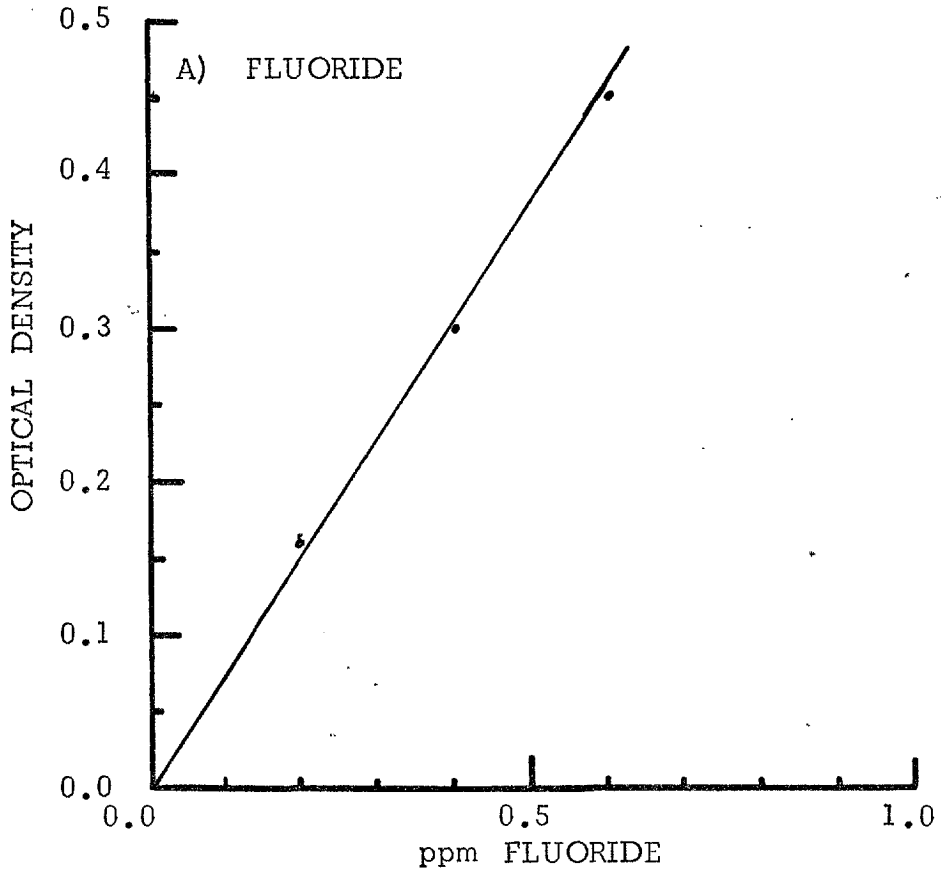
5.3. METHOD OF ANALYSIS

Ten grammes of −53.5 μm ground rock material were placed in a 500 ml. plastic screw-top jar and fifty ml. of deionised water added. The jar was continuously agitated at room temperature for thirty six hours to remove water-soluble fluoride and chloride. After this time the suspension was allowed to settle for four hours and then the supernatant water was filtered, under pressure, through a 0.45 μ Millipore filter into a Buchner collecting flask and used for the following determinations:

(a) Colourimetric Determination of Fluorine

Ten millilitres of the filtered solution was placed in a small diffusion bottle and 5 ml. of analar perchloric acid added to it. A filter-paper wick, moistened with one drop of 0.5N sodium hydroxide solution, was then suspended above the liquid and the bottle sealed. Diffusion was allowed to proceed for twenty four hours at 50°C.

At the end of the diffusion period the paper absorber was removed to a beaker and leached with 10 ml of 0.1M sodium succinate solution. After allowing this to stand for about five minutes, ten millilitres of a mixture of 2×10^{-3}M Lanthanum nitrate and 2.2×10^{-3}M alizarin fluorine blue were added to the beaker and the mixture transferred to a 50 ml. volumetric flask and diluted to the mark with deionised water. The optical density of the solution was measured at 625 nμ. in 1cm. quartz cells. The calibration curve for quantitative determination of fluorine is shown in Fig. 5.1a.



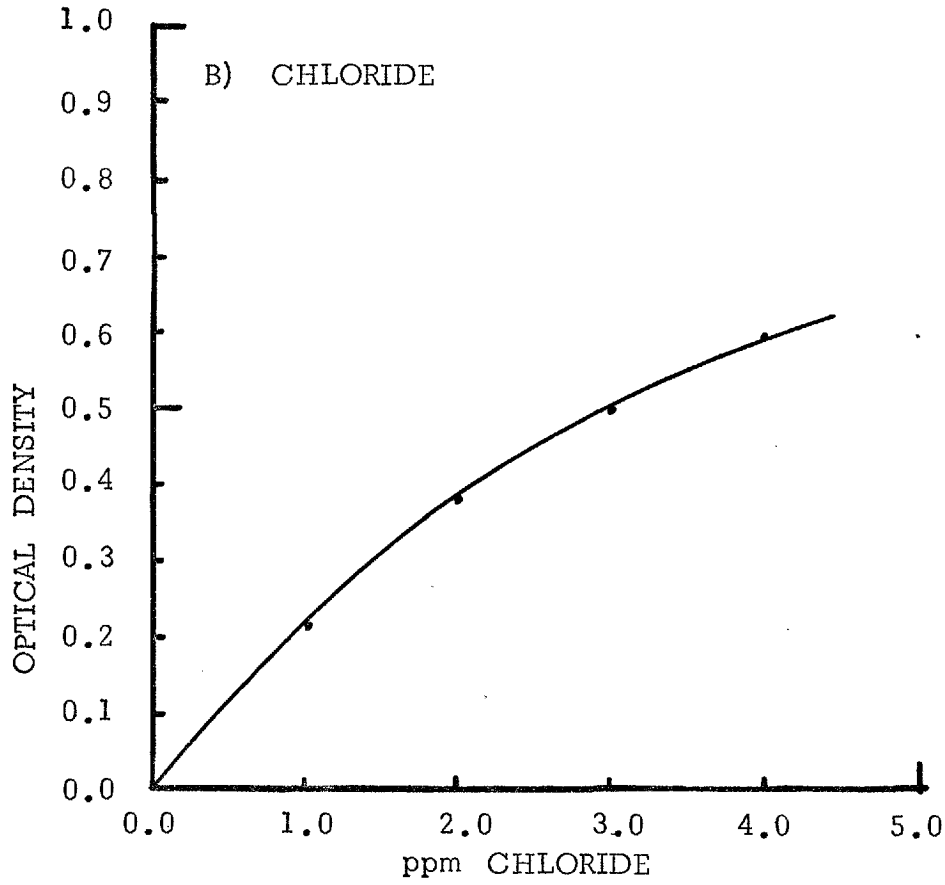


FIG ... 5.1 DIAGRAM OF THE CALIBRATION CURVES FOR FLUORIDE AND CHLORIDE ANALYSIS

(b) Turbidimetric Determination of Chloride.

0.2 ml of 0.05N silver nitrate solution and 1ml. of 1N HNO_3 were transferred to a 1cm. quartz spectrophotometer cell and 5 ml. of the filtered rock solution added. A slight turbidity formed and the optical density of this was measured at 400 mμ. The calibration curve for the quantitative determination of chloride is shown in Fig. 5.1b.

5.4. DISCUSSION OF THE METHOD OF ANALYSIS.

Experiments were carried out to ascertain the effects of time and light on the optical densities of the standard solutions of fluoride and suspensions of chloride. It was discovered that, once the fluoride colour complex had formed, the solution could be left for period of up to five days without any change. After this period some deterioration was noted and the optical densities of the standards fell, relative to fresh standards. However the chloride standards proved more unstable. A series of chloride standards were made up and analysed every minute for eight minutes. The calibration graphs obtained are illustrated in Fig. 5.2. This graph change from the normal convex to concave outline when the standard solution is left for periods longer than one minute is probably due to the formation of flocculated colloidal masses in suspension. A plot of relative changes in optical density of the standards with time, Fig. 5.3. indicates this possible flocculating effect to a much greater extent. During a four minute standing period, a 10 p p m chloride suspension gradually increases in optical density and then, after some six minutes, settles down to a standard level. It appears that for periods of up to four

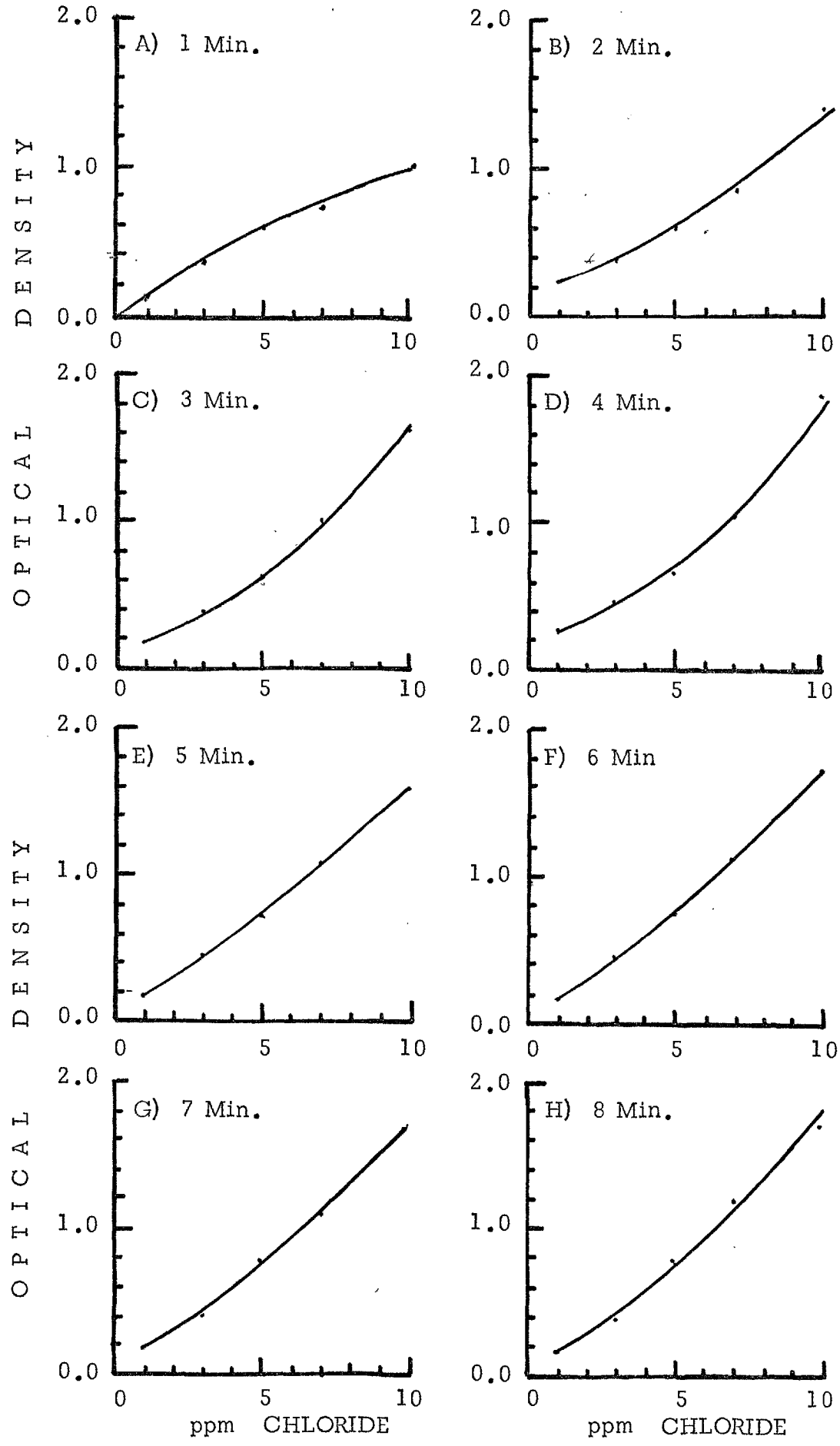


FIG ... 5.2

DIAGRAM SHOWING THE VARIATION WITH TIME OF OPTICAL DENSITY OF STANDARD COLLOIDAL SUSPENSIONS OF SILVER CHLORIDE

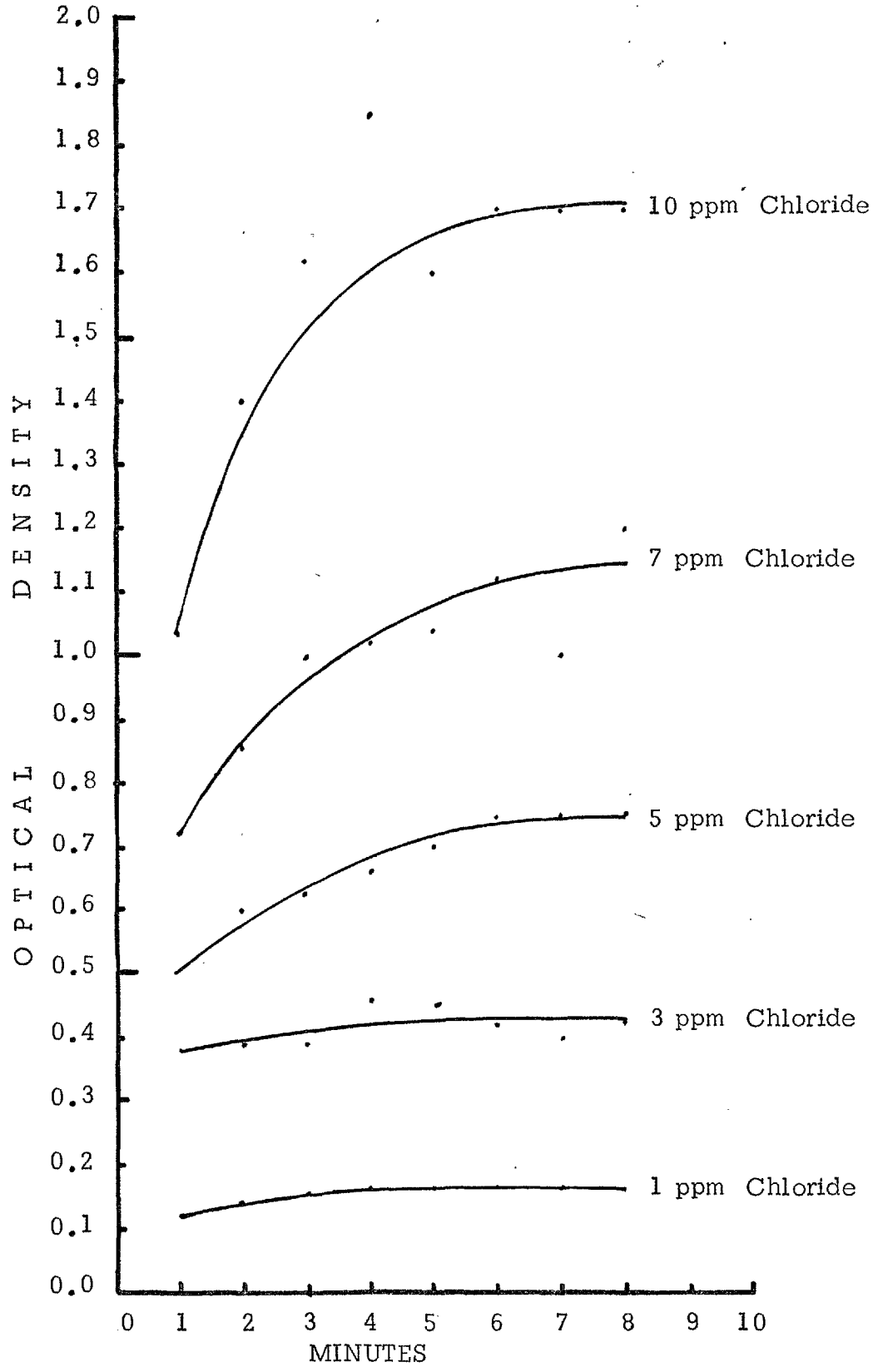


FIG ... 5.3 DIAGRAM OF THE RELATIVE VARIATION WITH TIME OF OPTICAL DENSITY OF STANDARD COLLOIDAL SUSPENSIONS OF SILVER CHLORIDE.

minutes standing, a gradual increase in $AgCl_2$ in suspension is taking place until a maximum level of optical density for the solution is obtained. The optical density then falls quite dramatically as if precipitation is taking place and then settles out to a uniform level, indicating a possible equilibrium condition. The lower concentration standards also show this effect but to a much more supressed level.

On the basis of this evidence it was decided to analyse all solutions individually, immediately after the addition of all reagents, and to run a standard solution with each unknown to further eliminate the possibility of error.

For complete standardization of the chloride method, rock standards G.1 and W.1. were also analysed for chloride.

5.5. ANALYSIS OF G.1 and W.1 FOR CHLORIDE.

Two hundred milligrammes of G.1 and W.1 were first boiled with 25 ml. of conc. nitric acid. The solution was then centrifuged to precipitate all suspended rock material and split into two, one half being used as a reference blank. 0.2 ml of 0.05N. $AgNO_3$ solution was added to a quartz spectrographic cell and 5 ml. of the nitric acid rock leach added to this. The optical density of the suspension was read at 400 nμ, taking care that less than one minute had elapsed after the addition of all reagents.

The following results were obtained for duplicate analyses of G.1 and W.1.

G.l.	Chloride content	W.l.	Chloride content
	109 p p m		256 p p m
	103 p p m		245 p p m

Cloride content of G.l and W.l. had been carried out by neutron activation analysis and recorded in the literature (Fleischer). The analyses obtained were as follows:-

G.l.	Chloride content	W.l.	Chloride analysis
	90 p p m		191 p p m
	63 p p m		187 p p m
	130 p p m		270 p p m
	19 p p m		256 p p m
			206 p p m

As can be seen, agreement in the literature is poor, nonetheless a reasonable correlation between literature results and the present study does exist.

5.6. ANALYSIS OF ROCK MATERIAL FROM KEEL FOR FLUORINE AND CHLORINE.

Eighty nine samples of drillcore, from nine different drill-holes, were prepared and analysed for fluorine, chlorine, sodium potassium, calcium and magnesium. The results obtained are summarized for D.D.H.K.1. and D.D.H.K.14. in Fig. 5.4. Here, there can be seen to be a reasonably sympathetic relationship between sodium and chlorine, which would be expected in marine sediments; the chloride values are however much lower than the sodium values. There does not appear to be any other inter-element relationship. Sodium, potassium, calcium and magnesium concentrations are very high, relative to fluorine and chlorine, and the presence of soluble carbonates and bicarbonates of

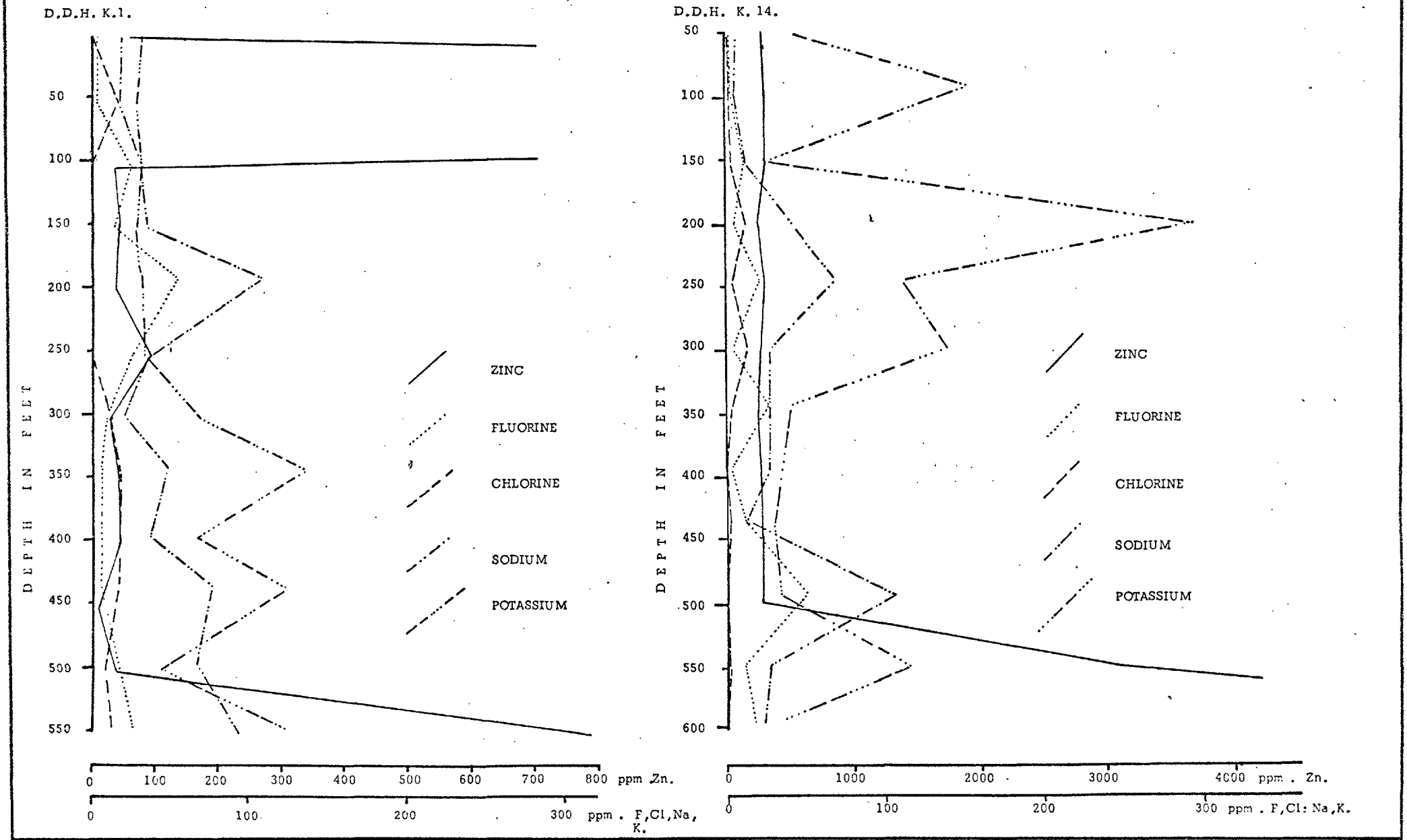


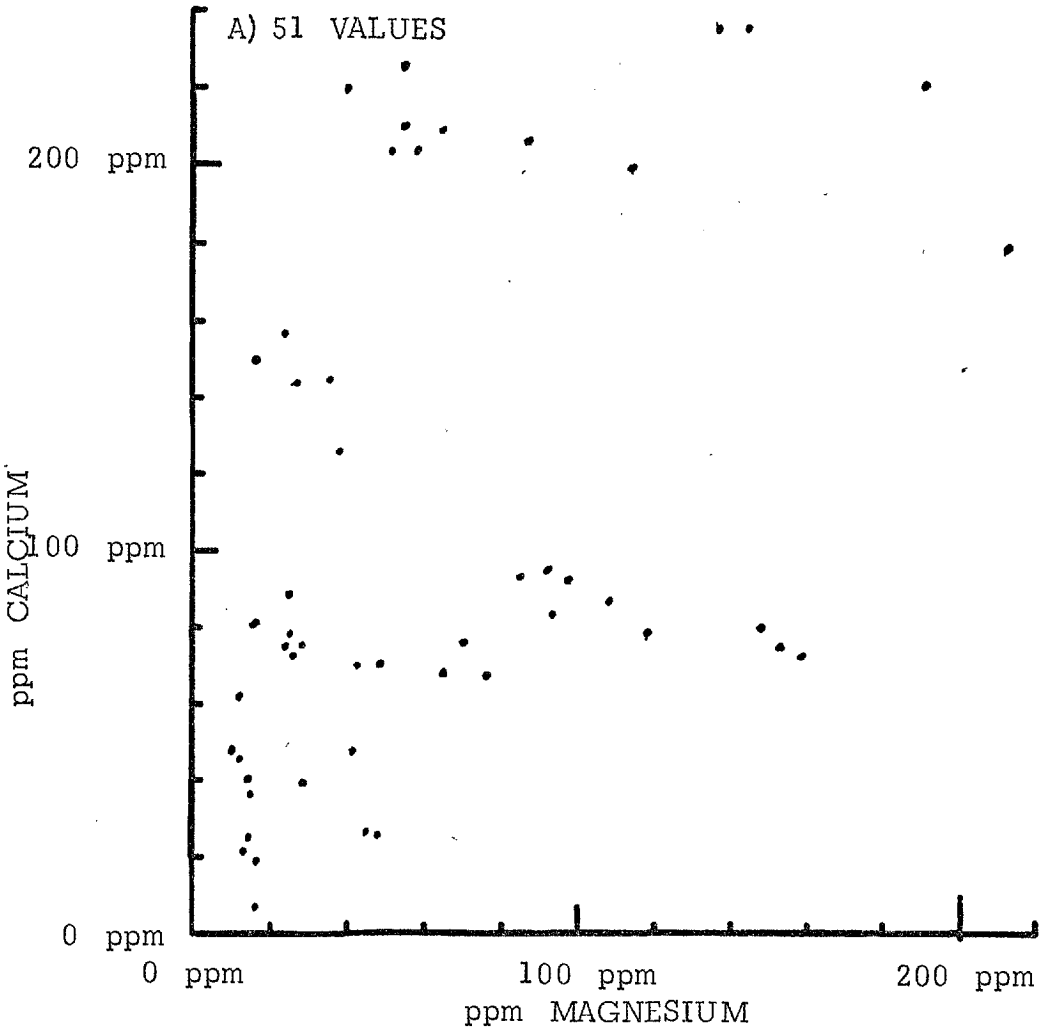
FIG ... 5.4

DIAGRAM ILLUSTRATING THE RELATIONSHIP BETWEEN ZINC , SODIUM , POTASSIUM , FLUORINE , CHLORINE IN D.D.H. 1 , & D.D.H. 14 , KEEL PROSPECT , COUNTY LONGFORD , IRELAND.

these elements is suspected in the drillcore material.

Absolutely no relationship between fluorine and chlorine, Fig. 5.5b, or between fluorine, chlorine and the extent of base metal mineralization, Fig. 5.4, can be found. Specific element relationships in the leach from ground drillcore were plotted to try and make more sense of the results. Fig. 5.5b shows a plot of fluorine against chlorine and Fig. 5.5a, a plot of calcium against magnesium. As can be seen from both these diagrams, absolutely no relationship exists. Fluorine to zinc and chloride to zinc, Fig. 5.4., also show no sensible relationship. An investigation into the total rock mercury and its relationship to chloride was also carried out. This experiment it was hoped, would further determine the existence of $HgCl_2$ and HgCl in the drillcore material (Chapter 8). However it was not really expected to yield any information, as the relative amounts of chloride would be vastly in excess of mercury and any mercury to chloride relationship that did exist could not be picked up in a method with such high detection limits. No relationship was found between mercury and chlorine.

Complete fluoride analysis was not undertaken as fluorite, unrelated to the mineralizing phase in the Keel area, was almost ubiquitously present in small amounts in Keel sediments, as indeed it is present in most marine sediments. These amounts, however, would be enough to mask any fluoride introduced with the mineralization by circulating connate or hydrothermal waters and would easily mask any primary dispersed fluoride halo. Original rock chloride in the sediments would also be enough to mask any chloride introduced with mineralization and therefore total chloride analysis was not undertaken.



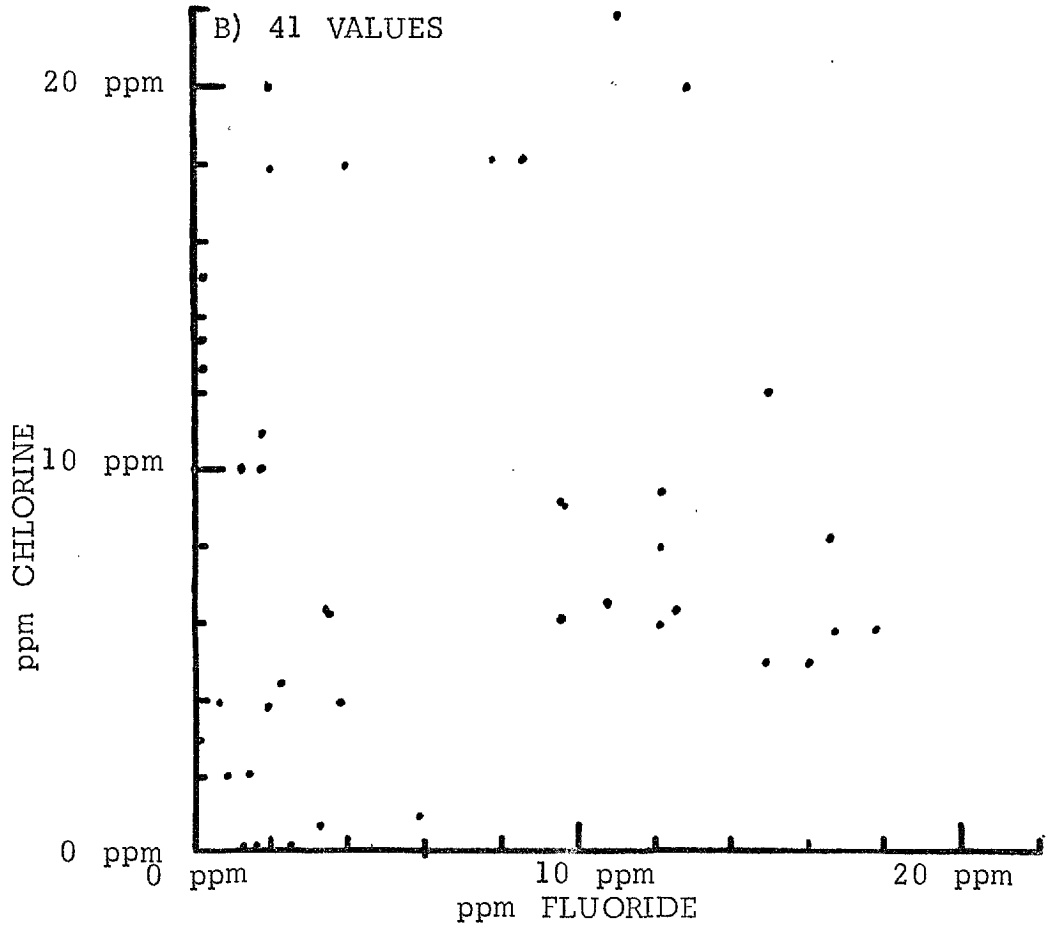


FIG ... 5.5

DIAGRAM OF THE RELATIONSHIP OF CALCIUM TO MAGNESIUM & CHLORINE TO FLUORINE IN COLD WATER LEACHES FROM KEEL DRILLCORE

Considering that the area around Keel is predominantly one of carbonate and clastic marine sediments, all the levels of fluorine and chlorine obtained during this study, can quite easily be explained as being original constituents of the host rocks and no introduction by hot, circulating hydrothermal waters is needed to explain their existence. It can therefore be concluded that primary dispersion of fluorine and chlorine in the wallrocks surrounding the Keel prospect is non existent and no relationship to base metals can be seen.

CHAPTER 6.

TRACE ELEMENT DISTRIBUTION IN SPHALERITE, GALENA AND PYRITE, FROM THE KEEL PROSPECT.

6.1. INTRODUCTION.

The preceding chapters have dealt primarily with primary dispersion of trace elements and major elements in the wallrocks surrounding the Keel zinc-cadmium prospect. This study has not proved a particularly rewarding line of research. During the investigation however, it was found that sphalerite contained anomalously high concentrations of certain trace elements, cadmium being one example. Because of this, it was decided to investigate the trace element distribution in the three main sulphide minerals, sphalerite, galena and pyrite at Keel in much greater detail and,as a consequence, possibly provide parameters on which a theory of ore-genesis could be based.

Patterson (1970) has already carried out an investigation into the distribution of Cd, Fe, Mn, Cu, Ag, Sb, Ti and V in nine sphalerite, two galena and four pyrite samples. This analytical programme however, was not comprehensive enough to draw anything but broad conclusions from.

6.2. ANALYTICAL METHOD.

(a) Sample Preparation

Approximately 200 g . samples of mineralized rock were crushed in a manganese-steel jaw-crusher and the -210 μm + 494 μm fraction sieved out and reserved. Several polished sections of this crushed material were prepared and carefully examined using a reflected light microscope in an attempt to ascertain if any contamination

from the jaw-crusher could be found. The results were negative. The - 210 μm + 494 μm fraction was then shaken with 200 ml. aliquots of deionised water until the latter was clear and free from suspended material; the residue was then dried between filter papers. Small portions of this clean - 210 μm + 494 μm material were then slowly poured into tetrabromoethane, specific gravity 2.97 g./cc., and centrifuged. The lighter fraction, consisting predominantly of gangue minerals, was then discarded and the heavy minerals retained. The specific gravities of various minerals at Keel are shown below and compared to tetrabromoethane.

MINERAL	SPECIFIC GRAVITY g./cc
TETRABROMOETHANE (T.B.E.)	2.97
SPHALERITE	4.102
GALENA	7.50
PYRITE	5.00
QUARTZ	2.20
DOLOMITE	2.80
CALCITE	2.60

Approximately 5 g. of heavy mineral were separated from each hand specimen in the above way. The minerals were then washed with acetone to remove any T.B.E. and allowed to dry. Each 5 g. sample was then transferred to a 100 ml. conicle flask and allowed to stand for 24 hours at room temperature in 50 ml. of 0.01N. hydrochloric acid.

This removed any adhering calcite on the grains, without attacking the sulphides themselves; after this the grains were washed with deionised water to remove acid, and allowed to dry. When dry the solid was slowly fed into a Franz magnetic separator and split into five fractions, depending upon the magnetic properties of the minerals. The settings on the magnetic separator used are shown below:-

	TILT	INCLINATION	AMPERE	REMOVES
(1)	1^{o}	18^{o}	1.1	Quartz and Carbonate gangue
(2)	2^{o}	18^{o}	1.1	Iron rich gangue and pyrite
(3)	3.5^{o}	18^{o}	1.1	Yellow sphalerite and galena
(4)	5.5^{o}	18^{o}	1.1	Intermediate sphalarite and galena
(5)	9.0^{o}	18^{o}	1.1	Dark iron rich sphalerite

After this, splits 2, 3, 4 and 5 were hand picked, using a binocular microscope, to remove any visible contamination. Galena and pyrite were also hand picked from each fraction. In this way, galena, pyrite and three colour varieties of sphalerite were obtained.

6.4 ANALYSIS

Each sample was thoroughly ground in an agate pestle and mortar. Fifty milligramme portions of the ground mineral were then mixed with an equal weight of high purity carbon powder, containing 0.04% palladium as an internal standard, and burnt to completion at 9 amps. The complete burn took

approximately 1 min. 30 seconds. The optical spectrograph used has been described in Chapter 3. Spectra were recorded on Kodak N.40 plates, a seven step sector (ratio 2:1) being employed for plate calibration. Line densities were read on an A.R.L. microphotometer and converted to relative intensities; the method is described in Ahrens and Taylor, (1961). The spectral lines used are shown in Table 6.6.

Working curves were constructed by means of specpure* mixes of the elements to be determined, diluted in zinc sulphide, lead oxide and ferric oxide bases. The precision of the method is within $\pm$ 15% relative.

Analytical results for sphalerite, galena and pyrite are shown in Tables 6.1 - 6.4 inclusive.

COMPARISON OF ATOMIC ABSORPTION AND OPTICAL SPECTROGRAPH.

In order to obtain information as to the accuracy of analysis of these minerals by the optical spectrograph method, it was decided to run a test series of samples on atomic absorption and compare results. Table 6.5. shows the results obtained after analysis of twenty-two samples of sphalerite. The reproducibility of cadmium and iron results can be seen to be excellent; silver, manganese and copper, good; while lead, magnesium and calcium are not very good at all. However, there is enough general agreement with the important trace elements, and a good indication that the values obtained on optical spectrograph are quite acceptable and reproducible by another analytical method. This

* Registered trade mark, Johnson Matthey Chemicals Ltd.

TABLE ... 6.1.

SEMIQUANTITATIVE SPECTROGRAPHIC ANALYSIS OF SELECTED SPHALERITES FROM KEEL PROSPECT, COUNTY LONGFORD, IRELAND

SAMPLE NUMBER	Cd	Ga	Ag	Ni	Co	Sb	Ba	Cu	Ca	Ti	In	Ge	Fe	Si	Pb	Mg	Mn
2116	10760	21.5	1	trace	n.d.	n.d.	<1.0	53	35.0	n.d.	n.d.	n.d.	3450	59	1090	10.5	32.0
2117	10640	86.0	157	11.0	15.0	640	7.5	650	n.d.	1.5	2.0	20.0	13800	10000	7170	3.3	37.0
2118	9900	100.0	310	4.0	24.0	786	3.5	780	trace	28.0	2.0	24.0	15500	4000	2650	49.0	43.5
2119	7900	42.5	15	2.0	15.0	n.d.	6.5	150	142.0	3.5	5.0	9.0	6900	10000	3900	133.0	30.0
2120	7100	43.5	4	9.0	24.0	n.d.	0.1%	125	58.5	4.0	42.5	n.d.	7100	10000	6200	49.5	15.0
2121	8000	38.0	5	trace	n.d.	n.d.	15.5	12	1870.0	2.0	n.d.	n.d.	6300	750	590	790.0	123.0
2122	8800	3.5	13	trace	trace	n.d.	23.5	27	216.0	7.5	8.0	n.d.	7080	3750	267	100.0	32.5
2123	8810	trace	9	trace	trace	n.d.	8.0	19	492.0	7.0	n.d.	n.d.	5700	970	4450	215.0	62.0
2124	7800	101.0	230	trace	13.0	1220	2.0	620	n.d.	1.5	2.0	18.0	15200	8700	2650	2.0	42.0
2125	9300	7.0	10	trace	9.0	n.d.	5.5	18	56.0	3.0	n.d.	n.d.	2950	95	50	26.5	105.0
2126	8900	54.5	300	23.0	4.0	1210	86.0	875	37.5	26.0	5.0	17.5	16200	4300	4200	255.0	105.0
2127	9150	30.0	103	31.5	trace	715	285.0	16	n.d.	36.5	n.d.	4.5	9600	10000	3200	34.0	61.5
2128	10000	59.5	95	17.5	trace	730	13.0	425	n.d.	60.0	2.0	8.5	10700	7700	10000	15.0	67.0
2129	7300	49.5	45	18.0	trace	trace	87.0	160	n.d.	6.5	trace	2.0	9000	3500	820	12.0	52.0
2130	7600	60.0	330	10.0	trace	1320	40.0	760	n.d.	6.5	trace	40.0	16200	2070	3750	41.5	54.5
2131	6600	52.0	225	10.0	trace	1330	17.5	810	n.d.	13.0	6.0	39.0	15500	3400	4350	7.0	52.0
2132	8800	43.5	3	3.0	20.5	n.d.	n.d.	42	n.d.	1.0	4.5	n.d.	5600	770	5050	9.0	48.0
2133	9100	1.0	2	trace	trace	n.d.	trace	11	222.0	1.5	trace	n.d.	4300	152	94	123.0	40.0
2134	10700	trace	5	trace	trace	n.d.	trace	17	515.0	3.5	n.d.	n.d.	4550	330	3650	200.0	78.0
2135	7300	5.4	1	5.5	3.0	n.d.	13.0	51	n.d.	trace	4.0	n.d.	4660	33	162	3.0	38.5
2137	11100	3.5	2	trace	17.5	n.d.	trace	20	n.d.	3.5	4.0	n.d.	4950	49	2550	2.0	31.0
2138	9100	44.5	84	57.0	4.5	218	110.0	295	trace	11.5	7.0	n.d.	13500	2570	4300	84.0	76.0
2139	7700	60.0	265	7.5	5.5	860	trace	990	trace	3.5	n.d.	42.0	19000	940	3000	trace	59.5
2140	11800	20.5	55	22.5	21.0	670	24.0	530	n.d.	17.0	4.0	11.5	9400	6700	10000	25.5	39.5
2141	12700	152.0	197	80.0	16.0	800	11.0	1042	n.d.	31.5	20.0	21.5	18400	4465	4150	103.0	49.5
2142	10600	90.0	252	7.5	10.5	875	16.0	810	n.d.	5.0	28.5	33.0	18500	2900	2350	22.0	57.0
2143	10000	47.0	192	7.6	16.0	710	4.5	523	n.d.	5.0	trace	22.5	16200	2450	10000	8.0	44.5
2145	8070	25.0	162	2.5	10.5	684	16.5	682	n.d.	44.0	2.0	28.5	17500	4500	1490	14.0	51.0

(N.B. Results expressed as p.p.m. unless otherwise stated)

((n.d. Looked for in sample but not detected. trace. Detected in sample but not measureable))

TABLE...6.2.

SEMIQUANTITATIVE SPECTROGRAPHIC ANALYSIS OF SELECTED SPHALERITES FROM THE KEEL PROSPECT, COUNTY LONGFORD, IRELAND

SAMPLE NUMBER	Cd	Ga	Ag	Ni	Co	Sb	Ba	Cu	Ca	Ti	In	Ge	Fe	Si	Pb	Mg	Mn
2146	8400	43.0	119	14.0	15.0	710	18.0	395	n.d.	24.0	7.0	17.0	12600	3200	1490	15.5	32.0
2147	6800	56.5	222	10.0	6.0	202	17.0	790	2470	47.5	3.5	32.5	19300	2220	2620	999.0	250.0
2148	8000	50.0	73	5.0	16.5	840	8.5	756	n.d.	1.5	n.d.	39.0	16400	2000	6100	5.0	48.0
2149	6800	51.0	264	10.5	5.0	720	107.0	880	n.d.	41.5	n.d.	34.0	17000	10000	8100	22.5	48.0
2150	6300	61.5	252	4.0	4.0	930	24.0	906	n.d.	5.5	n.d.	44.0	19600	3250	4650	1.0	57.0
2151	9200	65.0	252	2.5	6.0	900	12.5	620	n.d.	3.5	n.d.	33.0	16000	900	2600	1.0	44.0
2152	10800	11.5	21	10.0	19.5	trace	52.0	218	n.d.	15.0	3.0	7.5	7900	8300	10000	20.0	26.5
2153	10700	42.5	112	11.0	16.0	325	14.0	750	n.d.	7.0	trace	24.0	15500	4400	4200	5.0	51.0
2154	10500	44.0	325	44.0	21.0	1150	15.0	1370	n.d.	4.5	trace	21.0	9600	5500	10000	27.0	33.0
2155	5950	47.0	180	23.5	6.0	700	64.0	1070	370	52.0	7.5	41.5	15700	5550	6600	395.0	310.0
2156	8750	31.0	170	20.5	17.0	430	6.5	490	n.d.	14.0	trace	17.0	12700	8300	10000	23.0	36.5
2157	8350	55.0	142	4.0	13.5	437	2.5	630	n.d.	1.5	trace	26.0	17600	480	2200	trace	49.0
2158	9800	66.5	292	2.0	11.5	920	23.0	700	92	12.0	12.0	31.0	15200	10000	6100	57.5	55.5
2159	9500	70.5	193	2.0	13.5	870	trace	675	n.d.	trace	trace	26.0	17600	162	10000	trace	53.0
2160	7100	61.0	293	2.5	5.5	700	21.5	970	n.d.	8.0	trace	46.5	19300	3100	10000	trace	53.0
2161	6150	26.5	56	23.0	3.5	114	101.0	285	n.d.	12.0	n.d.	n.d.	13200	6400	1140	20.0	84.0
2162	8750	22.0	56	21.0	16.5	185	25.0	855	n.d.	13.5	n.d.	n.d.	8900	6100	10000	22.0	38.5
2163	8100	14.0	49	8.0	18.5	93	23.5	150	n.d.	30.0	n.d.	n.d.	8400	3250	10000	12.5	18.0
2164	10500	96.0	235	3.0	13.5	157	trace	790	n.d.	2.0	18.0	36.0	17600	3050	2800	8.5	55.0
2165	8700	59.0	228	2.0	9.0	860	11.5	630	76	13.0	9.0	21.5	13200	10000	5300	54.0	50.0
2166	8450	66.5	230	2.5	7.5	1050	11.5	690	n.d.	5.0	n.d.	33.5	15100	520	6300	2.0	38.5
2167	13600	88.0	247	3.0	13.5	547	trace	760	n.d.	8.5	17.5	24.0	16800	2880	4950	9.0	50.0
2168	7200	20.0	52	17.5	4.0	108	83.0	115	n.d.	8.0	trace	trace	7900	3250	675	9.0	51.0
2169	8800	116.0	210	2.0	8.5	920	12.5	690	65	13.5	11.0	28.5	14700	10000	2600	61.0	53.0
2170	10500	70.0	227	trace	12.0	622	n.d.	710	n.d.	4.5	17.5	34.5	18300	3200	2820	5.0	52.5
2171	8450	30.5	212	19.5	4.5	810	92.0	675	103	26.5	4.0	25.5	15400	3100	2960	22.5	95.0
2172	9650	60.0	230	4.5	6.0	880	11.0	600	n.d.	2.5	n.d.	29.5	14200	435	2630	2.5	36.5

(N.B. Results expressed as p.p.m. unless otherwise stated)

((n.d. Looked for in sample but not detected. trace. Detected in sample but not measureable))

TABLE...6.3.

SEMIQUANTITATIVE SPECTROGRAPHIC ANALYSIS OF SELECTED SPHALERITES FROM THE KEEL PROSPECT, COUNTY LONGFORD, IRELAND.

SAMPLE NUMBER	Co	Ni	Ag	Cu	Cd	Ti	Ge	In	Ga	Fe	Sb	Pb	Mn
2241	10.5	5.0	180	260	9200	7.5	n.d.	175	245	12250	1150	530	56.0
2242	3.0	trace	47	99	18500	3.5	n.d.	n.d.	4	7800	trace	90	21.5
2243	8.5	5.0	260	540	11000	11.5	9.0	n.d.	21	11750	860	890	19.5
2244	trace	n.d.	390	999	13750	8.5	23.5	n.d.	110	16500	1350	780	32.0
2245	12.0	5.0	190	200	16500	10.5	20.0	34	180	16000	1070	1150	100.0
2246	4.0	6.5	210	235	13500	3.5	30.0	n.d.	120	17000	1300	340	76.0
2248	n.d.	10.0	22	44	16000	trace	n.d.	n.d.	180	31000	n.d.	810	90.0
2249	n.d.	n.d.	n.d.	n.d.	n.d.	trace	n.d.	n.d.	n.d.	6000	n.d.	110	95.0
2250	12.0	n.d.	7	27	16000	n.d.	n.d.	31	4	10000	n.d.	1650	50.0
2251	33.0	12.0	120	600	13000	18.0	trace	n.d.	40	12500	n.d.	2750	20.0
2253	trace	47.0	350	999	12000	18.0	27.5	n.d.	72	20000	980	1150	53.0
2254	n.d.	trace	700	770	14500	n.d.	n.d.	n.d.	8	14000	1950	155	78.0
2255	7.0	11.5	19	55	7900	n.d.	9.0	23	7	5400	n.d.	580	14.5
2256	8.5	4.5	140	230	4600	n.d.	n.d.	n.d.	25	10000	600	540	22.0
2262	24.0	n.d.	9	125	10500	25.0	n.d.	15	26	5700	n.d.	680	115.0
2263	n.d.	12.0	62	340	14500	36.0	n.d.	10	33	7000	n.d.	310	11.5
2264	trace	trace	125	439	7800	10.5	11.0	n.d.	74	12700	590	370	85.0
2265	trace	n.d.	550	210	9200	trace	n.d.	n.d.	30	7800	395	140	46.0
2267	15.5	trace	220	999	20000	22.5	n.d.	190	245	15500	1200	870	37.0
2269	19.5	n.d.	70	660	11000	trace	22.0	n.d.	120	16700	450	1150	60.0
2270	32.0	210.0	250	1000	14000	n.d.	trace	n.d.	250	40200	1230	950	79.0
2271	19.0	5.5	800	1000	15000	640.0	n.d.	n.d.	300	19000	2800	980	42.0
2272	30.0	130.0	275	1000	11000	30.0	18.5	n.d.	65	21000	730	3300	25.5
2273	trace	trace	7	40	9000	24.0	n.d.	31	trace	4700	n.d.	350	15.5
2274	26.0	trace	11	51	10300	3.5	n.d.	n.d.	6	6700	n.d.	110	11.0
2275	8.0	16.5	82	680	18700	n.d.	17.0	23	58	13700	280	2100	23.0
2278	7.0	n.d.	560	1000	13300	8.5	15.0	n.d.	35	15500	1250	1450	31.0
2281	12.5	n.d.	82	440	14000	trace	15.5	9.0	160	12500	700	780	77.0

(N.B. Results expressed as p.p.m. unless otherwise stated)

((n.d. Looked for in sample but not detected. trace. Detected in sample but not measureable))

TABLE...6.4.

SEMIQUANTITATIVE SPECTROGRAPHIC ANALYSIS OF SELECTED SPHALERITES, PYRITES & GALENAS FROM THE KEEL PROSPECT, COUNTY LONGFORD, IRELAND.

SAMPLE NUMBER	Co	Ni	Ag	Cu	Cd	Ti	Ge	In	Ga	Fe	Sb	Pb	Mn
SPHALERITE													
2283	n.d.	n.d.	76	105	13700	34.0	n.d.	n.d.	18	6700	trace	3600	850.0
2285	5.0	9.0	200	640	11500	15.0	n.d.	n.d.	100	11500	960	1600	34.0
2286	13.0	6.5	400	620	12500	trace	n.d.	n.d.	110	14000	1270	720	33.0
2288	trace	135.0	310	1000	7100	trace	n.d.	n.d.	29	37000	11700	3700	36.0
2289	n.d.	trace	72	110	14700	28.0	n.d.	n.d.	14	13000	trace	285	1000.0
2290	n.d.	5.5	15	24	4850	trace	n.d.	n.d.	n.d.	3300	trace	460	54.0
2291	14.5	7.0	10	34	6500	trace	n.d.	n.d.	n.d.	5400	trace	1400	28.0
2293	trace	n.d.	260	1000	13500	19.5	17.0	n.d.	71	11590	800	1400	75.0
2294	27.5	14.0	120	510	14000	16.0	14.0	n.d.	36	10750	n.d.	2500	21.0
PYRITE													
2144	18.0	111.0	41	13	n.d.	530.0	n.d.	29.5	9		n.d.	2500	1000.0
2259	n.d.	98.0	52	34	trace	63.0	n.d.	n.d.	n.d.		n.d.	1175	3.0
2261	n.d.	n.d.	72	n.d.	n.d.	n.d.	n.d.	n.d.	n.d.		960	3500	50.0
2279	n.d.	16.5	64	230	n.d.	76.0	n.d.	n.d.	n.d.		n.d.	980	190.0
GALENA													
2239	n.d.	5.0	1000	8	trace	4.0	n.d.	n.d.	n.d.	trace	1700		44.0
2240	n.d.	trace	650	3	trace	6.5	n.d.	n.d.	n.d.	trace	1700		23.0
2247	n.d.	n.d.	320	78	trace	9.0	n.d.	n.d.	n.d.	trace	760		trace
2252	n.d.	n.d.	340	4	trace	n.d.	n.d.	n.d.	n.d.	n.d.	520		n.d.
2260	n.d.	n.d.	1000	17	trace	12.0	n.d.	n.d.	n.d.	trace	1850		17.5
2276	n.d.	n.d.	470	5	23	6.5	n.d.	n.d.	n.d.	n.d.	1170		13.0
2277	n.d.	n.d.	230	8	260	5.5	n.d.	n.d.	n.d.	n.d.	540		3.5
2280	n.d.	n.d.	1000	52	260	3.0	19.0	n.d.	n.d.	n.d.	10500		trace
2282	n.d.	n.d.	1000	12	180	trace	25.0	n.d.	n.d.	370	1500		125.0
2284	n.d.	n.d.	1000	n.d.	n.d.	trace	n.d.	n.d.	n.d.	n.d.	1370		10.0
2287	n.d.	6.5	500	19	430	15.0	n.d.	n.d.	n.d.	6200	930		n.d.
2292	n.d.	n.d.	1000	9	trace	trace	n.d.	n.d.	n.d.	n.d.	2450		39.0

(N.B. Results expressed as p.p.m. unless otherwise stated)

((n.d. Looked for in sample but not detected. trace. Detected in sample but not measureable))

TABLE...6.5.

COMPARISON OF SPECTROGRAPHIC & ATOMIC ABSORPTION ANALYSES FOR SELECTED ELEMENTS IN SPHALERITES FROM KEEL PROSPECT, COUNTY LONGFORD, IRELAND.

SAMPLE NUMBER	Ag		Cd		Pb		Cu		Mn		Fe		Mg		Ca	
	A.A.	O.S.	A.A.	O.S.	A.A.	O.S.	A.A.	O.S.	A.A.	O.S.	A.A.	O.S.	A.A.	O.S.	A.A.	O.S.
C 16	n.d.	5	8812	10700	81	36	5	17	107	78	4000	4550	1022	200	2325	515
C 33	315	230	9407	7800	1013	2650	850	620	50	42	17198	15200	2	16	625	n.d.
C 10	n.d.	2	8758	9100	75	94	5	11	39	40	2570	4300	n.d.	123	35	222
C 18	292	162	6653	8200	288	265	885	780	61	44	16122	15500	83	49	n.d.	trace
C 25	n.d.	3	8866	8800	81	51	30	42	71	48	3750	5600	68	9	1015	n.d.
C 14	n.d.	10	9732	9540	75	68	98	138	34	40	4560	5500	56	43	668	346
404 B	113	103	6595	9150	394	320	245	155	57	62	7870	9600	20	33	n.d.	n.d.
404 I	425	300	7078	8900	369	420	855	875	100	105	15256	16200	360	255	46	38
404 T	464	330	6541	7600	269	375	1008	760	46	55	17636	16200	41	42	35	n.d.
405 T	411	225	6109	6600	469	435	1070	810	29	52	17528	15500	24	7	n.d.	n.d.
406 B	62	52	7351	7300	100	82	120	160	32	52	6520	7400	22	20	n.d.	n.d.
406 T	391	265	6788	7700	200	300	920	990	25	60	17960	19000	n.d.	n.d.	n.d.	trace
103 B	319	210	7893	8800	594	260	895	690	24	53	13093	14700	95	61	65	65
103 T	375	252	9948	10600	225	235	845	810	29	51	18502	18500	26	22	50	n.d.
77 B	37	21	8000	10800	4519	5000	220	218	25	27	6370	7900	11	20	n.d.	n.d.
77 T	102	49	7082	8100	681	1000	895	150	39	18	14716	8400	n.d.	13	n.d.	n.d.
64 T	320	235	10380	10500	365	280	840	790	43	55	17528	17600	65	9	85	n.d.
64 B	166	119	8542	8400	781	590	450	395	21	32	9270	12600	n.d.	16	n.d.	n.d.
93 T	388	192	10921	10000	3781	4000	610	523	32	45	17526	16200	16	8	50	n.d.
93 I	351	170	10000	8750	9985	6780	625	490	29	37	15797	12700	11	23	n.d.	n.d.
67 I	179	112	9623	10700	431	420	875	750	28	51	15256	15500	18	5	n.d.	n.d.
67 T	191	142	10165	8350	181	220	730	630	25	49	17528	17600	23	n.d.	n.d.	n.d.

(N.B. Results expressed as p.p.m.)

((n.d. Looked for in sample but not detected. trace. Detected in sample but not measureable))

study further indicates that there is general matrix compatibility between the standard series and the sphalerite samples.

The elements analysed for in Keel samples were:- Cd, Ga, Ag, Ni, Co, Sb, Ba, V, Cu, Cr, Ca, Sn, Mo, Ti, Bi, In, Ge, Fe, Si, As, Pb, Mg, Mn and Hg.

Mercury was the only element in the aforementioned series, which was not analysed using the optical spectrograph. The techniques for mercury analysis in sphalerite, galena and pyrite and the results obtained are therefore discussed prior to the main body of the optical spectrograph analytical work.

6.4. MERCURY IN SPHALERITE, GALENA AND PYRITE.

Mercury has been reported as occurring in sphalerite from several localities, some of which were compiled by Fleischer (1955), in a paper on the minor elements in some sulphide minerals. Mercury has been reported in sphalerite from Austria (Schroll, 1950-51; 1953); Bohemia (Kutina, 1953; Yak, 1951); France (DeLauney and Urbain, 1910); Spain (Pina de Rubies and Lopez de Azcona, 1937); Norway (Oftedal, 1940) and Sweeden (Gabrielson, 1945). Fryklund and Fletcher (1956), reported sphalerite from the Coeur d'Alene district, Idaho, containing up to 200 ppm mercury. Grip (1948), quotes a figure of 400 ppm maximum for mercury in sphalerite from Boliden, N. Sweeden and James (1962), also quotes several figures for mercury in sphalerite from various temperature deposits. Saukov, 1946 and Fursov, 1958 have reported mercury in sphalerite from the Soviet Union. The latter author has described a mercury anomaly derived from the oxidation of mercury rich sphalerite and galena. Ozevova, 1959, in the Karatu

district, also reported mercury aureoles around lead/zinc deposits derived from mercury bearing sphalerite, galena, tetrahedrite and baryte and concluded that mercury was probably present as a "diadochic substitute" in these minerals. Jolly and Heyl (1968), duscuss the analysis of seventy-six sphalerites from mineral districts in the central and eastern U.S.A., showing values ranging from 100 to 300,000 ppb mercury. They concluded that the presence of mercury as an integral part of the sphalerite precludes the supposition that it was the result of a more recent addition by replacement or by pore space fitting. Mercury was probably deposited directly from the ore solutions, co-precipitating with zinc in the sphalerite lattice, this precipitating zinc sulphide "scavenging" (Hawkes, 1957), traces of certain other elements from solution and also incorporating them into the crystal lattice.

The presence of mercury, as an integral part of the sphalerite lattice (Chapter 8), suggests that possibly Keel sphalerite is hydrothermal in origin. Mercury can theoretically be transported in ore solutions as the volatile chloride, mercury vapour, or in slightly alkaline sulphide solutions, as the complex ion (Krauskopf, 1951). The solubility of mercuric sulphide in pure water at pH 7 and 25°C is 1×10^{-17} grammes per litre and at 400°C is 3×10^{-15} grammes per litre (Verhoogen, 1938). Pure cool ground water has also been reported as being incapable of carrying much elemental mercury in solution (Hawkes and Webb 1962).

Tunell (1964), and Krauskopf (1951), suggest that the temperature of alkaline ore solutions depositing mercuric sulphide must be low, between 80°C and 250°C. Krauskopf has stated that mercuric sulphide

cannot exist in any system above 250°C that includes moving vapours, without high concentrations of mercury and sulphur. It is also doubtful whether mercury can exist as a complex sulphide ion in solutions at such temperatures. Krauskopf further suggests that, at temperatures where other sulphides precipitate, mercuric sulphide is unstable, so that its components are forced to travel to a cooler region before the compound can form. This seems to put an upper limit of formation on the Keel Sphalerite of 250°C. (Chapter 8).

6.4.1. ANALYSIS OF MERCURY IN SPHALERITE, GALENA AND PYRITE.

Quantitative analysis of mercury in sulphide minerals by atomic absorption techniques has always proved difficult, due to the interfering effect of the sulphide ion and the possible recombination of mercury with sulphur. To overcome these difficulties two analytical techniques were used.

(a) Total Mercury analysis in Sphalerite, Galena and Pyrite, using a $SnCl_2$ Reduction Technique.

(a1) Method.

The use of stannous chloride solution, to quantitatively reduce mercuric and mercurous salts in solution to elemental mercury, was investigated by Wormley (1860) and Jackson (1903).

The following is an account of the experimental procedure used by the author, for analysis of the mercury content of Keel sulphides.

0.5 gms. of - 210 µm + 494 µm crushed sphalerite were transferred to a 250 ml. quick fit flask and 50 ml of 4:1 nitric acid / perchloric acid added. The mixture was then refluxed at 150°C for four hours by which time a clear yellow

solution had been obtained and the evolution of nitrogen peroxide had ceased. One millilitre of this solution wae then traneferred to 50 ml. of deionised water in a dreschel bottle and 10 ml. of a 10% stannoue chloride solution in 10% hydrochloric acid, added. The addition of stannoue chloride effectively reducee all mercury salts to elemental mercury. This mercury was then flushed with air into a quartz cell pre-heated to 450°C. Here the abeorption of light of wavelength 2536.5 Å by mercury vapour, was meaeured. A quantitative determination of mercury in sphalerite was obtained by comparison of reeults with standards. All reeulte were recorded on a chart recorder output and analyses repeated in triplicate to obtain an indication of the precision of the analyeis. Results differing by more than 10% were rejected and the whole analysis repeated for that sample.

For analysis of galena, concentrated nitric acid was substituted for the nitric-perchloric mixture because of the formation of a lead chloride precipitate. Oxidation of lead sulphide to lead sulphate by concentrated nitric acid and its effects on mercury liberation are discussed under the galena subheading in this chapter.

(a2) Preparation and Calibration of Standards.

67.45 mg. of specpure* mercuric chloride were dissolved in 100 ml. of 10% nitric acid to give a 500 µg/ml mercury standard. From this standard stock solution, calibration standards of 2.0, 1.0, 0.5, 0.4, 0.2, 0.1 and 0.05 µg/ml. were made up. On the basis of these, a calibration graph, Fig. 6.1A was drawn up and also a calibration graph on the basis of µg Hg/litre of solution, Fig. 6.1B. These standard curves were obtained from mercury in a 10% HNO_3 base.

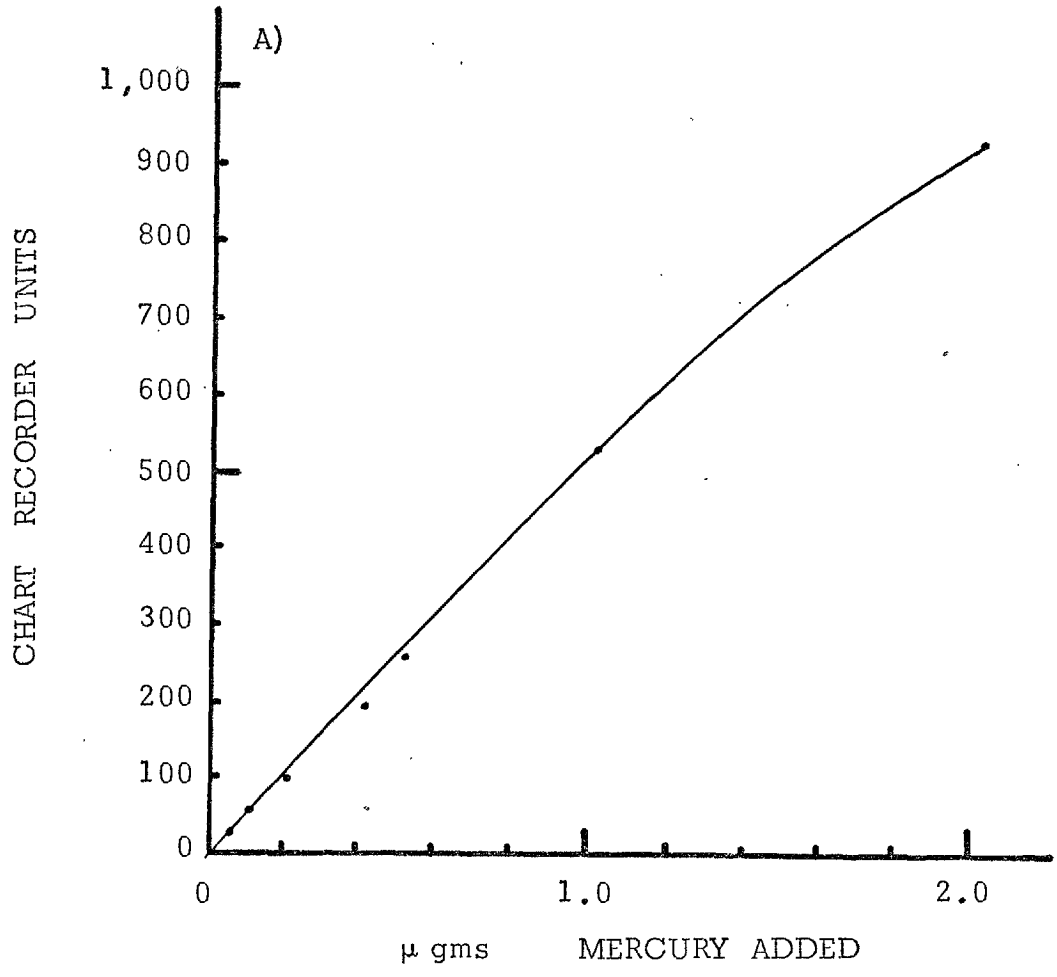
Two other solution bases for the mercury standards were also used to try and ascertain the best medium for keeping mercury in solution. An attempt was also made to try and ascertain the effect of age on the amount of mercury retained in solution in these different bases. The solution bases used were:-

(i) 10% Nitric acid

(ii) 0.05% Potassium permanganate solution

(iii) 0.05% Potassium permanganate plus 1% sulphuric acid solution.

The stannous chloride solution used for the mercury reduction was purged for four hours with air, prior to analysis, to remove any mercury associated with the original solid or acid and thus reduce blank values. Each standard series was then analysed to see the effects of different solution bases on mercury release.



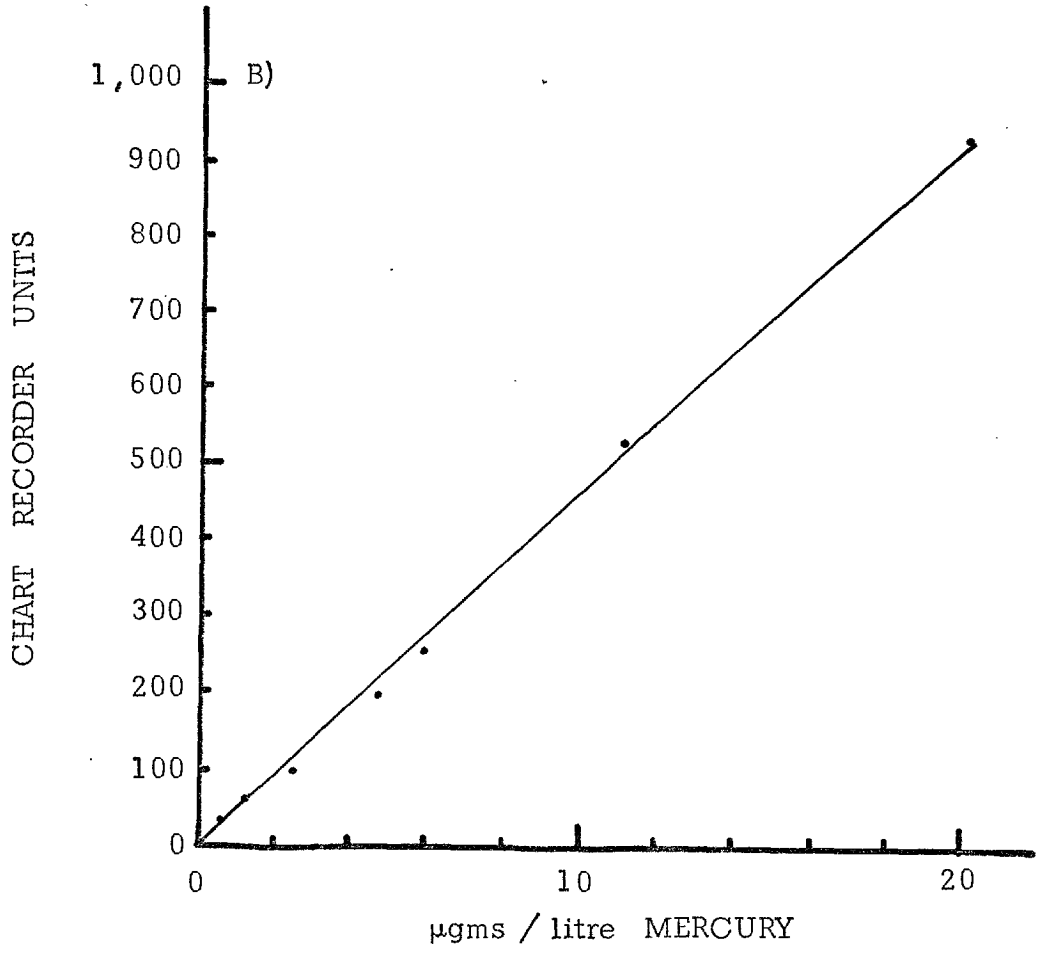


FIG . . . 6.1 MERCURY CALIBRATION CURVES FOR STANNOUS CHLORIDE METHOD OF MERCURY ANALYSIS

The results are shown below:

MERCURY CONCENTRATION	10% HNO_3	0.05% $KMnO_4$	0.05% $KMnO_4$ + 1% H_2SO_4
	(chart recorder deflections)		
0.2 µg	98.2	102.5	102.5
0.4 µg	258.1	250.0	235.8
2.0 µg	931.9	755.0	755.0

Units represent chart recorder scale.

As can be seen, the release of mercury from standards containing greater than 0.5 µg/ml. mercury remains reasonably linear for the 10% HNO_3 base, but drops off considerably in solutions ii and iii indicating possible retention properties of the glass in weak acid solution or retention properties of the Mn^{2+} ion.

An experiment to determine the effect of age on each of these standard solutions was also carried out using the 1 µg/ml. standard in each case. The original 1 µg/ml. standards were retained and fresh standards prepared each day for comparison to them. The results are displayed graphically in Fig. 6.2.

This experiment indicated that the mercury standards made up in 10% HNO_3 were by far the most stable and it is highly recommended that all mercury standards and samples should be stored in at least 10% HNO_3. The erratic behaviour of the 0.05% $KMnO_4$ and 0.05 $KMnO_4$ plus 1.0% H_2SO_4 standard solution bases can be attributed to mercury adsorbing and desorbing onto and from the glass walls of the containing vessels. This is probably due to the weaker acid of these two solutions

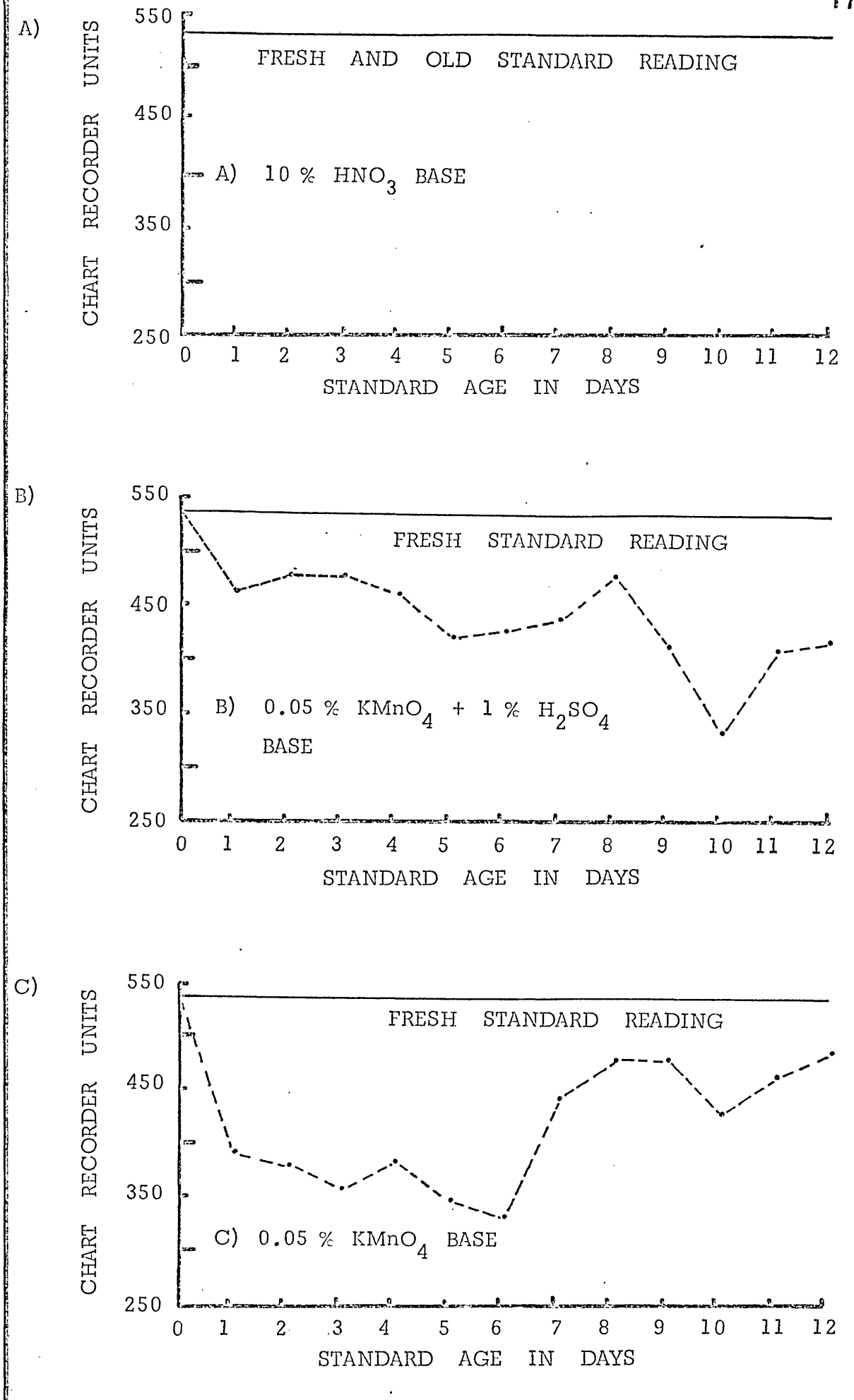


FIG ... 6.2

DIAGRAM ILLUSTRATING MERCURY RELEASE FROM A 0.1 μ gm / ml MERCURY STANDARD IN THREE DIFFERENT DILUTING MEDIUMS

not providing enough hydrogen ions to fill all vacant sites in the glass structure and consequently some of these have to be filled by mercury.

As a post-script it is worth noting that a 100 µg/litre standard made up in 10% HNO_3 still gave exactly the same value after 164 days as a 100 µg/litre freshly prepared standard.

(a3) The Effect of High Metal Levels in Solution on Mercury Analysis by the $SnCl_2$ Method.

Due to the fact that mercury being analysed in base metal sulphides could be considered as being in a base metal rich solution after the initial acid attack, an experiment was set up to test the effects of various metals on mercury release from solution. A 1 µg/ml mercury standard was used throughout this experiment. The following levels of metal contamination were added to this standard:-

(1) 20, 10, 5, 2 and 1 µg/ml Pt and Au

(2) 300, 200, 100, 10 and 1 µg/ml Ag

(3) 10,000, 1,000, 500, 200, 100, 10 and 1 µg/ml Fe, Cu, Zn, Mn and Pb.

It was found that concentrations of Fe, Cu, Zn, Mn and Pb at least 10,000 times in excess of the mercury concentration had no effect on the amount of mercury released from solution. However, Au and Pt had a considerable effect and Ag a marked, although lesser, effect, Fig. 6.3. In the author's opinion stannous chloride reduces the gold and platinum to metallic colloids and these either amalgamate with or adsorb mercury, likewise reduced to metal by the stannous chloride. The silver on the other hand forms colloidal silver chloride and the mercury adsorbs onto this colloid. The importance of keeping samples

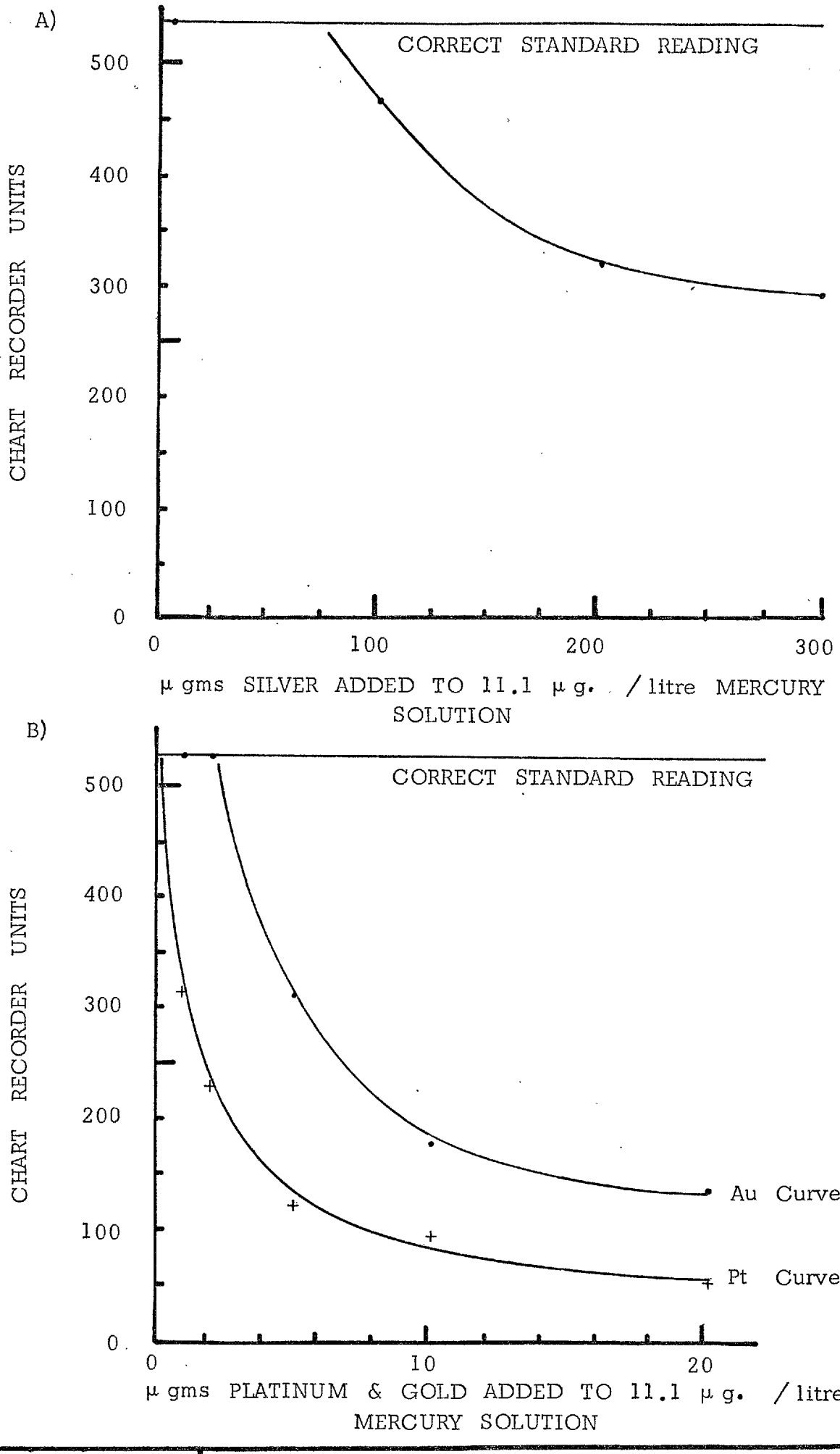


FIG ... 6.3

DIAGRAM ILLUSTRATING THE EFFECT OF Au , Pt & Ag ON MERCURY RELEASE FROM STANDARD SOLUTIONS

to be analysed for mercury away from any contact with platinum or gold equipment during the course of their preparation cannot therefore be over emphasised. The analysis of mercury in gold and platinum amalgams or near gold and platinum mineralization must also be treated with extreme care.

This method of acid digestion of sulphide material for mercury analysis suffers from none of the disadvantages of a method based on dry heat release of mercury and is to be recommended for mercury analysis in this type of material.

(a4) Analysis.

Initial work on precision of the analytical technique yielded the following information on two sphalerite standards, K23.379 and K407.T.

	SAMPLE K23.379 ppm. Hg	SAMPLE K407.T ppm. Hg
(1)	192	209
(2)	189	210
(3)	191	211
(4)	197	208
(5)	188	209
(6)	190	213
(7)	192	210
(8)	198	209
(9)	193	213
(10)	192	215
Mean of Results	192.2	210.7
Standard deviation	3.0	2.2

Whole crystals and crushed material were used for the test and results indicated no loss of mercury on crushing.

Having discovered that this method has an excellent precision, a series of 113 sphalerites were analysed for mercury. The results indicated that the distribution of mercury throughout the sphalerites of the deposit is very uniform, with a mean value of 226.5 ppm and a standard deviation of 34.4 ppm mercury. Four specimens of pyrite and twelve of galena were also analysed for mercury and, whereas the values were more erratic, broad general trends could be deduced. The analytical results were as follows:

PYRITE		GALENA			
Sample Number	ppm. Hg	Sample Number	ppm.Hg.	Sample Number	ppm.Hg
2144	7.21	2239	24.87	2271	14.58
2259	8.35	2240	18.38	2280	22.22
2261	14.45	2247	92.00	2282	26.36
2279	5.30	2252	18.27	2284	49.94
		2260	33.00	2287	32.47
		2276	44.75	2292	10.87

These results indicate that sphalerite is the primary host for mercury in the Keel deposit, followed by galena and then pyrite. Although the total concentration of mercury associated with sphalerite throughout the deposit is very uniform, there does appear to be an antipathetic relationship to ion content, Fig. 6.4., with mercury content slightly higher in the light sphalerite. In the vicinity of the underground workings the Fe/Hg relationship appears reasonably well defined, however, further away in drill core material this Fe/Hg relationship completely breaks down.

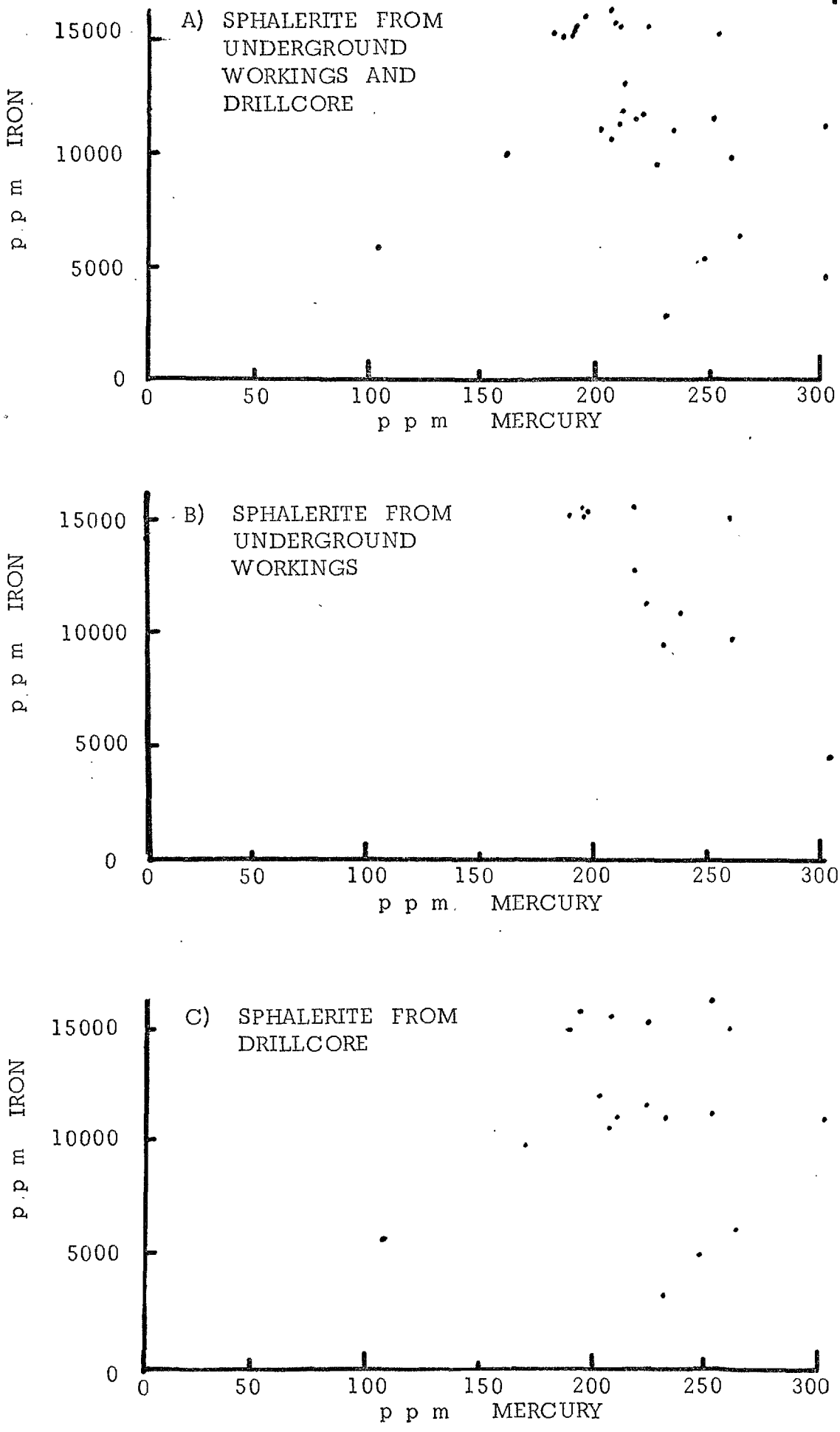


FIG ...6.4

DIAGRAM ILLUSTRATING THE RELATIONSHIP BETWEEN MERCURY AND IRON IN SPHALERITE FROM THE KEEL PROSPECT, COUNTY LONGFORD.

6.4.2. MERCURY ANALYSIS OF SOLID MINERAL SAMPLES.

The second method of mercury analysis in sulphide material involves volatilization of mercury by heat from the sulphide lattice. The mineral to be analysed is heated to 800°C, in a sealed chamber, for 1.5 minutes. The gases evolved are flushed into a quartz absorption cell by air, where the absorption of light, of wavelength 2536.5 Å by mercury vapour, is measured. Unfortunately the sulphide mineral itself breaks down, as is typified by sphalerite in the following equations:

(i) $2ZnS + 3O_2 = 2ZnO + 2SO_2$

(ii) $2SO_2 + O_2 = 2SO_3$

In excess oxygen, reaction (ii) can take place.

It was found that the SO_2 evolved was also flushed through into the absorption cell and also absorbed 2536.5 Å light. It was therefore necessary to remove SO_2 from the system and this was accomplished by two methods.

(α) Selective Removal of SO_2 in the Flow System.

After heating the sulphide mineral the gases evolved were flushed with air through an in-line dreschel bottle containing a mixture of 80 ml. of 0.05% $KMnO_4$ plus 0.1% H_2SO_4 solution.

The following reaction took place.

(a) $2KMnO_4 + 3H_2SO_4 = K_2SO_4 + 2MnSO_4 + 3H_2O = 5 [O]$

(b) $SO_2 + H_2O + [O] = H_2SO_4$

(c) $2KMnO_4 + 3H_2SO_4 + 5SO_2 + 5H_2O = K_2SO_4 + 2MnSO_4 + 5H_2SO_4 + 3H_2O$

The SO_2 was removed from the system and mercury passed on to be analysed. To avoid any moisture droplets being carried over into the analysis cell and dispersing light, a glass fibre filter pad was placed in the gas stream. The mercury and air was also passed through another tube furnace at 900°C to split up any recombined mercury or mercury molecules.

It was necessary however, to recalibrate the apparatus for this method, as a certain amount of mercury was absorbed by the $KMnO_4$ / H_2SO_4 mixture. The effects of washing the evolved gases with both water and permanganate are shown in Fig. 6.5.

(β) Selective Removal of Sulphur Dioxide in the Sample Heating Chamber.

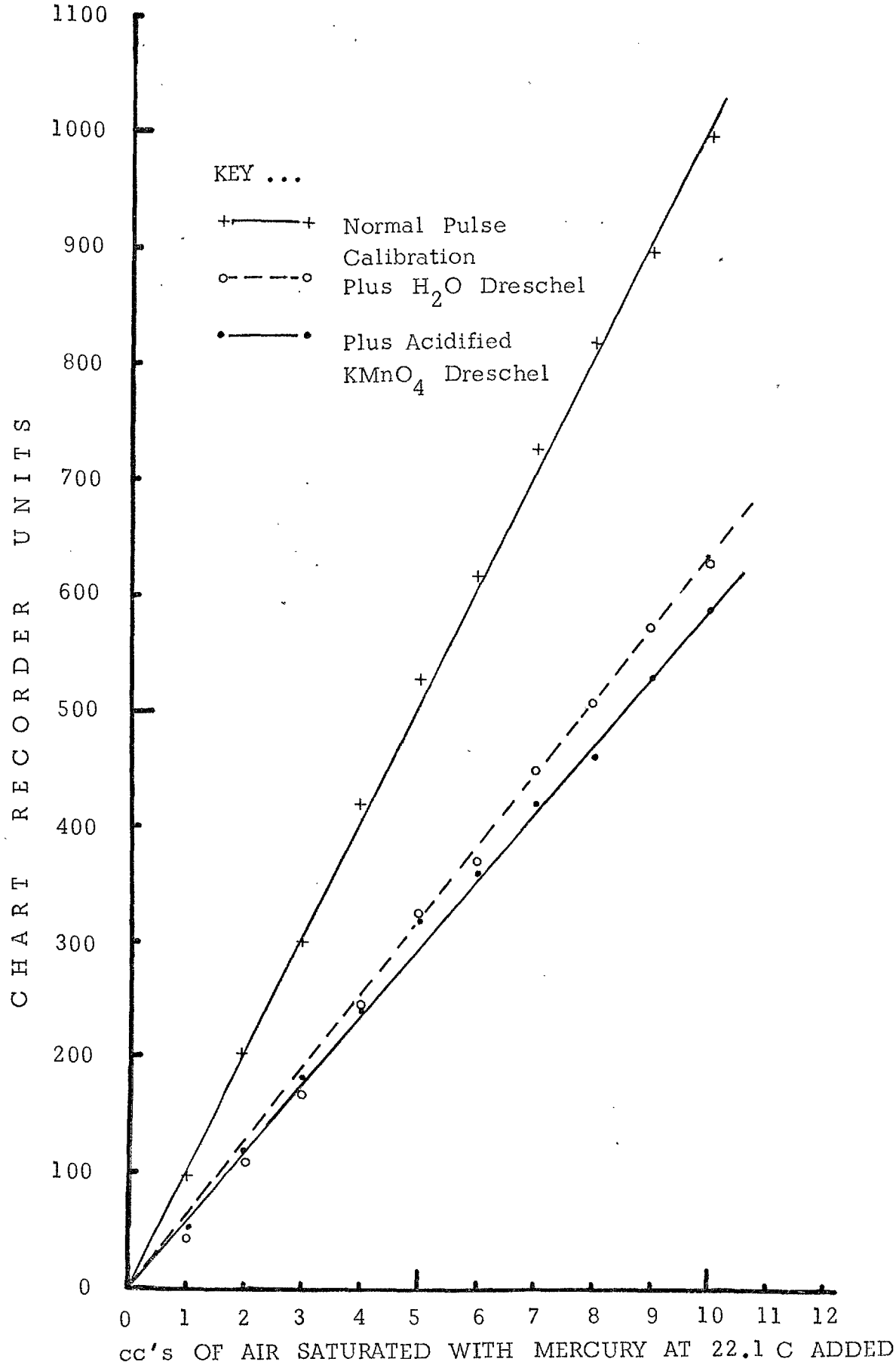
The removal of sulphur dioxide, inside the sample heating chamber, was carried out by mixing the sulphide sample with calcium carbonate. 50 milligrammes of - 210 μm sample were mixed with 950 milligrammes of - 210 μm calcium carbonate in an agate pestle and mortar. 500 milligrammes of this mixture were then transferred to a heating boat and heated to 800°C for 1.5 minutes and the evolved gases flushed into the mercury analysis chamber.

The following reactions took place inside the sample chamber.

$$2ZnS + 3O_2 = 2ZnO + 2SO_2$$

$$2CaCO_3 + 2SO_2 + O_2 = 2CaSO_4 + 2CO_2$$

The SO_2 was therefore removed from the system and mercury allowed to pass on into the absorption cell. The complete removal of SO_2 was tested by bubbling the evolved gases through acidified potassium permanganate solution.



(N.B. 1 cc of air saturated with mercury at 22.1 C contains 0.0157 μ g. mercury)

FIG ... 6.5	EFFECT OF WATER AND ACIDIFIED POTASSIUM PERMANGANATE SOLUTION ON THE MERCURY CALIBRATION GRAPH

Comparison of techniques indicates that the mercury detected by the acid digestion method is some five times as high as that detected in the same sample by simple heating without $CaCO_3$ and some three times that detected using $CaCO_3$. This indicates that the nearest complete breakdown of sulphide minerals is accomplished by acid attack. It also indicates that sphalerite, at least, is not completely broken down after 1.5 minutes at 800°C although the use of $CaCO_3$ does seem to speed up the breakdown process. The time and temperature needed for complete breakdown of the sphalerite lattice is discussed in detail in Chapter 8.

As a result of all these experiments it was decided that an acid attack would be used for analysis of mercury in samples of sulphide minerals throughout the course of this study.

6.4.3. TEMPERATURE OF FORMATION OF KEEL SPHALERITE ON THE BASIS OF MERCURY CONTENT.

On the basis of the analysis of 113 sphalerite samples for mercury it was shown that the mean value for mercury in sphalerite was 226.6 ppm. This high level does not necessarily indicate a low temperature of deposition for the sphalerite. However mercuric sulphide does exist in association with the sphalerite (Chapter 8) and according to Krauskopf (1951) mercuric sulphide cannot exist in any system above 250°C unless there are very high concentrations of mercury and sulphur. Tunell (1964) agrees that the temperature of alkaline ore solutions depositing mercuric sulphide must be between 80°C and 250°C. Analytical data on the Central Kentucky sphalerites shows these minerals to contain between 8 and 200 ppm. mercury and Edwin Roedder (1964) suggests, on the basis of fluid inclusion studies, that their temperature of deposition was below 120°C. Sphalerite from the

higher temperature mineral deposits in Maine, New York, Maryland Connecticut and New Hampshire (Jolly and Heyl, 1964) contain between 5 and 70 ppm mercury. This evidence would suggest that the Keel sphalerite was the result of low temperature deposition from saline brines. Chemical evidence will be presented in Chapter 8 suggesting a lower limit of deposition of 150°C. Evidence will also be presented in Chapter 8 confirming the presence of mercury as a lattice constituent of sphalerite and not, as could be supposed, bound up in included tetrahedrite/tennantite in the sphalerite.

6.5. TRACE ELEMENTS IN SPHALERITE FROM KEEL.

(a) Cadmium.

A table of analyses of cadmium, germanium and gallium in sphalerite from Central Kentucky, Central Tennessee (Jolly and Heyl 1964) and Keel is given below. America sphalerites were analysed by J. Harris of the U.S.G.S. in 1962 and 1964.

ELEMENT	CENTRAL KENTUCKY 37 Samples ppm	CENTRAL TENNESSEE 6 Samples ppm	KEEL 57 Samples ppm
Cd	13,400	13,000	10,223
Ge	280	200	17
Ga	90	150	65

El Shazly (1957) analysed 54 epigenetic and 9 syngenetic sphalerites from the British Isles. He confirmed cadmium to be present in quantities ranging from 300 to 10,000 ppm with a mean value of 1,000 - 5,000 ppm. El Shazly suggests that indium, manganese and

TABLE ... 6.6.

WAVELENGTHS OF THE SPECTRAL LINES USED IN THE DETERMINATION OF MINOR ELEMENT CONCENTRATIONS IN SPHALERITE FROM KEEL.

ELEMENT	WAVELENGTH Å	DETECTION LIMIT p p m
Pd	3421.24	INTERNAL STANDARD
Ag	3382.89	1
As	2860.45	1000
Ba	4554.04	1
Bi	3067.71	15
Ca	3179.33	25
Cd	3261.06	50
Co	3453.51	3
Cr	4254.35	1
Cu	3273.96	2
Cu	2961.16	100
Fe	2929.00	100
Ga	2943.64	1
Ge	3039.06	1
In	3039.36	1
Mg	2802.69	2
Mn	2798.27	2
Mo	3170.34	1
Ni	3414.76	2
Pb	2833.07	10
Sb	2877.92	100
Si	2881.58	10
Sn	3175.01	5
Ti	3008.02	2
V	3185.00	2
Zn	3035.78	INTERNAL STANDARD
Hg	2536.52	1 p p b

tin concentrations vary somewhat sympathetically with temperature and gallium germanium and antimony vary antipathetically with temperature, however he suggests no temperature relationship with cadmium concentration.

Warren and Thompson (1945) state the average cadmium concentration in sphalerite from East Canada, Newfoundland, Greenland and Eastern U.S.A. to be less than 3,000 ppm , and sphalerite from Western U.S.A. and Mexico to be 4,300 ppm . Fryklund and Fleischer (1956) found an average of 4,000 ppm cadmium in 59 sphalerites from Coeur d'Alene mine Idaho and at Broken Hill Australia, Edwards (1955) reports 2,400 ppm cadmium in sphalerite. In Ireland the cadmium content of sphalerite seems to have a regional variation , (Patterson, 1970; Morrissey, Davis and Steed, 1971); at Silvermines the cadmium content of sphalerite is approximately 2,500 ppm increasing northwards to 4,300 ppm at Tynagh (Morrissey, 1970) until further northwards still a value of 10,223 ppm at Keel is attained.

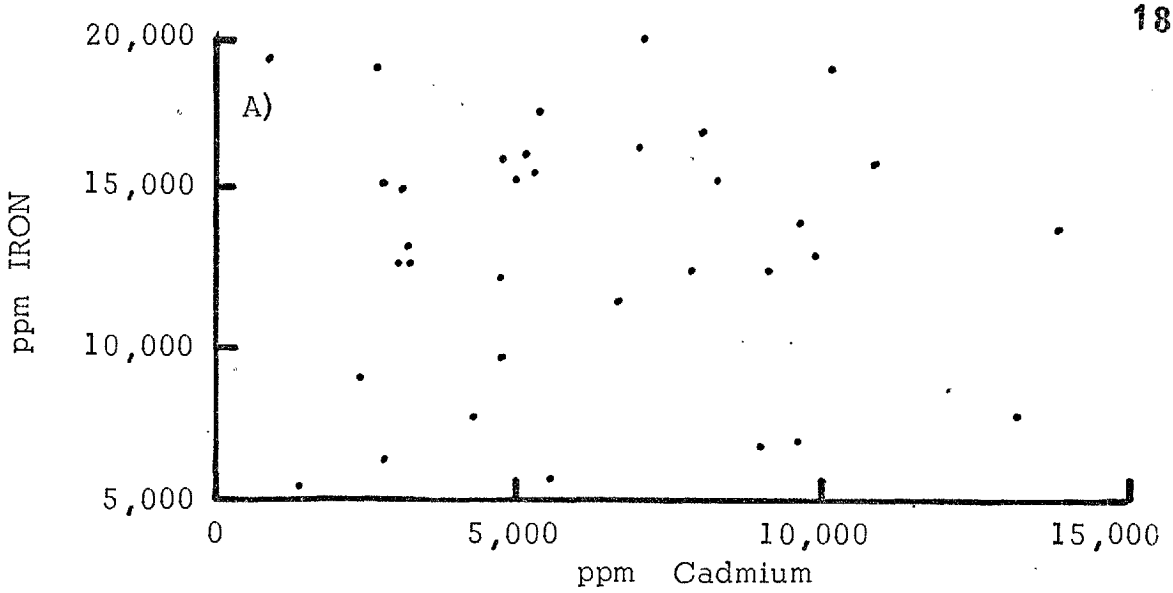
Opinion is somewhat divided as to whether or not cadmium is sympathetic or antipathetic with temperature increase. Stoiber suggests that cadmium is sympathetic with temperature and quotes high temperature Tuscany sphalerite with cadmium content of 12,300 ppm to support this. Traill believes the opposite and quotes low temperature sphalerite from Mill Close,Derbyshire,with cadmium content of 10,000 ppm to support his view. El Shazly opp.cit. found only 3,000 ppm cadmium in sphalerite from this deposit.

Attempts to relate iron and cadmium content to temperature of formation of sphalerite have so far failed,and Kullerud's quantification of the iron in sphalerite Geothermometer has been proved inaccurate (Boorman 1967, Barton and Skinner 1967).

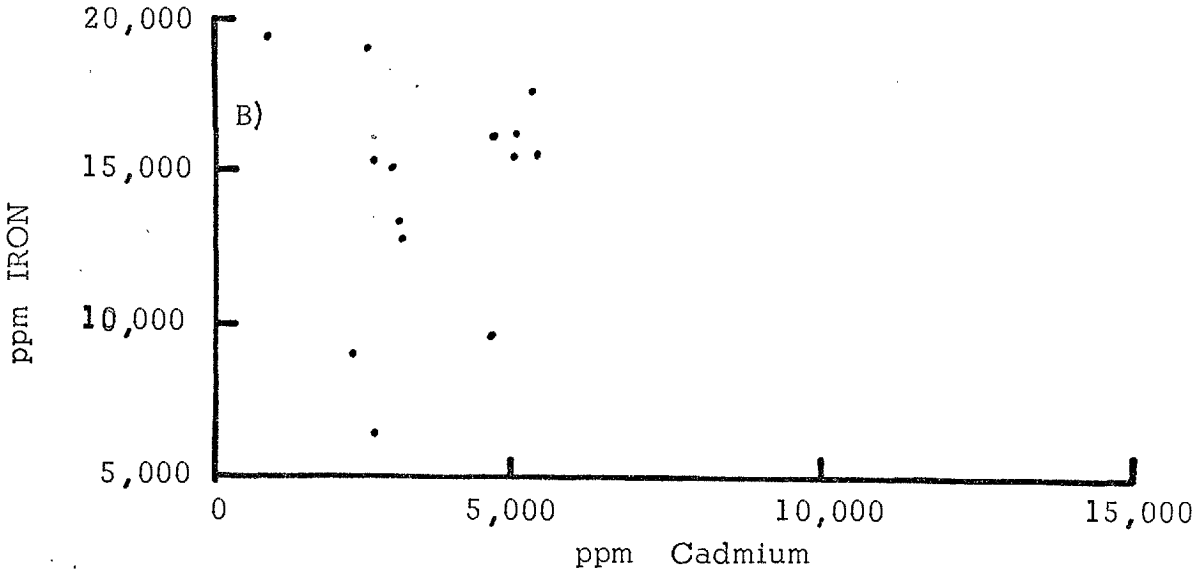
Boyle and Jambor (1963), in their work on sphalerites from Keno Hill and Galena Hill, found no relation between either cadmium or iron and temperature. This complete lack of relationship between iron and cadmium is very well displayed by Keel sphalerite, , Fig. 6.6.

The crustal abundance of cadmium has been estimated by Green (1959) as 0.15 ppm and by Brooks and Ahrens (1961) as 0.08 ppm . Zinc/cadmium ratios also seem to vary throughout the literature. Sandell and Goldick (1943) give a value of 500:1 and Rankhama and Sahama (1949) a value of 900:1. Kullerud (1953) and Edwards (1955), together with several other workers in the field, have however indicated the existence of complete isomorphism in the CdS/ZnS system and thus theoretically a complete transition from sphalerite to greenockite being possible. Mookerjee, (1962) however, states that this theoretical system does not appear to exist in nature. Mookerjee added sodium chloride to his ZnS/CdS system and produced two distinct mineralogical phases; he also found that the cadmium content of his sphalerite phase varied between 1,000 and 5,000 ppm , values quite common in sphalerite from many ore deposits.

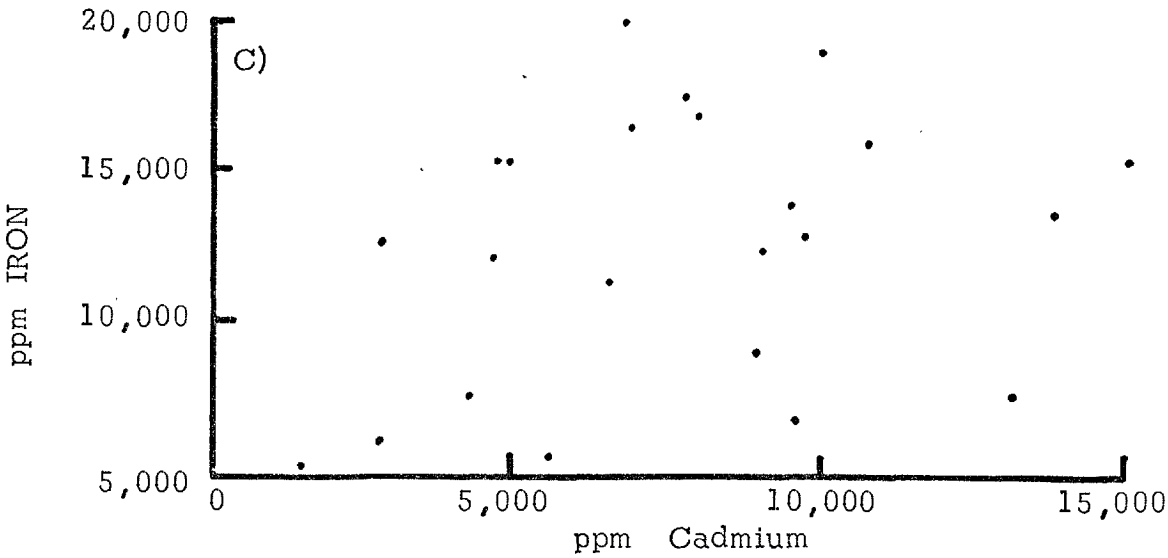
Ivanov (1964) suggested that high temperature skarn type lead-zinc deposits and low temperature silver deposits have cadmium - rich sphalerites but that the cadmium concentration in sphalerite depends on factors more complex than temperature alone. He also suggested that cadmium in low temperature sphalerite has an inverse relation to the concentration of Cl^- ions in solution. This would explain the cadmium-poor ores associated with hydrothermal solutions derived from mafic magmas rich in chlorine. Ivanov further concluded that cadmium may be enriched in ores deposited in carbonate sequences but that the degree of concentration of cadmium in the hydrothermal



A) Sphalerite from Underground & Drillcore



B) Sphalerite from Underground Workings



C) Sphalerite from Drillcore

FIG ...6.6

DIAGRAM ILLUSTRATING CADMIUM / IRON RELATIONS IN MATERIAL FROM DRILLCORE & UNDERGROUND WORKINGS

solution is really the determining factor in the degree of concentration of cadmium in the ore.

Edwin Roedder (1960) analysed fluid inclusions from zoned sphalerite crystals and found a sympathetic decrease in salinity with decrease in filling temperatures. Thus there is a general indication that with decreasing salinity and hence decreasing temperature of deposition, there may be an increase in the cadmium content of the sphalerite. However, other authors, Warren and Thompson (1945) and Fryklund and Fletcher (1956), like Ivanov, consider that the concentration of cadmium in the ore is solely determined by the concentration of cadmium in the ore forming solution. In the authors opinion there is no necessity to look for another reason for the concentration of cadmium in Keel sphalerite. This indicates the distinct possibility of a single ore fluid being responsible for all the sphalerite mineralization at Keel , with the centre of the plumbing system in the vicinity of the underground workings, due to the localization of greenockite and cinnabar there. Because of the high mercury content of Keel sphalerite, this latter is considered to be of low temperature origin, and further trace element information supporting this view will be presented in this Chapter.

(b) Germanium and Gallium.

El Shazly (1957) reports that gallium was present in three quarters of the sphalerites he examined and was present in all the sphalerites from the lower temperature deposits. However he finds a total absence of gallium in sphalerites from the higher temperature deposits of Cornwall, France, Portugal and Livuei Nigeria. Graton and Harcourt (1935), Stoiber (1940) and Warren and Thompson (1945) agree that gallium is a common trace element in low temperature sphalerites. Stoiber (1940) and Fleischer (1955) also suggest that germanium is most concentrated in sphalerites where the temperatures of formation are the lowest.

Table 6.7. following,gives the gallium, germanium iron and cadmium values for two sets of sphalerite samples. Each set has been divided into three on the basis of colour and magnetic properties. Each sample set came from the same hand specimen.

TABLE 6.7.

SAMPLE NUMBER	COLOUR	ppm. TRACES			
		Ga	Ge	Cd	Fe
(404B) 2127	Light	30.0	4.5	9150	9600
(404I) 2126	Intermediate	54.5	17.5	8900	16200
(404T) 2130	Dark	60.0	40.0	7600	16200
(67B) 2162	Light	22.0	N.D.	8750	8900
(67I) 2153	Intermediate	42.5	24.0	10700	15500
(67T) 2157	Dark	55.0	26.0	8350	17600

The analyses of gallium and germanium are most interesting, the gallium varying between 30 and 60 ppm in sphalerite samples 404 and between 22 and 55 in sphalerite samples 67. This variation is sympathetic with increased darkness of sphalerite and consequent increase in iron content. The variation is however at maximum 2.5 times. Germanium on the other hand varies very considerably, the variation also being sympathetic with increase in iron content of sphalerite. This latter characteristic was reported for yellow and black sphalerites from central Kentucky by Jolly and Heyl (1968). The latter authors also reported a similar order of magnitude difference in the gallium analyses; this however, was not confirmed at Keel. El Shazly (1957) detected germanium in varying amounts (5-500 ppm) in practically all his sphalerites from the lower temperature deposits, but discovered a virtual absence of the element from the higher temperature deposits.

(c) Silver.

The concentration of silver in Keel sphalerite is shown in Tables 6.1 - 6.4. Table 6.8 below shows the distribution of antimony, silver and copper in the two sphalerite series used previously.

TABLE 6.8.

SAMPLE NUMBER	COLOUR	ppm TRACES		
		Sb	Ag	Cu
(404B) 2127	Light	715	103	16
(404I) 2126	Intermediate	1210	300	875
(404T) 2130	Dark	1320	300	760
(67B) 2162	Light	185	56	855
(67I) 2153	Intermediate	325	112	750
(67T) 2157	Dark	437	142	630

The mean values of antimony, silver and copper in sphalerite from Keel are given in Table 6.9. El Shazly (1957) detected silver in nearly all his sphalerites in amounts varying from 1 - 1000 ppm. The author's analysis of Keel sphalerite shows similar limits. Patterson (1970) reports values of silver in Keel sphalerite up to only 3.2 ppm, although these values are based on only seven analyses, while for one other sphalerite at Keel he gives a value of 250 ppm which was attributed to included tetrahedrite. Jolly and Heyl (1968) give values of silver in American sphalerites from 0.5 ppm, in a low temperature deposit in Central Kentucky, to 1,000 ppm, in a high temperature deposit in Maine.

At Keel, low values of silver are usually associated with low values of antimony and copper, confirming Patterson's view that silver is tied up in argentiferous tetrahedrite. However, samples do occur with values of up to 62 ppm silver (Sample 2263) and 100 ppm antimony, copper, 340 ppm and lead 310 ppm, suggesting that more than the 3.5 ppm silver calculated by Patterson may be held in the sphalerite lattice.

TABLE ... 6.9

MEAN AND STANDARD DEVIATION VALUES FOR TRACE ELEMENT CONCENTRATIONS IN KEEL SPHALERITE .

ELEMENT	MEAN ppm	STANDARD DEVIATION ppm
Ag	166	150
As	n.d.	n.d.
Ba	60	46
Bi	n.d.	n.d.
Ca	105	360
Cd	10223	3059
Co	13	8
Cr	n.d.	n.d.
Cu	489	367
Fe	12954	6386
Ga	65	58
Ge	18	14
In	9	26
Mg	77	177
Mn	54	42
Mo	n.d.	n.d.
Ni	18	32
Pb	3179	2874
Sb	723	1250
Si	5973	2956
Sn	n.d.	n.d.
Ti	18	65
V	n.d.	n.d.
Hg	227	34

n.d. Below detection limit of element in ZnS .

Results based on the analysis of 113 sphalerites

Smith, (1963) reports silver values from Zewar to range from 12 to 110 ppm with antimony being entirely absent.

(d) Antimony.

Antimony was detected in the majority of Keel sphalerites, Tables 6.1 - 6.4, in amounts ranging from 93 - 11,700 ppm. A mean value of 723 ppm was calculated from these results. El Shazly indicates that, in his opinion, antimony is present in the lower temperature deposits rather than the higher temperature ones and suggests a possible antipathetic relation to temperature for this element. Considering the partitioning of trace elements between the three major sulphide minerals at Keel Fig. 6.7., and Table 6.10, antimony seems to be preferentially associated with galena. It is interesting to note that silver is also preferentially associated with galena and it is most probable that the high antimony and silver content of both the galena and sphalerite from Keel is indicative of no more than tetrahedrite inclusions in both minerals. However the possibility of lattice substitution of antimony for zinc in the sphalerite lattice must not be discounted as these elements have very similar ionic radii:- Sb^{3+}, 0.76 Å and Zn^{2+}, 0.74 Å. (Mason, 1966).

(e) Copper.

Copper was detected in all sphalerites analysed and ranges from 11 ppm - + 1000 ppm with a mean value of 489 ppm. Patterson (1970) suggests that high copper values are indicative of included tetrahedrite. However the copper/antimony relationship is far from consistent suggesting that other factors, such as exsolutions of chalcopyrite, which are

present in all Keel sphalerite, could be a major contributing factor to the high copper content of some sphalerites. Computer analysis of the data on trace elements in sphalerite, shows a very good correlation between iron and copper, indicating that chalcopyrite exsolutions could indeed be a major contributing factor to the high copper values. Warren and Thompson (1945) come to the same conclusion as Oftedal (1940), that is, that there is no reason to postulate a chemical relationship between copper and sphalerite. Fleischer (1955) gives analytical data on some 297 sphalerites with copper concentrations ranging up to 5%. His conclusion is also that this copper represents nothing more than exsolved copper minerals, with chalcopyrite as the most important.

Patterson (1970) finds pale sphalerite at Keel to contain 15 - 27 ppm copper and 3,500 ppm iron and on the basis of polished section studies indicates that pale sphalerite is most unlikely to contain exolved chalcopyrite. Patterson's highest value of copper in Keel sphalerite was 660 ppm, with an iron content of 15,000 ppm in the same sample, a dark sphalerite. The author has found eleven specimens of clear, honey coloured sphalerite at Keel containing 100 ppm copper and 9,000 ppm iron; it cannot therefore be said that the honey coloured sphalerite at Keel is most unlikely to contain exsolved chalcopyrite. This view is also supported by the excellent correlation coefficient between Cu and Fe in Table 6.12.

Patterson (1970) also concludes in his summary on copper in Keel sphalerite that "No copper values occur between 27 ppm and 115 ppm". He goes on to suggest that sphalerite containing up to 27 ppm does so in solid solution, while that containing 115 ppm and greater, contains chalcopyrite exsolutions. Here again it is worth noting that more than twelve sphalerites from this study, analysed by

the author, were found with copper values between 27 ppm and 115 ppm. An extensive thin section study and polished section study of the sphalerites was not carried out by the author, so that no upper limits on the copper concentration required in sphalerite before exsolution takes place, can be given. However, chalcopyrite blebs were seen in both honey coloured or dark sphalerite. It must therefore be suggested that whereas tetrahedrite does contain high amounts of copper at Keel, the correlation of high copper content of Keel sphalerite with exolved chalcopyrite blebs must not be discounted.

(f) Iron.

The iron content of Keel sphalerite varies between 0.29% and 4.0% with a mean value of 1.3%. This iron variation can be correlated with a colour variation in the sphalerite, the lighter sphalerite containing less iron than the darker. It is interesting to note however, that iron content/colour relationships, even within the one deposit, cannot be specifically quantified. Sample 2163, a dark sphalerite, contains 0.84% iron with its light, honey coloured equivalent, from the same hand specimen, containing 0.79% iron, (Sample 2152).

Manning (1967), investigating the iron content of sphalerite, concluded that iron was distributed between interstitial octahedral sites and substitial tetrahedral sites. This indicates that iron can exist in both fourfold and eightfold co-ordination within the sphalerite lattice. He further concluded that the octahedrally co-ordinated iron is in the ferric state, while the tetrahedrally co-ordinated iron was in the ferrous state. This theory would account for

the fact that, within a deposit, where the co-ordination chemistry of iron within the individual sphalerites would be similar, colour is more clearly associated with iron content. On the basis of this information, it can be said that any attempted correlation between iron content of sphalerite and colour, should always be restricted to a single deposit.

Jolly and Heyl (1968) find sphalerite from Central and Eastern Tennessee and Central Kentucky to contain between 0.1 and 0.5% iron, sphalerite from the Kentucky/Illinois region to contain 1.2 - 4.2% iron and sphalerite from Maine to contain 5 - 10% iron. These three groups are listed in order of increasing temperature of deposition. However, the use of a Fe - Zn - S system geothermometer (Kullerud, 1953) has been discredited, Boorman (1967) and Barton and Skinner (1967), and no attempt is made in this text to draw any conclusions about temperature of formation for Keel sphalerite, on the basis of its iron content.

(g) Manganese.

Manganese is present in all 113 sphalerites analysed, Tables 6.1 - 6.4, and varies between 7.5 ppm and 1,000 ppm, with a mean of 53.9 ppm. Two specimens contained anomalously high manganese, 2289 and 2283, containing 1,000 ppm and 850 ppm; all other sphalerites contained manganese much nearer the mean value. Of the eight sphalerites from Keel analysed by Patterson, five were below his detection limit of 30 ppm and the other three were 50 ppm, 77 ppm and 250 ppm respectively. Jolly and Heyl (1968) quote values of 1 - 20 ppm Mn for sphalerite from Central Tennessee and Central Kentucky, 10 - 20 ppm Mn from the Kentucky/Illinois district and North Carolina and, 200 - 3000 ppm

from Maine. This indicates a sympathetic relationship between manganese and increasing temperature of deposition of sphalerite.

El Shazly (1957) finds, in his analysis of sphalerite from various British localities, that manganese tends to vary sympathetically with temperature, being highest, 300 - 5,000 ppm in the high temperature deposits of Cornwall, France, Portugal, and Nigeria and virtually absent from the low temperature deposits of the Pennines, Flintshire and Caernarvonshire. In the low and medium temperature siliceous veins of Cardiganshire, the sphalerite contained an average of 150 ppm manganese, whereas close to the granites of the West of England, values of 1,000 - 5,000 ppm manganese are not uncommon. Jolly and Heyl (1968) confirm this observation with their data on high temperature Maine sphalerites. The average manganese value of 53.9 ppm for Keel sphalerites tends, in the light of this evidence, to suggest a low - medium low temperature of formation. It is however worth noting that at Keel the higher manganese values are usually associated with high calcium and magnesium values suggesting that the high manganese may only be due to inclusions of manganese-rich dolomite gangue in the sphalerite crystal.

(h) Titanium.

Titanium is present as a trace in the vast majority of Keel sphalerites and ranges from < 2 ppm to 640 ppm in one anomalously high sample. The mean value of 18.2 ppm is very close to Patterson's figures of 10 - 13 ppm, for the sphalerites he analysed. El Shazly (1957) reports titanium to be present only in his high temperature deposits, while Jolly and Heyl (1968) report 70 ppm titanium in the high temperature Maine sphalerite and 3 - 30 ppm Ti in the

low temperature Central Kentucky and Central Tennessee sphalerites. In a written communication to Jolly and Heyl (1967), Edwin Roedder states that on the basis of fluid inclusion studies on sphalerites from the central Kentucky veins, he had arrived at a temperature of less than 120°C for their deposition. If one can relate titanium content of sphalerite to its temperature of deposition, then Keel sphalerite must be of low temperature origin.

(i) Indium.

Indium is present in detectable amounts in approximately half the analysed sphalerites and assumes major significance in two of them, samples 2241 and 2267, which contain 174 ppm and 190 ppm indium respectively. These values however are anomalous as compared to the mean of 9.0 ppm. Jolly and Heyl report indium as occurring in only one of the New England veins in a concentration of 15 ppm and El Shazly expresses his belief that indium concentration is sympathetic with temperature. He quotes values of 700 ppm indium, in high temperature Nigerian sphalerite and a maximum of 100 ppm indium, in low temperature sphalerite from the north Pennines and Flintshire, to support this. On this evidence also, Keel sphalerite is typical of a low temperature deposit.

(j) Lead.

Lead was detected in all Keel sphalerites, Tables 6.1 - 6.4, and had a mean value of 3,200 ppm. This high concentration of lead is considered to be solely the result of mechanical inclusions of galena, or other lead salts, in the sphalerite crystal.

(k) Nickel.

Nickel is present in the majority of sphalerites and attains its maximum concentration of 210 ppm in sample 2270. This specimen also has the highest iron content of any sphalerite, 4.02%. On reference to Table 6.10 it can be seen that the partitioning of nickel is 3:1 in favour of pyrite and this high nickel value could be due to the presence of nickeliferous pyrite in the sphalerite crystal. The mean value of nickel in sphalerite is 17.7 ppm. El Shazly found no nickel in any of his sphalerites and Jolly and Heyl (1968) reported values of 15 ppm nickel in one sample of sphalerite from Central Kentucky and values of 9 and 4 ppm in two sphalerites from the Kentucky-Illinois district. These observations further suggest that the nickel in Keel sphalerite is probably the result of included nickeliferous pyrite.

(l) Cobalt.

Cobalt is slightly less abundant in Keel sphalerite than nickel, having a mean value of 12.6 ppm. Warren and Thompson (1945) found that cobalt is a characteristic element in low temperature sphalerite from Cumberland and high temperature sphalerite of New South Wales. Oftedal (1940) and Gabrielson (1945) found cobalt to increase with temperature in Norwegian and Swedish sphalerites and this fact is also brought out by Jolly and Heyl (1968) who give analyses of high temperature Maine sphalerites in which cobalt occurs in concentrations up to 200 ppm.

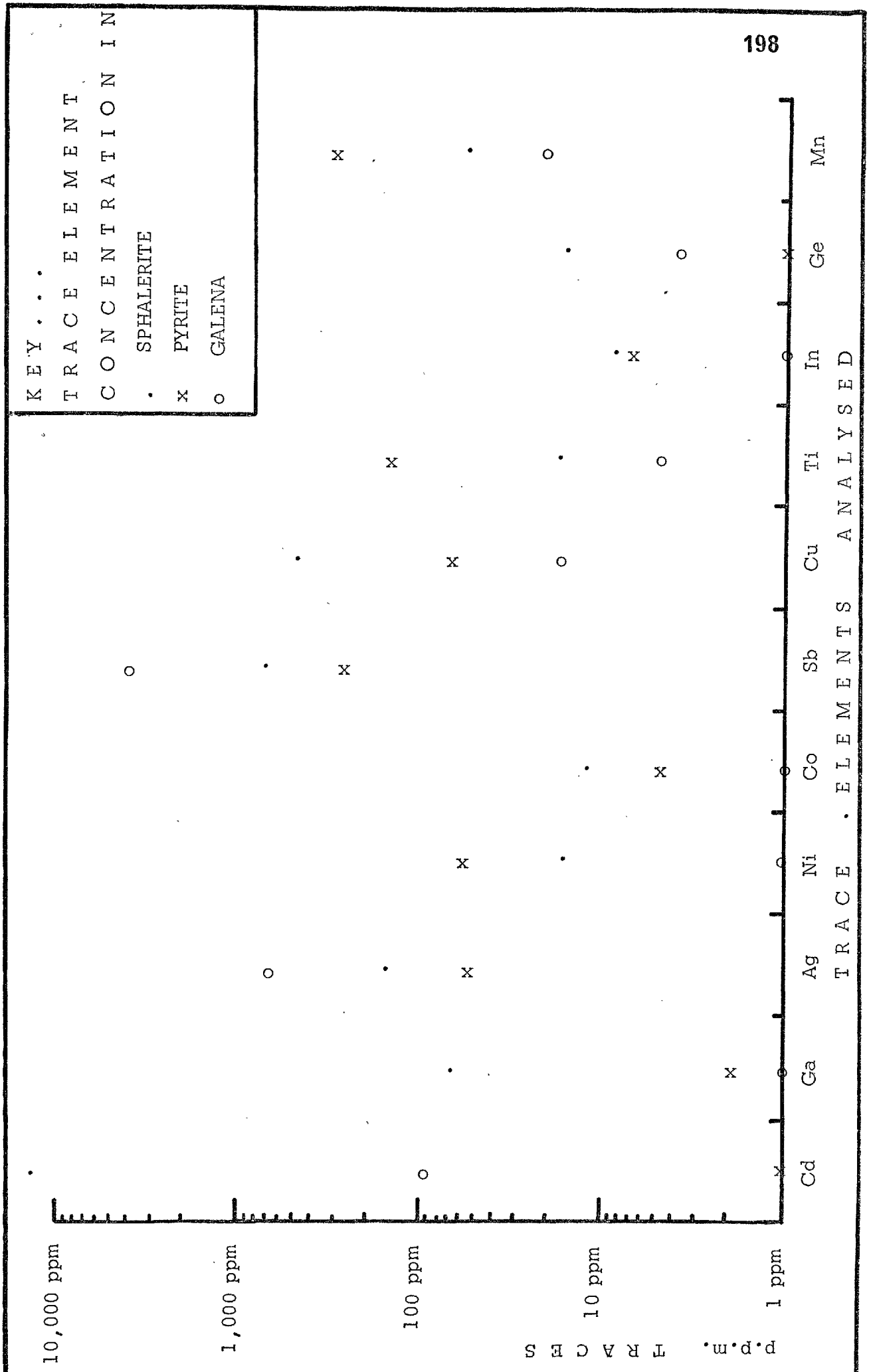


FIG ... 6.7 DIAGRAM SHOWING TRACE ELEMENT DISTRIBUTION IN SPHALERITE, GALENA & PYRITE, KEEL PROSPECT.

ELEMENT	MINERAL PYRITE	MINERAL GALENA	MINERAL SPHALERITE
CADMIUM	n.d.	96	10,223
GALLIUM	2	n.d.	65
SILVER	58	709	166
NICKEL	57	n.d.	18
COBALT	5	n.d.	13
ANTIMONY	240	2083	723
COPPER	69	18	488
TITANIUM	168	5	18
INDIUM	7	n.d.	9
GERMANIUM	n.d.	4	18
MANGANESE	301	23	54

TABLE . . . 6.10 DIAGRAM OF RELATIVE ABUNDANCES OF TRACE ELEMENTS IN SPHALERITE , GALENA & PYRITE , KEEL PROSPECT ,COUNTY LONGFORD , IRELAND .

(Results are mean values and expressed as p p m)

(m) Vanadium, Chromium, Tin and Molybdenum.

The trace elements do not attain significant amounts in any of the Keel sphalerites, being only just above detection limit.

(n) Bismuth and Arsenic.

Both these elements are always below detection limit for the optical spectrograph, in Keel sphalerite.

(o) Calcium, Magnesium, Silicon and Barium.

All these elements are present in varying amounts in Keel sphalerite, Tables 6.1 - 6.4., and represent inclusions of gangue minerals wihin the sphalerite crystal. El Shazly reports these traces also to be present in all of his sphalerites and for the same reasons. Jolly and Heyl record analyses in all their American sphalerites in which these trace elements also occur as included gangue minerals.

(p) Vertical Differences in Trace Element Assemblage in Keel Sphalerite.

Vertical zonation of trace elements in Keel sphalerite is also absent throughout the deposit. This is well substantiated by the comparison of trace elements in 37 sphalerites from 200' level and 37 sphalerites from the 500' level. Mean values of cadmium, iron, mercury and copper are shown in Table 6.11.

TABLE 6.11.

ELEMENT	200' LEVEL ppm	500' LEVEL ppm
Cadmium	10,026	10,129
Iron	13,870	14,444
Mercury	218.4	225.0
Copper	415.1	425.8

Variation in trace element assemblage in sphalerite is also not apparent laterally.

6.6. INTER-ELEMENT RELATIONSHIPS IN KEEL SPHALERITE.

A simple linear regression analysis of element relationships, for seventeen elements in fifty-nine samples of Keel sphalerite, was carried out by computer at Queen's University, Kingston, Ontario by S. Willington. A total of 136 inter-element relationships were investigated and the results are shown in Table 6.12 as correlation coefficients for the various inter-element relationships. In Table 6.12, those correlation coefficients bearing an asterisk represent, in the author's opinion, meaningful element relationships. Other high values for this correlation coefficient represent mere bunching of the data or very little variation in one parameter.

In all, seven inter-element relationships appear to be real, these are as follows:-

(1) Ag/Cu - Indicative of included tetrahedrite in the sphalerite.

(2) Cu/Fe - Indicative of included chalcopyrite in the sphalerite.

(3) Ca/Mg - Indicative of included dolomite in the sphalerite.

	Cd	Ga	Ag	Ni	Co	Sb	Ba	Cu	Ca	Ti	In	Ge	Fe	Si	Pb	Mg	Mn
Cd	-	0.368	0.208	0.094	0.069	-0.136	-0.287	-0.211	-0.185	0.225	0.381	-0.096	0.212	-0.040	-0.165	-0.111	0.176
Ga		-	0.368	-0.120	0.152	-0.023	-0.095	0.038	0.154	0.532	0.731	0.244	0.551	0.339	-0.098	-0.031	-0.107
Ag			-	-0.127	-0.030	0.240	-0.216	0.823*	-0.212	0.598	0.204	0.456	0.486	0.170	-0.080	-0.175	-0.087
Ni				-	-0.069	0.384	-0.028	-0.215	-0.867	-0.061	-0.003	-0.230	-0.026	0.045	-0.138	0.328	-0.194
Co					-	0.103	0.385	-0.058	0.304	0.110	-0.012	-0.207	0.222	0.396	0.222	-0.297	-0.154
Sb						-	-0.195	0.284	0.000	0.758	0.379	0.404	0.603	-0.113	-0.002	0.143	-0.113
Ba							-	-0.232	-0.206	-0.077	0.769	-0.426	-0.169	0.418	0.143	-0.056	-0.269
Cu								-	-0.272	0.170	-0.179	0.694*	0.799*	0.210	0.402	-0.201	0.032
Ca									-	-0.296	-0.390	-1.000	-0.096	-0.301	-0.255	0.947*	0.551
Ti										-	-0.081	-0.240	0.235	0.329	-0.070	-0.151	-0.000
In											-	-0.099	0.129	0.173	-0.288	0.069	-0.053
Ge												-	0.729*	-0.668*	-0.035	-0.131	0.151
Fe													-	0.264	0.084	-0.183	-0.027
Si														-	0.455	-0.208	-0.313
Pb															-	-0.217	-0.040
Mg																-	0.646*
Mn																	-

TABLE . . . 6 .12 TABLE ILLUSTRATING THE CORRELATION COEFFECIENTS OF TRACE ELEMENTS IN SPHALERITE FROM KEEL PROSPECT , COUNTY LONGFORD , IRELAND .

(4) Ge/Fe - Indicates possible substitution for iron in the sphalerite lattice, or replacement of iron in included chalcopyrite.

(5) Cu/Ge - Indicates replacement of iron in included chalcopyrite.

(6) Ge/Si - Indicates possible replacement of silicon in included silicate gangue material.

(7) Mn/Mg - Indicative of manganese rich included dolomite.

The observations really indicate that the inter-element relationships that do exist in Keel sphalerite, are mainly due to included sulphide minerals, chalcopyrite and sphalerite, or included silicate or dolomite gangue. It is also indicated that the distribution of other trace elements appears to be entirely arbitrary and apart from indicating broad general trends, gives very little information as to the metallogenesis of the deposit.

6.7. TRACE ELEMENTS IN GALENA FROM KEEL.

Table 6.10 shows the relative partitioning of trace elements between sphalerite, galena and pyrite at Keel. Here it can be seen that both silver and antimony are preferentially associated with galena. Twelve galena samples were used for this study and were prepared in exactly the same way as the sphalerites. The only difference was the preparation of standards, the galena standards being made up in a lead oxide and not zinc sulphide base. The minor elements looked for in Keel galena were as follows:

Cd, Ga, Ag, Ni, Sb, Ba, V, Cu, Cr, Ca, Sn, Mo, Ti, In, Bi, Ge, Fe, Si, As, Mg, Mn and Hg. Of these elements Co, In, Ga, V, Cr, Ca, Sn, Mo, Bi, As and Mg were always below detection limits

and silicon was only looked for in one sample and found to be 10,000 ppm. The spectral lines used and limits of detection of the minor elements in Keel galena and pyrite are shown in Table 6.13.

Mercury was not looked for on the spectrograph, but was analysed by the same methods as for mercury in sphalerite. One major problem however, occurred in the dissolution of galena by concentrated nitric acid prior to the stannous chloride reduction method. Sulphur was oxidised to sulphate and as a result insoluble lead sulphate precipitated. However, in the author's opinion the available mercury was all taken into solution in the nitric acid and not adsorbed onto the precipitated lead sulphate. The mercury results have already been discussed at the beginning of this chapter.

(a) Nickel.

Nickel is detected in trace amounts in two of the twelve specimens. One of these, 2287, contains the highest iron and titanium of any of the galenas and it is quite possible that nickel is present as a result of included nickelferous pyrite. Patterson (1970) found no nickel or iron in the two specimens of galena from Keel which he analysed. El Shazly on the other hand, found nickel to be commonly present in his galena samples, in quantities ranging from 10 - 200 ppm.

(b) Silver.

Keel galena contains, on average, 709 ppm silver. The higher silver contents correspond to high antimony and this, together with the fact that tetrahedrite does occur in Keel galena, Patterson (1970), points to mechanically

TABLE ...6.13

WAVELENGTHS OF THE SPECTRAL LINES USED IN THE DETERMINATION OF MINOR ELEMENTS IN PYRITE AND GALENA SAMPLES FROM KEEL IRELAND ,

ELEMENT	WAVELENGTH Å	D E T E C T I O N L I M I T S	
		PYRITE ppm	GALENA ppm
Pd	3421.24	INTERNAL	STANDARD
Ag	3382.89	1	1
As	2860.45	700	700
Ba	4554.04	1	1
Bi	3067.71	15	10
Ca	3179.33	25	25
Cd	3261.06	50	20
Co	3453.51	3	3
Cr	4254.35	1	1
Cu	3273.96	2	2
Cu	2961.16	100	100
Fe	2929.00	-	100
Ga	2943.64	3	3
Ge	3039.06	2	2
In	3039.36	500	2
Mg	2802.69	10	*
Mn	2798.27	2	2
Mo	3170.34	1	1
Ni	3414.76	3	2
Pb	2833.07	50	-
Sb	2877.92	200	50
Si	2881.58	10	10
Sn	3175.01	5	5
Ti	3008.02	10	2
V	3185.00	5	1
Hg	2536.52	1 ppb	1 ppb

\- Major Element * Masked by Lead Line

included tetrahedrite as the main source of silver. El Shazly suggests that, in the samples of galena from the British Isles analysed by him, he determined an average silver content of 100 ppm. He also drew attention to local high spots, Halkyn and Staffordshire, 100 - 200 ppm, Ireland, 300 ppm, Merioneth, 2,800 ppm, Cardigan, 866 ppm, Devon and Cornwall, 1,564 ppm.

(c) Antimony.

Antimony shows a marked preference for galena at Keel with the average antimony content of twelve galenas being 2,083 ppm. This is three times higher than the average in sphalerite. Oftedal (1940) shows antimony to increase with increasing temperature, and El Shazly shows values of 1,000 ppm in Cornish galenas in support of the same conclusion. However at Keel so much evidence points to a low temperature of formation of the deposit, that there is really no need to invoke any other reason than mechanically included tetrahedrite as a cause for high antimony in Keel galena.

(d) Copper.

Copper values are relatively low, 18 ppm being the mean, and are probably indicative of included tetrahedrite in the galena crystal.

(e) Cadmium.

Cadmium is present in minor amounts in eleven of the twelve galenas analysed. However its presence is probably due to included sphalerite and not to substitution for lead in the galena lattice.

(f) Titanium.

Titanium was present in all but one sample of galena and varied in concentration up to 15 ppm. El Shazly found titanium to vary from 1-200 ppm in his British galena, but to rarely exceed 50 ppm. He further comes to the conclusion that high values of titanium are encountered in galenas deposited at both low and high temperatures, indicating that temperature of deposition does not influence the distribution of titanium in galena. The highest titanium content of any of the Keel samples occurs in the same sample as the highest iron content and it is therefore probable that titanium concentration merely reflects the degree of pyrite contamination in the galena crystal.

(g) Germanium.

Germanium occurs in two of the twelve galena samples in concentrations of 19.0 and 25.0 ppm. The relation of germanium to silica in sphalerite has been well shown and the germanium concentration in galena is probably only a function of included silicate gangue material which, at least in one sample, reaches > 10,000 ppm.

(h) Iron.

Iron is seen to be present in only two of the galena samples. Unlike the iron in sphalerite, iron does not substitute for lead in the galena lattice and its presence in these two samples probably indicates included pyrite.

(i) Manganese.

Manganese is present as a trace in all but two of the twelve galena samples analysed. Its concentration varies up to 125 ppm. Calcium, magnesium and barium are, in the main, only present in low amounts, while silicon is present in high amounts as a contaminant. However the manganese in galena at Keel is probably attributable to the same cause as the manganese in sphalerite, that of being a constituent of contaminating dolomite gangue. However, it must be noted that these levels of manganese could be held in the galena lattice. El Shazly relates manganese in excess of 100 ppm. to high temperature of deposition and quotes Trewethen in Cornwall, with 500 ppm manganese in galena, to prove this. The general content of 50 ppm manganese in Keel galena therefore possibly points to a low temperature of deposition.

6.8. TRACE ELEMENTS IN PYRITE FROM KEEL.

Pyrite is the most common iron sulphide at Keel, but nonetheless is only of very minor distribution compared to sphalerite and galena. A table of spectral lines of elements looked for and limits of detection of those elements is shown in Table 6.13.

Four samples of pyrite were used in this study, standards being prepared in a similar way to those for galena and sphalerite, but using a ferric oxide base.

Mercury analysis was carried out by dissolving the sample in 4:1. nitric acid: perchloric acid and adding stannous chloride to a diluted aliquot of the final solution. The method of analysis and results have already been discussed in this chapter. Germanium, cadmium, tin and bismuth were not detected in any of the samples analysed.

When looking at the partitioning of elements between sphalerite, galena and pyrite, Table 6.10, it can be seen that manganese, titanium and nickel appear to be preferentially concentrated in pyrite and on reference to sample 2144, on which a complete analysis was carried out, vanadium, molybdenum and arsenic also appear to be preferentially concentrated in pyrite.

Manganese is seen to vary from 3 ppm - 1,000 ppm and is probably due to admixed dolomite. Lead values are consistantly high, 980-3,500 ppm, and probably only represent included galena, as lead will not substitute into the pyrite lattice. Antimony is only detected in one sample, 2261, this sample also having the highest lead content, and in the author's opinion this high antimony is a reflection of included tetrahedrite in the galena. Gallium and indium are probably present as lattice substitutes in pyrite. Titanium is high in the majority of pyrite and could indicate included rutile, however some degree of substitution in the pyrite lattice is possible due to the compatibility of ionic radii of the two elements.

ELEMENT	IONIC RADII	ELEMENT	IONIC RADII
Fe^{2+}	0.74 Å	Ti^{3+}	0.76 Å
Fe^{3+}	0.64 Å	Ti^{4+}	0.68 Å

Cadmium is present in sub-trace levels, and no specific values were obtainable for it. Copper values vary up to 230 ppm and probably represent increasing amounts of chalcopyrite in the pyrite crystal. Silver values are quite consistently similar, 41 - 72 ppm, but are all higher than Patterson's highest value of 29 ppm. It is quite possible that this silver is associated with included tetrahedrite in inclusions of galena within the pyrite. Nickel was detected in all but one sample of pyrite and cobalt in one sample. Arsenic is detected only in pyrite, although its presence in sphalerite was confirmed by alternative analysis, (Chapter 8). This arsenic is present as a lattice constituent of pyrite, a fact discussed in Chapter 8. Vanadium and molybdenum are also preferentially associated with pyrite but in very minor concentrations.

6.9. X-RAY ANALYSIS OF SPHALERITE, GALENA AND PYRITE.

A study was carried out on 32 samples of sphalerite, four samples of galena and four samples of pyrite in order to ascertain cell dimensions and to obtain any information about variation in these parameters throughout the deposit. It was also hoped to obtain information about the effect of trace element concentrations on these parameters.

(a) Sample Preparation.

Each mineral sample was carefully hand picked to avoid contamination and then ground to an ultra-fine powder in an agate mortar. A glass fibre, smeared with a thin film of vaseline, was then rolled in the sample powder until a

fine coating of the mineral was adherring to the fibre. This fibre was then mounted inside a Phillips 11cm. powder camera and exposed to Co Kα radiation,(λ 1.78890 Å), for twelve hours. Co Kα radiation was used because the only elements which absorb or scatter it to any degree are manganese, chromium and vanadium, none of which elements occur to any extent in the minerals being analysed. Powder photographs obtained were developed and fixed using standard methods but taking great care to obtain as near standard working conditions throughout the procedure as possible. Each photograph was interpreted using a vernier rule,and results converted to d-spacings using the appropriate tables. Sphalerite, galena and pyrite are all cubic minerals and have only one cell edge dimension. The true value of this cell edge was calculated exactly by plotting a series of cell edges,obtained by using the various values of d calculated,against the function

$$\frac{1}{2}\ \frac{\cos^2\theta}{\sin\theta} + \frac{\cos^2\theta}{\theta}$$ the

Taylor, Sinclair, Nelson and Riley extrapolation factor.

A digression is here necessitated to explain the use of this function .

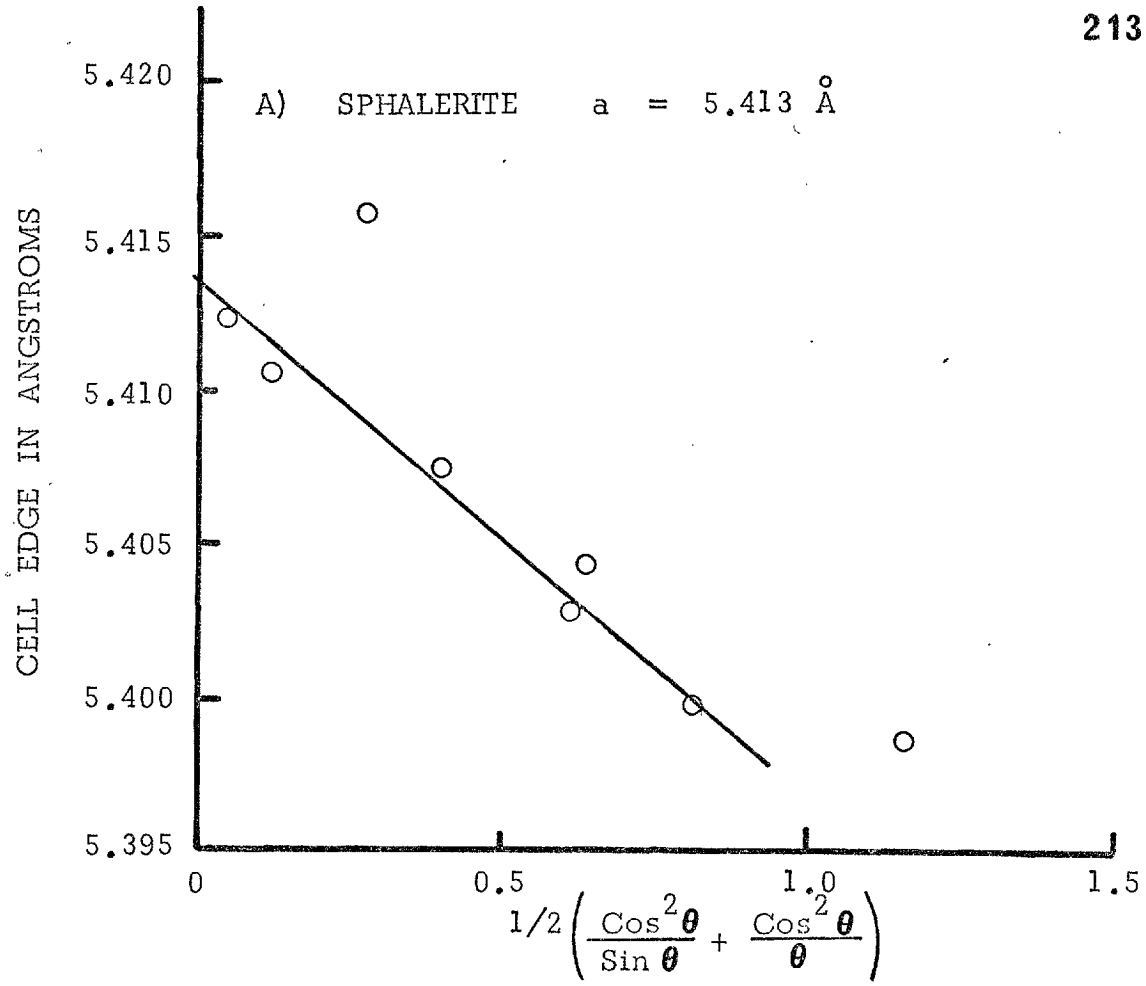
The position of the reflected arc on the powder photograph depends on the transparency of the specimen. If the crystal is absorbing,then only its surface regions can defract X-rays. The suppression of part of the reflected beam has the effect of narrowing the line on the photograph and of displacing its centre from the true centre of the reflection.

This effect decreases with increasing values of θ, vanishing completely at $\theta = 90^{o}$. In the laboratory X-ray instruments, the X-rays are sub-parallel and they diverge, and this divergence complicates greatly the angular dependence of the absorption error. Consequently techniques have been devised to eliminate this error and obtain an accurate value for the cell edge. Although the d value of a reflection whose glancing angle is 90^{o} cannot be measured, it is possible to extrapolate back to this value from those d values that can be measured. Taylor and Sinclair (1945) and Nelson and Riley (1945) have shown separately that by plotting the function

$$\frac{1}{2}\ \frac{\mathrm{Cos}^2\ \theta}{\mathrm{Sin}\ \theta} + \frac{\mathrm{Cos}^2\ \theta}{\theta} \quad \text{against}$$

equivalent a values, it is possible to obtain cell edge readings, free from interference, at $\theta = 90^{o}$. Figure 6.8a shows one such extrapolation for sphalerite and Figure 6.8b a similar extrapolation for galena.

Using the method, cell edges for sphalerite, galena and pyrite from Keel were calculated and compared with previously obtained data for similar minerals, Table 6.14. The mean value of the cell edge of 32 sphalerite samples was 5.416 Å and the standard deviation 0.0026 Å.



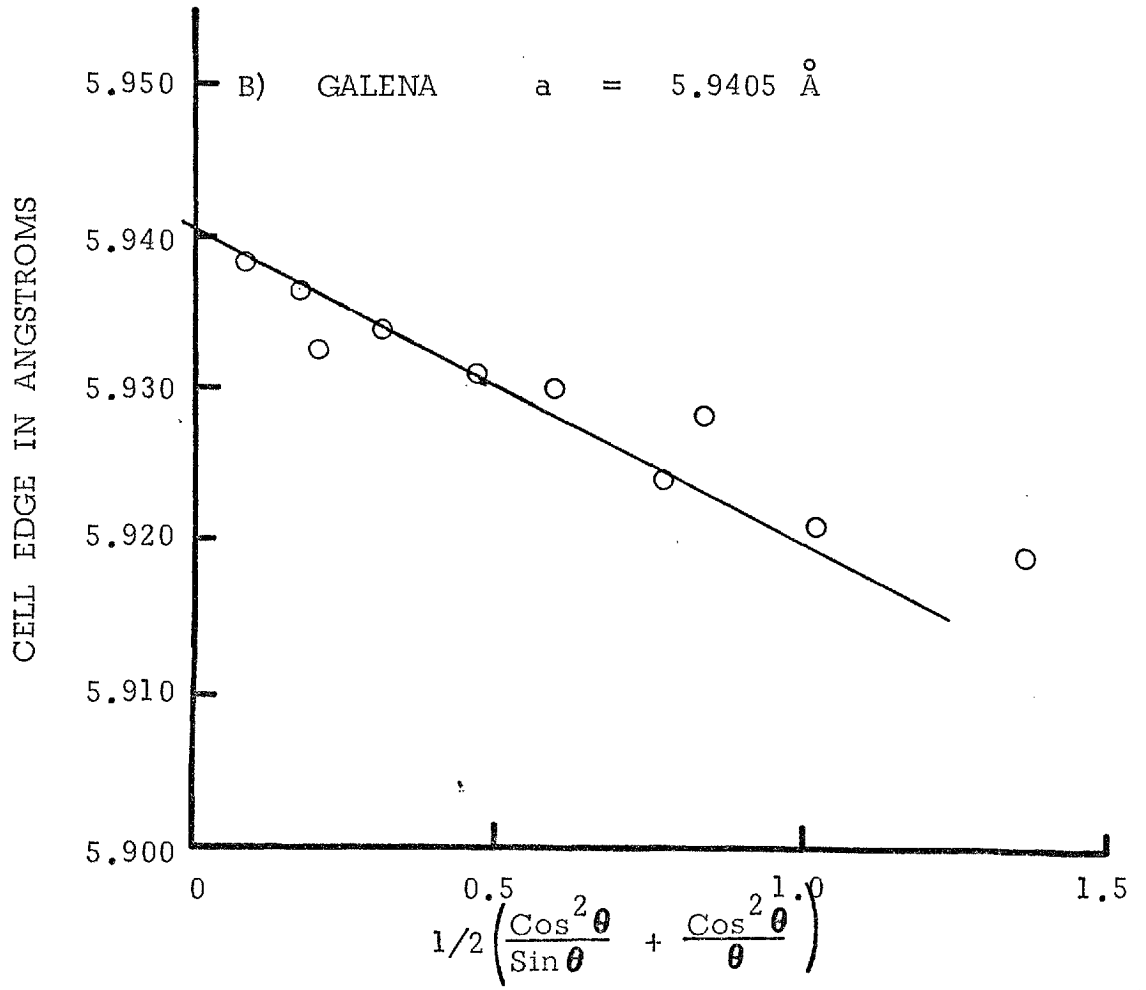


FIG ... 6.8

DIAGRAM ILLUSTRATING THE METHOD OF CALCULATING THE CELL EDGE OF SPHALERITE AND GALENA CRYSTALS

TABLE 6.14.

MINERAL	KEEL a SPACING	LITERATURE a SPACING		CRYSTAL SYSTEM
SPHALERITE	5.416 Å	5.411 Å		CUBIC
GALENA	5.938 Å	5.929 Å		CUBIC
PYRITE	5.389 Å	5.419 Å		CUBIC
WURTZITE	NONE	3.828 Å		HEXAGONAL
MARCASITE	NONE	4.445 Å	a	
		5.425 Å	b	ORTHORHOMBIC
		3.388 Å	c	

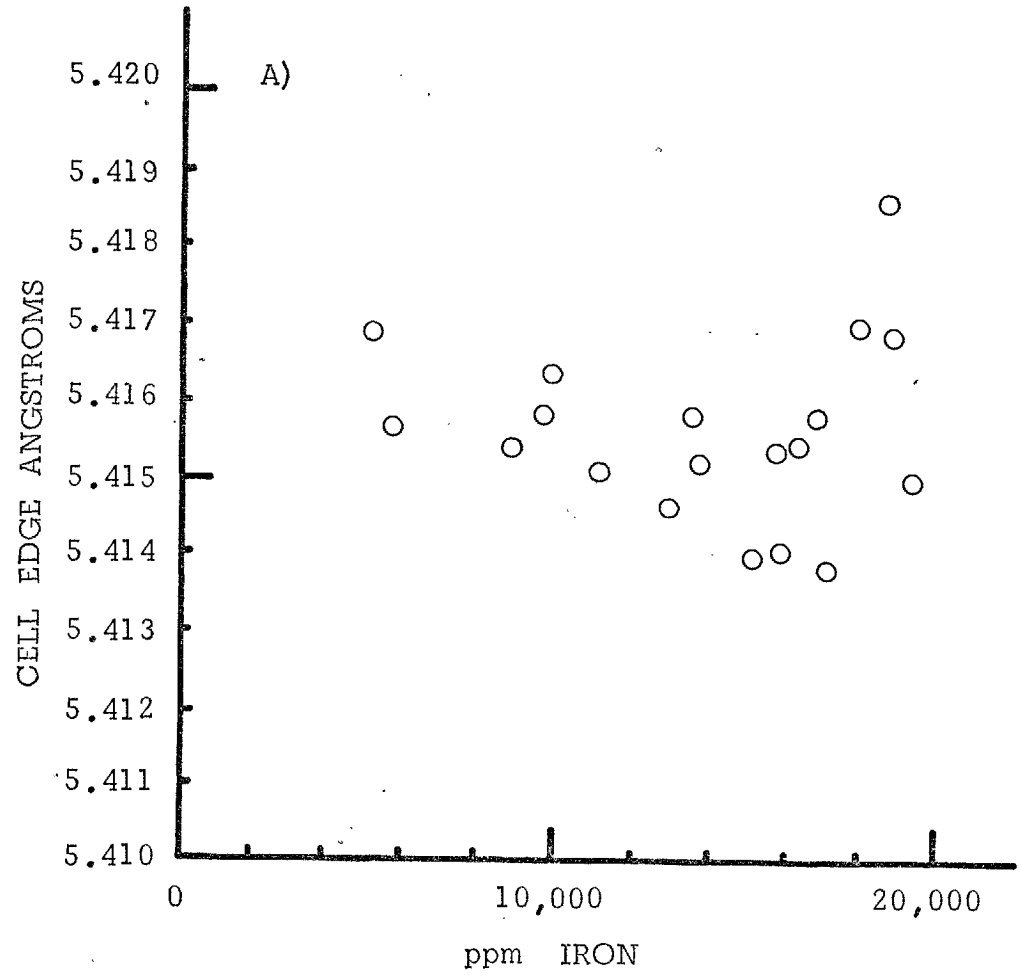
It was further decided to investigate the effects, if any, of varying amounts of trace elements on the unit cell characteristics of sphalerite. Consequently the concentrations of the major 'trace' elements, iron and cadmium, were plotted against cell edge of the sphalerite. The results obtained, Fig. 6.9, showed no detectable systematic variation of cell parameters with either increasing iron content or increasing iron plus cadmium content.

6.10. SUMMARY AND CONCLUSIONS.

On the basis of the trace element study of sphalerite, galena and pyrite within the Keel orebody, some very important facts emerge:-

(a) There is distinct partitioning of trace elements between the various minerals.

(b) The sphalerite and probably the galena and pyrite also, appear to conform to the trace element mineralogy of a low temperature deposit.



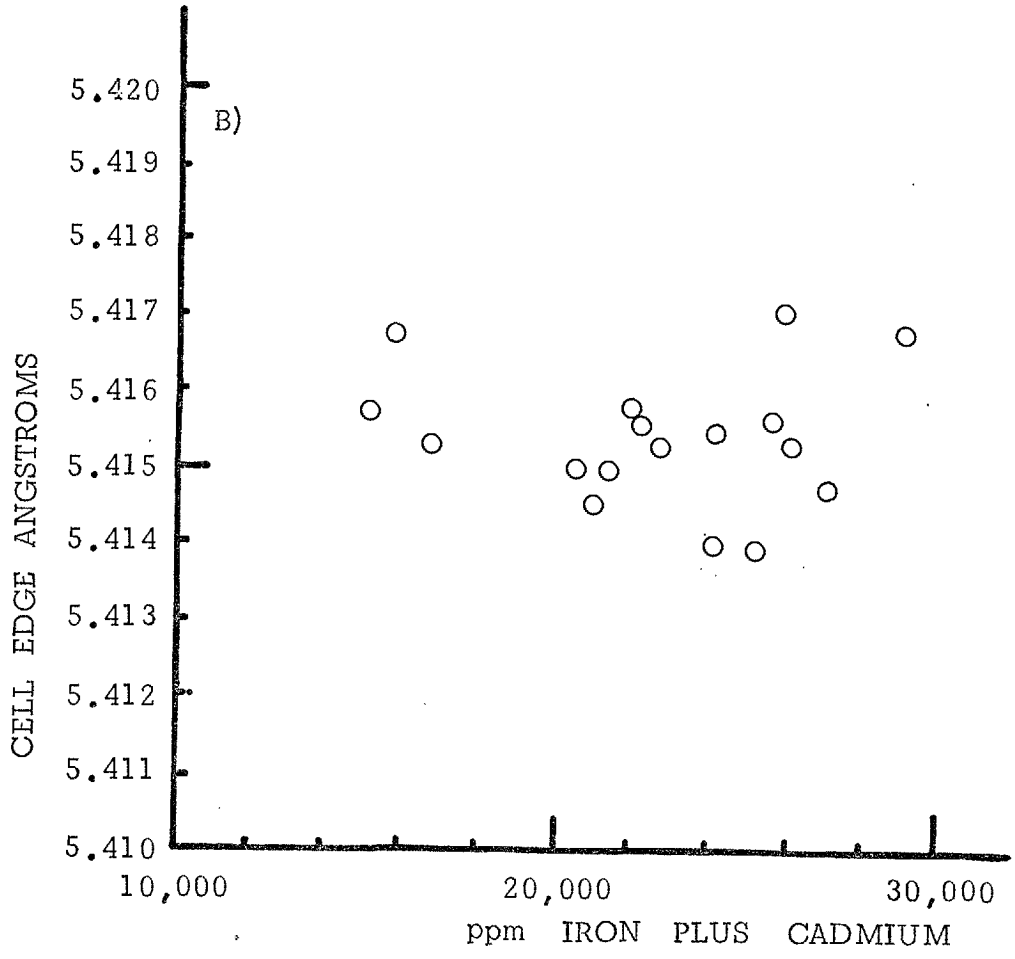


FIG ... 6.9

DIAGRAM ILLUSTRATING THE EFFECT OF INCREASING IRON AND CADMIUM CONCENTRATION ON THE CELL DIMENSIONS OF SPHALERITE

(c) Inter-element relationships in sphalerite appear to be a direct result of included gangue and sulphide minerals in the host crystal and not selective elemental substitution in the crystal lattice.

(d) There is no trace element zonation with depth in the Keel sphalerite.

(e) Mercury values in sphalerite are very uniform throughout the deposit.

(f) Colour variation in sphalerite is consistent with iron variation, although it cannot be said to be solely attributable to this cause.

(g) Cadmium values in sphalerite do not seem to be dependant upon iron concentration.

(h) Cadmium values in sphalerite are uniform throughout the extent of the underground workings, but vary in drillcore material.

(i) Germanium is found mainly in included chalcopyrite and silicate gangue material.

(j) Lattice characteristics of Keel sphalerite do not appear to be effected by differing concentrations in trace element content.

CHAPTER 7

SUMMARY AND CONCLUSIONS.

7.1. INTRODUCTION

This chapter serves as a review of the geological and geochemical information so far described.

7.2. GEOLOGY AND STRATIGRAPHY.

The Keel prospect is situated on a shelf area between the Lower Palaeozoic Longford Down Massif to the north and the Central (Dublin) Basin to the south. Its position is reflected both in the type of sedimentation and the environment of deposition. Metamorphic grade of the Lower Palaeozoics is low, with only minor sericitization and chloritization, the rocks also having weak cleavage. Rock types are alternating sequences of clastics and carbonates. The former are represented by conglomerates and sandstones and the latter by Reef and Bioclastic limestones. The sequence is capped by Calp Limestone, indicating a shallow water, low energy environment.

Faults are widespread throughout the area and faulting is sub-divided into three groups:

(1) Low angle, very light normal faults dipping at 25^{o} - 30^{o} and striking, more or less, east-west,

(2) High angle, east-west normal faults dipping south.

(3) North-south faults and associated joint systems.

These are post-ore faults.

7.3. MINERALIZATION.

Mineralization is associated with high angle, east-west, normal faults and there is abundant evidence that the ore is predominantly confined to the clastic sediments. Five of the thirteen major east-west faults, recognised by Patterson, were considered by him to be loci of important mineralization, namely C, D, G, H and K. The author also considers that the F fault should be included here.

A thick fault gouge exists between the Mixed Beds and Bioclastic Limestone and acted as an impermeable barrier to the mineralizing solutions during ore formation.

Sphalerite is the predominant ore mineral, although galena and pyrite do attain local significance. Sphalerite varies in colour from honey coloured"honey-blende" to black, this being in part a reflection of iron content. Texture also varies from disseminated inter-growths to coarse, well terminated crystals in vugs.

7.4. ORE GENESIS.

After the Hercynian Orogeny, ore solutions invaded the east-west trending faults and deposited base metal sulphides with apparent marked rapidity. The metals were probably gathered by scavenging brine solutions from the surrounding rocks and deposited in an area of high sulphur activity associated with the fault zones.

7.5. PRIMARY GEOCHEMISTRY.

An investigation into the primary dispersion of selected trace elements throughout the deposit was approached in three ways.

(1) The primary dispersion of Cu, Pb, Zn, Ag, Cd, Hg, Fe, Mn, Ca, Mg, Na and K in drill core material.

(2) The primary dispersion of Cu, Pb, Zn, Ag and Hg on the underground workings of the 200', 400' and 500' levels.

(3) The primary dispersion of cold-water-soluble fluorine and chlorine.

7.5.1.

The analysis of eight hundred rock samples for Cu, Pb, Zn, Ag, Cd, Hg, Fe, Mn, Ca, Mg, Na and K was carried out on drill core specimens, to try and obtain a broad picture of the primary dispersion of these elements throughout the prospect area. Previous work by Patterson (1970) indicated a marked degree of lateral metal zonation throughout the deposit, but this study did not confirm Patterson's findings.

Mg/Ca ratios in the limestones are low, $< 0.1:1$, and in the clastic sediments ratios are high, $> 1:1$. The fact that these high Mg/Ca ratios occur associated with mineralization is not, in the authors opinion, indicative of dolomitization associated with mineralization, but more of an association with rock type. Sodium/potassium ratios also show no relationship to mineralization.

High values of iron and manganese occur in the Upper Mixed Beds at Keel, in association with mineralization and faulting; low values occur in the limestones. This again reflects an association with rock type, rather than a correspondence with the extent of bass metal build up.

Lead and zinc mineralization is predominantly confined to fault zones throughout the deposit, and the Zn/Pb ratio is on the whole fairly uniform at © 33:1. However, a definite enrichment of lead, east of the shaft, is apparent and Zn/Pb ratios of 1:1 ars common in some sections of drill core in this area. The cadmium content of Keel sphalerite, © 1%, is very high for the Irish province. However the majority of rock material analysed gave a Zn/Cd ratio of approximately 62:1. Variations from this ratio do occur and up to 2% Cd can be found in some of the sphalerite.

The possible existence of a cadmium phase in the rocks of the deposit cannot, however, be over-looksd and Zn/Cd ratios as low as 25:1 are found in rock samples from the E fault zone on the 500' level. A broad association of zinc and msrcury is apparent for material from the underground workings but this relationship breaks down in drill core material. Total msrcury studies indicate a vague relationship between mercury and the proximity of sulphide ore on a broad scale. When specific values are used howsver, both antipathetic and sympathetic relationships are found.

7.5.2.

Three hundred and five rock samples from the underground workings of the prospect were analysed to investigate the primary dispersion of Cu, Pb, Zn, Ag and Hg on the 200', 400' and 500' levels. Sample distribution was as follows:

200' level, 142; 400' level, 62; 500' level, 101.

The 500' level is the deepest level of the Keel prospect and primary dispersion studies are complicated on this, as on all other levels, by the abundance of different lithologies. Analysis indicated that a broad sympathetic relationship exists between all base metals on this level; however, primary dispersion appears to be very limited and ore grade mineralization may drop to background in distances less than one inch. Mercury also appears to have little mobility and values of 50 ppb occur in fragments of wallrock, surrounded by massive sulphide mineralization with mercury values over 100 ppm.

The Zn/Pb ratio decreases northwards towards the Silurian inlier and the presence of greenockite in the E and D faults is indicated by their Zn/Cd ratios of 25:1 and 57:1 respectively. The actual sphalerite from these faults gives an approximate Zn/Cd ratio of 62:1.

The main feature of the 200' level is the C fault. This is an east-west normal fault, dipping south, which brings Bioclastic Limestone against Upper Mixed Beds and separates the two by a thick fault gouge. Mineralization has been dammed up against this fault. Again on the 200' level there appears to be a reasonably sympathetic relationship between base metals although no specific inter-element

correlations exist. The plans of the trace element distribution on the 200' level indicate that lead is far less abundant, here, than on the 500' level. Mercury also appears to have a lower concentration on this level, although the sphalerite contains approximately the same amount in its lattice as it does on the 500' level.

The underground workings of the 400' level have by far the smallest extent. They are mainly cut in Upper Quartz Sandstone and mineralization is abundant with high grade lead to the north of the shaft. Base metal relations are again sympathetic on this level.

7.5.3.

Colourimetric determination of water soluble fluoride and turbidimetric determination of water soluble chloride indicated that no relationship exists between these elements and the extent of base metal mineralization. Information also indicates that primary dispersion of fluorine and chlorine in the wallrocks surrounding the Keel prospect is non existent.

7.6. TRACE ELEMENT DISTRIBUTION IN SPHALERITE, GALENA AND PYRITE.

113 specimens of sphalerite, four of pyrite and twelve of galena, each weighing in excess of 500 mg., were separated from crushed rock material and analysed for Cd, Ga, Ag, Ni, Co, Sb, Ba, Cu Ca, Ti, In, Ge, Si, Mg, Mn, Hg, As, V, Cr, Sn, Mo, Bi, (Pb), (Zn) and (Fe) using a Hilger large quartz spectrograph. Comparative analyses of some of these samples by optical spectrograph and atomic absorption indicated a good agreement between techniques.

Analysis of sphalerites confirmed Pattersons' (1970) opinion, that high cadmium (>1%) is contained in the lattice of this mineral. Trace element values for all the minerals analysed can be seen in Tables 6.1 - 6.4, and the relative distribution of trace elements between sphalerite, galena and pyrite in Table 6.10. Sphalerite varies in colour from true honey coloured "honey-blende" to black, this colour variation being sympathetic with iron content, although not necessarily wholly dependent upon it.

The inter-element relationships which do exist in Keel sphalerite, (Cu/Ag; Cu/Ge; Cu/Fe; Ca/Mg; Ge/Fe; Ge/Si; Mn/Mg) appear to be a direct result of included gangue and sulphide minerals and not the result of substitution of these elements in the sphalerite lattice.

The sphalerite, and probably galena and pyrite also, appear to conform to the trace element mineralogy of a low temperature deposit.

7.7. CONCLUSIONS.

The lithological variation at Keel makes any study of the primary geochemistry extremely difficult. It is impossible to say at Keel, that there is any wide primary dispersion of any of the elements investigated, associated with the base metal build up of the area, nor is there any broad primary dispersion halo of total mercury around the deposit.

This investigation has led to the conclusion that primary dispersion patterns of any major significance do not exist, either on the broad scale of the drilled area, or on the detailed scale of the underground workings.

Investigation of the trace element content of the ore minerals has led to the conclusion that the major impurities, except cadmium and mercury, are present as included gangue and sulphide minerals and not as lattice substitutes. However, from this investigation it has been possible to postulate a temperature of formation of between 150°C and 250°C for the Keel deposit.

CHAPTER 8

MERCURY AND MERCURY COMPOUNDS IN THE PRIMARY ENVIRONMENT OF THE KEEL PROSPECT.

8.1. THE GEOCHEMISTRY AND ABUNDANCE OF MERCURY.

The geochemistry of mercury differs quite markedly from its sister elements in Group II of the Periodic Table, zinc and cadmium. Zinc and cadmium are present only as traces in early magmatic separates while mercury is almost absent. However, mercury does concentrate in the geologically young volcanic areas associated with low temperature hydrothermal solutions and hot springs (Rankama and Sahama, 1968).

Saukov (1946) suggests that the Hg^{2+} ion substitutes for both the Ca^{2+} and Ba^{2+} ions in calcite, dolomite and baryte, but suggests the greatest replacement is in sulphide minerals. Cinnabar, HgS, is the main sulphide mineral of mercury, but concentrations of metacinnabar, HgS and native mercury, Hg, are occasionally found; so too is calomel Hg_2Cl_2. Gold, tellurium, platinum and silver amalgams are known in nature and the oxide montroydite HgO, oxychlorides and mercury-halogens also occur as minerals.

Information concerning the abundance of mercury in chondrites is scarce, however Noddack and Noddack (1934) are quoted in Rankama and Sahama (1968) as estimating a figure of 10 ppb. Mercury is absent in the solar atmosphere, but due to its high volatility, is always present in our own. Goldschmidt (1937) estimates its abundance in igneous rocks as 500 ppb, while Sankov (1946) estimates 76 ppb

Table 8.1. gives average values for a set of igneous and sedimentary rocks. This information definitely suggests that there is enrichment of mercury in shales. This is due to the highly adsorptive nature of clay minerals in these sediments. Mercury evolved into the marine environment from such possible sources as submarine volcanic exhalations would therefore tend to concentrate in clay rich sediments and this could account for the low mercury content of sea water of 0.03 ppb. (Stock and Cucuel, 1934). During metamorphism and diagenesis, this adsorbed mercury could be dissociated and become available to anionic species in the sediment, forming, possibly, mercury compounds, e.g. $HgCl_2$ and HgS, depending upon the availability and activity of the anionic species present.

Rankama and Sahama (1968) noted that the "quantitative cycle" of mercury was inadequately known but concluded that the volatility of the element may play an important part in its dispersion. James (1962) has thoroughly dealt with the chemical and geochemical knowledge of mmercury up to that date and Evans (1971) has updated the information yet again. Boyle (1971) and Rankama and Sahama (1968) have produced meaningful diagrammatic representations of the mercury cycle in nature and these are reproduced in Figure 8.1.

8.2. PRIMARY DISPERSION OF TOTAL MERCURY AT THE KEEL PROSPECT.

Hawkes and Webb (1962) state that in permeable rocks, such as sandstone, limestone and dolomite, mercury can move great distances from its source as mercury vapour. It would therefore be reasonable to expect a broad halo of primary dispersed mercury in wallrocks surrounding lead-zinc ores. The extent of this anomaly and its shape

A) AVERAGE CONTENT OF MERCURY IN IGNEOUS ROCKS .

ROCK	MERCURY p p b
GABBRO (Stock and Cucuel , 1934)	77
GABBRO (Preuss , 1941)	98
BASIC EFFUSIVES (Saukov , 1946)	88
GRANITE (Stock and Cucuel , 1934)	80
GRANITE (Preuss , 1941)	10
ACIDIC INTRUSIVES (Saukov , 1946)	57

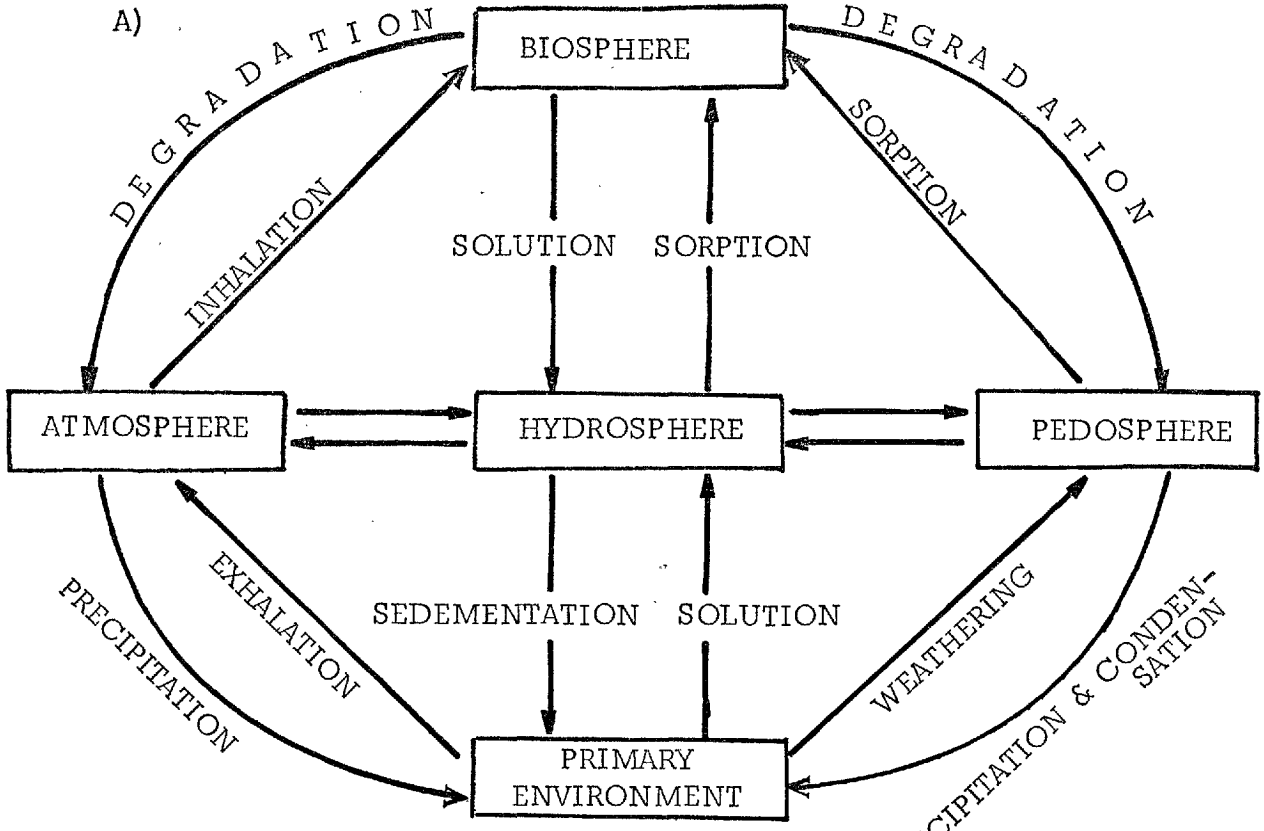
B) AVERAGE CONTENT OF MERCURY IN SEDIMENTARY ROCKS .

ROCK	MERCURY p p b
SANDSTONES , average (Preuss , 1941)	98
SANDSTONE (Stock and Cucuel , 1934)	30
SHALES average (Stock and Cucuel , 1934)	494
SHALES average (Preuss , 1941)	290
LIMESTONE (Stock and Cucuel , 1934)	30

After Rankama and Sahama 1968

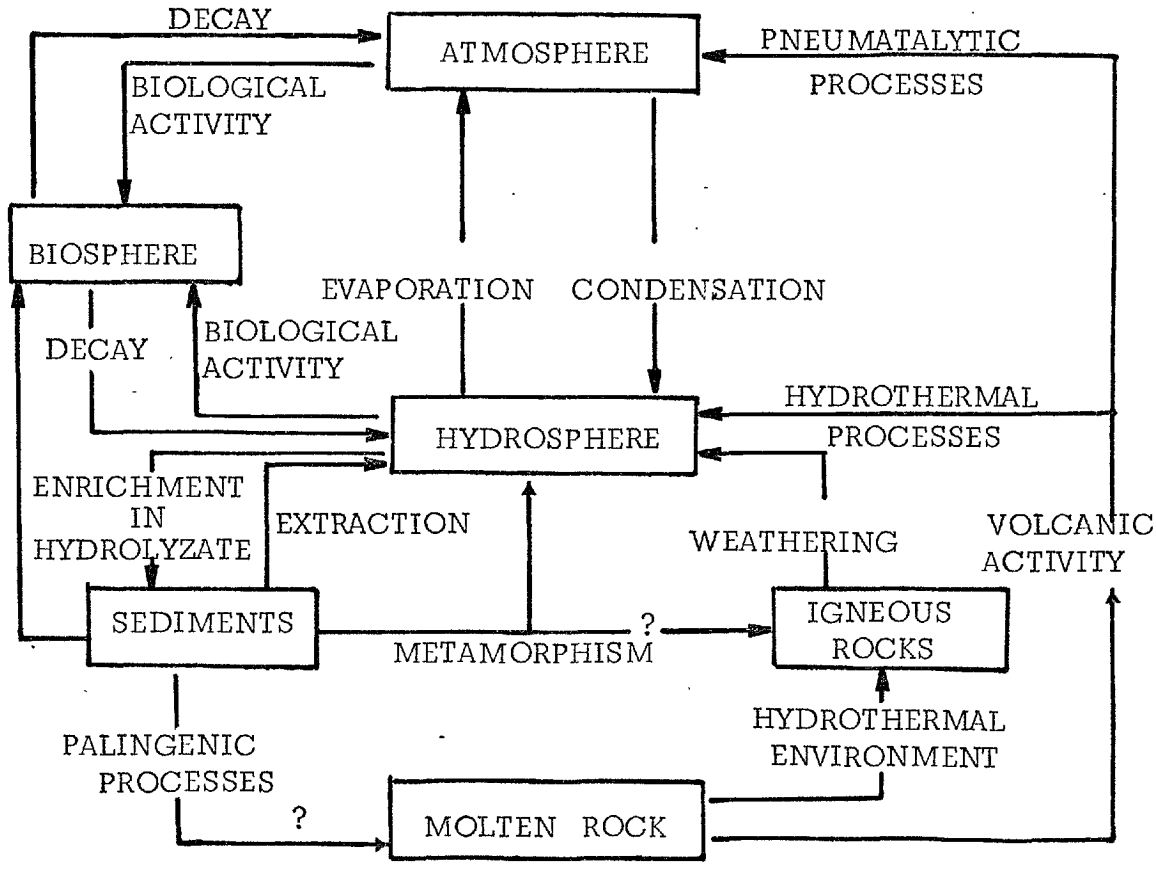
TABLE ...8.1 AVERAGE CONTENT OF MERCURY IN SEDIMENTARY AND IGNEOUS ROCKS .

A)



After Boyle (1971)

B)



After Rankama and Sahama (1968)

FIG ...8.1 THE CYCLES OF MERCURY

would be markedly dependent upon the physical characteristics of the host rocks.

Mercury anomalies have been detected in bedrock (Fursov, 1958, Ozerova, 1959., Frederick and Hawkes 1966), soil (Jolly and Heyl, 1968 Evans, 1971) and air (Barringer, 1964. Motycka, 1970) and several authors have pointed out the usefulness of mercury as an ore guide (James, 1964 and 1962). Barringer Research Ltd. of Toronto, Canada, have recorded anomalous mercury concentrations in the atmosphere over zinc soil anomalies in the Bruce Peninsular, Canada (Motycka, 1970). Anomalous atmospheric readings have also been recorded over the mineralized Cobalt, Ontario, area (A.R. Barringer pers. comm.). This confirms Williston's (1964) work, when he reported the atmospheric occurrence of mercury in California. As a further guide to mineral deposits, Friedrich and Hawkes (1966) have suggested that the mercury content of residual soils, but not of the unweathered rock, may be used as a guide to blind ore deposits in the Pachuca- Real del Monte district, Mexico.

James (1962), in his review on mercury, quotes Polikarpochkin (1957) as enumerating the most important factors influencing the formation of primary dispersion halos as:-

(1) Fissuring in the host rock

(2) Nature of the host rock:

  (a) Porosity

  (b) Chemical composition

(3) Properties of the elements forming the halo

(4) Properties of the mineralizing fluids

To these he adds:

(5) Depth:

(a) Variation in pressure

(b) Variation in temperature

Upon consideration of these points, together with the information gained in Chapter 6 that Keel sphalerite contains some 200 ppm mercury in solid solution, it is obvious that sufficient mercury was associated with the ore solutions at Keel to have produced a large halo in the wallrocks surrounding the mineralization. However, the information gained in Chapter three indicates that no definite mercury halo exists around the deposit. Although local anomalous values are encountered, mercury concentrations of < 50 ppb occur some half an inch away from massive mineralization with mercury concentration of > 100 ppm Very often, unless the actual sample containe sphalerite, galena or pyrite, its mercury content will be < 100 ppb. A sample some 6" away from massive mineralization can contain much less mercury than a sample several hundred feet away. This creates an extremely complex problem of interpretation of total mercury data.

The analysis of samples of rock material for total mercury was discussed in Chapter 3, and on the basis of this information Figs. 3.50 - 3.54 were compiled. These maps show the total mercury distribution on the five levels of Keel and do no more than indicate the existence of several anomalous samples. Specific mercury values for samples give no information as to the actual location of mineralization, with high and low mercury values alike being scattered over an area of $\frac{1}{2}$ mile by 1 mile. The absence of a meaningful primary dispersion mercury halo around the sphalerite veins of Keel is therefore very clear.

However, on the basis of information obtained during sample handling and preparation, it was concluded that a complex series of factors influenced the distribution of mercury at Keel. In order to try and explain these factors, a different approach to mercury analysis was undertaken.

8.3. PRIMARY DISPERSION OF MERCURY COMPOUNDS AT KEEL PROSPECT.

A small percentage of the information dealt with in the initial parts of this chapter, has been covered in chapters 3 and 4. However, for the sake of continuity, it is again quoted here.

(a) Sample Collection and Preparation.

Wallrock samples from the underground working, weighing in excess of one kilogramme, were collected and immediately stored inside sealed polythene bags and packed together in batches of ten. An effort was made to keep obviously mineralized and unmineralized samples apart. In the laboratory, each sample was scrubbed with ordinary tap water to remove surface contamination, then washed in deionised water and allowed to dry inside a large absorbant tissue at room temperature.

When dry, the sample was reduced to - 1550 μm in a manganese/steel jaw crusher and three size fractions were then sieved from this, - 210 μm, - 494 μm + 210 μm and - 1550 μm + 494 μm.

After each sample, the jaw crusher was cleaned by scrubbing with warm water and finally spraying with acetone to facilitate quick drying of the metal. Several polished sections of the - 494μm + 210 μm material were prepared and carefully examined under a reflected light microscope in an attempt to discover if any contamination from the jaw

crusher was being picked up. Initial results proved positive; however on changing jaw crusher, this contamination was soon removed. The initial samples were destroyed.

Under normal procedures, the jaw crusher is cleaned by running coarse sand through it, however as this sand was found to contain 1480 ppb (1480×10^{-9} g. /g. mercury), its use as an abrasive cleaner was discontinued.

The three different size fractions were stored in sealed Kraft paper bags, again in batches of ten taking similar precautions with respect to mineralized and unmineralized samples.

Drillcore samples, which consisted of short lengths of whole core, weighing about 1 Kg each, were handled in the same way.

The mercury analysis was carried out, initially, using the sensitive mercury vapour analyser designed by James and Webb (1964), a flow diagram of which is shown in Fig. 8.2. This instrument works on the atomic absorption principle, by measuring the relative absorption of light of wavelength 2536.5 Å by mercury vapour.

A sample of material was heated to 700°C for one minute and the evolved mercury was flushed through the apparatus ae a single pulse using air as the carrier gas. Additional analyses were carried out by Barringer Research Ltd., Toronto, Canada, using their own system of mercury analysis (Barringer, 1966).

This instrument used at the Royal School of Mines was initially calibrated by injecting known volumes of mercury saturated air, at known temperatures, into the gas stream. The absorption due to the mercury vapour was then measured on a voltmeter and a standard curve plotted

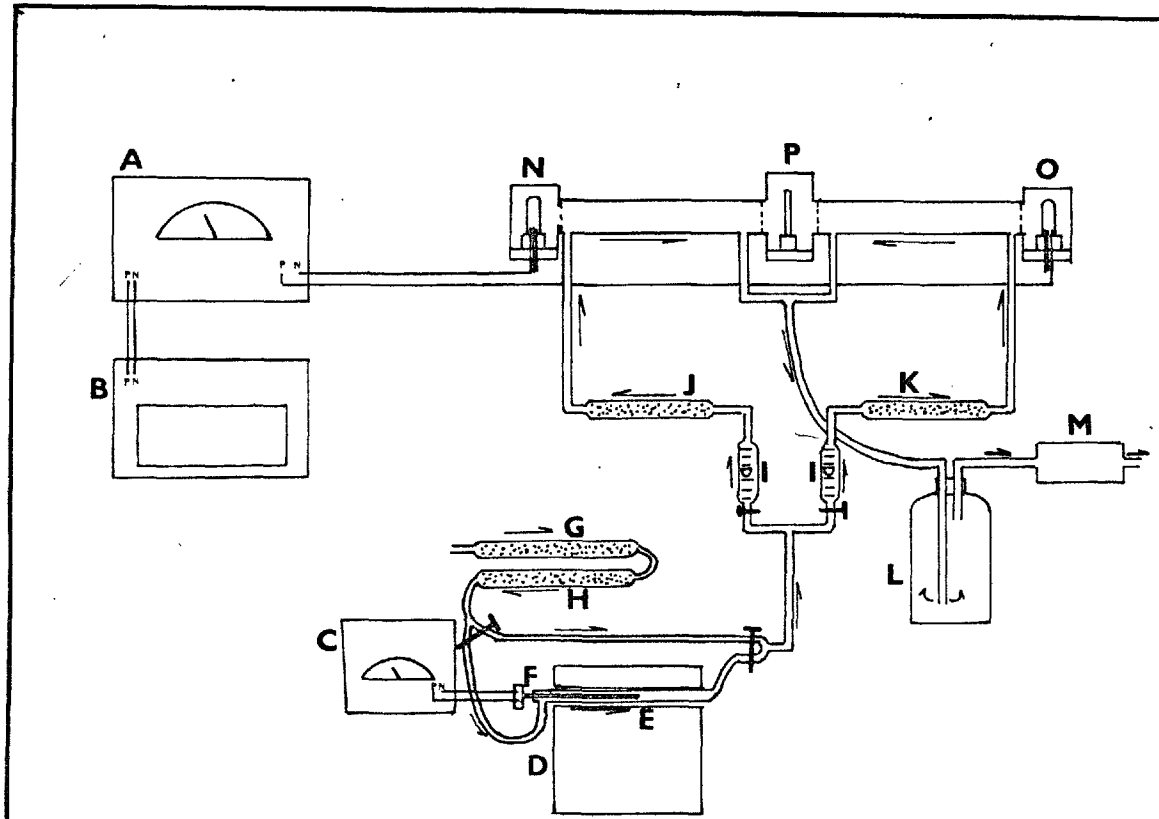


Fig . 8.2.

KEY :

A VOLTMETER
B CHART RECORDER
C THERMOCOUPLE
D TUBE FURNACE
E SAMPLE CHAMBER
F SILICA TUBE
G SILICA GEL
H ACTIVATED CHARCOAL
I FLOWMETERS
J GLASSWOOL
K PALLADIUM CHLORIDE ON GLASS WOOL
L ASPIRATOR
M PUMP
N RIGHT PHOTOCELL
O LEFT PHOTOCELL
P ULTRA-VIOLET SCOURCE

FLOW TAP

FLOW DIRECTION

DIAGRAM OF APPARATUS FOR CONTINUOUS MERCURY THERMAL RELEASE ANALYSIS

of voltmeter reading against µg./litre mercury. (Fig. 8.3).

When samples of the three mesh sizes were analysed, it was found that the mercury content varied with particle size, as shown in Table 8.2A.

This variation could be due to a combination of factors:-

(1) The mercury occurs as minute grains, possibly discrete mercury minerals, which tend to concentrate in the finer fraction.

(2) Concentration of friable minerals, particularly sphalerite, occurs in the finer fractions. Any ZnS lattice-held mercury would therefore also tend to concentrate in this fraction.

(3) Delay in release of mercury from the coarser material, due to a thermal gradient being set up, preventing release of mercury from the innermost parts of the larger grains during the one minute heating cycle. A diffusion gradient could also be set up in the coarser grains preventing mercury release.

After the analysis of the material from the underground workings of the prospect, a survey of the drillcore material from the west of the area was carried out. The results are shown in Table 8.2B.

Comparison of Tablee 8.2A and 8.2B shows that for both materials from the underground workings and for drillcore the lowest mercury contents occur in the - 1550 µm + 494 µm material; mercury content increases with decreasing particle size for samples from the underground workings and increases with increasing particle size for drillcore material. This, in the light of information available at the time, was thought to be due to a build up of pore and fracture held

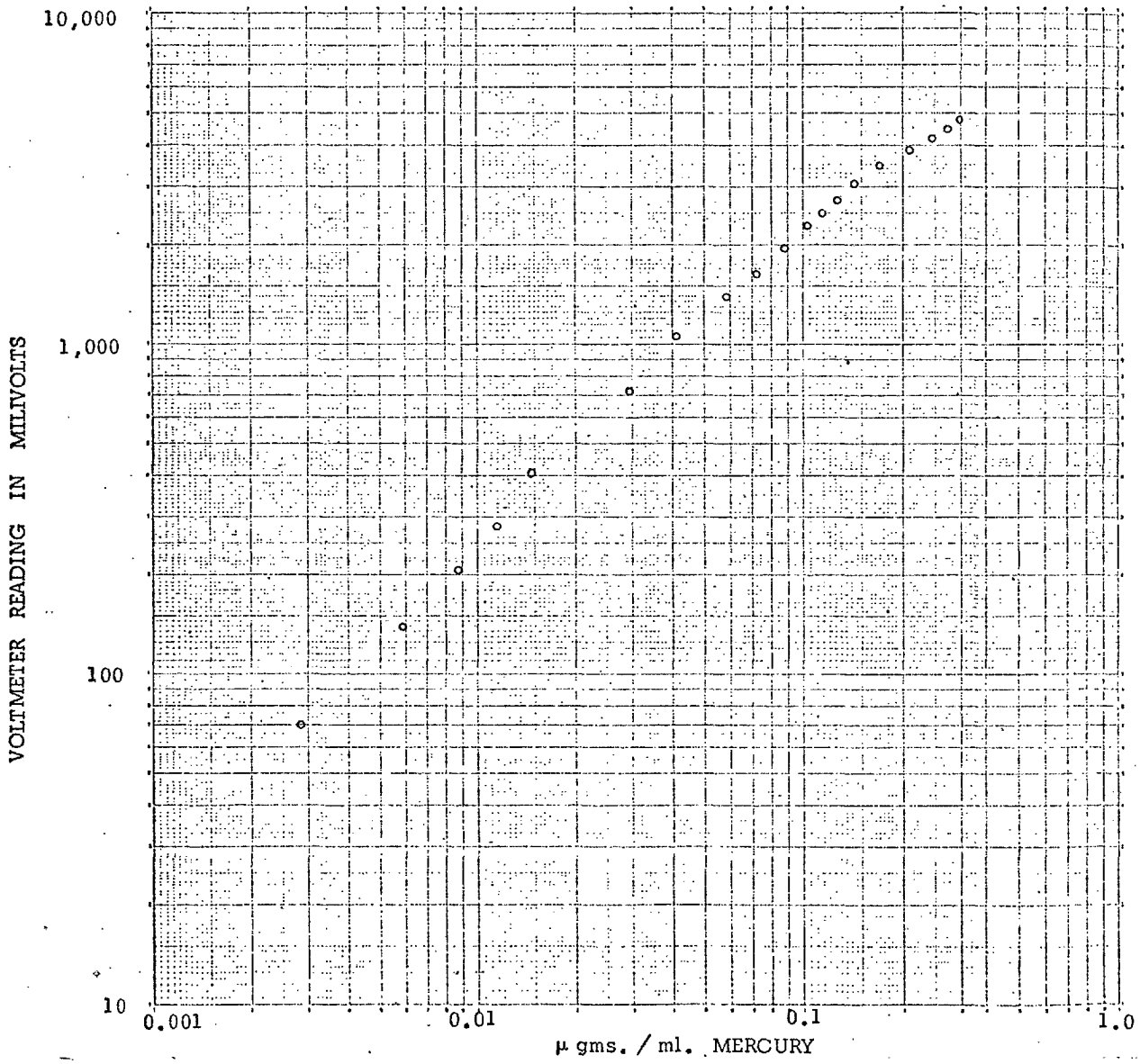


FIG ... 8. 3 CALIBRATION GRAPH FOR MERCURY ANALYSIS BY THE MERCURY VAPOUR INJECTION METHOD

TABLE ... 8.2

MERCURY CONTENT IN DIFFERENT SIZE FRACTIONS OF ROCK SAMPLES

A) FROM UNDERGROUND WORKINGS

SAMPLE	- 210 μ	- 494 μ + 210 μ	- 1550 μ + 494 μ
K 1	665	152	90
K 2	2575	280	174
K 3	2420	144	84
K 4	300	140	106
K 5	525	206	16
K 6	240	170	130
K 7	2855	1180	720
K 8	1330	160	80
K 9	705	184	116
K 10	2460	390	49
K 11	1075	216	139

B) FROM DRILLCORE

K 12	998	1560	1020
K 13	28	48	28
K 14	22	32	36
K 15	35	96	14
K 16	166	210	110
K 17	70	85	50
K 18	14	42	15
K 19	103	310	80
K 20	60	130	52
K 21	219	560	27
K 22	169	700	150
K 23	318	496	130
K 24	44	210	27
K 25	49	326	20
K 26	160	172	110
K 27	1675	2593	1020
K 28	66	74	30
K 29	44	236	25
K 30	33	57	14
K 31	141	280	100

RESULTS EXPRESSED AS p p b

mercury in drillcore material, away from the known area of mineralization, which was released in greater amounts the finer the material was crushed.

To test this possibility, - 1550 μm + 494 μm material both from the underground workings and from drillcore was ground for fifteen seconds in a Tema mill and then reanalysed for mercury. The results are shown in Tables 8.3A and 8.3B.

These results indicated that grinding increased the apparent mercury concentration in both sets of samples, and the increase in mercury content of some samples of drillcore material was substantially higher than the increase for the underground samples. The air inside the Tema mill was consequently analysed for mercury after the grinding procedure, in order to ascertain if the mine rock had lost more mercury than the drillcore, to the atmosphere inside the Tema mill. This experiment was carried out by substituting a 4 cm. thick perspex lid in place of the original silicon carbide Tema lid. Two holes were drilled through the lid in order to correspond to gaps between the grinding rings, Fig. 8.4. The holes were sealed with sellotape both inside and outside and the sellotape inside was pushed slightly into the hole so as to allow both outside and inside of the hole to be continuously sealed throughout grinding. After grinding a hypodermic needle was pushed through each hole and air from inside the mill was drawn into a 20 ml glass syringe. This air was then immediately transferred to the mercury analyser and the mercury content of this 20 ml sample measured. By knowing the original sample weight and the density of the specimen, together with the volume of the inside of the Tema mill, it was possible to calculate that from 4 - 13 nanogrammes of mercury per gramme of rock was lost and hence loss of mercury by volatilization

TABLE ...8.3

COMPARISON OF THE MERCURY CONTENT OF GROUND AND UNGROUND - 1550 μ + 494 μ MATERIAL FROM KEEL

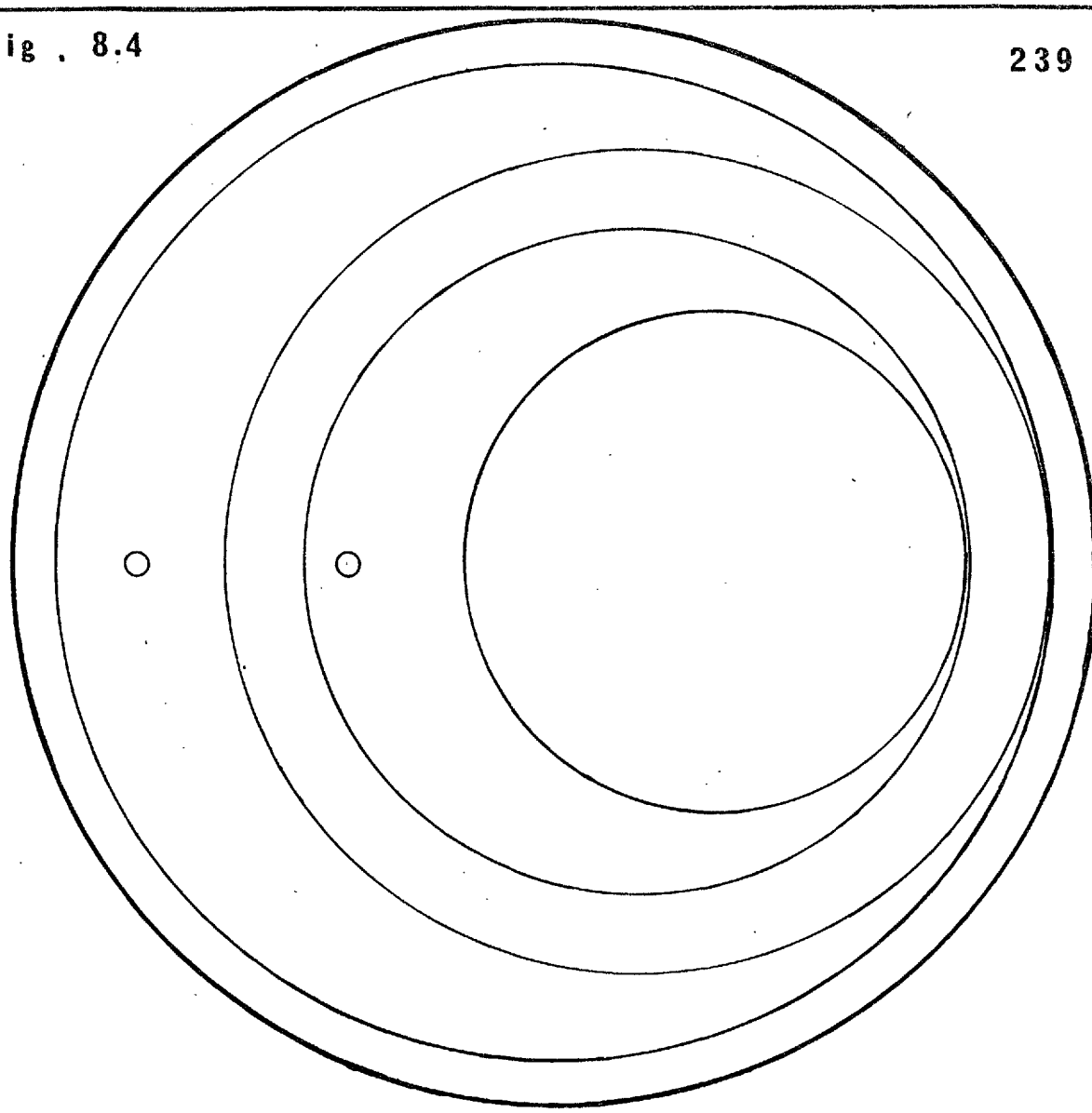
A) MATERIAL FROM THE UNDERGROUND WORKINGS

SAMPLE	GROUND	UNGROUND	GROUND / UNGROUND
K 1	178	90	1.98
K 2	1970	179	11.00
K 3	280	84	3.23
K 4	130	106	1.22
K 5	320	16	20.00
K 6	170	103	1.65
K 7	1420	720	1.97
K 8	380	80	4.75
K 9	296	116	2.55
K 10	483	49	9.85
K 11	980	139	7.05

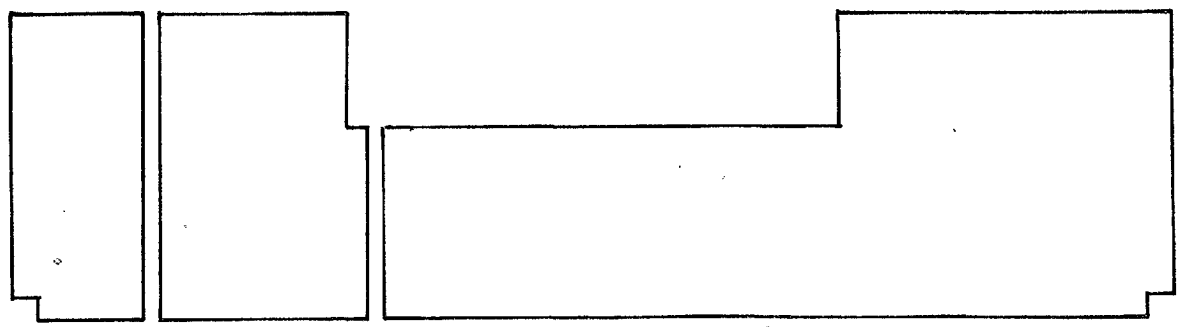
B) MATERIAL FROM DRILLCORE

K 12	2060	1020	2.00
K 13	210	28	7.50
K 14	240	36	6.70
K 15	1040	14	74.30
K 16	1840	110	16.70
K 17	546	50	10.90
K 18	480	15	32.00
K 19	1880	80	23.50
K 20	4200	52	80.70
K 21	6800	27	251.80
K 22	1560	150	10.40
K 23	6900	130	53.10
K 24	2100	27	77.80
K 25	1520	20	76.00
K 26	3400	110	30.90
K 27	7400	1020	7.30
K 28	3800	30	126.60
K 29	4200	25	168.00
K 30	1080	14	77.00
K 31	1600	100	16.00

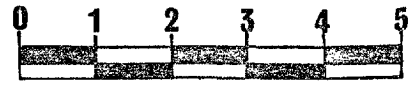
RESULTS EXPRESSED AS p p b



A PLAN VIEW OF MILL



B CROSS SECTION OF PERSPEX LID



SCALE IN CENTIMETRES

PERSPEX LID DESIGN FOR GAS EXTRACTION FROM A SEALED GRINDING MILL

during grinding was negligible. This fact indicated that the mercury in the drillcore samples was bound up just as tightly as that in samples from the underground workings, and that the distribution of mercury in rocks was governed by far more complex factors than a simple increase of elemental mercury in fractures and fissures.

(b) Initial Analytical Results.

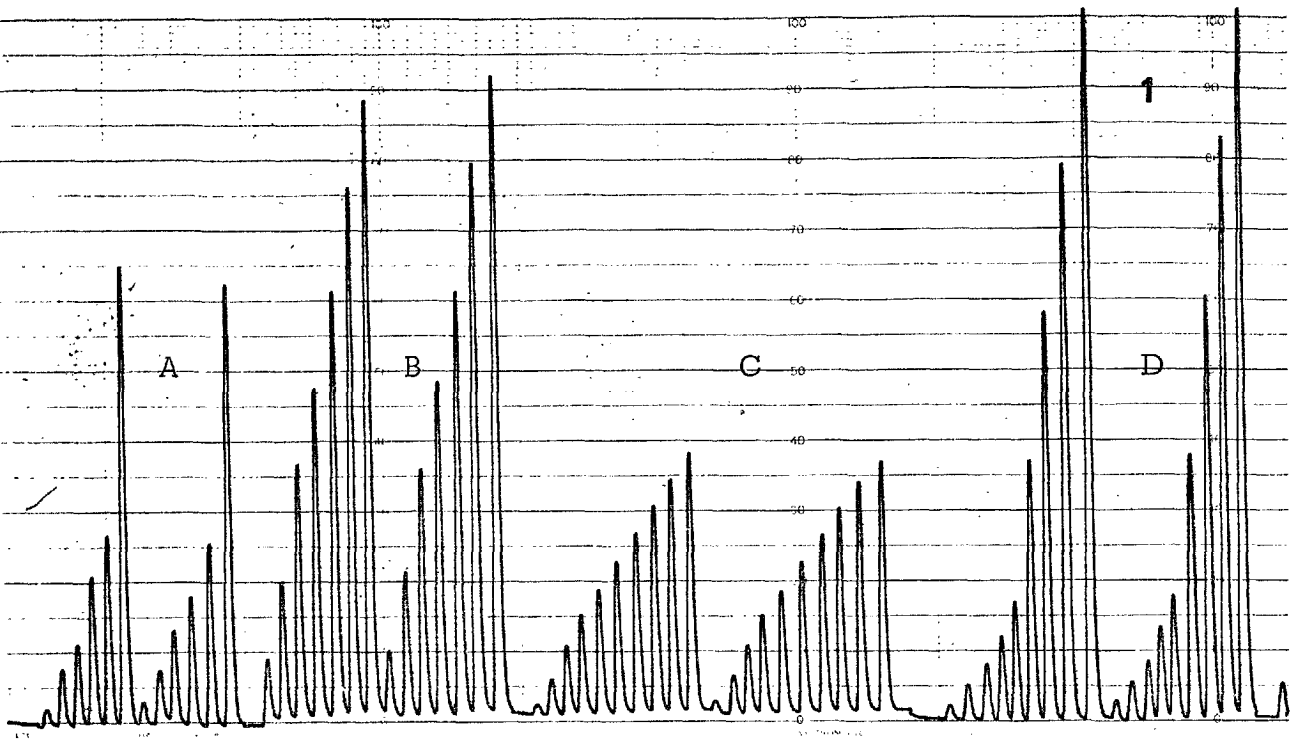
After careful consideration of the accumulated data, it was concluded that a specific distribution of mercury compounds may be the cause of the apparent analytical discrepancies between samples from the underground workings and drillcore material.

It was therefore decided to continue the work of Koksoy and Bradshaw (1967) and to modify the heating techniques for each sample. To do this, a heating cord was wound around an annealed pyrex tube to serve as a heating chamber. The cord was connected to a variable mains transformer by which input voltage to the cord, and consequently temperature of the cord, was varied. Temperatures of 450°C could be reached by this method and it was considered only a temporary set up to investigate the validity of the mercury compound theory.

5 g. samples of - 494 μm + 210 μm crushed rock material were placed in a nickel boat inside the heating chamber and the temperature increased. Temperature monitoring was carried out by means of a direct reading thermocouple placed directly in the sample inside the heating chamber. The temperature was increased in 10 volt steps, approximately 40°C steps, and the sample heated for one minute at each voltage setting. A time lag of approximately 1 minute between settings was required for the temperature to stabilize. After one minute heating, the evolved mercury was flushed in an air stream into the analytical equipment and the evolved mercury measured. Thus a

crude picture of mercury release with temperature could be built up, Fig. 8.6. The amount of mercury evolved at each step was measured on a chart recorder, this being connected in series with the analytical equipment. Because of the varying amounts of mercury released from the samples during the heating programme, several scale changes had to be made on both voltmeter and chart recorder, in order to attain maximum sensitivity at each point. Standardization of the equipment using a combination of chart recorder and voltmeter scales was therefore necessary, prior to sample analysis, Fig. 8.5. This standardization was carried out by injecting known quantities of mercury saturated air, at known temperatures, into the apparatus using an hypodermic syringe, and measuring the voltage difference between two photocells, Fig. 8.2. Table 8.4. explains the calibration graphs obtained.

As a result of these initial analyses, several distinct peaks for mercury release were obtained from the Keel rock material used, Fig. 8.6. On referring to the work of Koksoy and Bradshaw (1967) on mercury compounds around a cinnabar deposit in Western Turkey, it was possible to identify mercuric chloride, mercurous chloride and mercuric sulphide, together with another mercury phase which was released at much higher temperature than any of these and at a temperature too high for the heating cord to reach, Fig. 8.6C. It was also possible to identify one sample which appeared to contain two forms of mercury, mercuric sulphide and mercuric chloride, Fig. 8.6.A. Fig. 8.7 gives the temperatures of release of various mercury compounds analysed by the author. One other very important fact however, did emerge from the study and that was that the total amount of mercury released from each rock by this method was very much lower than the total obtained by whole rock total mercury analysis. This could have been due to several



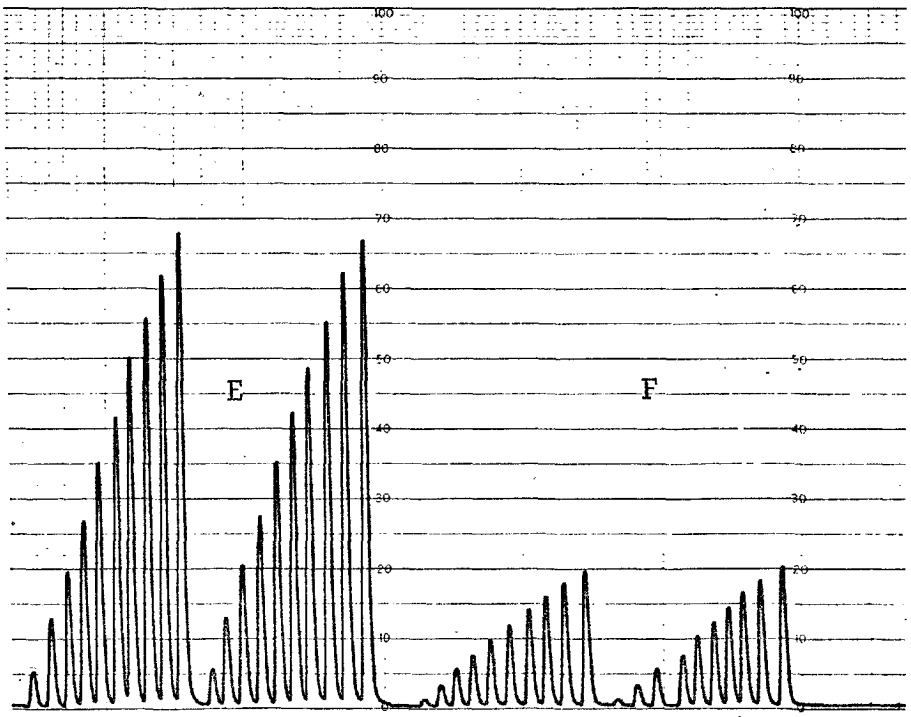


FIG ...8.5 CALIBRATION OF MERCURY ANALYSIS APPARATUS BY THE "MERCURY PULSE" METHOD.

	CHART RECORDER FULL SCALE	VOLTMETER FULL SCALE	CHART RECORDER DEFLECTION %	μ GMS. ADDED MERCURY	VOLUME OF MERCURY SATURATED AIR AT 20°C
A)	25 mv	10 mv	3.0	0.0027	0.2 ml
			7.6	0.0054	0.4 ml
			11.2	0.0081	0.6 ml
			17.8	0.0107	0.8 ml
			25.6	0.0135	1.0 ml
			62.3	0.0270	2.0 ml
B)	25 mv	30 mv	9.5	0.0135	1.0 ml
			20.0	0.0270	2.0 ml
			35.2	0.0405	3.0 ml
			47.5	0.0538	4.0 ml
			61.5	0.0675	5.0 ml
			76.2	0.0810	6.0 ml
			88.5	0.0945	7.0 ml
C)	25 mv	100 mv	2.5	0.0135	1.0 ml
			6.0	0.0270	2.0 ml
			10.7	0.0405	3.0 ml
			15.1	0.0538	4.0 ml
			18.8	0.0675	5.0 ml
			22.8	0.0810	6.0 ml
			26.8	0.0945	7.0 ml
			30.8	0.1080	8.0 ml
			34.6	0.1215	9.0 ml
			38.2	0.1350	10.0 ml
D)	50 mv	10 mv	2.7	0.0027	0.2 ml
			5.2	0.0054	0.4 ml
			8.6	0.0081	0.6 ml
			13.4	0.0107	0.8 ml
			17.9	0.0135	1.0 ml
			37.8	0.0270	2.0 ml
			60.4	0.0405	3.0 ml
			83.0	0.0538	4.0 ml
			102.0	0.0675	5.0 ml
E)	50 mv	30 mv	5.4	0.0135	1.0 ml
			13.0	0.0270	2.0 ml
			20.4	0.0405	3.0 ml
			27.5	0.0538	4.0 ml
			35.2	0.0675	5.0 ml
			42.3	0.0810	6.0 ml
			48.7	0.0945	7.0 ml
			55.2	0.1080	8.0 ml
			61.9	0.1215	9.0 ml
			68.0	0.1350	10.0 ml
F)	50 mv	100 mv	1.3	0.0135	1.0 ml
			3.2	0.0270	2.0 ml
			5.7	0.0405	3.0 ml
			7.7	0.0538	4.0 ml
			10.0	0.0675	5.0 ml
			12.0	0.0810	6.0 ml
			14.2	0.0945	7.0 ml
			16.1	0.1080	8.0 ml
			18.0	0.1215	9.0 ml
			20.1	0.1350	10.0 ml

TABLE . . 8.4 CALIBRATION OF MERCURY METER BY THE MERCURY PULSE METHOD USING VARIOUS CHART RECORDER / VOLTMETER SETTINGS TO OBTAIN MAXIMUM SENSITIVITY

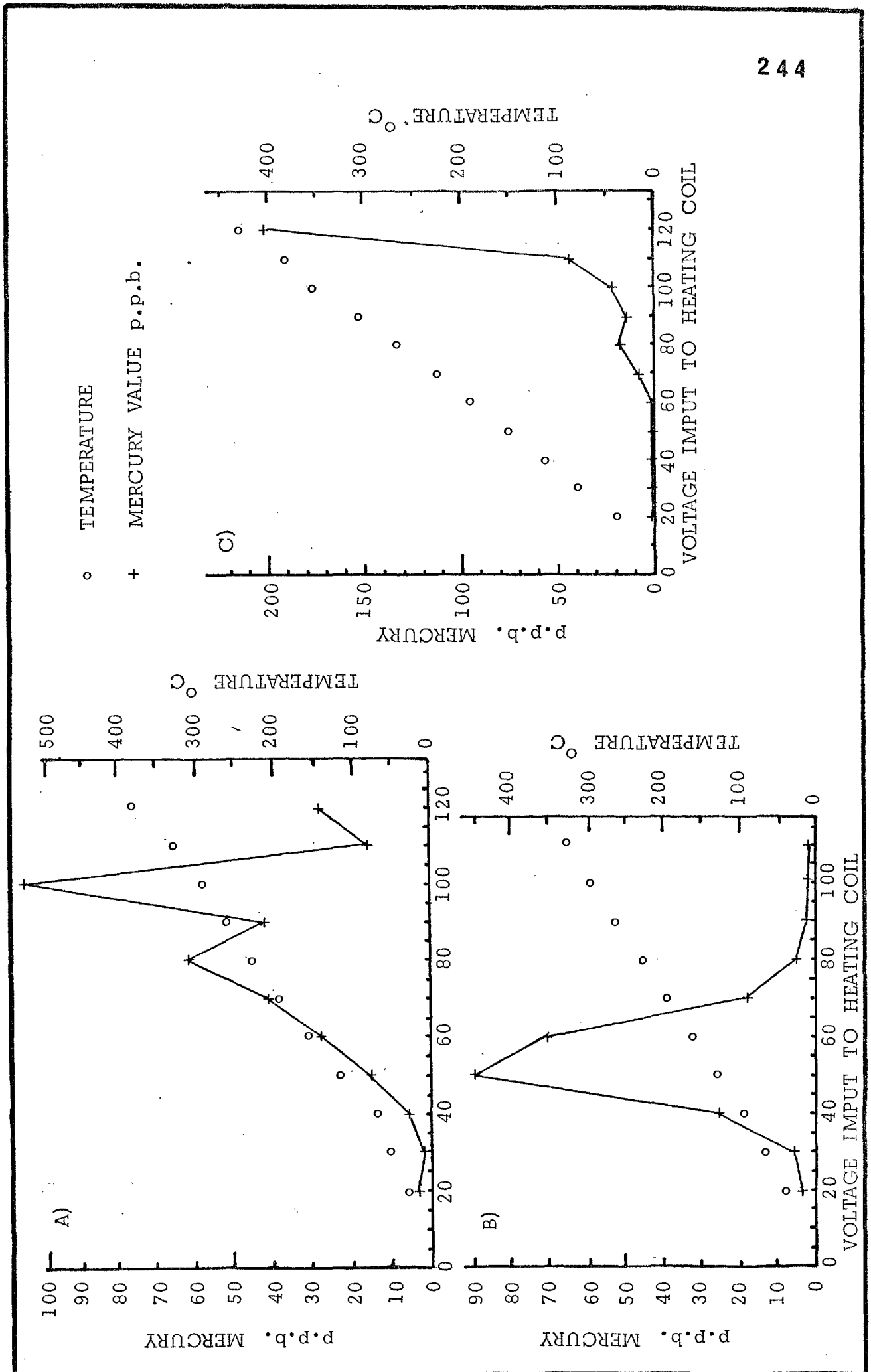
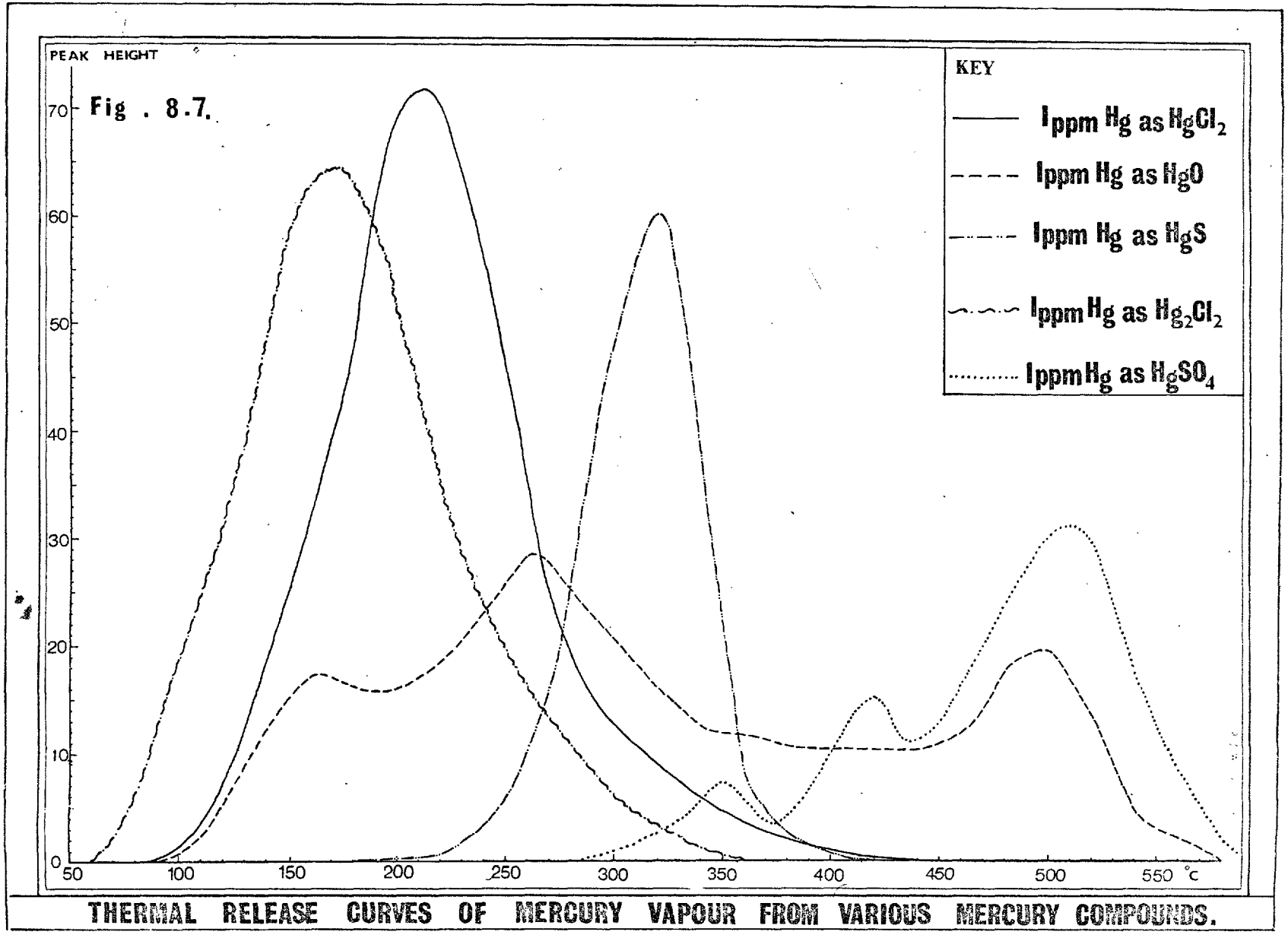


FIG ... 8.6

MERCURY RELEASE FROM CRUSHED ROCK MATERIAL UNDER "STEP - HEATING" VOLATILIZATION CONDITIONS



THERMAL RELEASE CURVES OF MERCURY VAPOUR FROM VARIOUS MERCURY COMPOUNDS.

factors:

(1) Mercury leakage from the heating chamber during heating.

(2) Absorption of mercury onto the walls of the heating chamber.

(3) All samples contained a high temperature form of mercury which was not released by this method.

(4) Recombination of mercury with its anions inside the heating chamber, prior to analysis.

(5) Oxidation of mercury vapour by the air and hence non absorption of light wavelength 2536.5 Å by mercuric oxide.

(6) Incorrect analysis by total mercury pulse method.

This initial survey however, suggested a possible reason for the lack of a sensible total mercury primary dispersion halo around Keel. It also indicated the inadequacies of the initial technique for investigating this, and the possible association of mercury compounds with base metal build up, to any degree of accuracy. It was therefore obvious that a new system of analysis would have to be designed if any meaningful research in this field was to be carried out.

(c) Continuous Flow, Thermal Dissociation of Mercury Compounds Analysis.

In order to carry out continuous flow thermal dissociation of mercury from its compounds, it was necessary to readapt the available mercury analysis equipment into a continuous mercury release monitoring device, Fig. 8.2. This was achieved by using a thermostatically controlled tube furnace to heat the sample, which was contained in a nickel boat inside a silica tube, to 800°C over a period of 45 minutes.

A thermocouple placed directly in the sample, inside the nickel boat, gave the temperature to within $\pm 5^{o}C$, while a variable scale, multispeed chart recorder enabled a continuous record of mercury release to be taken. Air, at the rate of four litres per minute was continuously flushed over the 1 g sample during the course of this heating run, Fig. 8.2. A great disadvantage with this equipment was the fact that the tube furnace, while taking only 45 minutes to reach $800^{o}C$, took four hours to cool, and no other furnace or heating equipment could be made available for these experiments. As a result, a maximum of four samples per sixteen hour working day could be analysed. Nonetheless a total of 1059 samples were analysed by this differential thermal release technique during the course of this study.

(d) Standardization of Equipment.

Synthetic standards containing 2.00, 1.00. 0.50, 0.25 and 0.125 ppm mercury, in the form of solid mercurous and mercuric chloride, mercuric sulphide, mercuric oxide and mercuric sulphate were prepared for comparison with the mercury release curves obtained from the Keel rocks. Each standard was made by successively diluting the spectrographically pure mercury salt in each base. It was not feasible to use elemental mercury in the preparation of standards of this type, due to homogenisation difficulties and oxidation; however, a qualitative standard was prepared.

As the thermal release characteristics of the various salts might be modified by the rock matrices, each set of standards was prepared in each of the synthetic rock bases listed in Table 8.5. To remove any mercury contamination, each base was heated to $900^{o}C$ for

TABLE ... 8.5

COMPOSITION OF ROCK STANDARD BASES USED IN MERCURY COMPOUND ANALYSIS

BASE	SiO_2	$CaO/CaCO_3$	Fe_2O_3	CARBON
A	100%			
B	90%	10%		
C	80%	15%	5%	
D	80%	15%		5%
E	75%	15%	5%	5%

TABLE ... 8.6

TEMPERATURES OF MERCURY RELEASE PEAKS

COMPOUND	PEAK 1	PEAK 2	PEAK 3
MERCURY	80°C		
MERCUROUS CHLORIDE	170°C		
MERCURIC CHLORIDE	220°C		
MERCURIC SULPHIDE	300°C		
MERCURIC OXIDE	160°C	255°C	495°C
MERCURIC SULPHATE	350°C	420°C	510°C

24 hours and reground to - 53.5 μm before addition of each mercury compound.

The mercury release characteristics of these compounds did not appear to be greatly modified by the synthetic bases, and their thermal release characteristics are shown in Fig. 8.7, and approximate peak temperatures are tabulated in Table 8.6.

From these results the possibility of qualitative identification of these compounds in natural material is opened up. Calibration curves on the basis of the prepared standards were also calculated and these are shown in Fig. 8.8. The temperature of maximum peak height and curve area is specific for each mercury compound and, by comparing the results on Fig. 8.8 for mercuric sulphide and for mercuric chloride, it can be seen that a sample containing 0.54 ppm mercury in the form of mercuric chloride will give an equal sub-curve area to one containing 1 ppm mercury in the form of mercuric sulphide. Thus two samples containing equal amounts of mercury, but one having the mercury in the form of mercuric chloride and the other in the form of mercuric sulphide will give different values unless specific calibration curves for mercuric chloride and mercuric sulphide are used for their quantification.

One extra qualitative standard was made from natural cinnabar to test the dissociation characteristics of the natural material against the synthetic mercuric sulphide. The dissociation curves of the two samples are shown in Fig. 8.9.

The position of the major 300°C peak was again confirmed, but cinnabar produced a much slower decay slope. On this decay slope, two other peaks suddenly formed Fig. 8.9B. These peaks correspond to

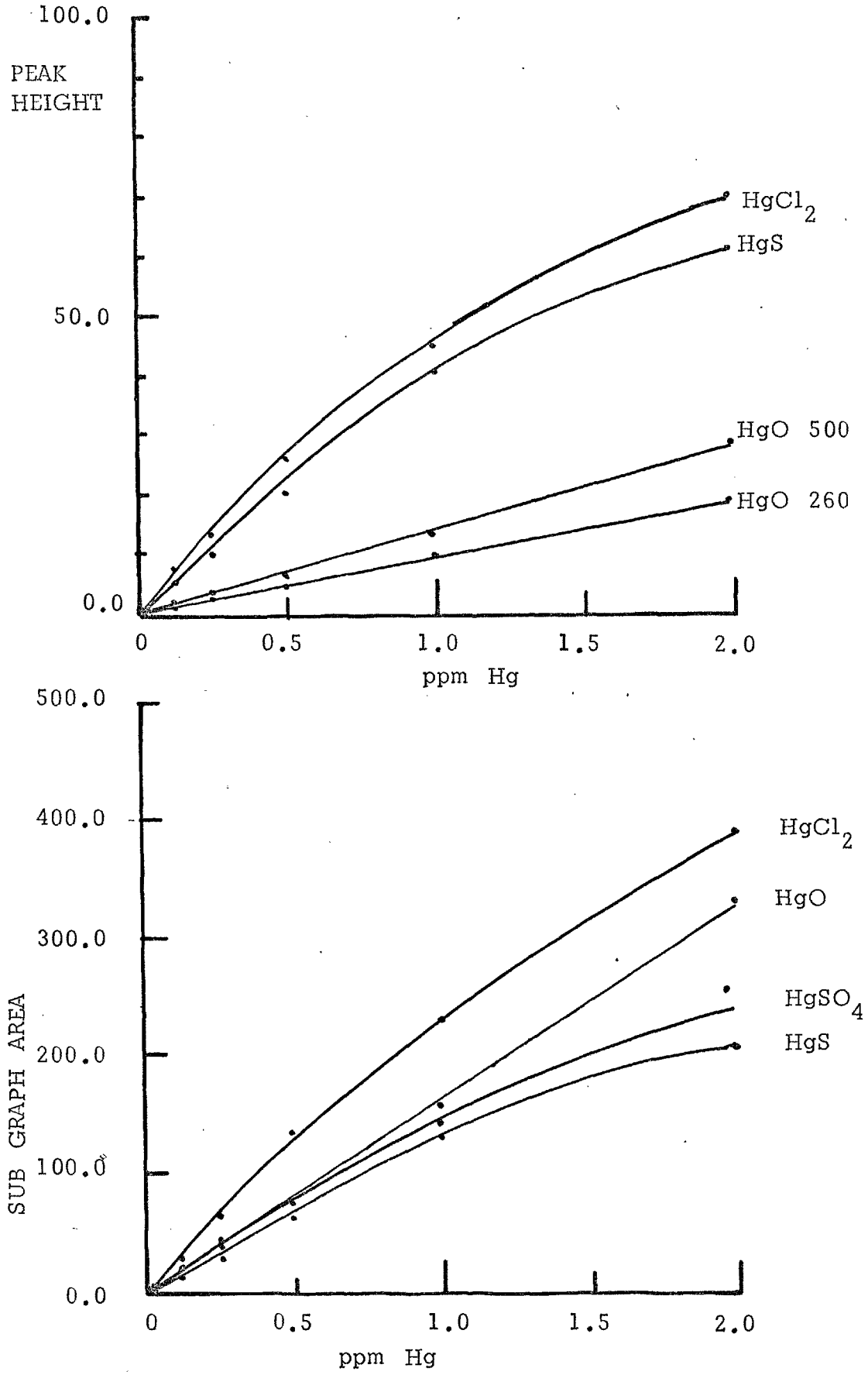
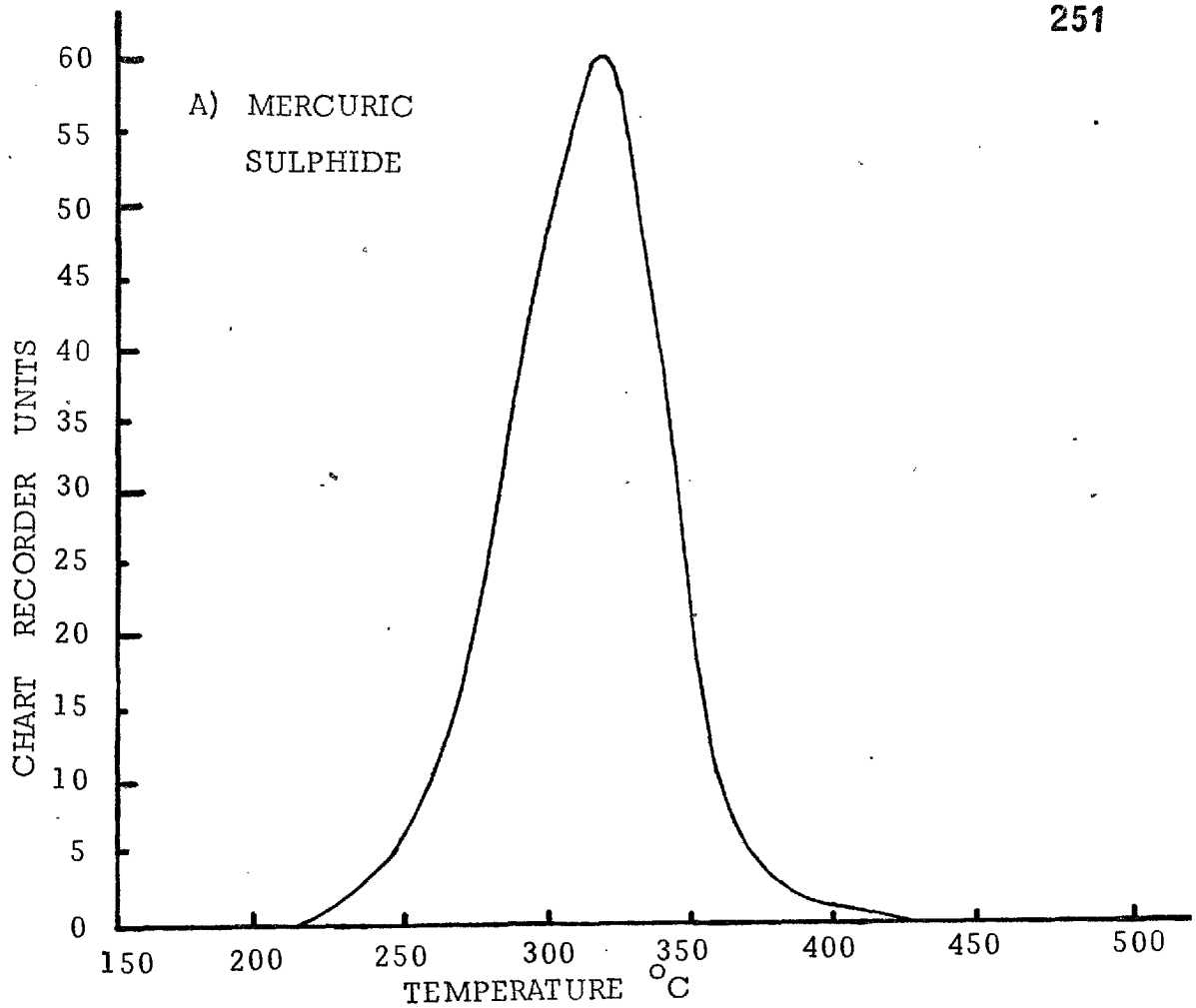


FIG ... 8.8 MERCURY COMPOUND CALIBRATION GRAPHS



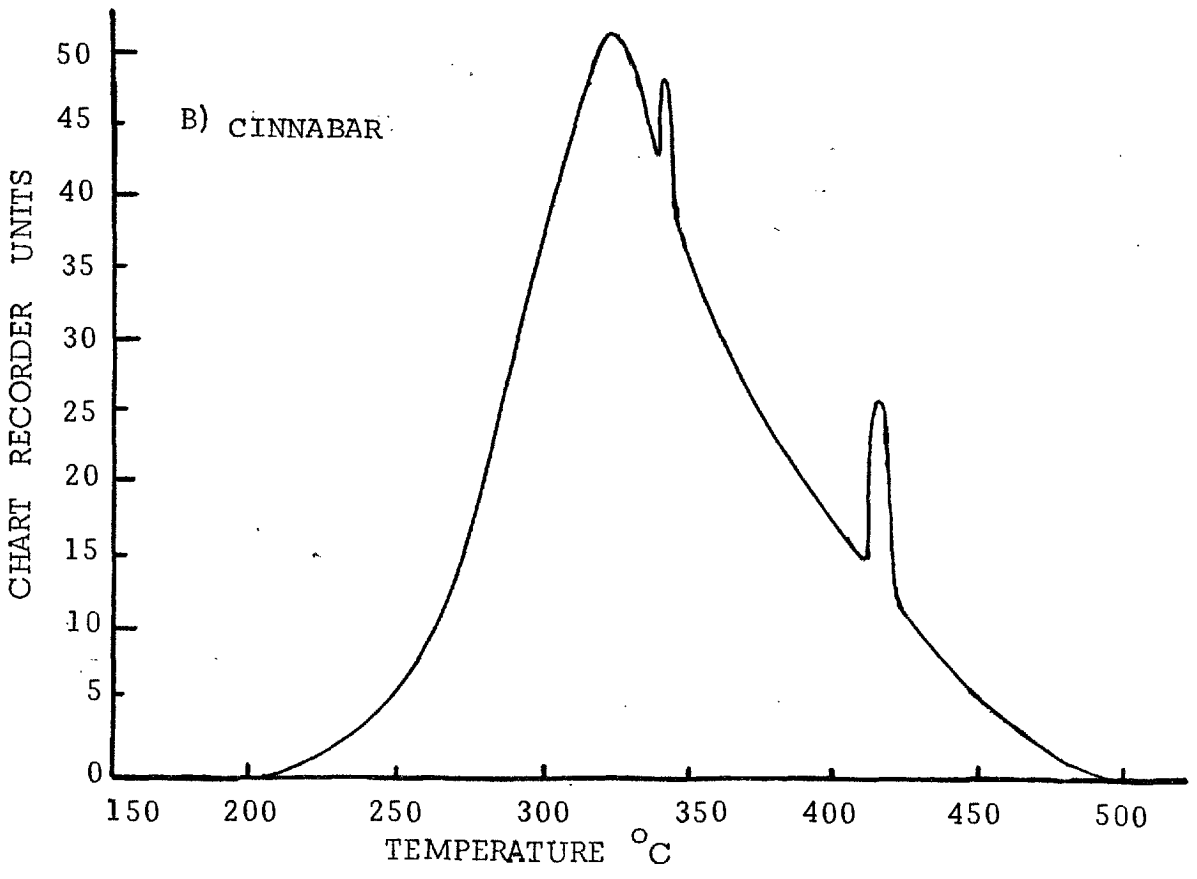


FIG ...8.9 DISSOCIATION CHARACTERISTICS OF CINNABAR AND MERCURIC SULPHIDE

the 350°C and 420°C peaks on the mercuric sulphate thermal dissociation trace, Fig. 8.7, and thus indicate the possible existence of mercuric sulphate admixed with the cinnabar, possibly as an oxidation product.

It was found that throughout the study where mercuric sulphate was encountered, except in one instance where it was intimately associated with anhydrite, the relative magnitudes of the peaks are opposite to the standards. In most cases only the 350°C and 420°C peaks occur and of these, the 350°C is almost invariably the stronger. This phenomenum is probably due to the fact that the naturally occurring mercuric sulphate is not in the same chemical form as that obtained from synthetic processes in the laboratory.

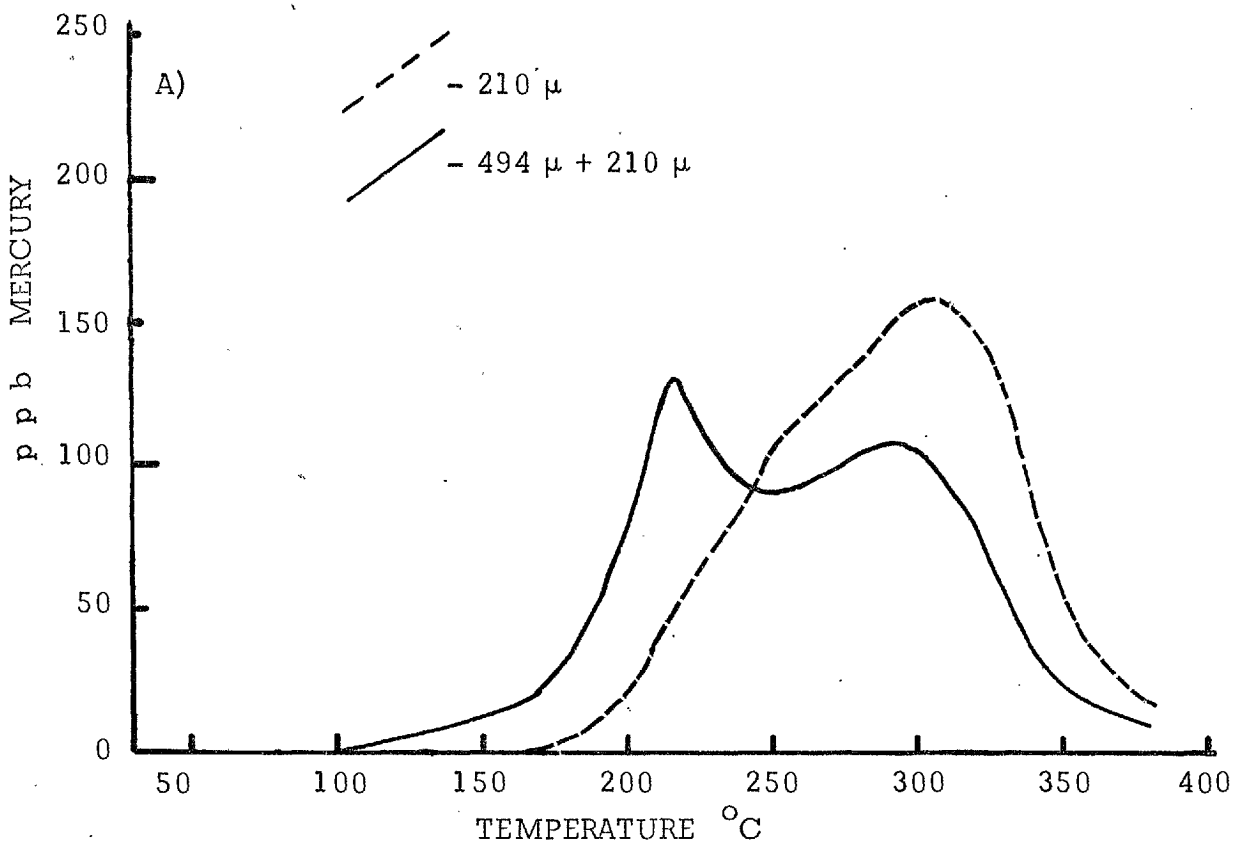
(e) One Possible Reason for Variation in Mercury Content with decreasing particle size in sieved, crushed rock material.

Initial work at Keel, using the conventional heating and pulse method of mercury analysis to determine mercury content of various size fractions of crushed rock material, produced the information tabulated in Table 8.2. These results for material from the the underground workings indicated a distinct increase in mercury values from the - 494 μm + 210 μm to - 210 μm fractions, with the - 1550 μm + 494 μm material being the lowest. The drillcore results, Table 8.2B, indicate the opposite, in that the increase in mercury values is from - 210 μm to - 494 μm + 210 μm, again the - 1550 μm + 494 μm material is the lowest in mercury content.

In the light of these results it was decided to run - 210 μm, - 494 μm + 210 μm and - 1550 μm + 494 μm material on the mercury thermal dissociation equipment, to try and ascertain whether these differences

represented selective volatilization of specific mercury compounds or pore held mercury, or whether the mercury in drillcore material was distributed in different ways from that in material from the underground workings. It must be remembered that the initial work on drillcore was carried out on samples over 1000 feet from known mineralization and consequently the term "drillcore" is here applied to this specific unmineralized material.

Results: Ten samples, five from drillcore and five from the underground workings were selected for analysis. Each sample was crushed in a manganese steel jaw crusher and sieved into the appropriate size fractions. Approximately one gramme of sample was weighed and mixed with approximately one gramme of freshly prepared calcium oxide (see section 2 in this chapter). The sample was not ground, and the mixing was carried out on weighing paper the whole of the mixture being transferred to the heating chamber. Three samples are used here to describe exactly what results were obtained. The - 1550 μm + 494 μm material gave extremely erratic and unreproducible results, mercury being released in a series of pulses from the rock and not as a simple release peak. This type of release is thought to be due to mercury degassing from individual particles following decrepitation. Consequently the release traces obtained from this - 1550 μm + 494 μm material were almost meaningless, Fig. 8.10B. However analysis of this material did lend support to the theory that a diffusion gradient, and probably a thermal gradient also, existed in this coarser fraction, suppressing the release of mercury. This would probably contribute greatly to the low values of total mercury obtained from this material by the original mercury analysis method.



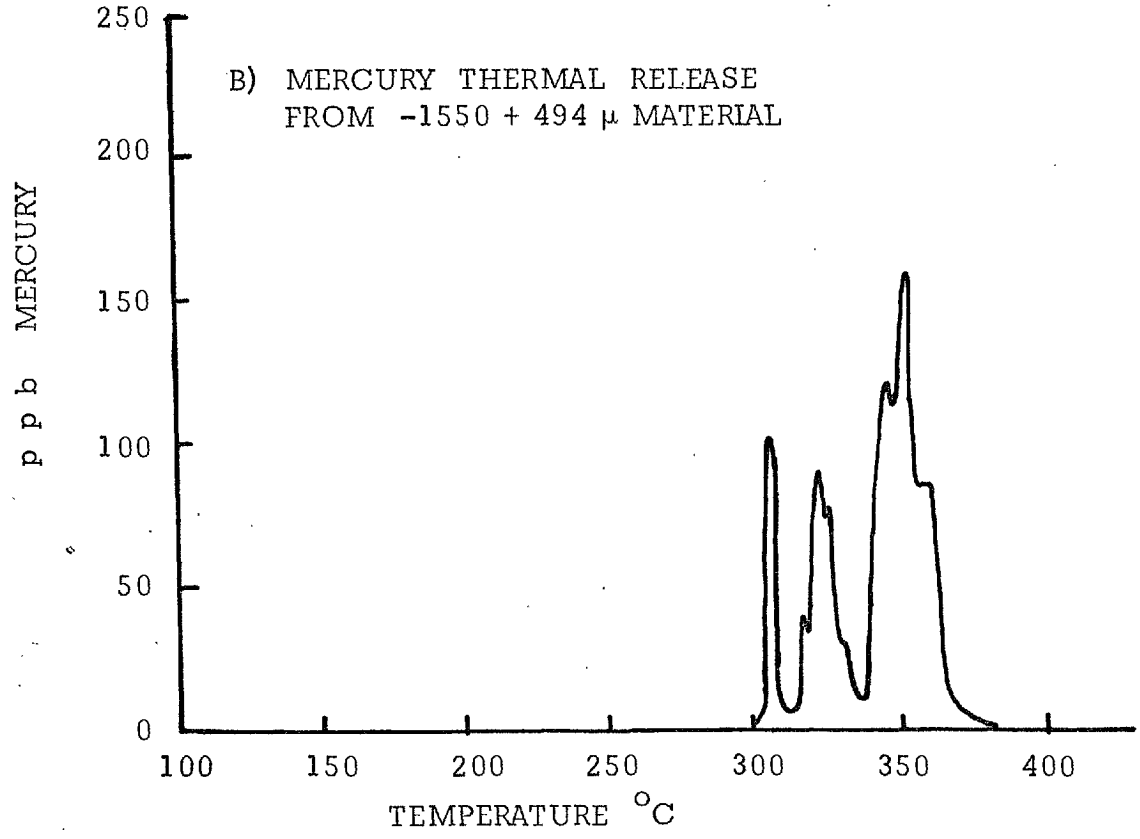


FIG ...8.10

DIAGRAM ILLUSTRATING THE EFFECT OF PARTICLE SIZE ON MERCURY THERMAL RELEASE CHARACTERISTICS

Fig. 8.10A indicates the situation where a rock from drill-core material at some distance from known mineralization, displays increased mercury content with decreasing particle size. When the two size fractions were analysed by the total mercury pulse method, the following results were obtained:

- 210 μm fraction 176.5 ppb
- 494μm + 210 μm fraction 293.3 ppb

The two fractions were then analysed by the mercury thermal dissociation method and the peaks quantitatively estimated for total mercury using the appropriate calibration graph. This sample originated from a mixed mercuric chloride and mercuric sulphide zone. The following results were obtained:

- 210 μm fraction: mercury as $HgCl_2$ - not detectable
  mercury as HgS - 135 ppb
  TOTAL - 135 ppb
- 494 μm + 210 μm fraction: mercury as $HgCl_2$ - 72 ppb
  mercury as HgS - 85 ppb
  TOTAL - 159 ppb

This indicates the same general trend as other drillcore material in the initial survey, once the total mercury has been calculated from the mercury compound data. Total mercury data shows the opposite trend. In this sample, crushing has apparently volatilized the mercuric chloride component of the rock mercury, thus lowering the mercury level, while at the same time decrease in particle size has allowed more mercuric sulphide greater access to the surface.

Thus the diffusion gradient problem has decreased and although mercury in the form of mercuric chloride has been lost from the finer fractions in the crushing procedure, the newly available mercuric sulphide has almost compensated for this.

This selective volatilization of mercury compounds on crushing is well exemplified by the following two examples. Sample 1, Fig. 8.11A, is material from the extremity of the chloride/sulphide zone (see distribution of mercury compounds in Keel rocks, section g.). When total rock mercury was calculated on this sample the following results were obtained:

- 210 µm fraction	215 ppb
- 494 µm + 210 µm fraction	1400 ppb

The results for the same sample calculated from the mercury thermal dissociation graphs, Fig. 8.11A., were as follows:

- 210 µm fraction	mercury as $HgCl_2$	500 ppb
	mercury as HgS	750 ppb
	TOTAL	1250 ppb
- 494 µm + 210 µm fraction,	mercury as $HgCl_2$	2405 ppb
	mercury as HgS	373 ppb
	TOTAL	2778 ppb

In this case, both methods of analysis indicate that the - 494 µm + 210 µm fraction has a higher mercury content than the - 210 µm fraction although specific amounts differ. The reason for this enrichment in the - 494 µm + 210 µm material can easily be seen, Fig. 8.11A. This fraction has a large proportion of its total mercury tied up as mercuric chloride; when the rock is crushed the

majority of this mercuric chloride is apparently volatilized. The mercuric sulphide component is slightly increased for reasons already discussed. However, this increase in mercuric sulphide is insufficient to compensate for the loss of mercury from mercuric chloride and therefore the rock has a greater value of total mercury in the coarser fraction.

Apparently local spot heating, by percussive grain on grain impact in the jaw crusher, creates enough local heat to volatilize the mercuric chloride from the finer particles. However temperatures are not elevated sufficiently to totally volatilize mercuric sulphide. In order to try and detect mercury in the atmosphere above the jaw crusher during crushing, air from inside the jaw cavity was drawn into a 20 ml. glass syringe and injected into the analysis apparatus. However no mercury was detected in any of the air samples taken. This could be due to a variety of reasons:

(1) The mercury had recombined with chloride ions.

(2) The mercury had combined with oxygen to form mercurous or mercuric oxides

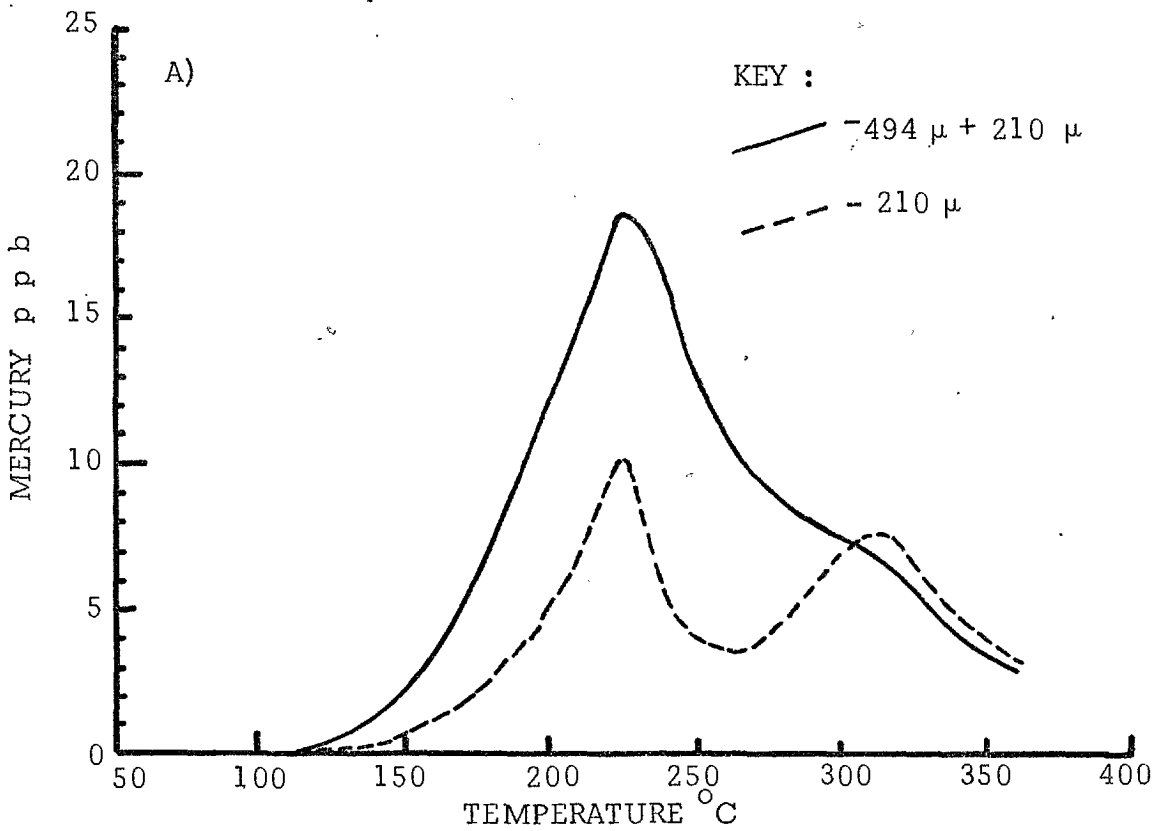
(3) The dissociated atoms had recombined to form molecules

(4) The mercury had amalgamated with, or condensed on, the jaws of the jaw crusher.

A rock from the underground workings was tested next. The release traces obtained are shown in Fig. 8.11B. The total mercury analyses for both fractions of this rock were as follows:

- 210 μm fraction 1780 ppb

- 494 μm + 210 μm fraction 720 ppb



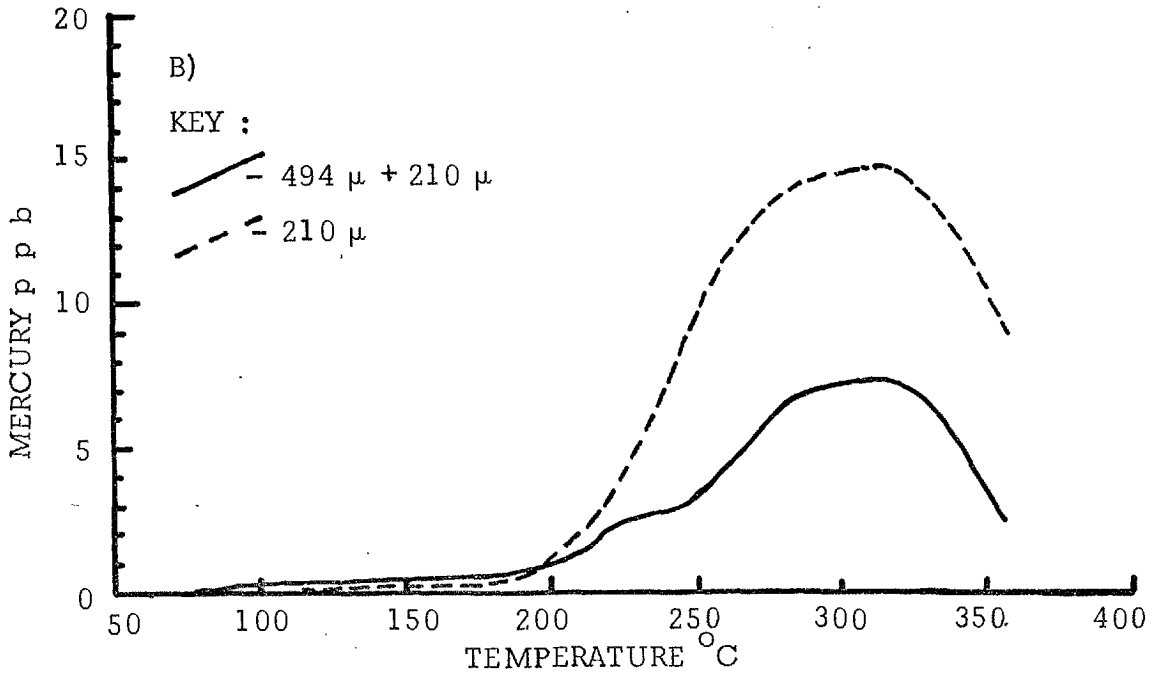


FIG ... 8.11

VARIATION OF MERCURY CONTENT WITH FRACTION IN CRUSHED ROCK MATERIAL FROM CHLORIDE-RICH & SULPHIDE-RICH AREAS KEEL PROSPECT , IRELAND

The results for the same sample calculated from the mercury thermal dissociation graphs, Fig. 8.11B, were as follows:

- 210 μm fraction	mercury as $HgCl_2$	nil
	mercury ae HgS	1610 ppb
	TOTAL	1610 ppb
- 494 μm + 210 μm fraction	mercury as $HgCl_2$	25 ppb
	mercury as HgS	595 ppb
	TOTAL	620 ppb

This indicates a significant increase in mercury with decreasing particle size. The reason for this increase can be seen in Figure 8.11B, as being due to an increase in HgS. Thus crushing here has increased the available mercury by decreasing particle size, and overcoming diffusion and thermal gradients within the particle.

These results give a possible explanation for the variation of mercury content of various particle sizes from crushed rock material.

On referring to Table 8.3A and B, it can be seen that, when the - 1550 μm + 494 μm material was ground in a Tema Mill, there was a substantial increase in mercury content of the residual ground material. When this material was analysed by mercury thermal dissociation analysis this increase was again shown; in this case however, where found, both mercuric chloride and mercuric sulphide had increased. This fact indicates that, whereas crushing appears to produce enough local heat to volatilize $HgCl_2$, the grinding technique does not. It must be pointed out however, that grinding continued for only 15 seconds and no experimentation was carried out to ascertain the effects of prolonged grinding on selective volatilization of mercury compounds.

This basic experimentation however,leads to the following conclusion. Both grinding and crushing procedures must produce local heat and it is improbable that crushing produces more heat than grinding. The mechanical process of grinding,however,is abrasive rather than percussive. Therefore the process of grinding may lead to a gradual build up of heat throughout the whole sample bulk and the process of crushing gives rise to local hot spots. If grinding is not continued for long periods,insufficient heat may be built up to volatilize mercury from mercuric chloride, whereas the generation of localized heat could accomplish this. Thus grinding - 1550 μm + 494 μm crushed rock material for fifteen seconds does not appear to volatilize much mercury. It does,however,substantially increase the apparent mercury content of the material by decreasing the particle size and consequently making the various mercury compounds much easier to volatilize.

As a result of this experimentation it was decided to use -494 μm + 210 μm material for all the mercury thermal dissociation analyses carried out.

f. Results.

This section is conveniently divided into two parts. The first will deal with the distribution of mercury compounds in the Keel environment and the second will deal with the distribution of mercury in sphalerite galena, and pyrite, and the effect of the release of mercury from the lattices of these minerals,on the thermal dissociation traces of the rocks.

g. Identification and Distribution of Mercury Compounds in the Primary Environment of the Keel Prospect.

Using a thermal dissociation technique, some 780 samples of drillcore and 279 samples of rock material from the underground workings, were analysed for mercury compounds. On the basis of these analyses it was found that mercuric chloride, mercuric sulphide and mercuric oxide were the predominant mercury compounds at Keel, with mercurous chloride occurring in one area on the 500 foot level. Mercuric sulphate and native mercury were also found, but very infrequently. Adsorbed mercury is dealt with under the soils section of this chapter.

Two major dissociation patterns emerged from the rocks in which mercury compounds were found.

(A) Single release peak at

A1 75 - 85°C

A2 160 - 175°C

A3 205 - 230°C

A4 295 - 320°C

(B) Double release peaks at

B1 205 - 230°C and 295 - 320°C

B2 260 - 275°C and 500 - 520°C

These forms of dissociation will be dealt with in turn.

A1 represents elemental mercury being released from pore spaces, cracks and fissures, within the rock. Mercury, however, was found in only three of the samples analysed, and in each case, in concentrations less than 50 ppb.

A2 represents mercurous chloride;

A3 can be seen to correspond to the release pattern of mercuric chloride;

A4 corresponds to mercuric sulphide.

The B1 dissociation curves are a mixture of mercuric chloride and mercuric sulphide; while B2 dissociation curves represent mercuric oxide.

The magnitude of the 160°C peak of the standard oxide is extremely suppressed in natural samples, and its presence is only occasionally indicated by a minor change in slope of the initial release curve. A triple peaked oxide dissociation curve is primarily associated with some samples from a decomposed zone at Keel, in which ferric oxides are also present. The release of mercury from these latter gives a mercury dissociation curve peaking at 420°C. Mercuric oxide is also present, associated with an area of faulting on the 200' level, Fig. 8.14.

The dissociation characteristics of mercuric sulphate in the natural sample, as already stated for mercuric sulphate in cinnabar, differ somewhat from the synthetic standard. The possibility of the existence in nature of peculiar mercuric sulphate complexes, for example $HgSO_4 \cdot H_2O$ and non-stoichiometric mercuric sulphate species, could possibly give rise to this variation in thermal breakdown characteristics. However, as this compound is only of very minor importance at Keel, an investigation into the reasons for the different characteristics was not carried out.

As a result of this study, three major divisions of the Keel rocks were made, on the basis of their mercury compounds. These

divisions can be seen in Figs. 8, 12A, B and C. These figures are taken directly from chart recorder traces, and the vertical lines, separating portions of the peak, represent changes in chart recorder scale, Fig. 8.5. Fig. 8.12D shows a fourth zone. This sample comes from the underground workings of the prospect, and the significance of the peak at 600°C is discussed in Section 2.

The significance of these sulphide and chloride peaks is that they give information of a quite fundamental nature. If their spatial distribution is plotted on plans of the underground levels of the prospect area, a direct relationship to the distribution of the known areas of sulphide mineralization becomes apparent, Figs. 8.13 - 8.17. No attempt as to a finite quantitative distribution of total mercury was made on these diagrams, as the whole essence of this type of study was to investigate the distribution of mercury compounds and their relation to sulphide mineralization, if such a relationship existed. Quantitative analysis of total mercury was, however, carried out by interpreting the peaks obtained, but is not part of this immediate study.

Areas of significantly low concentrations of mercury exist to the north, south-west and south of the map area. In the north, the mercury, where present, is in the form of mercuric sulphide, whereas, in the south and south-west, it is in the form of mercuric chloride, and is in direct association with higher mercuric chloride areas. Mercuric chloride build-up is predominantly confined to the south and south-west of the area, and its obvious relationship to the extent of the reef limestone is very apparent, especially on the 200' level, where it conforms closely to the relief boundary.

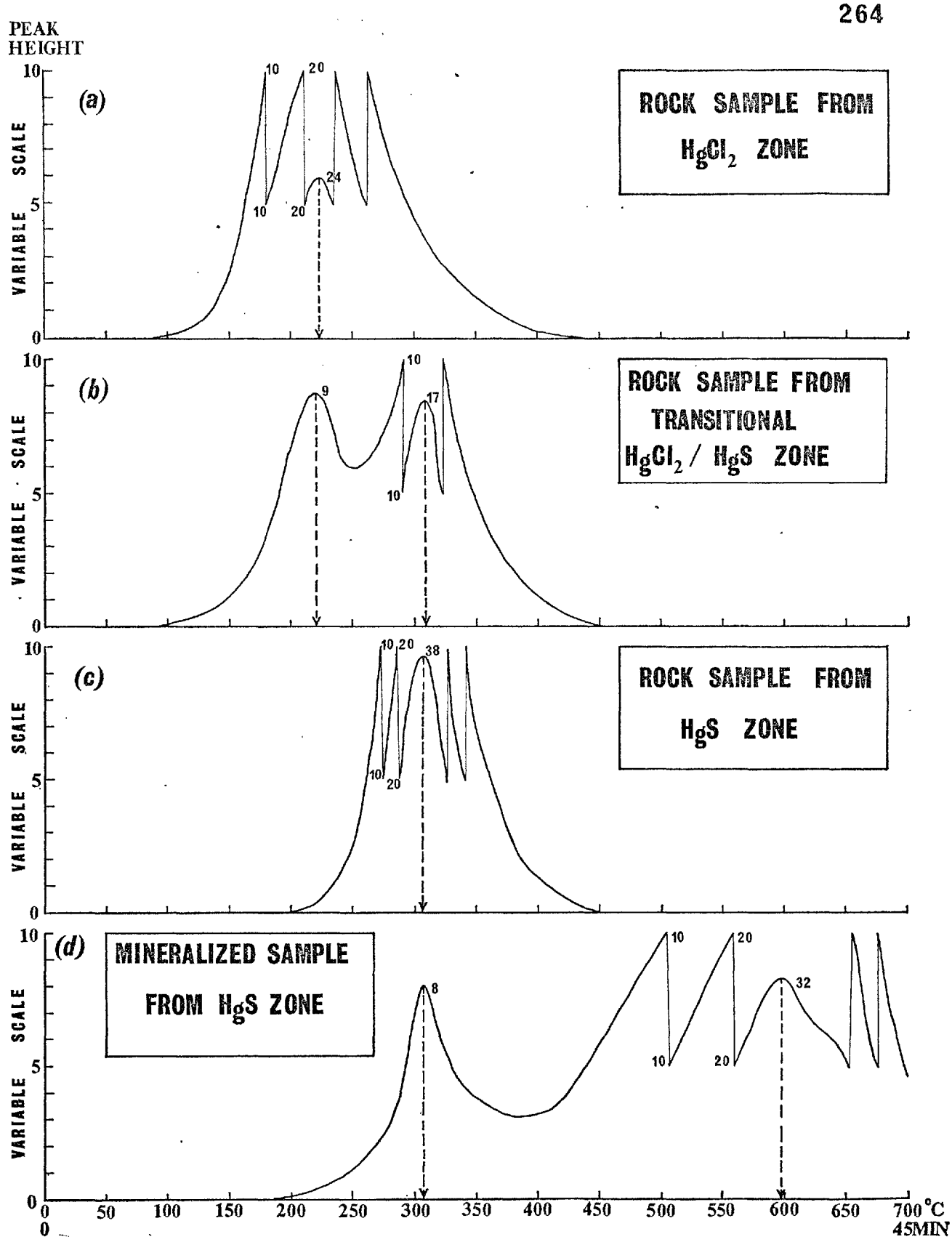


FIG ...8.12 THE VARIATION IN MERCURY THERMAL RELEASE PATTERN IN ROCK SAMPLES FROM THE DIFFERENT MERCURY COMPOUND ZONES, KEEL PROSPECT, COUNTY LONGFORD.

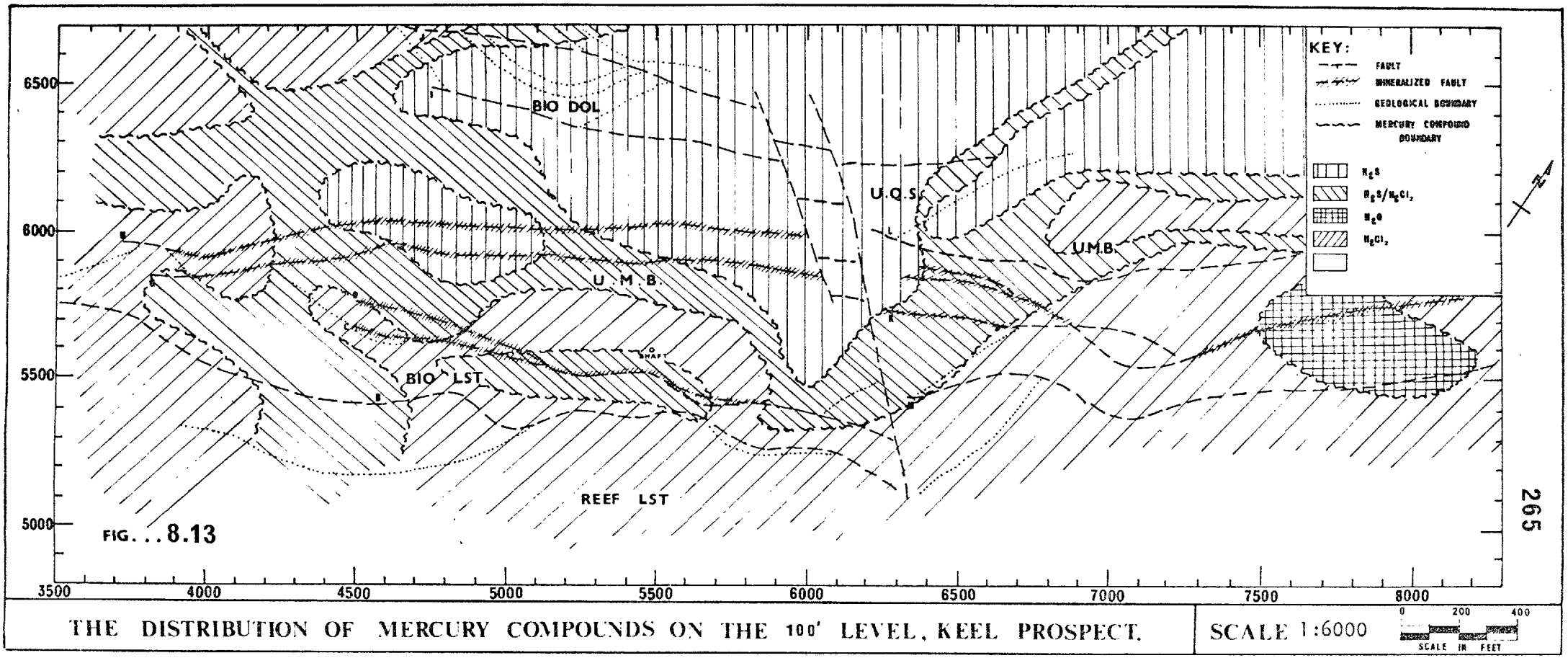


FIG. . . 8.13

THE DISTRIBUTION OF MERCURY COMPOUNDS ON THE 100' LEVEL, KEEL PROSPECT.

SCALE 1:6000

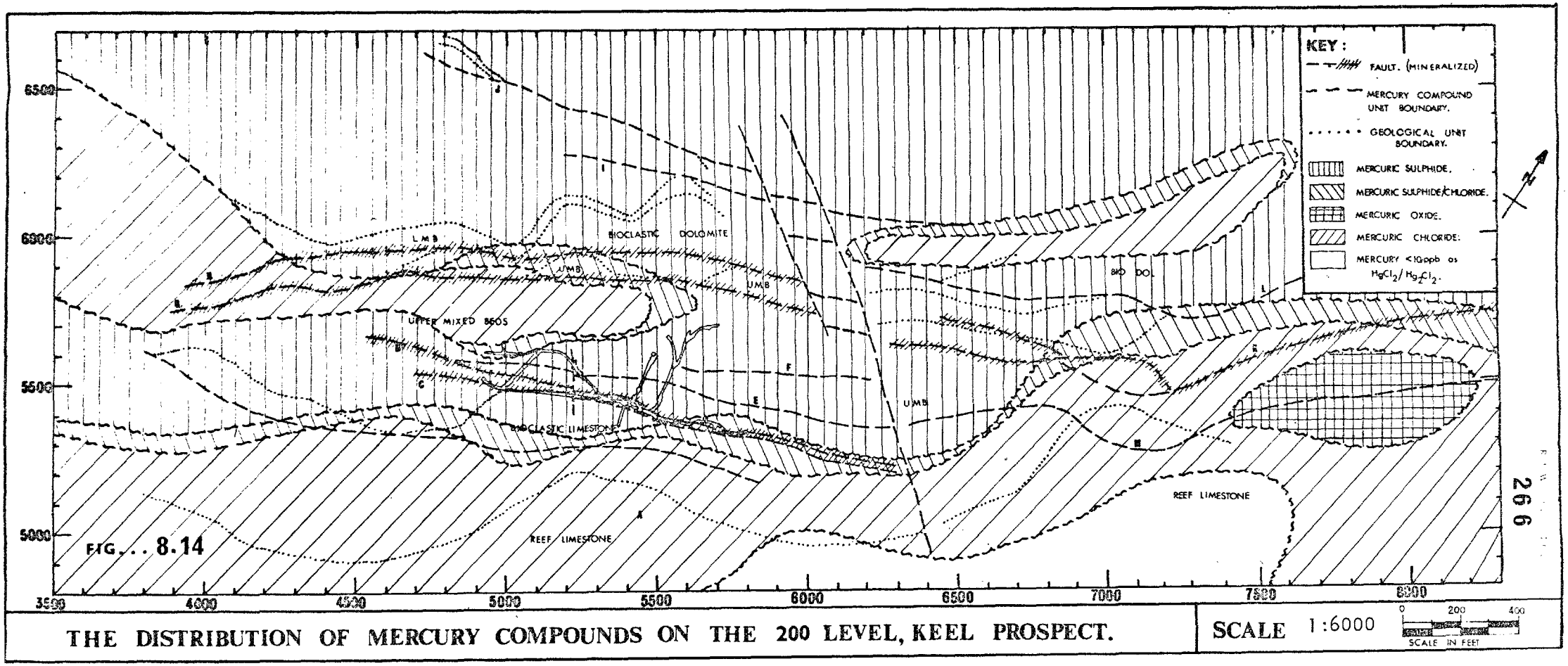


FIG... 8.14

THE DISTRIBUTION OF MERCURY COMPOUNDS ON THE 200 LEVEL, KEEL PROSPECT.

SCALE 1:6000

0 200 400
SCALE IN FEET

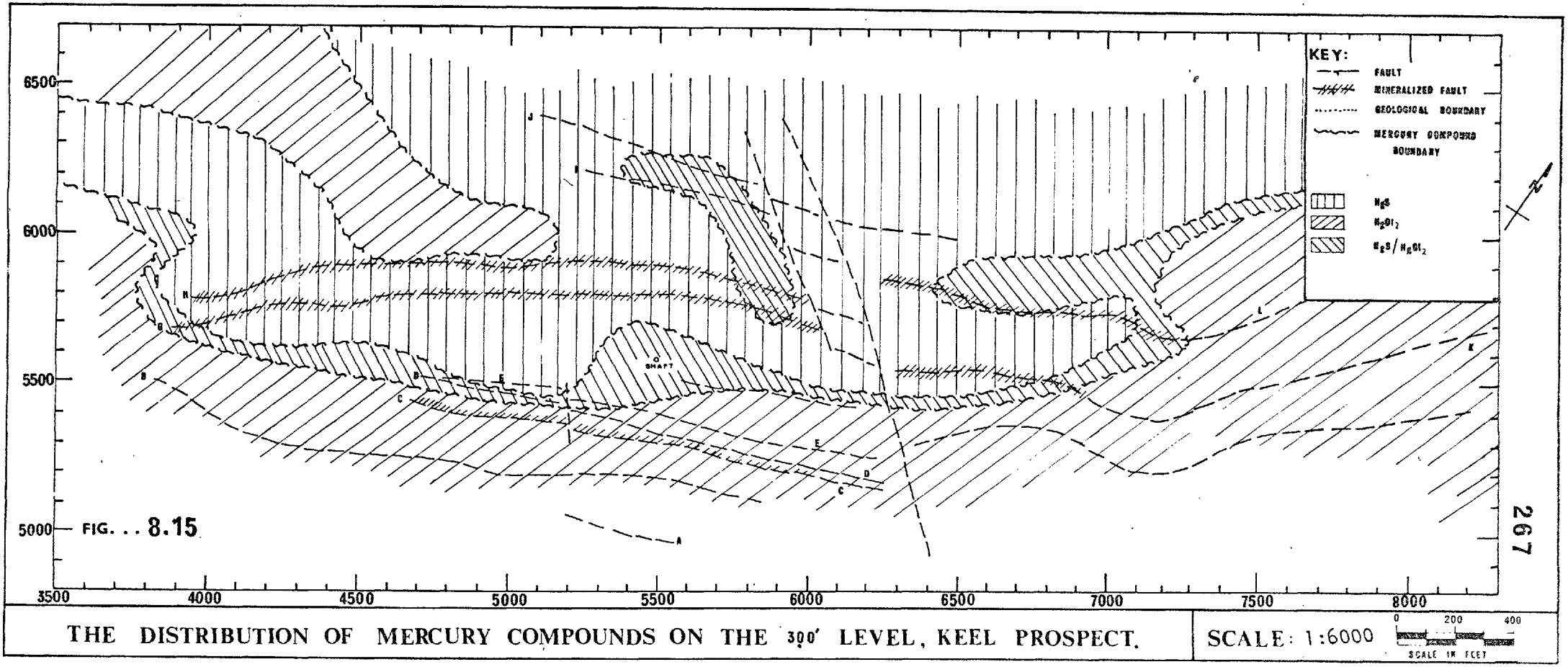


FIG. . . 8.15

THE DISTRIBUTION OF MERCURY COMPOUNDS ON THE 300' LEVEL, KEEL PROSPECT.

SCALE: 1:6000

0 200 400

SCALE IN FEET

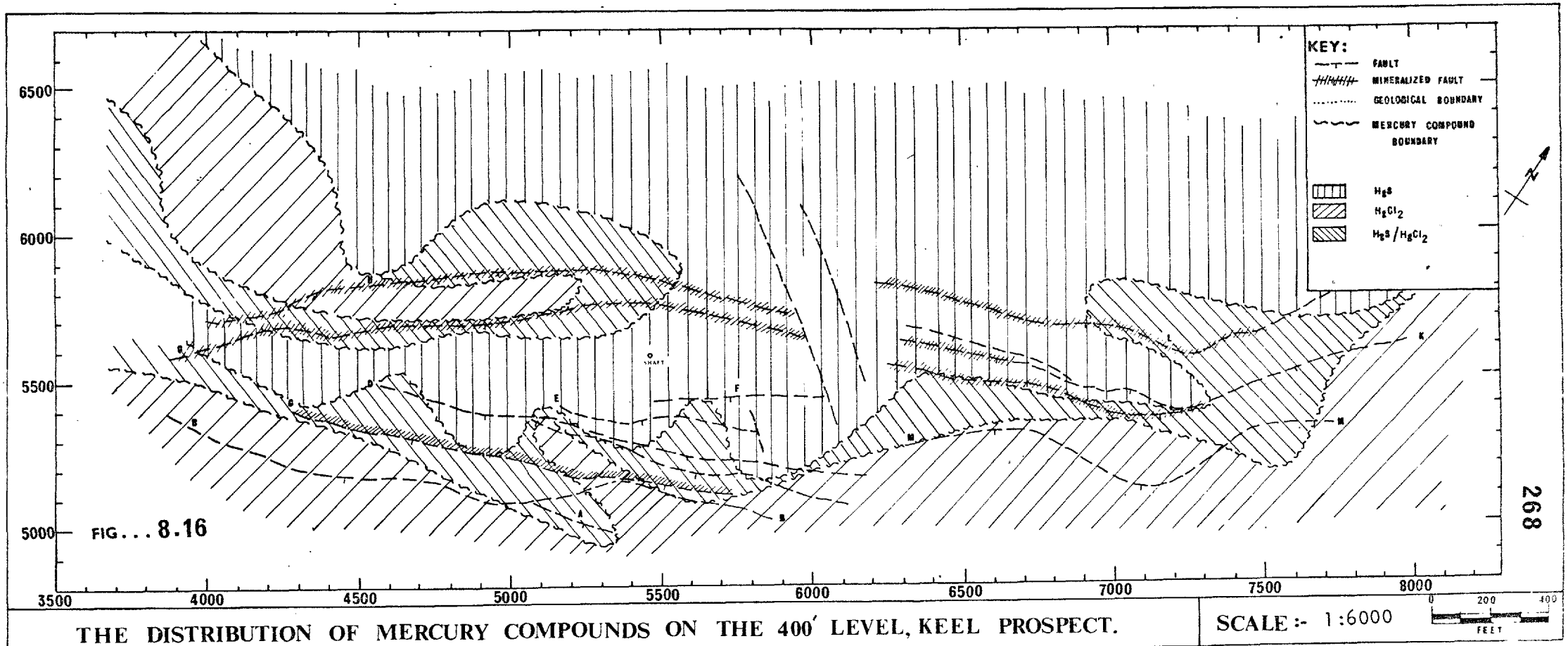


FIG... 8.16

THE DISTRIBUTION OF MERCURY COMPOUNDS ON THE 400′ LEVEL, KEEL PROSPECT.

SCALE :- 1:6000

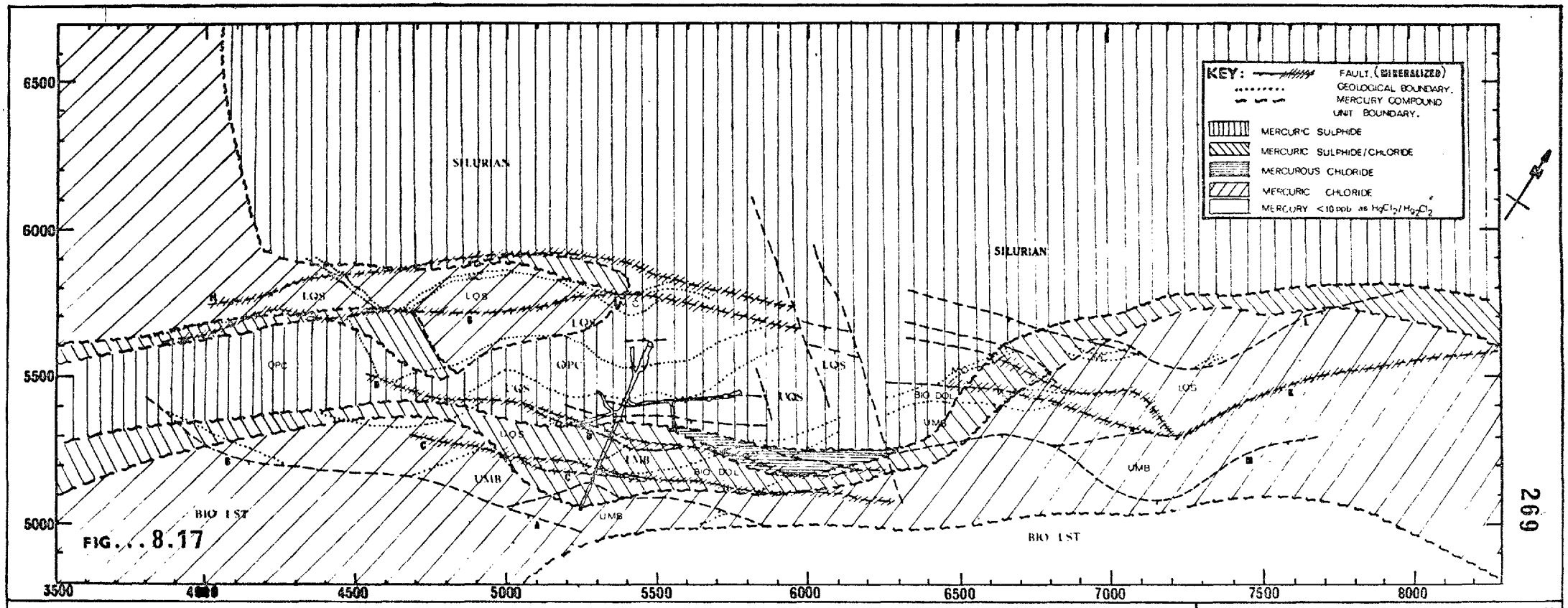


FIG. . . 8.17

THE DISTRIBUTION OF MERCURY COMPOUNDS ON THE 500 LEVEL, KEEL PROSPECT.

SCALE 1:6000

0 200 400

Separating the mercuric chloride zone from the mercuric sulphide zone, is an area of mixed mercuric sulphide and chloride. This zone appears to be very predominant on the 100' level, but is present on every other level, especially in the south of the area where the mercuric chloride halo is in close association with the reef boundary. In the west and south-west, however, the zone is far more sporadic in its distribution. This may be due to displacement by faulting in that area, which post-dates the mineralization and hence post-dates the emplacement of the mercury compound halos. Lack of drillhole information and the consequent inability to place precise boundary limits, also plays an important part in this patchy distribution picture of the mixed zone material. The mixed zone extends for some considerable distance into the underground workings on the 500' level, although the chloride component, in most cases, is extremely small. On the 200' level, the zone is only apparent at the eastern end of the drive east, and on the 400' level, is not found in the underground workings at all.

The ratio of mercuric chloride to mercuric sulphide appears to decrease as mineralization is approached, and is very low indeed in the underground workings, except at the southern end of the 500' level, where in one sample, mercuric chloride makes up 60% of the total rock mercury.

Mercuric oxide assumes prominence to the east of the area on the 100' and 200' levels. This oxide zone is, however, very closely associated with an area of faulting, and is probably a direct result of oxidation of the existing mercuric chloride in that area. The zone does not extend into the 300' level. A greater area of mercuric oxide is associated with an area of decomposed rock to the north-east, the

Decomposed Zone of Keel. The decomposition and oxidation, however, does not extend into the 100' level, and has been dealt with by D.S. Evans in a study on the secondary environment geochemistry at Keel, Evans (1972).

A zone of mercurous chloride is found, to a limited extent, on the 500' level, associated with an area of intense faulting and water flow, and probably represents in situ reduction of mercuric chloride in that area.

The information obtained from total mercury analysis, and mercury compound analysis is compared in Fig. 8.18. This figure shows mercury distribution on the 300' level of the prospect. As can be seen from the position of the mineralized faults, values of high total mercury do not always indicate a close association with mineralization, Fig. 8.18A. However, definite association of mineralization with areas, especially of predominantly mercuric sulphide and the high sulphide/low chloride regions of the mixed zone,can be clearly seen, Fig. 8.18B. The usefulness of mercury compound data to delimit specific areas of prospecting interest is therefore obvious, together with its advantage over conventional total mercury geochemical data.

The total mercury content of the bedrock tends to increase towards the underground workings, and also with increasing depth. High concentrations occur where mineralization is encountered, and also, occasionally, in the mercuric chloride zone, where no mineralization is found. Quite commonly, very low levels of total mercury occur only half an inch away from massive sulphide mineralization, whereas high values can exist throughout a complete drillhole in the unmineralized chloride zone. It is therefore of primary importance to identify the actual type of mercury compound giving rise to the anomaly.

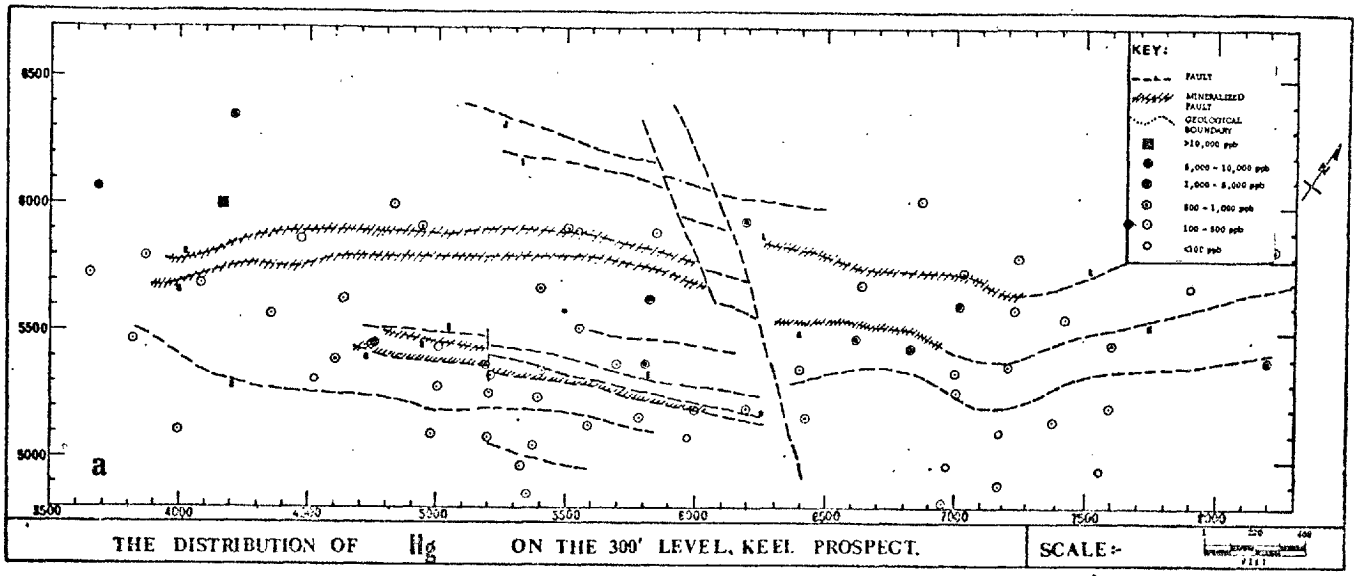
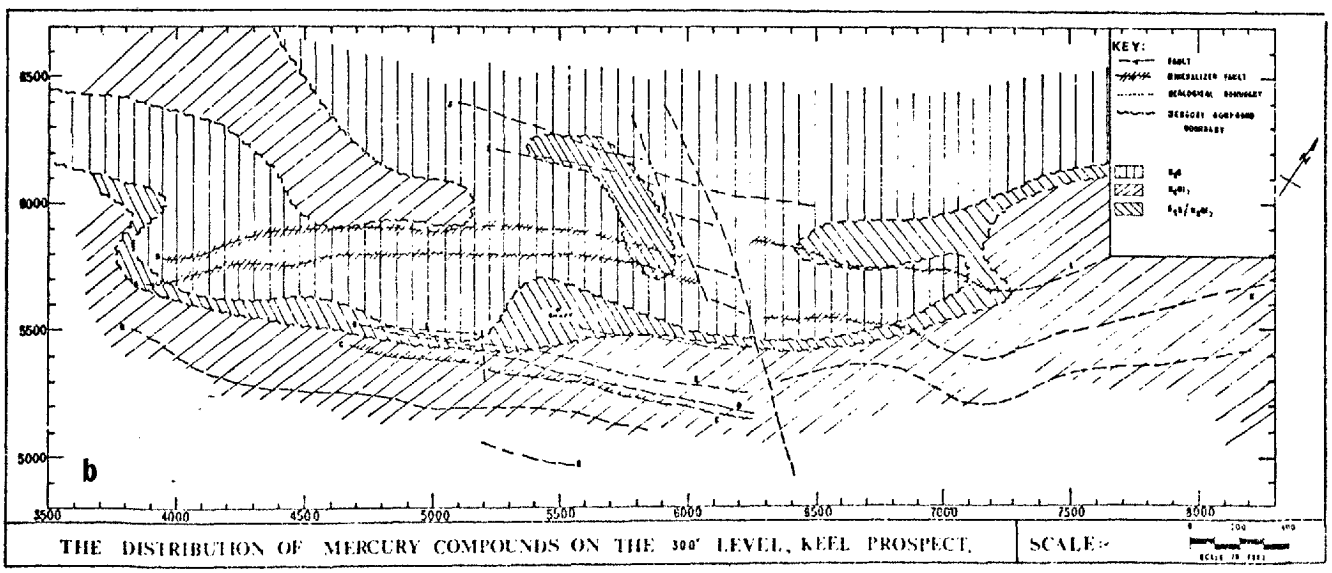


Fig . 8.18. COMPARISON OF TOTAL MERCURY AND MERCURY COMPOUND DATA



At Keel, as the mineralization is characteristically fault controlled and the distribution of mercury compounds appears to be aligned with the faults, it appears that the mercury compound distribution has been directly effected by the process or processes which gave rise to mineralization of the area. Evidence as to whether the mercury came directly from the mineralizing solutions, or whether it built up in the area, prior to mineralization and was later modified, is purely tentative.

Mineralization occurs in the Silurian to the south of the area (Chapter 3), and this suggests the possibility of the introduction of mineralizing solutions from depth. Although there appears to be no definite mineral zonation at Keel, there are signs that the Pb/Zn ratio increases with depth, and also on a level going northwards towards the Silurian inlier, (Chapters 3 and 4).

This tentatively points to a possible metal zonation and, as a consequence, an introduction of mineralizing solutions from depth, with precipitation of the least soluble sulphide, galena, first. The faulted zones at Keel also represent a potential area of increased sulphur activity, so that, when chloride rich waters encountered the faulted region, base metal sulphides were gradually precipitated. The precipitation occurred predominantly in the faults that acted as natural channels for migrating solutions. Disseminated sulphides were also precipitated throughout this sulphur active area. As the sulphides were both insoluble and stable, a gradual build up of base metal sulphides could occur by continuous precipitation from the migrating waters.

The halo of mercury compounds can therefore be interpreted as being due to one, or a combination of some of the following causes:

(1) Ground-waters, migrating from the marine Carboniferous sediments towards the faults on the southern side of the Silurian inlier, carried with them leached base metals and mercury in solution. When these solutions reached the faulted area, local precipitation, and build up of base metals, occurred, leading to disseminated sulphide mineralization. Immediately associated with the faulted area was an area of high sulphur activity, and once the soluble base metal salts and mercury salts encountered this, precipitation of base metal sulphides and mercuric sulphide occurred. Consequently, near the mineralization in the sulphur active area, all the mercury is converted to insoluble mercuric sulphide, while further away, a zone of mixed sulphide and chloride occurs where the activities of both ions were comparable. Further away still, a zone of mercuric chloride is present, where the activity of the sulphide ion was sufficiently low such that no mercuric sulphide was formed.

This suggests that the mercury halo was formed by successive replacement of mercuric chloride, transported towards the faulted area by migrating solutions, by mercuric sulphide, and that the mercury migrated from the extremities of the orebody, inwards.

(2) This theory of the genesis of the mercury compound halos is based on the fact that mercury was obviously present in the mineralizing solutions; 200 ppm is recorded in sphalerite as an average value (Chapter 6). Thus mercury, probably in either gaseous, chloride, or chloride complex form, migrated into the Carboniferous sediments

from the mineralizing solutions. Migration of zinc and lead into the rocks was by no means as pronounced, and conversion into insoluble galena and sphalerite took place predominantly within the faults themselves, leading to the extremely sharp cut-off of mineralization now seen. Build up of mercuric sulphide was greatest in closest proximity to the faults, but some of the mercury managed to migrate to the boundaries of the sulphur active area, where a build up of both mercuric sulphide and mercuric chloride was possible. Beyond this, sulphur activity was very much reduced and only mercuric chloride formed. This mercuric chloride could be considered as being predominantly natural rock mercury, and not connected with the mineralization at all. This hypothesis concludes with the suggestion that mercuric chloride is the natural form in which mercury exists in the clastic/carbonate facies of this section of the Carboniferous. It, however, does not take into account sediments which are rich in organic matter or syngenetic sulphides. The initial form of mercury in these sediments is still conjectural.

This being the case, the marine Silurian to the north of the area is anomalous, in that it contains mercuric sulphide but no mineralization. One explanation of this is based on the assumption that, when the Silurian was deposited, it did not contain trace mercury in the form of mercuric chloride. After sedimentation was completed, diagenesis and bacterial breakdown of sulphates to sulphides, and reduction of bisulphates and bisulphites to sulphides

increased the availability of the sulphide ion. Finally the Caledonian oregeny, which folded and faulted the Silurian, produced enough heat and pressure to sufficiently increase the sulphur activity to convert the soluble mercury salts to mercuric sulphide and fix it in the environment. Confirmation of the possibility of this hypothesis is given by the following series of experiments:

Four samples of two grammes each of rock standard base B, Table 8.5, were placed on watch glasses, each inside a separate pyrex desiccator, referred to hereafter as desiccators A, B, C, D.

Ten millilitres of deionised water were then poured into the base of each desiccator and three drops of redistilled mercury added to the water. Each rock base was then spiked with a solution, as tabulated, Table 8.7.

Each desiccator was covered and allowed to equilibrate at room temperature for one week. After this time the watch glasses were removed and dried at room temperature in separate desiccators over silica gel. Each sample was then analysed by the differential thermal release technique to ascertain which mercury compounds had formed. Analyses were performed in triplicate on samples of 500 mg.

The whole experiment was repeated twice more, once at 100°C and once at 140°C. At the latter two temperatures, constant re-additions of both mercury and water were required. After this the experiment had to be discontinued, due to the

TABLE ...8.7

	SOLUTION ADDED	COMPOUND FORMED AT ROOM TEMPERATURE	COMPOUND FORMED AT 100 °C	COMPOUND FORMED AT 100°C
A	1 ml. 2 % NaCl	$HgCl_2$ + v. minor HgO	$HgCl_2$	$HgCl_2$
B	1 ml. 2 % Na_2S	HgS	HgS	HgS
C	1 ml. Deionised Water	Hg vapour only	Hg vapour	Hg vapour
D	0.5 ml. 2 % NaCl 0.5 ml. 0.1 Na_2S	$HgCl_2$	$HgCl_2$	HgS

THE EFFECT OF HEAT ON THE REACTIONS $Hg^{2+} + S^{2-} \rightleftharpoons HgS$ AND $Hg^{2+} + 2Cl^- \rightleftharpoons HgCl_2$ AND ANION ACTIVITIES

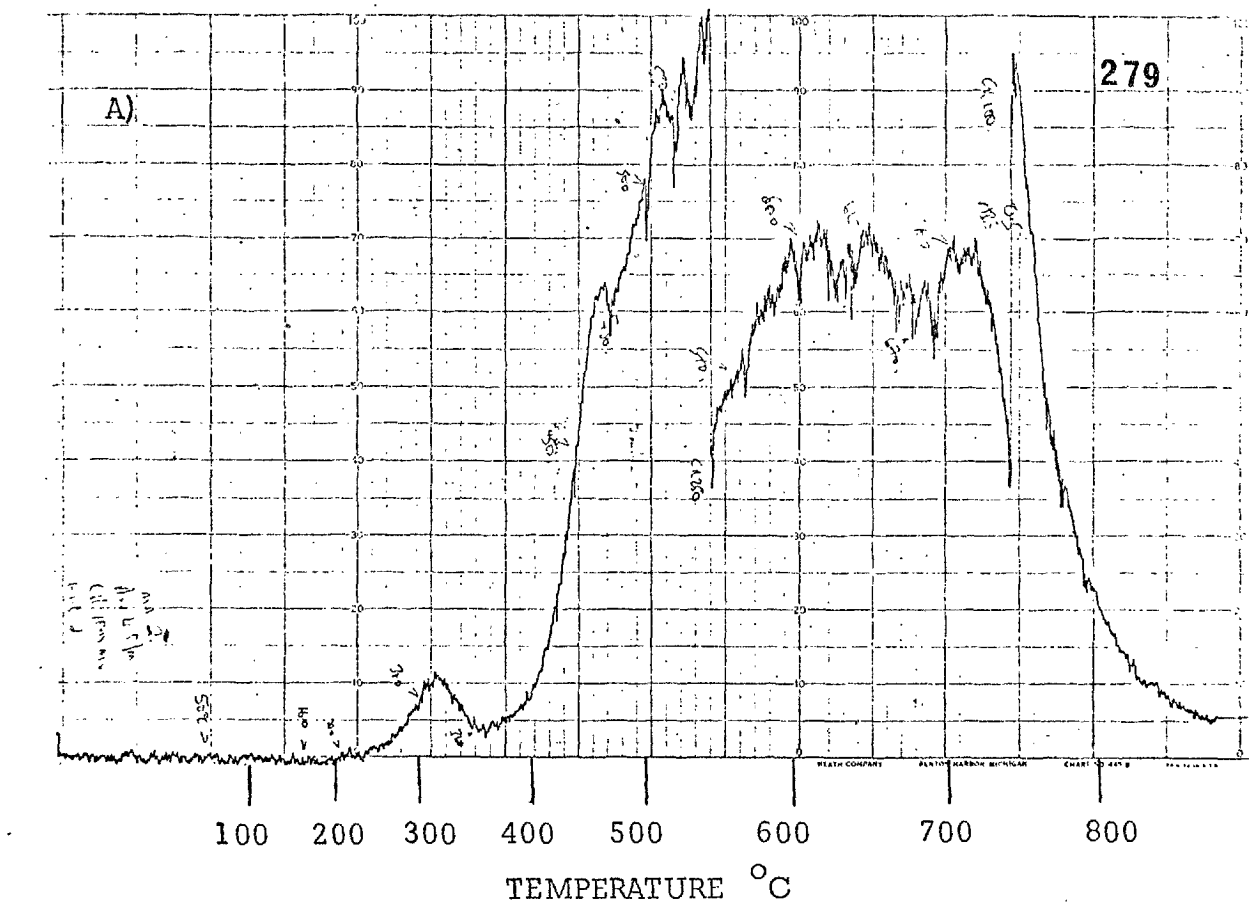
considerable volume of mercury being evolved and the inadequate safety precautions.

The experimental results, Table 8.7, indicate that extreme importance must be attached to the activities of the ions present and not their specific concentrations in the environment. It also indicates that mercuric chloride can exist in the presence of sulphur and sulphide ion, provided that the activity of the latter is sufficiently reduced. The activity of the sulphide ion is apparently greatly increased with increasing temperature.

h. Mercury in the Lattices of Sphalerite, Galena and Pyrite at Keel.

Initial experiments to obtain thermal release traces of mercury in sulphide rich material were unsuccessful, due to the interference of the S^{2-} anion. Release traces, such as Fig. 8.19A, were obtained. Here a rock, rich in both pyrite and sphalerite, was being analysed. The first peak, at approximately 310°C, can be seen to have a slightly erratic outline, but the major peak consisting of a series of minor jagged peaks at temperatures from 470°C to 720°C has an extremely erratic outline. Any attempt to classify these peaks under a single broad peak, and to identify the temperature of maximum release would be impossible.

To try and identify the cause of this behaviour, a simple experiment was set up, in which the gases evolved from the heating chamber were passed through acidified potassium permanganate solution.



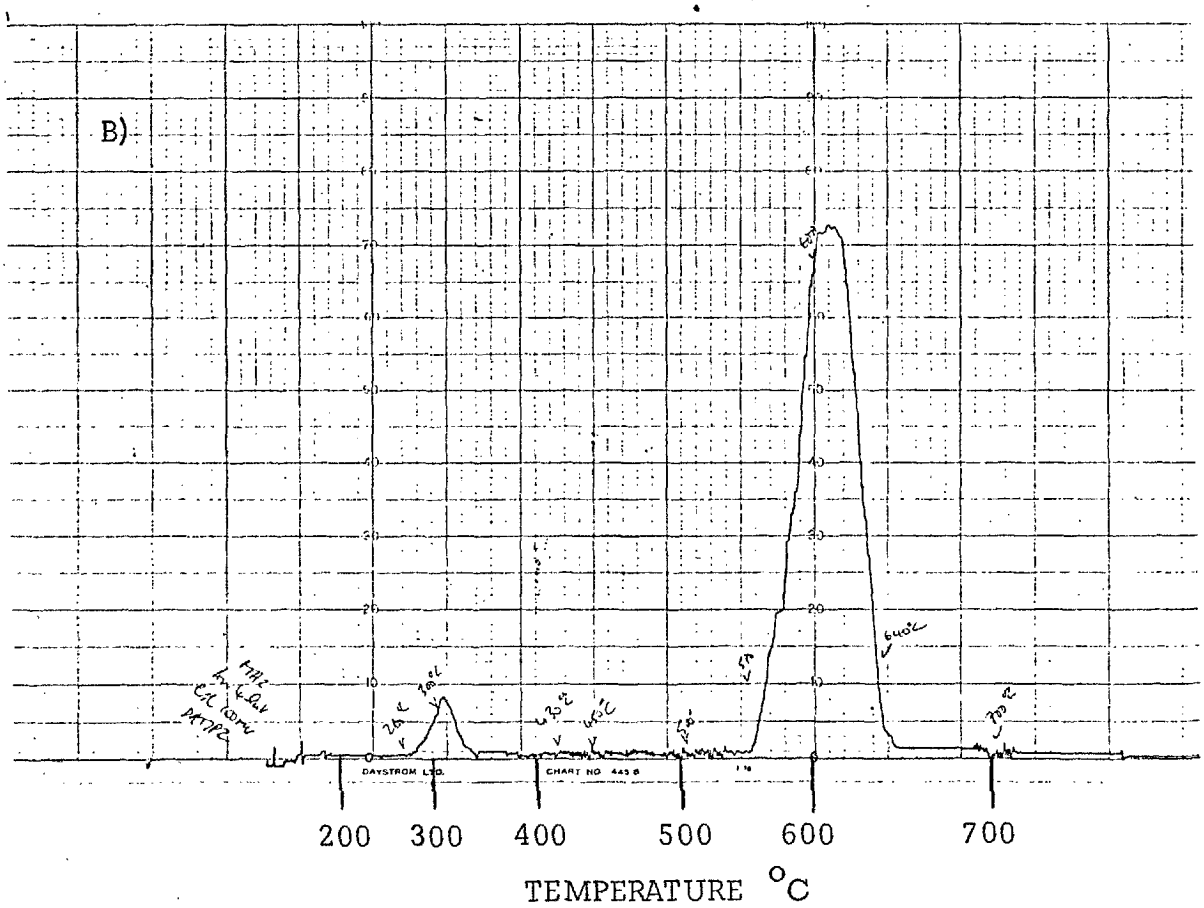


FIG ... 8.19 THE USE OF CALCIUM OXIDE TO REMOVE SULPHIDE INTERFERENCE IN MERCURY THERMAL DISSOCIATION ANALYSIS

When the sample temperature reached 420°C, the potassium permanganate solution became discoloured. The start of the discolouration corresponds closely to the beginning of the mercury release peak of Fig. 8.19A. The heating was continued and the permanganate solution removed; immediately a strong smell of sulphur dioxide was detected. The production of sulphur dioxide, as a by-product of the destruction of the sphalerite lattice, has been disucssed in Chapter 6.

It is therefore, extremely important to remove the sulphur dioxide from the system before the gases reach the mercury analysis cell. In the analysis of sulphide material, Chapter 6, the use of acidified potassium permanganate or water to either oxidise or dissolve the sulphur dioxide, has been discussed. Unfortunately, however, in these analyses, only a few milligrammes of sample were used, but in the analysis of sulphide material, one gramme of sample has to be used in order to detect the less concentrated low temperature mercury compounds. Due to this large quantity of sample, and consequent large volume of sulphur dioxide produced, (114 ml of SO_2 at S.T.P. are produced from the oxidation of 1 g. pure zinc sulphide), these methods failed. Calcium carbonate was now used but, irrespective of the weight added, it did not appear to react with the sulphur dioxide evolved.

A sample of calcium carbonate was heated to 900°C in a silica crucible for six hours, and allowed to cool in a desiccator to avoid contamination. An approximate 1 g. lump of this calcium oxide was then ground with one gramme of sample in an agate mortar, the exact weights of both calcium oxide and sample being known. The mixture was then transferred to a weighing paper and weighed, in order to calculate the exact weight of sample being transferred to the heating chamber.

$$\frac{\text{weight mixed sample + calcium oxide being analysed}}{\text{weight sample + weight calcium oxide originally taken}} \times \text{weight of sample} = \text{weight of sample being analysed}$$

By this method it was possible to obtain a quantitative analysis of mercury in the sulphide component of the sample.

When this sample + calcium oxide mix was now analysed by mercury thermal dissociation analysis, the results shown in Fig. 8.19B were obtained. The same sample was used to produce Fig. 8.19A as 8.19B, the only difference being the addition of calcium oxide to sample B.

The chemistry behind the reaction is as follows:

$$2\ ZnS + O_2 = 2\ ZnO + SO_2$$

$$2\ CaO + 2SO_2 + O_2 = 2Ca\ SO_4$$

The calcium sulphate breaks down at 1800°C and consequently is stable under these experimental conditions. The sulphur dioxide produced can therefore be considered as fixed throughout the experiment.

Due to the possibility of this sulphide ion interference, it was decided to run all samples mixed with an equal weight of calcium oxide, as a standard procedure.

The validity of assigning this 600°C peak to mercury released from the sphalerite lattice is now discussed.

A. The 600°C - 700°C Peak of Mercury Release.

The highest temperature peak on the mercury thermal dissociation graph was always associated with rocks containing reasonably high levels of zinc sulphide. This association led to the obvious assumption that

the peak represented mercury release from the sphalerite crystal. The identification of this peak was carried out in three ways.

(1) Thermal release data on separated sphalerite crystals.

Sphalerite crystals were separated from hand specimens by the method described in Chapter 6. The crystals were then ground to a fine powder and 50 mg. mixed with two grammes of calcium oxide. The mixture was transferred to a large plastic vial and two 1 cm. diameter plastic balls added. The vial was then thoroughly shaken for ten minutes to homogenise the mixture. 100 mg. of this mixture were then transferred to a nickel boat inside the heating chamber and the temperature gradually increased. The dissociation characteristics of these sulphide samples were exactly the same as the dissociation characteristics of this 600 - 700^{o}C peak found in the thermal dissociation traces of rock material.

(2) X.R.D. on portions of the heated rock material.

A 1g. portion of the - 494 μm + 210 μm fraction of the crushed rock material being analysed, was placed in a nickel boat inside a silica tube in the sample heating chamber. For this experiment a twin-tube tube-furnace was used. Inside the other tube was placed a 5g. sample of the same material. Both tubes of the tube-furnace were heated inside the same winding and therefore the temperature differential between the two tubes was negligible. Air was passed over both samples at the same rate, and at suitable points throughout the heating cycle, samples of - 494 μm + 210 μm material were taken from the 5 g. portion and reserved for X.R.D. analysis, Fig. 8.20. Each of these separate samples was

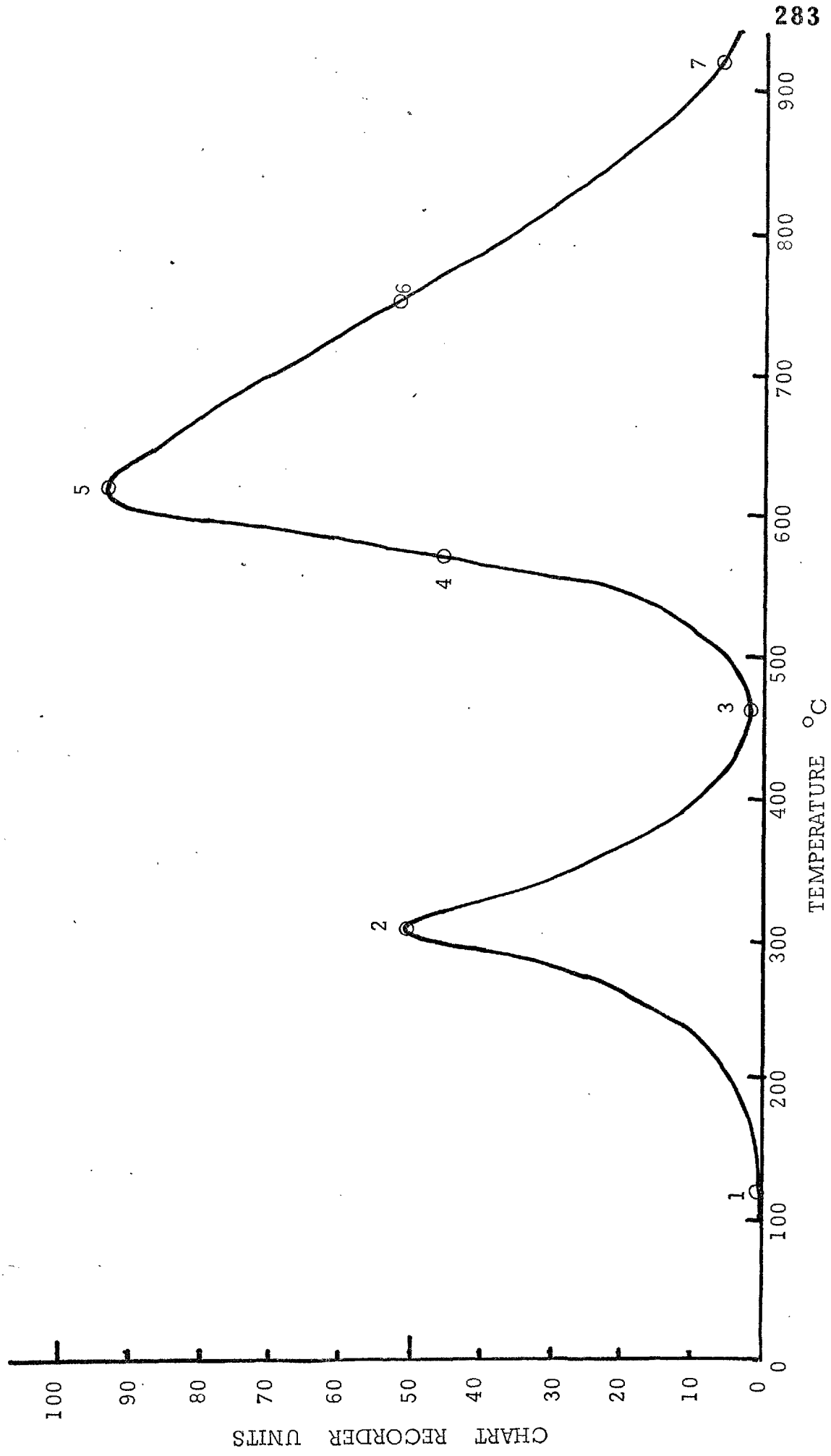


FIG ...8.20 DIAGRAM OF THE POSITIONS OF SAMPLES TAKEN FOR X - RAY ANALYSIS OF THERMAL BREAKDOWN OF THE ROCK MATRIX ON HEATING

then ground to an impalpable powder and made into a smear mount for X-ray analysis.

It was quite clear from the X-ray traces obtained that, between samples 3 and 6, zinc sulphide was rapidly being converted to zinc oxide, with associated breakdown in the sphalerite lattice. This method, however, was rather unsophisticated, and no exact temperature could be obtained for the breakdown sequence.

(3) High Temperature X-ray Analysis of Sphalerite.

This method was by far the most exact, accurate and meaningful, and determined exactly the temperature at which the sphalerite lattice broke down. The equipment was made available by Dr. J. Williamson of the Nuffield Research Group, Metallurgy Department, Imperial College.

The equipment consisted of a High Temperature Focussing Guinier Camera No. 115 - 503. 900 - 400, manufactured by Enraf-Nonius in Amsterdam, Holland. Heat was provided by a thermostatically controlled programmed heating furnace, with both entrance and exit slits for X-rays. The sample, consisting of sphalerite powder was pressed into a platinum gauze and mounted in a platinum-rhodium sample holder in the X-ray path. Cu K α radiation was used. Argon was flushed through the heating chamber throughout the heating programme. The furnace was set to heat from 200^{o}C - 800^{o}C in fifty hours over a programmed heating run. The temperature inside the furnace was measured by a thermocouple and converted to degrees Centigrade by use of standard tables. At set intervals after

starting the experiment, the position of the cassette, relative to the initial starting point, was measured, and a mark made on the film by means of a small flag, which was placed in the X-ray path to correspond to this, Fig. 8.21.

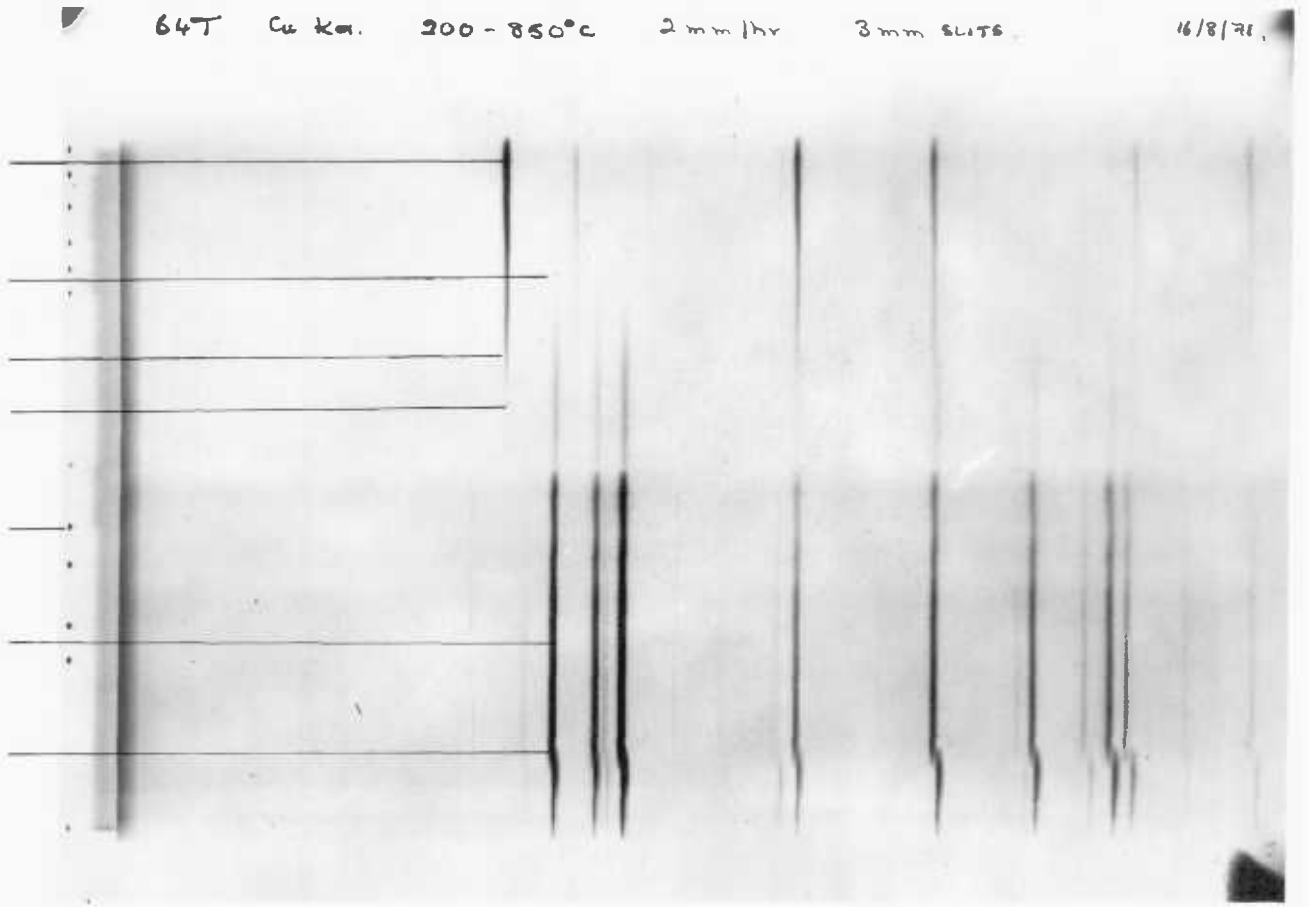
The diffracted X-rays are recorded on a film, which is placed in a movable carriage over the exit slit. At a given instant, only a small strip of film is exposed to the X-ray beam, the carriage containing the film gradually moving down over the exit slit. Eventually, after 50 hours, the whole film was exposed, Fig. 8.21. After processing, a film similar to that shown in Fig. 8.21. is obtained, with small flag marks representing time after starting. By knowing the position of these marks, and the temperature at which they were made, from the thermocouple, the temperature of the sample at these positions can be calculated. The change in the X-ray pattern can be clearly seen, Fig. 8.21, and when the temperatures of these changes were calculated, the following results were obtained:

Temperature of start of Zn O lattice picture	$470^{o}C \pm 6^{o}C$
Temperature of finish of Zn S lattice picture	$633^{o}C \pm 6^{o}C$
Temperature of position of equal intensity of Zn S and Zn O lattice picture	$593^{o}C \pm 6^{o}C$

From this data it can be seen that, on relating these temperatures to the thermal release diagram, Fig. 8.19A the temperature of the first appearance of Zn O is higher than the start of "mercury release", but is lower than the real temperature of mercury release, Fig. 8.19A. The data

FIG ...8.21

THERMAL X-RAY PHOTOGRAPH SHOWING DISSOCIATION OF SPHALERITE INTO ZINC OXIDE ON HEATING



for Fig. 8.21 were calculated on the appearance of the Zn O 100 plane, and the disappearance of the Zn S, 111 plane. This information, related to the true mercury release trace, Fig. 8.19B, definitely indicates that mercury, in the sphalerite lattice, could be associated with the 111 plane.

The SO_2 being released from breakdown of sphalerite, is first recorded at 360°C on the Fig. 8.19A trace. The fact that ZnO is not detected until 480°C on the X-ray film merely means that the initially formed Zn O is in too small a quantity to be detected on the film. Likewise, the last point of Zn S detection on the film, 633°C ± 6°C, is at a lower temperature than the position at which sulphur dioxide, and hence sphalerite breakdown, is detected, Fig. 8.19A at 840°C. However, on referring to Fig. 8.19B, the temperature at which mercury ceases to be released from sphalerite appears to be 645°C. We can therefore say that, as mercury ceases to be evolved from sphalerite at 645°C and the sphalerite 111 plane is completely broken down at 633°C ± 6°C, then mercury is entirely associated, in the sphalerite lattice, with the 111 plane. Breakdown of sphalerite continues up to 840°C, Fig. 8.19A, but is not accompanied by any further mercury release.

The temperature which is most important, and fortunately the temperature at which the most exact reading of temperature can be made, is the point of equal intensity of the Zn S 111 plane and Zn O 100 plane. This point should represent the position of peak on the mercury thermal release curve, Fig. 8.19B. This temperature is calculated as 593°C ± 6°C, and from the

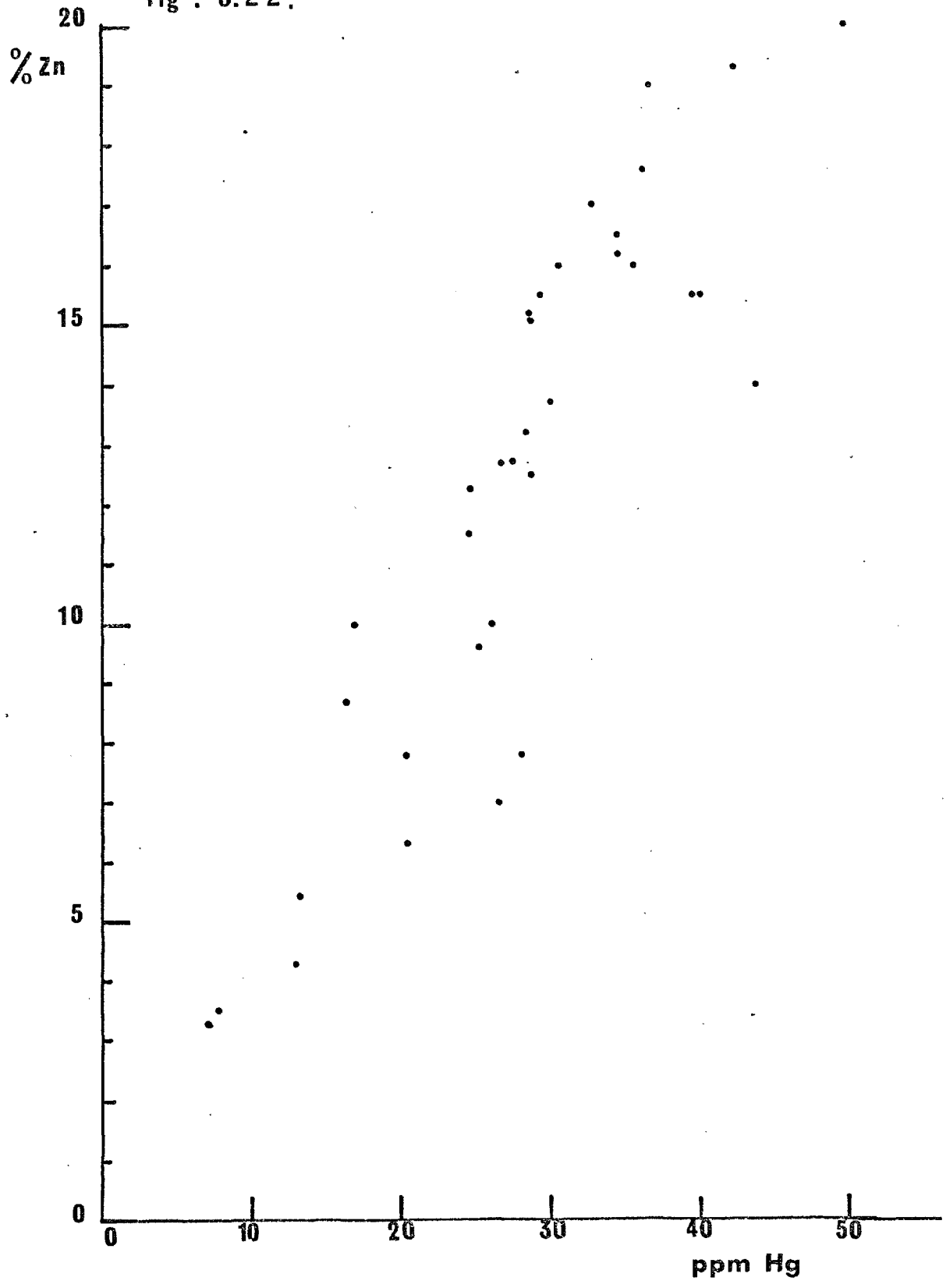
thermal dissociation graph as 610°C, Fig. 8.198. This further indicates that mercury in sphalerite is associated with the 111 plane. Other sphalerite crystals gave the position of this Zn O/Zn S equal intensity as 595 - 685°C, and this temperature always corresponds to the position of the peak on the thermal release trace. No reason could be found to explain the variation in temperature of sphalerite 111 lattice plane breakdown. Trace and major element analysis gave no reason as to why the differences occurred, and no relation to the distribution of the sphalerite in the prospect area, either laterally or vertically, could be found.

By taking the mercury released from the sphalerite lattice and calculating total mercury release from this, on the basis of the mercuric sulphide release graph, it is possible to obtain a far more accurate correlation between mercury and zinc in the rock, Fig. 8.22.

B. The 450°C Peak of Mercury Release.

This peak was found to occur in rocks containing large amounts of pyrite, and in order to try and associate the lattice breakdown of pyrite with this peak on thermal traces, it was again decided to run an X-ray programme. However, all available X-ray equipment at Imperial College, at this time, was using Cu Kα radiation. The Hot Wire Guinier Camera used Cu Kα radiation all the time, and as Cu Kα radiation is highly dispersed by iron, it is useless where pyrite is concerned. Two other methods for determination of mercury release from pure pyrite were used, one to be discussed here, and the other to be discussed in subsection 8.5 in this chapter.

Fig . 8.22.



RELATIONSHIP BETWEEN ZINC & MERCURY IN KEEL ROCK MATERIAL

(1) Thermal Analysis of Pure Pyrite.

Pyrite crystals were separated from host rocks and prepared for thermal dissociation analysis in the same way as described for sphalerites. The position of this mercury release peak occurred at 450°C. A further four samples were analysed in the same way and each gave the same temperature for the release peak. This in itself is enough to confirm the nature of the 450°C peak, but reference to section 8.5 should be made for further evidence.

C. The 520°C Peak of Mercury Release.

This peak was found to occur in rocks containing high amounts of galena. The only proof of its identity is offered by the thermal dissociation of pure galena, analysed by the same method as for pyrite and sphalerite, and the position of this dissociation was 520°C. Unfortunately thermal X-ray equipment was out of commission and no further confirmation was obtained.

8.4. SUMMARY.

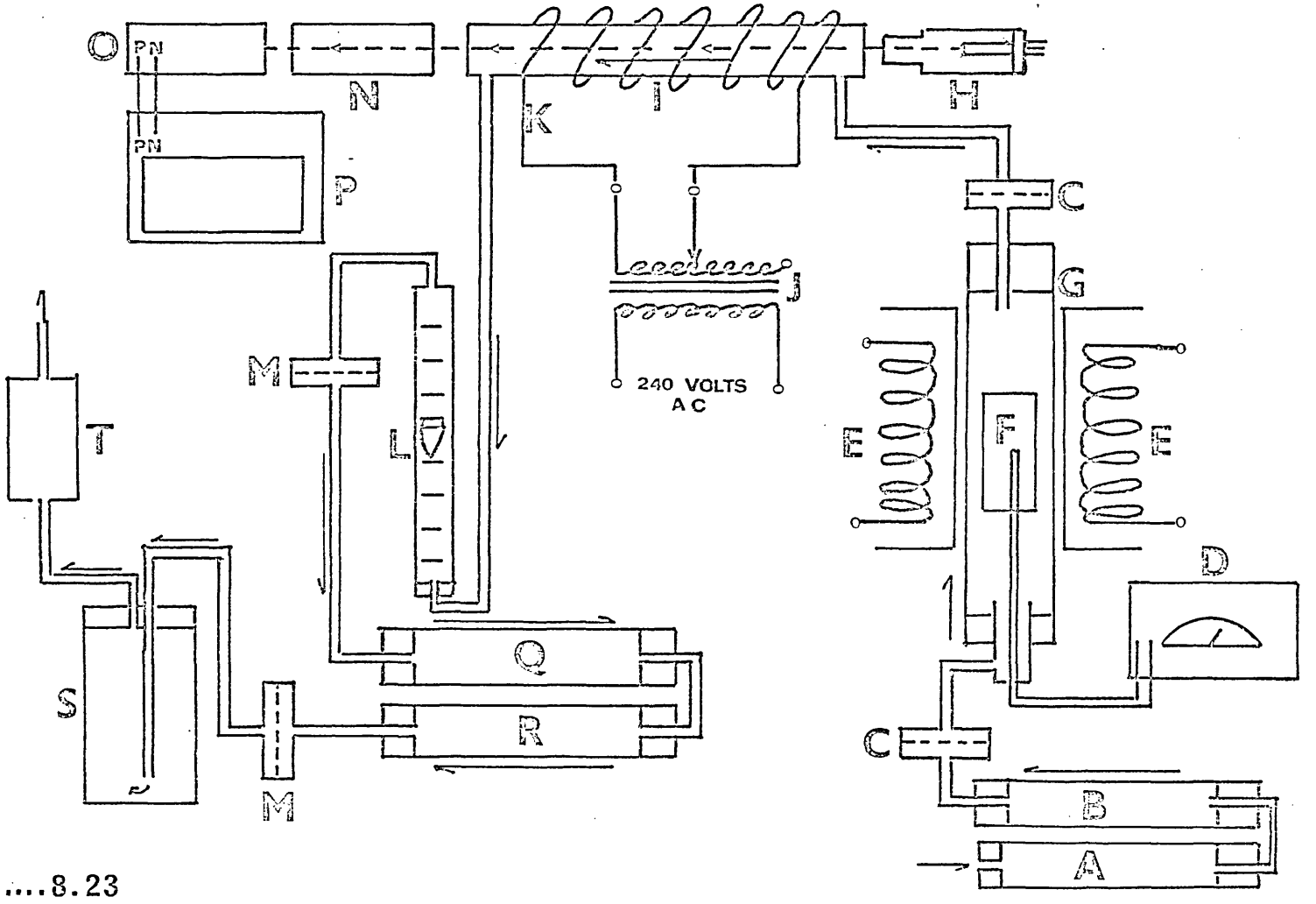
The information recorded here appears to be of primary geochemical significance. Standard geochemical methods of mercury analysis are clearly of great use in defining relatively broad areas of potential base metal mineralization. At Keel, bedrock zones containing mercuric chloride, which is closely associated with base metal concentrations, can give high total mercury values which may easily lead to misinterpretation of conventional geochemical data for total mercury. However, the method of differential mercury compound analysis can be used to identify those mercury compounds which are specifically associated with base metal

mineralization, and the potential area of sulphide mineralization may thus be outlined with increased confidence.

This approach, however, is still in its infancy, and a great deal more work needs to be done before it becomes a proven and worthwhile geochemical technique. Not only mercury, but other elements, and their compounds should be examined, in both primary and secondary environments

8.5. CONVERSION OF A SOUTHERN ANALYTICAL A. 3000 ATOMIC ABSORPTION SPECTROPHOTOMETER INTO CONTINUOUS MERCURY AND ARSENIC RELEASE MONITORING APPARATUS.

Towards the end of the survey, the analytical equipment being used became extremely troublesome, mainly because of the gradual breakdown of electrical components. As time was not available either to have the apparatus repaired, or to make the necessary repairs at Imperial College, it was decided to convert the A.3000 spectrophotometer. This was carried out by removing the burner and nebulizer unit, and replacing it by a silica cell, Fig. 8.23. This latter was wound with a heating wire in order to maintain a constant temperature of $450^{o}C \pm 10^{o}C$ within the cell. Conventional mercury and arsenic hollow cathode lampswere used as light sources. Air at the rate of 2.5 litres/minute was drawn over the sample. This air was scrubbed free of water, mercury and arsenic, by tubes A and B. Excess activated charcoal, being carried over in the gas stream from tube B, was removed by the glass fibre filter C. The sample on F was heated by a tube furnace E, and the temperature recorded on a direct reading thermocouple, D. Any particulate matter being carried over in the gas stream from G, was again filtered out by a silica fibre pad, C. The evolved mercury or arsenic was passed into the sample analysis chamber I, which was directly in the light path



KEY....

A	SILICA GEL
B	ACTIVATED CHARCOAL
C	GLASS FIBRE FILTER
D	THERMOCOUPLE
E	TUBE FURNACE
F	SAMPLE HOLDER
G	SILICA SAMPLE CHAMBER
H	Hg/As A.A. LAMP
I	QUARTZ CELL
J	VARIAC
K	HEATING WIRE
L	FLOW METER
M	$HgCl_2$/GLASS FIBRE FILTER
N	MONOCHROMATOR
O	PHOTOMULTIPLIER
P	CHART RECORDER
Q	$KMnO_4$ FILTER
R	ACTIVATED CHARCOAL
S	AIR RESERVOIR
T	FILTER PUMP

LIGHT PATH

DIRECTION OF GAS FLOW

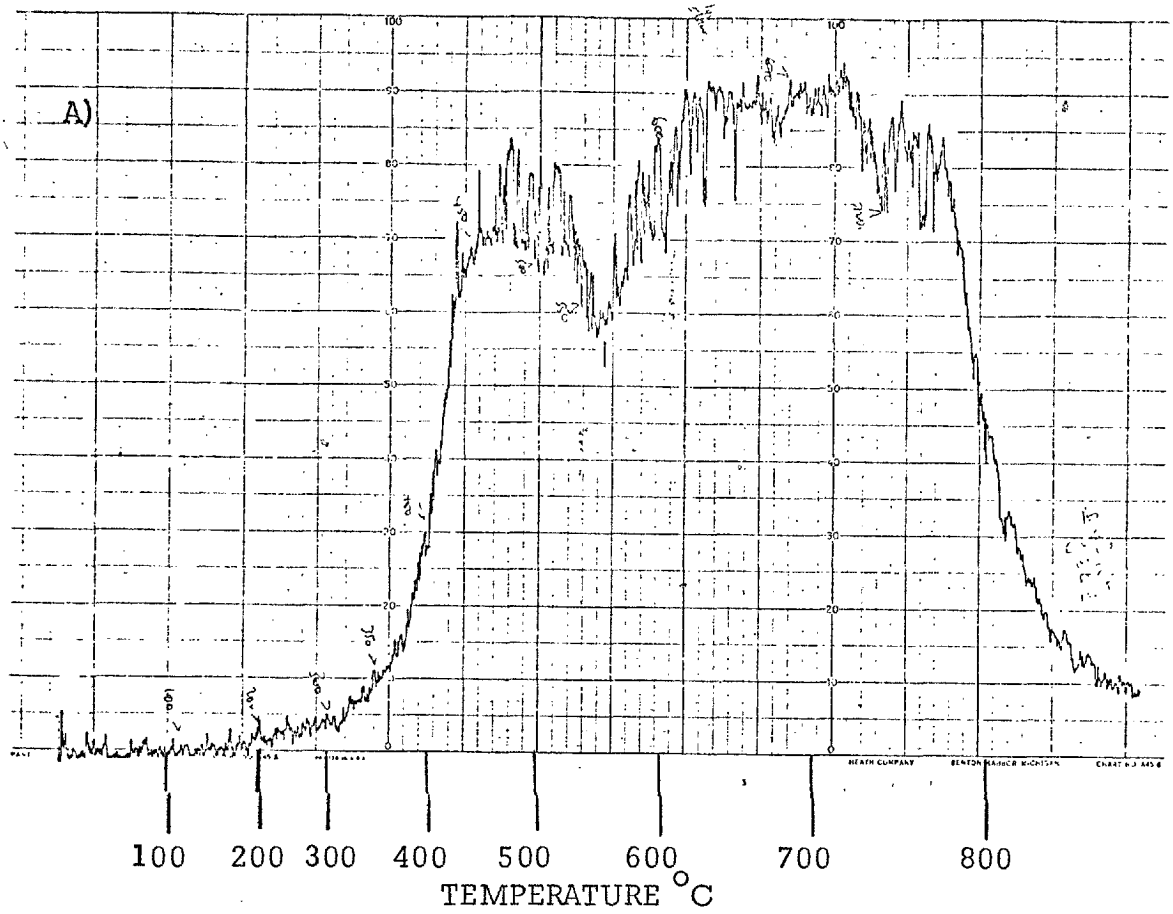
FIG....8.23

DIAGRAM OF APPARATUS FOR CONTINUOUS MERCURY & ARSENIC THERMAL RELEASE ANALYSIS

of the hollow cathode source, H. The absorption of this light by the vapour in the silica cell was measured by the photomultiplier, O, and recorded as a peak on the chart recorder P. The mercury standards already prepared were used. The air flow rate was measured on a flow valve L, placed directly after the sample cell. This arrangement ensured the shortest possible route for the evolved gases from the heating chamber, and also the least possible surface area for adsorption before analysis.

After analysis, the gases were again passed through an activated charcoal filter, R, to remove mercury. When arsenic was being analysed, another filter, Q, containing moistened potassium permanganate was placed before the activated charcoal filter. When arsenic comes into contact with moistened $KMnO_4$, As_2O_3 and AsH_3 are produced. These are either absorbed by the activated charcoal or on the mercuric chloride filter, M, where they are converted to arsenates. This is a modification of the Gutzeit technique for analysis of arsenic.

As this is a single beam instrument, the use of calcium oxide to remove S^{2-} interference is essential, both for arsenic and mercury analysis, Fig. 8.24. In this case, the same sample as used in the mercury analysis diagram, Fig. 8.19, is used. The suppression of interference, after the addition of calcium oxide, can be clearly seen, so too can the distribution of arsenic within the rock. The first peak of arsenic release occurs at 450°C, at exactly the same temperature of mercury release from pyrite. The second peak, at 620°C, is at the same temperature as release of mercury from the sphalerite lattice. It can therefore be said that arsenic, like mercury, is associated with the 111 plane in the sphalerite structure.



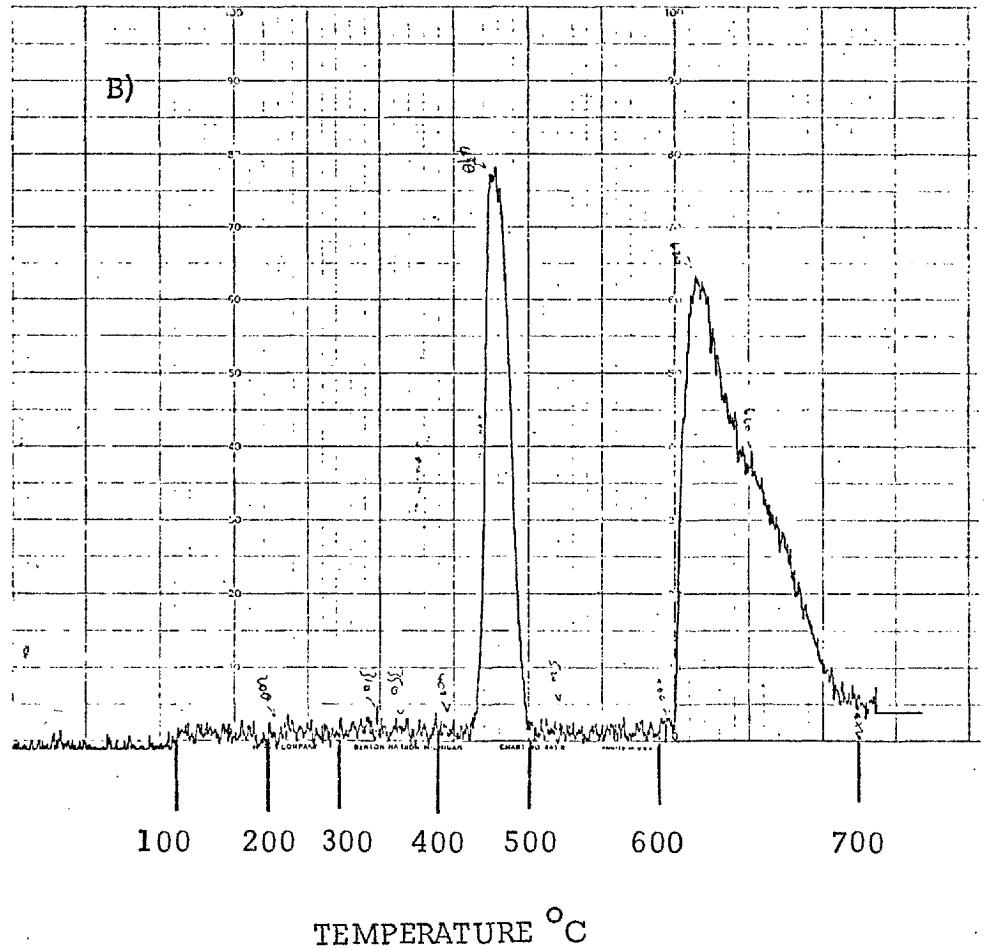


FIG ...8.24 THE USE OF CALCIUM OXIDE TO REMOVE SULPHIDE INTERFERENCE IN ARSENIC THERMAL DISSOCIATION ANALYSES

However, it can be clearly seen that, whereas mercury was predominantly associated with sphalerite, and was low in pyrite, (no mercury release occurring in Fig. 8.19B), arsenic is predominantly associated with pyrite. This is borne out by the spectrographic analysis of pyrite and sphalerite, in Chapter 6.

Unfortunately, time was not available for either a quantitative study of the distribution of arsenic in the Keel environment, nor for increasing the sensitivity of the apparatus (detection limit approximately 5 ppm), which clearly must be done before low levels of arsenic can be detected.

The peak of arsenic release in Fig. 8.24B, from pyrite, represents another proof of the fact that the 450^{o}C peak of mercury thermal release is indicative of mercury release from the pyrite lattice.

8.6. BASE METAL AND MERCURY COMPOUND DISTRIBUTION IN KEEL SOILS.

(1) Introduction.

During the Pleistocene epoch, glaciers advanced from the north-east and north-west to cover some 80% of Ireland during the Weischel glacial period.

Till composition of the Longford area suggests that local rocks are the main source of the glacial debris. An extensive X-ray diffraction programme, carried out by the author, confirmed this and also indicated the presence of quartz, calcite, dolomite, baryte, iron oxides, chlorite, illite, muscovite and feldspar. This investigation into till composition was carried out in order to try and relate possible changes in mineral composition and rock matrix, to mercury release peaks, evolved during thermal dissociation analysis.

A general soil map of Ireland was published in 1969, showing the Keel area to be in a group of reclaimed podzols. These soils represent cultivated podzols, in which both A and B horizons have been mixed. In the Keel area, however, soils range from a well drained podzolic type to ill-drained acid marsh and peat bog.

(2) Soil Geochemistry at Keel.

This aspect of metal distribution at Keel has been thoroughly investigated by Evans (1972). The purpose of this present study is, however, not to re-cover old ground, but to investigate the possible existence of mercury compounds in the soils overlying the Keel prospect. It was hoped that it may be possible to establish a relationship between mercury compounds in the soil and sub-cropping base metal mineralization. Analysis of the soil samples for copper, lead, zinc, cadmium, iron and manganese, was also necessary in order to try and establish a definite relationship between mercury compounds and sub-cropping mineralization, rather than to local spurious soil anomalies.

(3)(i) Sampling and Sample Preparation.

Samples were taken with a steel auger at depths of 24" - 30", two samples being collected at each site. Each sample was immediately stored in a sealed polythene bag and eventually dried at room temperature in a mercury free atmosphere. The samples were then broken down in a porcelain mortar, a - 210 µm portion being then sieved out and reserved for analysis.

(ii) Sample Drying.

In order to avoid loss of mercury or contamination during the drying period, an extensive experimental programme was undertaken to ascertain the most suitable conditions for sample drying. The same mercury compound standards, as were used for the mercury thermal dissociation method, were used throughout this experiment. The results are shown in Table 8.8.

These results indicate that although room temperature drying appears to be the most suitable, a low degree of heat can be used without significant loss of mercury. The study also indicated a definite possibility of sample intercontamination,by volatilized mercury from one sample, adsorbing onto another. Special precautions were therefore taken in drying the soil samples to avoid this intercontamination.

Each sample was placed on a watch glass and completely covered with a large filter paper, on top of which, a smaller watch glass of anhydrous calcium chloride, previously tested for mercury, was placed to absorb moisture. Both watch glasses were then completely covered with an inverted 400 ml. beaker and the whole allowed to dry, for 72 hours, at room temperature.

(4) Sample Analysis.

Exactly the same analytical technique was used for soil samples as was used for rocks. A lg. portion of the soil being analysed was mixed with lg. of calcium oxide and the whole gradually heated inside a thermostatically controlled tube furnace. A glass fibre filter was placed in - line, after the heating chamber, to filter out any particulate matter carried over in the air stream.

TABLE ...8.8

STANDARD	100°C	50°C	DRYING PERIOD
Hg gas	Total loss	Total loss	24 hours
$HgCl_2$ 1 ppm	16.5 % loss	3 % loss	24 hours
Hg_2Cl_2 1 ppm	24 % loss	5 % loss	24 hours
HgS 1 ppm	3 % loss	No loss	24 hours
HgO 1 ppm	4 % loss	No loss	24 hours

STANDARD	ROOM TEMPERATURE	DRYING PERIOD
Hg gas	25 % loss	72 hours
$HgCl_2$ 1 ppm	No loss	72 hours
Hg_2Cl_2 1 ppm	No loss	72 hours
HgS 1 ppm	No loss	72 hours
HgO 1 ppm	No loss	72 hours

THE EFFECTS OF HEAT ON MERCURY LOSS IN SAMPLE DRYING

(5) Results.

In all, 82 samples of soil from the immediate surroundings of the prospect shaft, Fig. 8.25, and 30 samples from a less detailed orientation traverse across the strike of the mineralization, Fig. 8.26, were taken. Analysis of these samples for Cu, Pb, Zn, Cd, Fe, Mn and Hg was carried out. Fig. 8.27 gives the concentration intervals into which the elements were divided for graphical presentation on the following maps. Appendix D gives the results obtained.

(5)(i) Copper.

Copper distribution shows no relationship to sub-cropping mineralized faults on either the detailed or orientation surveys, Figs. 8.28 and 8.29. The majority of copper values are between 10 and 50 ppm and only two are greater than this.

(5)(ii) Lead.

There is a distinct indication that an area about $\frac{1}{4}$ mile north-west of the Keel shaft has anomalous lead values, Fig. 8.30. It also corresponds to an area of sub-cropping mineralized faults. The outline of this anomaly is however far from distinct when investigated in detail, Fig. 8.31.

(5)(iii) Zinc.

A similar anomaly to that of lead became apparent on the zinc orientation survey, Fig. 8.32. A detailed survey over the site area indicated the existence of a pronounced zinc anomaly, with values from 1,000 - 5,000 ppm. The area to the west of the road also was higher in zinc than the area to the east, Fig. 8.33. On the basis of zinc values alone, this area would undoubtedly be recognised as anomalous.

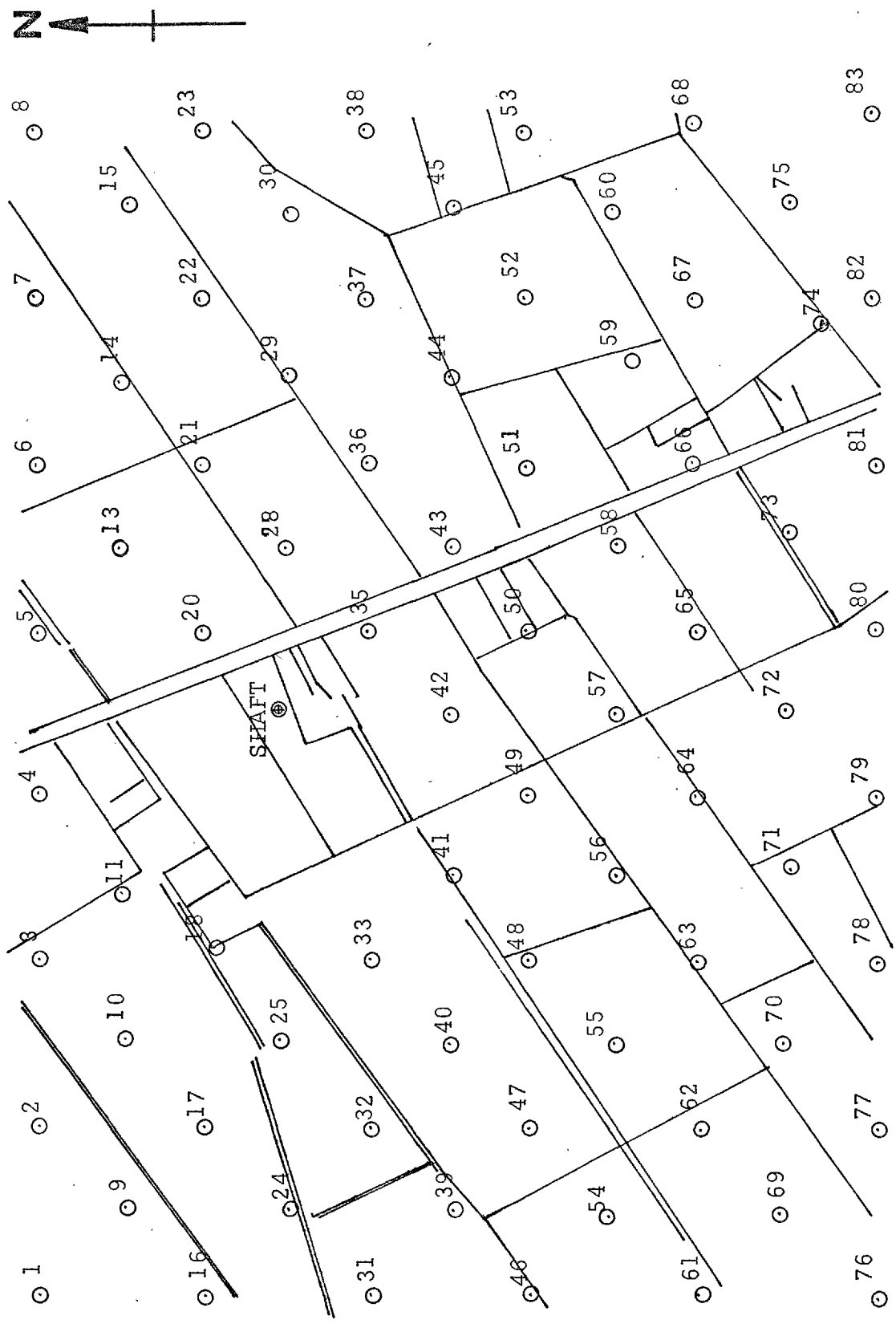


FIG ...8.25

PLAN OF SOIL SAMPLE LOCATIONS SURROUNDING THE KEEL SHAFT

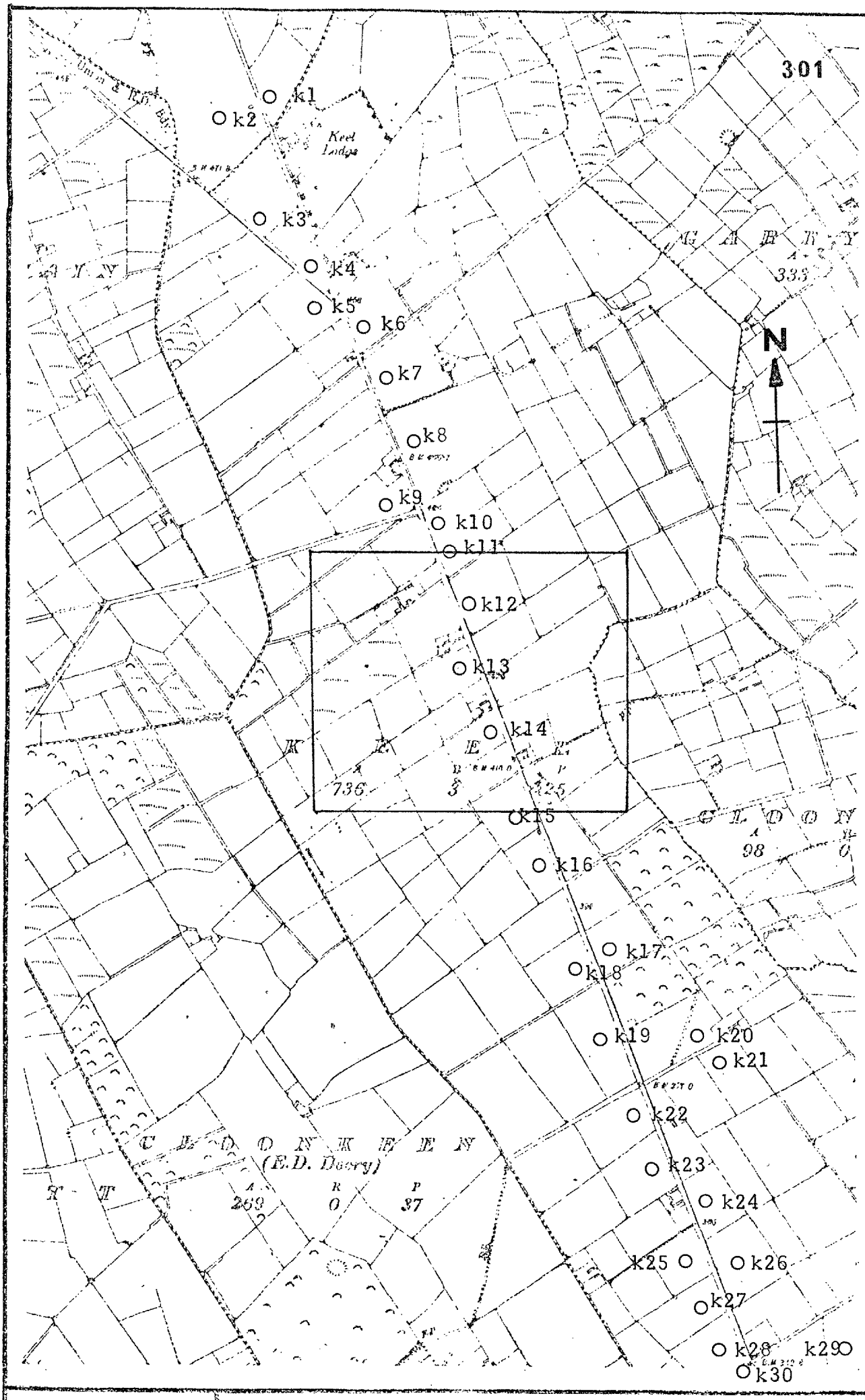


FIG ...8.26 SAMPLE POSITIONS ON ORIENTATION TRAVERSE

	ZINC	CADMIUM	LEAD
●	> 50,000	> 1000	> 10,000
◉	10,000 - 50,000	500 - 1,000	5,000 - 10,000
◎	5,000 - 10,000	100 - 500	1,000 - 5,000
⊙	1,000 - 5,000	50 - 100	500 - 1,000
⊙	500 - 1,000	10 - 50	100 - 500
○	< 500	< 10	< 100

	IRON	MANGANESE	COPPER
●	> 20,000	> 10,000	> 1,000
◉	18,000 - 20,000	5,000 - 10,000	500 - 1,000
◎	16,000 - 18,000	1,000 - 5,000	100 - 500
⊙	14,000 - 16,000	500 - 1,000	50 - 100
⊙	12,000 - 14,000	100 - 500	10 - 50
○	10,000 - 12,000	<100	< 10

Results expressed in p p m

	MERCURY
●	> 10,000
◉	5,000 - 10,000
◎	1,000 - 5,000
⊙	500 - 1,000
⊙	100 - 500
○	< 100

Results expressed in p p b

* : SOIL CONTAINS SOME HgS

FIG ...8.27 CONTOUR INTERVALS OF ELEMENT CONCENTRATION IN KEEL SOIL

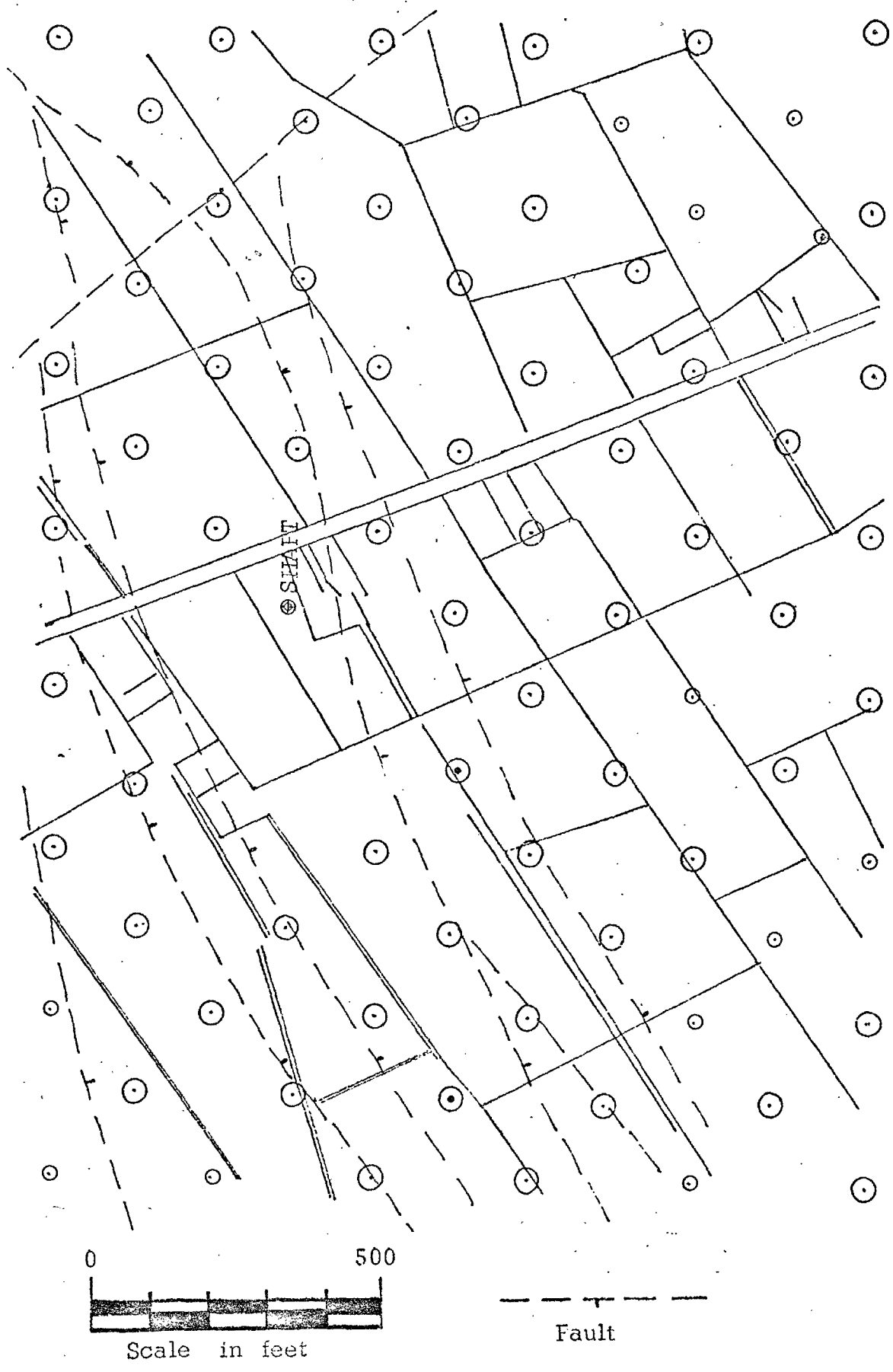


FIG ... 8.28 COPPER DISTRIBUTION IN SHAFT AREA

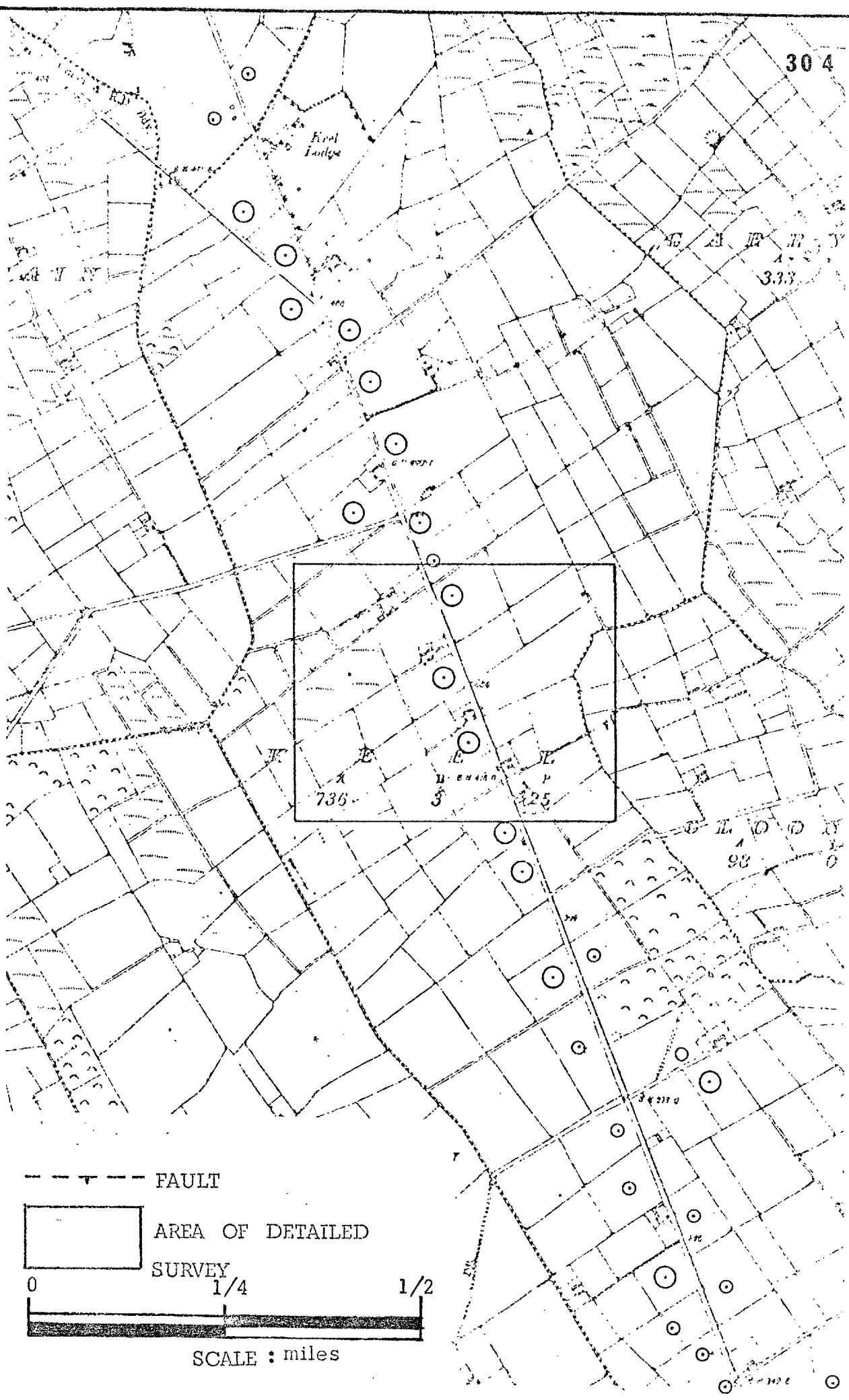


FIG ... 8.29 COPPER DISTRIBUTION ON ORIENTATION TRAVERSE

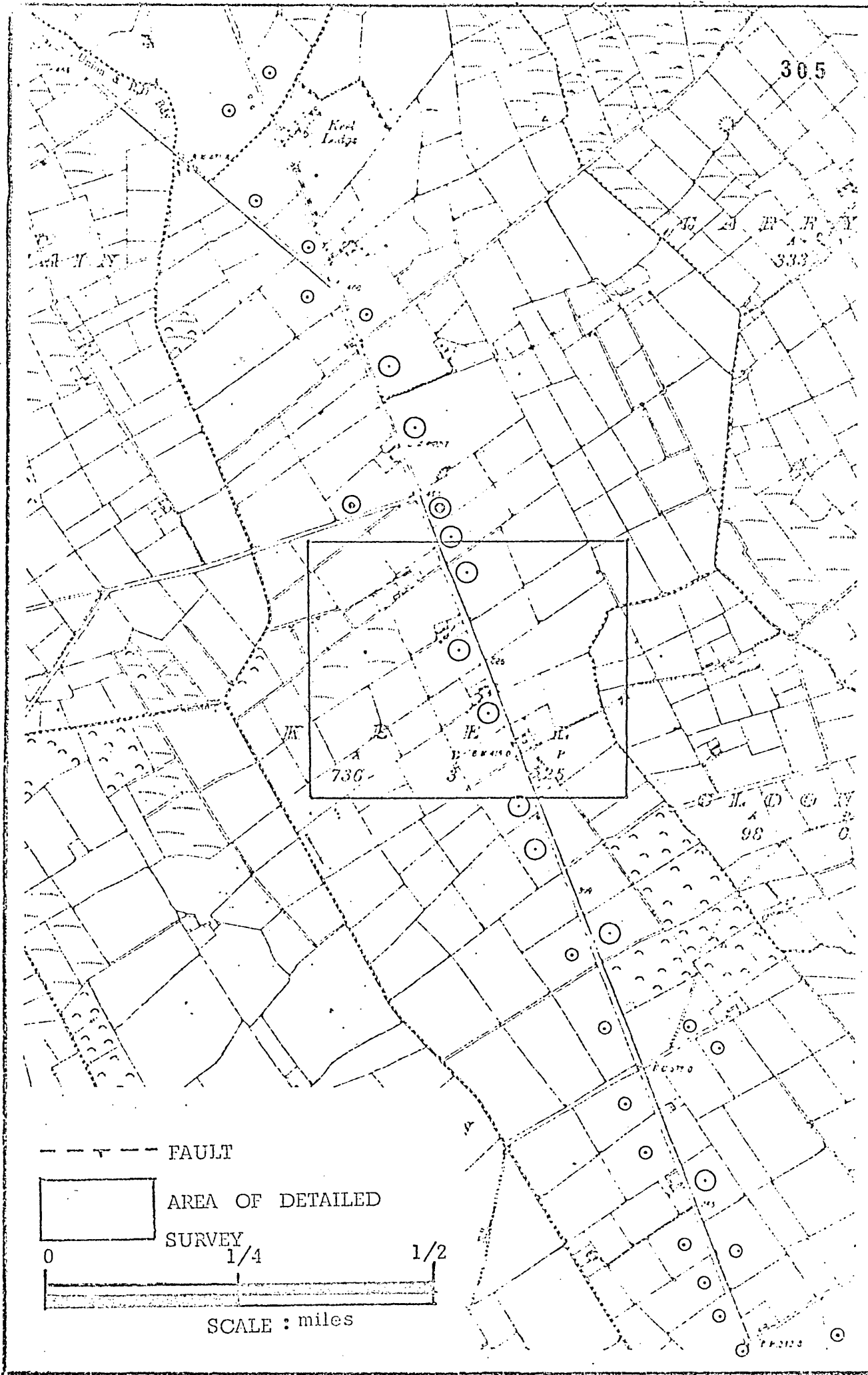


FIG ... 8.30 LEAD DISTRIBUTION ON ORIENTATION TRAVERSE

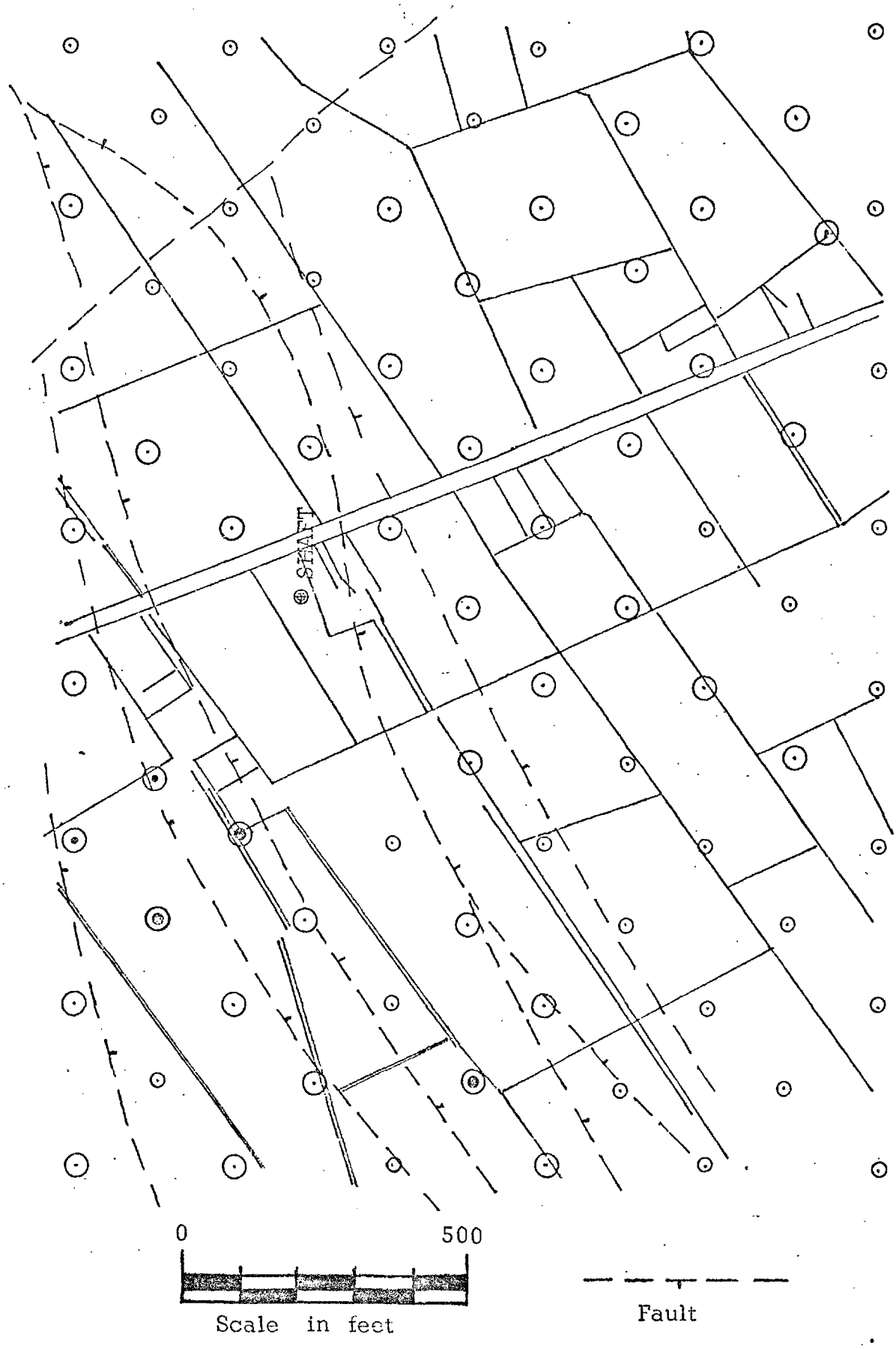


FIG ... 8.31 LEAD DISTRIBUTION IN SHAFT AREA

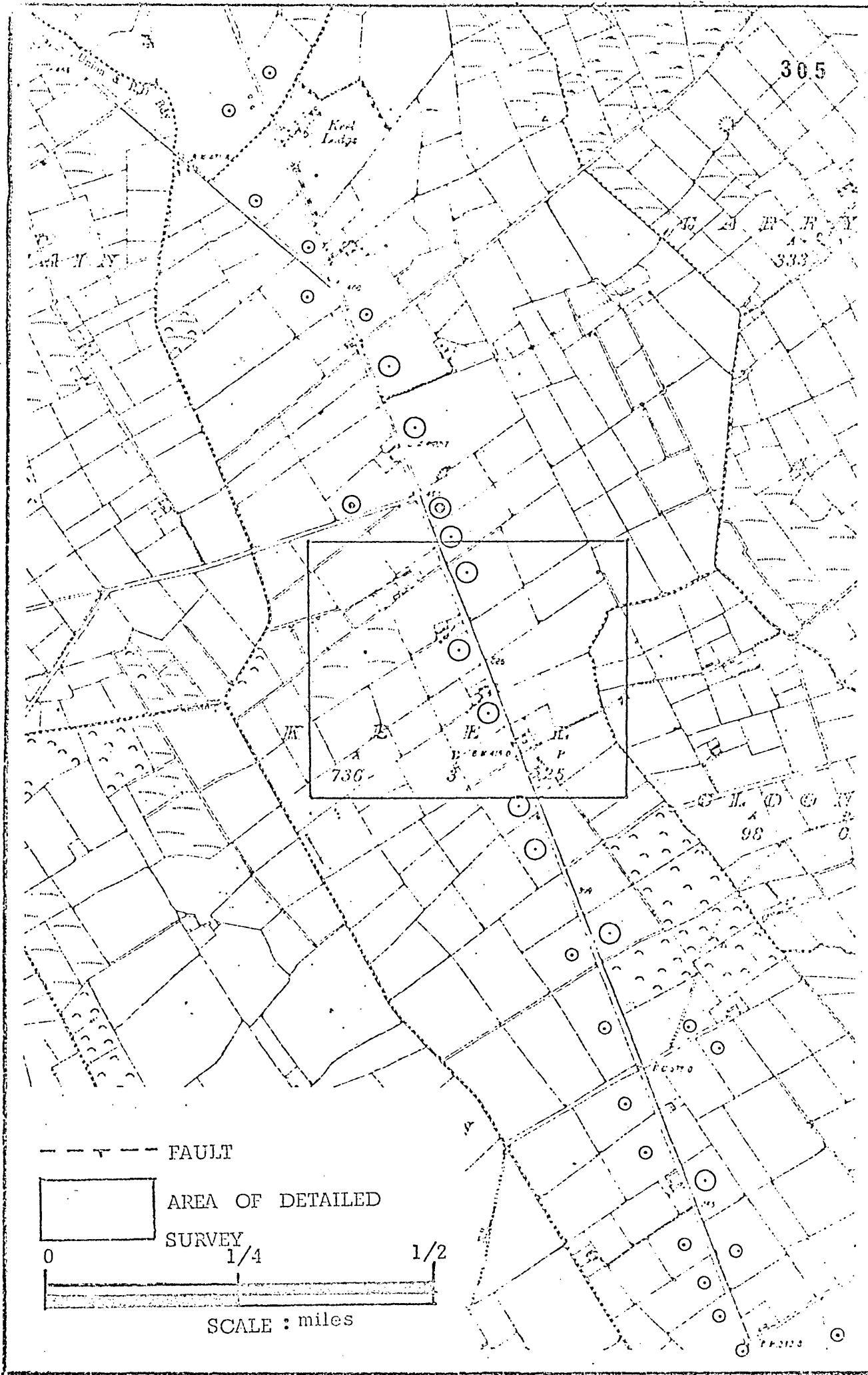


FIG ... 8.30 LEAD DISTRIBUTION ON ORIENTATION TRAVERSE

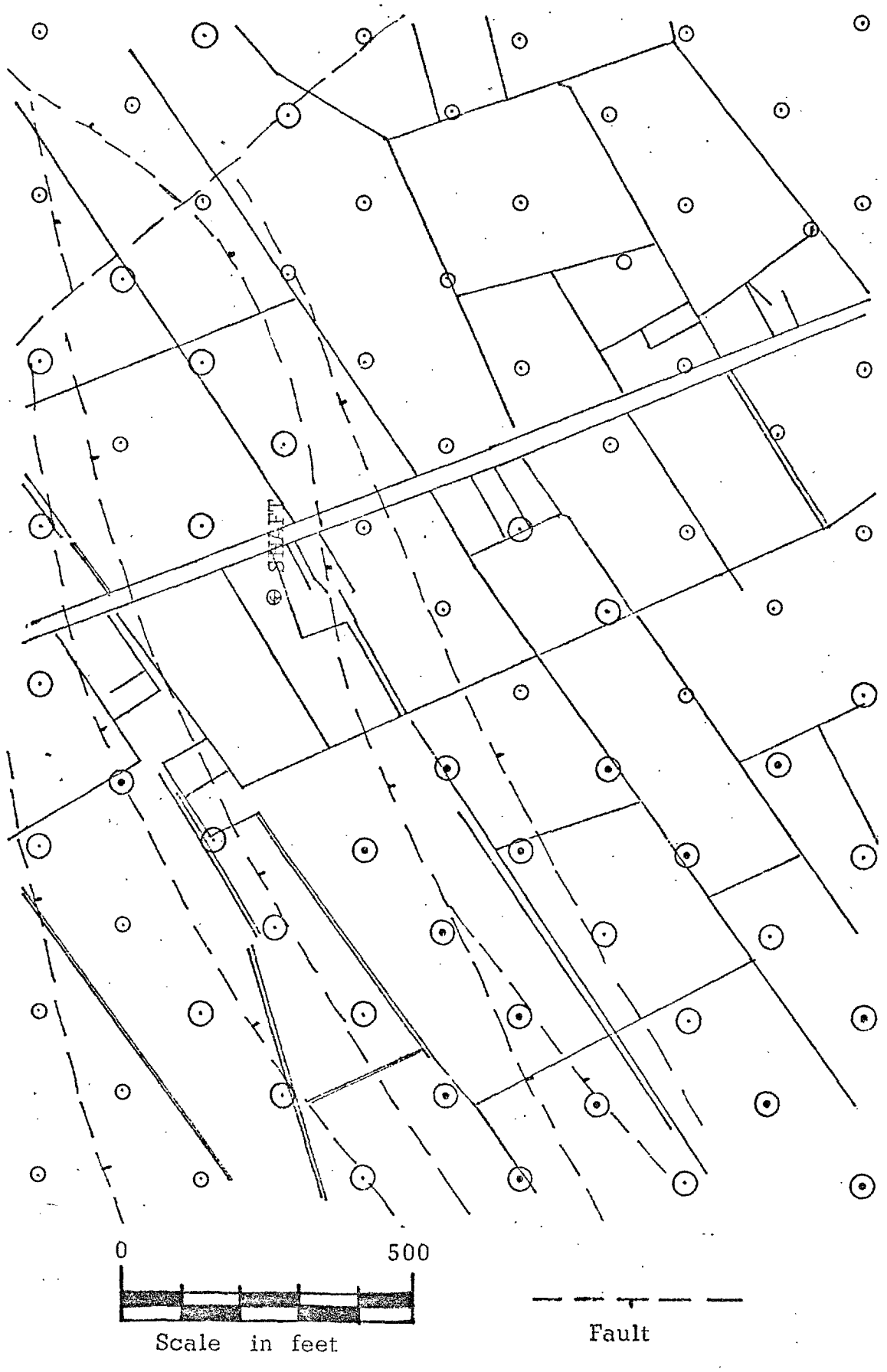


FIG ... 8.33 ZINC DISTRIBUTION IN SHAFT AREA

(5)(iv) Cadmium.

The orientation traverse line gives no indication of base metal build up in the area, Fig. 8.34. All cadmium values are below 10 ppm. The detailed survey however, picks up an anomalous area to the west of the shaft with values up to 1,000 ppm cadmium overlying sub-cropping mineralization, Fig. 8.35. When compared to the Zn/Cd ratio for rocks, this high value of cadmium compared to zinc must represent extreme secondary enrichment. No real relationship between zinc, lead or cadmium can be found in this soil survey.

(5)(v) Iron.

Iron shows very little relationship to any of the elements investigated. All values fall between 1% and 2%, 1.6-1.8% being an average, Figs. 8.36 and 8.37.

(5)(vi) Manganese.

Manganese distribution also shows very little; however two samples in the soil above the decomposed zone, Fig. 3.38, give values of 1,000 ppm manganese. In the detailed survey, Fig. 8.39, the decomposed zone is again picked out to the north-east of the shaft.

(5)(vii) Mercury and Mercury Compounds.

Because only limited time was available for this soil analysis programme, selected samples only were analysed for mercury and mercury compounds. Twelve samples from the orientation traverse and 27 samples from the detailed survey were selected, Figs. 8.40 and 8.41.

1g. of each of the soils was mixed with 1g. of calcium oxide. The mixture was then analysed by the thermal dissociation technique described in this chapter. Two new

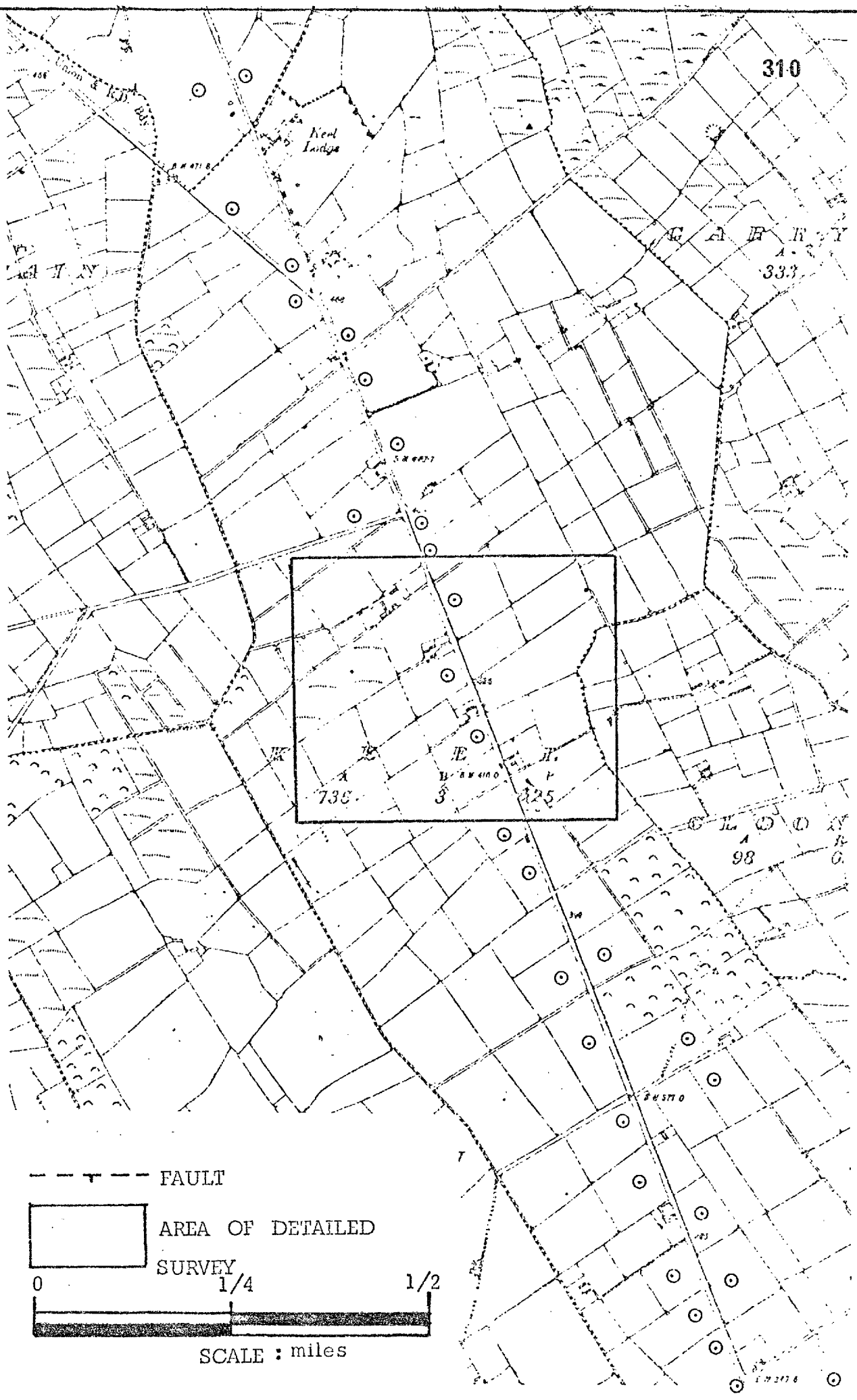


FIG ... 8.34 CADMIUM DISTRIBUTION ON ORIENTATION TRAVERSE

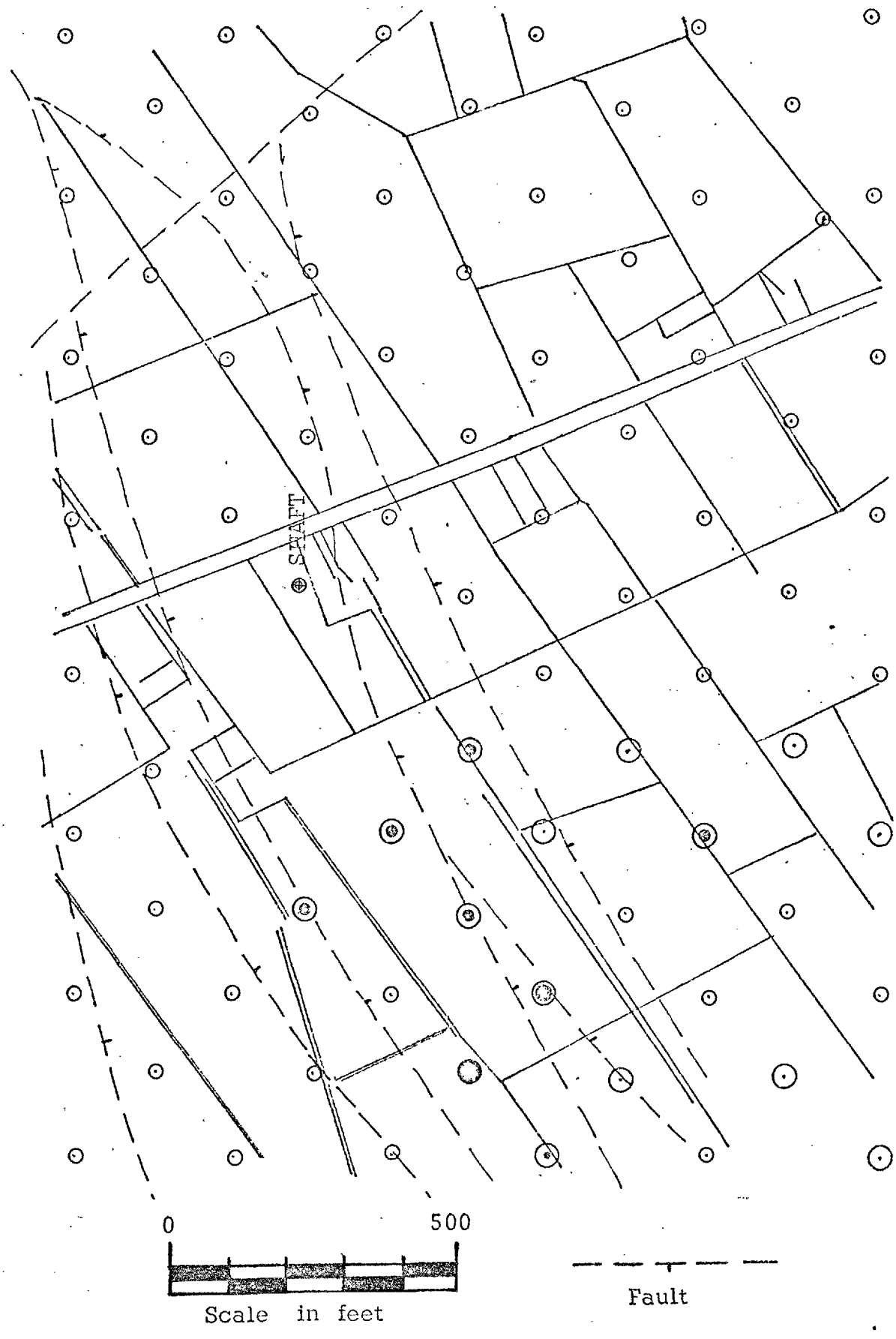


FIG ... 8.35 CADMIUM DISTRIBUTION IN SHAFT AREA

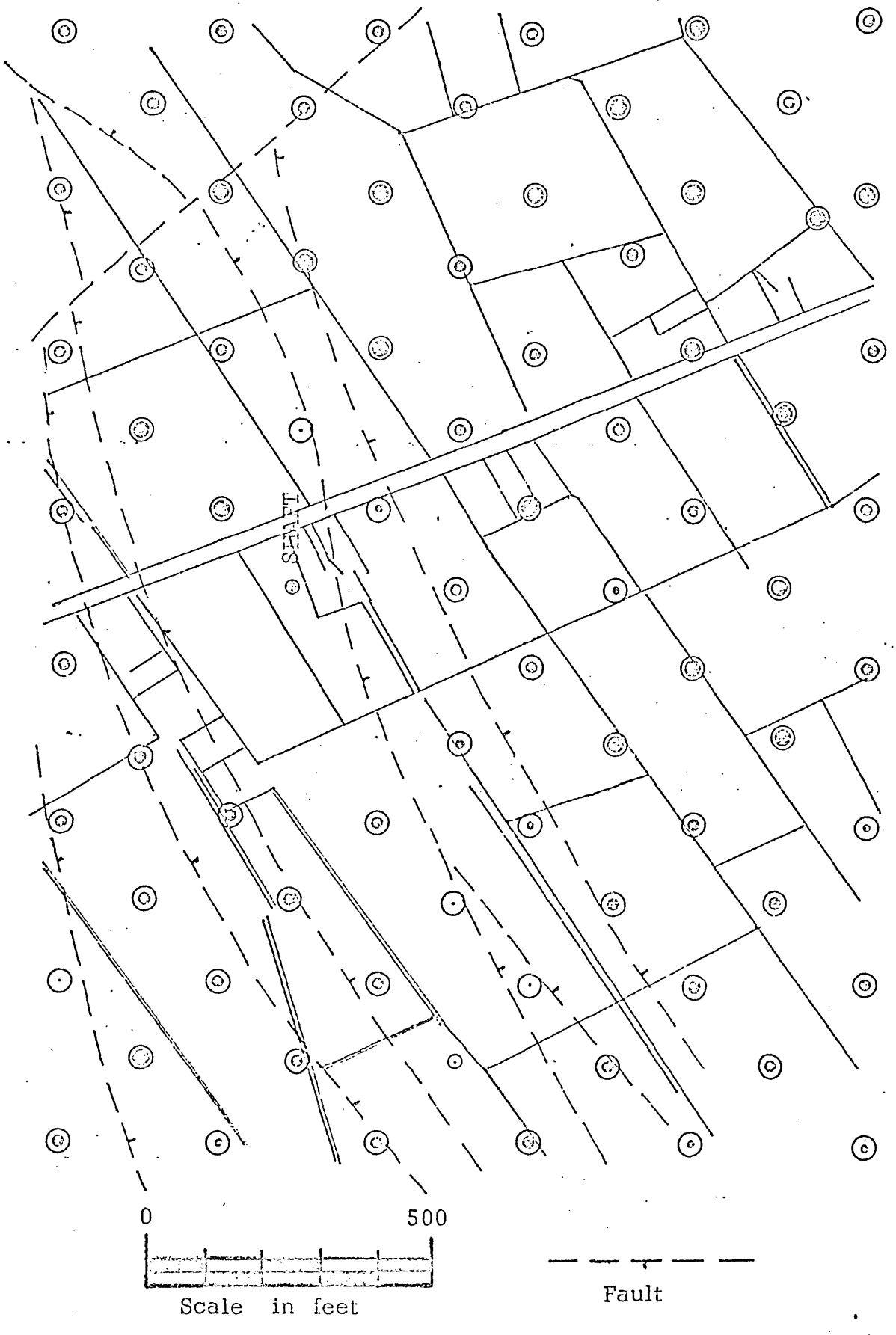


FIG ... 8.36 IRON DISTRIBUTION IN SHAFT AREA

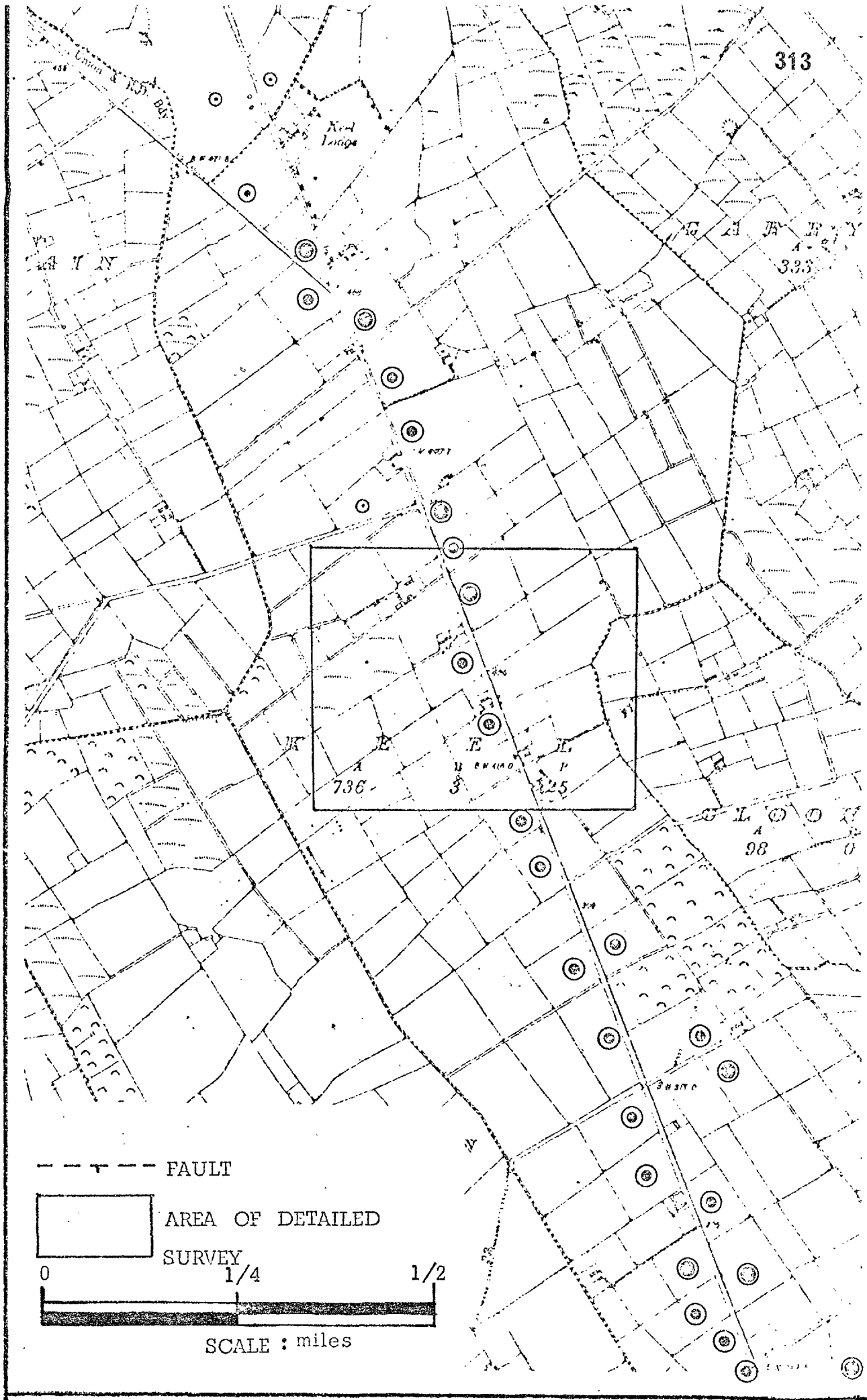


FIG ... 8.37 IRON DISTRIBUTION ON ORIENTATION TRAVERSE

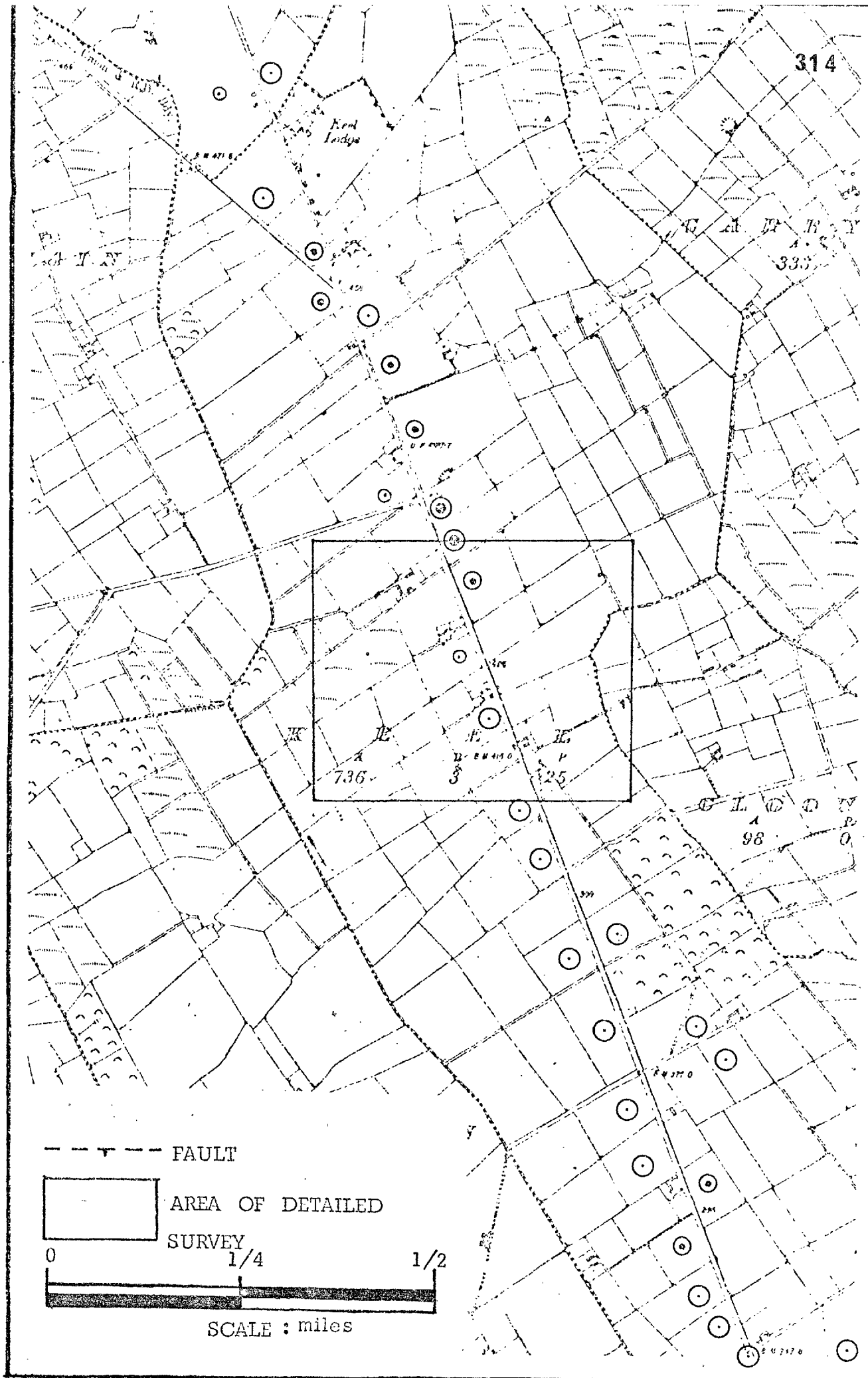


FIG ...8.38 MANGANESE DISTRIBUTION ON ORIENTATION TRAVERSE

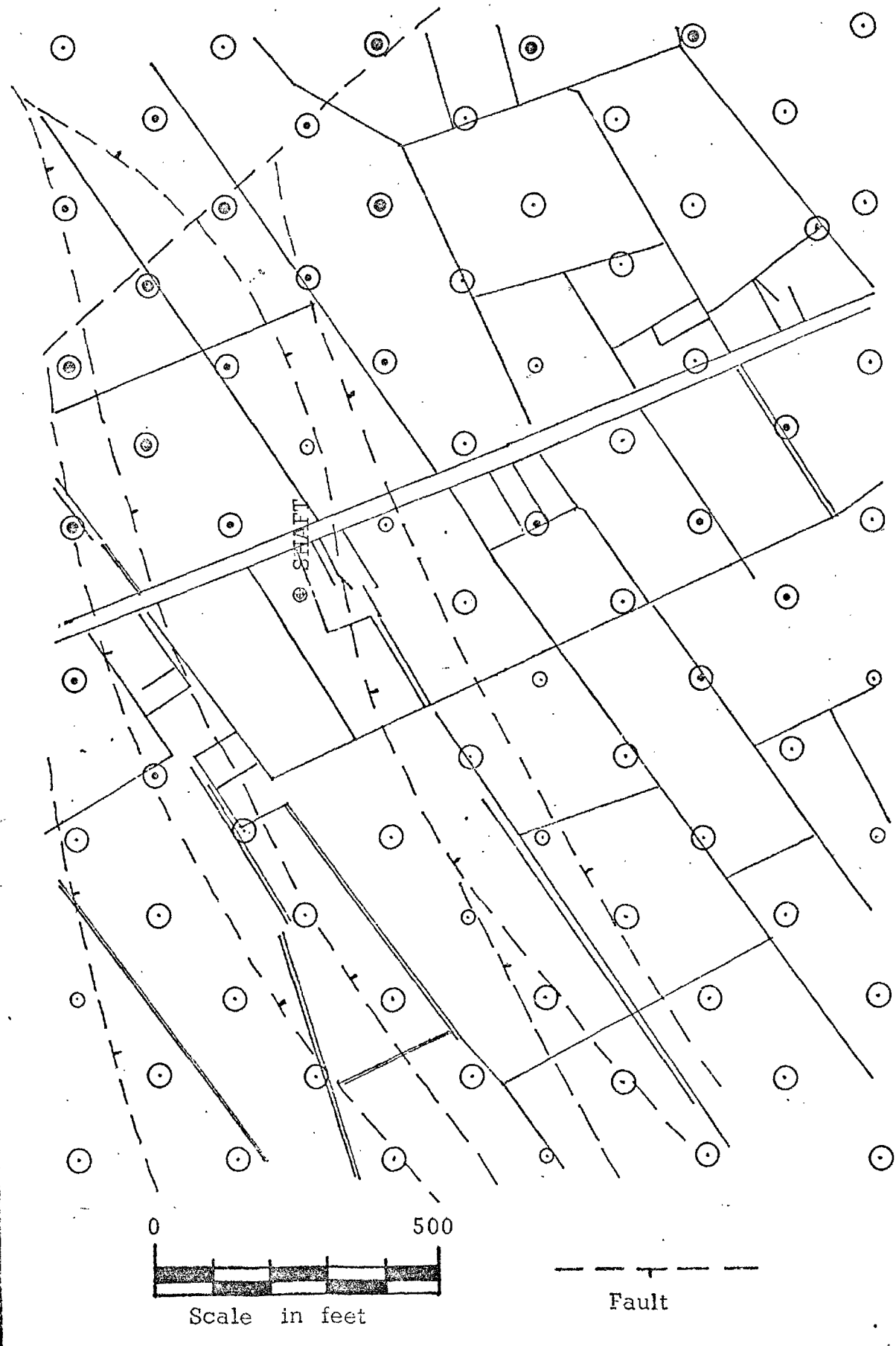


FIG ...8.39 MANGANESE DISTRIBUTION IN SHAFT AREA

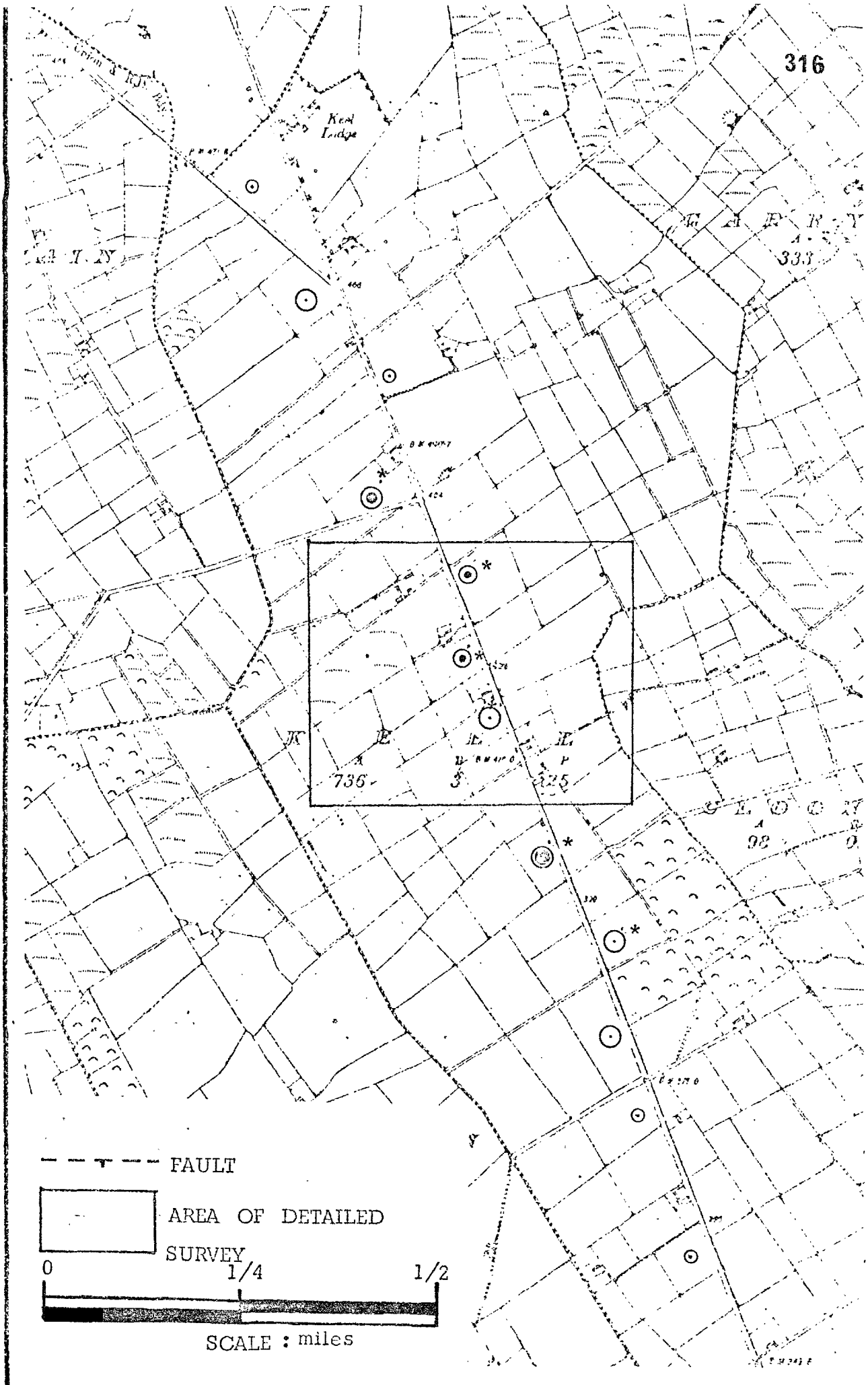


FIG ... 8.40

MERCURY AND MERCURY COMPOUND DISTRIBUTION ON ORIENTATION SURVEY

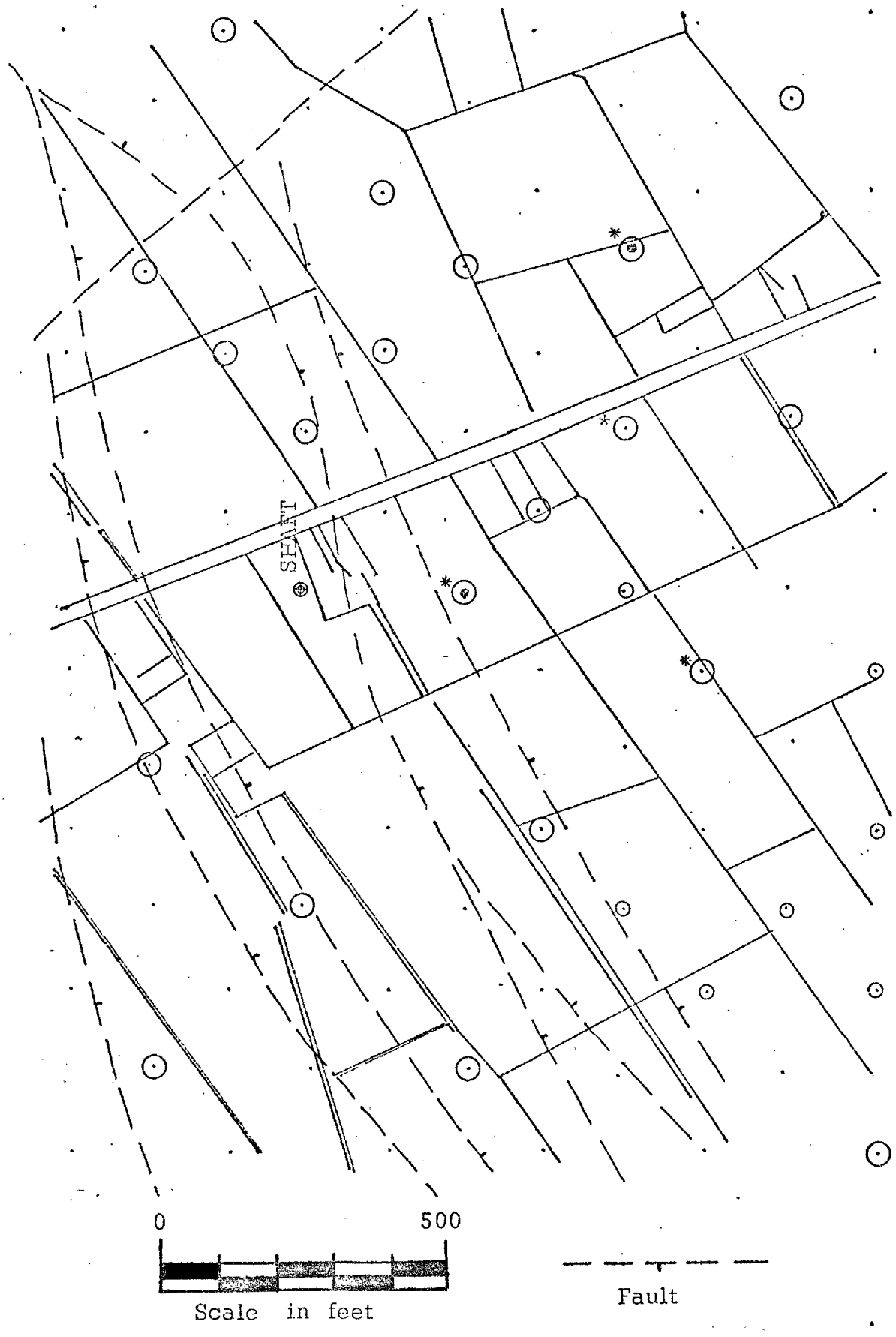


FIG ... 8.41 MERCURY AND MERCURY COMPOUND DISTRIBUTION IN SHAFT AREA

peaks, which did not occur in rocks, were found to predominate in soils. These were:

(a) 270°C Peak.

This peak was present in all the soil samples and varied in peak temperature between 240°C and 270°C . It was distinguished from $HgCl_2$ and HgS by the character of its total release trace, Fig. 8.42A. Mercury started to be evolved at 190°C - 200°C. and rose very sharply to a peak value and then quickly declined. For comparison with the $HgCl_2$ and HgS release traces, see Fig. 8.7. X.R.O. traces of the soils revealed a predominance of clay minerals and it was assumed that the 270°C peak could be due to release of adsorbed mercury from clay minerals.

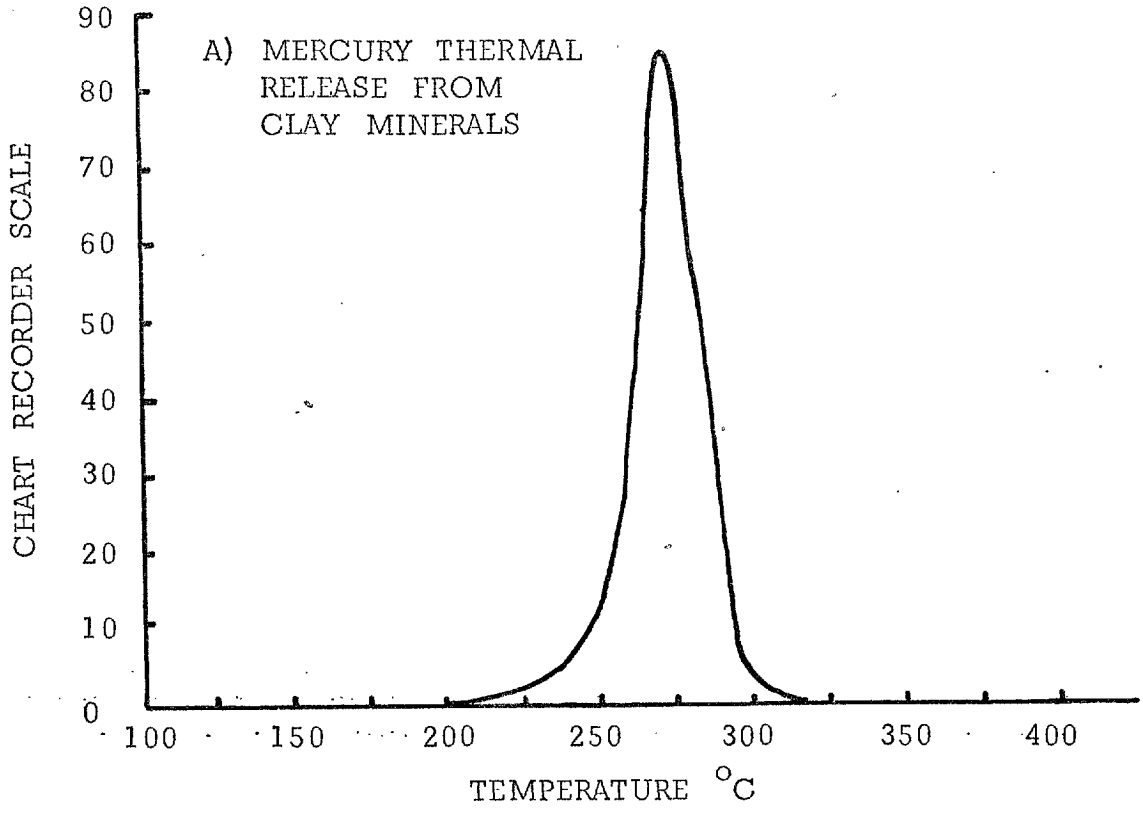
To test this possibility, ten grammes of Kaolinite, montmorillonite, keiselghur, Fullers earth and calcite, were weighed into five separate 1 litre, stoppered measuring cylinders. Eight hundred millilitres of a 100 µg/litre mercury solution were then added. The cylinders were then continuously agitated for three weeks. After this, the suspensions were filtered, dried and analysed for mercury by the thermal dissociation method. The results obtained were far from conclusive, except for montmorillonite, whence a very sharp peak, plateauing at 270°C, was obtained. It is obvious that much more work must be done before adequate classification of this peak is obtained. Nonetheless, it is the opinion of the author that this peak is due to release of adsorbed mercury from clay minerals.

(b) 430°C Peak.

A second peak at 430°C was found to predominate in iron rich soils, Fig. 8.42B. This correlated with a similar peak in drillcore material from the Decomposed Zone, where iron concentration, as ferric oxide, was greater than 25%. The temperature of mercury release from pyrite is 450°C.

(c) Results.

In the orientation survey, Fig. 8.40, an area associated with the mineralized zone is well picked out by samples containing some mercuric sulphide. The concentration intervals for mercury on Figs. 8.40 and 8.41, refer to total mercury and not to just mercuric sulphide. Asterisks indicate the samples containing some mercuric sulphide. The actual analysis of these soil samples is shown in Table 8.9. Sample K16, Fig. 8.40, contains over 5,000 ppb mercury, 8,955 ppb HgS and 187 ppb adsorbed, by far the highest concentration of HgS in any soil sample. If the base metal concentrations of the same sample are now looked at, they show no anomalies, (Cu, 11 ppm; Pb, 139 ppm; Zn, 536 ppm). Sample K9 on the other hand, contains over 1,000 ppb mercury, 842 ppb HgS and 2121 ppb adsorbed. This sample also has anomalous base metal concentrations, (Cu, 22 ppm; Pb, 1959 ppm, Zn, 1055 ppm). The HgS in this sample is probably more related to sub-cropping mineralization than that of sample K16. Associated with sample K9, samples K10 and K11 also contain HgS and these three together suggest a distinct possibility of sub-cropping mineralization.



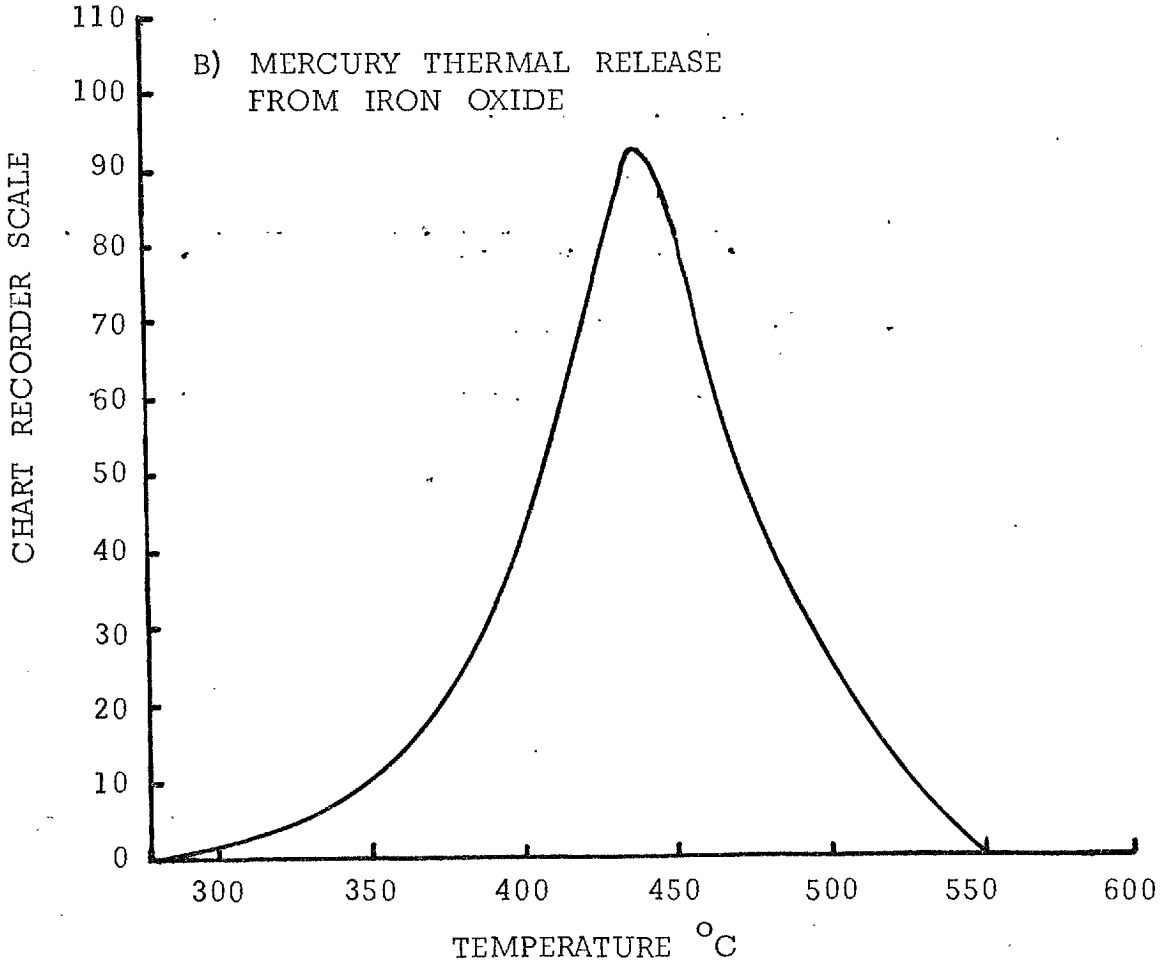


FIG ...8.42 MERCURY THERMAL RELEASE CHARACTERISTICS FROM CLAY MINERALS AND IRON OXIDES

TABLE ... 8.9

ANALYSIS OF MERCURY AND MERCURY COMPOUNDS IN KEEL SOILS

SAMPLE	CLAY ADSORBED MERCURY	MERCURIC SULPHIDE
k 3	26 ppb	
k 5	110 ppb	
k 7	69 ppb	
k 9	2121 ppb	842 ppb
k 12	380 ppb	290 ppb
k 13	280 ppb	400 ppb
k 14	120 ppb	100 ppb
k 16	187 ppb	8955 ppb
k 17	189 ppb	135 ppb
k 19	312 ppb	
k 22	95 ppb	
k 25	52 ppb	
9	280 ppb	
11	439 ppb	
14	312 ppb	
21	113 ppb	
23	222 ppb	
25	211 ppb	
28	240 ppb	
36	326 ppb	
37	500 ppb	
39	380 ppb	
42	76 ppb	469 ppb
44	115 ppb	
48	149 ppb	
50	204 ppb	
55	22 ppb	
57	206 ppb	69 ppb
58	120 ppb	100 ppb
59	110 ppb	520 ppb
62	13 ppb	50 ppb
64	68 ppb	50 ppb
70	31 ppb	
73	121 ppb	

The detailed survey, Fig. 8.41, indicates a further anomalous area to the south, samples 58,59 and 64,however the lateral extent is not very great. Of the twenty seven samples analysed for mercury in this survey, only four contained any HgS. It is obvious from comparison of Fig. 8.40 and 8.41,that the orientation survey has outlined the area of sub-cropping mineralization, while the detailed survey has not clarified it.

A far more extensive and detailed programme, designed to look into the distribution of mercury compounds in the soil, must obviously now be of primary importance for future research. The present study indicates that there is a definite possibility of identifying mercury compounds in soils. The reasons for their presence or absence and their relation to base metal mineralization, should be thoroughly investigated and interpreted before evaluation of this technique for secondary environment geochemical prospecting can be made. Further investigation is however beyond the scope of this present feasibility study.

CHAPTER 9

SUMMARY AND CONCLUSIONS

9.1. SUMMARY

In view of the role of mercury as a pathfinder element for potential areas of sulphide mineralization, the distribution of the metal in the vicinity of Keel has been assessed from analyses of drill cores and subsurface workings. Although the regional enrichment of mercury has been established in the rocks, the relationship between zinc and mercury was found to be highly erratic, with little correlation between the total mercury content and the proximity of sulphide ore. In view of the possible loss of mercury during sample preparation, and consequent masking of the relationship between mercury and base metals, an extensive study was undertaken in order to decide the best method of sample preparation and analysis. This study resulted in an analytical method being developed by which the identification of mercury compounds in unground rock material was made possible.

The quantitative identification of mercury in distinct compounds at the sub-microgramme level was accomplished by comparing atomic absorption of mercury, released during controlled continuous heating of unground rock samples, with thermal release curves, derived from rock standards, prepared from inorganic mercury compounds mixed with various synthetic rock bases.

The analysis of samples closely associated with mineralization has defined a zone in which mercury is present as mercuric sulphide, whereas in samples further from mineralization mercuric chloride is the dominant species. A transition zone of mixed mercuric sulphide/mercuric chloride is also present in places.

Analysis of mercury in sulphide rich material has been accomplished by the addition of an equal weight of calcium oxide to the sample. By this method it has been possible to overcome interference due to sulphur dioxide and sulphur trioxide molecular absorption and to identify individual mercury release curves which are associated with the breakdown of specific minerals in the Keel area. Consequently, by the isolation of these peaks it has been possible to obtain far more meaningful mercury/base metal associations.

9.2. CONCLUSIONS.

(a) An area of mercury enrichment has been established in bedrock at Keel, although no definite total mercury halo appears to exist around the actual deposit, the relation of total mercury to total base metal also being somewhat haphazard. High levels of mercury are found in areas far removed from base metal build up. However, this mercury has been established as being in the form of mercuric chloride. The reverse is true for some samples taken from the underground workings of the prospect, where low levels of total mercury are found in rocks adjacent to massive sulphide mineralization. This mercury has however been identified as always being in the form of mercuric sulphide.

(b) On the basis of total mercury analysis it was found that different size fractions of the same original crushed rock material from the underground workings of the prospect, increased in total mercury value with decreasing fraction size. The corresponding sieved size fractions of the majority of crushed drill core samples increased in total mercury value with increasing fraction size.

Short periods of grinding - 1550 μm + 494 μm material in a Tema mill do not appear to volatilize much mercury, while crushing appears to generate enough "local heat" to volatilize mercury from the more highly volatile mercury compounds in the finest material.

(c) The - 494 μm + 210 μm sieved crushed rock material is ideal for mercury analysis. Thermal diffusion gradients are apparent in the - 1550 μm + 494 μm crushed material, giving erratic mercury thermal release patterns.

(d) The thermal release characteristics of mercury, mercurous chloride, mercuric chloride, mercuric sulphide, mercuric oxide and mercuric sulphate are specific and characteristic for each compound.

The composition of rock bases used for diluting the analytical standards does not appear to greatly modify the thermal release characteristics of the mercury compounds. Using this technique, both qualitative and quantitative identification of mercury compounds in rock material is possible.

Recombination of mercury with its dissociated anions, or with oxygen from the air flushing gas, does not appear to be uniform between mercury compounds, although it is specific for each individual compound.

(e) By the use of a variable scale chart recorder and variable scale voltmeter placed in series, the optimum response for a given amount of mercury, released from crushed rock material during the heating programme, can be obtained at all times.

(f) From results obtained by the analysis of crushed rock material, by the mercury thermal dissociation technique, it is possible to divide the Keel deposit into three major mercury compound zones.

(1) A mercuric sulphide zone, which always appears to be associated with areas of sulphide mineralization.

(2) A mercuric chloride zone, which always appears to be further removed from the site of base metal build up.

(3) A mixed mercuric chloride/mercuric sulphide zone, separating the previous two zones, and which is also usually associated with base metal build up.

In addition to these three zones, two minor zones have also been recognised.

A mercuric oxide zone is found associated with an area of decomposed rocks, the Decomposed Zone, at Keel and also associated with an area of faulting to the south-east.

With reference to geological plans of the Keel prospect there appears to be a definite alignment between the distribution of mercury compounds and the east-west mineralized faults.

(g) The conversion of mercury into mercuric chloride or mercuric sulphide is dependent upon the specific activity of the associated anions and not only on their abundance. It is thus possible for mercuric chloride to exist in association with sulphide ions, provided that the activity of the sulphide ion is below that of the chloride ion. When the activity of the sulphide ion becomes greater than that of the chloride ion, mercuric sulphide, not mercuric chloride is formed.

(h) It is possible to identify mercury released from the lattices of sphalerite, galena and pyrite. By relating this mercury to the specific mineral from which it was released, it is possible to produce meaningful mercury/base metal relationships.

(i) The analysis of mercury in sulphide rich samples has been made extremely difficult by the absorption of light of 2536.5 Å by evolved SO_2 and SO_3. It was found that by mixing freshly prepared calcium oxide with the sulphide rich sample that sulphur was removed from the system, as calcium sulphate; this latter remaining inert to temperatures up to 1300°C. The use of calcium oxide therefore makes it possible to analyse mercury in sulphide rich material without fear of SO_2 and SO_3 molecular absorption.

(j) It is possible to quantitatively analyse arsenic released from both pyrite and sphalerite.

(k) A preliminary study of the distribution of mercury compounds in the soil at Keel has identified the presence of mercuric sulphide. This suggests a further possible adaptation of mercury thermal dissociation technique in the secondary environment.

9.3. SUGGESTIONS FOR FURTHER RESEARCH.

A great deal more research needs to be done on the distribution of not only mercury and its compounds,but other elements and their compounds,in both primary and secondary environment around many other ore deposits in both different geological and climatological environments.

A step forward in this direction is at present being taken in the Applied Geochemistry Research Group at the Royal School of Mines by W. T. Meyer and K. Lam Shang Leen who, using a radio frequency induced argon plasma have been able to identify specific distributions of cadmium, silver and lead compounds in soils over mineralized areas in various parts of Ireland.

9.4. SUGGESTIONS FOR IMPROVEMENT OF MERCURY THERMAL DISSOCIATION EQUIPMENT.

A geared radio frequency induction heater or fast cooling furnace needs to be used instead of a tube furnace,to heat the samples so that the slow cooling rate and consequent slow sample turnover is overcome. In this way it should be possible to analyse in excess of fifty samples per day instead of the four a day now possible.

REFERENCES

CHAPTERS 1 , 2 , 3 , 4 , 5 , 6 & 7 .

Ahrens , L . H . & Taylor , S . R . , 1961 . Spectrochemical Analysis . Pergamon Press , London . p . 454

Barnes , H . L . & Czamanske , G . K . , 1967 . Solubilities and transport of ore minerals , (Paper in Geochemistry of Hydrothermal ore deposits , Barnes , H . L . editor) , pp . 334 - 381 .

Barth , T . F . W . & Bruun , B . , 1945 . Studies on the igneous rock complex of the Oslo region . Ch . IV , Fluorine in the Oslo petrographic province . Skrifter Norske Videnskaps - Akad . Oslo , 1 Mat . - Naturv . Klasse , No . 8 .

Barton , P . B . & Skinner , B . J . , 1967 . Sulphide mineral stabilities , (Paper in Geochemistry of Hydrothermal ore deposits , Barnes , H . L . editor) . Holt , Rinehart & Winston , New York .

Berry , L . G . & Thompson , R . M . , 1962 . X - Ray powder data for ore minerals : The Peacock Atlas . Mem . Geol . Soc . Amer . No . 85 .

Boorman , R , S . , 1967 . Subsolidus studies in the ZnS - FeS - FeS_2 system, Econ. Geol., v.62, pp. 614 - 632 .

Boyle , R . W . & Jambor , J . L . , 1963 . The geochemistry and geothermometry of sphalerite in the Pb - Zn - Ag lodes of the Keno Hill - Galena Hill area , Yukon . Can . Min . 7 , pt. 3 pp . 479 - 496 .

Brooks , R . R . & Ahrens , L . H . 1961 . Some observations on the distribution of thallium, cadmium and bismuth in silicate rocks and the significance of covalency on their degree of association with other elements. Geochim. Cosmochim. Acta, 23 , pp. 100 - 115 .

Davidson , C . F . , 1966 . Some genetic relationships between ore deposits and evaporites . Trans . Inst . Min . Metall . Vol . 75 , pp. B 216 - 229

De Launay , L . & Urbain , G . , 1910 . Recherches sur la metallogenie des blendes et des mineraux qui en derivent . Soc . Geol . France Bull . , v . 10 , pp . 787 - 795 .

Dunham , K . C . , 1966 . Role of juvenile solutions , connate waters and evaporitic brines in the genesis of lead - zinc - fluorine - barium deposits . Trans . Inst . Min . Metall . Vol . 75 , pp. B 226 - 229

Edwards , A . B . , 1955 . Cadmium in the Broken Hill lode . Proc . Aust . Inst . Min . Metall . , no . 176 , pp . 71 - 96 .

El Shazly , E . M . , 1951 . The application of spectrographic analysis of minerals to the metallogenesis of lead / zinc ores . Ph.D. thesis , University of London .

El Shazly , E . M . , Webb , J . S . , Williams , D . , 1957 . Trace elements in sphalerite , galena and associated minerals from the British Isles . Trans . Inst . Min . Metall . , vol . 66 , pp . 241 - 271 .

Fleischer , M . , 1955 . Minor elements in some sulphide minerals , Econ . Geol . , 50 th . Anniv . Vol . 2 , pp . 970 - 1024 .

Fleischer , M . 1969 . U . S . G . S . standards . Additional data on rocks G 1 . &W 1 . 1965 - 1967 . Geochim . Cosmochim. Acta, v. 33, pp. 65 - 79.

Follingsbee , R . E . et al 1967 . Pine Point : N.W.T. Canada ; a lead zinc deposit formed from hydrothermal connate brines ? I.A.G.O.D. Symposium , St . Andrews , 1967 . Abstract in Trans . Min . Metall . vol . 76 , p . B 222 .

Fryklund , V . C . & Fletcher , J . D . , 1956 . Geochemistry of sphalerite from the Star Mine , Coeur d'Alene district , Idaho . Econ . Geol . vol . 51 , no . 3 , pp . 223 - 247 .

Fursov , V . Z . , 1958 . Halos of dispersed mercury as prospecting guides at the Achisai lead / zinc prospects . Geokhimiya . (English translation) , no . 3 , pp . 338 - 345 .

Gabrielson , O . , 1945 . Studier over elementfordelningen i zinkblanden fran svenska fyndorter - Studies on the distribution of elements in Sweedish sphalerites . Sveriges Geol . Udersokning Arsbok 39 , no . 1 , series C , no . 468 , p . 52 . (English summary) .

Graton , L . C . & Harcourt , G . A . , 1935 . Spectrographic evidence on origin of ores of Mississippi Valley Type . Econ . Geol . vol . 30 , no . 7 , pp . 800 - 824 .

Green , J . , 1959 . Geochemical tables of the elements for 1959 . Bull . Geol . Soc . Amer . , 70 , pp . 1127 - 1184 .

Grip , E . , 1948 . On the occurrence of mercury in Boliden and in some other sulphide deposits in North Sweeden . Sveriges Geologiska Undersokning Arsbok , 42 , no. 8 , series C , no . 499 .

Hawkes , H . E . , 1957 . Principles of geochemical prospecting U . S . Geol . Survey Bull . , 1000 - F , pp . 225 - 355 .

Hawkes , H . E . & Webb , J . S ., 1962 . Geochemistry in mineral exploration : Harper and Row , New York .

Hillebrand , Lundell , Bright & Hoffman , 1953 . Applied inorganic analysis , 2 nd. edition . John Wiley & Sons .

Ivanov , V . V . , 1964 . Distribution of cadmium in ore deposits : Geokhimiya , (English Translation) no . 4 , pp . 757 - 768 .

Jackson , F . , 1903 . The delicacy of tests employed for the detection of metals . J. Amer. Chem. Soc. vol . 25 , p . 922 .

James , C . H . , 1962 . A review of the geochemistry of mercury (excluding analytical aspects) and it's application to geochemical prospecting . I . C . S . T . Geochem . Prosp . Res . Centre Tech . Comm . No . 41 .

Jolly , J . L . & Heyl , A . V . , 1964 . Mineral paragenesis and zoning in the Central Kentucky mineral district . Econ . Geol . vol . 59 , no . 4 , pp . 596 - 624 .

Jolly , J . L . & Heyl , A . V . , 1966 . Mercury in sphalerite from Central Kentucky & Central Tennessee (abs .) Geol . Soc . Amer . Special Paper 87 , pp . 251 - 252 .

Jolly , J . L . & Heyl , A , V . , 1968 . Mercury and other trace elements in sphalerite and wallrocks from Central Kentucky , Tennessee and Appalachian zinc districts . U . S . Geol . Survey Bull . 1252 - F , pp . 1 - 29 .

Krauskopf , K . B . , 1951 . Physical chemistry of quicksilver transportation in vein fluids . Econ . Geol . vol . 46 , no . 5 , pp . 498 - 524 .

Kullerud , G . , 1953 . The FeS - ZnS system - a geological thermometer . Norsk . Geol . Tidsk . , vol . 32 , pp . 61 - 147 .

Kutina , J . , 1953 . Mikroskopischer und spektrographischer Beitrag zur Frage der Entstehung einiger Kolloidalstrukturen von Zinkblende und Wurtzit . Geologie , vol . 1 , no . 6 , pp . 436 - 452 .

Manning , P . G . , 1967 . Absorption spectra of Fe^{3+} in octahedral sites in sphalerite . Can . Mineral . vol . 9 , pt. 1 , pp . 57 - 64 .

Miller , A . R . , et al , 1966 . Hot brines and recent iron deposits in deeps of the Red Sea . Geochim . Cosmochim. Acta, v. 30, pp. 341 - 360 .

Mookherjee , A . , 1962 . Certain aspects of the geochemistry of cadmium . Geochim . Cosmochim. Acta, v.26, pp. 351 - 360 .

Morrissey , C . H . , 1970 . The mineralogy , structure and origin of the lead - zinc - copper residual orebody at Tynagh , County Galway , Ireland . Ph.D. thesis , University of London .

Morrissey , C . H . , Davis , G . R . , Steed , G . M . , 1971 . Mineralization in the Lower Carboniferous of Central Ireland . Trans . Inst . Min . Metall . Vol . 8 , sect . B , pp . B173 - 186 .

Nelson , J . B . & Riley , D . P . , 1945 . An experimental investigation of extrapolation methods in the derivation of accurate unit - cell dimensions of crystals . Proc . Phys . Soc . Lond . vol . 57 , pp . 160 - 177 .

Oftedal , I . , 1940 . Untersuchungen uber die Nebenbestandteile von Erzmineralien norwegischer Zinkblende - fuhrender Vorkommen : Norske Videnskaps Akad . , Skr . , Math . - Naturw . Kl ., no . 8 , p . 103 .

Ozerova , N . A . , 1959 . The use of primary dispersion holos of mercury in the search for lead - zinc deposits . Geokhimiya (English translation) , no . 7 , pp . 793 - 802 .

Patterson , J . M . , 1970/71 , Geology and mineralization of the Keel area , County Longford , Republic of Ireland . Ph.D. thesis , University of London .

Pina de Rubies , S . & Lopez de Azcona , J . M . , 1937 . Relacion entre el color y la composicion espectroquimica de la blende de Aliva , Picos de Europa . Soc . espanola fis . quim . , Anal . , vol . 35 , pp . 180 - 186 .

Rankhama , K . & Sahama , T . G . , 1950 . Geochemistry . University of Chicago Press , Chicago , p . 915 .

Robinson , W . O . & Edgington , G . , 1946 . Fluorine in soils . Soil Sci . Vol . 61 , p . 341 .

Roedder , E . , 1960 . Studies of primary fluid inclusions in sphalerite crystals from the OH vein , Creede , Colorado . Abstract in Econ . Geol ., vol ,55 . p.1337 .

Sandell , E . B . & Goldich , S . S . , 1943 . The rarer metallic constituents of some American igneous rocks . J . Geol . vol . 51 , pp . 99 - 115 & pp . 167 - 189 .

Saukov , A . A . , 1946 . (Geochemistry of mercury) : Akad . Nauk . U.S.S.R. , Inst , Geol . Nauk . Trudy , no . 78 , Mineral Geokhim . Ser . 17 , p . 129 (in Russian) .

Schroll , E . , 1950 / 51 . Spurenenelementparagenese (Mikroparagenese) ostalpiner Zinkblenden : Osterreich . Akad . Wiss . m Math . - Naturw . Kl ., Anz . Jahrg . 87 , pp . 21 - 25 ; Anz . Jahrg . 88 , pp . 6 - 12 . (Chem . Abs . 745,313 & 11,083 (1953)) .

Schroll , E . , 1953 . Uber Minerale und Spurenelemente , Verenzung und Enstehung der Blei - Zink Lagerstatte Bleiberg - Kreuth , Karten , Osterreich . Osterreich mineralog . Gesell . , Mitt ., Sanderheft no . 2 , p. 1 - 60

Shepherd , E . E . , 1940 . Note on the fluoride content of rocks and ocean bottom samples . Am.J.Sci. v.238 pp. 117 - 128 .

Smith , A . W . , 1963 . The geology and mineralization of the Zawar lead - zinc deposit , India . Ph.D. thesis University of London .

Stoiber , R . E . , 1940 . Minor elements in sphalerite . Econ . Geol . vol . 35 , no . 4 , pp . 501 - 519 .

Taylor , A . & Sinclair , H . , 1945 . On the determination of lattice parameters by the Debye - Scherrer method , Proc . Phys . Soc . Lond . vol . 57 , pp . 126 - 135 .

Tunell , G . , 1964 . Chemical processes in the formation of mercury ores and ores of mercury and antimony . Geochim . Cosmochim. Acta, v.28, pp. 1019 - 1038.

Traill , J . G . , 1939 . The geology and development of Mill Close Mine , Derbyshire . Econ . Geol . vol . 34 , pp . 851 - 889 .

Verhoogen , J . , 1938 . Thermodinamical calculations of the solubility of some important sulphides upto 400 °C . Econ . Geol . vol . 33 , no . 1 , pp . 34 - 51 .

Warren , H . V . & Thompson , R . M . , 1945 . Sphalerite from Western Canada . Econ . Geol . vol . 40 , no . 5 , pp . 309 - 335 .

White , D . E . , 1965 . Saline waters of sedimentary rocks . In fluids in subsurface environments . Mem . Ass . Petrol . Geol ., 4 , pp . 342 - 366 .

White , D . E . , Hem , J . D . & Waring , G . A . 1963 . Data of geochemistry , 6 th. edition , Chap . F , Chemical composition of subsurface waters . Prof . Pap . U.S. Geol . Surv . 440 - F , p . 67 .

Wormley , T . G . 1860. Notes on the chemical reactions of corrosive sublimate . Chem . News vol . 2 , p . 182 .

Yak , L . , 1951 . Sphalerite and apatite from Chvaletice , E . Bohemia . Acad . Tcheque Sci . Internat ., Classe sci . math ., nat , e med ., vol . 52 , pp . 53 - 68 .

CHAPTERS 8 & 9 .

Barringer , A . R . , 1964 . Developments towards the remote sensing of vapours as an airborne and space exploration tool . Third symposium on remote sensing of the environment , Univ . of Michegan , pp . 279 - 292 .

Barringer , A . R . , 1966 . Interference free spectrometer for high sensitivity mercury analysis of soils , rocks & air . Trans . Instn . Min . Metall . vol . 75 , sect . B , pp . B 120 - 124 .

Boyle , R . W . , 1971 . The land environment . Can . Min . & Metall . Bull . vol . 64 , no . 712 , pp . 46 - 50 .

Bradshaw , P . D . M . & Koksoy , M . , 1968 . Primary dispersion of mercury from cinnabar and stibnite deposits , Western Turkey . Trans . XXIII Int . Geol . Cong . vol . 7 , pp . 341 - 355 .

Bratt , J . ? 1967 . Mercury and mercury compounds . Kirk - Othmer Encyclopedia of chemical technology . Second edition , 13 , pp . 218 - 249 .

Dvornikov , A . G . , Vasilevskaya , A . E . & Shcherbakov , V . P . 1963 . Mercury dispersion aureoles in the soils of the Nagol'nyi Range . Geochemistry , pp . 501 - 509 .

Evans , D . S . , 1972 . Secondary dispersion of mercury and associated elements at Keel , Eire . Ph.D. thesis , University of London .

Friedrich , G . H . & Hawkes , H . E . , 1966 . Mercury as an ore guide in the Pachuca - Real del Monte district , Hidalgo , Mexico . Econ . Geol . vol . 61 , pp . 744 - 753 .

Friedrich , G . H . & Hawkes , H . E . , 1966 . Mercury dispersion halos as ore guides for massive sulphide deposits , West Shasta district , California . Mineralium deposita , 2 , pp . 77 - 88 .

Fursov , V . Z . , 1958 . Halos of dispersed mercury as prospecting guides in the Achisai lead / zinc deposit , Geokhimiya . (English translation) , no . 3 , pp.338-345 .

Goldschmidt , V . M . , 1937 . Geochemische Verteilungsgesetze der Elemente . 1X . Die Mengenverhaltnisse der Elemente und der Atom - Arten . Skrifter Norske Videnskaps - Akad . Oslo , 1 . Mat . - naturv . Klasse , no . 4 .

Hawkes , H . E . & Williston , S . H . , 1962 . Mercury vapour as a guide to lead - zinc - silver deposits . Min . Congr . J . 48 , pp . 30 - 32 .

Hawkes , H . E . & Webb , J . S . , 1962 . Geochemistry in mineral exploration . Harper Row , New York .

James , C . H . 1962 . A review of the geochemistry of mercury (excluding analytical aspects) and it's application to geochemical prospecting . I.C.S.T. Geochem . Prosp . Res . Centre , Tech . Comm . no . 41 .

James , C . H . & Webb , J . S . , 1964 . Sensitive mercury vapour meter for use in geochemical prospecting . Trans . Inst . Min . Metall . vol . 73 , pp. 633 - 641 .

James , C . H . , 1964 . The potential role of mercury in modern geochemical prospecting . Min . Mag . pp.23 - 32 .

Koksoy , M . 1967 . Dispersion of mercury and other elements from mineral deposits in Turkey. Ph.D. thesis , University of London .

Koksoy , M . , Bradshaw , P . D . M . & Tooms , J . S . , 1967 . Notes on the determination of mercury in geological samples . Trans . Inst . Min . Metall . vol . 76 , Sect . B , pp . 121 - 124 .

Manning , D . C . , 1970 . Non - flame methods for mercury determination by atomic absorption , a review . A . A . Newsletter , 9 , no . 5 , pp . 77 - 99 .

Mellor , J . W . , 1963 . A comprehensive treatise on inorganic and theoretical chemistry . Vol . lV , pp . 694 - 1049 , & Vol . lX , pp . 1 - 338 . Longmans London .

Motycka , J . , 1970 Airborne mercury spectrometer . Barringer Research , 3 , no . 3 , pp . 6 - 7 .

Noddack , I . & Noddack , W . , 1934 . Die geochemischen Verteilungskoeffizienten der Elemente . Svensk Kem . Tid . 46 , p . 173 .

Ozerova , N . A . 1959 . The use of primary dispersion halos of mercury in the search for lead zinc deposits . Geokhimiya , no , 7 , pp . 638 - 645 . (Russian Text) . English translation : Geochemistry , no . 7 , pp. 793-802.

Patterson , J . M . , 1970 . Geology and mineralization of the Keel area , County Longford , Republic of Ireland . Ph.D. thesis , University of London .

Polikarpochkin , V . V . , 1957 . Primary dispersion halos and their prospecting significance . Proc . First All - Union Conf . on geochemical methods of prospecting for ore deposits . (Ed . Krasnikov , V . I .) , Translation into English : English Science Translation Service , University of Alabama .

Preuss , E . , 1941 . Beitrage zur spektralanalytischen methodik . 11 . Bestimmung von Zn , Cd , Hg , In , Tl , Ge , Sn , Pb , Sb , und Bi , durch frakhonierte distillation . Z . angew . Mineral . 3 , p . 8 .

Rankama , K . & Sahama , T . G . , 1968 . Geochemistry . pp . 94 - 263 & pp . 715 - 718 . Univ . Chicago Press .

Sandell , E . B . , 1959 . Colorimetric determination of trace metals . Interscience Pub . Co . Inc . New York .

Saukov , A . A . , 1946 . Geochemistry of mercury . Trudy Inst . Geol . Nauk . Akad . S.S.S.R. Min . Geochem . Ser.No. 17 .

Stock , A . 7 Cucuel , F . 1934 . Die verbreitung des quecksilbers . Naturwissenchaften 22 , p . 390 .

Vaughn , W . W . & Mc Carthy , J . H . Jr. , 1964 . An instrumental technique for the determination of sub - microgramme concentrations of mercury in soils , rock & gas . Prof . Pap . U.S. Geol . Surv . 501 - D , pp . D 123 - 127 .

Watling , R . J . , 1972 . Identification of trace mercury compounds in rocks as a guide to sulphide mineralization at Keel , Eire . Tech . Comm .(in) Trans . Inst . Min . Metall . vol . 81 , sect. B , pp . B47 - 48 .

Watling , R . J . , 1972 . Trace identification of mercury compounds as a guide to sulphide mineralization at Keel , Eire. (In press) Proc . lV Internat . Geochem . Symp . London , April , 1972 .

Williston , S . H . , 1964 . The mercury halo method of exploration . Engineering and Mining Journal , 165 , No. 5 , pp . 98 - 101 .

Williston , S . H . , 1968 . Mercury in the atmosphere .
Jour . Geophys . Research , 73 , No . 22 , pp . 7051 - 7055 .

APPENDIX A

Sample Preparation and Methods of Analysis for Cu, Pb, Zn, Ag, Fe, Mn, Ca, Mg, Na and K, by Atomic Absorption and Atomic Emission Analysis.

A.1. SAMPLE PREPARATION

Each rock sample was reduced to - 1550 μm in a manganese steel jaw crusher. The crushed material from a sample was then thoroughly homogenised and then split into two, one half was then ground to - 53.5 μm using a silicon carbide Tema Mill. Samples of this ground half were used for the following analyses:

A.2 SAMPLE DIGESTION.

0.5 g. of the homogenised - 53.5μm sample were accurately weighed and transferred to a 100 ml. Teflon* beaker. To this, 20 ml. of a 4:1 mixture of conc nitric acid/conc perchloric acid were added and a watch glass placed over the beaker to prevent loss of sample by spitting. The watch glass also made the beaker into a crude reflux system. The beaker was now heated on either a thermostatically controlled hot-plate or suspended above a thermostatically controlled sand bath at 190°C - 200°C for four hours.

A variation of this technique was employed when dealing with samples rich in carbonate material. Here, 20 ml. of 40% hydrofluoric acid were added initially and 20 ml. of 4:1 conc HNO_3/conc. $HClO_4$ later. The addition of the hydrofluoric acid allowed the formation of insoluble calcium and magnesium fluorides which coated the carbonate grains and allowed slow dissolution of the carbonate instead of the vigorous dissolution and

consequent loss of sample which would have accompanied the addition of nitric and perchloric acids to a carbonate. Watch glasses were not used in the presence of hydrofluoric acid.

In the non carbonate digestion, after four hours refluxing, the watch glasses were removed and 20 ml. of 40% hydrofluoric acid added to decompose any silicates present. The whole was then evaporated to dryness at 190°C. When dry, 2 ml of perchloric acid were added to the residue to decompose any remaining fluorides and the whole again evaporated to dryness.

To the dry residue, 25 ml of 2N hydrochloric acid were added and the whole heated at 105°C until a clear solution had been obtained. This solution was then transferred to a 50 ml volumetric flask and diluted to the mark with repeated washings from the beaker.

*Teflon: A registered trade mark for poly tetra-fluor ethylene.

A.3. SAMPLE ANALYSIS.

Each sample was analysed for Cu, Pb, Zn, Ag, Fe, Mn, Ca and Mg. by atomic absorption and Na and K by atomic emission. These ten elements were divided into four groups for sample analysis.

(i) Elements sprayed directly in IN HCl

(ii) Elements sprayed in ammonia/ammonium carbonate solution.

(iii) Elements sprayed in IN. HCl plus 1% lanthanum solution.

(iv) Elements redissolved in conc. nitric acid and sprayed in 1% nitric acid solution.

(i) Cu, Pb, Zn, Ag, Fe and Mn.

The wavelengths used and optimum concentration ranges for these elements are shown in Table A.1.

(ii) Na and K.

(iia) Preparation of Ammonia/Ammonium Carbonate Solution.

10 g. of solid ammonium carbonate were weighed out and added to 500 ml. of deionised water (D.I.W.) in a 1 litre beaker. To this, 100 ml of ammonium hydroxide solution (S.G. 0.880 g./ml.) were added and the whole stirred until the ammonium carbonate had dissolved. The solution was then transferred to a 1 litre volumetric flask and diluted to the mark with D.I.W.

(iib) Reasons for the use of Ammonia/Ammonium Carbonate Solution.

(1) Interfering iron and aluminium cations were precipitated as insoluble R_2O_3 or hydrated oxides from the alkaline solution.

(2) Interfering calcium and magnesium cations were precipitated as insoluble $CaCO_3$ and $MgCO_3$ by the ammonium carbonate.

(iic) Preparation of samples for Atomic Emission Analysis.

All samples analysed for sodium and potassium were sprayed in a 10% solution of the ammonia/ammonium carbonate mixture. The wavelengths used and optimum concentration of the elements are shown in Table A.1.

TABLE ... A 1

OPTIMUM CONCENTRATION RANGES AND SPECTRAL LINES USED FOR Cu , Pb , Zn , Ag , Fe , Mn , Na , K , Ca , Mg . ANALYSIS .

ELEMENT	OPTIMUM CONCENTRATION RANGE ppm	WAVELENGTH Å
a)		
Cu	0 - 10	3247.5
Pb	0 - 40	2170.0
Zn	0 - 3	2138.6
Ag	0 - 4	3280.7
Fe	0 - 20	2483.3
Mn	0 - 10	2794.8
b)		
Na	0 - 4	5890.0
K	0 - 4	7664.9
c)		
Ca	0 - 10	4226.7
Mg	0 - 2	2852.1

(iiic) Preparation of Samples for Mg and Ca Analysis.

All samples analysed for magnesium and calcium were sprayed in a 1 % lanthanum chloride solution. Wavelengths used and optimum concentration ranges are shown in Table A1.

(iv) Pb and Ag.

Samples containing high levels of Ag and Pb were redissolved in conc. nitric acid to avoid precipitation of insoluble $PbCl_2$ and $AgCl_2$. Difficulties were experienced in dissolving some samples with high Pb, as oxidation of the sulphide anion by the nitric acid produced a sulphate and led to the precipitation of insoluble $PbSO_4$

Samples were diluted and sprayed in 1% HNO_3 solution; wavelengths and optimum concentration ranges are shown in Table A1.

(iii) Ca and Mg

(iiia) Preparation of 10% Lanthanum chloride solution.

100 g. of lanthsnum oxide were added to 300 ml. of D.I.W. and 200 ml. of conc. hydrochloric acid slowly added. A vigorous reaction took place with the production of a great amount of heat; a clear solution was finally obtained. This solution when cool was transferred to a 1 litre volumetric flask and made up to the mark with D.I.W.

(iiib) Reasons for the use of Lanthanum Solution and Precautions.

Because of the abundance of aluminium ions in solution and the ease with which calcium and magnesium aluminates form, (Calcium and Magnesium aluminates are not broken down in the air/acetylene flame), lanthanum was added to allow the formation of lanthanum aluminate and consequent removal of aluminium from the system.

The production of a white, milky solution after the addition of the lanthanum chloride solution usually indicates the presence of free fluoride ion and the production of insoluble lanthanum fluoride. In such a case , the sample should be redissolved, and 10 ml. of perchloric acid added in the final fuming cycle to make sure that all the fluoride has been decomposed, before addition of the 25 ml of 2N. HCl.

APPENDIX . B .

ANALYTICAL RESULTS FROM THE INITIAL SAMPLE PREPARATION STUDY

SAMPLE	- 210 µm	- 494 + 210 µm	- 1550 + 494 µm	CALCULATED TOTAL	TRUE TOTAL
1	39	36	15	30	28
2	75	15	5	32	38
3	42	41	28	37	30
4	68	53	20	47	27
5	54	17	14	28	28
6	40	25	11	25	20
7	265	150	96	170	172
8	30	26	82	46	10
9	21	10	2	11	9
10	10	15	14	13	18
11	15	3	9	9	7
12	25	5	2	11	10
13	60	41	21	41	58
14	26	25	11	21	36
15	36	10	14	17	37
16	42	18	15	25	28
17	104	27	24	52	45
18	25	10	9	15	25
19	16	12	10	12	10
20	20	15	7	14	15
21	117	91	26	78	78
22	90	46	41	59	100
23	102	9	15	42	51
24	193	98	50	114	127
25	31	44	27	34	36
26	682	720	600	667	650
27	35	22	15	24	29
28	29	13	25	22	20
29	85	37	36	53	46
30	144	10	12	55	150
31	36	17	10	21	30
32	188	169	110	156	150
33	138	140	116	131	139
34	334	248	210	297	270
35	54	11	5	23	40
36	305	260	149	238	270
37	104	51	27	61	69

TABLE A COPPER

Results expressed in p p m

SAMPLE	- 210 µm	- 494 + 210 µm	- 1550 + 494 µm	CALCULATED TOTAL	TRUE TOTAL
1	99	46	22	56	52
2	125	10	10	48	51
3	58	46	15	39	43
4	89	27	5	40	45
5	55	42	12	36	35
6	210	160	18	129	125
7	290000	215600	1519	169040	151800
8	1600	27	15	547	65
9	77	49	9	45	31
10	<5	15	5	7	31
11	<5	26	12	13	34
12	154	141	36	77	108
13	197	150	27	125	100
14	72	59	10	47	33
15	7	17	27	17	43
16	2100	1820	596	1505	1620
17	53200	49610	12160	38323	25500
18	480	210	26	239	46
19	1200	970	190	787	470
20	<5	52	21	24	20
21	24	16	25	22	42
22	157	138	59	118	121
23	49200	17700	2196	23032	16700
24	229671	167500	52875	150015	95720
25	1764	273	127	721	596
26	585225	525000	375000	495075	470510
27	6889	2500	196	3195	410
28	300	132	15	149	27
29	24921	18906	19955	21261	21650
30	169975	158750	25975	118233	79200
31	55944	27500	492	27979	6250
32	241821	220937	986	154581	21750
33	130045	134375	11057	91826	65000
34	480870	301562	26979	269801	79575
35	43452	19531	41520	34834	36275
36	304200	217187	45870	189086	96785
37	124362	95625	210	73399	1575

TABLE B ZINC

Results expressed in p p m

SAMPLE	- 210 μm	- 494 + 210 μm	- 1550 + 494 μm	CALCULATED TOTAL	TRUE TOTAL
1	1360	516	290	722	532
2	128	79	10	72	64
3	72	27	15	38	52
4	56	97	52	68	100
5	80	105	25	70	80
6	3400	2160	1050	2203	1540
7	101000	7325	290	36250	5800
8	72	26	20	39	52
9	40	21	17	26	16
10	52	34	15	26	16
11	<5	10	27	12	12
12	320	186	45	184	92
13	92	91	150	111	68
14	40	26	290	119	80
15	48	190	27	88	100
16	264	216	152	211	240
17	2316	1970	286	1524	1532
18	108	115	93	105	120
19	5400	3960	1095	3485	2620
20	16	70	70	52	72
21	64	27	180	90	72
22	116	180	25	107	164
23	12000	9925	156	7360	3560
24	5219	1918	1065	2735	2150
25	2267	1342	970	1526	1065
26	3140	1638	35	1604	956
27	2975	1122	1075	1724	1957
28	2647	930	27	1201	580
29	17530	7488	296	8438	4960
30	27544	16808	2280	15514	9750
31	5870	4488	2175	4178	5350
32	14526	13888	9725	12713	12750
33	80682	69975	7671	52776	59950
34	7306	4088	3865	5086	5751
35	1444	532	95	690	456
36	22532	17468	4968	14989	15135
37	9399	6635	1027	5687	4950

TABLE C LEAD

Results expressed in ppm

SAMPLE	- 210 µm	- 494 + 210 µm	- 1550 + 494 µm	CALCULATED TOTAL	TRUE TOTAL
1	103	97	25	75	65
2	7893	7500	9600	8331	8500
3	5143	4605	4350	4699	5450
4	5443	5200	4200	4998	5500
5	8143	7500	6975	7539	7750
6	12143	12100	12975	12406	13000
7	12093	14000	12750	12948	14750
8	75	63	27	55	55
9	295	220	190	235	232
10	191	105	85	127	100
11	162	140	110	137	118
12	357	327	357	347	338
13	113	107	100	107	99
14	7600	7200	7350	7385	11500
15	3600	4950	7796	5449	6650
16	406	290	197	298	200
17	128	107	29	88	70
18	128	101	57	95	89
19	26	19	10	18	20
20	434	390	486	437	305
21	262	197	92	184	118
22	235	196	151	194	178
23	21	10	21	17	25
24	78	50	46	58	78
25	59	16	27	34	25
26	52	28	14	31	30
27	2 200	2000	2010	2006	2000
28	85	25	50	53	50
29	79	13	60	50	27
30	64	13	10	29	54
31	155	166	140	154	160
32	56	19	12	29	30
33	94	63	47	68	76
34	67	19	40	42	52
35	81	23	12	39	49
36	85	84	49	76	56
37	299	350	200	283	325

TABLE D MANGANESE

Results expressed in ppm

SAMPLE	- 210 µm	- 494 + 210 µm	- 1550 + 494 µm	CALCULATED TOTAL	TRUE TOTAL
1	3252	7250	2671	4391	4600
2	37400	2958	1537	13965	28000
3	28000	25300	1005	18102	21000
4	27600	26725	26150	26825	23000
5	36400	31500	21650	29850	30200
6	28400	27750	22530	26227	26000
7	33000	29725	27625	30117	31000
8	14400	13125	297	9335	8000
9	2820	1917	1050	1929	2000
10	10500	7650	2165	6772	4000
11	6700	5960	2425	5028	3400
12	13500	9732	4530	9254	7800
13	37000	151	2050	13076	3200
14	35100	29650	15975	26908	27400
15	32800	29625	25750	29392	28600
16	21600	21000	10500	17700	13000
17	5600	4970	975	3848	3000
18	41100	35000	32000	36033	36000
19	1850	1880	1550	1760	1200
20	10200	7950	5350	7833	6600
21	16800	15975	9750	14175	12400
22	38500	36200	32500	35733	35200
23	1930	1853	1210	1664	1680
24	5164	4200	2056	3807	3920
25	6149	5200	1327	4225	4750
26	10664	12800	7800	10421	9755
27	21650	11500	6397	10182	10950
28	3377	2500	1516	2426	2158
29	3578	2700	2850	3043	3268
30	7900	6700	2452	5684	5207
31	1865	1500	980	1448	1416
32	3739	6200	1215	3718	2625
33	4446	4200	2975	3874	3980
34	7151	6500	26	4554	5287
35	3578	2500	1275	2451	2985
36	4444	3500	2780	3575	4150
37	5076	2780	3575	4150	4080

TABLE E IRON

Results expressed in ppm

SAMPLE	- 210 µm	- 494 + 210 µm	- 1550 + 494 µm	CALCULATED TOTAL	TRUE TOTAL
1	52500	41650	26150	40100	41850
2	123000	137000	127000	129000	130000
3	110000	105050	105150	149733	108500
4	135000	127500	121500	128000	121000
5	97500	83500	79500	86833	79000
6	158500	151000	171750	160417	166000
7	107000	97650	97500	100717	101000
8	2500	990	14725	6072	10500
9	11250	9750	8580	9860	8850
10	126	50	1175	450	2000
11	9100	8900	5325	7775	7000
12	20100	21750	15160	19003	17750
13	3850	3500	2000	3117	2500
14	175500	175000	141000	163833	139500
15	69500	63800	50500	57933	56000
16	22250	21700	1975	15308	12350
17	1900	850	2100	1617	600
18	2550	2150	2515	2405	2250
19	16	20	12	16	16
20	21300	11975	11550	12925	15600
21	1290	8900	5300	5163	7050
22	2800	2175	2159	2375	2222
23	<5	596	1580	692	1600
24	15	5	10	10	15
25	831	10	532	458	765
26	260	12	210	161	210
27	39532	77500	39500	52177	42575
28	1206	<5	120	443	1137
29	1278	<5	500	594	1560
30	718	<5	280	334	890
31	14918	15900	15325	15381	15350
32	623	5	516	381	340
33	1223	28	1515	922	1510
34	1479	45	1060	861	734
35	1073	<5	105	395	770
36	2504	990	2510	2001	1915
37	10460	14750	15105	13420	12535

TABLE F CALCIUM

Results expressed in ppm

SAMPLE	- 210 µm	- 494 + 210 µm	- 1550 + 210 µm	CALCULATED TOTAL	TRUE TOTAL
1	1760	1693	1525	1641	1470
2	97975	97050	97175	97367	97200
3	84975	79600	78500	81025	80000
4	107475	115000	100000	107492	98000
5	57975	59175	51950	56367	55100
6	106475	112150	90750	106242	99400
7	57975	59175	61650	60375	63300
8	6625	6250	426	4435	5100
9	2365	1897	2120	2127	1980
10	5840	5151	4165	5052	3750
11	2886	2935	2075	2632	1720
12	5801	4951	4105	4953	4300
13	25740	22200	25950	22456	22000
14	95647	95750	95350	95582	95200
15	54307	51300	50600	52069	49500
16	4050	5216	3260	4175	3670
17	1530	900	897	1109	1000
18	3259	1650	1750	1920	2120
19	487	526	435	482	600
20	4221	1517	2975	2904	2900
21	5021	3850	3955	4275	3500
22	23595	21550	20750	21965	19200
23	750	600	510	620	570
24	511	800	863	725	730
25	454	480	412	449	450
26	176	91	185	151	200
27	45180	41200	41500	42627	42700
28	666	659	693	670	615
29	419	300	525	415	420
30	1197	1280	1150	1209	1050
31	531	500	500	510	560
32	169	200	184	184	180
33	889	550	790	743	873
34	404	100	592	365	416
35	368	180	370	306	200
36	2274	2830	2198	2434	2170
37	8487	9200	4932	7540	5690

TABLE G MAGNESIUM

Results expressed in ppm

SAMPLE	- 210 µm	- 494 + 210 µm	- 1550 + 494 µm	CALCULATED TOTAL	TRUE TOTAL
1	24950	31600	25300	27283	28000
2	23500	23950	22150	23200	22500
3	24375	23500	23900	23925	23675
4	21375	21075	25150	22553	21125
5	25000	26200	27175	26125	29250
6	6000	5735	5965	5900	5525
7	4500	4100	4700	4433	4000
8	41250	51250	39750	44083	60750
9	21750	23775	21255	22260	24875
10	31500	41500	29750	34250	42250
11	28500	26200	21000	25233	24125
12	25000	29700	21110	25370	34500
13	65000	72000	65050	67350	83250
14	10875	10950	11900	11242	11550
15	26250	37300	31500	31685	47000
16	21750	17150	22700	20533	15125
17	11250	9695	15195	12047	8250
18	60000	72000	61750	61442	65500
19	17000	16000	17950	16983	15175
20	1925	17175	17560	12222	18375
21	25500	29500	27500	27500	31000
22	55500	59695	41575	52257	66750
23	19500	18255	17975	18577	17250
24	1102	6945	5937	4664	4962
25	1520	3358	2569	2479	2390
26	489	458	500	482	470
27	19095	14500	1327	11641	14900
28	2146	14788	4172	7037	5315
29	1400	1483	1400	1428	1425
30	1846	2883	2775	2501	2500
31	2397	8166	4950	5172	3750
32	848	4549	3150	2849	2520
33	1428	8166	9320	6305	6516
34	692	2315	2530	1842	2415
35	1642	11500	9700	7614	7900
36	879	345	390	541	490
37	2900	2012	3194	2885	3121

TABLE H POTASSIUM

Results expressed in ppm

SAMPLE	- 210 µm	- 494 + 210 µm	- 1550 + 494 µm	CALCULATED TOTAL	TRUE TOTAL
1	10300	11270	10450	10685	10275
2	780	5470	7325	4608	5790
3	3830	8963	7961	6918	8220
4	3535	9761	7045	6777	8685
5	11750	11750	10950	11483	12555
6	870	5120	4937	3642	4575
7	385	512	405	435	405
8	16850	15795	12575	15073	10069
9	9556	9900	10750	10030	9930
10	11250	13050	11975	12087	12750
11	12875	15732	10500	13036	11880
12	11000	11250	10500	13036	11880
13	8000	7832	8250	8061	7080
14	1250	1965	5325	2847	6450
15	4395	8168	5250	5938	9000
16	3135	4735	3050	3640	4275
17	3100	2715	2080	2623	1845
18	8125	8160	5965	7417	7095
19	1625	1375	960	1320	1005
20	7475	7950	8100	7842	8850
21	10250	11750	9000	10333	11325
22	6750	5210	4590	5517	4830
23	3000	2971	4625	3532	3870
24	1597	2145	1369	1704	1637
25	2415	1755	3280	2483	2780
26	618	330	790	579	720
27	2823	4680	2130	3211	3735
28	4371	3000	5130	4167	4798
29	2236	2415	1930	2194	1732
30	2842	5625	2125	3531	2849
31	2457	2970	2520	2648	2793
32	1277	1380	680	1112	1030
33	2510	2805	3520	2945	2971
34	842	750	800	797	750
35	3109	3465	1317	2630	2976
36	763	420	583	562	580
37	973	750	1241	1048	1070

TABLE I SODIUM

Results expressed in ppm

APPENDIX . C .

POLAROGRAPHIC TECHNIQUE AND PREPARATION OF ATOMIC ABSORPTION STANDARD SOLUTIONS .

APPENDIX C.

POLAROGRAPHIC TECHNIQUE.

From a small tube immersed in the solution, a stream of mercury drops was allowed to fall into a pool of mercury. A variable voltage was applied between the jet and the pool, and the resulting electrical current measured. By using a univector unit a voltage-current curve was obtained, and the position of the peak of the curve was characteristic of the nature of the ions present in solution, while from the height of the curve it was possible, by calibration under constant working conditions, to measure the concentration of the ions. The solution was contained in a glass cell, and a platinum wire, sealed through the bottom of the cell, dipped into a small pool of mercury in the cell holder, making connection between the mercury pool and the potentiometer. The connection between the potentiometer and the dropping mercury electrode was made through the mercury reservoir, which fed mercury to the latter.

The applied potential was measured, and by reference to standard tables of half wave potential in conjunction with the position of the element peak obtained from synthetic standards, it was possible to interpret the resulting curves. The half wave potential of cadmium is - 0.7 volts. and of lead is - 0.48 volts in the solution used for these experiments.

This method enabled any interferences by Ca, Mg, Na and K, to be overcome, as they simply cannot be read in acid solution.

Standards for atomic absorption analysis were made up for cadmium and lead from 1.0 - 10.0 ppm and 1.0 - 40.0 ppm respectively,

in: 1M HCl

1M HCl + 10 ppm Ca + 10 ppm Mg,

1M HCl + 100 ppm Ca + 100 ppm Mg,

1M HCl + 1,000 ppm Ca + 1,000 ppm Mg,

1M HCl + 5,000 ppm Ca + 5,000 ppm Mg,

1M HCl + 10,000 ppm Ca +10,000 ppm Mg,

The cadmium and lead values were read off on the most appropriate curve after the calcium and magnesium values had been obtained for each sample. This method eliminates incorrect results due to both viscosity and interfering ions.

Initial problems were encountered using the polarographic technique. The mercury in contact with the solution immediately formed a scum and gave erratic results. The action of hydrochloric acid, ferrous and ferric iron on mercury were tested and found to have no effect. Consequently two experiments were carried out to try and overcome this interference.

(a) Addition of 1M ammonia/ammonium chloride and 0.01% gelatine.

This solution was designed to bring down R_2O_3 as hydroxide, and eliminate any effect they had on the mercury. No improvement was found.

(b) Addition of 0.5M sodium-potassium tartrate and ascorbic acid.

This solution was designed to complex any available R_2O_3 and rare earths, and also to reduce any ions not complexed by the tartrate. By addition of this solution all interference with the mercury was stopped.

APPENDIX . D .

FLUORINE AND CHLORINE ANALYSIS OF SELECTED DRILL CORE SAMPLES

(Numbers correspond to sample positions in the analytical file in the Mining Geology Department , Royal School of Mines , London .)

TABLE ... A .

FLUORINE AND CHLORINE ANALYSIS ON SELECTED DRILL CORE SAMPLES

SAMPLE	F	Cl	SAMPLE	F	Cl
935	12.0	3.6	970	2.0	60.0
936	6.2	4.2	971	1.7	170.0
937	15.5	1.1	972	n.d.	170.0
938	19.0	1.8	973	n.d.	45.0
939	9.5	1.5	974	3.4	1.0
940	3.0	1.8	975	2.8	8.0
941	4.5	8.5	976	2.6	n.d.
942	4.7	1.5	977	1.5	n.d.
943	2.5	13.5	978	4.2	n.d.
944	1.3	9.6	979	1.6	n.d.
945	3.7	13.0	980	1.9	20.0
946	1.3	21.0	981	1.9	4.0
947	0.8	13.9	982	0.7	2.0
948	2.0	17.0	983	1.7	10.0
949	1.9	12.0	984	11.1	4.0
950	4.4	37.0	985	3.2	20.0
951	1.5	84.0	986	13.0	4.0
952	n.d.	66.0	987	4.0	25.0
953	3.0	187.0	988	n.d.	3.0
954	n.d.	48.0	989	1.0	11.0
955	2.2	90.0	990	n.d.	50.0
956	2.6	41.0	991	1.2	10.0
957	3.6	44.0	992	n.d.	17.0
958	3.3	10.0	993	n.d.	13.0
959	4.6	10.6	994	n.d.	4.0
960	10.5	8.6	995	1.2	2.0
961	10.0	9.3	996	2.3	5.0
962	n.d.	10.7	997	n.d.	3.0
963	6.4	38.0	998	16.2	5.0
964	4.2	20.0	999	n.d.	25.0
965	0.1	7.5	1000	n.d.	14.0
966	n.d.	4.0	1001	n.d.	55.0
967	1.1	n.d.	1002	n.d.	25.0
968	5.8	1.0	1003	12.7	10.0
969	2.0	35.0	1004	18.7	6.0
1005	17.9	16.0	1015	9.1	147.0
1006	17.6	8.0	1016	9.5	23.0
1007	9.3	18.0	1017	11.1	22.0
1008	12.5	27.0	1018	10.9	7.0
1009	11.3	15.0	1019	7.8	30.0
1010	10.7	61.0	1020	8.5	18.0
1011	9.7	6.0	1021	11.1	9.0
1012	9.7	9.0	1022	n.d.	62.0
1013	13.1	10.0	1023	11.3	6.0
1014	14.7	14.0			

n.d. : Below detection limit. Results expressed in ppm .

SAMPLE	- 210 μm	- 494 + 210 μm	- 1550 + 494 μm	CALCULATED TOTAL	TRUE TOTAL
1	3252	7250	2671	4391	4600
2	37400	2958	1537	13965	28000
3	28000	25300	1005	18102	21000
4	27600	26725	26150	26825	23000
5	36400	31500	21650	29850	30200
6	28400	27750	22530	26227	26000
7	33000	29725	27625	30117	31000
8	14400	13125	297	9335	8000
9	2820	1917	1050	1929	2000
10	10500	7650	2165	6772	4000
11	6700	5960	2425	5028	3400
12	13500	9732	4530	9254	7800
13	37000	151	2050	13076	3200
14	35100	29650	15975	26908	27400
15	32800	29625	25750	29392	28600
16	21600	21000	10500	17700	13000
17	5600	4970	975	3848	3000
18	41100	35000	32000	36033	36000
19	1850	1880	1550	1760	1200
20	10200	7950	5350	7833	6600
21	16800	15975	9750	14175	12400
22	38500	36200	32500	35733	35200
23	1930	1853	1210	1664	1680
24	5164	4200	2056	3807	3920
25	6149	5200	1327	4225	4750
26	10664	12800	7800	10421	9755
27	21650	11500	6397	10182	10950
28	3377	2500	1516	2426	2158
29	3578	2700	2850	3043	3268
30	7900	6700	2452	5684	5207
31	1865	1500	980	1448	1416
32	3739	6200	1215	3718	2625
33	4446	4200	2975	3874	3980
34	7151	6500	26	4554	5287
35	3578	2500	1275	2451	2985
36	4444	3500	2780	3575	4150
37	5076	2780	3575	4150	4080

TABLE E IRON

Results expressed in ppm

APPENDIX

ANALYSES OF SOIL SAMPLES ON DETAILED SHAFT SURVEY

SAMPLE	Cd	Cu	Pb	Mn	Zn	Fe
1	<1	3	123	116	153	16477
2	<1	8	221	31	39	13657
3	2	25	633	260	666	17657
4	8	16	426	575	861	17159
5	7	22	467	1382	818	16716
6	5	16	164	1351	540	17711
7	2	11	139	546	264	16219
8	4	11	90	371	226	17324
9	1	11	33	124	99	18006
10	1	19	1377	118	279	16772
11	2	25	762	631	1163	17767
12	3	19	303	130	295	16606
13	2	19	204	1255	399	18246
14	2	11	90	1175	730	17380
15	1	14	90	526	251	16643
16	<1	5	139	127	166	15297
17	2	16	467	575	861	16600
18	8	46	2368	342	864	16569
20	1	30	402	898	579	18320
21	1	22	49	620	562	16753
22	<1	25	57	1127	289	18117
23	6	11	57	201	619	17564
24	1	11	761	124	226	16760
25	200	19	238	141	958	16192
28	4	16	164	59	779	13583
29	<1	38	16	790	272	18135
30	3	22	33	980	661	17767
31	2	11	400	631	579	18810
32	12	14	90	1120	861	16500
33	181	33	57	150	1322	17066
35	1	16	115	76	274	15002

SAMPLE	- 210 µm	- 494 + 210 µm	- 1550 + 210 µm	CALCULATED TOTAL	TRUE TOTAL
1	1760	1693	1525	1641	1470
2	97975	97050	97175	97367	97200
3	84975	79600	78500	81025	80000
4	107475	115000	100000	107492	98000
5	57975	59175	51950	56367	55100
6	106475	112150	90750	106242	99400
7	57975	59175	61650	60375	63300
8	6625	6250	426	4435	5100
9	2365	1897	2120	2127	1980
10	5840	5151	4165	5052	3750
11	2886	2935	2075	2632	1720
12	5801	4951	4105	4953	4300
13	25740	22200	25950	22456	22000
14	95647	95750	95350	95582	95200
15	54307	51300	50600	52069	49500
16	4050	5216	3260	4175	3670
17	1530	900	897	1109	1000
18	3259	1650	1750	1920	2120
19	487	526	435	482	600
20	4221	1517	2975	2904	2900
21	5021	3850	3955	4275	3500
22	23595	21550	20750	21965	19200
23	750	600	510	620	570
24	511	800	863	725	730
25	454	480	412	449	450
26	176	91	185	151	200
27	45180	41200	41500	42627	42700
28	666	659	693	670	615
29	419	300	525	415	420
30	1197	1280	1150	1209	1050
31	531	500	500	510	560
32	169	200	184	184	180
33	889	550	790	743	873
34	404	100	592	365	416
35	368	180	370	306	200
36	2274	2830	2198	2434	2170
37	8487	9200	4932	7540	5690

TABLE G MAGNESIUM

Results expressed in ppm

TRACE ELEMENT ANALYSIS OF SOIL SAMPLES ON ORIENTATION SURVEY

SAMPLE	Cd	Cu	Pb	Mn	Zn	Fe
k1	1	3	67	28	36	8515
k2	1	1	22	849	171	9897
k3	3	13	16	189	75	16034
k4	3	13	57	682	148	18522
k5	<1	11	65	504	59	17859
k6	1	16	41	155	101	18301
k7	2	16	180	835	237	17490
k8	1	33	361	657	295	16126
k9	1	16	836	73	260	9178
k10	1	22	1959	3124	1055	18559
k11	6	5	401	1526	541	17610
k12	1	30	402	898	579	18320
k13	1	16	115	76	274	15002
k14	3	27	131	368	326	17324
k15	3	14	123	609	160	18449
k16	<1	11	139	416	536	15887
k17	1	8	107	181	140	16624
k18	1	11	98	495	185	17914
k19	2	8	98	303	159	17159
k20	2	3	74	339	89	16495
k21	<1	11	90	492	139	19610
k22	2	8	25	473	178	17730
k23	1	8	98	247	140	16587
k24	2	8	106	569	158	17785
k25	3	16	66	558	100	18504
k26	2	3	16	467	84	19168
k27	3	3	<5	337	75	17159
k28	1	<1	16	410	76	17675
k29	1	8	<5	399	131	19094
k30	3	<1	25	331	701	16661

Results expressed in ppm